



Design of Cold-formed Steel Structures

Eurocode 3: Design of Steel Structures
Part 1-3: Design of Cold-formed Steel Structures

Dan Dubina
Viorel Ungureanu
Raffaele Landolfo



ECCS
CECM
E K B

WILEY-BLACKWELL

Ernst & Sohn
A Wiley Company

ECCS Eurocode Design Manuals

DESIGN OF COLD-FORMED STEEL STRUCTURES

ECCS EUROCODE DESIGN MANUALS

ECCS EDITORIAL BOARD

Luis Simões da Silva (ECCS)

António Lamas (Portugal)

Jean-Pierre Jaspart (Belgium)

Reidar Bjorhovde (USA)

Ulrike Kuhlmann (Germany)

DESIGN OF STEEL STRUCTURES

Luis Simões da Silva, Rui Simões and Helena Gervásio

FIRE DESIGN OF STEEL STRUCTURES

Jean-Marc Franssen and Paulo Vila Real

DESIGN OF PLATED STRUCTURES

Darko Beg, Ulrike Kuhlmann, Laurence Davaine and Benjamin Braun

FATIGUE DESIGN OF STEEL AND COMPOSITE STRUCTURES

Alain Nussbaumer, Luís Borges and Laurence Davaine

Design of Cold-formed Steel Structures

Dan Dubina, Viorel Ungureanu and Raffaele Landolfo

AVAILABLE SOON

DESIGN OF COMPOSITE STRUCTURES

Markus Feldman and Benno Hoffmeister

DESIGN OF JOINTS IN STEEL AND COMPOSITE STRUCTURES

Jean-Pierre Jaspart, Klaus Weynand

INFORMATION AND ORDERING DETAILS

For price, availability, and ordering visit our website www.steelconstruct.com.
For more information about books and journals visit www.ernst-und-sohn.de

DESIGN OF COLD-FORMED STEEL STRUCTURES

Eurocode 3: Design of Steel Structures
Part 1-3 – Design of Cold-formed Steel
Structures

Dan Dubina
Viorel Ungureanu
Raffaele Landolfo



ECCS
CECM
E K S

 **WILEY-BLACKWELL**

 **Ernst & Sohn**
A Wiley Company

Design of Cold-formed Steel Structures

1st Edition, 2012

Published by:

ECCS – European Convention for Constructional Steelwork

publications@steelconstruct.com

www.steelconstruct.com

Sales:

Wilhelm Ernst & Sohn Verlag für Architektur und technische Wissenschaften
GmbH & Co. KG, Berlin

All rights reserved. No parts of this publication may be reproduced, stored in a retrieval system, or transmitted in any form or by any means, electronic, mechanical, photocopying, recording or otherwise, without the prior permission of the copyright owner.

ECCS assumes no liability with respect to the use for any application of the material and information contained in this publication.

Copyright © 2012 ECCS – European Convention for Constructional Steelwork

ISBN (ECCS): 978-92-9147-107-2

ISBN (Ernst & Sohn): 978-3-433-02979-4

Legal dep.: 348490/12 - Printed in Multicomp Lda, Mem Martins, Portugal

Photo cover credits: BRITT Ltd., Timisoara, Romania.

TABLE OF CONTENTS

FOREWORD	xi
PREFACE	xiii
Chapter 1	
<u>INTRODUCTION TO COLD-FORMED STEEL DESIGN</u>	1
1.1 General	1
1.2 Cold-formed steel sections	4
1.2.1 Types of cold-formed steel sections	4
1.2.2 Manufacturing	9
1.2.3 Some peculiar characteristics of cold-formed steel sections	12
1.3 Peculiar problems of cold-formed steel design	15
1.3.1 Buckling strength of cold-formed steel members	15
1.3.2 Torsional rigidity	20
1.3.3 Web crippling	21
1.3.4 Ductility and plastic design	22
1.3.5 Connections	22
1.3.6 Design assisted by testing	23
1.3.7 Design standards	23
<i>1.3.7.1 North American Cold-formed Steel Specification, 2001 Edition (AISI, 2001) and 2007 Edition (AISI, 2007)</i>	23
<i>1.3.7.2 Australian/New Zealand Standard – AS/NZS 4600, 2005 Edition (AS/NZS, 2005)</i>	25
<i>1.3.7.3 Eurocode 3 – Design of Steel Structures, Part 1.3 – General Rules, Supplementary Rules for Cold-formed Thin Gauge Members and Sheeting</i>	26
1.3.8 Fire resistance	27
1.3.9 Corrosion	28

TABLE OF CONTENTS

1.3.10 Sustainability of cold-formed steel construction	28
1.4 Main applications of cold-formed steel	31
1.4.1 Advantages of cold-formed steel in building construction	31
1.4.1.1 Advantages during construction	31
1.4.1.2 Advantages in service	32
1.4.2 Applications	34
Chapter 2	
BASIS OF DESIGN	47
<hr/>	
2.1 General	47
2.2 Limit state design	49
2.3 Actions on structures. Combinations of actions	53
2.3.1 Verification at the Ultimate Limit State	54
2.3.2 Verification at the Serviceability Limit State	57
2.3.2.1 Deflections	60
2.3.2.2 Dynamic effects	63
2.4 Materials	65
2.4.1 General	65
2.4.2 Structural steel	67
2.4.2.1 Material properties of base material	67
2.4.2.2 Material properties of cold-formed sections and sheeting	68
2.4.2.3 Thickness and thickness tolerances	72
2.5 Methods of analysis and design	73
2.5.1 Methods of analysis – Global frame analysis	73
2.5.2 Finite Element Methods (FEM) for analysis and design	77
2.5.3 Design assisted by testing	80
2.6 Imperfections	85
2.6.1 Imperfections for global analysis of frames	85
2.6.2 Imperfections for analysis of bracing systems	90
2.6.3 Role of imperfections in advanced numerical simulation	91
2.6.3.1 Section imperfections	93
2.6.3.2 Residual stresses	94

Chapter 3		
BEHAVIOUR AND RESISTANCE OF CROSS SECTION		97
3.1	General	97
3.2	Properties of gross cross section	100
3.2.1	Nominal dimensions and idealisation of cross section	100
3.2.2	Net geometric properties of perforated sections	104
3.2.3	Dimensional limits of component walls of cold-formed steel sections	107
3.2.4	Modelling of cross section component walls for analysis	110
3.3	Flange curling	111
3.4	Shear lag	114
3.5	Local buckling	116
3.5.1	Sectional buckling modes in thin-walled sections	116
3.5.2	Elastic buckling of thin plates	118
3.6	Distortional buckling: analytical methods for predicting elastic distortional buckling stresses	129
3.6.1	The method given in EN 1993-1-3:2006	130
3.7	Design against local and distortional buckling according to EN 1993-1-3	132
3.7.1	General	132
3.7.2	Plane elements without stiffeners	133
3.7.3	Plane elements with edge or intermediate stiffeners	136
3.7.3.1	<i>General</i>	136
3.7.3.2	<i>Plane elements with edge stiffeners</i>	139
3.7.3.2.1	<i>Conditions</i>	139
3.7.3.3.2	<i>General procedure</i>	140
3.7.3.3	<i>Plane elements with intermediate stiffeners</i>	162
3.7.3.3.1	<i>Conditions</i>	162
3.7.3.3.2	<i>General procedure</i>	163
3.7.3.4	<i>Trapezoidal sheeting profiles with intermediate stiffeners</i>	165
3.7.3.4.1	<i>General</i>	165

TABLE OF CONTENTS

3.7.3.4.2	<i>Flanges with intermediate stiffeners</i>	166
3.7.3.4.3	<i>Webs with up to two intermediate stiffeners</i>	169
3.7.3.4.4	<i>Sheeting with flange stiffeners and web stiffeners</i>	174
3.8	Resistance of cross sections	175
3.8.1	General	175
3.8.2	Axial tension	176
3.8.3	Axial compression	180
3.8.4	Bending moment	185
3.8.4.1	<i>Elastic and elastoplastic resistance with yielding at the compressed flange</i>	185
3.8.4.2	<i>Elastic and elastoplastic resistance with yielding at the tension flange only</i>	188
3.8.4.3	<i>Effects of shear lag</i>	188
3.8.5	Shear force	192
3.8.6	Torsional moment	194
3.8.7	Local transverse forces	203
3.8.7.1	<i>General</i>	203
3.8.7.2	<i>Cross sections with a single unstiffened web</i>	204
3.8.7.3	<i>Cross sections with two or more unstiffened webs</i>	214
3.8.7.4	<i>Stiffened webs</i>	217
3.8.8	Combined tension and bending	218
3.8.9	Combined compression and bending	220
3.8.10	Combined shear force, axial force and bending moment	224
3.8.11	Combined bending moment and local load or support reaction	231
Chapter 4		
<u>BEHAVIOUR AND DESIGN RESISTANCE OF BAR MEMBERS</u> 239		
4.1	General	239
4.2	Compression members	241
4.2.1	Theoretical background	241
4.2.1.1	<i>Ideal elastic members</i>	241

4.2.1.2	<i>Imperfect member</i>	248
4.2.1.3	<i>Class 4 sections: local-global interactive buckling</i>	253
4.2.2	Buckling resistance of uniform members in compression. Design according to EN 1993-1-3	259
4.2.2.1	<i>Flexural buckling</i>	260
4.2.2.2	<i>Torsional buckling and flexural-torsional buckling</i>	262
4.3	Buckling strength of bending members	277
4.3.1	Theoretical background	277
4.3.2	Design according to EN 1993-1-3	289
4.3.2.1	<i>Lateral-torsional buckling of members subject to bending</i>	289
4.3.2.2	<i>Simplified assessment methods for beams with restraints in building</i>	291
4.4	Buckling of members in bending and axial compression	299
4.4.1	Theoretical background	299
4.4.2	Design of beam-columns according to EN 1993-1-1 and EN 1993-1-3	303
4.4.2.1	<i>General method for lateral and lateral-torsional buckling of structural components</i>	311
4.5	Beams restrained by sheeting	324
4.5.1	General. Constructional detailing and static system	324
4.5.2	Modelling of beam-sheeting interaction	329
4.5.3	Design of beams restrained by sheeting according to EN 1993-1-3	333
4.5.3.1	<i>Design criteria</i>	334
4.5.3.2	<i>Design resistance</i>	336
4.5.3.3	<i>Rotational restraint given by the sheeting</i>	342
4.5.4	Simplified design of purlins	346
4.6	Design of beams at serviceability limit states	363
Chapter 5		
SHEETING ACTING AS DIAPHRAGM		367
5.1	Introduction	367

TABLE OF CONTENTS

5.2	General design considerations for diaphragm action	372
5.2.1	Conditions and restrictions for the use of stressed skin design	372
5.2.2	Types of diaphragms	375
5.2.3	Irregular roof chape	377
5.2.4	Design criteria	378
5.2.4.1	<i>Diaphragm flexibility</i>	378
5.2.4.2	<i>Diaphragm strength</i>	380
5.2.5	Interaction of diaphragm action and rigid-jointed frames	381
5.2.6	The danger of ignoring stressed skin action in conventional construction	381
5.3	Design procedures for sheeting acting as diaphragm	382
5.3.1	Design expressions for shear flexibility of diaphragm	382
5.3.1.1	<i>Sheeting spanning perpendicular to length of diaphragm</i>	382
5.3.1.2	<i>Sheeting spanning parallel to length of diaphragm</i>	394
5.3.2	Design expression for shear strength of diaphragms	397
5.3.2.1	<i>Sheeting spanning perpendicular to length of diaphragms</i>	397
5.3.2.2	<i>Sheeting spanning parallel to length of diaphragms</i>	402
5.3.2.3	<i>Buckling strength of sheeting in shear</i>	404
5.3.2.3.1	<i>General</i>	404
5.3.2.3.2	<i>Global shear buckling</i>	405
5.3.2.3.3	<i>Local shear buckling</i>	406
5.3.2.4	<i>Effect of combined loads</i>	407
5.3.3	Diaphragms with openings	407
5.3.3.1	<i>Discrete openings</i>	408
5.3.3.1.1	<i>Requirements for discrete openings</i>	408
5.3.3.1.2	<i>Flexibility of diaphragms with discrete openings</i>	409

5.3.3.1.3	<i>Strength of diaphragms with discrete openings</i>	409
5.3.3.2	<i>Strip openings</i>	410
5.3.4	Two skin envelopes	410
5.4	Interaction of the shear diaphragms with supporting framing	412
5.4.1	General	412
5.4.2	Elastic design of framing	413
5.4.2.1	<i>Rectangular frames: all frames loaded</i>	413
5.4.2.2	<i>Pitched roof frames: all frames loaded</i>	415
5.4.2.3	<i>One frame loaded</i>	417
5.4.3	Plastic design of framing	418
5.4.3.1	<i>Rectangular frames</i>	418
5.4.3.2	<i>Pitched roof frames</i>	419
5.4.4	Modelling of diaphragm effect for frame analysis	420
5.5	Diaphragm action of sandwich panels	422
Chapter 6		
STRUCTURAL LINER TRAYS		437
6.1	Introduction	437
6.2	Design procedures for cassette sections	442
6.2.1	General	442
6.2.2	Axial compression	443
6.2.3	Moment resistance	444
6.2.3.1	<i>Bending with the narrow flange in compression (wide flange in tension)</i>	444
6.2.3.2	<i>Bending with the wide flange in compression</i>	447
6.2.4	Behaviour in shear	449
6.3	Design procedures for cassette panels acting as diaphragm	453
6.3.1	Cassettes spanning horizontal to the length of diaphragm (liner tray shear panels)	453
6.3.2	Some peculiar problems for design of wall panels of cassettes spanning vertically to the length of diaphragm	455
6.4	Combined effects	457

TABLE OF CONTENTS

Chapter 7

CONNECTIONS	463
7.1 Introduction	463
7.2 Fastening techniques of cold-formed steel constructions	465
7.2.1 Mechanical fasteners	465
7.2.1.1 <i>Mechanical fasteners for sections</i>	466
7.2.1.2 <i>Mechanical fasteners for sheeting</i>	477
7.2.1.3 <i>Mechanical fasteners for sandwich panels</i>	478
7.2.2 Welding	480
7.2.2.1 <i>Fusion arc welding</i>	481
7.2.2.2 <i>Resistance welding</i>	483
7.2.2.3 <i>Behaviour of cold-formed steel welds</i>	484
7.2.3 Fastening based on adhesive bonding	486
7.3 Mechanical properties of connections	487
7.4 Design of connections	489
7.4.1 General design considerations	489
7.4.2 Design of connections with mechanical fasteners	491
7.4.2.1 <i>General rules</i>	492
7.4.2.2 <i>Design of bolted connections</i>	498
7.4.2.3 <i>Design of connections with self-tapping screws</i>	508
7.4.2.4 <i>Design of connections with blind rivets</i>	519
7.4.2.5 <i>Design of connections with fired pins</i>	520
7.4.3 Design of welded connections	523
7.4.3.1 <i>General design and workmanship consideration</i>	523
7.4.3.2 <i>Design of spot welds</i>	524
7.4.3.3 <i>Fillet lap welds</i>	526
7.4.3.4 <i>Arc spot welds</i>	528
7.5 Design assisted by testing of cold-formed steel connections	536
7.5.1 General	536
7.5.2 Fasteners in shear	537
7.5.3 Fasteners in tension	539
7.5.4 Evaluation of test results	540

7.5.4.1	<i>General</i>	540
7.5.4.2	<i>Evaluation of tests results according to Annex A of EN 1993-1-3</i>	541
7.5.4.3	<i>Evaluation of test results under static loads according to European Recommendations</i>	546
Chapter 8		
BUILDING FRAMING		557
<hr/>		
8.1	General information	557
8.2	Introduction	557
8.3	Construction systems	558
8.4	Stick built constructions	563
8.4.1	Foundation	563
8.4.2	Floors	564
8.4.3	Wall studs	567
8.4.4	Roof	569
8.4.5	On-site construction	570
8.5	Conceptual design	573
8.5.1	Architectural design	573
8.5.2	Thermal insulation	577
8.5.3	Soundproofing	578
8.5.4	Fire resistance	581
8.5.5	Vibration	583
8.5.6	Durability	584
8.5.7	Sustainability	587
8.6	Structural design	589
8.6.1	Structural conception	589
8.6.2	Design under vertical loads	592
8.6.2.1	<i>Design of floors</i>	593
8.6.2.2	<i>Design of walls</i>	595
8.6.2.3	<i>Sheathing-braced design for vertical loads</i>	597
8.6.3	Design under horizontal loads	598
8.6.3.1	<i>“All-steel” lateral bracing</i>	599
8.6.3.2	<i>Structural behaviour of sheathed diaphragm</i>	601
8.6.4	Specific design manuals	606

TABLE OF CONTENTS

8.6.4.1 <i>Prescriptive method for residential cold-formed steel framing</i>	606
8.6.4.2 <i>Workpack design for steel house</i>	607
8.7 Case study: residential building	608
8.7.1 Architectural design	608
8.7.2 Conceptual design	611
8.7.2.1 <i>Floor assembly</i>	612
8.7.2.2 <i>Wall assembly</i>	614
8.7.3 Structural design	617
8.7.3.1 <i>Reference codes</i>	617
8.7.3.2 <i>Loads</i>	617
8.7.4 Design checking	620
8.7.4.1 <i>Joist</i>	620
8.7.4.2 <i>Studs</i>	624
8.7.5 Details	626
REFERENCES	633

FOREWORD

Following pioneering research in the 1940s, research into cold-formed steel intensified in the 1970s and led to numerous national European design specifications, and subsequently the preparation of Part 1-3 of Eurocode3 (EN1993-1-3) for cold-formed steel structures. Now a Euronorm, EN1993-1-3 is fully embedded in the Eurocode framework.

This book serves as a reference text for design engineers using EN1993-1-3. It forms part of the suite of ECCS Eurocode Design Manuals prepared in recent years for other parts of EN1993 and other Eurocodes to aid the implementation of Eurocodes in European states. The book draws on the authors' considerable experience with designing cold-formed steel structures, both as academics and practitioners, and strikes a balance between theory and practice.

Applications of cold-formed steel have broadened over the years. Cold-formed steel is now used as primary structural elements, as in steel framed residential buildings, steel storage racks, portal frames, and tubular truss and frame structures, and as secondary structural elements, as in roofing and wall systems featuring purlins, girts and corrugated steel sheeting. Additionally, integrated building systems have been developed, such as cassettes, as have stressed skin principles for designing the building envelope.

The design of cold-formed steel is perceived to be challenging by many structural engineers because the thinness of the steel leads to buckling and failure modes not found in the design of hot-rolled and fabricated steel structures. Furthermore, roll-forming techniques have developed rapidly in recent decades and spawned highly optimised cross sections featuring intermediate stiffeners and complex lip stiffeners, which are not easily designed using conventional methods. The book covers the design of structural members of complex shapes and connections as well as the design of integrated structural solutions, such as cassettes, and design using stressed

skin principles. The structural behaviour and design to EN1993-1-3 are explained and numerous worked examples are included to guide or enable a cross-check for structural design engineers.

The final Chapter 8 deserves a special mention as it addresses the comprehensive range of considerations other than structural to be made in cold-formed steel construction, including thermal transmission and sound, serviceability, durability, sustainability and recyclability. Methods of design for single and multi-storey housing are explained in detail, concluding with a comprehensive worked example of a residential building.

This book presents a landmark in the development of guidelines for the structural design of cold-formed steel. It is arguably the most extensive reference available for designing cold-formed steel structures to EN1993-1-3, and will serve the structural engineering community well in adapting to the expanding range of residential and industrial applications of cold-formed steel.

Kim Rasmussen

Chairman, Centre for Advanced Structural Engineering, University of Sydney

PREFACE

The use of cold-formed steel members in building construction began in the 1850s in both the United States and Great Britain. In the 1920s and 1930s, acceptance of cold-formed steel as a construction material was still limited because there was no adequate design standard and there was limited information on material use in building codes. One of the first documented uses of cold-formed steel as a building material is the Virginia Baptist Hospital, constructed around 1925 in Lynchburg, Virginia, USA. The building structure was composed by masonry and the floors supported by cold-formed steel built-up joists of back- to- back lipped channel sections. Only some 20 years later, only, Lustron Corporation built in Albany, New York, with almost 2500 steel-framed homes, with the framing, finishes, cabinets and furniture made from cold-formed steel. These inexpensive houses were built for the veterans returning from the World War II. This was the beginning of *cold-formed steel adventure* in building.

In recent years, cold formed steel sections are used more and more as primary framing components. Wall stud systems in housing, trusses, building frames or pallet rack structures are some examples. As secondary structural systems they are used as purlins and side rails or floor joists, as well as in building envelopes. Cassette sections in modern housing systems play simultaneously the role of primary structure and envelope. Profiled decking is widely used as basic components in composite steel-concrete slabs.

Cold-formed steel members are efficient in terms of both their stiffness and strength. Additionally, because the base steel is thin, even less than 1mm thick when high strength steel is used, the members are lightweight. The use of thinner sections and high strength steel leads to design problems for structural engineers which may not normally be encountered in routine structural steel design. Further, the shapes which can be cold-formed are often considerably more complex than hot-rolled steel shapes such as I-

sections and plain channel sections. The cold-formed sections commonly have mono-symmetric or point symmetric shapes, and normally have stiffening lips on flanges and intermediate stiffeners in wide flanges and webs. Both simple and complex shapes can be formed for structural and non-structural applications.

Cold-formed steel design is dominated by two specific problems, i.e. (1) *stability behaviour*, which is dominant for design criteria of thin sections, and (2) *connecting technology*, which is specific and influences significantly the structural performance and design detailing.

Special design standards have been developed to cover the specific problems of cold-formed steel structures. In the USA, the Specification for the design of cold-formed steel structural members of the American Iron and Steel Institute was first produced in 1946 and has been regularly updated based on research to the most recent 2007 edition, AISI S100-07, entitled *North American Specification for Design of Cold-Formed Steel Structural Members*.

In Europe, the ECCS Committee TC7 originally produced the European Recommendations for the design of light gauge steel members in 1987 (ECCS, 1987). This European document has been further developed and published in 2006 as the European Standard Eurocode 3: *Design of steel structures. Part 1-3: General Rules. Supplementary rules for cold-formed thin gauge members and sheeting* (EN 1993-1-3, 2006).

In Australia and New Zealand, the last version of specification for the design of cold-formed steel structures, AS/NZS 4600, was published in December 2005, and the review of cold-formed steel design specification could be continued around the world.

The market share of cold-formed structural steelwork continues to increase in the developed world. The main reasons can be found in the improving technology of manufacture and corrosion protection which leads, in turn, to an increased competitiveness of resulting products as well as new applications. Recent studies have shown that the coating loss for galvanised

steel members is sufficiently slow, and indeed slows down to effectively zero, than a design life in excess of 60 years can be guaranteed.

The range of use of cold-formed steel sections specifically as load-bearing structural components is very wide. Besides building applications, cold-formed steel elements can be met in the Automotive industry, Shipbuilding, Rail transport, in Aircraft industry, Highway engineering, Agricultural and Industry equipment, Office equipment, Chemical, Mining, Petroleum, Nuclear and Space industries.

This book is primarily concerned with the design of cold-formed steel members and structures in building construction in Europe. For this reason it is mainly focused on the EN 1993-1-3, and the related parts of EN 1993 (e.g. EN 1993-1-1, EN 1993-1-5, EN 1993-1-8, etc.).

Generally, the book contains the theoretical background and design rules for cold-formed members and connections, accompanied by design oriented flow charts and worked examples for common building application.

The book was conceived primarily as a technical support for structural engineers in design and consulting offices, but it is expected to be of interest and useful for students and staff members of structural engineering faculties, as well as, for engineers working in steelwork industry.

Dan Dubina

Viorel Ungureanu

Raffaele Landolfo

Chapter 1

INTRODUCTION TO COLD-FORMED STEEL DESIGN

1.1 GENERAL

Cold-formed steel products are found in all aspects of modern life. The use of these products are multiple and varied, ranging from “tin” cans to structural piling, from keyboard switches to mainframe building members. Nowadays, a multiplicity of widely different products, with a tremendous diversity of shapes, sizes, and applications are produced in steel using the cold-forming process.

The use of cold-formed steel members in building construction began about the 1850s in both the United States and Great Britain. However, such steel members were not widely used in buildings until 1940.

In recent years, it has been recognised that cold-formed steel sections can be used effectively as primary framing components. In what concerns cold-formed steel sections, after their primarily applications as purlins or side rails, the second major application in construction is in the building envelope. Options for steel cladding panels range from inexpensive profiled sheeting for industrial applications, through architectural flat panels used to achieve a prestigious look of the building. Light steel systems are widely used to support curtain wall panels. Cold-formed steel in the form of profiled decking has gained widespread acceptance over the past fifteen years as a basic component, along with concrete, in composite slabs. These are now prevalent in the multi-storey steel framed building market. Cold-formed steel members are efficient in terms of both stiffness and strength. In addition,

because the steel may be even less than 1 mm thick, the members are light weight. The already impressive load carrying capabilities of cold-formed steel members will be enhanced by current work to develop composite systems, both for wall and floor structures.

The use of cold-formed steel structures is increasing throughout the world with the production of more economic steel coils particularly in coated form with zinc or aluminium/zinc coatings. These coils are subsequently formed into thin-walled sections by the cold-forming process. They are commonly called “Light gauge sections” since their thickness has been normally less than 3 mm. However, more recent developments have allowed sections up to 25 mm to be cold-formed, and open sections up to approximately 8 mm thick are becoming common in building construction. The steel used for these sections may have a yield stress ranging from 250 MPa to 550 MPa (Hancock, 1997). The higher yield stress steels are also becoming more common as steel manufacturers produce high strength steel more efficiently.

The use of thinner sections and high strength steels leads to design problems for structural engineers which may not normally be encountered in routine structural steel design. Structural instability of sections is most likely to occur as a result of the thickness of the sections, leading to reduced buckling loads (and stresses), and the use of higher strength steel typically makes the buckling stress and yield stress of the thin-walled sections approximately equal. Further, the shapes which can be cold-formed are often considerably more complex than hot-rolled steel shapes such as I-sections and unlippped channel sections. Cold-formed sections commonly have mono-symmetric or point-symmetric shapes, and normally have stiffening lips on flanges and intermediate stiffeners in wide flanges and webs. Both simple and complex shapes can be formed for structural and non-structural applications as shown in Figure 1.1. Special design standards have been developed for these sections.

In the USA, the Specification for the design of cold-formed steel structural members of the American Iron and Steel Institute was first produced in 1946 and has been regularly updated based on research to the most recent 2007 edition (AISI, 1996, 1999, 2001, 2004, 2007). The first edition of the unified *North American Specification* (AISI, 2001) was prepared and issued in 2001, followed by *Supplement 2004: Appendix 1*,

Design of Cold-Formed Steel Structural Members Using Direct Strength Method (AISI, 2004). It is applicable to the United States, Canada and Mexico for the design of cold-formed steel structural members. In 2007, the second edition of the *North American Specification for the Design of Cold-Formed Steel Structural Members* was issued (AISI, 2007). The document was prepared on the basis of the 2001 edition of the Specification, the Supplement 2004 to the 2001 Specification, and subsequent developments. The new and revised provisions provide up-to-date information for the design of cold-formed steel structural members, connections, assemblies, and systems.

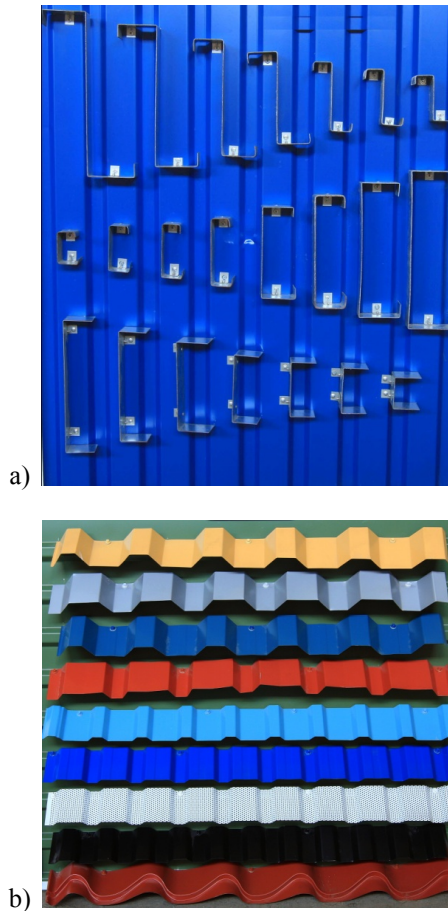


Figure 1.1 – Collection of cold-formed steel sections shapes:
a) sections for cold-formed steel structural members; b) profiled sheets

In Europe, the ECCS Committee TC7 originally produced the European Recommendations for the design of light gauge steel members in 1987 (ECCS, 1987). This European document has been further developed and published in 2006 as the European Standard Eurocode 3: *Design of steel structures. Part 1-3: General Rules. Supplementary rules for cold-formed thin gauge members and sheeting* (CEN, 2006a).

In Australia and New Zealand, a revised limit states design standard AS/NZS4600 for the design of cold-formed steel structures was published in December 2005 (AS/NZS 4600:2005).

The market share of cold-formed structural steelwork continues to increase in the developed world. The reasons for this include the improving technology of manufacture and corrosion protection which leads, in turn, to the increase competitiveness of resulting products as well as new applications. Recent studies have shown that the coating loss for galvanised steel members is sufficiently slow, and indeed slows down to effectively zero, that a design life in excess of 60 years can be guaranteed.

The range of use of cold-formed steel sections specifically as load-bearing structural components is very wide, encompassing residential, office and industrial buildings, the automobile industry, shipbuilding, rail transport, the aircraft industry, highway engineering, agricultural and industry equipment, office equipment, chemical, mining, petroleum, nuclear and space industries.

This book is primarily concerned with the design of cold-formed steel members and structures in building construction in Europe and for this reason it is based on the European Design Code EN1993-1-3 (CEN, 2006a).

1.2 COLD-FORMED STEEL SECTIONS

1.2.1 Types of cold-formed steel sections

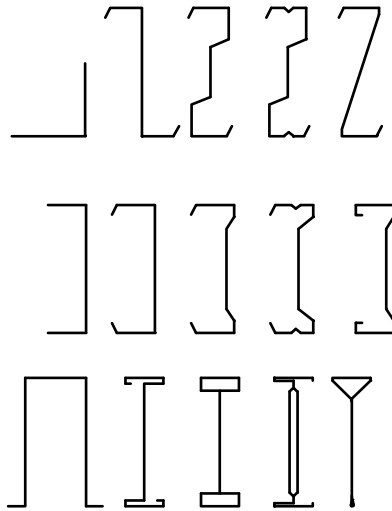
Cold-formed members and profiled sheets are steel products made from coated or uncoated hot-rolled or cold-rolled flat strips or coils. Within the permitted range of tolerances, they have constant or variable cross section.

Cold-formed structural members can be classified into two major types:

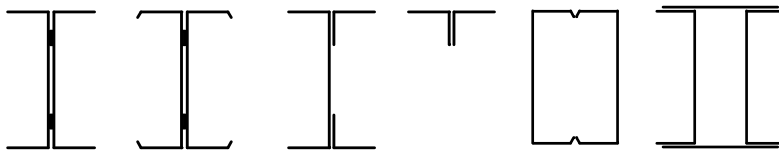
- Individual structural framing members;
- Panels and decks.

Individual structural members (bar members) obtained from so called “long products” include:

- single open sections, shown in Figure 1.2a;
- open built-up sections (Figure 1.2b);
- closed built-up sections (Figure 1.2c).



a) Single open sections



b) Open built-up sections

c) Closed built-up sections

Figure 1.2 – Typical forms of sections for cold-formed structural members

Usually, the depth of cold-formed sections for bar members ranges from 50 – 70 mm to 350 – 400 mm, with thickness from about 0.5 mm to 6 mm. Figure 1.3 shows, as an example, some series of lipped channel and “sigma” sections (www.kingspanstructural.com/multibeam/ – Multibeam products).

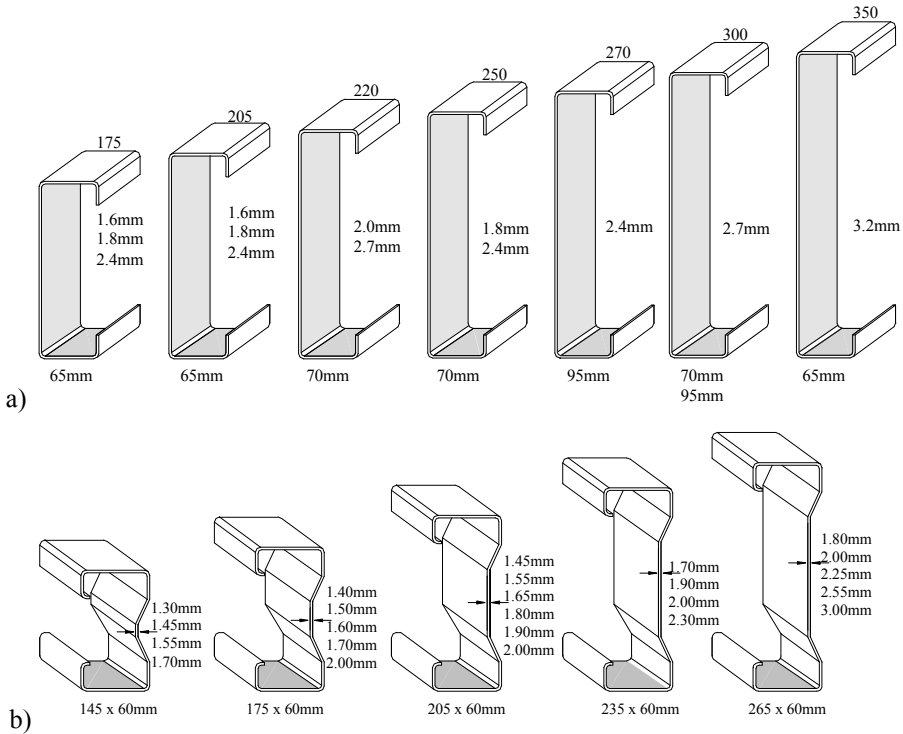


Figure 1.3 – Multibeam sections: a) Lipped Channels; b) Σ sections

6 Panels and decks are made from profiled sheets and linear trays (cassettes) as shown in Figure 1.4. The depth of panels usually ranges from 20 to 200 mm, while thickness is from 0.4 to 1.5 mm.

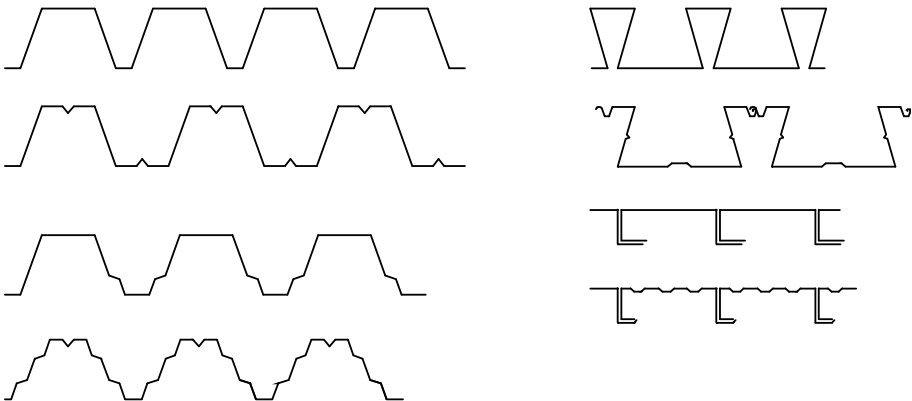


Figure 1.4 – Profiled sheets and linear trays

Figure 1.5 shows examples of Rannila corrugated sheets for roofing, wall cladding systems and load-bearing deck panels.

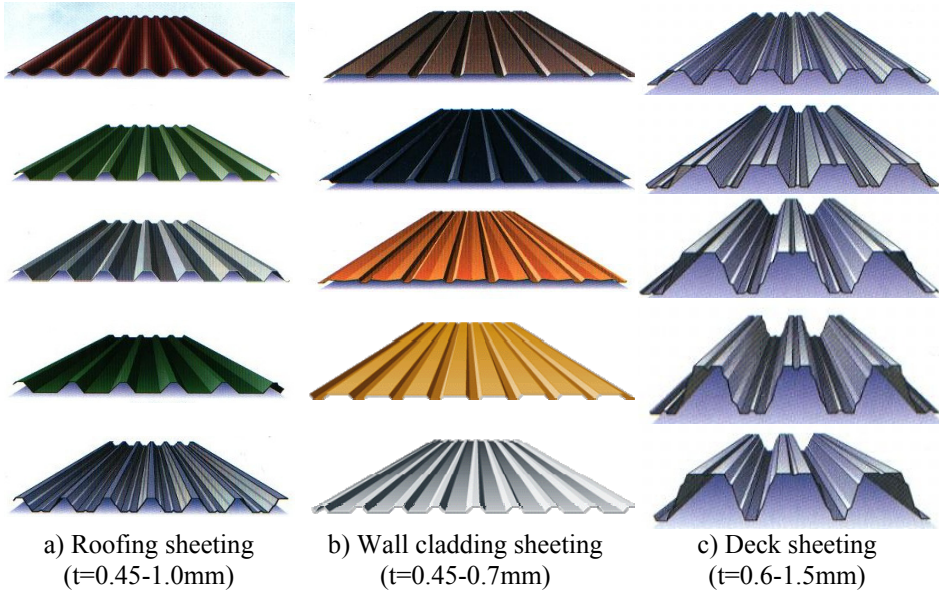


Figure 1.5 – Rannila sheeting products

In order to increase the stiffness of both cold-formed steel sections and sheeting, edge and intermediate stiffeners are used (Figure 1.6); they can be easily identified in examples from Figures 1.3 and 1.5.

7

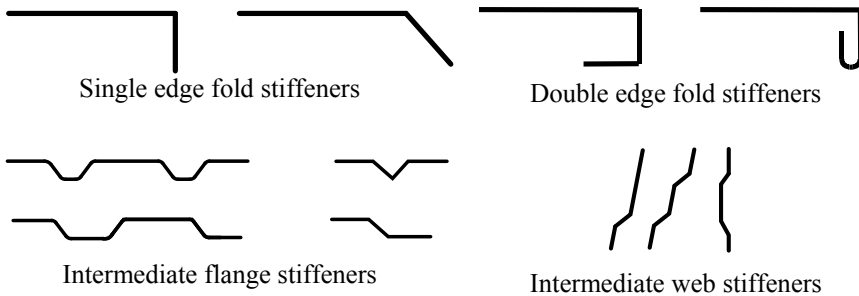


Figure 1.6 – Typical forms of stiffeners for cold-formed members and sheeting

In general, cold-formed steel sections provide the following advantages in building construction (Yu, 2000):

- As compared with thicker hot-rolled shapes, cold-formed steel members can be manufactured for relatively light loads and/or short spans;
- Nestable sections can be produced, allowing for compact packaging and shipping;
- Unusual sectional configurations can be produced economically by cold-forming operations (see Figure 1.1), and consequently favourable strength-to-weight ratios can be obtained;
- Load-carrying panels and decks can provide useful surfaces for floor, roof, and wall construction, and in other cases they can also provide enclosed cells for electrical and other conduits;
- Load-carrying panels and decks not only withstand loads normal to their surfaces, but they can also act as shear diaphragms to resist force in their own planes if they are adequately interconnected to each other and to supporting members.

Compared with other materials such timber and concrete, the following qualities can be realised for cold-formed steel structural members.

- Lightness;
- High strength and stiffness;
- Ability to provide long spans, up to 12 m (Rhodes, 1991);
- Ease of prefabrication and mass production;
- Fast and easy erection and installation;
- Substantial elimination of delays due to weather;
- More accurate detailing;
- Non-shrinking and non-creeping at ambient temperatures;
- Formwork unnecessary;
- Termite-proof and rot-proof;
- Uniform quality;
- Economy in transportation and handling;
- Non-combustibility;
- Recyclable material.

The combination of the above-mentioned advantages can result in cost saving in construction.

1.2.2 Manufacturing

Cold-formed members are normally manufactured by one of two processes. These are:

- Roll forming;
- Folding and press braking.

Roll forming consists of feeding a continuous steel strip through a series of opposing rolls to progressively deform the steel plastically to form the desired shape. Each pair of rolls produces a fixed amount of deformation in a sequence of type shown in Figure 1.7a. Each pair of opposing rolls is called a stage as shown in Figure 1.7. In general, the more complex the cross sectional shape, the greater the number of stages required. In the case of cold-formed rectangular hollow sections, the rolls initially form the section into a circular section and a weld is applied between the opposing edges of the strip before final rolling (called sizing) into a square or rectangular shape.

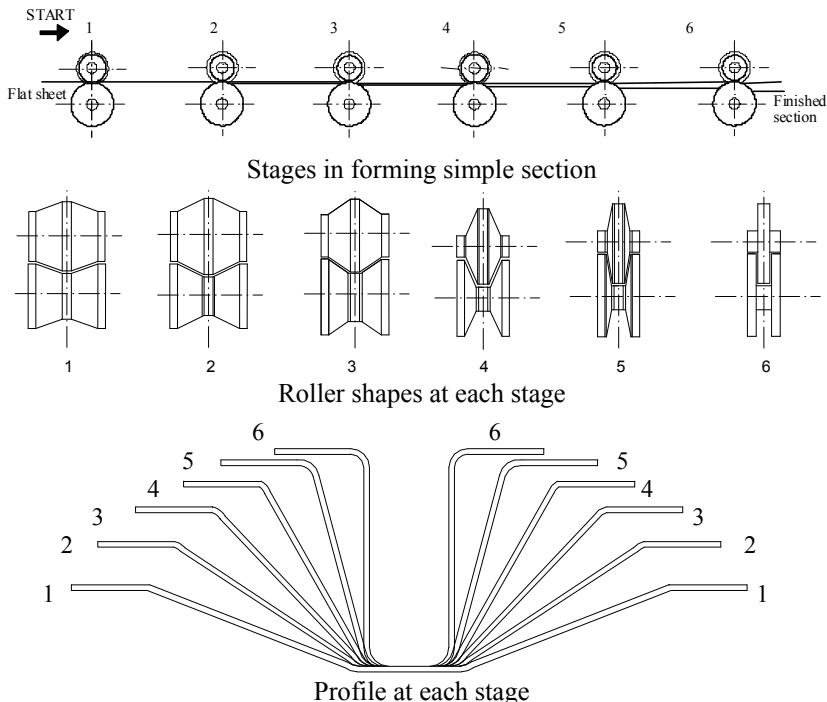


Figure 1.7 – Stages in roll forming a simple section (Rhodes, 1991)

Figures 1.8 (a and b) shows two industrial roll forming lines for long products profiles and sheeting, respectively.

A significant limitation of roll forming is the time taken to change rolls for a different size sections. Consequently, adjustable rolls are often used which allows a rapid change to a different section width or depth.

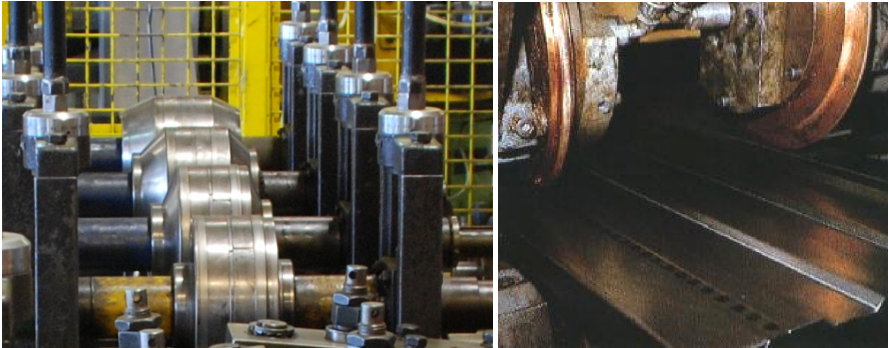


Figure 1.8 – Industrial roll forming lines

Folding is the simplest process, in which specimens of short lengths, and of simple geometry are produced from a sheet of material by folding a series of bends (see Figure 1.9). This process has very limited application.

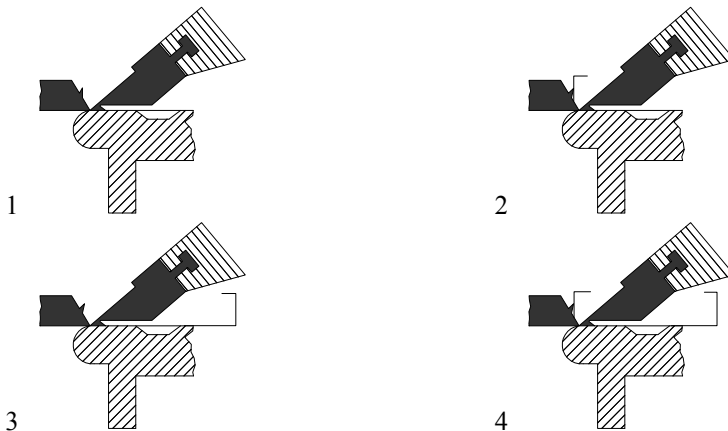


Figure 1.9 – Forming of folding

Press braking is more widely used, and a greater variety of cross sectional forms can be produced by this process. Here a section is formed from a length of strip by pressing the strip between shaped dies to form the profile shape (see Figure 1.10). Usually each bend is formed separately. The

set up of a typical brake press is illustrated in Figure 1.11. This process also has limitations on the profiled geometry which can be formed and, often more importantly, on the lengths of sections which can be produced. Press braking is normally restricted to sections of length less than 5 m although press brakes capable of producing 8 m long members are in use in industry.

Roll forming is usually used to produce sections where very large quantities of a given shape are required. The initial tooling costs are high but the subsequent labour cost is low. Brake pressing is normally used for low volume production where a variety of shapes are required and the roll forming costs cannot be justified.

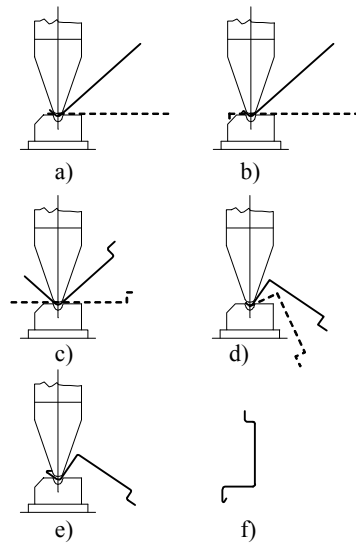


Figure 1.10 – Forming steps in press braking process



Figure 1.11 – Industrial brake press

1.2.3 Some peculiar characteristics of cold-formed steel sections

Compared to hot-rolled steel sections, the manufacturing technology of cold-formed steel sections induces some peculiar characteristics. First of all, cold-forming leads to a modification of the stress-strain curve of the steel. With respect to the virgin material, cold-rolling provides an increase of the yield strength and, sometimes, of the ultimate strength that is important in the corners and still appreciable in the flanges, while press braking leave these characteristics nearly unchanged in the flanges. Obviously, such effects do not appear in case of hot-rolled sections, as shown in Table 1.1 (Rondal, 1988).

Table 1.1 – Influence of manufacturing process on the basic strengths of hot and cold-formed profiles

Forming method		Hot rolling	Cold forming	
			Cold rolling	Press braking
Yield strength	Corner	--	high	high
	Flange	--	moderate	--
Ultimate strength	Corner	--	high	high
	Flange	--	moderate	--

12

The increase of the yield strength is due to strain hardening and depends on the type of steel used for cold rolling. On the contrary, the increase of the ultimate strength is related to strain aging, that is accompanied by a decrease of the ductility and depends on the metallurgical properties of the material.

Design codes provide formulas to evaluate the increase of yield strength of cold-formed steel sections, compared to that of the basic material.

Hot-rolled profiles are affected by residual stresses, which result from air cooling after hot-rolling. These stresses are mostly of membrane type, they depend on the shape of sections and have a significant influence on the buckling strength. Therefore, residual stresses are the main factor which causes the design of hot-rolled sections to use different buckling curves in European design codes (CEN, 2005a).

In the case of cold-formed sections the residual stresses are mainly of flexural type, as Figure 1.12 demonstrates, and their influence on the

buckling strength is less important than membrane residual stresses as Table 1.2 shows (Bivolaru, 1993).

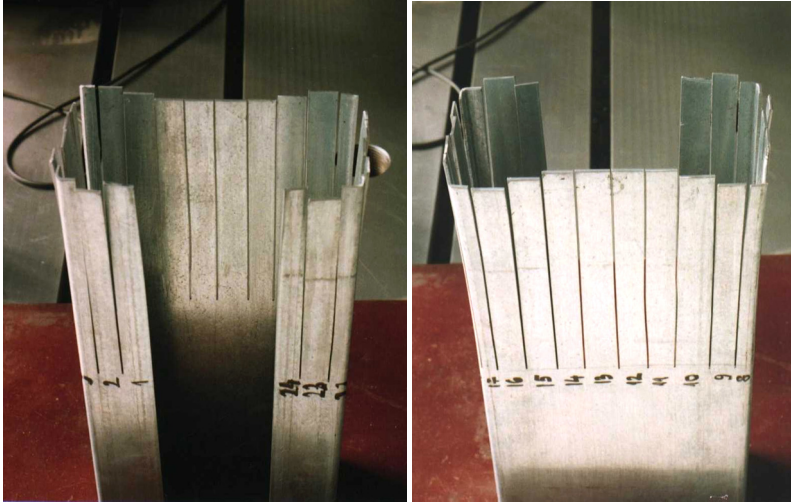


Figure 1.12 – Evidence of flexural residual stresses in a lipped channel cold-formed steel section (Bivolaru, 1993)

On the other hand, cold rolling produce different residual stresses in the section when compared with press braking, as shown in Table 1.2, so the section strength may be different in cases where buckling and yielding interact (Rondal, 1988).

Table 1.2 – Type magnitude of residual stress in steel sections

Forming method	Hot rolling	Cold forming	
		Cold rolling	Press braking
Membrane residual stresses (σ_{rm})	high	low	low
Flexural residual stresses (σ_{rf})	low	high	low

Experimental evidence shows more complex actual distributions of residual stresses. Figure 1.13 (a to c) presents the distribution of measured residual stress for a cold-formed steel angle, channel and lipped channel (Rondal *et al*, 1994).

The European buckling curves have been calibrated using test results on hot formed (rolled and welded) steel sections, obtained during a large

experimental program in Europe in the 1960's (Sfintesco, 1970). These curves are based on the well-known Ayrton-Perry formula, in which the imperfection factor α was correspondingly calibrated (Rondal & Maquoi, 1979).

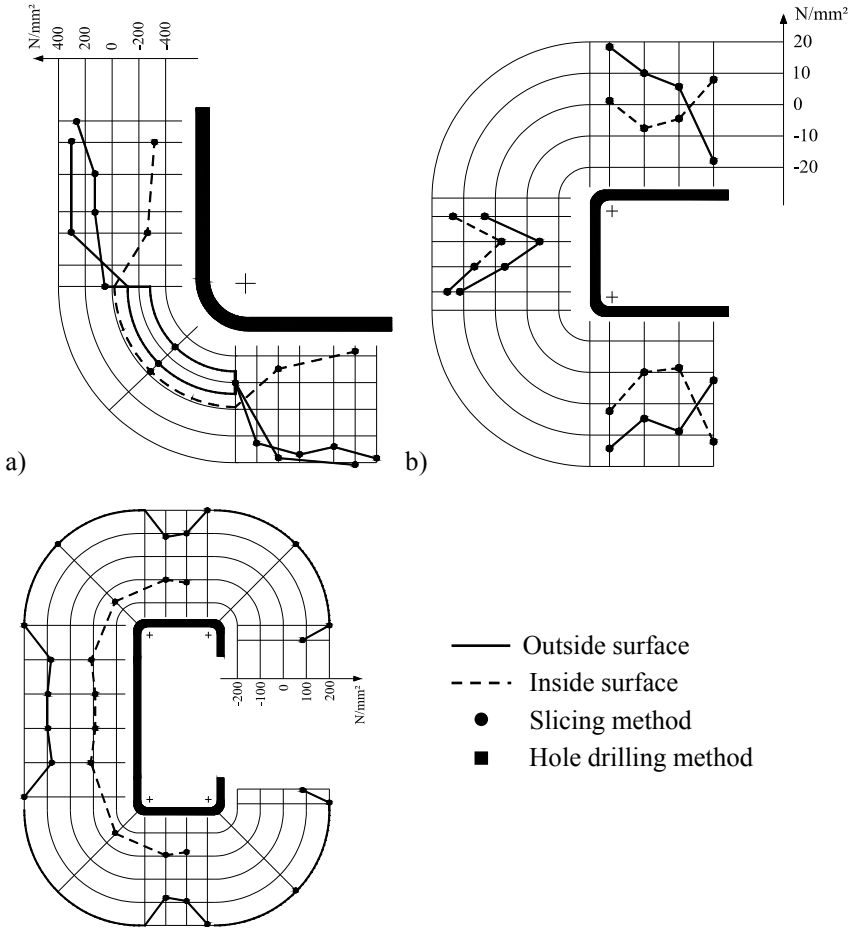


Figure 1.13 – Measured residual stress in cold-formed steel sections: a) cold-rolled angle; b) cold-rolled C profile; c) press braked U profile (Rondal *et al*, 1994)

Due to the fact the mechanical properties of cold-formed sections – e.g. cold-forming effect and residual stresses – are different to those of hot-rolled ones, different buckling curves should be justified (Dubina, 1996). Nowadays both numerical and experimental approaches are available to calibrate appropriate α factors for cold-formed sections (Dubina, 2001) but,

for the sake of simplicity of the design process, the same buckling curves as for hot formed sections are still used (CEN, 2005a and CEN, 2006a).

1.3 PECULIAR PROBLEMS OF COLD-FORMED STEEL DESIGN

The use of thin-walled sections and cold-forming manufacturing effects can result in special design problems not normally encountered when hot-rolled sections are used. A brief summary of some special problems in cold-formed steel design are reviewed in the following (Dubina, 2005).

1.3.1 Buckling strength of cold-formed steel members

Steel sections may be subject to one of four generic types of buckling, namely local, global, distortional and shear. Local buckling is particularly prevalent in cold-formed steel sections and is characterised by the relatively short wavelength buckling of individual plate element. The term “global buckling” embraces Euler (flexural) and flexural-torsional buckling of columns and lateral-torsional buckling of beams. It is sometimes termed “rigid-body” buckling because any given cross section moves as a rigid body without any distortion of the cross section. Distortional buckling, as the term suggests, is buckling which takes place as a consequence of distortion of the cross section. In cold-formed sections, it is characterised by relative movement of the fold-lines. The wavelength of distortional buckling is generally intermediate between that of local buckling and global buckling.

It is a consequence of the increasing complexity of section shapes that local buckling calculation are becoming more complicated and that distortional buckling takes on increasing importance.

Local and distortional buckling can be considered as “sectional” modes, and they can interact with each other as well as with global buckling (Dubina, 1996). Figure 1.14 shows single and interactive (coupled) buckling modes for a lipped channel section in compression. The results have been obtained using an elastic eigen-buckling FEM analysis.

For given geometrical properties of member cross section, the different buckling modes depend by the buckling length, as shown in Figure 1.15 (Hancock, 2001).

The curves shown in Figure 1.15 have been obtained using an elastic Finite Strip (FS) software, analysing and describing the change of buckling strength versus buckle half-wavelength.

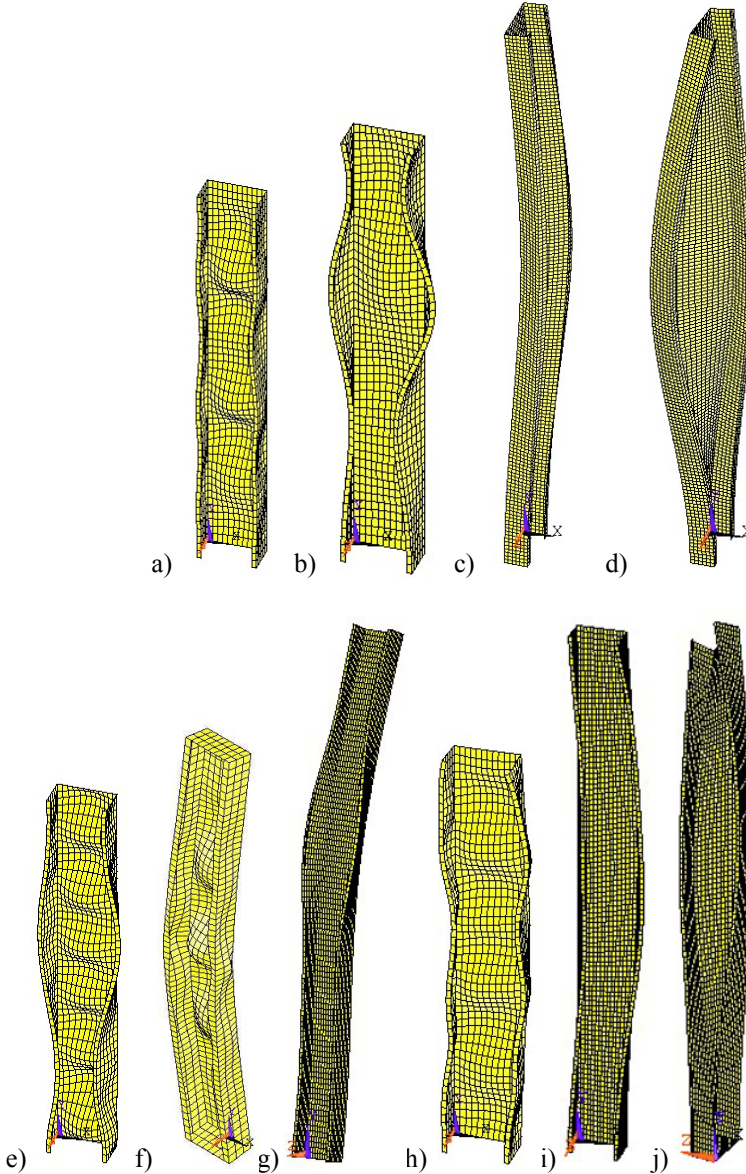


Figure 1.14 – Buckling modes for a lipped channel in compression

Single modes: a) local (L); b) distortional (D); c) flexural (F); d) flexural-torsional (FT); Coupled (interactive) modes: e) L + D; f) F + L; g) F + D; h) FT + L; i) FT + D; j) F + FT (Dubina, 2002)

A first minimum (Point A) occurs in the curve at a half-wavelength of 65 mm and represents *local* buckling in the mode shown. The local mode consists mainly of deformation of the web element without movement of the line junction between the flange and lip stiffener. A second minimum also occurs at a point B at a half-wavelength of 280 mm in the mode shown. This mode is the *distortional* buckling mode since movement of the line junction between the flange and lip stiffener occurs without a rigid body rotation or translation of the cross section. In some papers, this mode is called a *local-torsional* mode. The distortional buckling stress at point B is slightly higher than the local buckling stress at point A, so that when a long length fully braced section is subjected to compression, it is likely to undergo local buckling in preference to distortional buckling. The section buckles in a flexural or flexural-torsional buckling mode at long wavelengths, such as at points C, D and E. For this particular section, flexural-torsional buckling occurs at half-wavelengths up to approximately 1800 mm beyond which flexural buckling occurs.

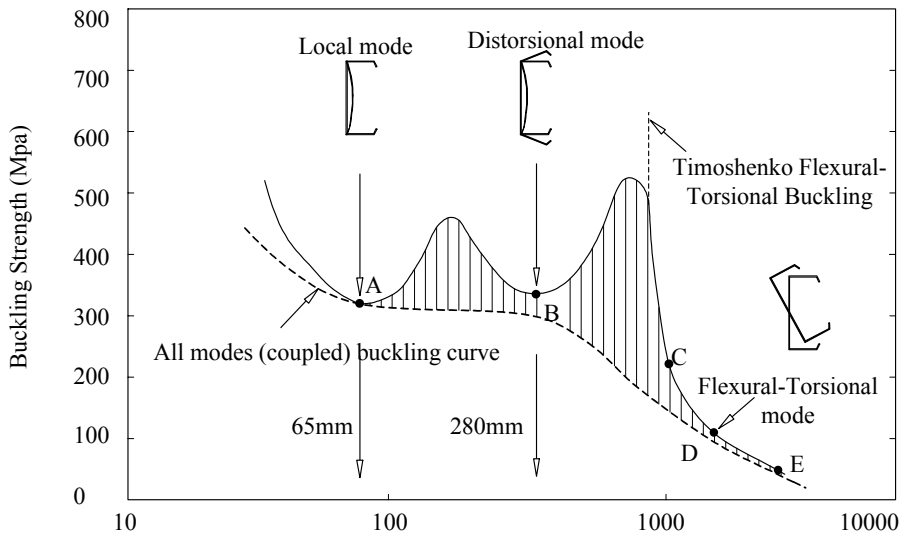


Figure 1.15 – Buckling strength versus half-wavelength for a lipped channel in compression (Hancock, 2001)

The dashed line in Figure 1.15, added to the original figure, qualitatively shows the pattern of *all modes* or *coupled mode*.

The effect of interaction between sectional and global buckling modes results in increasing sensitivity to imperfections, leading to the erosion of the

theoretical buckling strength (see hachured zones in Figure 1.15). In fact, due to the inherent presence of imperfection, buckling mode interaction always occurs in case of thin-walled members.

Figure 1.16 shows the difference in behaviour of a *thick-walled* slender bar in compression (Figure 1.16a), and a *thin-walled* bar (Figure 1.16b); they are assumed, theoretically, to have the same value of their gross areas. Both cases of an ideal perfect bar and a geometric imperfect bar are presented.

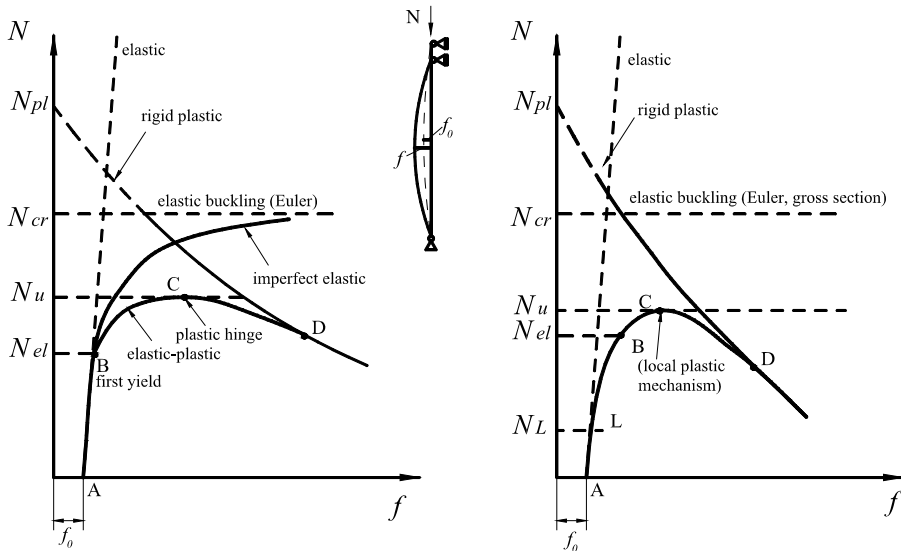


Figure 1.16 – Behaviour of (a) slender thick-walled and (b) thin-walled compression bar

Looking at the behaviour of a *thick-walled* bar it can be seen that it begins to depart from the elastic curve at point B when the first fibre reaches the yield stress, N_{el} , and it reaches its maximum (ultimate) load capacity, N_u , at point C; after which the load drops gradually and the curve approaches the theoretical rigid-plastic curve asymptotically. The elastic theory is able to define the deflections and stresses up to the point of first yield and the load at which first yield occurs. The position of the rigid-plastic curve determines the absolute limit of the load carrying capacity, above which the structure cannot support the load and remain in a state of equilibrium. It intersects the elastic line as if to say “thus far and no further” (Murray, 1985).

In case of a thin-walled bar, sectional buckling, e.g. local or distortional buckling, may occur prior to the initiation of plastification. Sectional buckling is characterised by the stable post-critical path and the bar does not fail as a result of this, but significantly lose stiffness. Yielding starts at the corners of cross section prior to failure of the bar, when sectional buckling mode changes into a local plastic mechanism quasi-simultaneously with the occurrence of global buckling (Dubina, 2000). Figure 1.17, obtained by advanced FEM simulation, clearly shows the failure mechanism of a lipped channel bar in compression (Ungureanu & Dubina, 2004).

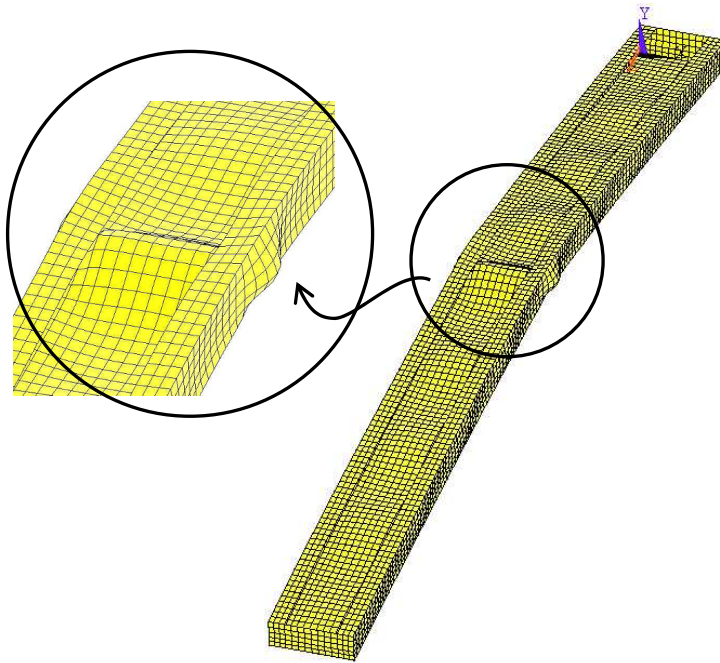


Figure 1.17 – Failure mode of a lipped channel in compression (Ungureanu & Dubina, 2004)

Figure 1.18 shows the comparison between the buckling curves of a lipped channel member in compression, calculated according to EN1993-1-3 (CEN, 2006a), considering the fully effective cross section (i.e. no local buckling effect) and the reduced (effective) cross section (i.e. when local buckling occurs and interacts with global buckling).

However the effectiveness of thin-walled sections, expressed in terms of load carrying capacity and buckling strength of compression walls of

beam and columns can be improved considerably by the use of edge stiffeners or intermediate stiffeners (see Figure 1.6).

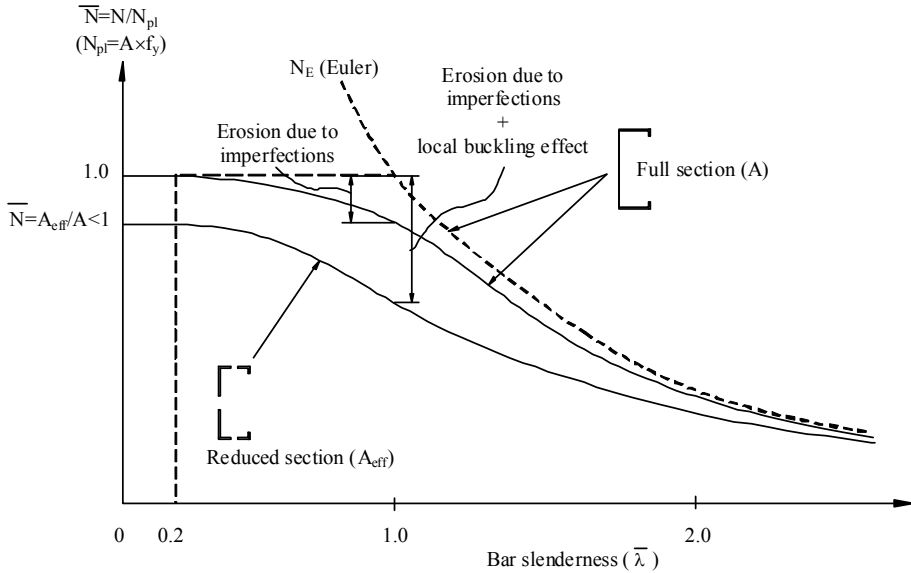


Figure 1.18 – Effect of local buckling on the member capacity

1.3.2 Torsional rigidity

Cold-formed sections are normally thin and consequently they have low torsional stiffness. Many of the sections produced by cold-forming are mono-symmetric and their shear centres are eccentric from their centroids as shown in Figure 1.19a. Since the shear centre of a thin-walled beam is the axis through which it must be loaded to produce flexural deformation without twisting, then any eccentricity of the load from this axis will generally produce considerable torsional deformations in a thin-walled beam as shown in Figure 1.19a. Consequently, thin-walled beams usually require torsional restraints either at intervals or continuously along the length to prevent torsional deformations. Often, this is the case for beams such as Z- and C- purlins which may undergo flexural-torsional buckling because of their low torsional stiffness, if not properly braced.

In addition, for columns axially loaded along their centroid axis, the eccentricity of the load from the shear centre axis may cause buckling in the flexural-torsional mode as shown in Figure 1.19b at a lower load than the

flexural buckling mode also shown in Figure 1.19b. Hence the checking for the flexural-torsional mode of buckling is necessary for such mono-symmetric columns.

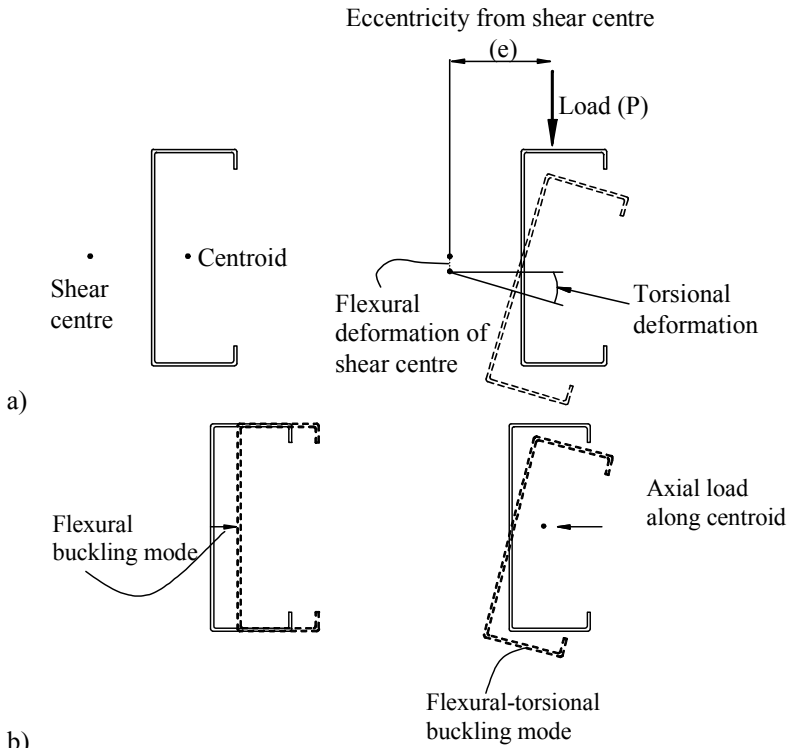


Figure 1.19 – Torsional deformations: a) eccentrically loaded lipped channel beam; b) axially loaded lipped channel column

1.3.3 Web crippling

Web crippling at points of concentrated load and supports can be a critical problem in cold-formed steel structural members and sheeting for several reasons. These are:

- in cold-formed steel design, it is often not practical to provide load bearing and end bearing stiffeners. This is always the case in continuous sheeting and decking spanning several support points;
- the depth-to-thickness ratios of the webs of cold-formed members are usually larger than for hot-rolled structural members;
- in many cases, the webs are inclined rather than vertical;

- the intermediate element between the flange, onto which the load is applied, and the web of a cold-formed member usually consists of a bend of finite radius. Hence the load is applied eccentrically from the web.

Special provisions are included in design codes to guard against failure by web crippling.

1.3.4 Ductility and plastic design

Due to sectional buckling mainly (cold-formed sections are of class 4 or class 3, at the most), but also due to the effect of cold-forming by strain hardening, cold-formed steel sections possess low ductility and are not generally allowed for plastic design. The previous discussion related to Figure 1.16b revealed the low inelastic capacity reserve for these sections, after yielding initiated. However, for members in bending, design codes allow to use the inelastic capacity reserve in the part of the cross section working in tension.

Because of their reduced ductility, cold-formed steel sections cannot dissipate energy in seismic resistant structures. However, cold-formed sections can be used in seismic resistant structures because there are structural benefits to be derived from their reduced weight, but only elastic design is allowed and no reduction of the shear seismic force is possible. Hence, in seismic design, a reduction factor $q = 1$ has to be assumed as stated in EN1998-1 (CEN, 2004).

1.3.5 Connections

Conventional methods for connections used in steel construction, such as bolting and arc-welding are available for cold-formed steel sections but are generally less appropriate because of the wall thinness, and special techniques more suited to thin materials are often employed. Long-standing methods for connecting two thin elements are blind rivets and self drilling, self tapping screws. Fired pins are often used to connect thin materials to a thicker supporting member. More recently, press-joining or clinching technologies (Predeschi *et al*, 1997) have been developed, which require no

additional components and cause no damage to the galvanising or other metallic coating. This technology has been adopted from the automotive industry and is successfully used in building construction. “Rosette” system is another innovative connecting technology (Makelainen & Kesti, 1999), applicable to cold-formed steel structures.

Therefore, connection design is more complex and challenging to the engineers.

1.3.6 Design assisted by testing

Cold-forming technology makes available production of unusual sectional configurations (see Figure 1.1). However, from the point of view of structural design, the analysis and design of such unusual members may be very complex. Structural systems formed by different cold-formed sections connected to each other (like purlins and sheeting, for instance) can also lead to complex design situations, not entirely covered by design code procedures. Of course, numerical FEM analysis is always available, but for many practical situations, modelling can be very complicate. For such complex design problems, modern design codes permit the use of testing procedures to evaluate structural performances. Testing can be used either to replace design by calculation or combined with calculation. Only officially accredited laboratories, by competent authorities, are allowed to perform such tests and to delivery relevant certificates.

1.3.7 Design standards

Extensive research and product development in the past has led to national design specifications for cold-formed steel sections and structures in many countries. On the following, a summary review of main design specifications is presented.

1.3.7.1 North American Cold-formed Steel Specification, 2001 Edition (AISI, 2001) and 2007 Edition (AISI, 2007)

The first edition of the unified North American Specification was prepared and issued in 2001, together with commentaries. It is applicable to

the United States, Canada and Mexico for the design of cold-formed steel structural members.

This edition of the Specification was developed on the basis of the 1996 AISI Specification with the 1999 Supplement (AISI, 1999) and the 1994 Canadian Standard (CSA, 1994), which is based on Limit State Design (LSD), like in Europe and Australia.

Since the *Specification* is intended for use in Canada, Mexico and the United States, it was necessary to develop a format that would facilitate the allowance of unique requirements in each country. This resulted in a format that contained a basic document, Chapters A through G, intended for use in all three countries, and three country specific appendices, Appendix A – United States, Appendix B – Canada, and Appendix C – Mexico.

Three design methods are recognized: ASD – now termed Allowable Strength Design, LRFD – Load and Resistance Factor Design, and LSD – Limit States Design. The use of ASD and LRFD is limited to the US and Mexico; LSD is limited to Canada. LRFD and LSD are essentially the same except for differences in nomenclature, load factors, load combinations, and target reliability indexes. Equivalent LSD terminology is shown in brackets throughout the *Specification*.

A new design method for cold-formed steel members – the Direct Strength Method – has been developed by Schafer (2006) and adopted in 2004 as Appendix 1 of the *North American Specification for the Design of Cold-Formed Steel Structural Members* (AISI, 2004).

The second edition of the unified *North American Specification for the Design of Cold-Formed Steel Members* (AISI S100-07) was issued by American Iron and Steel Institute in 2007, together with *Commentary on North American Specification for the Design of Cold-Formed Steel Members* (AISI S100-07-C).

Also the 2007 editions of the AISI standards for cold-formed steel framing have been approved. It should be noted that the words “North American” are now in the titles of many of these standards. This was done to emphasize that these documents are intended for adoption throughout North America and use not just in the United States. In all such documents, provisions applicable to Canada were added. This work by the AISI Committee on Framing Standards includes the revision of six current standards and the issuing of two new standards, as follows:

Revised Standards:

- *AISI S200-07: North American Standard for Cold-Formed Steel Framing – General Provisions;*
- *AISI S211-07: North American Standard for Cold-Formed Steel Framing – Wall Stud Design;*
- *AISI S212-07: North American Standard for Cold-Formed Steel Framing – Header Design;*
- *AISI S213-07: North American Standard for Cold-Formed Steel Framing – Lateral Design;*
- *AISI S214-07: North American Standard for Cold-Formed Steel Framing – Truss Design;*
- *AISI S230-07: Standard for Cold-Formed Steel Framing – Prescriptive Method for One and Two Family Dwellings;*

New Standards:

- *AISI S201-07: North American Standard for Cold-Formed Steel Framing – Product Data;*
- *AISI S210-07: North American Standard for Cold-Formed Steel Framing – Floor and Roof System Design.*

1.3.7.2 Australian/New Zealand Standard – AS/NZS 4600, 2005 Edition (AS/NZS, 2005)

The Australian/New Zealand Standard is very similar to the AISI Specification since Section 1-5 correspond with Sections A to E of the AISI Specification. However, AS/NZS4600 only permits design by the limit states method (LSD), and not by the allowable stress method (ASD). In addition, because of the use of higher strength steels, additional provisions have been included for distortional buckling.

To summarise, the AS/NZS4600 differs from the AISI Specifications as follows:

- Use of high strength G550 cold-reduced steels less than 0.9mm thick for structural members (in addition to sheeting).
 - Distortional buckling of both flexural and compression members.
 - Blind rivets connections.
 - Testing provisions.
-

The Direct Strength Method was included in the 2005 edition of the *Australian/New Zealand Standard for cold-formed steel structures (AS/NZS4600:2005)*.

The 4th edition of *Design of cold-formed steel structures (to AS/NZS4600:2005)* by Hancock (2007), explains the basis of the design rules of AS/NZS 4600:2005 and deals with the large number of changes made to the standard since the 1996 version.

1.3.7.3 Eurocode 3 – Design of Steel Structures, Part 1.3 – General Rules, Supplementary Rules for Cold-formed Thin Gauge Members and Sheeting

EN1993-1-3 (CEN, 2006a) represents the unified European Code for cold-formed steel design, and contains specific provisions for structural applications using cold-formed steel products made from coated or uncoated thin gauge hot or cold-rolled sheet and strip. It is intended to be used for the design of buildings or civil engineering works in conjunction with EN1993-1-1 (CEN, 2005a) and EN1993-1-5 (CEN, 2006b). EN1993-1-3 permits only design by the limit states method (LSD).

The code provisions are limited to steel in the thickness range 1.0 – 8.0 mm for members, and 0.5 – 4.0 mm for sheeting. Thicker material may also be used provided the load-bearing capacity is determined by testing.

Member design provisions in EN1993-1-3 are not dissimilar from the AISI Specification, even though the notations and format of formulas are different, but generally include more advanced design provisions. In some areas such as plane elements in compression and with edge or intermediate stiffeners, the EN1993-1-3 design provisions are considerably more complex. Also, compared with the AISI S100-07 (2007) and AS/NZS4600 (2005) design codes, distortional buckling design is less explicitly presented in this code.

EN1993-1-3 includes in Chapter 10 design criteria for the following particular applications:

- Beams restrained by sheeting;
- Linear trays restrained by sheeting;
- Stressed skin design;
- Perforated sheeting.

The design provisions for these particular applications are often complex but may be useful for design engineers since they include detailed methodologies not available in other standards or specifications.

As application support of this code, the European Convention for Constructional Steel Work, ECCS, published in 2008 “Worked examples according to EN1993-1-3” (ECCS, 2008b). Previously, in 2000, ECCS also edited worked examples on the same topic (ECCS, 2000).

In 1995 the European Convention for Constructional Steelwork – ECCS published the *European Recommendations for the Application of Metal Sheeting acting as a Diaphragm* (ECCS, 1995).

1.3.8 Fire resistance

Due to the small values of section factor (i.e. the ratio of the heated volume to the cross sectional area of the member) the fire resistance of unprotected cold-formed steel sections is reduced. For the same reason fire protection with intumescent coating is not efficient.

Sprayed cementations or gypsum based coatings, while very efficient for other applications are, generally, not usable for galvanised cold-formed steel sections. However, cold-formed steel sections can be employed as beams concealed behind a suspended ceiling. In load bearing applications, fire resistance periods of 30 minutes can usually be achieved by one layer of “special” fire resistant plasterboard, and 60 minutes by two layers of this plasterboard, which possesses low shrinkage and high integrity properties in fire. Planar protection to floors and walls provides adequate fire resistance to enclosed sections, which retain a significant proportion of their strength, even at temperatures of 500 °C.

In light gauge steel framing, the board covering of walls and floors can protect the steel against fire for up to 120 minutes, depending on the board material and the number of boards. The choice of insulation material, mineral wool or rock wool is also crucial to fire strength.

Box protection of individual cold-formed steel sections used as beams and columns is provided in much the same way as with hot-rolled sections.

Non-load bearing members require less fire protection, as they only have to satisfy the “insulation” criterion in fire conditions. Ordinary plasterboard may be used in such cases.

1.3.9 Corrosion

The main factor governing the corrosion resistance of cold-formed steel sections is the type and thickness of the protective treatment applied to the steel rather than the base metal thickness. Cold-formed steel has the advantage that the protective coatings can be applied to the strip during manufacture and before roll forming. Consequently, galvanised strip can be passed through the rolls and requires no further treatment.

Steel profiles are typically hot dip galvanised with 275 gram of zinc per square meter (Zn 275), corresponding to a zinc thickness of 20 μm on each side. The galvanising layer is sufficient to protect the steel profiles against corrosion during the entire life of a building, if constructed in the correct manner. The most severe effects of corrosion on the steel occur during transport and outdoors storage. When making holes in hot dip galvanised steel framing members, normally no treatment is needed afterwards since the zinc layer possesses a healing effect, i.e. transfers to unprotected surfaces.

Hot dip galvanising is sufficient to protect the steel profiles against corrosion during the life of a building. The service life of hot dip galvanised steel studs was studied by British Steel and others (John, 1991). The loss in zinc weight will be around 0.1 g/m^2 per year indoors. A similar study was also carried out for steel floors above crawl spaces with plastic sheeting on the ground. Results showed that a zinc weight of 275 g/m^2 is sufficient to provide a durability of around 100 years.

1.3.10 Sustainability of cold-formed steel construction

Sustainability is one of the greatest challenges of the modern world. Sustainability includes environmental, economic and social aspects, all contributing to a durable development of the society.

The building industry plays an important role both in national economies and in the sustainable development of the world in general. Sustainable constructions have different priorities and purposes in various countries. Sustainable construction can be regarded as a subset of sustainable development and contains a wide range of issue, i.e.: re-use of existing built

assets, design for minimum waste, reduction of resources and energy consumption and of pollution.

Steel as construction material plays an important role as component for buildings and engineering structures, and it has a wide range of applications. On the other hand, steel is the most recycled material and from the total production in the world, almost half is obtained from waste material.

The steel construction sector has a great deal to offer sustainable development. Like other industrial activities, steel construction works for continuously improvement in terms of sustainability. The following guiding principles for sustainable constructions can be emphasized (Plank & Dowling 2003):

- Understand what sustainable development means for clients and customers;
- Use whole-life thinking, best value considerations and high quality information to inform your decision making;
- Design for flexibility to extend building lifetimes and, where possible, further extend the life of buildings by renovation and refurbishment;
- Design and construct with maximum speed and minimum disruption around the site;
- Design to minimize operational impacts (e.g. energy use);
- Design for demountability, to encourage future re-use and recycling of products and materials;
- Engage organizations within your supply chain about sustainability development;
- Select responsible contractors who have embraced sustainable development principles.

Light gauge steel framed houses are usually built by using different solutions for interior and exterior cladding. This approach is widespread and accounts for an important and increasing market share in the US, Japan, Australia and Europe.

Burstrand (2000) presents the reasons in choosing light gauge steel framing from an environmental point of view:

- Light gauge steel framing is a dry construction system without organic materials. Dry construction significantly reduces the risk of moisture problems and sick building syndrome;
- Steel, gypsum and mineral wool are closed cycle materials;
- Every material used in light gauge steel framing (steel, gypsum and mineral wool) can be recycled to 100%;
- It is possible to disassemble the building components for re-use;
- Light gauge steel framing means less energy consumption during production than equivalent housing with a framework of concrete poured on-site;
- Light gauge steel framing only uses about a fourth of the amount of raw materials used for equivalent masonry-concrete homes;
- Less waste means a cleaner work site and a low dead weight of building components ensures a good working environment;
- Low dead weight leads to reduced transport needs.

In what concerns the building envelopes they should be energy-positive, adaptable, affordable, environmental, healthy, intelligent and durable. The envelope is essential in ensuring the comfort and energy savings of the system taken as a whole and has to provide as much as possible a uniform “wrapping” of the steel structure in order to avoid and/or control thermal bridging.

Ungureanu *et al* (2011) present a practical application of integration of environmental impact into design of buildings, by means of a case-study. The example compares the environmental impact for a single-family house, designed in two situations: classic structure, by considering a masonry house and, the same house, designed using lightweight steel profiles. The impact analyses were performed at different levels: (i) construction, (ii) construction and end-of-life, (iii) life cycle including maintenance and, (iv) the life cycle including maintenance and consumable goods.

Figure 1.20 presents the environmental impact for the two solutions of the single-family house for construction phase only. In a direct comparative impact analysis, for traditional house, higher impact values for most of the impact indicators (categories) result, while aggregated into a single score (inner figure), leading to an overall score for the light gauge steel framed house less than half of the global score of the traditional house.

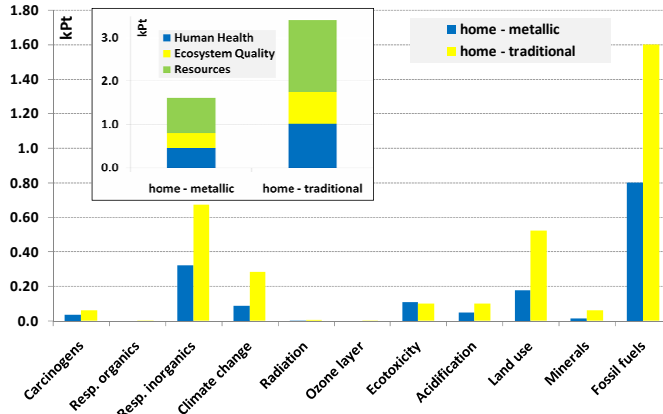


Figure 1.20 – Comparison on environmental impact for light gauge steel framed house and traditional house (Ungureanu *et al*, 2011)

As a main conclusion of the study, it could be stated that dwellings with cold-formed steel structural elements represents a good alternative to masonry houses, not only with respect to structural requirements but also in considering the environmental impact assessment.

1.4 MAIN APPLICATIONS OF COLD-FORMED STEEL

1.4.1 Advantages of cold-formed steel in building construction

Cold-formed steel sections are used widely in building construction. The advantages of cold-formed sections are highlighted in §1.2.1. In the series entitled “Light Steel”, the Steel Construction Institute (SCI) published a guide on *Building Design using Cold-Formed Steel Sections: Construction Detailing and Practice* (Grub & Lawson, 1997). In this guide, the following representative list of advantages of using constructional cold-formed steelwork for building, during construction and service are presented (Grub & Lawson, 1997).

1.4.1.1 Advantages during construction

- Easily assembled into a wide range of structural and architectural forms. Standard connection details are available;

- Good and readily available infra-structure of installation skills and connection methods;
- Largely prefabricated components produced in a factory environment. Members can be delivered cut to length and with bolt holes;
- Assembly on site is relatively simple. Bundles of sections can be lifted by crane. Individual members and sub-frames can be man-handled into place easily;
- Fast speed of construction is achieved, leading to savings in site preliminaries and early return on capital;
- Modifications can be made on site (subject to approval of the designer);
- Efficient use of material leads to competitive construction and to savings in material costs;
- Good design information, and well developed Codes for design as for all steel in construction;
- Efficient design and detailing methods with possibility of interaction and transfer of information on computer disk between the designer and fabricator;
- Can be fire protected relatively easily. Fire rated plasterboards provide up to 120 minutes fire resistance;
- Site checks are minimised;
- The “dry” kit of parts ensures early occupancy with fewer problems later;
- Positive connection between frames and components by welded or mechanically fixed joints;
- Largely unaffected by site conditions;
- Good strength to weight ratio helps with Construction Design and Management (CDM) regulations for man-handling of components.

1.4.1.2 Advantages in service

- Slender and efficient structures may be created in a wide range of forms e.g. portals, trusses, arches, etc.
 - Longer spans can be achieved than with timber. Open roofs spaces can also be created. Removable internal partitions provide flexible use of space;
-

- Stiff structure with good serviceability performance i.e. control of deflections, vibrations, etc.
- Service holes can be provided for routing and re-routing of cables and pipes;
- Attachments can be made easily. Replacement sections are readily available;
- No contribution to fire load;
- Good fire resistance is achieved, and protection materials can be easily replaced after fire;
- Good thermal insulation and avoidance of condensation, if properly detailed and insulated;
- Good acoustic insulation;
- Reduced heat loss through narrow cold-bridge path (some sections are slotted to reduce the heat loss);
- Easy visual inspection and maintenance;
- Long life due to galvanising layer. Sole plated may need additional protection in some applications;
- No hidden defects which might lead to sudden failure, as has affected other materials;
- No long term creep or shrinkage problems, which might otherwise lead to cracking of finishes, etc.;
- No change in material properties over the life of the structure;
- Robust against small explosions or impact or seismic action;
- High environment protection due to long service life, re-use and recycling, waste minimising after dismantling (Burstand, 2000).

It has to be emphasised that light steel framing is often the only solution in many situations, for example in over-roofing or in adding of a storey to a building where additional loading on the existing structure and foundations must be minimised.

On the other hand, framing elements in cold-formed steel may also be combined with hot-rolled steel sections in areas where longer spanning capabilities or greater load capacities are required.

In multi-storey steel buildings, if moment resisting frames are used, significant structural benefits, under wind and earthquake actions can be derived, from the shear resistance of cold-formed steel cladding panels (Mazzolani & Piluso, 1996).

1.4.2 Applications

The most common application of cold-formed steel sections are summarised on the following:

Roof and wall members

Traditionally, a major use of cold-formed steel has been as purlins and girts to support the cladding in industrial type buildings (see Figure 1.21). These are generally based on the Z-section (and its variants) which facilitates incorporation of sleeves and overlaps to improve the efficiency of the members in multi-span applications. Special shapes are made for eaves members etc.



a)



b)

Figure 1.21 – Z and C sections used as: a) purlins; b) girts

Steel framing

An increasing market for cold-formed steel sections is in site-assembled frames and panels for walls and roofs, and stand-alone buildings. This approach has been used in light industrial and commercial buildings and in mezzanine floors of existing buildings (see Figure 1.22).

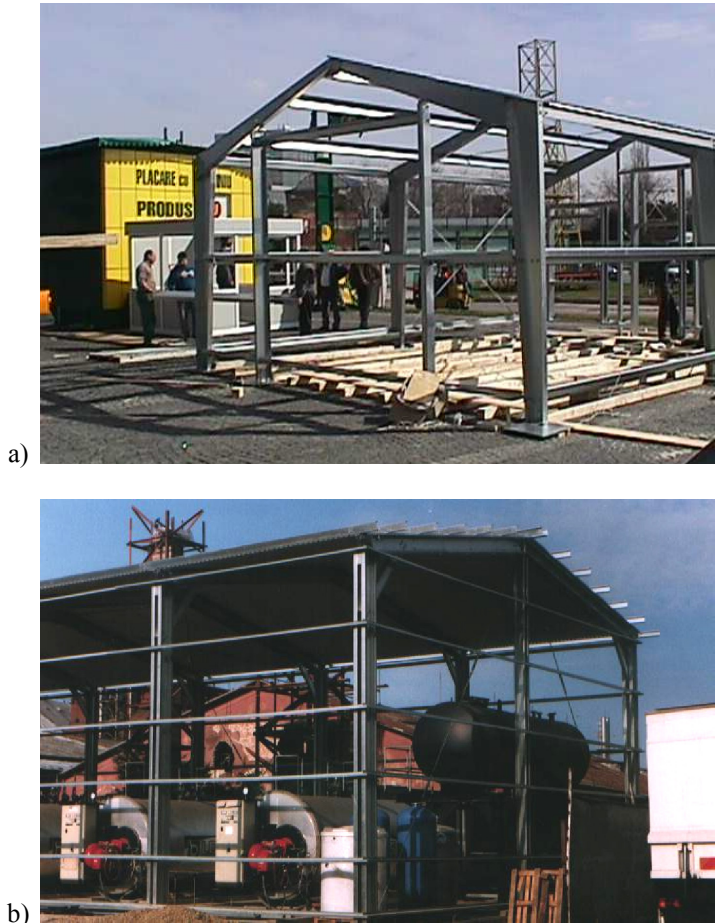


Figure 1.22 – Cold-formed steel framing
a) Single open section *GALCOROM* system; b) Built-up channel section frames

Wall partitions (see Figure 1.23)

A special application is for very light sections used in conjunction with plasterboard panels in stud wall partitioning to form a thin robust wall.



a)



b)

Figure 1.23 – Wall partition inside of building
a) Steel house skeleton; b) Shear resistant stud wall

Large panels for housing

Wall panels can be factory-built and assembled into housing units on site. This is an extension of the approach used for timber framing, called “wall stud” system (see Figures 1.24, 1.25, 1.26).

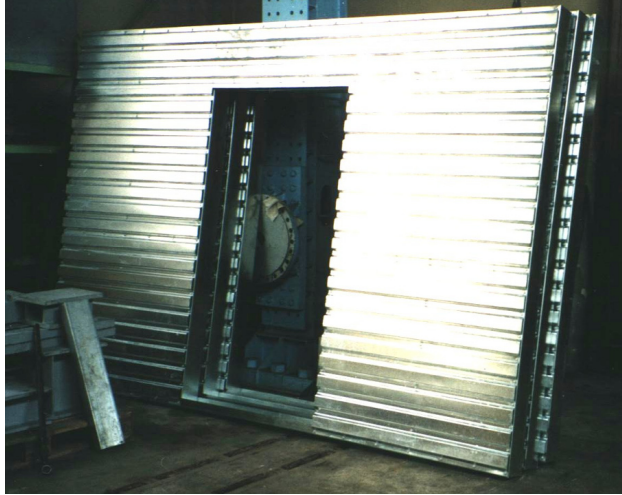


Figure 1.24 – Wall stud panels made of cold-formed steel sections



a)



b)

Figure 1.25 – Installing of prefabricated units



Figure 1.26 – Wall stud housing system with prefabricated cold-formed steel wall panels

Floor joists (see Figures 1.27)

Cold-formed sections may be used as an alternative to timber joists in floors of modest span in domestic and small commercial buildings.



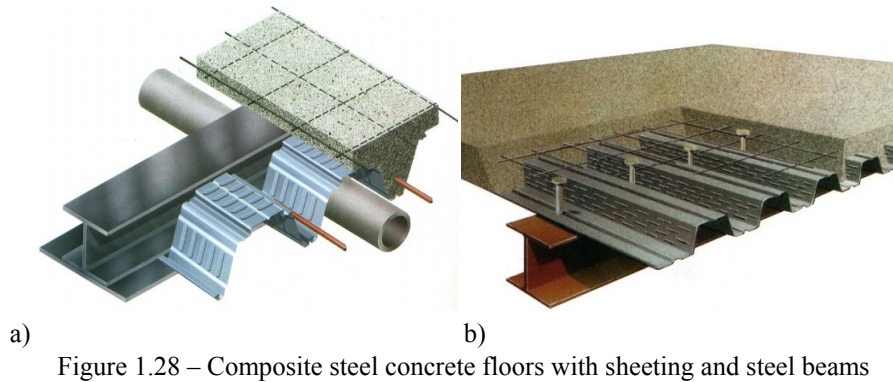
a)



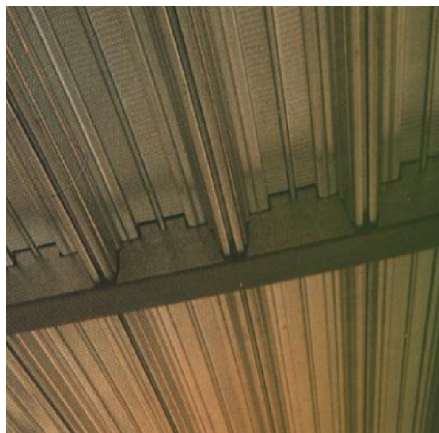
b)

Figure 1.27 – Cold-formed steel joist positioned on the load bearing wall stud structure

Floor decking for composite steel concrete slabs in multi-storey frame building (see Figures 1.28 and 1.29)



a) Decking structure and re-bar for a composite concrete steel structure



b) Positioning of sheeting on steel beams
Figure 1.29 – Composite steel concrete floor

Trusses (see Figures 1.30, 1.31, 1.32)

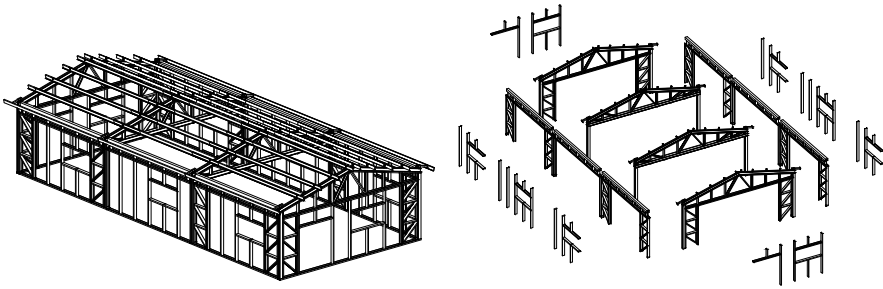
There are a number of manufacturers of lattice girder and truss systems using cold-formed steel sections like SADEF, METSEC, LINDAB, HAMBRO and others.



Figure 1.30 – Roof truss using C bolted sections (Constanta, Romania)



Figure 1.31 – Trusses made of double built-up channel section for a penthouse structure (Alcatel Timisoara, Romania)



a)



b)

Figure 1.32 – Wall Stud Modular System (WSMS) for small and medium size building facilities using trusses for roof structure and resistance against horizontal actions:a) structural concept; b) framing structure; c) building completed (Dubina *et al*, 2001a)

Frames with bolted beam-to-column joints for industrial buildings (Figure 1.33)



Figure 1.33 – Pitched roof portal frame made by built-up sections (back-to-back C bolted connected by stitches, Dubina *et al*, 2001b): a) general view; b) built-up column; c) joint detailing for ridge; d) joint detailing for eaves

Frameless steel building (Figure 1.34)

Steel folded plates, barrel vaults and truncated pyramid roofs are examples of systems that have been developed as so called frameless

buildings (i.e. those without beams and which rely partly on “stress skin” action).

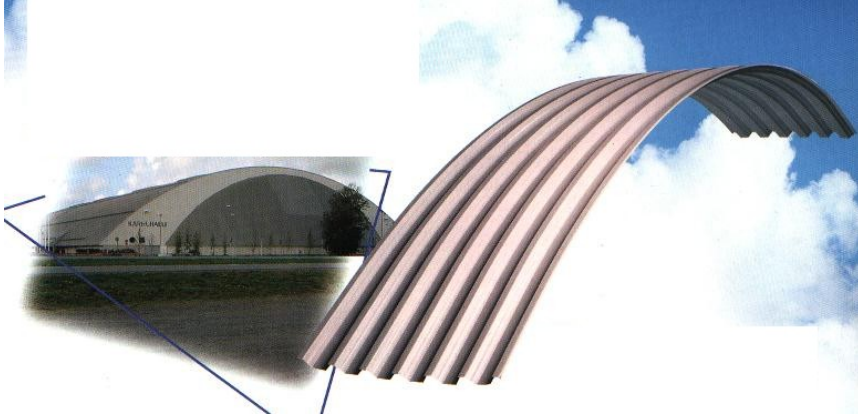


Figure 1.34 – Cylindrical self-bearing sheeting structure (Rannila System)

Storage racking

Storage racking systems for use in warehouses and industrial buildings are made from cold-formed steel perforated sections. Most systems have special clip attachments or bolted joints for easy assembly, as shown in Figures 1.35 and 1.36.



Figure 1.35 – Storage rack systems (http://en.wikipedia.org/wiki/Pallet_racking)



Figure 1.36 – Members and joint detailing for a storage rack systems system

Space Frames (see Figure 1.37)

A space frame (a three-dimensional truss) using cold-formed steel sections.



Figure 1.37 – Three-dimensional truss made by cold-formed steel sections
(<http://en.wikipedia.org/wiki/File:WikiCFSbuilding.jpg>)

Prefabricated buildings (see Figure 1.38)

The transportable prefabricated building unit (such as the ubiquitous site hut) is a common application of the use of cold-formed steel. Other applications are as prefabricated “toilet pod” units in multi-storey buildings.



Figure 1.38 – Prefabricated modular units used for schools and offices: a) American School in Bucharest (<http://www.algeco.ro/>); b) Office building (<http://www.algeco.ro/>); c) Sea Container Group, Constanta – Romania (<http://www.containex.ro/>)

The present book provides to the reader calculation procedures accompanied by relevant numerical examples to be able to design all types of application presented above.

For some specific type of constructions, like residential and industrial buildings, design examples including constructional detailing are presented.

Chapter 2

BASIS OF DESIGN

2.1 GENERAL

The Eurocodes as European unified design rules for structures are part of the European Standard Family comprising also product standards, testing standards, standards for execution, European Technical Approvals and European Technical Approval Guidelines. A key feature of all these standards is consistency that has been obtained by correlated definitions of material and product properties and by basing any calculative way of defining structural properties on test evaluations. As a consequence, all rules in Eurocode 3 are justified by test evaluations with a standardised method that provides full transparency into the harmonisation works and allows new innovative design approaches (Sedlacek & Müller, 2006).

For steel structures, the relevant parts of European standard family are shown in Figure 2.1.

EN1993-1-3 gives design requirements for cold-formed thin gauge members and sheeting. It applies to cold-formed steel products made from coated or uncoated thin gauge hot or cold-rolled sheet or strip, that have been cold-formed by such processes as cold-rolled forming or press-braking. The execution of steel structures, including cold-formed thin gauge members and sheeting, is covered in EN1090. The calculation rules given in this standard are only valid if the tolerances of the cold-formed members comply with EN1090-2 (CEN, 2008) specific provisions.

This European Standard EN1090 specifies requirements for execution of steel structures, in order to ensure adequate levels of mechanical

2. BASIS OF DESIGN

resistance and stability, serviceability and durability. The requirements are expressed in terms of execution classes.

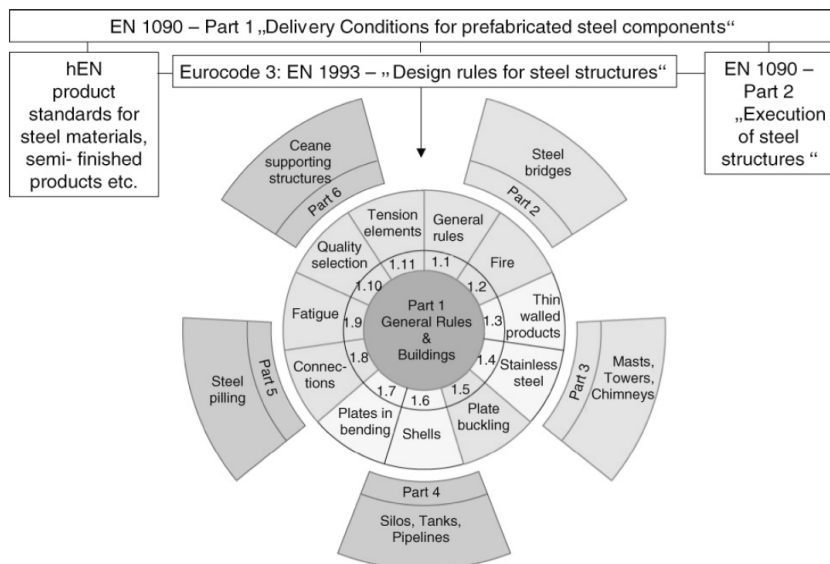


Figure 2.1 – Standard system for steel structures (Sedlacek & Müller, 2006)

The structure shall be designed such that deterioration over its design working life does not impair the performance of the structure below that intended, having due regard to its environment and the anticipated level of maintenance. In order to achieve an adequately durable structure, the following should be taken into account (see EN1990):

- the intended or foreseeable use of the structure;
- the required design criteria;
- the expected environmental conditions;
- the composition, properties and performance of the materials and products;
- the properties of the soil;
- the choice of the structural system;
- the shape of members and the structural detailing;
- the quality of workmanship, and the level of control;
- the particular protective measures;
- the intended maintenance during the design working life.

The environmental conditions shall be identified at the design stage so that their significance can be assessed in relation to durability and adequate provisions can be made for protection of the materials used in the structure.

The effects of deterioration of material, corrosion and fatigue where relevant should be taken into account by appropriate choice of material, or by structural redundancy and by the choice of an appropriate corrosion protection system.

This chapter describes the principles and requirements for safety, serviceability and durability of structures according to EN1990, based on the limit state concept used in conjunction with a partial factor method.

As shown in Chapter 1, the cold-formed steel structures are, usually, thin-walled. This means, in the design for Ultimate Limit State, the stability criteria must be of concern. Also, since the structures will be slender, particular attention has to be paid to Serviceability Limit State criteria, e.g. for deflection limits and vibrations. On the other hand, the complex shapes of cross sections and the special connecting technologies, might involve testing in design, either to check the solutions, either to calibrate the design formulas or to model safety coefficients. On this purpose the Annex D of EN1990 and Chapter 9 of EN1993-1-3 (CEN, 2006a) will be considered.

2.2 LIMIT STATE DESIGN

Limit states design provides the basic framework within which the performance and probability of failure of a structure can be assessed against various limiting conditions. Formulating a limit state should take into account the inherent variability of loads, materials, construction practices and approximations made in design, which involves the concept of probability.

The central concepts of limit state design, as shown by MacGinley & Ang (1992), are that:

1. All the separate conditions that make a structure unfit for use are taken into account. These are the separate limit states;
 2. The design is based on the actual behaviour of materials and performance of structures and members in service;
-

2. BASIS OF DESIGN

3. Ideally, design should be based on statistical methods with a small probability of the structure reaching a limit state.

Concept (1) means that the structure should not overturn under applied loads and its members and joints should be strong enough to carry the forces to which they are subjected. In addition, other conditions such as excessive deflection of beams or unacceptable vibration, though not in fact causing collapse, should not make the structure unfit for use.

In *concept (2)* the strengths are calculated using elastic or plastic¹ theory and post-buckling behaviour is taken into account. The effect of imperfections on design strength is also included. It is recognized that calculations cannot be made in all cases to ensure that limit states are not reached.

Concept (3) implies recognition of the fact that: (i) loads and material strengths vary and are different in reality from the nominal values assumed in design, (ii) approximations are made in design and (iii) imperfections are introduced during fabrication and erection. The effect of these factors on the strength of the structure can only be realistically assessed in statistical terms. Partial factors of safety are introduced to take account of the uncertainties in loads, materials strengths, etc. mentioned above.

Since a limit state approach to design involves the use of a number of specific terms, simple definitions of the more important of these are provided in Table 2.1 (Nethercot, 1991).

50

Table 2.1 – Definition of basic limit states terminology (Nethercot, 1991)

Term	Definition
A limit state	A condition beyond which the structure would become less than completely fit for its intended use. If this happens, the structure is said to have entered a limit state
The ultimate or safety limit state	Inability to sustain any increase in load
The serviceability limit state	Loss of utility and/or requirement for remedial action
Characteristic loads	Those loads which have an acceptability small probability of not being exceeded during the lifetime of the structure
The characteristic strength of a material	The specific strength below which not more than a small percentage (usually 5%) of the results of tests may be expected to fall

¹ usually does not apply to thin-walled sections (e.g. class 3 and class 4)

Partial safety factor	The factors applied to characteristic loads, and properties of materials to take account of the probability of the loads being exceeded and the assessed design strength not being reached.
The design load or factored load	The characteristic load multiplied by the relevant partial factor
The design strength	The characteristic strength divided by the appropriate partial safety factor for the material

The design for limit states shall be based on the use of structural and load models for relevant limit states. It shall be verified that no limit state is exceeded when relevant design values for

- actions,
- material properties, or
- product properties, and
- geometrical data

are used in these models. The verifications shall be carried out for all relevant design situations and load cases. The requirements for limit states should be achieved by using the partial factor method.

A limit state is formally defined by the description of a condition for which a particular structural member or an entire structure fails to perform the function that is expected of it. From the point of view of a structural designer, four types of limit states are considered for steel structures, namely:

- ultimate limit state (ULS);
- serviceability limit state (SLS);
- fatigue limit state (FLS);
- accidental limit state (ALS).

According with EN1990 (CEN, 2002a), a distinction shall be made between ultimate limit states and serviceability limit states. Appropriate partial factors shall be adopted for ultimate limit states and serviceability limit states.

ULS typically represents the collapse of the structure due to loss of structural stiffness and strength. Such loss of capacity may be related to:

1. strength (including general yielding, rupture, buckling and transformation into a mechanism);
2. stability against overturning and sway;

3. fracture due to fatigue;
4. brittle fracture.

When an ultimate limit state is reached, the whole structure or part of it collapses.

SLS conventionally represents failure states for normal operations due to deterioration of routine functionality. SLS considerations in design may address:

1. deflection;
2. vibration (for example wind-induced oscillation, floor vibration);
3. repairable damage due to fatigue;
4. corrosion and durability.

The serviceability limit states, when reached, make the structure or part of it unfit for normal use but do not indicate that collapse has occurred.

All relevant limit states should be considered, but usually it will be appropriate to design on the basis of strength and stability at ultimate loading and then check that deflection is not excessive under serviceability loading.

The general condition of structural reliability with respect to ultimate or serviceability limit states may be expressed using the following inequality:

$$E_d < R_d \quad (2.1)$$

where E_d is the design value of the load effect E , while R_d is the design value of the resistance R . Both E and R are random variables.

A structure must be designed to resist all loads expected to act on the structure during its service life. Thus, the design of a structure require a balance of necessary reliability and reasonable economy.

The limit state design approach simply provides a framework within which explicit and separate consideration is given to a number of distinct performance requirements. The limit state design format bases the design of a structure on the probability and mode of failure, or impaired serviceability, and the probability of the occurrence and variation of the load. Using this concept, the structure is characterized by its overall resistance, which leads to a better understanding of the structural behaviour than working with arbitrary equivalent values which is the case with allowable stress design methods. For example, the failure of a column is described by the buckling

resistance, rather than by an equivalent allowable stress which relates to the buckling load.

Particularly, when designing cold-formed steel building structures, the designer has to manage five peculiar problems connected with ULS design criteria, which characterise the behaviour and performance of thin-walled sections. These specific issues are summarised in Chapter 1 and refer mainly to:

- local instability and strength of sections;
- interactive instability and influence of specific imperfection;
- connecting technology and related design procedures;
- reduced capacity with reference to ductility, plastic design and seismic resistance;
- fire resistance.

The first two types of problems are addresses in Chapters 3, 4 and 7, while the last two types of problems are addressed in Chapter 1, §§1.3.4 and §§1.3.8, respectively. However, more detailed knowledge is necessary to understand the fire and seismic performances of such structures. Fire, because it is really a weakness of steel structures in general, and seismic, because it is important for a large number of countries, where earthquakes may occur.

2.3 ACTIONS ON STRUCTURES. COMBINATIONS OF ACTIONS

The European standards *EN1991: Actions on structures* provides comprehensive information on all actions that should normally be considered in the design of buildings and other civil engineering works.

It is in four main parts, the first part being divided into sub-parts that cover densities, self-weight and imposed loads, actions due to fire, snow, wind, thermal actions, loads during execution and accidental actions, i.e.:

- EN1991-1-1. Eurocode 1: Actions on structures - Part 1-1: General actions - Densities, self-weight, imposed loads for buildings (CEN, 2002b);
 - EN1991-1-2. Eurocode 1: Actions on structures - Part 1-2: General actions - Actions on structures exposed to fire (CEN 2002c);
-

- EN1991-1-3. Eurocode 1: Actions on structures - Part 1-3: General actions - Snow loads (CEN, 2003a);
- EN1991-1-4:2005. Eurocode 1: Actions on structures - Part 1-4: General actions - Wind actions (CEN, 2005b);
- EN1991-1-5:2003. Eurocode 1: Actions on structures - Part 1-5: General actions - Thermal actions (CEN, 2003b);
- EN1991-1-6:2005. Eurocode 1: Actions on structures - Part 1-6: General actions - Actions during execution (CEN, 2005c);
- EN1991-1-7:2006. Eurocode 1: Actions on structures - Part 1-7: General actions - Accidental actions (CEN, 2006c);.

Additionally, each country issued National Annexes to the Eurocodes which provide information on design situations and load arrangements to be used for different locations. The remaining three parts cover traffic loads on bridges, actions by cranes and machinery and actions in silos and tanks.

The European standard *EN1990 Eurocode – Basis of structural design* (CEN, 2002a) provides combination rules for actions. Partial factors for actions and combination coefficients, ψ , used for verification of the ultimate limit state and for verification of the serviceability limit state are considered in accordance with the recommendations given in EN1990.

Two sets of conditions should be considered in accordance with the partial factor method by verifying that the design load effect does not exceed:

- the design resistance of an element/structure in the *Ultimate Limit State*;
- the relevant criteria for the *Serviceability Limit State*.

For the selected design situations and identified limit states, critical load cases should be determined.

2.3.1 Verification at the *Ultimate Limit State*

Ultimate limit states concern safety, such as load-carrying resistance and equilibrium, when the structure reaches the point where it is substantially unsafe for its intended purpose. The designer should ensure that the maximum resistance of a structure (or element of a structure) is adequate to sustain the maximum actions (loads or deformations) that will be imposed

upon it with a reasonable margin of safety. For steelwork design, the principal aspects which must be checked are resistance (including yielding, buckling, and transformation into a mechanism) and stability against overturning. In some cases it will also be necessary to consider other possible failure modes such as fracture due to material fatigue and brittle fracture. However, the material fatigue and brittle fracture limit states can be ignored for simple building structures and neither are discussed in detail in this book.

According to EN1990, four types of ultimate limit states are distinguished: (1) strength; (2) stability; (3) second order effects; (4) fatigue. Equation (2.1) has to be satisfied in which E_d is the design value of the effect of actions such as internal force, moment or a vector representing several internal forces or moments and R_d is the design value of the corresponding resistance.

For each load case, design values E_d for the effect of actions shall be determined from combination rules, involving the design values of actions given in Table 2.2.

For the case of thin-walled cold-formed steel structures the variability of permanent actions G may be neglected, considering that G does not vary significantly during the design working life of the structure and its coefficient of variation is small. In these circumstances G_k should be taken equal to the mean value. No upper value $G_{k,sup}$ or lower value $G_{k,inf}$ will be considered.

Table 2.2 – Design values of actions for use in the combination of actions (CEN, 2002a)

Design situation	Permanent actions	Variable actions		Seismic actions
		Leading variable action	Accompanying variable action	
Persistent and Transient	$\gamma_{G,j} \cdot G_{k,j}$	$\gamma_{Q,1} \cdot Q_{k,1}$	$\gamma_{Q,i} \cdot \psi_{0,i} \cdot Q_{k,i}$	–
Seismic	$G_{k,j}$	–	$\psi_{2,i} \cdot Q_{k,i}$	$\gamma_I A_{Ek}$ or A_{Ed}

The combination of effects of actions to be considered should be based on:

- the design value of the leading variable action, and
- the design combination values of accompanying variable actions.

2. BASIS OF DESIGN

The design values given in Table 2.2 shall be combined using the following rules:

- (1) *persistent or transient design situations for verifications other than those relating to fatigue (fundamental combinations)*

$$\sum_{j \geq 1} \gamma_{G,j} \cdot G_{k,j} + \gamma_{Q,1} \cdot Q_{k,1} + \sum_{i > 1} \gamma_{Q,i} \psi_{0,i} \cdot Q_{k,i} \quad (2.2)$$

- (2) *seismic design situations*

$$\sum_{j \geq 1} G_{k,j} + A_{Ed} + \sum_{i \geq 1} \psi_{2,i} \cdot Q_{k,i} \quad (2.3)$$

where:

- $G_{k,j}$ characteristic value of a permanent actions j ;
- $Q_{k,1}$ characteristic value of the leading variable action 1;
- $Q_{k,i}$ characteristic value of the accompanying variable action i ;
- A_{Ek} characteristic value of seismic action;
- A_{Ed} design value of seismic action $A_{Ed} = \gamma_I A_{Ek}$;
- $\gamma_{G,j}$ partial factor for permanent action j ;
- γ_I importance factor (see EN1998-1)
- $\gamma_{Q,1}$ partial factor for leading variable action 1;
- $\gamma_{Q,i}$ partial factor for variable action i ;
- ψ_0 factor for combination value of a variable action;
- ψ_1 factor for frequent value of a variable action
- ψ_2 factor for quasi-permanent value of a variable action.

The partial safety factors for the ultimate limit state for actions on building structures are given in Table 2.3.

Table 2.3 – Partial safety factors for actions on building structures for persistent and transient design situations (CEN, 2002a)

Permanent actions	Variable actions	
	Leading variable action	Accompanying variable action
$\gamma_{G,j} = 1.35$	$\gamma_{Q,1} = 1.5$	$\gamma_{Q,i} = 1.5$

The recommended values of ψ factors for the more common actions may be obtained from Table 2.4.

Table 2.4 – Combination coefficients for buildings, ψ_0 for the normal design situation, ψ_1 and ψ_2 for accidental design situations (CEN, 2002a)

Variable action	ψ_0	ψ_1	ψ_2
Imposed loads in buildings			
category A: domestic, residential areas	0.7	0.5	0.3
category B: offices	0.7	0.5	0.3
category C: congregation areas	0.7	0.7	0.6
category D; shopping areas	0.7	0.7	0.6
category E: storage areas	1.0	0.9	0.8
Traffic loads in buildings			
category F: traffic area – vehicle weight $\leq 30\text{kN}$	0.7	0.7	0.6
category G: traffic area – $30\text{kN} < \text{vehicle weight} \leq 160\text{kN}$	0.7	0.5	0.3
category H: roofs	0	0	0
Snow loads on buildings (for sites located at altitude H $>1000\text{m}$ above sea level) (see EN1991-1-3)	0.7	0.5	0.2
Snow loads on buildings (for sites located at altitude H $>1000\text{m}$ above sea level)	0.5	0.5	0
Wind loads on buildings (see EN1991-1-4)	0.6	0.2	0
Temperature (non-fire) in buildings (see EN1991-1-5)	0.6	0.5	0

The design of cold-formed members and sheeting shall be in accordance with the general rules given in EN1990 and EN1993-1-1. Appropriate partial factors shall be adopted for ultimate limit states and serviceability limit states.

For verifications by calculation at ultimate limit states the partial factor γ_M shall be taken as follows:

- resistance of cross sections to excessive yielding including local and distortional buckling: γ_{M0} ;
- resistance of members and sheeting where failure is caused by global buckling: γ_{M1} ;
- resistance of net sections at fastener holes: γ_{M2} .

The following numerical values are recommended by EN1993-1-3 for the use in buildings: $\gamma_{M0} = 1.00$; $\gamma_{M1} = 1.00$; $\gamma_{M2} = 1.25$. Numerical values for γ_{Mi} may be defined in the National Annexes.

2.3.2 Verification at the *Serviceability Limit State*

The serviceability limit state is generally concerned with ensuring that deflections are not excessive under normal conditions of use. In some cases

it may also be necessary to ensure that the structure is not subject to excessive vibrations. Both deflection and vibration are associated with the stiffness rather than strength of the structure. For steel structures, adequate stiffness is generally ensured by calculating deflections and ensuring that these are less than stipulated limits. Vibrations will then only need to be considered for special cases, such as floors with long-spanning cold-formed steel joists.

The verification at the serviceability limit state must fulfil the following inequality:

$$E_d \leq C_d \quad (2.4)$$

where C_d is the serviceability constraint (for example admissible deflection) and E_d is the design value of the effects of actions specified in the serviceability criterion, determined on the basis of the relevant combination. The serviceability criteria for deformations and vibrations shall be defined:

- depending on the intended use;
- in relation to the serviceability requirements.

For verifications at serviceability limit states the partial factor $\gamma_{M,ser}$ should be used. The following numerical value is recommended for the use in buildings: $\gamma_{M,ser} = 1.00$. Numerical values for $\gamma_{M,ser}$ may be defined in the National Annexes.

58

The combinations of actions to be taken into account in the relevant design situations should be appropriate for the serviceability requirements and performance criteria being verified. Three combinations of actions for serviceability limit states are defined by the following expressions:

a) Characteristic combination:

$$\sum_{j \geq 1} G_{k,j} + Q_{k,1} + \sum_{i > 1} \psi_{0,i} \cdot Q_{k,i} \quad (2.5)$$

b) Frequent combination:

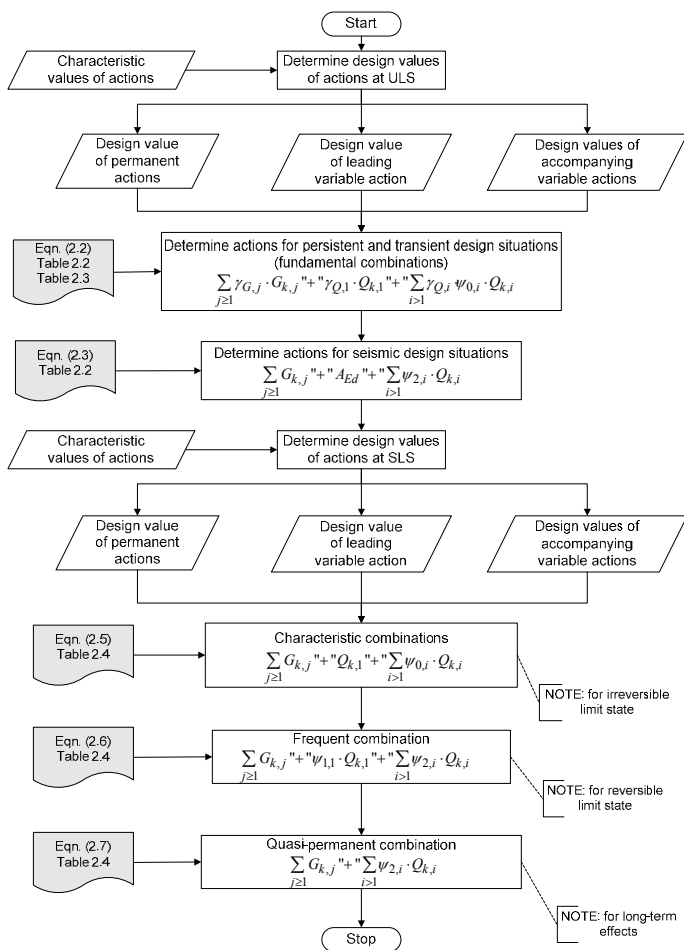
$$\sum_{j \geq 1} G_{k,j} + \psi_{1,1} \cdot Q_{k,1} + \sum_{i > 1} \psi_{2,i} \cdot Q_{k,i} \quad (2.6)$$

c) Quasi-permanent combination:

$$\sum_{j \geq 1} G_{k,j} + \sum_{i > 1} \psi_{2,i} \cdot Q_{k,i} \tag{2.7}$$

The serviceability limit states in buildings should take into account criteria related, for example, to floor stiffness, differential floor levels, storey sway or/and building sway and roof stiffness. Stiffness criteria may be expressed in terms of limits for vertical deflections and for vibrations. Sway criteria may be expressed in terms of limits for horizontal displacements.

Flowchart 2.1 presents the procedure to choose the governing combination of actions according to EN1990 (adapted version, AccessSteel, 2006). Examples of load combinations are presented in Chapter 8.



Flowchart 2.1 – The procedures to choose the governing combination of actions according to EN1990 (adapted version, SF012a-EN-EU, AccessSteel, 2006)

2.3.2.1 Deflections

At the serviceability limit state, the calculated deflection of a member or of a structure is seldom meaningful in itself since the design assumptions are rarely realised. This is because, for example:

- the actual load may be quite unlike the assumed design load;
- beams are seldom "simply supported" or "fixed". Rather, in reality, a beam is usually in some intermediate condition;
- the steelwork may be stiffened by other building components such as floors and walls.

If the functioning or damage of the structure, or damage of the finishes or non-structural members (e.g. partition walls, claddings) is being considered, the verification for deflection should take account of those effects of permanent and variable actions that occur after the execution of the member or finish concerned.

According to EN1993-1-1, §§7.2 and EN1990 – Annex A1.4, deflection limits should be specified for each project and agreed to by the client. As is mentioned in §§7.2 of EN1993-1-1, the National Annex to EN 1993-1-1 may specify these limits.

Calculated deflections should be compared with specified maximum values, which will depend upon circumstances. Eurocode 3 tabulates limiting vertical deflections for beams in six categories as follows:

60

- roofs generally;
- roofs frequently carrying personnel other than for maintenance;
- floors generally;
- floors and roofs supporting plaster or other brittle finish or non-flexible partitions;
- floors supporting columns (unless the deflection has been included in the global analysis for the ultimate limit state);
- situations in which the deflection can impair the appearance of the building.

Vertical deflections are presented schematically in Figure 2.2, where:

w_c is the precamber in the unloaded structural member;

w_1 is the initial part of the deflection under permanent loads of the relevant combination of actions;

- w_2 is the long-term part of the deflection under permanent loads, not to be considered for single storey steel buildings;
- w_3 is the additional part of the deflection due to the variable actions of the relevant combination of actions;
- w_{tot} is the total deflection as sum of w_1 , w_2 , w_3 ;
- w_{max} is the remaining total deflection taking into account the precamber.

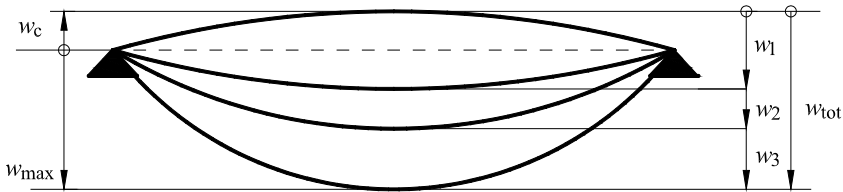


Figure 2.2 – Definition of vertical deflections

For buildings, the recommended limits for vertical deflections are given in Table 2.5, in which L is the span length of the beam (ENV1993-1-1 (CEN, 1992)). For cantilever beams, the length L to be considered is twice the projecting length of the cantilever.

Table 2.5 – Recommended limiting values for vertical deflections

Conditions	Deflection limits	Deflection limits
	w_{max}	w_3
Roofs generally	$L/200$	$L/250$
Roofs frequently carrying personnel other than for maintenance	$L/250$	$L/300$
Floors generally	$L/250$	$L/300$
Floors or roofs supporting plaster or other brittle finish or non-flexible partitions	$L/250$	$L/350$
Floors supporting columns (unless the deflection has been included in the global analysis for the ultimate limit state)	$L/400$	$L/500$
Cases where w_{max} may impair the appearance of the building	$L/250$	-

Another important aspect of serviceability limit state design is ponding. These additional checks should be based on the load combinations for the Ultimate Limit States. To ensure the correct discharge of rainwater from a flat or nearly flat roof, the design of all roofs with a slope of less than 5% should be checked to ensure that rainwater cannot collect in pools.

2. BASIS OF DESIGN

Precambering of beams may reduce the likelihood of rainwater collecting in pools, provided that rainwater outlets are appropriately located.

Where the roof slope is less than 3%, additional calculations should be made to check that collapse cannot occur due to the weight of water:

- either collected in pools which may be formed due to the deflection of structural members or roofing material,
- or retained by snow.

Horizontal frame deflection limits are also specified in ENV1993-1-1 (CEN, 1992). The horizontal frame deflection are represented schematically in Figure 2.3, where u is the overall horizontal displacement over the building height H and u_i is the horizontal displacement over a storey height H_i .

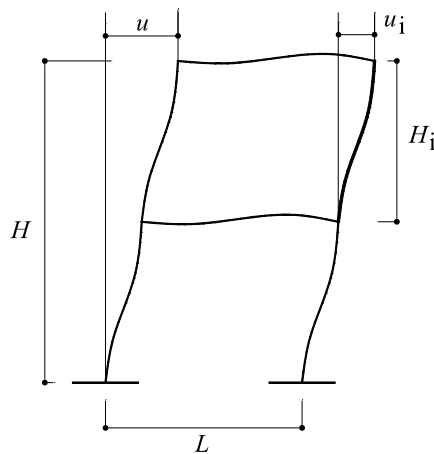


Figure 2.3 – Definition of horizontal displacements

The recommended limiting values for horizontal deflection are given in Table 2.6.

Table 2.6 – Recommended limiting values for horizontal deflections

Conditions	Limits
Portal frames without gantry cranes: Single storey buildings with no particular requirements regarding the deflection	
- Deflection at the top of the columns	$H/150$
- Difference of deflection between two consecutive portal frames	$L/150$
Member supporting metal cladding	
- Post	$H/150$

- Rail	$L/150$
Other single storey buildings: Buildings with particular requirements regarding the deflection (brittle walls, appearance...)	
- Deflection at the top of the columns	$H/250$
- Difference of deflection between two consecutive portal frames	$L/200$
Multi-storey buildings	
- Deflection in each storey	$H/300$
- Deflection on the structure as a whole	$H/500$

2.3.2.2 Dynamic effects

The dynamic effects to be considered at the serviceability limit state are vibration caused by machinery and self-induced vibrations. Resonance can be avoided by ensuring that the natural frequencies of the structure (or any part of it) are sufficiently different from those of the excitation source. The oscillation and vibration of structures on which the public can walk should be limited to avoid significant discomfort to the users. This situation can be checked by performing a dynamic analysis and limiting the lowest natural frequency of the floor.

To achieve satisfactory vibration behaviour of buildings and their structural members under serviceability conditions, the following aspects, amongst others, should be considered:

- the comfort of the user;
- the functioning of the structure or its structural members (e.g. damage to cladding, sensitivity of building contents to vibrations).

Possible sources of vibration that should be considered include walking, synchronized movements of people, machinery, ground borne vibrations from traffic, and wind actions. These, and other sources, should be specified for each project and agreed to by the client.

In case of light gauge steel structures the control of vibrations under dynamic loads can be a crucial problem.

Eurocode 3 recommends a lower limit of 3 cycles per second for floors over which people walk regularly, with a more severe limit of 5 cycles per second for floors used for dancing or jumping, such as gymnasia or dance halls. An alternative method is to ensure adequate stiffness by limiting deflections to appropriate values.

In United States current practice is based on the recommendation of the National Association of Home Builders, which limits the span deflection to $L/480$ under specified uniform live loads, where L is the span length (Xu *et al.*, 2000).

Vibration limits are best expressed in terms of acceleration, as a percentage of the acceleration due to gravity (g). The limit depends primarily on the context, that is, on what people are doing when they experience the vibration. For example, people sitting or lying down in offices or residences find distinctly perceptible vibration (accelerations of about 0.5% g) unacceptable, whereas those taking part in an activity such as aerobics will accept much greater vibration (about 10% g). People dining beside a dance floor or standing in a shopping mall will find vibrations that fall between these two extremes (about 2% g) acceptable (Allen & Pernica, 1998). Generally, it is not the participants in a particular activity or event who are most disturbed by floor vibration, but those who are located in adjacent spaces, as they find it annoying or disruptive to their own activities.

If the vibration is very large (more than 20% g), and occurs frequently, then fatigue failure of the floor can occur. To prevent collapse due to fatigue or overloading, the National Building Code of Canada (NBC–1995) requires a dynamic analysis of a floor structure if it has a natural frequency of less than 6 Hz.

64

The primary factors affecting the design of floor structures for rhythmic activities are (Allen & Pernica, 1998):

- *Span*. The longer the floor span the lower the natural frequency;
- *Storey height*. The taller the columns supporting the floor on which the rhythmic activity takes place the lower the natural frequency of the floor;
- *Walking Vibration*. Walking vibration, which is largely dependent on the type of floor construction, is also an important consideration in the design of floor structures of most buildings.

Most floor vibration problems are caused by resonance and, for light-frame construction, sudden deflections due to footsteps. Light-frame floors of cold-formed steel joists with a wood deck typically have floor frequencies of between 10 Hz and 30 Hz. Someone walking across a floor can be a source of annoyance to a person sitting in a room because of the jolts caused

by sudden changes in floor elevation produced by each footstep. Vibration can usually be controlled by stiffening the floor structure, although sometimes the problems can be addressed by adding damping or by isolating equipment. Proper placement of an activity (e.g., aerobics) or machinery in the building is the most important consideration.

More recently, in the frame of the RSFC Project *Human induced Vibrations of Steel Structures (HIVOSS)* (RFS2-CT-2007-00033:2007) theoretical methods for vibration design of floors have been elaborated. The procedure provided in this guideline provides a simplified method for determining and verifying floor designs for vibrations due to walking. The guideline focuses on simple methods, design tools and recommendations for the acceptance of vibration of floors which are caused by people during normal use. The given design and assessment methods for floor vibrations are related to human induced vibrations, mainly caused by walking under normal conditions. The guideline focuses on the prediction and evaluation of vibration at the design level.

2.4 MATERIALS

2.4.1 General

Material properties play an important role in the performance of structural members. Consequently, it is important to be familiar with the mechanical properties of the steel sheets, strip, plates, or flat bars generally used in cold-formed steel construction before designing this type of steel structural member.

From a structural standpoint, the most important properties of steel are (Yu, 2000): (1) Yield point or yield strength; (2) Tensile strength; (3) Stress–strain characteristics; (4) Modulus of elasticity, tangent modulus, and shear modulus; (5) Ductility; (6) Weldability; (7) Fatigue strength; (8) Toughness. In addition, formability and durability are also important properties for thin-walled cold-formed steel structural members.

According to EN1993-1-3 the design of cold-formed members and profiled sheets fabricated from steel material shall conform with the steel grades and standards listed in Table 2.7a.

2. BASIS OF DESIGN

Table 2.7a – Nominal values of basic yield strength f_{yb} and ultimate tensile strength f_u

Type of steel	Standard	Grade	f_{yb} (N/mm ²)	f_u (N/mm ²)
Hot rolled products of non-alloy structural steels. Part 2: Technical delivery conditions for non-alloy structural steels	EN 10025: Part 2	S 235	235	360
		S 275	275	430
		S 355	355	510
Hot-rolled products of structural steels. Part 3: Technical delivery conditions for normalized/normalized rolled weldable fine grain structural steels	EN 10025: Part 3	S 275 N	275	370
		S 355 N	355	470
		S 420 N	420	520
		S 460 N	460	550
		S 275 NL	275	370
		S 355 NL	355	470
Hot-rolled products of structural steels. Part 4: Technical delivery conditions for thermo-mechanical rolled weldable fine grain structural steels	EN 10025: Part 4	S 420 NL	420	520
		S 460 NL	460	550
		S 275 M	275	360
		S 355 M	355	450
		S 420 M	420	500
		S 460 M	460	530
		S 275 ML	275	360
		S 355 ML	355	450
		S 420 ML	420	500
		S 460 ML	460	530

Examples of steel grades that may conform to the requirements of EN1993-1-3 are given in Table 2.7b.

Table 2.7b – Nominal values of basic yield strength f_{yb} and ultimate tensile strength f_u

Type of steel	Standard	Grade	f_{yb} (N/mm ²)	f_u (N/mm ²)
Cold reduced steel sheet of structural quality	ISO 4997	CR 220	220	300
		CR 250	250	330
		CR 320	320	400
Continuous hot dip zinc coated carbon steel sheet of structural quality	EN 10326	S220GD+Z	220	300
		S250GD+Z	250	330
		S280GD+Z	280	360
		S320GD+Z	320	390
		S350GD+Z	350	420
Hot-rolled flat products made of high yield strength steels for cold forming. Part 2: Delivery conditions for thermo-mechanically rolled steels	EN 10149: Part 2	S 315 MC	315	390
		S 355 MC	355	430
		S 420 MC	420	480
		S 460 MC	460	520
		S 500 MC	500	550
		S 550 MC	550	600
		S 600 MC	600	650
		S 650 MC	650	700
S 700 MC	700	750		

		S 260 NC	260	370
		S 315 NC	315	430
	EN 10149: Part 3	S 355 NC	355	470
		S 420 NC	420	530
Cold-rolled flat products made of high yield strength micro-alloyed steels for cold forming		H240LA	240	340
		H280LA	280	370
	EN 10268	H320LA	320	400
		H360LA	360	430
		H400LA	400	460
Continuously hot-dip coated strip and sheet of steels with higher yield strength for cold forming		H260LAD	240	340
		H300LAD	280	370
	EN 10292	H340LAD	320	400
		H380LAD	360	430
		H420LAD	400	460
Continuously hot-dipped zinc-aluminium (ZA) coated steel strip and sheet		S220GD+ZA	220	300
		S250GD+ZA	250	330
	EN 10326	S280GD+ZA	280	360
		S320GD+ZA	320	390
		S350GD+ZA	350	420
Continuously hot-dipped aluminium-zinc (AZ) coated steel strip and sheet		S220GD+AZ	220	300
		S250GD+AZ	250	330
	EN 10326	S280GD+AZ	280	360
		S320GD+AZ	320	390
		S350GD+AZ	350	420
Continuously hot-dipped zinc coated strip and sheet of mild steel for cold forming		DX51D+Z	140	270
	EN 10327	DX52D+Z	140	270
		DX53D+Z	140	270

All steels used for cold-formed members and profiled sheets should be suitable for cold-forming and welding, if needed. Steels used for members and sheets to be galvanized should also be suitable for galvanizing. The nominal values of material properties should be adopted as characteristic values in design calculations.

2.4.2 Structural steel

2.4.2.1 Material properties of base material

The nominal values of yield strength f_{yb} or ultimate tensile strength f_u should be obtained:

- a) either by adopting the values $f_y = R_{eh}$ (upper yield strength) or $R_{p0.2}$ (proof strength) and $f_u = R_m$ (tensile strength) direct from product standards, or
- b) by using the values given in Table 2.7a and b, or
- c) by appropriate tests.

Where the characteristic values are determined from tests, such tests should be carried out in accordance with EN10002-1 (CEN, 2001). The coupons should be taken at random from the concerned lot of steel and the orientation should be in the length of the structural element. The characteristic values should be determined on the basis of a statistical evaluation in accordance with Annex D of EN 1990.

2.4.2.2 Material properties of cold-formed sections and sheeting

The manufacturing process plays a governing role for some characteristics that have an influence on the buckling behaviour of the profiles. First of all, it leads to a modification of the stress-strain curve of the steel. With respect to the virgin material, cold-rolling provides an increase of the yield strength and, sometimes, of the ultimate strength that is important in the corners and still appreciable in the flanges, while press braking leaves these characteristics nearly unchanged in the flanges. Obviously, such effects do not appear in case of hot-rolled sections, as shown in Table 1.1 (Rondal, 1988).

The increase of the yield strength is due to strain hardening and depends on the type of steel used for cold-rolling. On the contrary, the increase of the ultimate strength is related to strain aging, which is accompanied by a decrease of the ductility and depends on the metallurgical properties of the material.

Another important aspect is related to the fact that the cold-forming process (roll-forming and press-braking) is applied to the flat steel sheets. The flat steel sheet has already experienced the coiling, uncoiling and flattening process. Cold-rolled steel sheets are first coiled into rolls for storage. They are subsequently uncoiled from the roll and forced to become a flat sheet before cold-forming forces are applied. The residual stresses in a cold-formed section are therefore derived from two sources: the coiling, uncoiling and flattening process (referred to simply as the coiling–uncoiling

process) and the cold-forming process. The predictions of residual stresses in cold-formed sections can thus be separated into two tasks: the prediction of residual stresses from the coiling and uncoiling process involving pure bending of the steel sheet and the prediction of the residual stresses from the cold-bending process (Quach *et al*, 2004).

Some producers of cold-formed steel sections are using a cold rolling mill technology in order to reduce the thickness of base sheeting. Special attention should be paid to such steels because cold reducing produces, depending of the rate of thickness reduction, lead to significant changes of the initial base material properties due to strain hardening effects (e.g. significant increase of f_y and decrease of ductility). The cold-forming process of the sections, applied after cold-reducing of the thickness of steel strips, will affect supplementary the same mechanical properties.

EN1993-1-3 provides formulas to evaluate the increase of yield strength of cold-formed steel sections, compared to that of basic material.

The increased yield strength due to cold forming may be taken into account as follows:

- in axially loaded members in which the effective cross sectional area A_{eff} equals the gross area A_g ;
- in determining A_{eff} the yield strength f_y should be taken as the basic yield strength f_{yb} .

Special attention should be paid to the fact that some heat treatments (especially annealing) might induce a reduced yield strength lower than the basic yield strength f_{yb} . In other cases the basic yield strength f_{yb} should be used.

The average yield strength f_{ya} of a cross section due to cold working may be determined from the results of full size tests. Alternatively the increased average yield strength f_{ya} may be determined by calculation using the following formulas:

$$f_{ya} = f_{yb} + (f_u - f_{yb}) \frac{knt^2}{A_g} \quad \text{but} \quad f_{ya} \leq \frac{(f_u + f_{yb})}{2} \quad (2.8)$$

where:

A_g is the gross cross sectional area;

2. BASIS OF DESIGN

- k is a numerical coefficient that depends on the type of forming as follows: (a) $k = 7$ for roll forming; (b) $k = 5$ for other methods of forming;
- n is the number of 90° bends in the cross section with an internal radius $r \leq 5t$ (fractions of 90° bends should be counted as fractions of n);
- t is the design core thickness of the steel material before cold-forming, exclusive of metal and organic coatings.

The average yield strength f_{ya} may be utilised in determining:

- the cross section resistance of an axially loaded tension member;
- the cross section resistance and the buckling resistance of an axially loaded compression member with a fully effective cross section;
- the moment resistance of a cross section with fully effective flanges.

Example 2.1: Compute the average yield strength, f_{ya} , due to cold working by roll forming, for the lipped channel section given in Figure 2.4 subjected to tension.

The dimensions of the cross section and the material properties are:

Total height	$h = 120 \text{ mm}$
Total width of flange	$b = 40 \text{ mm}$
Total width of edge fold	$c = 15 \text{ mm}$
Internal radius	$r = 3 \text{ mm}$
Nominal thickness	$t_{nom} = 2.0 \text{ mm}$
Steel core thickness	$t = 1.96 \text{ mm}$
Steel grade	S280GD+Z
Basic yield strength	$f_{yb} = 280 \text{ N/mm}^2$
Ultimate strength	$f_u = 360 \text{ N/mm}^2$
Modulus of elasticity	$E = 210000 \text{ N/mm}^2$
Poisson's ratio	$\nu = 0.3$
Gross cross section area:	$A_g = 435 \text{ mm}^2$

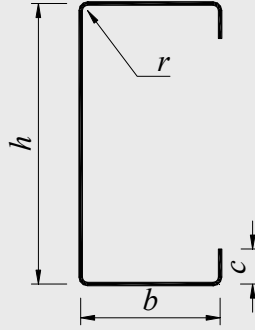


Figure 2.4 – General dimensions for a lipped channel section

The average yield strength f_{ya} :

$$f_{ya} = f_{yb} + (f_u - f_{yb}) \frac{kn t^2}{A_g} = 280 + (360 - 280) \times \frac{7 \times 4 \times 1.96^2}{435} = 300 \text{ N/mm}^2 \text{ but}$$

$$f_{ya} \leq \frac{f_u + f_{yb}}{2} = \frac{360 + 280}{2} = 320 \text{ N/mm}^2$$

where:

k – coefficient depending on the type of forming; $k = 7$ for roll forming

n – the number of 90° bends in the cross section with an internal radius $r \leq 5t$; $n = 4$;

$$f_{ya} = 300 \text{ N/mm}^2 < \frac{f_u + f_{yb}}{2} = 320 \text{ N/mm}^2$$

71

To determine the moment resistance of a cross section with fully effective flanges, the cross section may be subdivided into m nominal plane elements, such as flanges. Expression (2.8) may then be used to obtain values of increased yield strength $f_{y,i}$ separately for each nominal plane element i , provided that:

$$\frac{\sum_{i=1}^m A_{g,i} f_{y,i}}{\sum_{i=1}^m A_{g,i}} \leq f_{ya} \quad (2.9)$$

where

$A_{g,i}$ is the gross cross sectional area of nominal plane element i , and when calculating the increased yield strength $f_{y,i}$ using the expression (2.8) the bends on the edge of the nominal plane elements should be counted with half their angle for each area $A_{g,i}$.

2.4.2.3 Thickness and thickness tolerances

The provisions for design by calculation given in Part 1-3 of EN1993 may be used for steel within given ranges of core thickness t_{cor} . The following values are recommended:

- for sheeting and members: $0.45 \text{ mm} \leq t_{cor} \leq 15 \text{ mm}$
- for connections: $0.45 \text{ mm} \leq t_{cor} \leq 4 \text{ mm}$

Thicker or thinner material may also be used, provided the load bearing resistance is determined by design assisted by testing.

The steel core thickness t_{cor} should be used as design thickness, where

$$t = t_{cor} \quad \text{if} \quad tol \leq 5\% \quad (2.10a)$$

$$t = t_{cor} \cdot \frac{100 - tol}{95} \quad \text{if} \quad tol > 5\% \quad (2.10b)$$

$$\text{with} \quad t_{cor} = t_{nom} - t_{metallic \ coatings} \quad (2.10c)$$

where

tol is the tolerance expressed in % (it is positive if the measured thickness is less than the nominal value);

t_{nom} is the nominal sheet thickness after cold forming. It may be taken as the value of t_{nom} of the original sheet, if the calculative cross sectional areas before and after cold forming do not differ more than 2%; otherwise the notional dimensions should be changed.

2.5 METHODS OF ANALYSIS AND DESIGN

2.5.1 Methods of analysis – Global frame analysis

The aim of global frame analysis is to determine the distribution of the internal forces and the corresponding deformations in a structure subjected to a specified loading. Achieving this purpose requires the adoption of adequate models which incorporate assumptions about the behaviour of the structure and in particular of its component members and joints.

Global analysis of frames is conducted on a model based on many assumptions including those for the structural model, the geometric and material behaviour of the structure and of its members and the behaviour of the sections and of the joints.

Once the analysis is completed, a number of design checks of the frame and its components (members and joints) must be performed. These checks depend on the type of analysis performed and the type of cross section verification (i.e. ultimate limit state criteria) used.

The determination of the actual load-deformation response generally requires the use of a sophisticated analysis method. For practical purposes, assumptions for the frame and its component member and joint models are made that permit a safe bound for the ultimate load to be obtained. Hence models range from the simple linear elastic analysis or the rigid-plastic analysis to the most complex, elastoplastic analysis, which can provide a close representation of the real behaviour of the structure.

The first important distinction that can be made between the methods of analysis is the one that separates elastic and plastic methods. Whilst elastic analysis can be used in all cases, the use of plastic analysis is subject to some restrictions. Another important distinction is between methods which make allowance for and those which neglect the effects of the actual displaced configuration of the structure. They are referred to as second-order theory and first-order theory based methods respectively. While the second-order theory can be adopted in all cases, the first-order theory may be used only either when the displacement effects of the structural behaviour are negligible or when they can be incorporated in some other way.

The methods for global analysis are: (1) First-order elastic analysis; (2) Second-order elastic analysis; (3) Elastic-perfectly plastic analysis (Second-order theory); (4) Elastoplastic analysis (second-order theory); (5) Rigid-plastic analysis (first-order theory).

According to EN1993-1-1 (CEN, 2005a), the internal forces and displacements may be determined using either a global elastic analysis or a global plastic analysis (clause 5.4.1(1)). Finite element analysis is also possible but is not specifically covered in EN1993-1-1, reference being made to EN1993-1-5 (CEN, 2006b). Global elastic analysis is based on the assumption of a linear stress-strain relation for steel, whatever the stress level in the structure is (see clause 5.4.2(1) of EN1993-1-1). Elastic global analysis may be used in all cases, provided that the provisions in Section 5.1 of EN1993-1-1 are met. Global plastic analysis assumes progressive yielding of some cross sections of the structures, normally leading to plastic hinges and a redistribution of forces within the structure. In this type of analysis it is mandatory that the cross sections where plastic hinges occurs possess sufficient rotation capacity. The adopted stress-strain relation for steel is a bi-linear elastoplastic relationship, although more precise relationship may be adopted (see §§5.4.3 of EN1993-1-1).

One important parameter in choosing the methods for global analysis is the cross section of the elements of the frame. EN1993-1-1 defines four classes of cross section. The class into which a particular cross section falls depends upon the slenderness of each element (defined by a width-to-thickness ratio) and the compressive stress distribution i.e. uniform or linear. The classes are defined in terms of performance requirements for resistance of bending moments (see Figure 2.5):

Class 1: cross sections are those which can form a plastic hinge with the required rotational capacity for plastic analysis.

Class 2: cross sections are those which, although able to develop a plastic moment, have limited rotational capacity and are therefore unsuitable for structures designed by plastic analysis.

Class 3: cross sections are those in which the calculated stress in the extreme compression fibre can reach yield but local buckling prevents the development of the plastic moment resistance.

Class 4: cross sections are those in which local buckling limits the moment resistance (or compression resistance for axially loaded

members). Explicit allowance for the effects of local buckling is necessary.

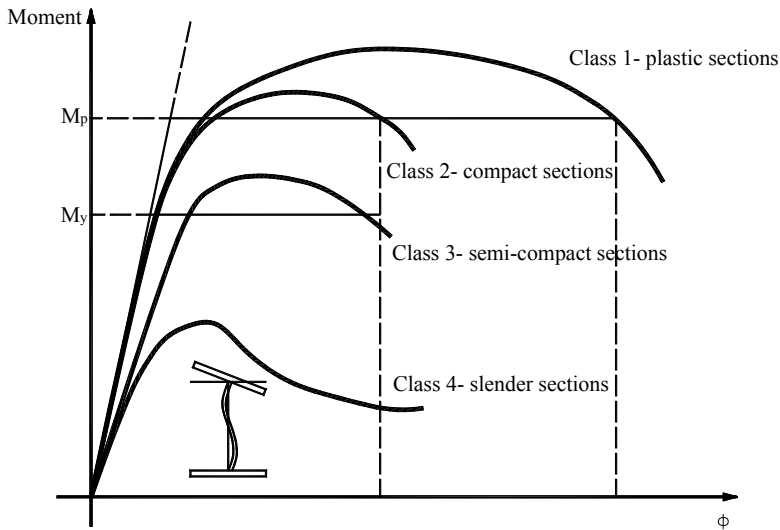


Figure 2.5 – Cross section behaviour classes

Thin-walled cold-formed steel members are usually made by sections of class 4 or, at most, of class 3. Compared with hot-rolled sections (of class 1 or 2), they are characterised by a reduced post-elastic strength and, as a consequence, by a reduced ductility (e.g. they do not have sufficient plastic rotation capacity to form plastic hinges, as shown in Figure 2.5). For this reason, only elastic global frame analyses is usually of interest.

First order analysis may be used for the structure, if the increase of the relevant internal forces or moments or any other change of structural behaviour caused by deformations can be neglected. This condition may be assumed to be fulfilled, if the following criterion is satisfied:

$$\alpha_{cr} = \frac{F_{cr}}{F_{Ed}} \geq 10 \text{ for elastic analysis} \quad (2.11)$$

where

- α_{cr} is the factor by which the design loading would have to be increased to cause elastic instability in a global mode;
- F_{Ed} is the design loading on the structure;

2. BASIS OF DESIGN

F_{cr} is the elastic critical buckling load for the global instability mode based on initial elastic stiffness.

The effects of the deformed geometry (second-order effects) shall be considered if they increase the action effects significantly or modify significantly the structural behaviour.

Portal frames with shallow roof slopes and unbraced beam-and-column type plane frames in buildings may be checked for sway mode failure with first order analysis if the criterion (2.11) is satisfied for each storey. For these structures α_{cr} may be calculated using the following approximate formula, provided that the axial compression in the beams or rafters is not significant:

$$\alpha_{cr} = \left(\frac{H_{Ed}}{V_{Ed}} \right) \left(\frac{h}{\delta_{H,Ed}} \right) \quad (2.12)$$

where

H_{Ed} is the design value of the horizontal reaction at the bottom of the storey to the horizontal loads and notional horizontal loads (see Figure 2.6);

V_{Ed} is the total design vertical load on the structure on the bottom of the storey (see Figure 2.6);

$\delta_{H,Ed}$ is the horizontal displacement at the top of the storey, relative to the bottom of the storey, when the frame is loaded with horizontal loads (e.g. wind) and notional horizontal loads which are applied at each floor level (see Figure 2.6);

h is the storey height (see Figure 2.6).

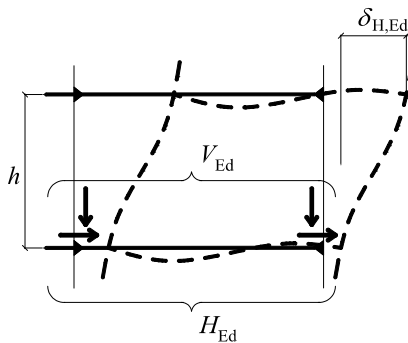


Figure 2.6 – Parameters for calculation of α_{cr} in multi-storey buildings

When a frame is analysed using an elastic method, the in-plane second-order effects can be allowed for by using:

- a) first-order analysis, “amplified sway moment method”;
- b) first-order analysis, “Iterative method”;
- c) first-order analysis, with sway-mode buckling length.

2.5.2 Finite Element Methods (FEM) for analysis and design

The Finite Element Method (FEM) is widely used in design of structures. Annex C of EN1993-1-5 gives guidance on the use of FE-methods for ultimate limit state design, serviceability limit state design and fatigue verifications of plated structures. The FE-modelling may be carried out either for: (1) the component as a whole or (2) a substructure as a part of the whole structure. Also, design of members and details can be assisted by numerical simulations (e.g. numerical testing). The choice of the FE-method depends on the problem to be analysed.

The key categories of computational analysis that were first devised for use in EN 1993-1-6 (CEN, 2007) are recommended for wide use for all structures (Rotter, 2011):

- LBA: Linear elastic bifurcation analysis, obtaining the lowest eigenvalue for the system;
- MNA: Materially non-linear analysis, using small displacement theory (no change of geometry), and an ideal elastoplastic constitutive model for the material;
- GNA: Geometrically non-linear analysis of the elastic perfect structure;
- GMNA: Geometrically and materially non-linear analysis of the perfect structure;
- GMNIA: Geometrically and materially non-linear analysis with explicit imperfections.

“Geometrically non-linear” means an analysis that takes full account of the change in geometry, both in kinematic and equilibrium relationships, whether this be a small change in one dimension or a gross inversion of the complete structure. Similarly it is expected that in a GMNA or GMNIA analysis, the material model will be fully non-linear and not simply an ideal elastoplastic model, unless this truly represents the material response. The

classic image of the load-displacement curves given by these analyses is shown in Figure 2.7.

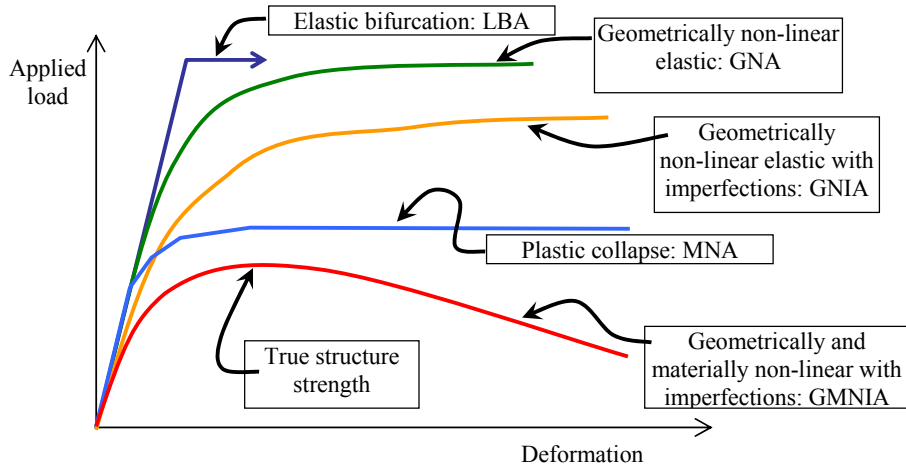


Figure 2.7 – Load-displacement curves found using different analyses of the same structure (Rotter, 2011)

In using FEM for design special care should be taken in:

- the modelling of the structural component and its boundary conditions;
- the choice of software and documentation;
- the modelling of imperfections;
- the modelling of material properties;
- the modelling of loads;
- the choice of limit state criteria;
- the choice of partial factors to be applied.

The choice of FE-models (shell models or volume models) and the size of mesh determine the accuracy of results. For validation, sensitivity checks with successive refinement may be carried out.

The boundary conditions for supports, interfaces and applied loads should be chosen such that results obtained are conservative. Geometric properties should be taken as nominal.

Where imperfections need to be included in the FE-model these imperfections should include both geometric and structural imperfections. Unless a more refined analysis of the geometric imperfections and the

structural imperfections is carried out, equivalent geometric imperfections may be used. The direction of the applied imperfection should be such that the lowest resistance is obtained. In combining imperfections a leading imperfection should be chosen and the accompanying imperfections may have their values reduced to 70%.

Material properties should be taken as characteristic values. Depending on the accuracy and the allowable strain required for the analysis the following assumptions for the material behaviour may be used:

- a) elastoplastic without strain hardening;
- b) elastoplastic with a nominal plateau slope;
- c) elastoplastic with linear strain hardening;
- d) true stress-strain curve modified from test results.

The loads applied to the structures should include relevant load factors and load combination factors. For simplicity a single load multiplier α may be used.

Thin-walled cold-formed steel members are characterised by the following instability modes: local buckling of the walls, distortional buckling of the cross section or global buckling of the member. For relevant member lengths an interaction of these modes can occur. The structural design of thin-walled cold-formed steel members is strongly dependent on the analysis of the stability and, consequently, the elastic stability behavior has to be obtained as accurate as possible, in order to produce safe and reliable results to be applied in design procedures.

For this, one can apply direct formulations previously obtained from the theory of elastic stability, as for the case of the global buckling, or take advantage of computational programs that allow general stability analysis by solving the fundamental eigenvalue problem, related to the bifurcation-type stability behavior. The general solution of the first order stability problem for the case of thin-walled members can be easily accessed, with the help of finite element method – based programs.

Alternative computational solutions have been developed, on the basis of numerical models other than the FEM, such as the general beam theory method (GBT) and the finite strip method (FSM).

Generalized Beam Theory is an extension to conventional engineering beam theory that allows cross section distortion to be considered. Stability

analysis of thin-walled members may also be performed using GBT. GBT was originally developed by Schardt (1989), then extended by Davies *et al* (1994a,b; 1995, 1996), and has over the last several years been an active focus of Silvestre & Camotim (2002a, 2002b, 2003). It has a short solution time and the method is applicable for both pin-ended and fixed-ended members. Generalized Beam Theory has a user friendly program for use developed at the TU Lisbon called GBTUL (<http://www.civil.ist.utl.pt/gbt/>), that performs elastic buckling (bifurcation) and vibration analyses of prismatic thin-walled members.

Another alternative to determine the elastic buckling loads of thin-walled cold-formed members is the freely available open source program CUFSM tool (<http://www.ce.jhu.edu/bschafer/cufsm/>). CUFSM employs the semi-analytical finite strip method to provide solutions for the cross section stability of such members (Schafer & Ádány, 2006). The new version CUFSM 4.04 applies to members with general end boundary conditions. The constrained finite strip method (cFSM) is also fully implemented in this version.

Other software packages that provide the same solutions are available, e.g. CFS (www.rsgsoftware.com) and THIN-WALL (<http://sydney.edu.au/engineering/civil/case/thinwall.shtml>).

In case of thin-walled cold-formed members, when the interaction of local-overall or distortional-overall buckling is the purpose of an analysis, GNIA or GMNIA, with shell finite elements are recommended. For connecting details, in almost all the cases, MNA with 3D finite elements can be used.

An useful reference for a good guidance in design of steel structures using FEM is the book of Kidmann & Krauss (2011).

2.5.3 Design assisted by testing

Design assisted by testing may be used instead of design by calculation. Section 9 of EN1993-1-3 may be used to apply the principles for design assisted by testing given in EN1990 and in Section 2.5 of EN1993-1-1, with additional specific requirements for cold-formed members and sheeting. Annex A of EN1993-1-3 gives standardised procedures for testing

and evaluation for a number of tests commonly required in cold-formed steel design. The procedures refer to:

- tests on profiled sheets and liner trays;
- tests on cold-formed members;
- tests on structures and portions of structures;
- tests on beams torsionally restrained by sheeting;
- evaluation of test results to determine design values.

For testing fasteners, Chapter 9 of EN1993-1-3 makes reference to older documents of ECCS–TC7, e.g. Publications no. 21 and no. 42. In 2008, an updated version of Publication 21 of ECCS was published (ECCS, 2008a).

If design assisted by testing is used either to replace design by calculation or combined with calculation, the testing shall be performed by a testing body approved by the competent authority, or by a body officially notified, or officially accredited, or by a body with equal status and with a quality system. The testing may be realized in the producer's laboratory under the control of competent authority.

Testing may be undertaken under any of following circumstances:

- a) if the properties of steel are unknown;
- b) if it is desired to take account of the actual properties of the cold-formed member or sheet;
- c) if adequate analytical procedures are not available for designing the component by calculation alone;
- d) if realistic data for design cannot otherwise be obtained;
- e) if it is desired to check the performance of an existing structure or structural component;
- f) if it is desired to build a number of similar structures or components on the basis of a prototype;
- g) if confirmation of consistency of production is required;
- h) if it is desired to determine the effects of interaction with other structural components;
- i) if it is desired to determine the effects of the lateral or torsional restraint supplied by other components;
- j) it is desired to prove the validity and adequacy of an analytical procedure;

- k) if it is desired to produce resistance tables based on tests, or on a combination of testing and analysis;
- l) if it is desired to take into account practical factors that might alter the performance of a structure, but are not addressed by the relevant analysis method for design by calculation.

Tensile testing of steel should be carried out in accordance with EN10002-1. Testing of other steel properties should be carried out in accordance with the relevant European Standards. The characteristic values should be determined on the basis of a statistical evaluation in accordance with Annex D of EN 1990.

As already presented in §§2.1, all rules in Eurocode 3 are justified by test evaluations with a standardised method. The central role of the test evaluation for the development of sustainable design rules with sufficient stability and continuity for steel structures is demonstrated in Figure 2.8 (Sedlacek & Müller, 2006), by the following steps:

1. Prefabricated steel components to be tested experimentally shall have properties representative for a larger population and comply with the requirements of the Product Standards for materials and semi-finished products and with the execution rules in EN1090-2. These representative properties make them suitable to determine representative resistance values $R_{exp,i}$.
2. For interpreting the test results an engineering model $R(X)$ is applied that allows us to determine by calculation the resistance properties $R_{calc,i}$ of the test components using the measured parameters X_i .
3. The plotting of the ratios $(R_{exp} / R_{calc})_i$ versus X_i demonstrates the quality of the engineering model (the ratios should be independent of X_i variations, i.e. horizontal lines).
4. By direct comparison of $R_{exp,i}$ and $R_{calc,i}$ the mean value correction R_m and the scatter distribution s_δ can be found. These values allow estimation of the initial value $R_k = R_{5\%}$ and the design value R_d , for which the recommended value of the reliability index $\beta = 3.8$ and the weighting factor $\alpha_R = 0.8$ for the resistance are used.
5. From R_k and R_d the γ_M -value for the particular problem can be obtained, or as suggested in Eurocode 3.
6. The initial characteristic value is then corrected to comply with the partial factor γ_{Mi} chosen as $R_k = \gamma_{Mi} R_d$.

- Finally, the statistical parameters obtained from this test evaluation allow the determination of quality requirements for the product standards and execution standards to comply with the γ_M values.

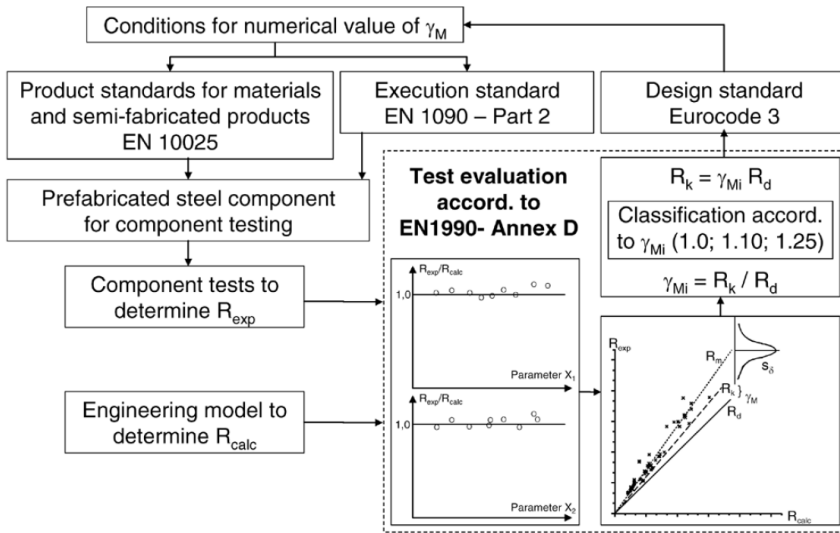


Figure 2.8 – Determination of characteristic values R_k and γ_M values from tests (Sedlacek & Müller, 2006)

This method has been used to justify the characteristic values of strength and also the numerical values of the partial factors γ_M recommended in Eurocode 3 (CEN, 2005a). Figure 2.9 gives a survey on the various recommended γ_M values associated with the different ductile failure modes distinguished in Eurocode 3 (Sedlacek & Müller, 2006). It also shows that test evaluations were performed to determine the design strength functions R_d depending on the yield strength f_y or the tensile strength f_u according to the relevant failure mode in the first instance, whereas the characteristic values R_k were obtained from R_d by multiplying with the recommended γ_M -values.

All test evaluations have demonstrated that the model uncertainty s_δ of any engineering model R is the main controlling parameter for γ_M , so that the format $R_d = R_k / \gamma_M$ used in Eurocode 3 is also justified from the statistical point of view.

2. BASIS OF DESIGN

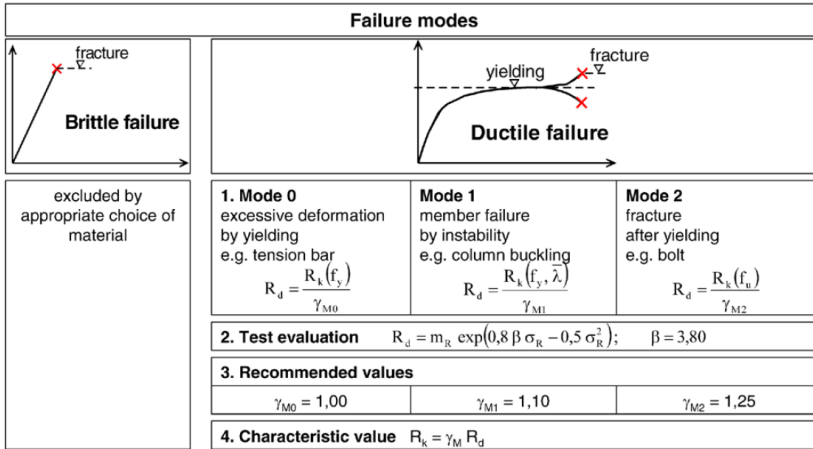


Figure 2.9 – Procedure to obtain reliable values R_k (Sedlacek & Müller, 2006)

Dubina (2008), based on the results obtained at the “Politehnica” University of Timisoara, shows how test results can be used to solve and validate some complex problems of analysis and design of cold-formed steel structures. Four complex problems of analysis and/or design of cold-formed steel structures have been solved using testing, i.e.:

- Calibration of imperfection factor for interactive local-overall buckling of cold-formed steel compression members. On this purpose, test results collected from literature, ECBL approach, and statistical data processing procedure of Annex Z from ENV1993 (actually, replaced by Annex D of EN1990) have been used;
- Experimental calibration of stiffness of joints in cold-formed steel trusses. Tests on single-bolt lap joints and on structural T-joints have been used to calibrate the stiffness calculation formula. Afterwards, a full-scale test on a truss module has been used to validate the proposal;
- Analysis and design of cold-formed steel pitched-roof portal frames. First, a test campaign on ridge and knee joints was performed in order to characterize their behaviour and performance. Based on these test results, the component method from EN1993-1-8 has been adopted for cold-formed steel joints calculation in terms of stiffness and strength. In the second phase, full-scale tests on frame units have been used to evaluate and confirm the global analysis models;

- Analysis and design of cold-formed steel framing houses. Tests on shear panels and fastening systems combined with numerical simulations have been carried out in order to propose a design approach based on the shear walls capacity and 3D analysis. Next, in situ vibration measurements on a building structure, in subsequent stages of erection, have been used to evaluate the contribution of finishing and to validate the design approach.

In all these four problems, tests only or accompanied by numerical simulations have been used to find the proper solutions and/or to validate them. In fact, without tests, the solutions of these problems would be very difficult, say impossible, to be found.

2.6 IMPERFECTIONS

All structures are in reality imperfect. The term “imperfection” refer equally to cross section and member geometry, to residual stresses, to yield strength distribution across the section, to support conditions and to load introduction. Excepting the last two types of imperfections, which are of mechanical type, the geometrical and material imperfections are functions of sheet width and thickness, and of the forming process. Rondal (1988) has analysed the difference between hot-rolled and cold-formed sections, expressed in terms of characteristic imperfections. The different nature of imperfections, associated with the slenderness of component walls, leads to a different instability behaviour of cold-formed sections compared to hot-rolled sections. Specific buckling curves should be used for cold-formed steel sections instead of the curves specified for hot-rolled sections.

2.6.1 Imperfections for global analysis of frames

Appropriate allowance must be made to account for the effects of practical imperfections in the global analysis, in the analysis of bracing systems and in member design. Practical imperfections, which include residual stresses, are geometrical imperfections such as lack of verticality, lack of straightness, lack of fit and unavoidable eccentricities present in practical joints.

Allowance for these imperfections may be achieved by incorporating suitable geometric imperfections with values which reflect all types of imperfection. According to EN1993-1-1 the following imperfections should be taken into account in the global analysis of all frames:

- a) global imperfections for frames and bracing systems,
- b) local imperfections for individual members.

The effects of member imperfections may be neglected when carrying out the analysis of non-sway frames. For sway frames with slender columns it may be required to incorporate member imperfections in the analysis.

The effects of global frame imperfections must be accounted for in the global analysis in the form of an equivalent geometric imperfection, i.e. an initial sway (see Figure 2.10(a)). The assumed shape of global imperfections and local imperfections may be derived from the elastic buckling mode of a structure in the plane of buckling considered. Both in- and out-of-plane buckling including torsional and flexural-torsional buckling with symmetric and asymmetric buckling shapes should be taken into account in the most unfavourable direction and form. The resulting forces and moments shall be used for member design.

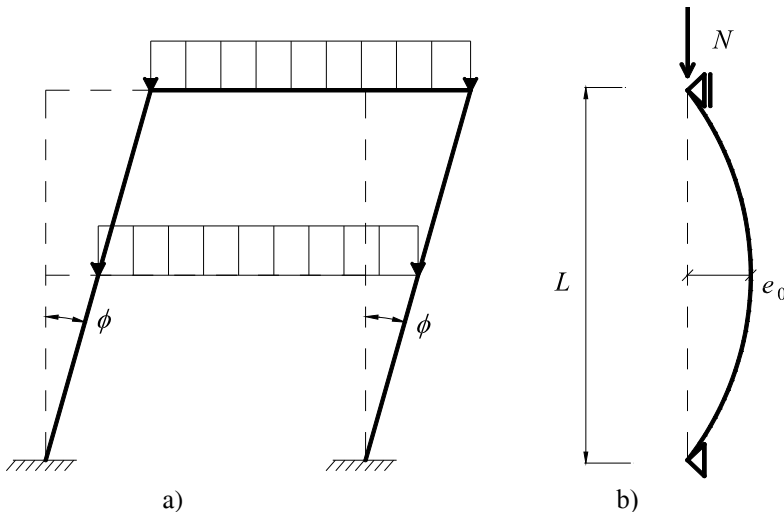


Figure 2.10 – a) Global frame imperfections; b) Local member imperfections

The frame imperfections are treated as a load case to be used in conjunction with the critical load combinations acting on the frame. The

initial sway imperfections apply in all horizontal directions, but need only be considered in one direction at a time. Particular attention should be paid to cases of anti-symmetric sways on two opposite faces which may introduce torsional effects. The assumed shape of global imperfections and local imperfections may be derived from the elastic buckling mode of a structure in the plane of buckling considered.

These global imperfections can also be accounted for by introducing equivalent lateral loads at the floor levels.

For frames sensitive to buckling in a sway mode, the effect of imperfections should be allowed for in frame analysis by means of an equivalent imperfection in the form of an initial sway imperfection and individual bow imperfections of members. The imperfections may be determined from:

a) *global initial sway imperfections*, see Figure 2.11:

$$\phi = \phi_0 \cdot \alpha_h \cdot \alpha_m \quad (2.13)$$

where

ϕ_0 is the basic value: $\phi_0 = 1/200$;

α_h is the reduction factor for height h applicable to columns:

$$\alpha_h = \frac{2}{\sqrt{h}} \quad \text{but} \quad \frac{2}{3} \leq \alpha_h \leq 1.0;$$

h is the height of the structure in meters;

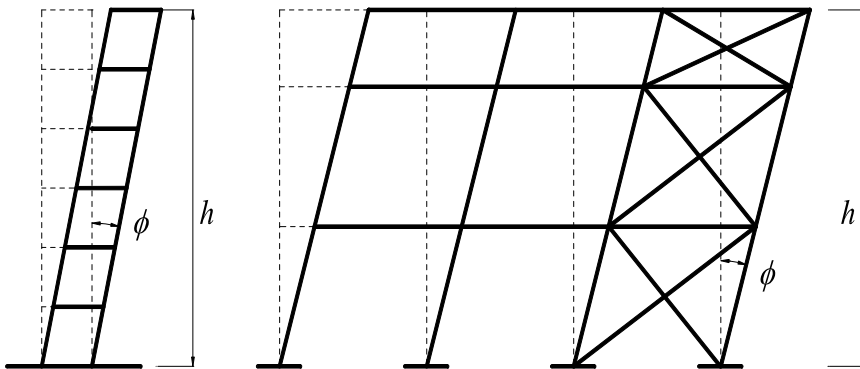


Figure 2.11 – Equivalent sway imperfections

2. BASIS OF DESIGN

α_m is the reduction factor for the number of columns in a row:

$$\alpha_m = \sqrt{0.5 \left(1 + \frac{1}{m} \right)}$$

m is the number of columns in a row, including only those columns which carry a vertical load N_{Ed} not less than 50% of the average value of the axial force in the columns in the vertical plane considered.

b) relative initial local bow imperfections of members for flexural buckling

$$e_0 / L \quad (2.14)$$

where L is the member length. The values e_0 / L may be specified in the National Annexes. The recommended values given by EN1993-1-1 are presented in Table 2.8, with reference to the EN1993-1-1 column buckling curves.

Table 2.8 – Design values of initial local bow imperfection for elastic analysis

Buckling curve	e_0/L
a ₀	1/350
a	1/300
b	1/250
c	1/200
d	1/150

The appropriate equivalent bow imperfection for a given member depends on the relevant buckling curve, the method of analysis and the type of cross section verification used. It is usual to represent the initially bowed member by two or more rigid connected straight elements. Moments and forces for design are thus generated at intermediate points along the member.

The local member imperfection (bowing) to be used is shown in Figure 2.10(b). It can be seen that its effect is the same as that due to the actual deflection of the member itself due to bending and axial load (i.e. a P - δ effect).

The effects of member imperfections may be neglected when carrying out elastic global analyses of frames, except in some specific cases of

slender members. For those cases for which it can be neglected, the effect is presumed to be included in the appropriate buckling formula.

The cases for which member imperfections must be explicitly modelled are the members in sway frames subjected to axial compression which have moment-resisting connections and in which:

$$\bar{\lambda} > 0.5 \sqrt{\frac{A \cdot f_y}{N_{Ed}}} \tag{2.15}$$

where

N_{Ed}	is the design value of the compressive force;
$\bar{\lambda} = \sqrt{A \cdot f_y / N_{cr}}$	is the in-plane non-dimensional slenderness calculated for the member considered as hinged at its ends;
N_{cr}	is the Euler buckling load for the member calculated using the buckling length equal to the system length.

The incorporation of the initial local member imperfections in the global analysis leads to the modification of the member forces and moments along the entire length of the members (compared to when imperfections are not included).

As an alternative method the effects of initial sway imperfection and local bow imperfections may be replaced by systems of equivalent horizontal forces, introduced for each column (see Figure 2.12).

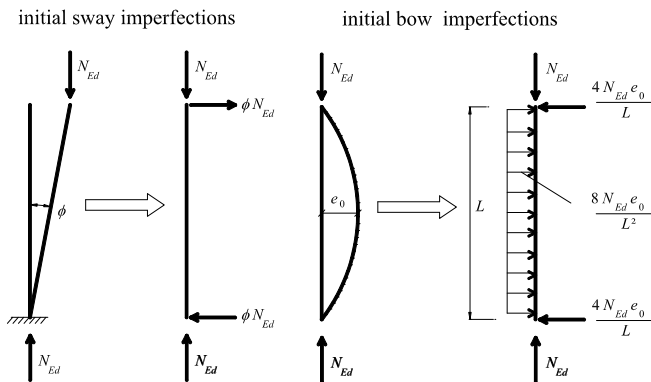


Figure 2.12 – Replacement of initial imperfections by equivalent horizontal forces

The procedure used for determining these forces is the same as that for obtaining the equivalent lateral load to account for the $P-\Delta$ sway effect due to the loading applied to the structure. The equivalent horizontal forces at each roof and floor level are calculated by multiplying the vertical load applied at each level by the initial sway imperfection. They may be applied in any horizontal direction, but only in one sway direction at a time.

The equivalent horizontal forces obtained by multiplying the vertical reactions by the initial sway imperfections are applied at the supports (in the opposite direction to those applied at the other levels) so that the equivalent horizontal forces on the entire frame form a closed system, i.e. the net equivalent horizontal force applied to the entire structure becomes zero.

The possible torsional effects on a structure caused by anti-symmetric sways at two opposite faces, should also be considered, see Figure 2.13.

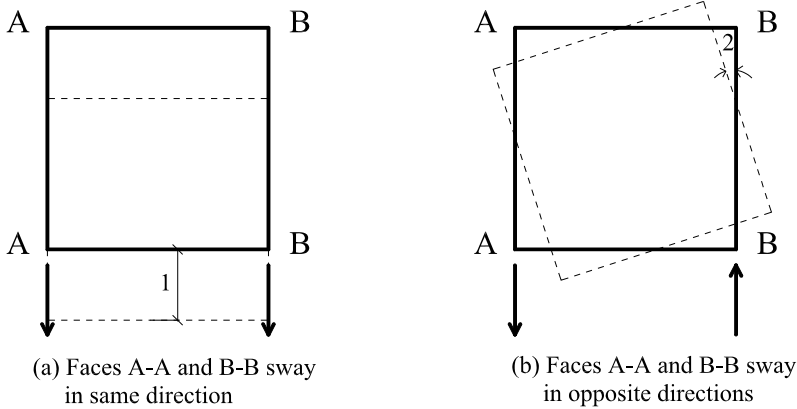


Figure 2.13 – Translational and torsional effects (plan view):
 1) translational sway; 2) rotational sway

2.6.2 Imperfections for analysis of bracing systems

In the analysis of bracing systems which are required to provide lateral stability within the length of beams or compression members, the effects of imperfections should be included by means of an equivalent geometric imperfection of the members to be restrained, in the form of an initial bow imperfection:

$$e_0 = \alpha_m L / 500 \tag{2.16}$$

where L is the span of the bracing system and $\alpha_m = \sqrt{0.5 \left(1 + \frac{1}{m}\right)}$, in which m is the number of members to be restrained.

For convenience, the effects of the initial bow imperfections of the members to be restrained by a bracing system, may be replaced by an equivalent stabilizing force, as shown in Figure 2.14:

$$q_d = \sum N_{Ed} \cdot 8 \cdot \frac{e_0 + \delta_q}{L^2} \quad (2.17)$$

where δ_q is the in-plane deflection of the bracing system due to q_d plus any external loads calculated from first order analysis (δ_q may be taken as 0 if second order theory is used).

In addition, when the restrained members are spliced, the bracing system shall be capable of resisting a local force applied to it at that point by each beam or compression member which is spliced.

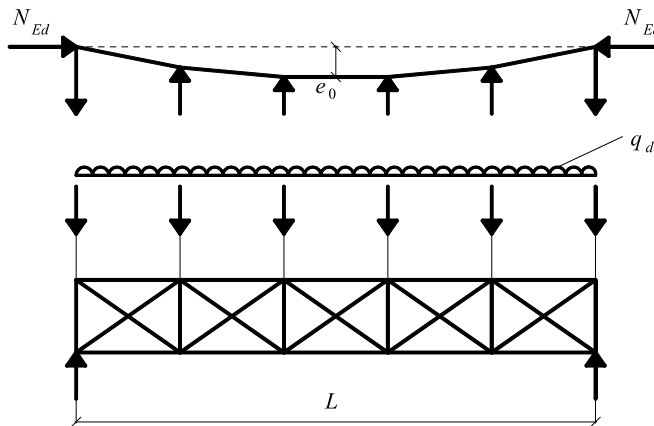


Figure 2.14 – Imperfections for bracing systems

2.6.3 Role of imperfections in advanced numerical simulation

When numerical non-linear analysis (e.g. Finite Element Method – FEM or Finite Strip Method – FSM) is used to simulate the behaviour or to evaluate the effective properties of a cold-formed steel section, the effect of imperfections must always be considered.

Due to the sectional local and/or distortional buckling (see §§1.3.1), the behaviour of thin-walled cold-formed steel members is highly non-linear.

When a geometrical non-linear analysis is performed, some kind of initial disturbances (e.g. imperfection) is necessary in determining the strength of the member.

Two kinds of imperfections are characterising the behaviour of cold-formed steel sections i.e.:

- geometrical imperfections, sectional and along the member;
- residual stress and change of yield strength due to cold forming.

When initial imperfections are used to invoke geometric non-linearity, the shape of imperfections can be determined by eigen-buckling analysis and may be chosen affine to the relevant local, distortional or overall buckling modes of the cross section or member. Consequently, until now the geometrical imperfections are introduced in numerical models using equivalent sine shapes with wavelength corresponding to relevant instability modes. Rasmussen & Hancock (1988) and, recently, Schafer & Peköz (1998a), proposed numerical models to generate automatically geometrical imperfection modes. Schafer *et al* (1998b) used a probabilistic analysis in order to evaluate the frequency and magnitude of imperfections.

Maximum measured imperfections, can be conservatively used as amplitude in sine shapes to predict lower bound strength by analysis (Rasmussen & Hancock, 1988). While it is true that larger imperfections do not always mean lower strength if the eigenmode shape used in the analysis does not characterise the most unfavourable imperfect shape of the member, generally, the strength decreases as the magnitude of the imperfection increases. Of course, the use of a maximum value of sine shape imperfection is a simplification. On this aim a systematic analysis, in order to study the effect of geometric imperfection size and shape, was presented by Dubina & Ungureanu (2002). In fact, since the maximum imperfections are not periodic along the length of a member, using the maximum imperfection as a magnitude for the buckling shapes is quite conservative. Despite, these drawbacks, the maximum imperfections provide a reasonable criterion for a lower bound strength analysis. It is also useful to underline a conclusion by Bernard *et al* (1999), who demonstrated statistically that significant geometrical imperfections may exist in thin-walled members at short and

medium wavelengths, leading to a reduction of the load carrying capacity. This means the sectional (e.g. local and distortional) buckling modes, singly or coupled with overall ones are mainly affected.

In the following the codification rules of both geometrical imperfections and residual stresses, suggested by Schafer & Peköz (1998a) to be used in computational modelling of cold-formed steel sections, are presented.

2.6.3.1 Section imperfections

Geometric imperfections refer to deviations from the “perfect” or “nominal” geometry. Imperfections of cold-formed steel members include bowing, warping, and twisting as well as local deviations. Local deviations are characterized by dents and regular undulation of plate elements. Collected data on geometric sectional imperfection are divided by Schafer & Peköz (1998a) in two categories: type 1, maximum local imperfection in a stiffened element and type 2, maximum deviation from straightness for a lip stiffened or unstiffened flange (see Figure 2.15). Based on statistical analysis of existing imperfection measurements, Schafer & Peköz proposed simple rules for sections less than 3 mm in thickness, and width/thickness (b/t) less than 200 for *type 1* imperfections and $b/t < 100$ for *type 2* imperfections.

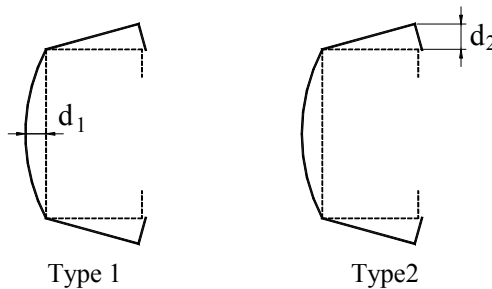


Figure 2.15 – Sectional imperfections (Schafer & Peköz, 1998a)

For a *type 1* imperfections a simple linear regression based on the plate width yielded the approximate expression:

$$d_1 \approx 0.006 \cdot b \quad (2.18a)$$

2. BASIS OF DESIGN

where b is width or depth of the web. An alternative rule based on an exponential curve fit in the thickness, t , is:

$$d_1 \approx 6 \cdot t \cdot e^{-2t} \quad (d_1 \text{ and } t \text{ in mm}) \quad (2.18b)$$

For *type 2* imperfections the maximum deviation from straightness is approximately equal to the plate thickness:

$$d_2 \approx t \quad (2.18c)$$

In what concerns the overall sinusoidal imperfection (bar deflection), the magnitude of 1/1500 times the member length, L , which corresponds to the statistical mean of imperfections of carbon steel columns as suggested by Bjorhovde (1972), can be used, or the conservative value of $L/1000$ proposed by the ECCS Recommendations (ECCS, 1978), can be used.

For the case of lateral-torsional buckling of thin-walled beams both initial deflection and initial twisting may be significant. For this purpose, the Australian Standard AS4100:1990 proposes recommendations for the initial deflection, f_0 , and initial twist, ϕ_0 , as follows:

$$1000 \cdot f_0 / L = 1000 \cdot \phi_0 \cdot (M_{cr} / N_{cr} L) = -1 \quad \text{for } \lambda_{LT} \geq 0.6 \quad (2.19a)$$

$$1000 \cdot f_0 / L = 1000 \cdot \phi_0 \cdot (M_{cr} / N_{cr} L) = -0.001 \quad \text{for } \lambda_{LT} < 0.6 \quad (2.19b)$$

where

- N_{cr} is the column elastic critical buckling (Euler) load about the minor axis;
- M_{cr} is the elastic critical moment for lateral-torsional buckling;
- λ_{LT} is the lateral-torsional slenderness;
- L is the length of the member.

2.6.3.2 Residual stresses

In cold-formed steel members, residual stresses and increase in yield strength results from the manufacturing process and tend to compensate each other.

Adequate computational modelling of residual stresses is troublesome. Inclusion of residual stresses (at the integration points of the model for instance) may be complicated, and selecting an appropriate magnitude is made difficult by the lack of data. As a result, residual stresses are often excluded altogether, or the stress-strain behaviour of the material is modified to approximate the effect of residual stresses.

In hot-rolled steel members, residual stresses do not vary markedly through the thickness, which means the membrane residual are dominant, while in cold-formed members residual stresses are dominated by a “flexural”, or through thickness variation (see Table 1.1, §§1.2.3). This variation of residual stresses leads to early yielding at the faces of cold-formed steel plates. Through-thickness residual stresses are implicitly considered when obtaining the stress-strain curve from coupon tests, and lead to a roundedness of the stress-strain curve near the yield point.

Residual stress can be idealised as a summation of two types: flexural and membrane (see Figure 2.16).

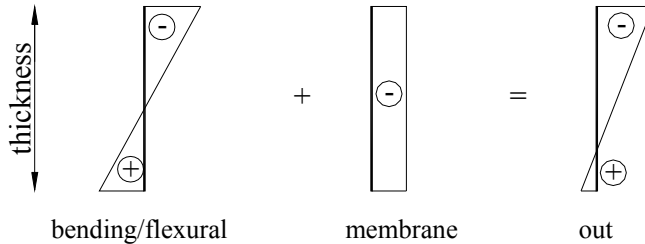


Figure 2.16 – Idealisation of residual stress (Schafer & Peköz, 1998a)

Membrane residual stresses are more prevalent in roll-formed members than press-braked members. Compressive membrane residual stresses cause a direct loss in compressive strength. Significant membrane residual stresses exist primarily in corner regions. Counteracting this effect, the yield stress, f_y , is enhanced in corner regions due to significant cold work during forming. If large membrane residual stresses are modelled in the corners or other heavily worked zones, then increased yield stress in these regions should be modelled as well. Conversely, if membrane residual stresses are ignored, the enhancement of the yield stress should not be included. Further study is needed to assess how much these two effects counteract one another.

Flexural residual stresses. As stated in §§1.2.3, flexural residual stresses are much more significant in cold-formed steel sections than the membrane ones. For member buckling (overall modes) their influence is usually not important. However, sectional buckling strengths, mainly the local and distortional buckling strengths can be significantly influenced.

Large magnitude of flexural residual stresses in cold-formed sections are regularly observed – residual stresses equal to $50\%f_y$ are not uncommon. Measured flexural residual stresses also experience a large degree of variability.

For the purpose of numerical analysis Schafer & Peköz (1998a) proposed the approximate and conservative average distributions of flexural residual stresses, as shown in Figure 2.17.

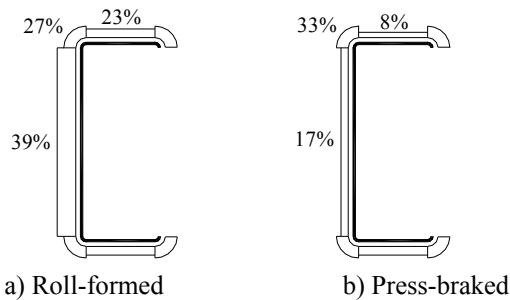


Figure 2.17 – Average flexural residual stress as percentage of f_y (Schafer & Peköz, 1998a)

When a highly refined numerical analysis is performed, both residual stresses and actual distribution of yield strength over the full cross section, taking into account the influence of cold-forming have to be considered.

Numerical studies have shown the reduced influence of flexural residual stresses on the ultimate strength of sections. Moreover, Rasmussen & Hancock (1993) observed that tension and compression coupons cut from finished tubes curved longitudinally as a result of through-thickness flexural residual stresses, and that straightening of the coupons as part of the testing procedure approximately reintroduced the flexural residual stresses. Therefore, when the material properties of the cross section are established from coupons cut from within the section, the effect of flexural residual stresses is inherently present, and are not require to be explicitly defined in the finite element model (Gardner & Nethercot, 2001).

Chapter 3

BEHAVIOUR AND RESISTANCE OF CROSS SECTION

3.1 GENERAL

The individual components of cold-formed steel members are usually so thin with respect to their widths that they buckle at stress levels less than the yield point when subjected to compression, shear, bending or bearing. Local buckling of such elements is therefore one of the major considerations in cold-formed steel design.

It is well known that, compared to other kinds of structures, thin plates are characterised by a stable post-critical behaviour (see Figure 3.1). Consequently, cold-formed steel sections, which can be regarded as an assembly of thin plates along the corner lines, will not necessarily fail when their local buckling stress is reached and they may continue to carry increasing loads in excess of that at which local buckling occurs.

As already shown in Figure 1.16 of Chapter 1, Figure 3.2 summarises the difference in behaviour of a thick-walled slender bar in compression (see Figure 3.2a), and a thin-walled one (see Figure 3.2b). Both cases of ideal perfect bar and imperfect bar are presented.

Figure 3.3 illustrates examples of local buckling patterns of beams and columns (Yu, 2000).

In order to account for local buckling, when the resistance of cross sections and members is evaluated and checked for design purposes, the effective section properties have to be used. However, for members in tension the full section properties are used. The appropriate use of full and

3. BEHAVIOUR AND RESISTANCE OF CROSS SECTION

effective cross section properties is explained in this section.

Local buckling of individual walls of cold-formed steel sections is a major design criterion and, consequently, the design of such members should provide sufficient safety against failure by local instability with due consideration given to the post-buckling strength of structural components (e.g. walls).

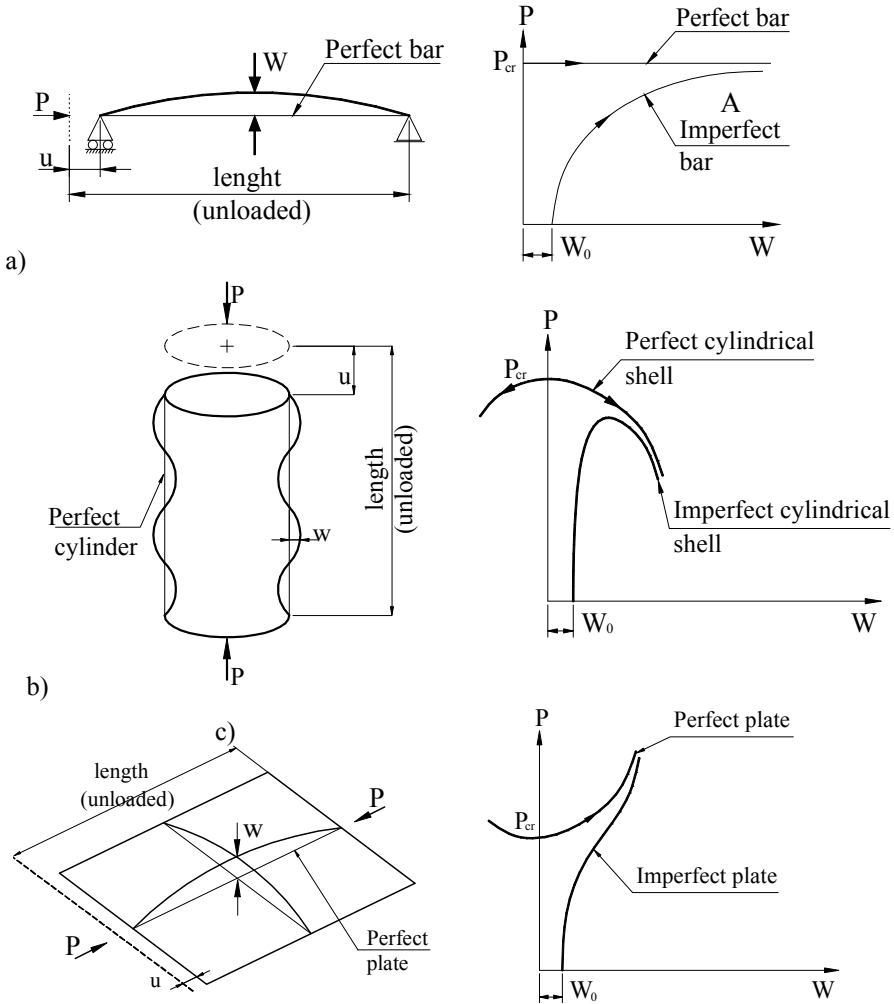


Figure 3.1 – Post-critical behaviour of elastic structures:

- a) columns: indifferent post-critical path;
- b) cylinders: unstable post-critical path;
- c) plates: stable post-critical path

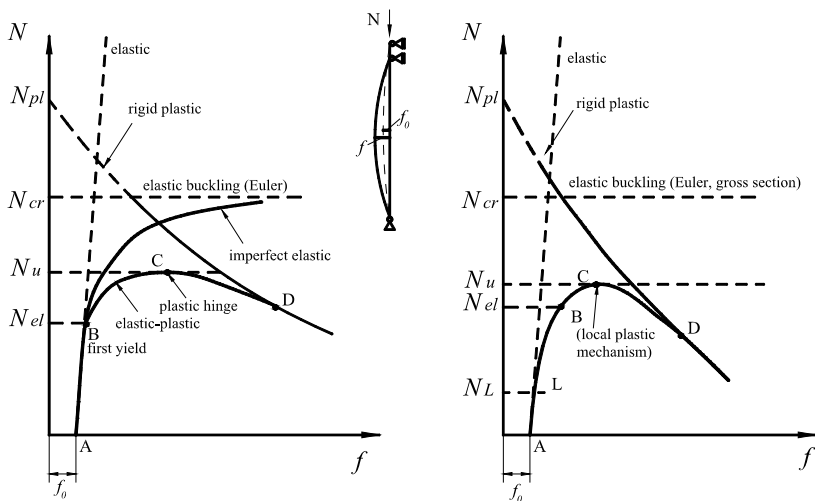


Figure 3.2 – Behaviour of (a) slender tick-walled and (b) thin-walled compression bar

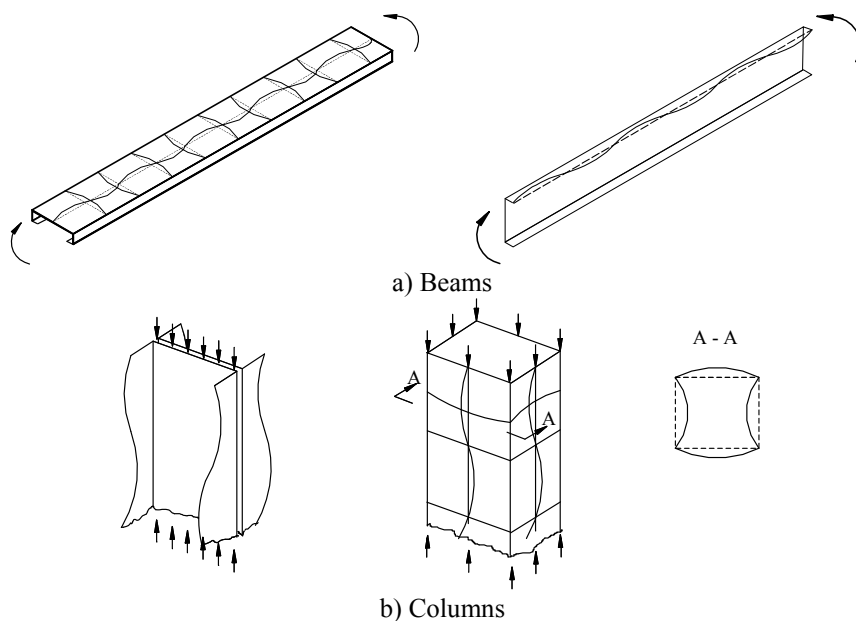


Figure 3.3 – Local buckling of compression walls of cold-formed steel section

The present section provides details of the calculation procedure for the evaluation of cross section resistance for the following design actions:

- axial tension;
- axial compression;

- bending moment;
- combined bending and axial tension;
- combined bending and axial compression;
- torsional moment;
- shear force;
- local transverse forces;
- combined bending moment and shear force;
- combined bending moment and local transverse force.

Both local buckling and distortional buckling (sectional instability modes) effects on the cross section strength will be examined.

3.2 PROPERTIES OF GROSS CROSS SECTION

3.2.1 Nominal dimensions and idealisation of cross section

The properties of the gross cross section shall be determined using specified nominal dimensions (width and thickness) of the walls and stiffeners composing the cross section (see Figure 3.4).

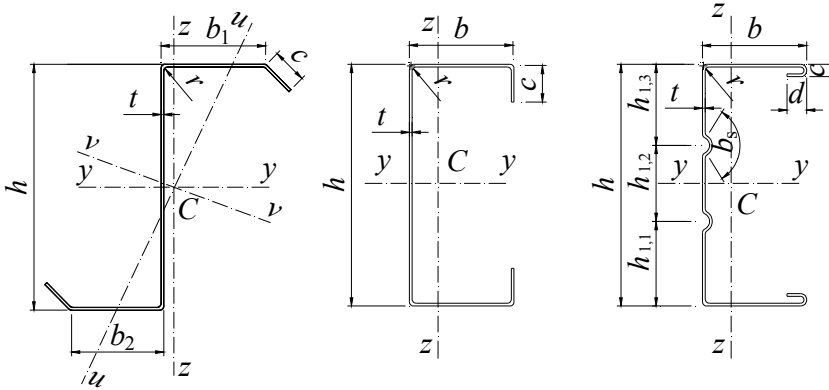


Figure 3.4 – Nominal dimensions of gross cross section

Due to the manufacturing process, cold-formed steel sections have rounded corners. The notional flat widths of plane elements shall be measured from the midpoints of the adjacent corner elements as indicated in Figure 3.5 (CEN, 2006a).

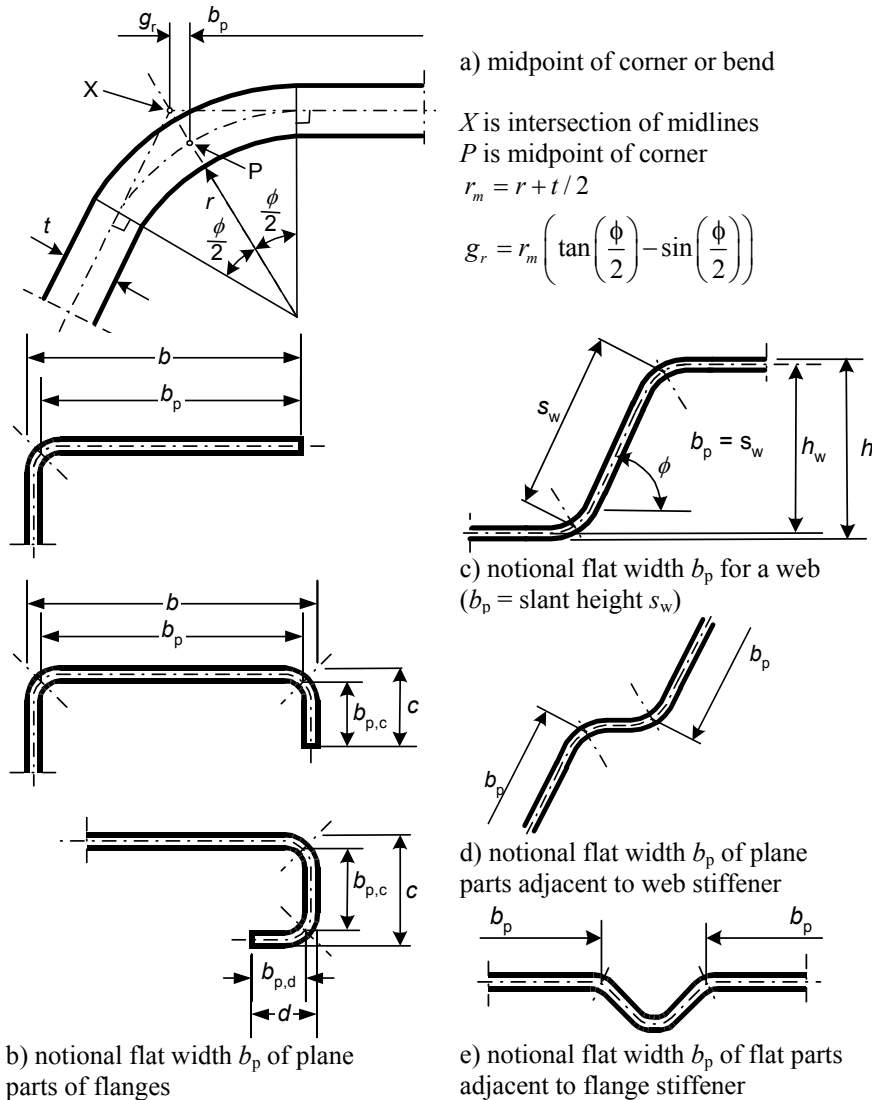


Figure 3.5 – Notional widths of plane cross section parts b_p allowing for corner radii

Since many cold-formed steel sections have thin walls and small radii then in many cases of practical design, the determination of section properties can be simplified by assuming that the material is concentrated at the mid-line of the section and the corners are replaced by the intersections of flat elements. The accuracy of these assumptions may be illustrated by considering the lipped channel section shown in Figure 3.6. Figure 3.7a and 3.7b (Rhodes, 1991) illustrate the effects of using the simplified “mid-line”

3. BEHAVIOUR AND RESISTANCE OF CROSS SECTION

cross section on the geometrical properties of the gross cross section. In these figures, $A_g/A_{g,m-l}$ denotes the ratio of the area calculated considering the round corners versus the “mid-line” one, while $I_g/I_{g,m-l}$ correspondingly refers to second order moment of the area. As can be seen, the errors are small if radius and thickness are small, but they are significant and lead to an overestimation of the geometric properties if both thickness and radii are large.

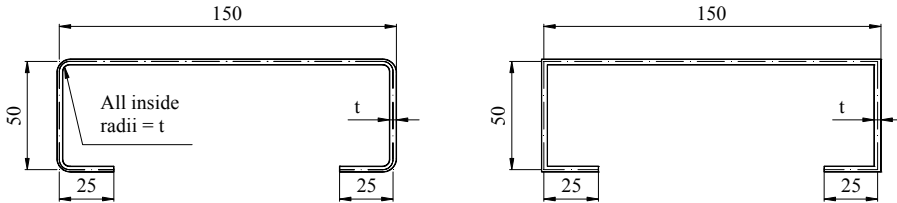


Figure 3.6 – Lipped channel section

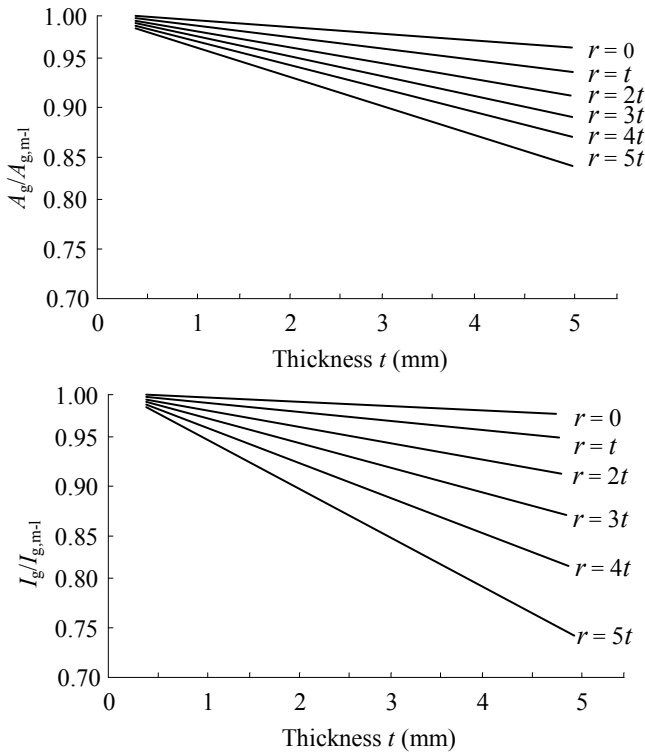


Figure 3.7 – Effect of inside radius on calculated geometrical properties of lipped channel section

Generally, in order to avoid the overestimation of area and second moment of area the influence of rounded corners on section properties shall be taken into account. This may be done (CEN, 2006a) with sufficient accuracy by reducing the properties calculated for the same cross section with sharp corners (see Figure 3.8) using following approximations:

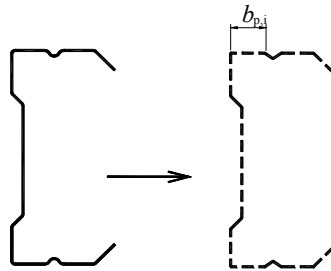
$$A_g \approx A_{g,sh} \cdot (1 - \delta) \tag{3.1a}$$

$$I_g \approx I_{g,sh} \cdot (1 - 2\delta) \tag{3.1b}$$

$$I_w \approx I_{w,sh} \cdot (1 - 4\delta) \tag{3.1c}$$

with:

$$\delta = 0.43 \cdot \frac{\sum_{j=1}^n r_j \frac{\phi_j}{90^\circ}}{\sum_{i=1}^m b_{p,i}} \tag{3.1d}$$



Actual cross section Idealized cross section
 Figure 3.8 – Approximate allowance for rounded corners

where

- A_g is the area of the gross cross section;
- $A_{g,sh}$ is the value of A_g for a cross section with sharp corners;
- $b_{p,i}$ is the notional flat width of plane element i for a cross section with sharp corners;
- I_g is the second moment of area of the gross cross section;
- $I_{g,sh}$ is the value of I_g for a cross section with sharp corners;
- I_w is the warping constant of the gross cross section;
- $I_{w,sh}$ is the value of I_w for a cross section with sharp corners;

3. BEHAVIOUR AND RESISTANCE OF CROSS SECTION

- ϕ is the angle between two plane elements, in degrees;
 m is the number of plane elements;
 n is the number of curved elements;
 r_j is the internal radius of curved element j .

The reductions given by eqn. (3.1) may also be applied in calculating the geometrical properties of the effective cross section, provided that the notional flat widths of the plane walls are measured to the points of intersection of their midlines.

As stated in EN1993–1–3, when the internal radius $r > 0.04t \cdot E / f_y$, then the resistance of the cross section should be determined by tests. However, for practical design purposes, EN1993–1–3 in §§5.1, allows the influence of rounded corners to be ignored if the following conditions are fulfilled:

$$r \leq 5 \cdot t \quad (3.2a)$$

and

$$r \leq 0.10 \cdot b_p \quad (3.2b)$$

3.2.2 Net geometric properties of perforated sections

The net geometrical properties of a cross section, or of an element of a cross section, shall be taken as its gross cross section properties minus the appropriate deduction for all fastener holes and other openings.

In the evaluation of the section properties of members in bending or compression, holes made specifically for fasteners such as screws, bolts, etc., may be neglected when the hole is filled with material and able to transfer load. However, for openings or holes in general, the reduction in cross sectional area and cross sectional properties caused by such holes or openings should be taken into account. This may be accomplished either by testing or by analysis. If the section properties are to be evaluated analytically, they should be calculated considering the net cross section, which has the most detrimental arrangement of holes, which is not necessarily the same cross section for bending analysis and compression analysis. This is illustrated in Figure 3.9, where for the channel section shown the net cross section $A-A$ has a smaller area than the net cross section

$B-B$, and is therefore critical with regard to axial loading. For loading about the $x-x$ axis, the second moment of area and the section modulus of cross section $B-B$ however are less than those of section $A-A$, and so for bending strength section $B-B$ is critical.

In the case of tension members, fasteners do not effectively resist the tension loading, which is tending to open the fastener holes, and holes made for fasteners must also be taken into consideration.

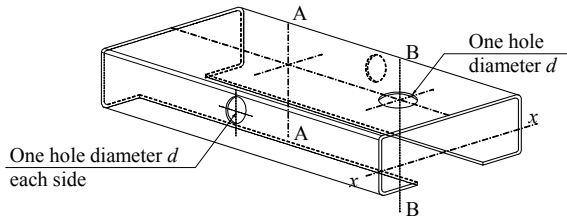


Figure 3.9 – Channel section with holes (Rhodes, 1991)

In determining the net area of tension members, the cross section having the largest area of holes should be considered. The area that should be deducted from the gross cross sectional area is the total cross sectional areas of all holes in the cross section. In determining the area of fastener holes the nominal hole diameter should be used. In the case of countersunk holes, the countersunk area should be deducted.

In case of a member in tension, which has staggered holes, the weakening effects of holes which are not in the same cross section, but close enough to interact with the holes in a given cross section should be taken into account. If two lines of holes are far apart from another line of holes, they have not any effect on the strength of the section at the position of the other line of holes. If the lines are close, then each line of holes affects the other one. In such a case (see Figure 3.10), the area that should be deducted from the gross cross sectional area is the greater of:

- a) the deduction of non-staggered holes, along the section 1-1 in Figure 3.10, i.e.

$$A_{net,1-1} = b_p \cdot t - 2 \cdot d \cdot t \quad (3.3a)$$

- b) the sum of the sectional area of all holes in any diagonal or zigzag line extending progressively across the member or element (i.e. along the

3. BEHAVIOUR AND RESISTANCE OF CROSS SECTION

section 2–2 in Figure 3.10), minus an allowance for each gauge space p in the chain of holes. This allowance shall be taken as $0.25s^2/p$, but not more than $0.6s \cdot t$, where:

- p is the gauge space, i.e. the distance measured perpendicular to the direction of load transfer, between the centres of two consecutive holes in the chain;
- s is the staggered pitch, i.e. the distance, measured parallel to the direction of the load transfer, between the centres of the same two holes;
- t is the thickness of the material.

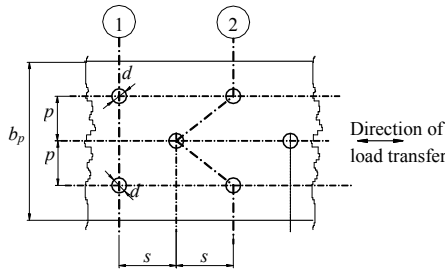


Figure 3.10 – Staggered holes and appropriate net cross section

Therefore, the net area for section 2–2 in Figure 3.10 is calculated as follows:

$$A_{net,2-2} = b_p \cdot t - (2 \cdot d \cdot t - 2 \cdot 0.25 \cdot s^2 \cdot \frac{t}{p}) = b_p \cdot t - 2 \cdot (d - 0.5 \cdot \frac{s^2}{p}) \cdot t \quad (3.3b)$$

In case of cross sections such as angles with holes in more than one plane, the spacing p shall be measured along the centre line of thickness of the material, as shown in Figure 3.11 for the case of staggered holes in the two legs.

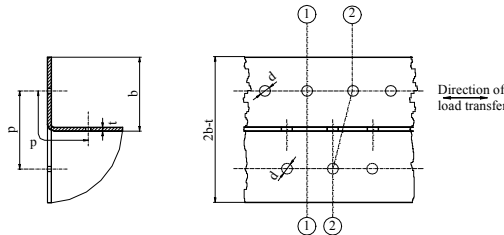


Figure 3.11 – Angles with staggered holes in both legs

In a built-up member (e.g. battened, laced, etc.) where the critical chains of holes in each component part do not correspond with the critical chain of holes for the member as a whole, the resistance of any connecting component joining the parts between such chains of holes shall be taken into account in determining the resistance of the member.

However, no general rules can be given for perforated members (periodic pattern of holes) because the resistance is influenced by the form and pattern of the perforation.

3.2.3 Dimensional limits of component walls of cold-formed steel sections

Cold-formed steel sections are composed by thin walls, which can be unstiffened or stiffened, i.e.:

1. *Unstiffened compression walls.* An unstiffened compression wall is a flat compression element that is stiffened at only one edge parallel to the direction of stress. As shown in Figure 3.12, the leg of an angle section and the compression flange of a channel section or zed section are unstiffened compression elements.

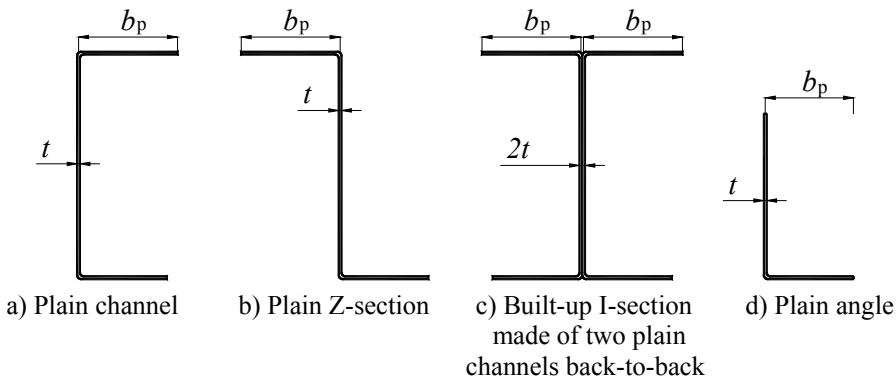


Figure 3.12 – Sections with unstiffened walls

2. *Stiffened or partially stiffened compression walls.* A stiffened or partially stiffened compression wall is a compression element of which both edges parallel to the direction of stress are stiffened either by a web, flange, stiffening lip or intermediate stiffener, see Figure 3.13.

3. BEHAVIOUR AND RESISTANCE OF CROSS SECTION

3. *Multiple-stiffened walls.* A multiple-stiffened wall is a flat element in compression that is stiffened between webs, or between a web and a stiffened edge, by means of intermediate stiffeners which are parallel to the direction of stress (see Figure 3.14). The portion between adjacent stiffeners or between a web and an intermediate stiffener or between an edge and an intermediate stiffener is called a “sub-element”.

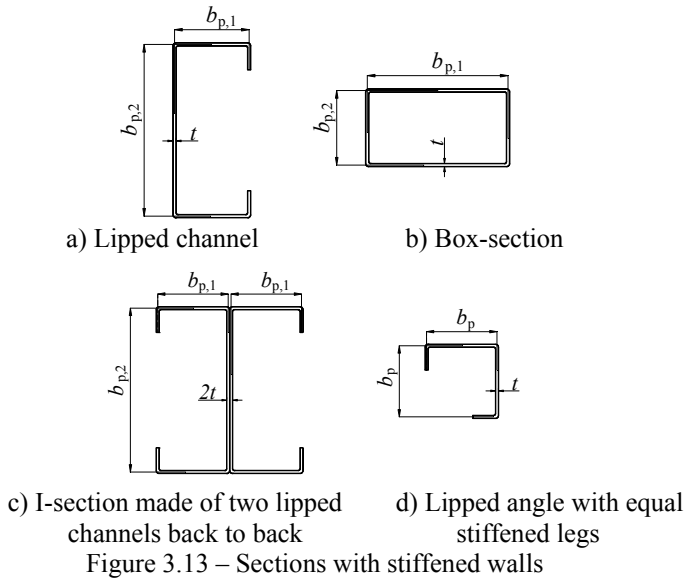


Figure 3.13 – Sections with stiffened walls

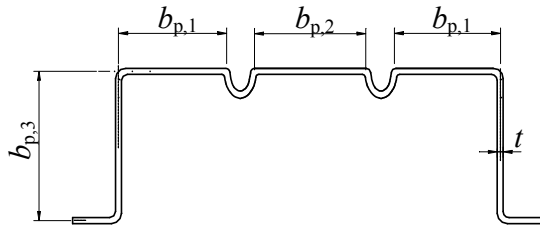


Figure 3.14 – Section with multiple-stiffened wall

The provisions for design by calculations given in this book, which corresponds to those of EN1993-1-3, shall not be applied to cross sections with width-to-thickness ratios (wall slenderness) greater than the maximum values shown in Table 3.1.

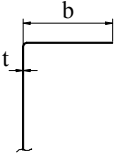
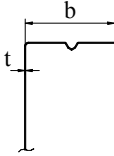
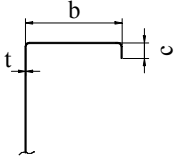
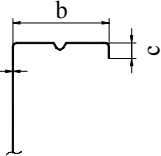
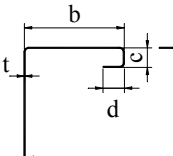
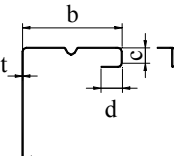
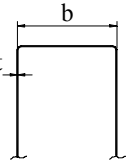
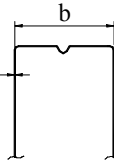
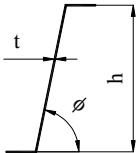
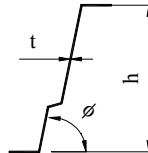
In order to provide sufficient stiffness and to avoid primary buckling of the stiffener itself, the sizes of stiffeners should be in the following ranges:

$$0.2 \leq c/b \leq 0.6 \tag{3.4a}$$

$$0.1 \leq d/b \leq 0.3 \tag{3.4b}$$

in which the dimensions b , c and d are as shown in Table 3.1. If $c/b \leq 0.2$, then $c = 0$, and if $d/b \leq 0.1$, then $d = 0$. To some extent, the limiting slenderness values shown in Table 3.1 are arbitrary. They do, however, reflect a long-time experience and are intended to define practical ranges of application (Winter, 1970).

Table 3.1 – The maximum width-to-thickness ratios

		$b/t \leq 50$
		$b/t \leq 60$ $c/t \leq 50$
		$b/t \leq 90$ $c/t \leq 50$ $d/t \leq 50$
		$b/t \leq 500$
		$45^\circ \leq \phi \leq 90^\circ$ $h/t \leq 500 \sin \phi$

The limiting b/t value of 60 for compression flanges having one longitudinal edge connected to a web and the other edge stiffened by a simple lip is based on the fact that if the b/t ratio of such a flange exceeds 60, a simple lip with relatively large depth would be required to stiffen the flange (Winter, 1970). The local instability of the lip would necessitate a

reduction of the bending capacity to prevent premature buckling of the stiffening lip.

The limiting b/t value of 90 for compression flanges with other than simply lip stiffeners indicates that thinner flanges with large b/t ratios are flexible and liable to be damaged in transport, handling and erection. The same is true for the limiting b/t value of 500 for stiffened compression elements with both longitudinal edges connected to other stiffened elements and for the limiting b/t value of 50 for unstiffened compression elements. In fact, wider flange are not unsafe to use, but when the b/t ratio of stiffened flanges exceeds 250, they are likely to develop noticeable deformation at the full design strength, without affecting the ability of the member to develop the required strength. In both cases the maximum b/t ratio is set at twice that ratio at which first noticeable deformations are likely to appear, based on observations of such members during tests. These upper limits will generally keep such deformations to reasonable limits.

Cross section with larger width-to-thickness ratios than those shown in Table 3.1 may also be used, provided that their resistance in the ultimate limit states and their behaviour in serviceability limit states are verified by relevant testing procedures or appropriate calculations, which must produce evidence that the safety level accepted by the EN1993-1-3 code can be assumed. When effective cross section properties are determined by testing or calculations the limitations of stiffener dimensions, e.g. eqns. (3.4), do not apply.

3.2.4 Modelling of cross section component walls for analysis

The calculation procedures for the effective geometric properties of cross sections, presented in this book, according to EN1993-1-3, have to be applied to component walls of sections as discussed further in §§3.7. The cross section properties are calculated as the sum of the properties of the component element.

The interaction between the component walls of a cold-formed steel-section can be considered by using an appropriate modelling of their junctions and contribution of stiffeners. Consequently, when geometrical properties of cross sections are determined by calculation the models shown in Table 3.2 may be applied. The rigidity of rotational and translational

springs used to simulate the stiffening effect of adjacent walls or stiffeners can be evaluated by testing or by calculation.

Table 3.2 – Modelling of elements of a cross section (CEN, 2006a)

Type of element	Model	Type of element	Model

3.3 FLANGE CURLING

In beams that have unusually wide and thin but stable flanges, i.e. primarily tension flanges with large b/t ratios, there is a tendency for these flanges to curl under bending. That is, the portion of these flanges most remote from the web (edges of I beams, centre portions of flanges of box or hat beams) tend to deflect toward the neutral axis, as illustrated in Figure 3.15.

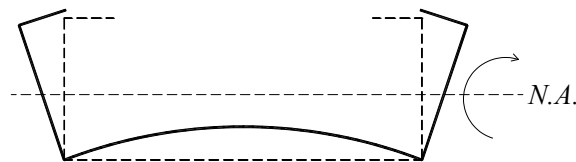


Figure 3.15 – Flange curling of channel section beam

The curling is due to the effect of longitudinal curvature of the beam and bending stress in flanges. The first study of this phenomenon was

3. BEHAVIOUR AND RESISTANCE OF CROSS SECTION

presented by George Winter (1940). The phenomenon can be easily explained with reference to the behaviour of a wide flange I-beam in pure bending (see Figure 3.16). The transverse component p of the flange force ($\sigma_a \cdot t$) per unit width can be determined by:

$$p = \frac{\sigma_a \cdot t \cdot d\phi}{dl} = \frac{\sigma_a \cdot t}{\rho} = \frac{\sigma_a \cdot t}{E \cdot I / M} \quad (3.5)$$

where

- σ_a is the average (mean) bending stress in flange;
- E is the modulus of elasticity;
- I is the second moment of the beam area;
- $b_f, h, t, dl, d\phi$ and ρ as shown in Figure 3.16.

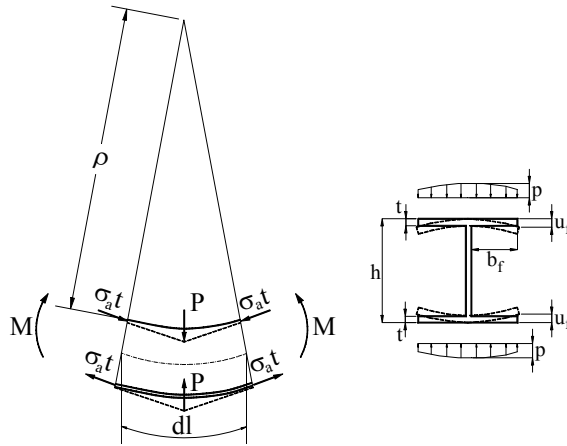


Figure 3.16 – Flange curling of I-beam subjected to bending

If the value of the transverse component p is considered to be a uniformly distributed load applied on the flange, the deflection of curling at the outer edge of the flange, u , can be computed considering flange as a cantilever plate (Yu, 2000):

$$u_f = \frac{p \cdot b_f^4}{8 \cdot D} = 3 \cdot \left(\frac{\sigma_a}{E} \right)^2 \cdot \left(\frac{b_f^4}{t^2 \cdot d} \right) \cdot (1 - \nu^2) \quad (3.6)$$

where

- u_f is flange deflection of outer edge;

D is flexural rigidity of plate, $D = E \cdot t^2 / 12 \cdot (1 - \nu^2)$;
 ν is Poisson's ratio.

The ECCS Recommendations (ECCS, 1987; the predecessor of EN1993-1-3) provide the following formula for calculating the curling displacement, applicable to both compression and tensile flanges, both with and without stiffeners:

$$u_f = 2 \cdot \frac{\sigma_a^2 \cdot b_f^4}{E^2 \cdot t^2 \cdot z} \quad (3.7)$$

In eqn. (3.7), b_f is one half of the distance between webs in box and hat sections, or the width of the portion flange projecting from the web (see Figure 3.17), z is the distance of flange under consideration from neutral axis (N.A.), while the other notations are defined as in eqn. (3.6).

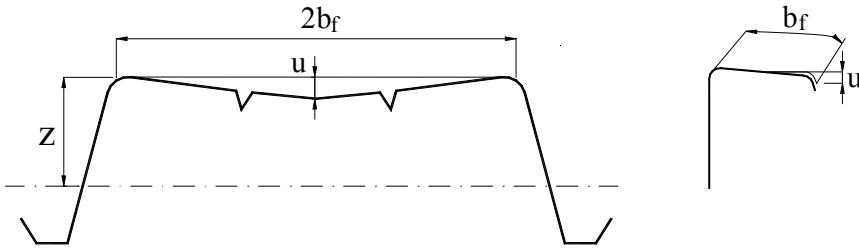


Figure 3.17 – Geometrical parameters of flange curling

When the actual stress in the flange has been calculated for the effective cross-section, the mean value of the stress, σ_a , is obtained by multiplying the stress for the effective cross-section by the ratio of the effective flange area to the gross flange area.

In order to limit the curling effect both AISI S100-07 and ASNZ-4600:2005 provide an upper bound formula for the half width flange, b_f , i.e.

$$b_f \leq \sqrt{\frac{0.06t \cdot d \cdot E}{\sigma_a}} \cdot \sqrt[4]{\frac{100 \cdot u_f}{d}} \quad (3.8)$$

where d is the depth of the cross section, the other notations being as above.

Flange curling is in general highly dependent on the flange width-to-thickness ratio, but also varies significantly with web depth and, indeed, the

general geometry of the section. Beams with shallow webs and small tension elements are particularly prone to flange curling.

Flange curling can be neglected in calculations if the deflection u_s is not greater than 5% of the depth of cross section. Equation (3.8) assures the curling is less than $0.05d$.

Accounting for flange curling, when $u_s > 0.05d$, implies a rather involved analysis. The major effect of flange curling is to displace the flange centre towards the neutral axis, thus reducing the stress on the flange towards the centre. This can, if required be taken into account by an iterative approach in which the stress at different positions is recalculated depending on the curling deflections at that point. In the case of compression elements the curling effects only produce large deflections for wide thin flanges, which are ineffective near the centre in any case so that the degree of curling does not make appreciable difference to the beam capacity. For tension flanges, the difference can be more substantial.

One type of compression flange for which flange curling can have a very significant effect is the intermediately stiffened element, in which the regions near the stiffener and the stiffener itself are highly effective in resisting load. Such elements usually have high width-to-thickness ratios.

However, the maximum width-to-thickness ratios given in Table 3.1 significantly reduce the curling effect.

In some ways, flange curling can be regarded as a kind of initial imperfection.

3.4 SHEAR LAG

For the beams of usual shapes, the normal stresses are induced in the flanges through shear stresses transferred from the web to the flange. These shear stresses produce shear strains in the flange which, for ordinary dimensions, have negligible effects. However, if the flanges are unusually wide (relative to their length) these shear strains have the effect of decreasing the normal bending stresses in the flange with increasing distance from the web. This phenomenon is known as shear lag (see Figure 3.18).

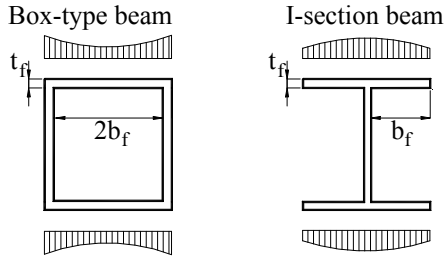


Figure 3.18 – Normal bending stress distribution in both compression and tension flanges of short beams due to shear lag

The simplest way of accounting for this stress variation in design is to replace the non-uniformly stressed flange, of actual width b , ($b \approx 2 \cdot b_f$), by a reduced (effective) width subjected to uniform stress (Winter, 1970).

Shear lag is important for beams with large flanges subjected to concentrated loads on fairly short spans; the smaller the span-to-width ratio, the larger the effect. For beams supporting uniform loads, shear lag is usually negligible except when the L/b_f ratio is less than about 10, as shown in Figure 3.19 (Winter, 1940).

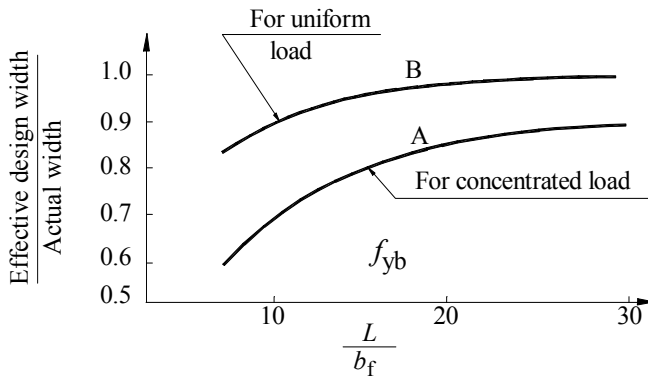


Figure 3.19 – Analytical curves for determining effective width of flange of short span beams (Winter, 1940)

Where the span of the beam, L , is less than $30b_f$ and the beam supports a concentrated load, or several loads spaced greater than $2b_f$, the effective design width of a flange, whether in tension or compression, shall be limited to the values given in Table 3.3. These values were obtained by Winter in early 1940s (Winter, 1940), and actually are included in American (AISI S100-07) and Australian/New Zealand design codes (AS/NZS-4600:2005).

3. BEHAVIOUR AND RESISTANCE OF CROSS SECTION

Table 3.3 – Maximum ratio of effective design width to actual width for short wide flange beams

L/b_1	Ratio	L/b_1	Ratio
30	1.00	14	0.82
25	0.96	12	0.78
20	0.91	10	0.73
18	0.89	8	0.67
16	0.86	6	0.55

where, L is the full span for simple beams; or distance between inflection points for continuous beams; or twice the length of cantilever beam.

The values of effective width ratios given in Table 3.3 are those corresponding to Curve A of Figure 3.19. For uniform load, it can be seen from Curve B of Figure 3.19 that the width reduction due to shear lag for any practicable width-span ratio is so small as to be effectively negligible.

According to EN1993-1-5, the effect of shear lag shall be taken into account in flanges of flexural members if the length L_e between the points of zero bending moment is less than $50b_f$.

The phenomenon of shear lag is of considerable consequence in naval architecture and aircraft design. However, in cold-formed steel construction, beams are infrequently so wide that significant reductions are required.

3.5 LOCAL BUCKLING

116

3.5.1 Sectional buckling modes in thin-walled sections

Sectional instability modes refer to local and distortional buckling. These modes are called “sectional” (Ungureanu & Dubina, 1999) because they affect the shape and resistance of member cross sections. Local buckling of a plane element (e.g. a wall of a cold-formed steel section) when both edges remain straight in the longitudinal direction, as shown in Figures 3.20a and 3.21a, is characterised by half-wavelengths comparable with the element width.

Distortional buckling of sections involves rotation of the lip/flange components about the flange/web junction as shown in Figure 3.20 (b and c). Distortional buckling is also known as “stiffener buckling” or “local-torsional buckling”. In this case, the web and lip/flange distortional buckling occur at the same half-wavelength which is larger than the local buckling

half-wavelength. In members with intermediately stiffened elements distortional buckling is characterized by a displacement of the intermediate stiffer normal to the plane of the element (see Figure 3.21b).

Web buckling involves single curvature transverse bending of the web (Schafer & Peköz, 1999). Distortional buckling can occur due to insufficient edge stiffeners.

Local buckling is a phenomenon which characterises the behaviour of thin plates, and is solved accordingly. Distortional buckling is treated either as a problem of elastic critical buckling of a long sheet (e.g. the flange/lip assembly) on an elastic foundation (see CEN, 2006a) or as a problem of lateral-torsional buckling of a flange/lip section column (Schafer & Peköz, 1999).

Both local and distortional buckling may interact with overall buckling modes (e.g. flexural or flexural-torsional modes). These type of interaction are classified as “strong” or “moderate” and, due to imperfections, they are characterised by a significant erosion of the theoretical critical bifurcation load, which can reach 50% to 30% (Dubina, 1996).

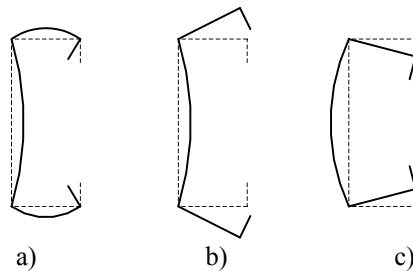


Figure 3.20 – Local and distortional buckling of a lipped channel section in compression: a)-Local buckling mode; b) and c) distortional buckling modes

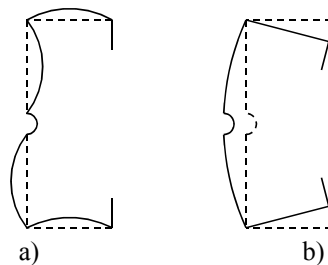


Figure 3.21 – Local and distortional buckling of a lipped channel with web intermediate stiffener: a) local buckling mode; b) distortional buckling mode

Local buckling can occur either simultaneously with distortional buckling, or at higher or lower loads. The two modes can interact too but the post-critical coupled mode is stable and, consequently, the local and distortional buckling strengths can be assessed independently of whether they occur simultaneously. Therefore, in design codes and also in this book, these two problems are treated separately.

3.5.2 Elastic buckling of thin plates

Considering a simply supported square plate subjected to uniform compression stress in one direction, it will buckle in a single curvature in both directions, as shown in Figure 3.22.

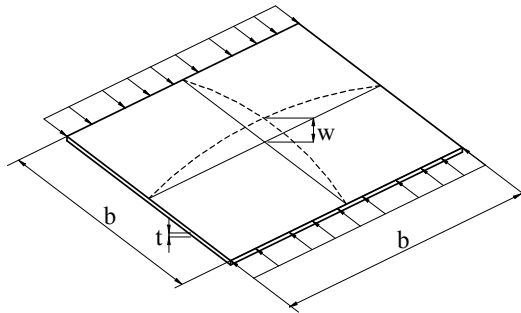


Figure 3.22 – Square simply supported thin plate in compression

However, in the case of an individual compression wall of a cold-formed thin-walled section the length of the element is much larger than the width (see Figure 3.23). This type of buckling is called “local” because the length of buckles is comparable to the dimensions of the cross section.

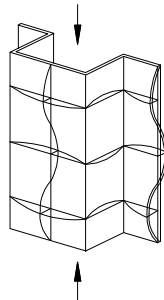


Figure 3.23 – Local buckling of component walls of a cold-formed thin-walled section

Local buckling does not normally result in failure of the section as does Euler flexural buckling of a column (see and compare Figures 3.1 (a) and (c)).

A plate subjected to uniform compressive strain between rigid frictionless platens will deform after buckling as shown in Figure 3.24a and will redistribute the longitudinal membrane stress from uniform compression to those shown in Figure 3.24b.

This will occur irrespective of whether the plate is a stiffened or an unstiffened element. The plate element will continue to carry load although with stiffness reduced to 40.8% of the initial linear elastic value for a square stiffened element, and to 44.4% for a square unstiffened element (Bulson, 1970). However, the line of action of the compressive force in an unstiffened element will move towards the stiffened edge in the post-buckling range.

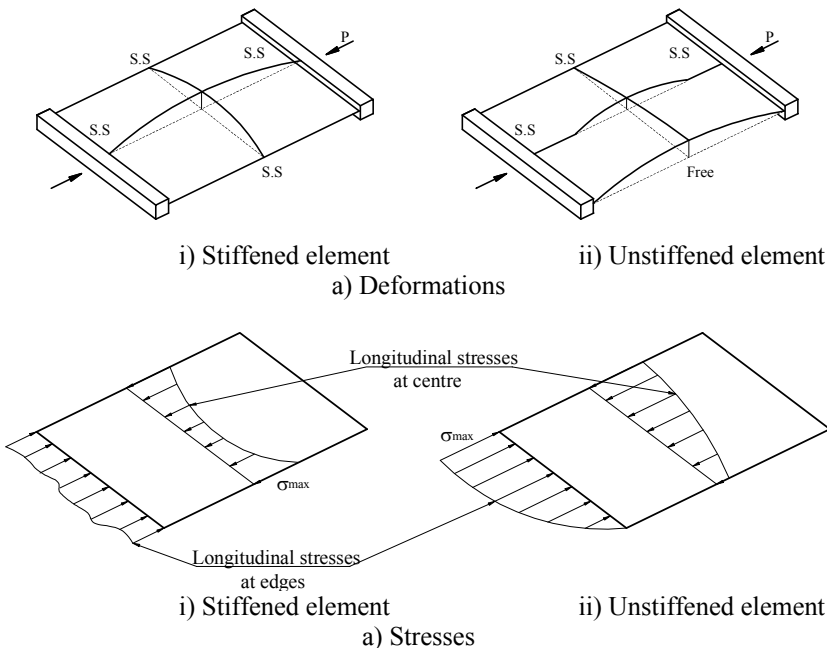


Figure 3.24 – Post-buckling behaviour of stiffened and unstiffened plate element (Hancock, 1998)

The mechanism of the post-buckling action can be easily visualized using a “Strut and Tie” grid model for the simply supported square plate in compression as shown in Figure 3.24 (Winter, 1970). It represents a square portion of the compression flange of the hat section in Figure 3.23,

3. BEHAVIOUR AND RESISTANCE OF CROSS SECTION

corresponding to a half-wave and is equivalent to the square plate shown in Figure 3.22.

If the compression struts are simple columns, unsupported except at the ends, they would buckle and collapse simultaneously and independently of each other under equal end loads. However, collapse of the struts in the grid model is prevented by the ties anchored at the sides of the grid which provide a “membrane” type action. Consequently the model shown in Figure 3.25 (and the plate that it represents) will not collapse when its theoretical buckling stress, σ_{cr} , is reached. This is in contrast to independent columns, which develop large deflections and fail once buckling starts. The ability to support loads beyond the buckling load is known as post-buckling strength. Essentially, in the grid model, the centre struts (or strips) deflect the most and tend to transfer part of their loads to their less deflected neighbours, while the struts (or strip) near the edge continue to resist increasing load with hardly any additional deflection.

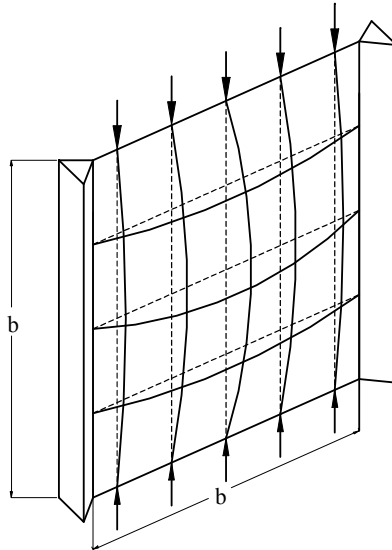


Figure 3.25 – “Strut and Tie” grid model of a plate simply supported along its edges and subjected to end loading

This explains the shape of stress diagrams shown in Figure 3.24b. In fact, in the pre-buckling phase stresses are uniformly distributed (see Figure 3.26a), while after buckling they become non-uniform (see Figure 3.26b) and continuously concentrate near the supported edges as the load increases,

until the yield strength is reached (see Figure 3.26c) and the plate starts to fail.

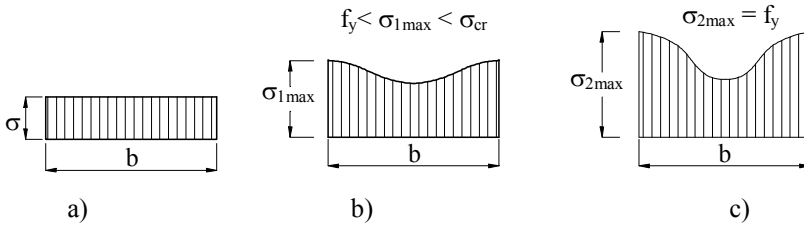


Figure 3.26 – Consecutive stress distribution in stiffened compression elements: a) pre-critical stage; b) intermediate post-critical stage; c) ultimate post-critical stage

The behaviour of an ideal (e.g. perfect) and an actual (imperfect) plate is shown in Figure 3.27.

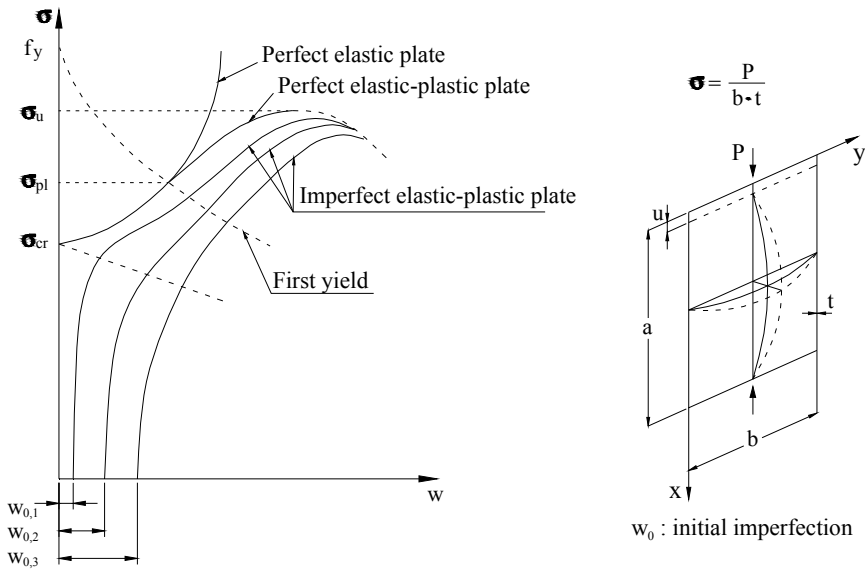
Considering the stress-deflection curve for the ideal plate, it can be observed that in the pre-critical range $\sigma < \sigma_{cr}$, the plate behaviour is linear, characterised by a plane stress state, whereas when the critical stress point is reached, $\sigma = \sigma_{cr}$, the plate suddenly loses rigidity (see Figure 3.27b) and significant increase of deflection occurs (see Figure 3.27a). The post-critical path depends on the edge support conditions, applied stress distribution (e.g. uniform or non-uniform compression) and material characteristics. The behaviour may continue to remain elastic ($\sigma_{cr} < \sigma < f_y$) and due to “membrane lag” effect (simulated by the tie effect in Figure 3.25) a stabilizing action occurs due to which post-critical stress reserve is available. The behaviour of the plate in this range is described by non-linear equations of stress equilibrium and strain compatibility, well known as Von Karman-Marguerre equations (von Karman, 1910; Marguerre, 1938). The “membrane lag” is the explanation for the non-linear elastic behaviour within this range.

When first yield is reached at the point $\sigma = \sigma_{pl}$, the stress-displacement curve changes curvature, and the plate starts its elastoplastic behaviour. In the domain $\sigma \leq \sigma_{pl}$, the unloading path is fully reversible. For this reason, the point $\sigma = \sigma_{pl}$ is also called the “reversibility” point (Bourrier & Brozzetti, 1996). The behaviour at this point corresponds to the stress distribution (c) in Figure 3.26.

In the range $\sigma > \sigma_{pl}$ the plate rapidly loses stiffness and soon reaches the ultimate strength, f_u . To account for the reduced stiffness of the plate in the post-critical range, the plate behaviour within this range is not governed

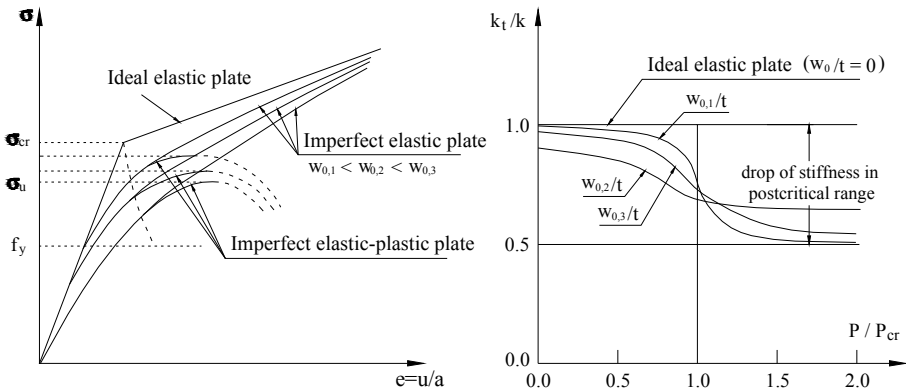
3. BEHAVIOUR AND RESISTANCE OF CROSS SECTION

by the elastic modulus, E , but by the “tangent modulus”, E_t , or by the “secant modulus” E_s (Bleich, 1952; Stowell, 1948; Gerard, 1946). In fact, due to the small plate thickness, the post-elastic strength reserve of cold-formed steel plates is usually not significant and may not be considered in practice. Therefore, for practical design purposes, the ultimate strength reference point was taken as $\sigma = \sigma_{pl}$. Consequently one speaks about the “post-critical” strength of thin steel plates, but does not speak about their post-elastic strength.



122

a) Stress vs. deflection



b) Stress vs. axial strain

c) Axial stress vs. stiffness

Figure 3.27 – Behaviour of ideal and actual simply supported plate in uniaxial stress

When both geometrical and material imperfections are present (e.g. initial deflections and residual stresses for instance), which is the case for actual plates, the behaviour is characterised by a smooth deformation process, as seen in Figure 3.27: the greater the initial deflection w_0 (to be regarded here as an equivalent imperfection), the smoother is the $\sigma - w$ curve. In fact, in practice it is really difficult to catch the points σ_{cr} and σ_{pl} , and often during tests σ_u is taken as σ_{cr} and vice versa. Therefore for the imperfect thin plate, the $\sigma_{cr} - \sigma_u$ range is really small.

The elastic post-buckling behaviour of the plate can be analysed by using large deflection theory. For this purpose, the following differential equation was introduced by von Karman in 1910:

$$\begin{aligned} \frac{\partial^4 \omega}{\partial x^4} + 2 \cdot \frac{\partial^4 \omega}{\partial x^2 \partial y^2} + \frac{\partial^4 \omega}{\partial y^4} = \\ = \frac{t}{D} \cdot \left(\frac{\partial^2 F}{\partial y^2} \cdot \frac{\partial^2 \omega}{\partial x^2} - 2 \cdot \frac{\partial^2 F}{\partial x \partial y} \cdot \frac{\partial^2 \omega}{\partial x \partial y} + \frac{\partial^2 F}{\partial x^2} \cdot \frac{\partial^2 \omega}{\partial y^2} \right) \end{aligned} \quad (3.9)$$

where F is the Airy stress function defining the median fibre stress of the plate,

$$\sigma_x = \frac{\partial^2 F}{\partial y^2} \quad (3.10a)$$

$$\sigma_y = \frac{\partial^2 F}{\partial x^2} \quad (3.10b)$$

$$\tau_{xy} = \frac{\partial^2 F}{\partial x \partial y} \quad (3.10c)$$

It has been found that the solution of the differential equation for large deflections has little application in practical design because of its complexity. For this reason, the concept of “*effective width*” was introduced by von Karman *et al* in 1932. In this approach, instead of considering the non-uniform distribution of stress, $\sigma_x(y)$, over the entire width of the plate b , it was assumed that the total load, P , is carried by a fictitious effective width, b_{eff} , subjected to a uniformly distributed stress equal to the edge stress, σ_{max} , as shown in Figure 3.28. The width b_{eff} is selected so that the area under the

3. BEHAVIOUR AND RESISTANCE OF CROSS SECTION

curve of the actual non-uniform stress distribution is equal to the sum of the two parts of the equivalent rectangular shaded area with a total width b_{eff} and an intensity of stress equal to the edge stress σ_{max} , that is,

$$P = \sigma_{med} \cdot b \cdot t = \int_0^b \sigma_x(y) \cdot t \cdot dy = \sigma_{max} \cdot b_{eff} \cdot t \tag{3.11}$$

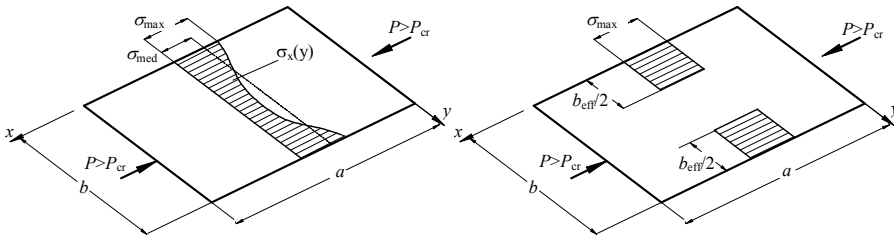


Figure 3.28 – Stress distribution in simply supported plate, uniaxially compressed: a) actual stress distribution; b) equivalent stress distribution based on the “effective width” approach

The magnitude of effective width, b_{eff} , changes as the magnitude of σ_{max} , changes (see Figure 3.29). Therefore the minimum effective width results when σ_{max} equals to f_y (see Figure 3.26c).

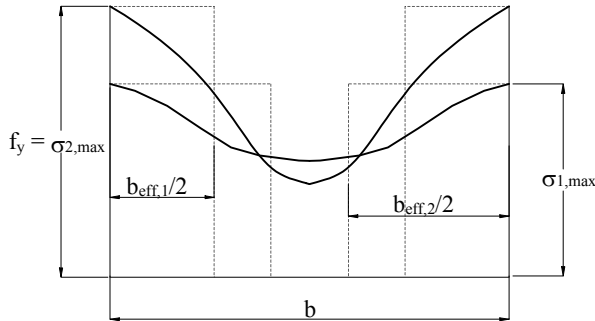


Figure 3.29 – Change of effective width in terms of maximum edge stress

In the limit $\sigma_{max} = f_y$, it may also be considered that the effective width b_{eff} represents a particular width of the plate for which the plate strength is achieved when the applied stress ($\sigma_{max} = f_y$) causes buckling. Therefore for a long plate, the value of b_{eff} to be used for strength design may be determined from eqn. (3.13) as follows:

$$\sigma_{max} = f_y = \frac{k_\sigma \cdot \pi^2 \cdot E}{12 \cdot (1 - \nu^2) \cdot (b_{eff}/t)^2} = \sigma_{cr,eff} \quad (3.12)$$

or

$$b_{eff} = \frac{\sqrt{k_\sigma} \cdot \pi}{\sqrt{12 \cdot (1 - \nu^2)}} \cdot t \cdot \sqrt{\frac{E}{f_y}} \quad (3.13)$$

or

$$b_{eff} = C \cdot t \cdot \sqrt{\frac{E}{f_y}} \quad (3.14)$$

where

$$C = \sqrt{k_\sigma \cdot \pi^2 / 12 \cdot (1 - \nu^2)} \quad (3.15)$$

is a constant for a given type of plate element, depending of the value of buckling coefficient, k_σ .

If $k_\sigma = 4$ and $\nu = 0.3$, $C = 1.9$, and eqn. (3.14) becomes:

$$b_{eff} = 1.9 \cdot t \cdot \sqrt{\frac{E}{f_y}} \quad (3.16)$$

which represents the von Karman formula for the design of stiffened elements as derived in 1932.

125

Since the critical elastic buckling stress of the complete plate is given by,

$$\sigma_{cr} = \frac{k_\sigma \cdot \pi^2 \cdot E}{12 \cdot (1 - \nu^2) \cdot (b/t)^2} \quad (3.17)$$

then by substitution

$$\frac{b_{eff}}{b} = \sqrt{\frac{\sigma_{cr}}{f_y}} \quad (3.18)$$

The relative or reduced plate slenderness, $\bar{\lambda}_p$, is defined as:

$$\bar{\lambda}_p = \sqrt{\frac{f_y}{\sigma_{cr}}} = \frac{1.052}{\sqrt{k}} \cdot \frac{b}{t} \cdot \sqrt{\frac{f_y}{E}} = \frac{b/t}{28,4 \cdot \varepsilon \cdot \sqrt{k}} \quad (3.19)$$

3. BEHAVIOUR AND RESISTANCE OF CROSS SECTION

where: $\varepsilon = \sqrt{235/f_y}$.

At the end, the effective width, b_{eff} , of a thin wall (e.g. plate) in compression, of width b , is calculated with the following formula:

$$b_{eff} = \rho \cdot b \quad (3.20)$$

where

$$\rho = \frac{b_{eff}}{b} = \frac{1}{\lambda_p} \leq 1 \quad (3.21)$$

and is the reduction factor of the plate within the post-buckling range.

Equation (3.20) is in fact another form of the initial von Karman formula given by eqn. (3.13). Equation (3.18) gives the effective width in the ultimate limit state (see Figure 3.26c). In the intermediate post-buckling stage, when $\sigma_{cr} < \sigma_{max} < f_y$, (see Figure 3.26b) the effective width can be obtained from:

$$b_{eff} = C \cdot t \cdot \sqrt{\frac{E}{\sigma_{max}}} \quad (3.22)$$

or

$$\frac{b_{eff}}{b} = \sqrt{\frac{\sigma_{cr}}{\sigma_{max}}} \quad (3.23)$$

with the corresponding relative slenderness of the plate defined as,

$$\bar{\lambda}_p = \sqrt{\frac{\sigma_{max}}{\sigma_{cr}}} \quad (3.24)$$

Equation (3.15) for C , which for plates simply supported on both longitudinal edges (i.e. $k_\sigma=4$) leads to the value of 1.9, was confirmed by test of plates with large b/t ratios. Consequently, for plates with intermediate b/t ratios, in 1946 Winter proposed to replace the expression for C with:

$$C = 1.9 \cdot \left[1 - 0.415 \cdot \left(\frac{t}{b} \right) \cdot \sqrt{\frac{E}{f_y}} \right] \quad (3.25)$$

which leads to the well-known effective width equation

$$\rho = \frac{b_{eff}}{b} = \sqrt{\frac{\sigma_{cr}}{f_y}} \cdot \left(1 - 0.22 \cdot \sqrt{\frac{\sigma_{cr}}{f_y}} \right) \leq 1 \quad (3.26)$$

or, in terms of relative plate slenderness, $\bar{\lambda}_p$,

$$\rho = \frac{b_{eff}}{b} = \frac{1}{\bar{\lambda}_p} \cdot \left(1 - \frac{0.22}{\bar{\lambda}_p} \right) \quad (3.27)$$

The effective width depends on both edge stress σ_{max} and b/t ratio. The plate is fully effective when $\rho = 1$, i.e. $b = b_{eff}$. It is easy to show that this happens when $\bar{\lambda}_p \leq 0.673$ (see Figure 3.30) or

$$\frac{b}{t} < \left(\frac{b}{t} \right)_{lim} = 16.69 \cdot \varepsilon \cdot \sqrt{k_\sigma} \quad (3.28)$$

with

$$\varepsilon = \sqrt{235 / f_y} \quad (3.29)$$

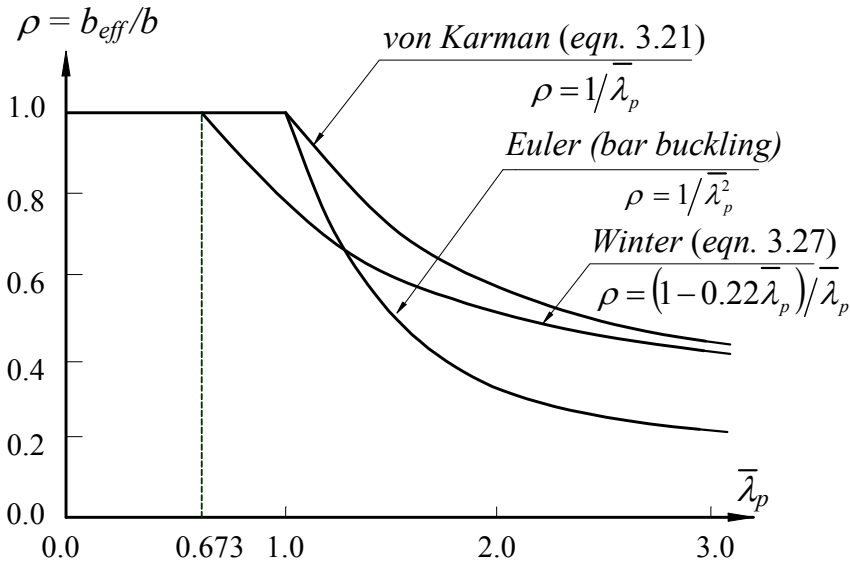


Figure 3.30 – Reduction factor, ρ , vs. relative plate slenderness, $\bar{\lambda}_p$, relationship

3. BEHAVIOUR AND RESISTANCE OF CROSS SECTION

If $k_\sigma=4$ and $k_\sigma=0.425$ are substituted into eqn. (3.28) for simply supported edge stiffened or web type plate elements, and for unstiffened plate elements with a free longitudinal edge, or flange type elements, respectively, the following limiting b/t ratios are obtained:

- web type elements

$$\left(\frac{b}{t}\right)_{\text{lim}} = 38.3 \cdot \varepsilon \quad (3.30)$$

- flange type elements

$$\left(\frac{b}{t}\right)_{\text{lim}} = 12.5 \cdot \varepsilon \quad (3.31)$$

The limiting b/t ratios for the usual steel grades S235, S275 and S355 are shown in Table 3.4.

Table 3.4 – $(b/t)_{\text{lim}}$ values for stiffened and unstiffened plate elements

Steel grade	f_y (N/mm ²)	Type of plate element	
		Stiffened	Unstiffened
S235	235	38	12.5
S275	275	35	11.5
S355	355	31	10

The effective or equivalent width method leads to simple design rules and gives an indication of the behaviour of the plate as the ultimate condition is approached. However, it is difficult to prove the validity of this approach, especially due to approximate nature of the initial assumptions made by von Karman in regard with the two “edge strips” which defined the effective part of the plate. Therefore, Winter semi-empirically adapted the von Karman formula and replaced eqn. (3.21) in order to fit better with test results.

The Winter formula (3.27) for the effective width is used in the major design code provisions for thin-walled steel structures (CEN, 2006a; AISI S100-07; AS/NZS 4600:2005). Despite its semi-empirical nature, the Winter formula leads to quite satisfactory results for stiffened (web type) plate elements. However, for unstiffened (flange type) plate elements, this formula used with a buckling coefficient equal to 0.425 or 0.43 is too conservative both for strength and stiffness. Alternative proposals were made by several authors (von Karman *et al*, 1932; Fischer & Zhu, 1996).

3.6 DISTORTIONAL BUCKLING: ANALYTICAL METHODS FOR PREDICTING ELASTIC DISTORTIONAL BUCKLING STRESSES

Intuition for local buckling behaviour is relatively straightforward: as width-to-thickness (b/t) ratios increase, the local buckling critical stress becomes lower. This fact serves the engineer well in designing for local buckling. A similar intuition for distortional buckling is not as straightforward.

Distortional buckling of compression members with C cross sections is governed by the rotational stiffness at the web/flange junction; deeper webs are more flexible and thus provide less rotational stiffness to the web/flange juncture. This results in earlier distortional buckling for deep webs. If the flange is narrow, local buckling of the web occurs at wavelengths close to distortional buckling of the flange and the distortional mode forms at lower stresses than local buckling. If the flange is excessively wide, local buckling is not the concern, but rather the size of the stiffener require to keep the flange in place is the concern. For practical stiffener lengths, wide flange also lead to low distortional stresses. Longer lips are beneficial against flange distortion but become too sensitive for local buckling.

The wavelength of distortional buckling is generally intermediate between those of local and overall modes, like Figure 3.31 shows.

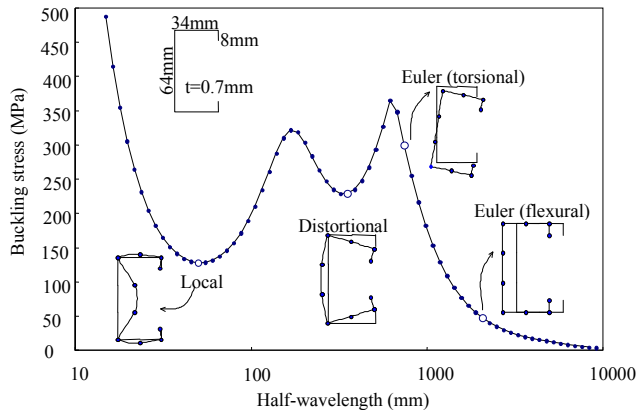


Figure 3.31 – Elastic buckling modes vs. half-wavelengths curve for a lipped channel column (Finite Strip Analysis by Schafer, 2001)

Manual calculation methods for predicting the elastic distortional buckling stress of simple sections such as C- and rack-sections have been presented, e.g. by Law & Hancock (1897) and Schafer & Peköz (1999). However, manual calculation methods for distortional buckling are relatively cumbersome. Numerical methods, such as the finite element method (FEM), or the finite strip method (FSM) have been found to be efficient methods for determining elastic buckling stresses for both local and distortional buckling. The finite strip method has proved to be a useful approach because it has a short solution time compared to the finite element method and does not require discretisation in the longitudinal direction. The finite strip method assumes simply supported end boundary conditions and is applicable to longer sections where multiple half-waves occur along the section length.

Generalized Beam Theory (GBT) is an extension of conventional engineering beam theory, allowing cross section distortion to be considered (Silvestre & Camotim, 2002a, b, 2003). It has a short solution time and the method is applicable for both pin-ended and fixed-ended members. A user friendly GBT program has been developed at the Technical University of Lisbon called GBTUL (<http://www.civil.ist.utl.pt/gbt/>), which performs elastic buckling and vibration analyses of prismatic thin-walled members.

An alternative program to perform the elastic buckling analysis of thin-walled members is CUFSM (<http://www.ce.jhu.edu/bschafer/cufsm/>). CUFSM employs the semi-analytical finite strip method to provide solutions for the cross section stability of thin-walled members (Schafer & Ádány, 2006).

3.6.1 The method given in EN1993-1-3:2006

EN1993-1-3 does not provide explicit provisions for distortional buckling. However, a calculation procedure can be obtained from the interpretation of the rules given in the code for plane elements with edge or intermediate stiffeners in compression.

The design of compression elements with either edge or intermediate stiffeners is based on the assumption that the stiffener behaves as a compression member with continuous partial restraint. This restraint has a spring stiffness that depends on the boundary conditions and the flexural stiffness of the adjacent plane elements of the cross section. The spring

stiffness of the stiffener may be determined by applying a unit load per unit length to the cross section at the location of the stiffener, as illustrated in Figure 3.32. The rotational spring stiffness C_θ characterizes the bending stiffness of the web part of the section. The spring stiffness K per unit length may be determined from:

$$K = u / \delta \tag{3.32}$$

where δ is the deflection of the stiffener due to the unit load u .

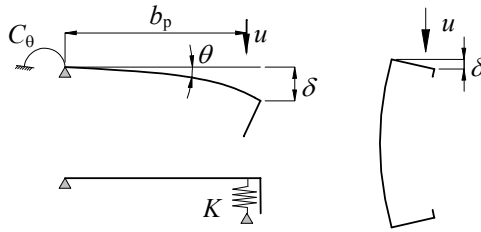


Figure 3.32 – Determination of the spring stiffness K according to EN1993-1-3

The elastic critical buckling stress for a long strut on an elastic foundation, in which the preferred wavelength is free to develop, is given by Timoshenko & Gere (1961):

$$\sigma_{cr} = \frac{\pi^2 \cdot E \cdot I_s}{A_s \cdot \lambda^2} + \frac{I}{A_s \cdot \pi^2} K \cdot \lambda^2 \tag{3.33}$$

131

where

A_s and I_s are the effective cross sectional area and second moment of area of the stiffener according to EN1993-1-3, as illustrated in Figure 3.33 for an edge stiffener;

$\lambda = L / m$ is the half-wavelength; m is the number of half-wavelengths.

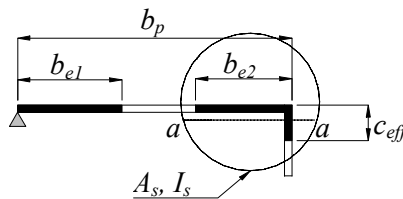


Figure 3.33 – Effective cross sectional area of an edge stiffener

The preferred half-wavelength of buckling for a long strut can be derived from eqn. (3.33) by minimizing the critical stress:

$$\lambda_{cr} = \sqrt[4]{\frac{E \cdot I_s}{K}} \quad (3.34)$$

For an infinitely long strut, the critical buckling stress can be derived, after substitution, as:

$$\sigma_{cr} = \frac{2 \cdot \sqrt{K \cdot E \cdot I_s}}{A_s} \quad (3.35)$$

Equation (3.35) is given in EN1993-1-3; thus, this method does not consider the effect of column length but assumes that it is sufficiently long for integer half-waves to occur. In the case of intermediate stiffeners, the procedure is similar, but the rotational stiffness due to adjacent plane elements is ignored and the stiffened plane element is assumed to be simply supported.

In fact, for elements with edge or intermediate stiffeners, the design against distortional buckling is limited to the checking of stiffener effectiveness (see §§3.7.2 for details). For more complete analysis, the code gives freedom for the designer to use numerical methods.

3.7 DESIGN AGAINST LOCAL AND DISTORTIONAL BUCKLING ACCORDING TO EN1993-1-3

3.7.1 General

According to EN1993-1-3, the followings general provisions must be considered when a section is designed against local or distortional buckling:

- (a) The effects of local and distortional buckling shall be taken into account in determining the resistance and stiffness of cold-formed members and sheeting;

- (b) Local buckling effects may be accounted for by using effective cross sectional properties, calculated on the basis of the effective widths of those elements that are prone to local buckling;
- (c) The possible shift of the centroidal axis of the effective cross section relative to the centroidal axis of the gross cross section shall be taken into account;
- (d) In determining resistance to local buckling, the yield strength f_y should be taken as f_{yb} ;
- (e) In determining the resistance of a cross section, the effective width of a compression element should be based on the compressive stress $\sigma_{com,Ed}$ in the element when the cross section resistance is reached;
- (f) Two cross sections are used in design: gross cross section and effective cross section of which the latter varies as a function of loading (compression, major axis bending etc.);
- (g) For serviceability verifications, the effective width of a compression element should be based on the compressive stress $\sigma_{com,Ed,ser}$ in the element under the serviceability limit state loading;
- (h) Distortional buckling shall be taken into account where it constitutes the critical failure mode.

3.7.2 Plane elements without stiffeners

The effective widths of compression elements shall be obtained from Table 3.5 for doubly supported compression elements or Table 3.6 for outstand compression elements (CEN, 2006b).

The notional flat width b_p of a plane element shall be determined as specified in §§3.2.1. In the case of plane elements in sloping webs, the appropriate slant height shall be used.

The reduction factor ρ used in Tables 3.5 and 3.6 to determine b_{eff} shall be based on the largest compressive stress $\sigma_{com,Ed}$ in the relevant element (calculated on the basis of the effective cross section and taking account of possible second order effects), when the resistance of the cross section is reached.

3. BEHAVIOUR AND RESISTANCE OF CROSS SECTION

Table 3.5 – Internal compression elements

Stress distribution (compression positive)				Effective width b_{eff}		
				$\psi = 1$ $b_{eff} = \rho \cdot b_p$ $b_{e1} = 0.5 \cdot b_{eff}; b_{e2} = 0.5 \cdot b_{eff}$		
				$1 > \psi \geq 0$ $b_{eff} = \rho \cdot b_p$ $b_{e1} = \frac{2}{5 - \psi} \cdot b_{eff}; b_{e2} = b_{eff} - b_{e1}$		
				$\psi < 0$ $b_{eff} = \rho \cdot b_c = \rho b_p / (1 - \psi)$ $b_{e1} = 0.4 \cdot b_{eff}; b_{e2} = 0.6 b_{eff}$		
$\psi = \sigma_2 / \sigma_1$	1	$1 > \psi > 0$	0	$0 > \psi > -1$	-1	$-1 > \psi \geq -3$
Buckling factor k_σ	4.0	$8.2 / (1.05 + \psi)$	7.81	$7.81 - 6.29\psi + 9.78\psi^2$	23.9	$5.98(1 - \psi)^2$

Table 3.6 – Outstand compression elements

Stress distribution (compression positive)				Effective width b_{eff}		
				$1 > \psi \geq 0$ $b_{eff} = \rho \cdot c$		
				$\psi < 0$ $b_{eff} = \rho \cdot b_c = \rho c / (1 - \psi)$		
$\psi = \sigma_2 / \sigma_1$	1	0	-1	$1 \geq \psi \geq -3$		
Buckling factor k_σ	0.43	0.57	0.85	$0.57 - 0.21\psi + 0.07\psi^2$		
				$1 > \psi \geq 0$ $b_{eff} = \rho \cdot c$		
				$\psi < 0$ $b_{eff} = \rho \cdot b_c = \rho c / (1 - \psi)$		
$\psi = \sigma_2 / \sigma_1$	1	$1 > \psi > 0$	0	$0 > \psi > -1$	-1	
Buckling factor k_σ	0.43	$0.578 / (\psi + 0.24)$	1.70	$1.7 - 5\psi + 17.1\psi^2$	23.8	

If $\sigma_{com,Ed} = f_{yb} / \gamma_{M0}$ the reduction factor ρ should be obtained according to EN1993-1-5, from the following:

- internal compression elements:

$$\rho = 1.0 \quad \text{for } \bar{\lambda}_p \leq 0.5 + \sqrt{0.085 - 0.055\psi} \quad (3.36a)$$

$$\rho = \frac{\bar{\lambda}_p - 0.055(3 + \psi)}{\bar{\lambda}_p^2} < 1.0 \quad \text{for } \bar{\lambda}_p > 0.5 + \sqrt{0.085 - 0.055\psi} \quad (3.36b)$$

- outstand compression elements (flange type):

$$\rho = 1.0 \quad \text{for } \bar{\lambda}_p \leq 0.748 \quad (3.37a)$$

$$\rho = \frac{\bar{\lambda}_p - 0.188}{\bar{\lambda}_p^2} < 1.0 \quad \text{for } \bar{\lambda}_p > 0.748 \quad (3.37b)$$

in which the plate slenderness $\bar{\lambda}_p$ is given by:

$$\bar{\lambda}_p = \sqrt{\frac{f_{yb}}{\sigma_{cr}}} = \frac{b_p/t}{28.4 \cdot \varepsilon \cdot \sqrt{k_\sigma}} \quad (3.38)$$

where

- k_σ is the relevant buckling factor from Tables 3.5 or 3.6;
- ε is the ratio $\sqrt{235/f_{yb}}$ with f_{yb} in N/mm²;
- ψ is the stress ratio;
- t is the thickness;
- σ_{cr} is the elastic critical plate buckling stress.

If $\sigma_{com,Ed} < f_{yb} / \gamma_{M0}$ the reduction factor ρ should be determined in a similar manner, but the reduced plate slenderness $\bar{\lambda}_{p,red}$ is given by:

$$\bar{\lambda}_{p,red} = \bar{\lambda}_p \cdot \sqrt{\frac{\sigma_{com,Ed}}{f_{yb} / \gamma_{M0}}} \quad (3.39)$$

However, when verifying the design buckling resistance of a member or performing a second order system analysis, for calculating the values of A_{eff} , e_N and W_{eff} the plate slenderness $\bar{\lambda}_p$ of an element should be based

either on its yield strength f_y or on $\sigma_{com,Ed}$ based on a 2nd order system analysis.

The application of the second approach generally requires an iterative procedure for the second order calculation in which the internal forces and moments are determined with the effective cross sections defined with the internal forces and moments determined from the previous iteration.

For effective width calculation at the serviceability limit states the reduction factor ρ should be determined in a similar manner, but using the reduced plate slenderness $\bar{\lambda}_{p,ser}$ given by:

$$\bar{\lambda}_{p,ser} = \bar{\lambda}_p \cdot \sqrt{\frac{\sigma_{com,Ed,ser}}{f_{yb}}} \quad (3.40)$$

where

$\sigma_{com,Ed,ser}$ is the largest compressive stress in the relevant element (calculated on the basis of the effective cross section) under the serviceability limit state loading.

In determining the effective width of a flange element subject to stress gradient, the stress ratio ψ used in Table 3.5 and Table 3.6 may be based on the properties of the gross cross section.

In determining the effective width of a web element the stress ratio ψ used in Table 3.5 may be obtained using the effective area of the compression flange but the gross area of the web.

The effective section properties may be refined by iteration, in which case the stress ratio ψ is based on the effective cross section of the previous iteration. The minimum number of iterations when dealing with stress gradients is two.

In the case of webs of trapezoidal profiled sheets under stress gradient, the simplified method given in §§3.7.3.4 may be used.

3.7.3 Plane elements with edge or intermediate stiffeners

3.7.3.1 General

The design of compression elements with edge or intermediate stiffeners shall be based on the assumption that the stiffener behaves as a

compression member with continuous partial restraint, with a spring stiffness that depends on the boundary conditions and flexural stiffness of the adjacent plane elements.

The spring stiffness of a stiffener should be determined by applying a unit load per unit length u as illustrated in Figure 3.34. The spring stiffness K per unit length may be determined from:

$$K = u / \delta \tag{3.41}$$

where

δ is the deflection of the stiffener due to the unit load u acting at the centroid (b_1) of the effective part of the stiffened part of the cross section.

In determining the values of the rotational spring stiffnesses C_θ , $C_{\theta 1}$ and $C_{\theta 2}$ from the geometry of the cross section, account should be taken of the possible effects of other stiffeners that exist in the same element, or on any other element of the cross section that is subject to compression.

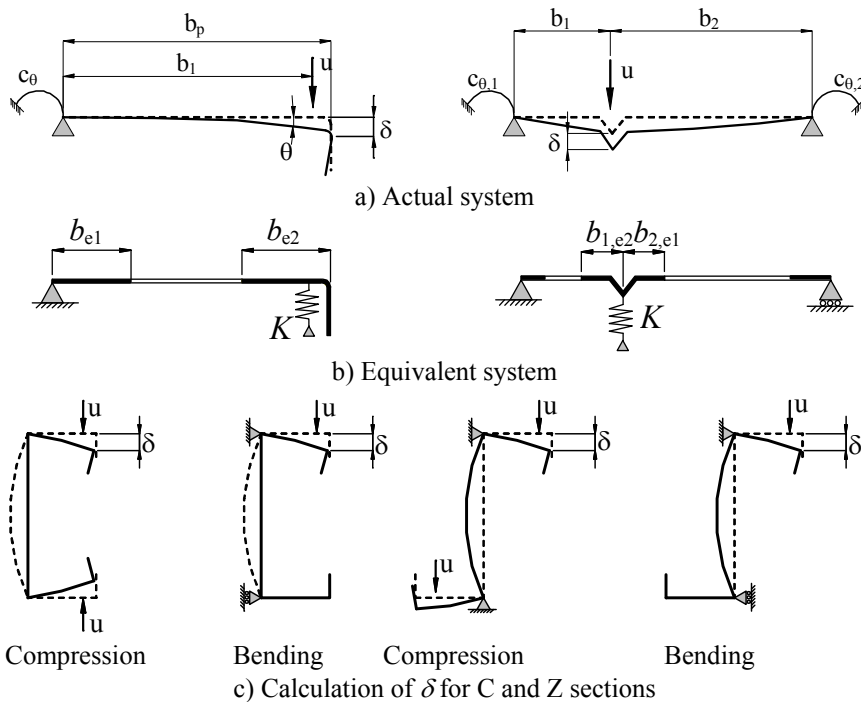


Figure 3.34 – Determination of spring stiffness

3. BEHAVIOUR AND RESISTANCE OF CROSS SECTION

For an edge stiffener, the deflection δ should be obtained from:

$$\delta = \theta \cdot b_p + \frac{u \cdot b_p^3}{3} \cdot \frac{12 \cdot (1 - \nu^2)}{E \cdot t^3} \quad (3.42)$$

with:

$$\theta = u \cdot b_p / C_\theta \quad (3.43)$$

In the case of the edge stiffeners of lipped C-sections and lipped Z-sections, C_θ should be determined with the unit loads u applied as shown in Figure 3.34c. This results in the following expression for the spring stiffness K_I for the flange 1:

$$K_I = \frac{E \cdot t^3}{4 \cdot (1 - \nu^2)} \cdot \frac{1}{b_1^2 \cdot h_w + b_1^3 + 0,5 \cdot b_1 \cdot b_2 \cdot h_w \cdot k_f} \quad (3.44)$$

where

b_1 is the distance from the web-to-flange junction to the gravity centre of the effective area of the edge stiffener (including the effective part b_{e2} of the flange) of flange 1 (see Figure 3.34a);

b_2 is the distance from the web-to-flange junction to the gravity centre of the effective area of the edge stiffener (including the effective part of the flange) of flange 2;

h_w is the web depth;

$k_f = 0$ if flange 2 is in tension (e.g. for a beam in bending about the y - y axis);

$k_f = A_{s2} / A_{s1}$ if flange 2 is in compression (e.g. for a member in axial compression);

$k_f = 1$ for a symmetric section in compression;

A_{s1} and A_{s2} are the effective area of the edge stiffener (including the effective part b_{e2} of the flange, see Figure 3.34b) of flange 1 and flange 2 respectively.

For an intermediate stiffener, the values of the rotational spring stiffnesses $C_{\theta 1}$ and $C_{\theta 2}$ may conservatively be taken as equal to zero, and the deflection δ may be obtained from:

$$\delta = \theta \cdot b_p + \frac{u \cdot b_1^2 \cdot b_2^2}{3 \cdot (b_1 + b_2)} \cdot \frac{12 \cdot (1 - \nu^2)}{E \cdot t^3} \quad (3.45)$$

The reduction factor χ_d for the distortional buckling resistance (flexural buckling of a stiffener) should be obtained from the relative slenderness $\bar{\lambda}_d$ from:

$$\chi_d = 1.0 \quad \text{if} \quad \bar{\lambda}_d \leq 0.65 \quad (3.46a)$$

$$\chi_d = 1.47 - 0.723 \cdot \bar{\lambda}_d \quad \text{if} \quad 0.65 < \bar{\lambda}_d \leq 1.38 \quad (3.46b)$$

$$\chi_d = \frac{0.66}{\bar{\lambda}_d} \quad \text{if} \quad \bar{\lambda}_d \geq 1.38 \quad (3.46c)$$

and

$$\bar{\lambda}_d = \sqrt{f_{yb} / \sigma_{cr,s}} \quad (3.46d)$$

where

$\sigma_{cr,s}$ is the elastic critical stress for the stiffener(s) from §§3.7.3.2, §§3.7.3.3 or §§3.7.3.4.

In the case of a plane element with an edge and intermediate stiffener(s), in the absence of a more accurate method the effect of the intermediate stiffener(s) may be neglected.

3.7.3.2 Plane elements with edge stiffeners

3.7.3.2.1 Conditions

An edge stiffener shall not be taken into account in determining the resistance of the plane element to which it is attached unless the following conditions are met:

- the angle between the stiffener and the plane element is between 45° and 135°;

3. BEHAVIOUR AND RESISTANCE OF CROSS SECTION

- the outstand width c is not less than $0.2b$, where b and c are as shown in Figure 3.35;
- the b/t ratio is not more than 60 for a single edge fold stiffener, or 90 for a double edge fold stiffener.

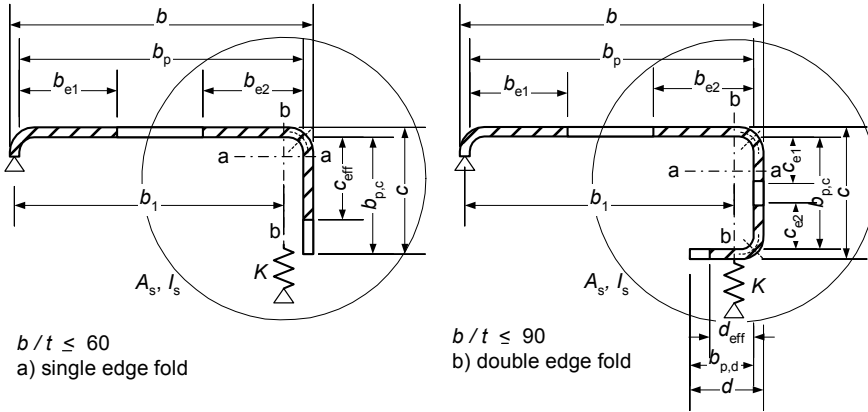


Figure 3.35 – Edge stiffeners

If the above criteria are met, the effectiveness of the stiffener may be determined from the general procedure given in §3.7.3.2.2.

3.7.3.2.2 General procedure

140

The cross section of an edge stiffener should be taken as comprising the effective portions of the stiffener (element c or elements c and d as shown in Figure 3.35) plus the adjacent effective portion, b_{e2} , of the plane element b_p .

The procedure, which is illustrated in Figure 3.36 and presented schematically in Flowcharts 3.1 and 3.2, should be carried out in steps as follows:

- Step 1:** Obtain an initial effective cross section for the stiffener using effective widths determined by assuming that the stiffener gives full restraint and that $\sigma_{com,Ed} = f_{yb} / \gamma_{M0}$;
- Step 2:** Use the initial effective cross section of the stiffener to determine the reduction factor for distortional buckling (flexural buckling of the stiffener), allowing for the effects of the continuous spring restraint;

Step 3: Optionally iterate to refine the value of the reduction factor for buckling of the stiffener.

Initial values of the effective widths b_{e1} and b_{e2} shown in Figure 3.35 should be determined from §§3.7.2 by assuming that the plane element b_p is supported on both longitudinal edges (see Table 3.5).

Initial values of the effective widths c_{eff} and d_{eff} shown in Figure 3.35 should be obtained as follows:

a) for a single edge fold stiffener:

$$c_{eff} = \rho \cdot b_{p,c} \quad (3.47a)$$

with ρ obtained from §§3.7.2, except using a value of the buckling factor k_σ given by the following:

- if $b_{p,c} / b_p \leq 0.35$:

$$k_\sigma = 0.5 \quad (3.47b)$$

- if $0.35 < b_{p,c} / b_p \leq 0.6$:

$$k_\sigma = 0.5 + \sqrt[3]{(b_{p,c} / b_p - 0.35)^2} \quad (3.47c)$$

b) for a double edge fold stiffener:

$$c_{eff} = \rho \cdot b_{p,c} \quad (3.47d)$$

with ρ obtained from §§3.7.2 with a buckling factor k_σ for a doubly supported element as per Table 3.5;

$$d_{eff} = \rho \cdot b_{p,d} \quad (3.47e)$$

and with ρ obtained from §§3.7.2 with a buckling factor k_σ for an outstand element as per Table 3.6.

The effective cross sectional area of the edge stiffener A_s should be obtained from:

$$A_s = t (b_{e2} + c_{eff}) \text{ or} \quad (3.48a)$$

$$A_s = t (b_{e2} + c_{e1} + c_{e2} + d_{eff}) \quad (3.48b)$$

respectively.

The elastic critical buckling stress $\sigma_{cr,s}$ for an edge stiffener should be obtained from:

$$\sigma_{cr,s} = \frac{2 \cdot \sqrt{K \cdot E \cdot I_s}}{A_s} \quad (3.49)$$

where

- K is the spring stiffness per unit length, see §§3.7.3.1;
- I_s is the effective second moment of area of the stiffener, taken as that of its effective area A_s about the centroidal axis $a-a$ of its effective cross section, see Figure 3.35.

The reduction factor χ_d for the distortional buckling (flexural buckling of a stiffener) resistance of an edge stiffener should be obtained from the value of $\sigma_{cr,s}$ using the method given in §§3.7.3.1.

If $\chi_d < 1$ the effective area calculation may be refined iteratively, starting the iteration with modified values of ρ obtained using the formulas of section §§3.7.2 with $\sigma_{com,Ed,i}$ equal to $\chi_d f_{yb} / \gamma_{M0}$, so that:

$$\bar{\lambda}_{p,red} = \bar{\lambda}_p \cdot \sqrt{\chi_d} \quad (3.50)$$

The reduced effective area of the stiffener $A_{s,red}$ allowing for flexural buckling should be taken as:

$$A_{s,red} = \chi_d \cdot A_s \cdot \frac{f_{yb} / \gamma_{M0}}{\sigma_{com,Ed}} \quad \text{but} \quad A_{s,red} \leq A_s \quad (3.51)$$

where

- $\sigma_{com,Ed}$ is compressive stress at the centreline of the stiffener calculated on the basis of the effective cross section.

In determining effective section properties, the reduced effective area $A_{s,red}$ should be represented by using a reduced thickness $t_{red} = t \cdot A_{red} / A_s$ for all the elements included in A_s .

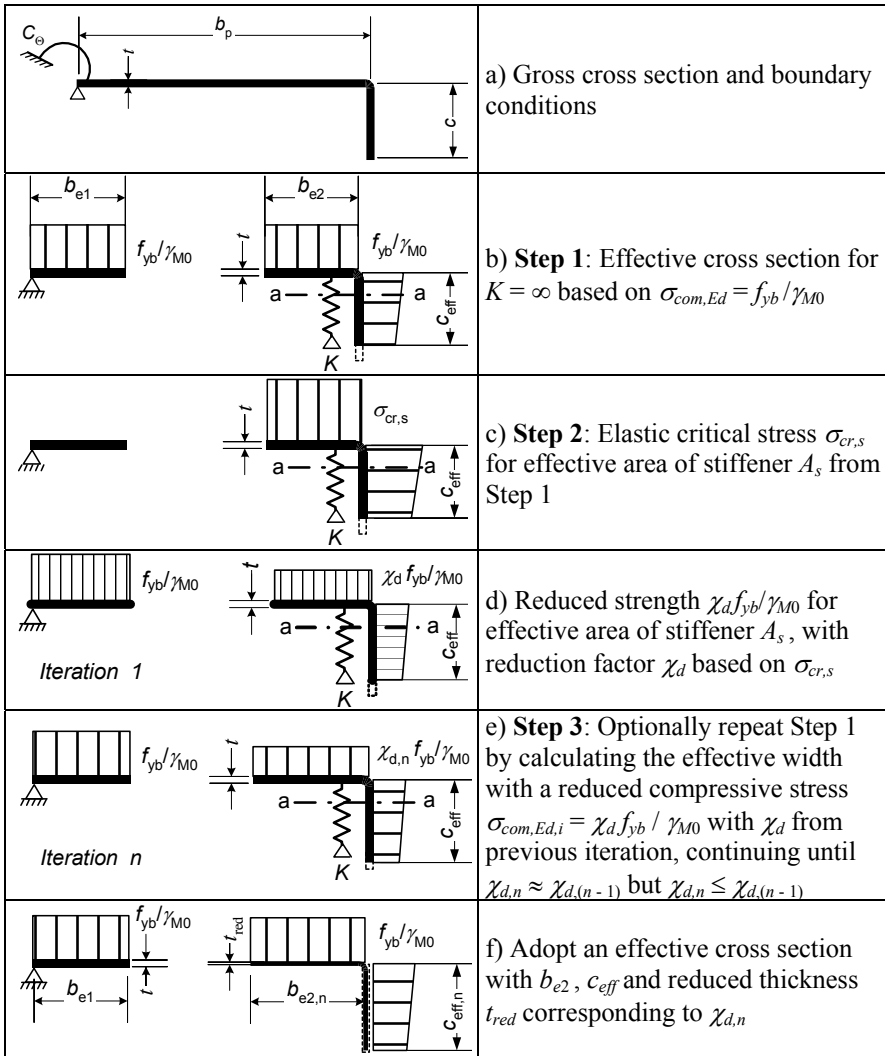
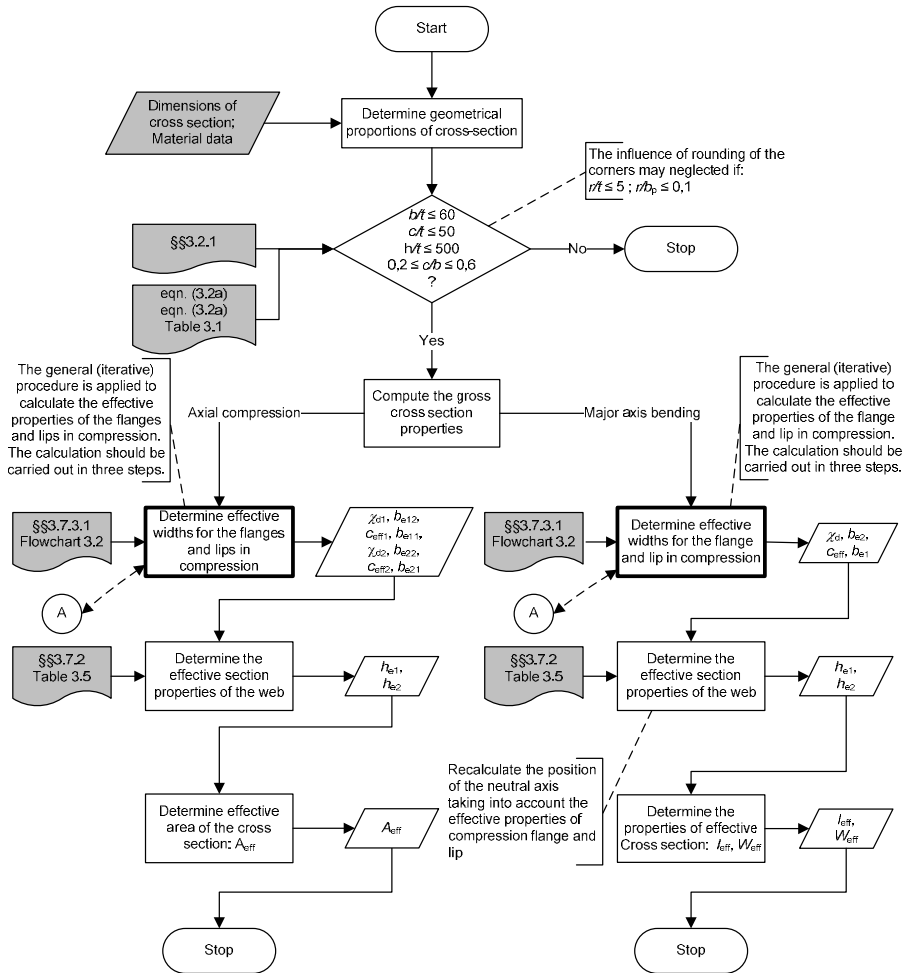


Figure 3.36 – Compression resistance of a flange with an edge stiffener

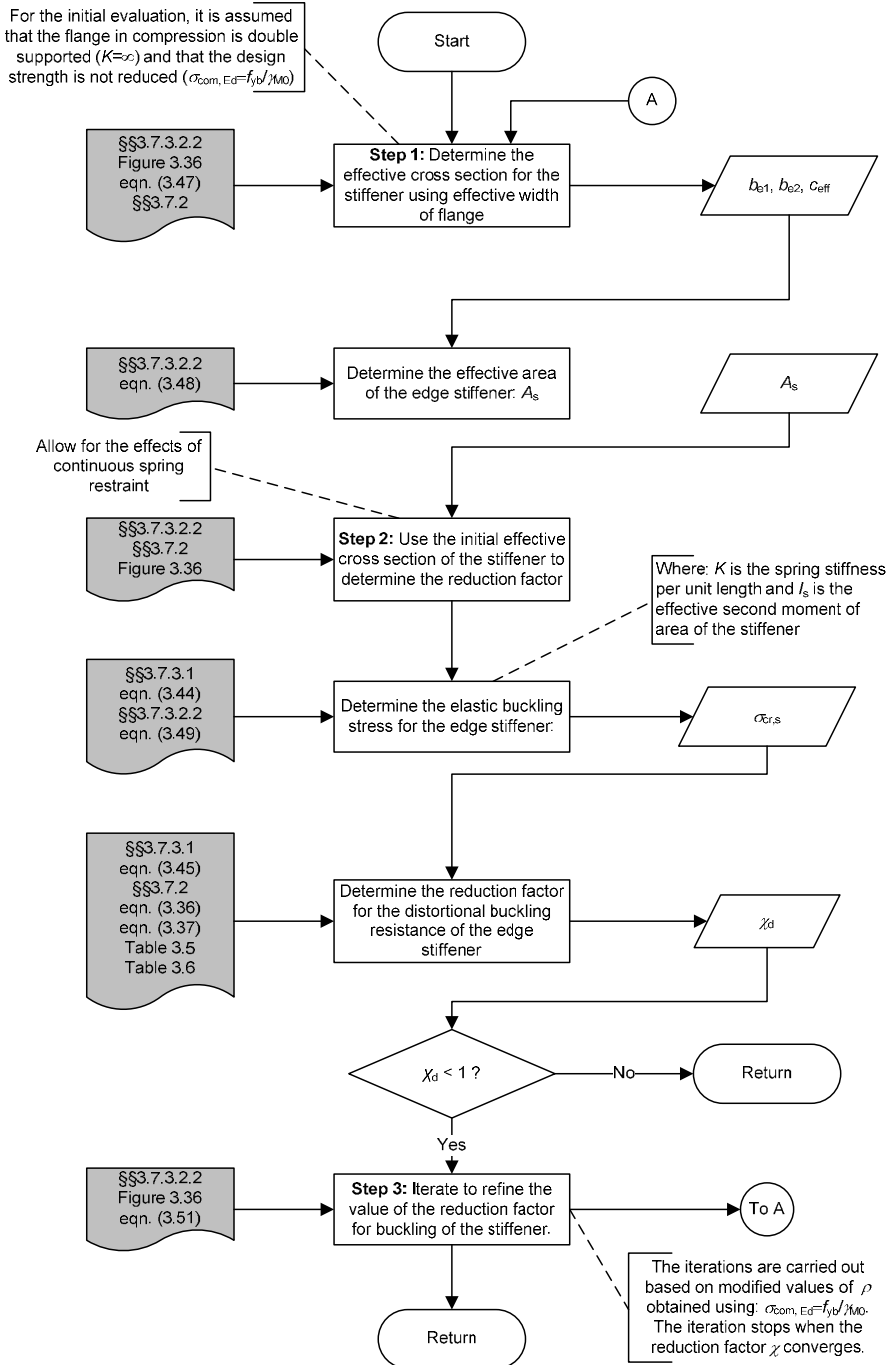
Flowcharts 3.1 and 3.2 present schematically the calculation of effective section properties for cold-formed steel sections under bending or compression. Examples 3.1 and 3.2 present detailed calculations of effective section properties for a cold-formed steel lipped channel sections in bending and compression, respectively.

3. BEHAVIOUR AND RESISTANCE OF CROSS SECTION



Flowchart 3.1 – Calculation of effective section properties for cold-formed steel sections under compression or bending (SF038a-EN-EU, AccessSteel 2006)

3.7 DESIGN AGAINST LOCAL AND DISTORTIONAL BUCKLING ACCORDING TO EN1993-1-3



Flowchart 3.2 – Effective section properties of the flange and lip in compression – General (iterative) procedure (SF038a-EN-EU, AccessSteel 2006)

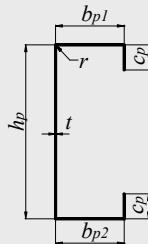
Example 3.1: Calculation of effective section properties for a cold-formed lipped channel section in bending

Basic Data

The dimensions of the cross section and the material properties are:

Total height	$h = 150 \text{ mm}$
Total width of flange in compression	$b_1 = 47 \text{ mm}$
Total width of flange in tension	$b_2 = 41 \text{ mm}$
Total width of edge fold	$c = 16 \text{ mm}$
Internal radius	$r = 3 \text{ mm}$
Nominal thickness	$t_{nom} = 1 \text{ mm}$
Steel core thickness (§§2.4.2.3)	$t = 0.96 \text{ mm}$
Basic yield strength	$f_{yb} = 350 \text{ N/mm}^2$
Modulus of elasticity	$E = 210000 \text{ N/mm}^2$
Poisson's ratio	$\nu = 0.3$
Partial factor (§§2.3.1)	$\gamma_{M0} = 1.00$

The dimensions of the section centre line are:



146

Web height	$h_p = h - t_{nom} = 150 - 1 = 149 \text{ mm}$
Width of flange in compression	$b_{p1} = b_1 - t_{nom} = 47 - 1 = 46 \text{ mm}$
Width of flange in tension	$b_{p2} = b_2 - t_{nom} = 41 - 1 = 40 \text{ mm}$
Width of edge fold	$c_p = c - t_{nom} / 2 = 16 - 1 / 2 = 15.5 \text{ mm}$

Checking of geometrical proportions

The design method of EN1993-1-3 can be applied if the following conditions are satisfied (§§3.2.3, Table 3.1):

$$\begin{aligned} b/t &\leq 60 & b_1/t &= 47/0.96 = 48.96 < 60 & - \text{OK} \\ c/t &\leq 50 & c/t &= 16/0.96 = 16.67 < 50 & - \text{OK} \\ h/t &\leq 500 & h/t &= 150/0.96 = 156.25 < 500 & - \text{OK} \end{aligned}$$

In order to provide sufficient stiffness and to avoid primary buckling of the stiffener itself, the size of stiffener should be within the following range (§§3.2.3, eqn. (3.4)):

$$\begin{aligned} 0.2 \leq c/b \leq 0.6 & & c/b_1 &= 16/47 = 0.34 & & 0.2 < 0.34 < 0.6 - \text{OK} \\ & & c/b_2 &= 16/41 = 0.39 & & 0.2 < 0.39 < 0.6 - \text{OK} \end{aligned}$$

The influence of rounding of the corners is neglected if (§§3.2.1, eqn. (3.2)):

$$\begin{aligned} r/t &\leq 5 & r/t &= 3/0.96 = 3.125 < 5 & - \text{OK} \\ r/b_p &\leq 0.10 & r/b_{p1} &= 3/47 = 0.06 < 0.10 & - \text{OK} \\ & & r/b_{p2} &= 3/41 = 0.07 < 0.10 & - \text{OK} \end{aligned}$$

Gross cross section properties

$$A_{br} = t(2c_p + b_{p1} + b_{p2} + h_p) = 0.96 \times (2 \times 15.5 + 46 + 40 + 149) = 255.36 \text{ mm}^2$$

Position of the neutral axis with respect to the flange in compression:

$$z_{b1} = \frac{[c_p(h_p - c_p/2) + b_{p2}h_p + h_p^2/2 + c_p^2/2]t}{A_{br}} = 72.82 \text{ mm}$$

Effective section properties of the flange and lip in compression

The general (iterative) procedure is applied to calculate the effective properties of the compressed flange and the lip (plane element with edge stiffener). The calculation should be carried out in three steps (§§3.7.3.2.2):

Step 1 (§§3.7.3.2.2, Figure 3.36b):

Obtain an initial effective cross section for the stiffener using effective widths of the flange determined by assuming that the compressed flange is doubly supported, the stiffener gives full restraint ($K = \infty$) and that design strength is not reduced ($\sigma_{com,Ed} = f_{yb} / \gamma_{M0}$).

3. BEHAVIOUR AND RESISTANCE OF CROSS SECTION

Effective width of the compressed flange (§§3.7.2)

The stress ratio: $\psi = 1$ (uniform compression), so the buckling factor is $k_\sigma = 4$ for internal compression element (§§3.7.2, Table 3.5).

$$\varepsilon = \sqrt{235/f_{yb}}$$

The relative slenderness:

$$\bar{\lambda}_{p,b} = \frac{b_{p1}/t}{28.4 \varepsilon \sqrt{k_\sigma}} = \frac{46/0.96}{28.4 \times \sqrt{235/350} \times \sqrt{4}} = 1.03$$

the width reduction factor is:

$$\rho = \frac{\bar{\lambda}_{p,b} - 0.055(3 + \psi)}{\bar{\lambda}_{p,b}^2} = \frac{1.03 - 0.055 \times (3 + 1)}{1.03^2} = 0.764 < 1$$

The effective width is:

$$b_{eff} = \rho b_{p1} = 0.764 \times 46 = 35.14 \text{ mm}$$

$$b_{e1} = b_{e2} = 0.5 b_{eff} = 0.5 \times 35.14 = 17.57 \text{ mm}$$

Effective width of the edge fold (§§3.7.3.2.2, eqn. (3.47))

The buckling factor is:

$$\text{if } c_p/b_{p1} \leq 0.35 : \quad k_\sigma = 0.5$$

$$\text{if } 0.35 < c_p/b_{p1} \leq 0.6 : \quad k_\sigma = 0.5 + 0.83 \sqrt[3]{(c_p/b_{p1} - 0.35)^2}$$

$$c_p/b_{p1} = 15.5/46 = 0.337 < 0.35 \quad \text{so} \quad k_\sigma = 0.5$$

The relative slenderness (§§3.7.2, eqn. (3.38)):

$$\bar{\lambda}_{p,c} = \frac{c_p/t}{28.4 \varepsilon \sqrt{k_\sigma}} = \frac{15.5/0.96}{28.4 \times \sqrt{235/350} \times \sqrt{0.5}} = 0.981$$

The width reduction factor is:

$$\rho = \frac{\bar{\lambda}_{p,c} - 0.188}{\bar{\lambda}_{p,c}^2} = \frac{0.981 - 0.188}{0.981^2} = 0.824, \quad \rho \leq 1$$

The effective width is (§§3.7.3.2.2, eqn. (3.47)):

$$c_{eff} = \rho c_p = 0.824 \times 15.5 = 12.77 \text{ mm}$$

Effective area of the edge stiffener (§§3.7.3.2.2, eqn. (3.48)):

$$A_s = t(b_{e2} + c_{eff}) = 0.96 \times (17.57 + 12.77) = 29.126 \text{ mm}^2$$

Step 2 (§§3.7.3.2.2, Figure 3.36c):

Use the initial effective cross section of the stiffener to determine the reduction factor, allowing for the effects of the continuous spring restraint.

The elastic critical buckling stress for the edge stiffener (§§3.7.3.2.2, eqn. (3.49)) is

$$\sigma_{cr,s} = \frac{2\sqrt{K E I_s}}{A_s}$$

where

K is the spring stiffness per unit length (§§3.7.3.1, eqn. (3.44)):

$$K = \frac{E t^3}{4(1-\nu^2)} \cdot \frac{1}{b_1^2 h_p + b_1^3 + 0.5 b_1 b_2 h_p k_f}$$

with:

b_1 – distance from the web to the centre of the effective area of the stiffener in compression (upper flange)

$$b_1 = b_{p1} - \frac{b_{e2} t b_{e2} / 2}{(b_{e2} + c_{eff}) t} = 46 - \frac{17.57 \times 0.96 \times 17.57 / 2}{(17.57 + 12.77) \times 0.96} = 40.913 \text{ mm}$$

$k_f = 0$ for bending about the y - y axis

$$K = 0.161 \text{ N/mm}^2$$

I_s is the effective second moment of area of the stiffener:

$$I_s = \frac{b_{e2} t^3}{12} + \frac{c_{eff}^3 t}{12} + b_{e2} t \left[\frac{c_{eff}^2}{2(b_{e2} + c_{eff})} \right]^2 + c_{eff} t \left[\frac{c_{eff}}{2} - \frac{c_{eff}^2}{2(b_{e2} + c_{eff})} \right]^2$$

$$\Rightarrow I_s = 457.32 \text{ mm}^4$$

so, the elastic critical buckling stress for the edge stiffener is

3. BEHAVIOUR AND RESISTANCE OF CROSS SECTION

$$\sigma_{cr,s} = \frac{2 \times \sqrt{0.161 \times 210000 \times 457.32}}{29.126} = 270.011 \text{ N/mm}^2$$

Thickness reduction factor χ_d for the edge stiffener

The relative slenderness (§§3.7.3.1, eqn. (3.46) and §§3.7.3.2.2, Figure 3.36d):

$$\bar{\lambda}_d = \sqrt{f_{yb}/\sigma_{cr,s}} = \sqrt{350/270.011} = 1.139$$

The reduction factor will be:

$$\text{if } \bar{\lambda}_d \leq 0.65 \quad \chi_d = 1.0$$

$$\text{if } 0.65 < \bar{\lambda}_d < 1.38 \quad \chi_d = 1.47 - 0.723 \bar{\lambda}_d$$

$$\text{if } \bar{\lambda}_d \geq 1.38 \quad \chi_d = 0.66/\bar{\lambda}_d$$

$$\Rightarrow 0.65 < \bar{\lambda}_d = 1.139 < 1.38 \quad \text{so } \chi_d = 1.47 - 0.723 \times 1.139 = 0.646$$

Step 3 (§§3.7.3.2.2, Figure 3.36e):

As the reduction factor for buckling of the stiffener is $\chi_d < 1$, iterate to refine the value of the reduction factor for buckling of the stiffener.

The iterations are carried out based on modified values of ρ obtained using (§§3.7.3.2.2, eqn. (3.50)):

$$\sigma_{com,Ed,i} = \chi_d f_{yb} / \gamma_{M0} \quad \text{and} \quad \bar{\lambda}_{p,red} = \bar{\lambda}_p \sqrt{\chi_d}$$

The iteration stops when the reduction factor χ converges.

Initial values (iteration 1):

$$\chi_d = 0.646$$

$$b_{e2} = 17.57 \text{ mm}$$

$$c_{eff} = 12.77 \text{ mm}$$

Final values (iteration n):

$$\chi_d = \chi_{d,n} = 0.614$$

$$b_{e2} = b_{e2,n} = 20.736 \text{ mm}$$

$$c_{eff} = c_{eff,n} = 12.77 \text{ mm}$$

Final values of effective properties for flange and lip in compression are:

$$\chi_d = 0.614 \quad b_{e2} = 20.736 \text{ mm} \quad c_{eff} = 12.77 \text{ mm}$$

$$\text{and } b_{e1} = 17.57 \text{ mm}$$

$$t_{red} = t\chi_d = 0,96 \times 0,614 = 0.589 \text{ mm} \quad (\S\S 3.7.3.2.2, \text{Figure 3.36f})$$

Effective section properties of the web

The position of the neutral axis with regard to the flange in compression:

$$h_c = \frac{c_p (h_p - c_p/2) + b_{p2} h_p + h_p^2/2 + c_{eff}^2 \chi_d/2}{c_p + b_{p2} + h_p + b_{e1} + (b_{e2} + c_{eff}) \chi_d} \quad h_c = 79.5 \text{ mm}$$

The stress ratio:

$$\psi = \frac{h_c - h_p}{h_c} = \frac{79.5 - 149}{79.5} = -0.874$$

The buckling factor (§§3.7.2, Table 3.5):

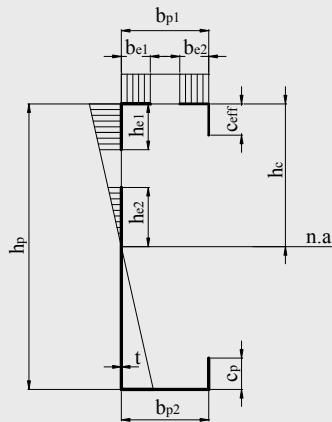
$$k_\sigma = 7.81 - 6.29\psi + 9.78\psi^2 \quad k_\sigma = 20.76$$

The relative slenderness:

$$\bar{\lambda}_{p,h} = \frac{h_p/t}{28.4 \varepsilon \sqrt{k_\sigma}} = \frac{149/0.96}{28.4 \times \sqrt{235/350} \times \sqrt{20.76}} = 1.464$$

The width reduction factor is:

$$\rho = \frac{\bar{\lambda}_{p,h} - 0.055(3 + \psi)}{\bar{\lambda}_{p,h}^2} = \frac{1.464 - 0.055 \times (3 - 0.874)}{1.464^2} = 0.629$$



3. BEHAVIOUR AND RESISTANCE OF CROSS SECTION

The effective width of the zone in compression of the web is:

$$h_{eff} = \rho h_c = 0.629 \times 79.5 = 50 \text{ mm}$$

Near the flange in compression:

$$h_{e1} = 0.4h_{eff} = 0.4 \times 50 = 20 \text{ mm}$$

Near the neutral axis:

$$h_{e2} = 0.6h_{eff} = 0.6 \times 50 = 30 \text{ mm}$$

The effective width of the web is:

Near the flange in compression:

$$h_1 = h_{e1} = 20 \text{ mm}$$

Near the flange in tension:

$$h_2 = h_p - (h_c - h_{e2}) = 149 - (79.5 - 30) = 99.5 \text{ mm}$$

Effective section properties

Effective cross section area:

$$A_{eff} = t[c_p + b_{p2} + h_1 + h_2 + b_{e1} + (b_{e2} + c_{eff})\chi_d]$$

$$A_{eff} = 0.96 \times [15.5 + 40 + 20 + 99.5 + 17.57 + (20.736 + 12.77) \times 0.614]$$

$$A_{eff} = 204.62 \text{ mm}^2$$

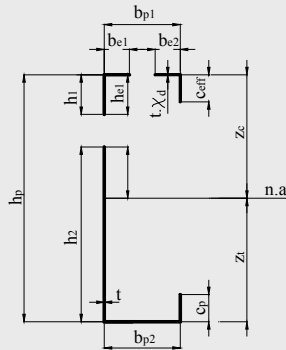
Position of the neutral axis with regard to the flange in compression:

$$z_c = \frac{t[c_p(h_p - c_p/2) + b_{p2}h_p + h_2(h_p - h_2/2) + h_1^2/2 + c_{eff}^2\chi_d/2]}{A_{eff}}$$

$$z_c = 85.75 \text{ mm}$$

Position of the neutral axis with regard to the flange in tension:

$$z_t = h_p - z_c = 149 - 85.75 = 63.25 \text{ mm}$$



Second moment of area:

$$I_{eff,y} = \frac{h_1^3 t}{12} + \frac{h_2^3 t}{12} + \frac{b_{p2}^3 t^3}{12} + \frac{c_p^3 t^3}{12} + \frac{b_{e1} t^3}{12} + \frac{b_{e2} (\chi_d t)^3}{12} + \frac{c_{eff}^3 (\chi_d t)^3}{12} + c_p t (z_t - c_p / 2)^2 + b_{p2} t z_t^2 + h_2 t (z_t - h_2 / 2)^2 + h_1 t (z_c - h_1 / 2)^2 + b_{e1} t z_c^2 + b_{e2} (\chi_d t) z_c^2 + c_{eff} (\chi_d t) (z_c - c_{eff} / 2)^2$$

$$I_{eff,y} = 668103 \text{ mm}^4$$

Effective section modulus:

- with regard to the flange in compression

$$W_{eff,y,c} = \frac{I_{eff,y}}{z_c} = \frac{668103}{85.75} = 7791 \text{ mm}^3$$

- with regard to the flange in tension

$$W_{eff,y,t} = \frac{I_{eff,y}}{z_t} = \frac{668103}{63.25} = 10563 \text{ mm}^3$$

Example 3.2: Calculation of effective section properties for a cold-formed lipped channel section in compression

Basic Data

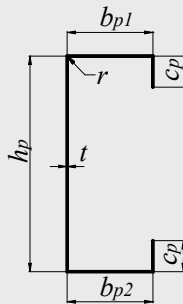
The dimensions of the cross section and the material properties are:

Total height $h = 150 \text{ mm}$

3. BEHAVIOUR AND RESISTANCE OF CROSS SECTION

Total width of upper flange	$b_1 = 47 \text{ mm}$
Total width of bottom flange	$b_2 = 41 \text{ mm}$
Total width of edge fold	$c = 16 \text{ mm}$
Internal radius	$r = 3 \text{ mm}$
Nominal thickness	$t_{nom} = 1 \text{ mm}$
Steel core thickness (§§2.4.2.3)	$t = 0.96 \text{ mm}$
Basic yield strength	$f_{yb} = 350 \text{ N/mm}^2$
Modulus of elasticity	$E = 210000 \text{ N/mm}^2$
Poisson's ratio	$\nu = 0.3$
Partial factor (§§2.3.1)	$\gamma_{M0} = 1.0$

The dimensions of the section centre line are:



154

Web height	$h_p = h - t_{nom} = 150 - 1 = 149 \text{ mm}$
Width of upper flange	$b_{p1} = b_1 - t_{nom} = 47 - 1 = 46 \text{ mm}$
Width of bottom flange	$b_{p2} = b_2 - t_{nom} = 41 - 1 = 40 \text{ mm}$
Width of edge fold	$c_p = c - t_{nom}/2 = 16 - 1/2 = 15.5 \text{ mm}$

Checking of geometrical proportions

The design method of EN1993-1-3 can be applied if the following conditions are satisfied (§§3.2.3, Table 3.1):

$b/t \leq 60$	$b_1/t = 47/0.96 = 48.96 < 60$	– OK
	$b_2/t = 41/0.96 = 42.71 < 60$	– OK
$c/t \leq 50$	$c/t = 16/0.96 = 16.67 < 50$	– OK
$h/t \leq 500$	$h/t = 150/0.96 = 156.25 < 500$	– OK

In order to provide sufficient stiffness and to avoid primary buckling of the stiffener itself, the size of stiffener should be within the following range (§§3.2.3, eqn. (3.4)):

$$0.2 \leq c/b \leq 0.6$$

$$c/b_1 = 16/47 = 0.34 \quad 0.2 < 0.34 < 0.6 - \text{OK}$$

$$c/b_2 = 16/41 = 0.39 \quad 0.2 < 0.39 < 0.6 - \text{OK}$$

The influence of rounding of the corners is neglected if (§§3.2.1, eqn. (3.2)):

$$r/t \leq 5 \quad r/t = 3/0.96 = 3.125 < 5 \quad - \text{OK}$$

$$r/b_p \leq 0.10 \quad r/b_{p1} = 3/46 = 0,065 < 0.10 - \text{OK}$$

$$r/b_{p2} = 3/40 = 0.075 < 0.10 - \text{OK}$$

Gross cross section properties

$$\begin{aligned} A_{br} &= t(2c_p + b_{p1} + b_{p2} + h_p) = \\ &= 0.96 \times (2 \times 15.5 + 46 + 40 + 149) = 255.36 \text{ mm}^2 \end{aligned}$$

Position of the centroidal axis with regard to the upper flange:

$$z_{b1} = \frac{[c_p(h_p - c_p/2) + b_{p2}h_p + h_p^2/2 + c_p^2/2]t}{A_{br}} = 72.82 \text{ mm}$$

Effective section properties of the flanges and lips in compression

The general (iterative) procedure is applied to calculate the effective properties of the compressed flange and the lip (plane element with edge stiffener). The calculation should be carried out in three steps (§§3.7.3.2.2):

Step 1 (§§3.7.3.2.2, Figure 3.36b):

Obtain an initial effective cross section for the stiffeners using effective widths of the flanges determined by assuming that the compressed flanges are doubly supported, the stiffener gives full restraint ($K = \infty$) and that design strength is not reduced ($\sigma_{com,Ed} = f_{yb} / \gamma_{M0}$).

3. BEHAVIOUR AND RESISTANCE OF CROSS SECTION

Effective width of the compressed flanges (§§3.7.2)

The stress ratio: $\psi = 1$ (uniform compression), so the buckling factor is: $k_\sigma = 4$ for internal compression element (§§3.7.2, Table 3.5).

$$\varepsilon = \sqrt{235/f_{yb}}$$

For the upper flange:

The relative slenderness:

$$\bar{\lambda}_{p,b1} = \frac{b_{p1}/t}{28.4 \varepsilon \sqrt{k_\sigma}} = \frac{46/0.96}{28.4 \times \sqrt{235/350} \times \sqrt{4}} = 1.03$$

The width reduction factor is:

$$\rho_1 = \frac{\bar{\lambda}_{p,b1} - 0.055(3 + \psi)}{\bar{\lambda}_{p,b1}^2} = \frac{1.03 - 0.055 \times (3 + 1)}{1.03^2} = 0.764$$

The effective width is:

$$b_{eff1} = \rho_1 b_{p1} = 0.764 \times 46 = 35.14 \text{ mm}$$

$$b_{e11} = b_{e12} = 0.5 b_{eff1} = 0.5 \times 35.14 = 17.57 \text{ mm}$$

For the bottom flange:

The relative slenderness:

$$\bar{\lambda}_{p,b2} = \frac{b_{p2}/t}{28.4 \varepsilon \sqrt{k_\sigma}} = \frac{40/0.96}{28.4 \times \sqrt{235/350} \times \sqrt{4}} = 0.895$$

The width reduction factor is:

$$\rho_2 = \frac{\bar{\lambda}_{p,b2} - 0.055(3 + \psi)}{\bar{\lambda}_{p,b2}^2} = \frac{0.895 - 0.055 \times (3 + 1)}{0.895^2} = 0.843$$

The effective width is:

$$b_{eff2} = \rho_2 b_{p2} = 0.843 \times 40 = 33.72 \text{ mm}$$

$$b_{e21} = b_{e22} = 0.5 b_{eff2} = 0.5 \times 33.72 = 16.86 \text{ mm}$$

Effective width of the edge fold (§§3.7.3.2.2, eqn. (3.47))

For the upper edge fold:

The buckling factor is:

$$\text{if } c_p/b_p \leq 0.35: \quad k_\sigma = 0.5$$

$$\text{if } 0.35 < c_p/b_p \leq 0.6: \quad k_\sigma = 0.5 + 0.83 \sqrt[3]{(c_p/b_p - 0.35)^2}$$

$$c_p/b_{p1} = 15.5/46 = 0.337 < 0.35 \text{ so } k_{\sigma1} = 0.5$$

The relative slenderness (§§3.7.2, eqn. (3.38)):

$$\bar{\lambda}_{p,c1} = \frac{c_p/t}{28.4 \varepsilon \sqrt{k_{\sigma1}}} = \frac{15.5/0.96}{28.4 \times \sqrt{235/350} \times \sqrt{0.5}} = 0.981$$

The width reduction factor is:

$$\rho_1 = \frac{\bar{\lambda}_{p,c1} - 0.188}{\bar{\lambda}_{p,c1}^2} = \frac{0.981 - 0.188}{0.981^2} = 0.824$$

The effective width is (§§3.7.3.2.2, eqn. (3.47)):

$$c_{eff1} = c_p \rho_1 = 15.5 \times 0.824 = 12.77 \text{ mm}$$

Effective area of the upper edge stiffener (§§3.7.3.2.2, eqn. (3.48)):

$$A_{s1} = t(b_{e12} + c_{eff1}) = 0.96 \times (17.57 + 12.77) = 29.13 \text{ mm}^2$$

157

For the bottom edge fold:

The buckling factor is:

$$c_p/b_{p2} = 15.5/40 = 0.388 > 0.35 \text{ so}$$

$$k_\sigma = 0.5 + 0.83 \sqrt[3]{(0.388 - 0.35)^2} = 0.594$$

The relative slenderness (§§3.7.2, eqn. (3.38)):

$$\bar{\lambda}_{p,c2} = \frac{c_p/t}{28.4 \varepsilon \sqrt{k_{\sigma2}}} = \frac{15.5/0.96}{28.4 \times \sqrt{235/350} \times \sqrt{0.594}} = 0.900$$

The width reduction factor is:

3. BEHAVIOUR AND RESISTANCE OF CROSS SECTION

$$\rho_2 = \frac{\bar{\lambda}_{p,c2} - 0.188}{\bar{\lambda}_{p,c2}^2} = \frac{0.900 - 0.188}{0.900^2} = 0.879$$

The effective width is (§§3.7.3.2.2, eqn. (3.47)):

$$c_{eff2} = c_p \rho_2 = 15.5 \times 0.879 = 13.62 \text{ mm}$$

Effective area of the bottom edge stiffener (§§3.7.3.2.2, eqn. (3.48)):

$$A_{s2} = t(b_{e22} + c_{eff2}) = 0.96 \times (16.86 + 13.62) = 29.26 \text{ mm}^2$$

Step 2 (§§3.7.3.2.2, Figure 3.36c):

Use the initial effective cross section of the stiffener to determine the reduction factor, allowing for the effects of the continuous spring restraint.

The elastic critical buckling stress for the edge stiffener is (§§3.7.3.2.2, eqn. (3.49)):

$$\sigma_{cr,s} = \frac{2\sqrt{K E I_s}}{A_s}$$

where

K is the spring stiffness per unit length,
 I_s is the effective second moment of area of the stiffener.

158

For the upper edge stiffener (§§3.7.3.1, eqn. (3.44)):

The spring stiffness is:

$$K_1 = \frac{E t^3}{4(1-\nu^2)} \cdot \frac{1}{b_1^2 h_p + b_1^3 + 0.5 b_1 b_2 h_p k_{f1}}$$

with

b_1 – distance from the web to the centre of the effective area of the stiffener in compression (upper flange)

$$b_1 = b_{p1} - \frac{b_{e12} t b_{e12}/2}{(b_{e12} + c_{eff}) t} = 46 - \frac{17.57 \times 0.96 \times 17.57/2}{(17.57 + 12.77) \times 0.96} = 40.91 \text{ mm}$$

b_2 – distance from the web to the centre of the effective area of the stiffener in compression (bottom flange)

$$b_2 = b_{p2} - \frac{b_{e22} t b_{e22}/2}{(b_{e22} + c_{eff2}) t} = 40 - \frac{16.86 \times 0.96 \times 16.86/2}{(16.86 + 13.62) \times 0.96} = 35.34 \text{ mm}$$

$$k_{f1} = \frac{A_{s2}}{A_{s1}} = \frac{29.26}{29.13} = 1.004 \text{ for a member in axial compression}$$

$$K_1 = 0.12 \text{ N/mm}^2$$

The effective second moment of area:

$$I_{s1} = \frac{b_{e12} t^3}{12} + \frac{c_{eff1}^3 t}{12} + b_{e12} t \left[\frac{c_{eff1}^2}{2(b_{e12} + c_{eff1})} \right]^2 + c_{eff1} t \left[\frac{c_{eff1}}{2} - \left[\frac{c_{eff1}^2}{2(b_{e12} + c_{eff1})} \right] \right]^2 = 457.32 \text{ mm}^4$$

so, the elastic critical buckling stress for the upper edge stiffener is

$$\sigma_{cr,s1} = \frac{2 \times \sqrt{0.12 \times 210000 \times 457.32}}{29.13} = 233.1 \text{ N/mm}^2$$

For the bottom edge stiffener (§§3.7.3.1, eqn. (3.44)):

The spring stiffness is:

$$K_2 = \frac{Et^3}{4(1-\nu^2)} \cdot \frac{1}{b_2^2 h_p + b_2^3 + 0.5 b_1 b_2 h_p k_{f2}},$$

$$k_{f2} = \frac{A_{s1}}{A_{s2}} = \frac{29.13}{29.26} = 0.996 \text{ for a member in axial compression}$$

$$K_2 = 0.151 \text{ N/mm}^2$$

The effective second moment of area:

$$I_{s2} = \frac{b_{e22} t^3}{12} + \frac{c_{eff2}^3 t}{12} + b_{e22} t \left[\frac{c_{eff2}^2}{2(b_{e22} + c_{eff2})} \right]^2 + c_{eff2} t \left[\frac{c_{eff2}}{2} - \left[\frac{c_{eff2}^2}{2(b_{e22} + c_{eff2})} \right] \right]^2 = 538.02 \text{ mm}^4$$

3. BEHAVIOUR AND RESISTANCE OF CROSS SECTION

so, the elastic critical buckling stress for the bottom edge stiffener is

$$\sigma_{cr,s2} = \frac{2 \times \sqrt{0.151 \times 210000 \times 538.02}}{29.26} = 282.33 \text{ N/mm}^2$$

Thickness reduction factor χ_d for the edge stiffener

For the upper edge stiffener:

The relative slenderness (§§3.7.3.1, eqn. (3.46) and §§3.7.3.2.2, Figure 3.36d):

$$\bar{\lambda}_{d1} = \sqrt{f_{yb} / \sigma_{cr,s1}} = \sqrt{350 / 233.1} = 1.225$$

The reduction factor will be:

$$\text{if } \bar{\lambda}_d \leq 0.65 \quad \chi_d = 1.0$$

$$\text{if } 0.65 < \bar{\lambda}_d < 1.38 \quad \chi_d = 1.47 - 0.723\bar{\lambda}_d$$

$$\text{if } \bar{\lambda}_d \geq 1.38 \quad \chi_d = 0.66 / \bar{\lambda}_d$$

$$0.65 < \bar{\lambda}_{d1} = 1.225 < 1.38 \quad \text{so} \quad \chi_{d1} = 1.47 - 0.723 \times 1.225 = 0.584$$

For the bottom edge stiffener:

The relative slenderness:

$$\bar{\lambda}_{d2} = \sqrt{f_{yb} / \sigma_{cr,s2}} = \sqrt{350 / 282.33} = 1.113$$

The reduction factor will be:

$$0.65 < \bar{\lambda}_{d2} = 1.113 < 1.38 \quad \text{so} \quad \chi_{d2} = 1.47 - 0.723 \times 1.113 = 0.665$$

Step 3 (§§3.7.3.2.2, Figure 3.36e):

As the reduction factor for buckling of the stiffener is $\chi_d < 1$, iterate to refine the value of the reduction factor for buckling of the stiffener. The iterations are carried out based on modified values of ρ obtained using (§§3.7.3.2.2, eqn. (3.50)):

$$\sigma_{com,Ed,i} = \chi_d f_{yb} / \gamma_{M0} \quad \text{and} \quad \bar{\lambda}_{p,red} = \bar{\lambda}_p \sqrt{\chi_d}$$

The iteration stops when the reduction factor χ_d converges.

For the upper edge stiffener:

<u>Initial values (iteration 1):</u>	<u>Final values (iteration n):</u>
$\chi_{d1} = 0.584$	$\chi_{d1} = \chi_{d1,n} = 0.622$
$b_{e12} = 17.57 \text{ mm}$	$b_{e12} = b_{e12,n} = 20.65 \text{ mm}$
$c_{eff1} = 12.77 \text{ mm}$	$c_{eff1} = c_{eff1,n} = 15.16 \text{ mm}$

For the bottom edge stiffener:

<u>Initial values (iteration 1):</u>	<u>Final values (iteration n):</u>
$\chi_{d2} = 0.665$	$\chi_{d2} = \chi_{d2,n} = 0.693$
$b_{e22} = 16.86 \text{ mm}$	$b_{e22} = b_{e22,n} = 18.92 \text{ mm}$
$c_{eff2} = 13.62 \text{ mm}$	$c_{eff2} = c_{eff2,n} = 15.49 \text{ mm}$

Final values of effective properties for flanges and lips in compression are:

For the upper flange and lip:

$$\chi_{d1} = 0.622, b_{e12} = 20.65 \text{ mm}, c_{eff1} = 15.16 \text{ mm} \text{ and } b_{e11} = 17.57 \text{ mm}$$

For the bottom flange and lip:

$$\chi_{d2} = 0.693, b_{e22} = 18.92 \text{ mm}, c_{eff2} = 15.49 \text{ mm} \text{ and } b_{e21} = 16.86 \text{ mm}$$

From §§3.7.3.2.2, Figure 3.36f, results:

$$t_{red,1} = t \chi_{d1} = 0.96 \times 0.622 = 0.597 \text{ mm}$$

$$t_{red,2} = t \chi_{d2} = 0.96 \times 0.693 = 0.665 \text{ mm}$$

Effective section properties of the web

The stress ratio: $\psi = 1$ (uniform compression), so the buckling factor is: $k_\sigma = 4$ for internal compression element (§§3.7.2, Table 3.5).

$$\varepsilon = \sqrt{235/f_{yb}}$$

The relative slenderness:

$$\bar{\lambda}_{p,h} = \frac{h_p/t}{28.4 \varepsilon \sqrt{k_\sigma}} = \frac{149/0.96}{28.4 \times \sqrt{235/350} \times \sqrt{4}} = 3.335$$

The width reduction factor is:

3. BEHAVIOUR AND RESISTANCE OF CROSS SECTION

$$\rho = \frac{\bar{\lambda}_{p,h} - 0.055(3 + \psi)}{\bar{\lambda}_{p,h}^2} = \frac{3.335 - 0.055 \times (3 + 1)}{3.335^2} = 0.280$$

The effective width of the web is:

$$h_{eff} = \rho h_p = 0.28 \times 149 = 41.72 \text{ mm}$$

$$h_{e1} = h_{e2} = 0.5 h_{eff} = 0.5 \times 41.72 = 20.86 \text{ mm}$$

Effective section properties

Effective cross section area:

$$A_{eff} = t \left[b_{e11} + b_{e21} + h_{e1} + h_{e2} + (b_{e12} + c_{eff1}) \chi_{d1} + (b_{e22} + c_{eff2}) \chi_{d2} \right]$$

$$A_{eff} = 117.37 \text{ mm}^2$$

Position of the centroidal axis with regard to the upper flange:

$$z_{G1} = \frac{t \left[c_{eff2} \chi_{d2} \left(h_p - \frac{c_{eff2}}{2} \right) + h_p (b_{e22} \chi_{d2} + b_{e21}) + \right.}{A_{eff}} \\ \left. + \frac{h_{e2} \left(h_p - \frac{h_{e2}}{2} \right) + \frac{h_{e1}^2}{2} + \frac{c_{eff1}^2 \chi_{d1}}{2} \right]}{A_{eff}} = 74.92 \text{ mm}$$

Position of the centroidal axis with regard to the bottom flange:

$$z_{G2} = h_p - z_{G1} = 149 - 74.92 = 74.08 \text{ mm}$$

3.7.3.3 Plane elements with intermediate stiffeners

3.7.3.3.1 Conditions

Intermediate stiffeners may be formed by grooves or bends. The stiffeners should be equally shaped and not more than two in number. If these criteria are met the effectiveness of the stiffener may be determined

from the general procedure given in §§3.7.3.3.2. All plane elements in a section should be calculated following clause §§3.7.2.

3.7.3.3.2 General procedure

The cross section of an intermediate stiffener should be taken as comprising the stiffener itself plus the adjacent effective portions of the adjacent plane elements $b_{1,e2}$ and $b_{2,e1}$ shown in Figure 3.37.

The procedure, which is illustrated in Figure 3.38, should be carried out in steps as follows:

- Step 1:** Obtain an initial effective cross section for the stiffener using effective widths determined by assuming that the stiffener gives full restraint and that $\sigma_{com,Ed} = f_{yb}/\gamma_{M0}$;
- Step 2:** Use the initial effective cross section of the stiffener to determine the reduction factor for distortional buckling (flexural buckling of an intermediate stiffener), allowing for the effects of the continuous spring restraint;
- Step 3:** Optionally iterate to refine the value of the reduction factor for buckling of the stiffener.

Initial values of the effective widths $b_{1,e2}$ and $b_{2,e1}$ shown in Figure 3.37 should be determined from §§3.7.2 by assuming that the plane elements $b_{p,1}$ and $b_{p,2}$ are supported on both longitudinal edges, see Table 3.5.

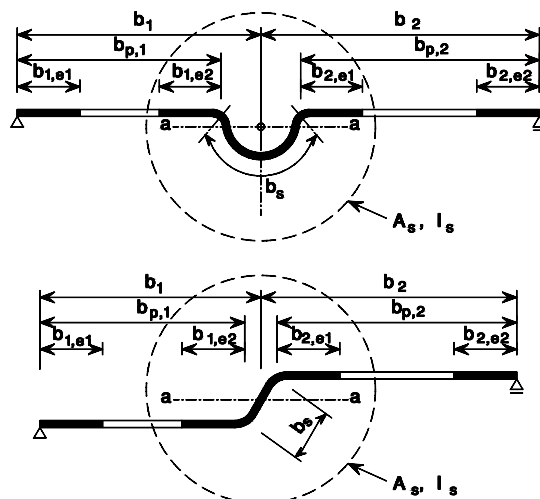


Figure 3.37 – Intermediate stiffeners

3. BEHAVIOUR AND RESISTANCE OF CROSS SECTION

The effective cross sectional area of an intermediate stiffener A_s should be obtained from:

$$A_s = t (b_{1,e2} + b_{2,e1} + b_s) \quad (3.52)$$

in which the stiffener width b_s is as shown in Figure 3.37.

The critical buckling stress $\sigma_{cr,s}$ for an intermediate stiffener should be obtained from:

$$\sigma_{cr,s} = \frac{2 \cdot \sqrt{K \cdot E \cdot I_s}}{A_s} \quad (3.53)$$

where

- K is the spring stiffness per unit length, see §§3.7.3.1.
- I_s is the effective second moment of area of the stiffener, taken as that of its effective area A_s about the centroidal axis $a-a$ of its effective cross section, see Figure 3.37.

The reduction factor χ_d for the distortional buckling resistance (flexural buckling of an intermediate stiffener) should be obtained from the value of $\sigma_{cr,s}$ using the method given in §§3.7.3.1.

If $\chi_d < 1$ the effective area calculation may optionally be refined iteratively, starting the iteration with modified values of ρ obtained using §§3.7.2 with $\sigma_{com,Ed}$ equal to $\chi_d f_{yb} / \gamma_{M0}$, so that:

$$\bar{\lambda}_{p,red} = \bar{\lambda}_p \cdot \sqrt{\chi_d} \quad (3.54)$$

The reduced effective area of the stiffener $A_{s,red}$ allowing for distortional buckling (flexural buckling of an intermediate stiffener) should be taken as:

$$A_{s,red} = \chi_d \cdot A_s \cdot \frac{f_{yb} / \gamma_{M0}}{\sigma_{com,Ed}} \quad \text{but} \quad A_{s,red} \leq A_s \quad (3.55)$$

In determining effective section properties, the reduced effective area $A_{s,red}$ should be represented by using a reduced thickness $t_{red} = t \cdot A_{red} / A_s$ for all the elements included in A_s .

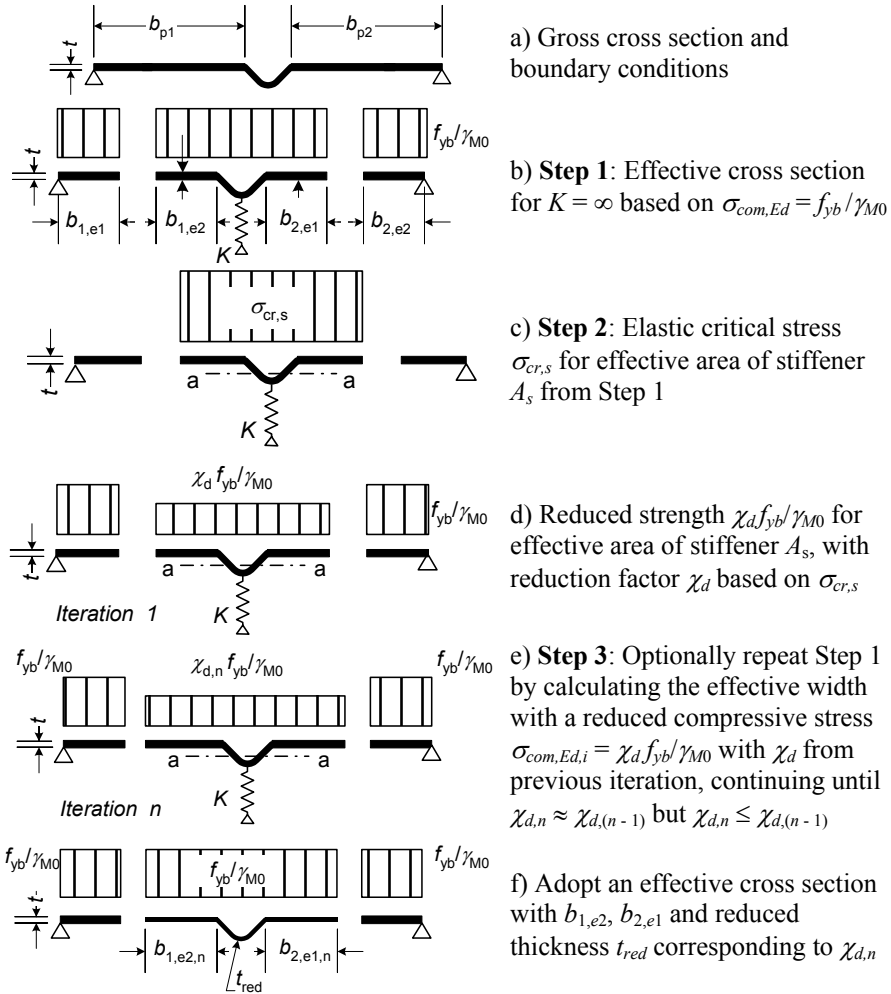


Figure 3.38 – Compression resistance of a flange with an intermediate stiffener

3.7.3.4 Trapezoidal sheeting profiles with intermediate stiffeners

3.7.3.4.1 General

This sub-clause §§3.7.3.4 should be used for trapezoidal profiled sheets, in association with §§3.7.3.3 for flanges and webs with intermediate flange stiffeners. Interaction between the buckling of intermediate flange stiffeners and intermediate web stiffeners should also be taken into account using the method given in §§3.7.3.4.4.

3.7.3.4.2 Flanges with intermediate stiffeners

If subject to uniform compression, the effective cross section of a flange with intermediate stiffeners should be assumed to consist of the reduced effective areas $A_{s,red}$ including two strips of width $0.5b_{eff}$ (or $15t$) adjacent to the stiffener (see Figure 3.39).

For one central flange stiffener, the elastic critical buckling stress $\sigma_{cr,s}$ should be obtained from:

$$\sigma_{cr,s} = \frac{4.2 \cdot k_w \cdot E}{A_s} \sqrt{\frac{I_s \cdot t^3}{4 \cdot b_p^2 \cdot (2 \cdot b_p + 3 \cdot b_s)}} \quad (3.56)$$

where

b_p is the notional flat width of plane element shown in Figure 3.39;

b_s is the stiffener width, measured around the perimeter of the stiffener, see Figure 3.39;

k_w is a coefficient that allows for partial rotational restraint of the stiffened flange by the webs or other adjacent elements. For the calculation of the effective cross section in axial compression the value $k_w = 1$;

A_s, I_s are the cross section area and the second moment of area of the stiffener cross section according to Figure 3.39.

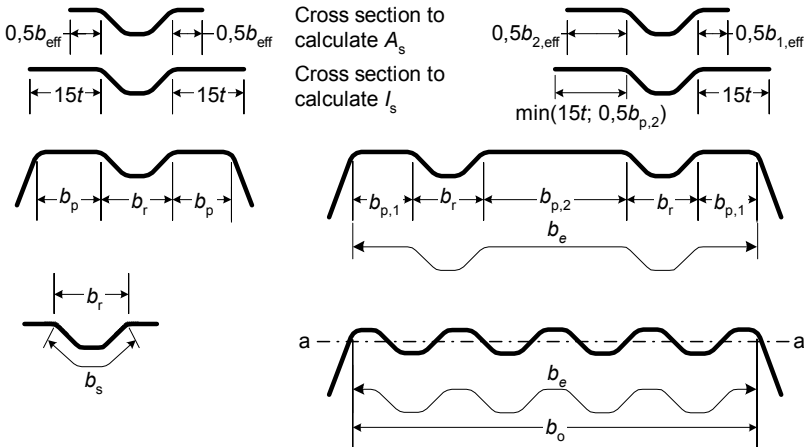


Figure 3.39 – Compression flange with one, two or multiple stiffeners

The eqn. (3.56) may be used for wide grooves provided that flat part of the stiffener is reduced due to local buckling and b_p in the eqn. (3.56) is replaced by the larger of b_p and $0.25(3b_p+b_r)$, see Figure 3.39. Similar method is valid for flange with two or more wide grooves.

For two symmetrically placed flange stiffeners, the elastic critical buckling stress $\sigma_{cr,s}$ should be obtained from:

$$\sigma_{cr,s} = \frac{4.2 \cdot k_w \cdot E}{A_s} \sqrt{\frac{I_s \cdot t^3}{8 \cdot b_1^2 \cdot (3 \cdot b_e - 4 \cdot b_1)}} \quad (3.57a)$$

with

$$b_e = 2b_{p,1} + b_{p,2} + 2b_s$$

$$b_1 = b_{p,1} + 0.5 b_r$$

where

$b_{p,1}$ is the notional flat width of an outer plane element, as shown in Figure 3.39;

$b_{p,2}$ is the notional flat width of the central plane element, as shown in Figure 3.39;

b_r is the overall width of a stiffener, see Figure 3.39;

A_s, I_s are the cross section area and the second moment of area of the stiffener cross section according to Figure 3.39.

For a multiple stiffened flange (three or more equal stiffeners) the effective area of the *entire flange* is

$$A_{eff} = \rho b_e t \quad (3.57b)$$

where ρ is the reduction factor according to §§3.7.2 for the slenderness $\bar{\lambda}_p$ based on the elastic buckling stress

$$\sigma_{cr,s} = 1.8E \sqrt{\frac{I_s t}{b_o^2 b_e^3}} + 3.6 \frac{Et^2}{b_o^2} \quad (3.57c)$$

where

I_s is the sum of the second moment of area of the stiffeners about the centroidal axis $a-a$, neglecting the thickness terms $bt^3/12$;

3. BEHAVIOUR AND RESISTANCE OF CROSS SECTION

- b_o is the width of the flange as shown in Figure 3.39;
 b_e is the developed width of the flange as shown in Figure 3.39.

The value of k_w may be calculated from the compression flange buckling wavelength l_b as follows:

- if $l_b / s_w \geq 2$:

$$k_w = k_{wo} \quad (3.58a)$$

- if $l_b / s_w < 2$:

$$k_w = k_{wo} - (k_{wo} - 1) \left[\frac{2l_b}{s_w} - \left(\frac{l_b}{s_w} \right)^2 \right] \quad (3.58b)$$

where

- s_w is the slant height of the web, see Figure 3.5(c).

Alternatively, the rotational restraint coefficient k_w may conservatively be taken as equal to 1.0 corresponding to a pin-jointed condition.

The values of l_b and k_{wo} may be determined from the following:

- for a compression flange with one intermediate stiffener:

$$l_b = 3.07^4 \sqrt{\frac{I_s \cdot b_p^2 \cdot (2 \cdot b_p + 3 \cdot b_s)}{t^3}} \quad (3.59)$$

$$k_{wo} = \sqrt{\frac{s_w + 2b_d}{s_w + 0.5b_d}} \quad (3.60)$$

with $b_d = 2b_p + b_s$.

- for a compression flange with two intermediate stiffeners:

$$l_b = 3.65^4 \sqrt{\frac{I_s \cdot b_1^2 \cdot (3 \cdot b_e - 4 \cdot b_1)}{t^3}} \quad (3.61)$$

$$k_{wo} = \sqrt{\frac{(2b_e + s_w) \cdot (3b_e - 4b_1)}{b_1 \cdot (4b_e - 6b_1) + s_w \cdot (3b_e - 4b_1)}} \quad (3.62)$$

The reduced effective area of the stiffener $A_{s,red}$ allowing for distortional buckling (flexural buckling of an intermediate stiffener) should be taken as:

$$A_{s,red} = \chi_d \cdot A_s \cdot \frac{f_{yb} / \gamma_{M1}}{\sigma_{com,ser}} \quad \text{but} \quad A_{s,red} \leq A_s \quad (3.63)$$

If the webs are unstiffened, the reduction factor χ_d should be obtained directly from $\sigma_{cr,s}$ using the method given in §§3.7.3.1.

If the webs are also stiffened, the reduction factor χ_d should be obtained using the method given in §§3.7.3.1, but with the modified elastic critical stress $\sigma_{cr,mod}$ given in §§3.7.3.4.4.

In determining effective section properties, the reduced effective area $A_{s,red}$ should be represented by using a reduced thickness $t_{red} = t \cdot A_{red} / A_s$ for all the elements included in A_s .

The effective section properties of the stiffeners at serviceability limit states should be based on the design thickness t .

3.7.3.4.3 Webs with up to two intermediate stiffeners

The effective cross section of the compression zone of a web (or other element of a cross section that is subject to stress gradient) should be assumed to consist of the reduced effective areas $A_{s,red}$ of up to two intermediate stiffeners, a strip adjacent to the compression flange and a strip adjacent to the centroidal axis of the effective cross section, see Figure 3.40.

The effective cross section of a web as shown in Figure 3.40 should be taken to include:

- a) a strip of width $s_{eff,1}$ adjacent to the compression flange;
- b) the reduced effective area $A_{s,red}$ of each web stiffener, up to a maximum of two;
- c) a strip of width $s_{eff,n}$ adjacent to the effective centroidal axis;
- d) the part of the web in tension.

3. BEHAVIOUR AND RESISTANCE OF CROSS SECTION

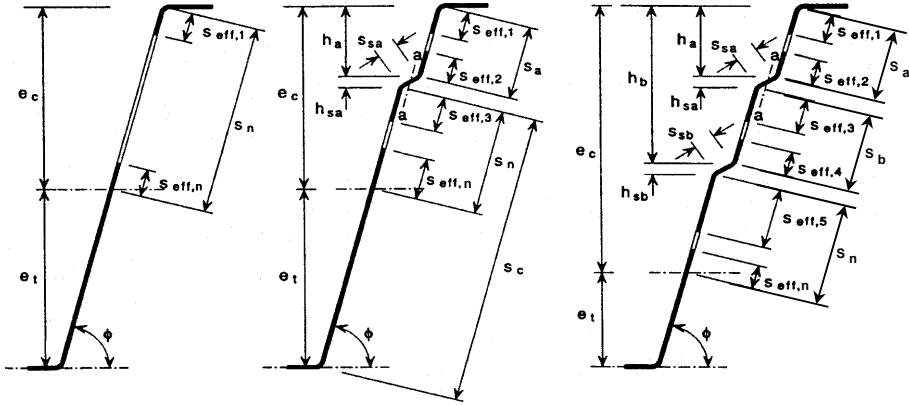


Figure 3.40 – Effective cross sections of webs of trapezoidal profiled sheets

The effective areas of the stiffeners should be obtained from the following:

- for a single stiffener, or for the stiffener closer to the compression flange:

$$A_{sa} = t (s_{eff,2} + s_{eff,3} + s_{sa}) \quad (3.64)$$

- for a second stiffener:

$$A_{sb} = t (s_{eff,4} + s_{eff,5} + s_{sb}) \quad (3.65)$$

170

in which the dimensions $s_{eff,1}$ to $s_{eff,n}$ and s_{sa} and s_{sb} are as shown in Figure 3.40.

Initially the location of the effective centroidal axis should be based on the effective cross sections of the flanges but the gross cross sections of the webs. In this case the basic effective width $s_{eff,0}$ should be obtained from:

$$s_{eff,0} = 0.76 \cdot t \sqrt{E / (\gamma_{M0} \cdot \sigma_{com,Ed})} \quad (3.66)$$

where

$\sigma_{com,Ed}$ is the stress in the compression flange when the cross section resistance is reached.

If the web is not fully effective, the dimensions $s_{eff,1}$ to $s_{eff,n}$ should be determined as follows:

$$s_{eff,1} = s_{eff,0} \quad (3.67a)$$

$$s_{eff,2} = (1 + 0.5h_a / e_c) s_{eff,0} \quad (3.67b)$$

$$s_{eff,3} = [1 + 0.5(h_a + h_{sa}) / e_c] s_{eff,0} \quad (3.67c)$$

$$s_{eff,4} = (1 + 0.5h_b / e_c) s_{eff,0} \quad (3.67d)$$

$$s_{eff,5} = [1 + 0.5(h_b + h_{sb}) / e_c] s_{eff,0} \quad (3.67e)$$

$$s_{eff,n} = 1.5s_{eff,0} \quad (3.67f)$$

where

e_c is the distance from the effective centroidal axis to the system line of the compression flange (see Figure 3.40),
and the dimensions h_a , h_b , h_{sa} and h_{sb} are as shown in Figure 3.40.

The dimensions $s_{eff,1}$ to $s_{eff,n}$ should initially be determined and then revised if the relevant plane element is fully effective, using the following:

- in an unstiffened web, if $s_{eff,1} + s_{eff,n} \geq s_n$ the entire web is effective, so revise as follows:

$$s_{eff,1} = 0.4s_n \quad (3.68a)$$

$$s_{eff,n} = 0.6s_n \quad (3.68b)$$

- in stiffened web, if $s_{eff,1} + s_{eff,2} \geq s_a$ the whole of s_a is effective, so revise as follows:

$$s_{eff,1} = \frac{s_a}{2 + 0.5h_a / e_c} \quad (3.69a)$$

$$s_{eff,2} = s_a \cdot \frac{1 + 0.5h_a / e_c}{2 + 0.5h_a / e_c} \quad (3.69b)$$

- in a web with one stiffener, if $s_{eff,3} + s_{eff,n} \geq s_n$ the whole of s_n is effective, so revise as follows:

$$s_{eff,3} = s_n \cdot \frac{1 + 0.5(h_a + h_{sa}) / e_c}{2.5 + 0.5(h_a + h_{sa}) / e_c} \quad (3.70a)$$

$$s_{eff,n} = \frac{1.5 \cdot s_n}{2.5 + 0.5(h_a + h_{sa}) / e_c} \quad (3.70b)$$

- in a web with two stiffeners:

- if $s_{eff,3} + s_{eff,4} \geq s_b$ the whole of s_b is effective, so revise as follows:

$$s_{eff,3} = s_b \cdot \frac{1 + 0.5(h_a + h_{sa})/e_c}{2 + 0.5(h_a + h_{sa} + h_b)/e_c} \quad (3.71a)$$

$$s_{eff,4} = s_b \cdot \frac{1 + 0.5h_b/e_c}{2 + 0.5(h_a + h_{sa} + h_b)/e_c} \quad (3.71b)$$

- if $s_{eff,5} + s_{eff,n} \geq s_n$ the whole of s_n is effective, so revise as follows:

$$s_{eff,5} = s_b \cdot \frac{1 + 0.5(h_b + h_{sb})/e_c}{2.5 + 0.5(h_b + h_{sb})/e_c} \quad (3.72a)$$

$$s_{eff,n} = \frac{1.5 \cdot s_n}{2.5 + 0.5(h_b + h_{sb})/e_c} \quad (3.72b)$$

For a single stiffener, or for the stiffener closer to the compression flange in webs with two stiffeners, the elastic critical buckling stress $\sigma_{cr,sa}$ should be determined using:

$$\sigma_{cr,sa} = \frac{1.05 \cdot k_f \cdot E \cdot \sqrt{I_s \cdot t^3 \cdot s_1}}{A_{sa} \cdot s_2 \cdot (s_1 - s_2)} \quad (3.73)$$

172

in which s_1 is given by the following:

- for a single stiffener:

$$s_1 = 0.9 (s_a + s_{sa} + s_c) \quad (3.74a)$$

- for the stiffener closer to the compression flange, in webs with two stiffeners:

$$s_1 = s_a + s_{sa} + s_b + 0.5(s_{sb} + s_c) \quad (3.74b)$$

with

$$s_2 = s_1 - s_a - 0.5s_{sa} \quad (3.74c)$$

where

k_f is a coefficient that allows for partial rotational restraint of the stiffened web by the flanges;

I_s is the second moment of area of a stiffener cross section comprising the fold width s_{sa} and two adjacent strips, each of width $s_{eff,1}$, about its own centroidal axis parallel to the plane web elements, see Figure 3.41. In calculating I_s the possible difference in slope between the plane web elements on either side of the stiffener may be neglected.

In the absence of a more detailed investigation, the rotational restraint coefficient k_f may conservatively be taken as equal to 1.0 corresponding to a pin-jointed condition.

For a single stiffener in compression, or for the stiffener closer to the compression flange in webs with two stiffeners, the reduced effective area $A_{sa,red}$ should be determined from:

$$A_{sa,red} = \frac{\chi_d \cdot A_{sa}}{1 - (h_a + 0.5 \cdot h_{sa}) / e_c} \quad \text{but} \quad A_{sa,red} \leq A_{sa} \quad (3.75)$$

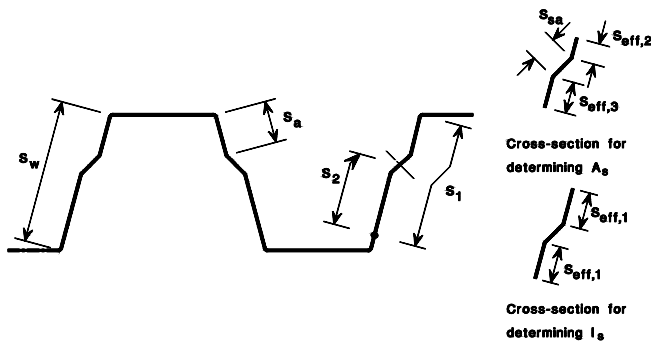


Figure 3.41 – Web stiffeners for trapezoidal profiled sheeting

If the flanges are unstiffened, the reduction factor χ_d should be obtained directly from $\sigma_{cr,sa}$ using the method given in §§3.7.3.1.

If the flanges are also stiffened, the reduction factor χ_d should be obtained using the method given in §§3.7.3.1, but with the modified elastic critical stress $\sigma_{cr,mod}$ given in §§3.7.3.4.4.

For a single stiffener in tension, the reduced effective area $A_{sa,red}$ should be taken as equal to A_{sa} .

For webs with two stiffeners, the reduced effective area $A_{sb,red}$ for the second stiffener, should be taken as equal to A_{sb} .

3. BEHAVIOUR AND RESISTANCE OF CROSS SECTION

In determining effective section properties, the reduced effective area $A_{sa,red}$ should be represented by using a reduced thickness $t_{red} = \chi_d t$ for all the elements included in A_{sa} .

The effective section properties of the stiffeners at serviceability limit states should be based on the design thickness t .

Optionally, the effective section properties may be refined iteratively by basing the location of the effective centroidal axis on the effective cross sections of the webs determined by the previous iteration and the effective cross sections of the flanges determined using the reduced thickness t_{red} for all the elements included in the flange stiffener areas A_s . This iteration should be based on an increased basic effective width $s_{eff,0}$ obtained from:

$$s_{eff,0} = 0.95 \cdot t \cdot \sqrt{\frac{E}{\gamma_{M0} \cdot \sigma_{com,Ed}}} \quad (3.76)$$

3.7.3.4.4 Sheeting with flange stiffeners and web stiffeners

In the case of sheeting with intermediate stiffeners in the flanges and in the webs, see Figure 3.42, interaction between the distortional buckling (flexural buckling of the flange stiffeners and the web stiffeners) should be allowed for by using a modified elastic critical stress $\sigma_{cr,mod}$ for both types of stiffeners, obtained from:

$$\sigma_{cr,mod} = \frac{\sigma_{cr,s}}{\sqrt[4]{1 + \left[\beta_s \frac{\sigma_{cr,s}}{\sigma_{cr,sa}} \right]^4}} \quad (3.77)$$

where

$\sigma_{cr,s}$ is the elastic critical stress for an intermediate flange stiffener, see §§3.7.3.4.2 for a flange with a single stiffener or with two stiffeners;

$\sigma_{cr,sa}$ is the elastic critical stress for a single web stiffener, or the stiffener closer to the compression flange in webs with two stiffeners, see §§3.7.3.4.3;

A_s is the effective cross section area of an intermediate flange stiffener;

A_{sa} is the effective cross section area of an intermediate web stiffener;

$\beta_s = 1 - (h_a + 0.5 h_{ha}) / e_c$ for a profile in bending;

$\beta_s = 1$ for a profile in axial compression.

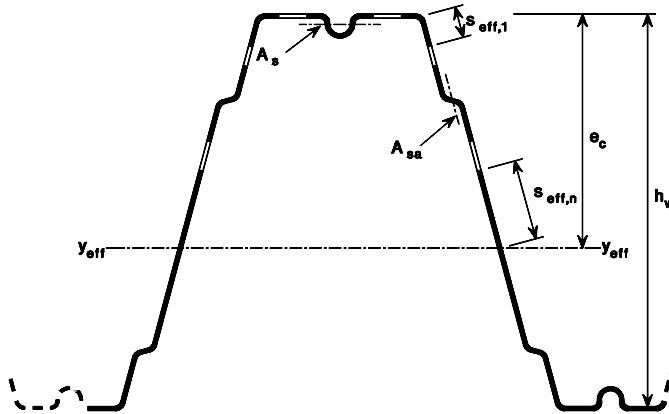


Figure 3.42 – Trapezoidal profiled sheeting with flange stiffeners and web stiffeners

3.8 RESISTANCE OF CROSS SECTIONS

3.8.1 General

The design values of the internal forces and moments at each cross section shall not exceed the design values of the corresponding resistances.

The design resistance of a cross section shall be determined either by calculation, using the methods given in this §3.8.1, or by design assisted by testing.

For design by calculation, the resistance of the cross section shall be determined for:

- axial tension, as given in §§3.8.2;
- axial compression, as given in §§3.8.3;
- bending moment, as given in §§3.8.4;
- shear force, as given in §§3.8.5;
- torsional moment, as given in §§3.8.6;
- local transverse forces, as given in §§3.8.7;
- combined bending and axial tension, as given in §§3.8.8;

3. BEHAVIOUR AND RESISTANCE OF CROSS SECTION

- combined bending and axial compression, as given in §§3.8.9;
- combined bending moment and shear force, as given in §§3.8.10;
- combined bending moment and local transverse force, as given in §§3.8.11.

Design assisted by testing may be used instead of design by calculation for any of these resistances. Design assisted by testing is particularly likely to be beneficial for cross sections with relatively high b_p/t ratios, e.g. in relation to inelastic behaviour, web crippling or shear lag.

For design by calculation, the effects of local buckling shall be taken into account by using effective section properties determined as specified in Section 3.7. In members with cross sections that are susceptible to cross sectional distortion, account shall be taken of possible lateral buckling of compression flanges and lateral bending of flanges generally.

3.8.2 Axial tension

The design value of the tension force N_{Ed} at each cross section should satisfy:

$$\frac{N_{Ed}}{N_{t,Rd}} \leq 1.0 \quad (3.78)$$

176

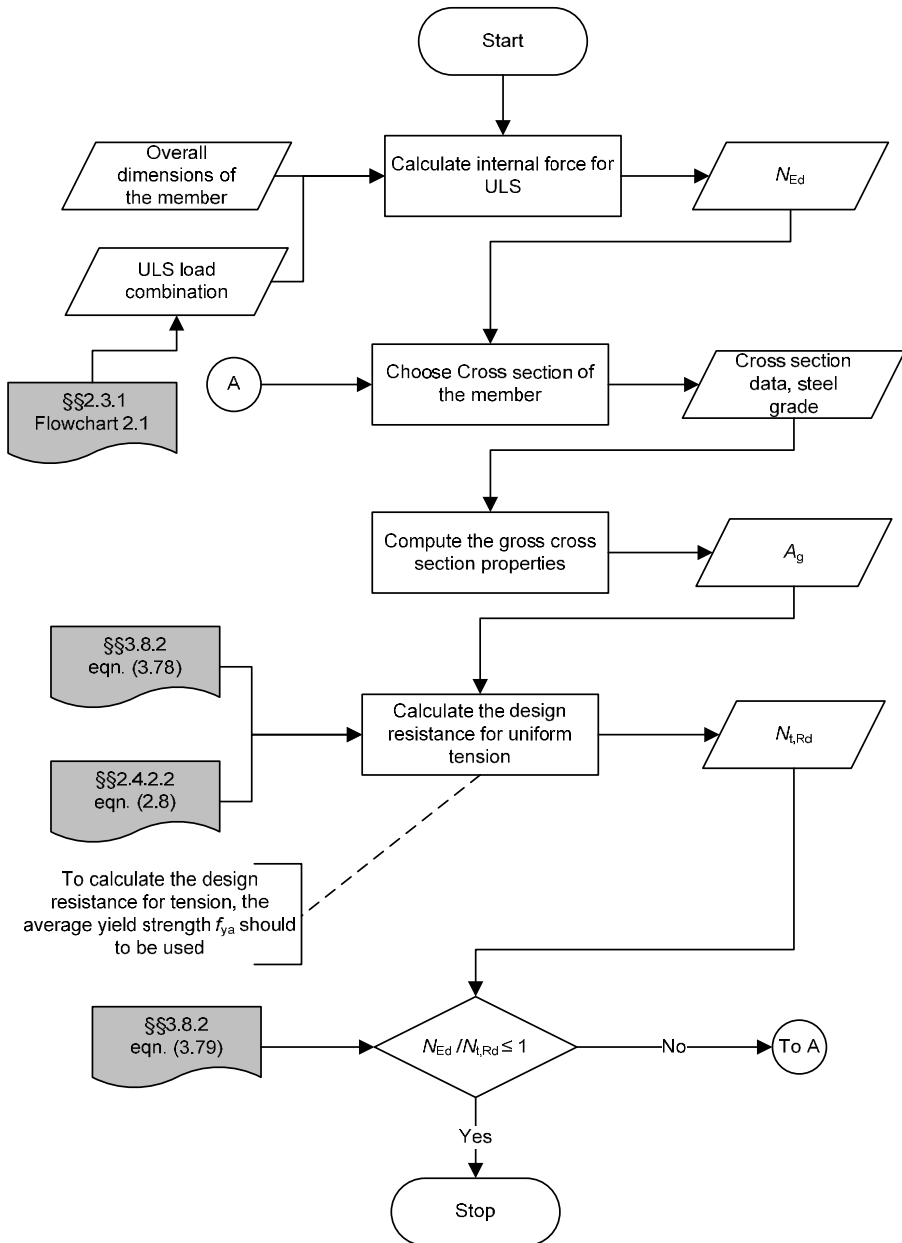
The design tension resistance of a cross section $N_{t,Rd}$ shall be determined from:

$$N_{t,Rd} = \frac{A_g \cdot f_{ya}}{\gamma_{M0}} \quad \text{but } N_{t,Rd} \leq F_{n,Rd} \quad (3.79)$$

where

- A_g is the gross area of the cross section;
- $F_{n,Rd}$ is the net-section resistance for the appropriate type of mechanical fastener;
- f_{ya} is the average yield strength (see §§2.4.2.2, eqn. (2.8)).

Flowchart 3.3 presents the schematically design of a cold-formed steel member in tension, while Example 3.3 present a numerical example.



Flowchart 3.3 – Design of a cold-formed steel cross section in tension (SF040a-EN-EU, Access Steel 2006)

3. BEHAVIOUR AND RESISTANCE OF CROSS SECTION

Example 3.3: Design of a cold-formed steel member in tension

Basic Data

Height of stud $H = 3.00 \text{ m}$

The dimensions of the cross section and the material properties are:

Total height $h = 150 \text{ mm}$

Total width of flange $b = 45 \text{ mm}$

Total width of edge fold $c = 16 \text{ mm}$

Internal radius $r = 3 \text{ mm}$

Nominal thickness $t_{nom} = 1.0 \text{ mm}$

Steel core thickness (§§2.4.2.3, eqn. (2.10)) $t = 0.96 \text{ mm}$

Basic yield strength $f_{yb} = 350 \text{ N/mm}^2$

Ultimate strength $f_u = 420 \text{ N/mm}^2$

Modulus of elasticity $E = 210000 \text{ N/mm}^2$

Poisson's ratio $\nu = 0.3$

Shear modulus $G = \frac{E}{2(1+\nu)} = 81000 \text{ N/mm}^2$

Partial factors (§§2.3.1) $\gamma_{M0} = 1.0$

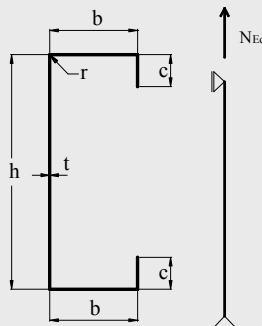
$\gamma_{M1} = 1.0$

178

Properties of the gross cross section

Gross cross section area: $A_g = 257 \text{ mm}^2$

The design value of the tension force on the stud $N_{Ed} = 68.26 \text{ kN}$



Resistance check of the cross section

The following criterion should be satisfied (§§3.8.2, eqn. (3.79)):

$$\frac{N_{Ed}}{N_{t,Rd}} \leq 1$$

where the design resistance of a cross section for uniform tension is (§§3.8.2, eqn. (3.78)):

$$N_{t,Rd} = \frac{f_{ya} A_g}{\gamma_{M0}}$$

f_{ya} – the average yield strength (§§2.4.2.2, eqn. (2.8))

$$f_{ya} = f_{yb} + (f_u - f_{yb}) \frac{knt^2}{A_g} \quad \text{but} \quad f_{ya} \leq \frac{f_u + f_{yb}}{2} = \frac{420 + 350}{2} = 385 \text{ N/mm}^2$$

where

k – coefficient depending on the type of forming; $k = 7$ for roll forming

n – the number of 90° bends in the cross section with an internal radius $r \leq 5t$; $n = 4$

$$f_{ya} = f_{yb} + (f_u - f_{yb}) \frac{knt^2}{A_g} = 350 + (420 - 350) \times \frac{7 \times 4 \times 0.96^2}{257} = 357 \text{ N/mm}^2$$

$$f_{ya} = 357 \text{ N/mm}^2 < \frac{f_u + f_{yb}}{2} = 385 \text{ N/mm}^2 \quad \text{– OK}$$

The design resistance will be:

$$N_{t,Rd} = \frac{f_{ya} A_g}{\gamma_{M0}} = \frac{357 \times 257}{1.0} = 91749 \text{ N} = 91.75 \text{ kN}$$

The resistance check is:

$$\frac{N_{Ed}}{N_{t,Rd}} = \frac{68.26}{91.75} = 0.744 < 1 \quad \text{– OK}$$

3.8.3 Axial compression

The design value of the compression force N_{Ed} at each cross section should satisfy:

$$\frac{N_{Ed}}{N_{c,Rd}} \leq 1.0 \quad (3.80)$$

The design compression resistance of a cross section $N_{c,Rd}$ shall be determined from the following:

- if its effective area A_{eff} is less than its gross area A_g :

$$N_{c,Rd} = \frac{A_{eff} \cdot f_{yb}}{\gamma_{M0}} \quad (3.81a)$$

- if its effective area A_{eff} is equal to its gross area A_g :

$$N_{c,Rd} = A_g \left(f_{yb} + (f_{ya} - f_{yb}) 4 \left(1 - \bar{\lambda}_e / \bar{\lambda}_{e0} \right) \right) / \gamma_{M0} \quad (3.81b)$$

but no more than $\frac{A_g \cdot f_{ya}}{\gamma_{M0}}$

where

A_{eff} is the effective area of the cross section, obtained from Section 3.7 by assuming a uniform compressive stress $\sigma_{com,Ed}$ equal to f_{yb}/γ_{M0} ;

f_{ya} is the average yield strength (see §§2.4.2.2, eqn. (2.8));

f_{yb} is the basic yield strength.

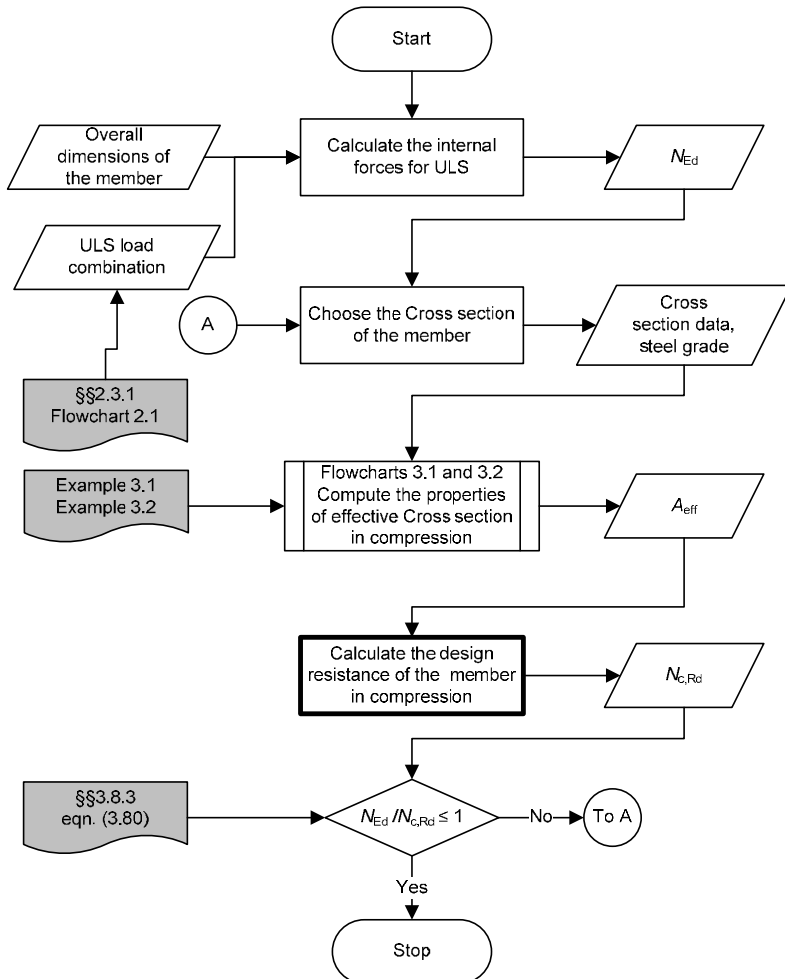
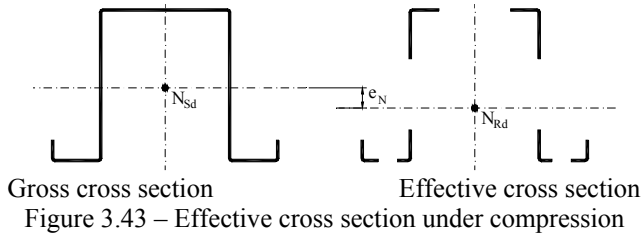
For plane elements $\bar{\lambda}_e = \bar{\lambda}_p$ and $\bar{\lambda}_{e0} = 0.673$, see §§3.7.2;

For stiffened elements $\bar{\lambda}_e = \bar{\lambda}_d$ and $\bar{\lambda}_{e0} = 0.65$, see §§3.7.3.

The internal axial force in a member shall be taken as acting at the centroid of its gross cross section. In determining A_{eff} , holes for fasteners at the column ends need not to be taken into account.

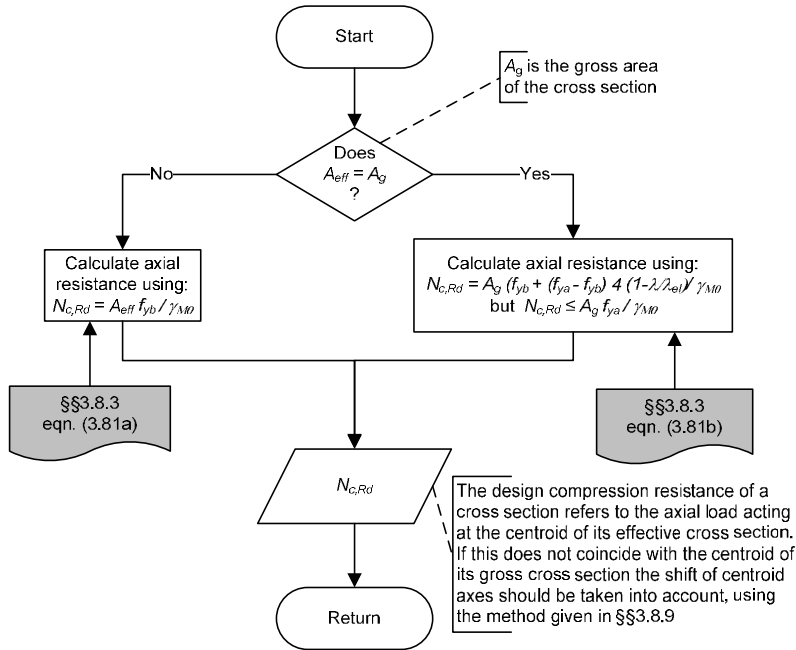
The resistance of a cross section to axial compression shall be assumed to act at the centroid of its effective cross section. If this does not coincide with the centroid of its gross cross section, the shift e_N of the centroidal axes (see Figure 3.43) shall be taken into account, using the method given in §§3.8.6. When the shift of the neutral axis increases the design capacity, then the shift should be neglected only if the shift has been calculated at the yield strength and not at the actual compressive stresses.

Flowcharts 3.4 and 3.5 present schematically the design of a cold-formed steel cross section in compression, while Example 3.4 presents a numerical example.



Flowchart 3.4 – Design resistance of a cold-formed steel cross section in compression (SF039a-EN-EU, Access Steel 2006)

3. BEHAVIOUR AND RESISTANCE OF CROSS SECTION



Flowchart 3.5 – Calculate the design resistance of the cross section in compression – $N_{c,Rd}$ (SF039a-EN-EU, Access Steel 2006)

Example 3.4: Design resistance of a cold-formed steel member in compression

182

Basic Data

Height of stud $H = 3.10$ m

Spacing between studs $S = 0.6$ m

Span of floor $L = 5$ m

Spacing between floor joists $S = 0.6$ m

Distributed loads applied to the floor:

dead load – lightweight slab 1.20 kN/m²

$$q_G = 1.20 \times 0.6 = 0.72 \text{ kN/m}$$

imposed load 2.50 kN/m²

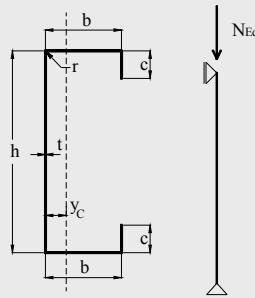
$$q_Q = 2.50 \times 0.6 = 1.50 \text{ kN/m}$$

Ultimate Limit State concentrated load

from upper level and roof: $Q = 14.0$ kN

The dimensions of one cross section and the material properties are:

Total height	$h = 150 \text{ mm}$
Total width of flange	$b = 45 \text{ mm}$
Total width of edge fold	$c = 15 \text{ mm}$
Internal radius	$r = 3 \text{ mm}$
Nominal thickness	$t_{nom} = 1 \text{ mm}$
Steel core thickness	$t = 0.96 \text{ mm}$



Basic yield strength	$f_{yb} = 350 \text{ N/mm}^2$
Modulus of elasticity	$E = 210000 \text{ N/mm}^2$
Poisson's ratio	$\nu = 0.3$
Shear modulus	$G = \frac{E}{2(1+\nu)} = 81000 \text{ N/mm}^2$
Partial factors (§§2.3.1)	$\gamma_{M0} = 1.0$ $\gamma_{M1} = 1.0$ $\gamma_G = 1.35$ – permanent loads $\gamma_Q = 1.50$ – variable loads

Derived data (section properties and action effects)

Properties of the gross cross section

Gross cross section area:	$A = 255 \text{ mm}^2$
Position of z - z axis of the gross cross section with respect to the web:	$y_c = 12.08 \text{ mm}$

Properties of the effective cross section (§§3.7.3, Flowcharts 3.1 and 3.2)

The properties of effective cross section were calculated following the procedures presented in Examples 3.1 and 3.2.

Effective area of the cross section in compression:

$$A_{eff} = 115 \text{ mm}^2$$

Position of z-z axis of the effective cross section with respect to the web:

$$y_{c,eff} = 16.28 \text{ mm}$$

Effective section modulus for bending about weak axis:

$$W_{eff,z,com} = 1561 \text{ mm}^3$$

$$W_{eff,z,ten} = 4127 \text{ mm}^3$$

The applied concentrated load on the stud (only compression) – §§2.3.1, Flowchart 2.1

$$N_{Ed} = (\gamma_G q_G + \gamma_Q q_Q) L + Q = (1.35 \times 0.72 + 1.50 \times 1.50) \times 5 + 14 = 30.11 \text{ kN}$$

Resistance check of the cross section (§§3.8.9)

The following condition should be satisfied:

$$\frac{N_{Ed}}{N_{c,Rd}} + \frac{M_{z,Ed} + \Delta M_{z,Ed}}{M_{cz,Rd,com}} \leq 1$$

184

where

$$N_{c,Rd} = A_{eff} f_{yb} / \gamma_{M0} \quad (\text{§§3.8.3, eqn. (3.81)})$$

$$M_{cz,Rd,com} = W_{eff,com} f_{yb} / \gamma_{M0} \quad (\text{§§3.8.4, eqn. (3.83a)})$$

$$\Delta M_{z,Ed} = N_{Ed} e_{Nz} \quad (\text{§§3.8.9})$$

e_{Nz} – is the shift of centroidal z-z axis

$$M_{z,Ed} = 0$$

$$e_{Nz} = y_{c,eff} - y_c = 16.28 - 12.08 = 4.2 \text{ mm}$$

The resistance check is:

$$\frac{30110}{115 \times 350 / 1.0} + \frac{0 + 30110 \times 4.2}{1561 \times 350 / 1.0} = 0.979 < 1 - \text{OK}$$

3.8.4 Bending moment

3.8.4.1 Elastic and elastoplastic resistance with yielding at the compressed flange

The design value of the bending moment M_{Ed} at each cross section should satisfy:

$$\frac{M_{Ed}}{M_{c,Rd}} \leq 1 \quad (3.82)$$

The moment resistance of a cross section for bending about a principal axis shall be obtained from the following:

- if the effective section modulus W_{eff} is less than the gross elastic section modulus W_{el} :

$$M_{c,Rd} = \frac{W_{eff} \cdot f_{yb}}{\gamma_{M0}} \quad (3.83a)$$

- if the effective section modulus W_{eff} is equal to the gross elastic section modulus W_{el} :

$$M_{c,Rd} = f_{yb} (W_{el} + (W_{pl} - W_{el})4(1 - \bar{\lambda}_{e,max} / \bar{\lambda}_{e0})) / \gamma_{M0} \quad (3.83b)$$

but not more than $W_{pl}f_{yb} / \gamma_{M0}$

where

f_{yb} is the basic yield strength;

$\bar{\lambda}_{e,max}$ is the slenderness of the element which correspond to the largest value of $\bar{\lambda}_e / \bar{\lambda}_{e0}$.

For stiffened elements $\bar{\lambda}_e = \bar{\lambda}_p$ and $\bar{\lambda}_{e0} = 0.5 + \sqrt{0.25 - 0.055(3 + \psi)}$

where ψ is the stress ratio;

For unstiffened elements $\bar{\lambda}_e = \bar{\lambda}_p$ and $\bar{\lambda}_{e0} = 0.673$, see §§3.7.2;

Equation (3.83b) is applicable provided that the following conditions are satisfied:

a) Bending moment is applied only about one principal axes of the cross section;

b) The member is not subjected to torsion or flexural-torsional or lateral-torsional or distortional buckling;

3. BEHAVIOUR AND RESISTANCE OF CROSS SECTION

c) The angle ϕ between the web (see Figure 3.50) and the flange is larger than 60° .

If the above conditions are not fulfilled the following expression may be used:

$$M_{c,Rd} = W_{el} f_{ya} / \gamma_{M0} \quad (3.84)$$

The effective section modulus W_{eff} shall be based on an effective cross section that is subject only to bending moment about the relevant principal axis, with a maximum stress $\sigma_{max,Ed} = f_{yb} / \gamma_{M0}$, allowing for the effects of local buckling as specified in Section 3.7. Where shear lag is relevant, allowance shall also be made for its effects as specified in §§3.8.4.3.

The stress ratio $\psi = \sigma_2 / \sigma_1$ used to determine the effective portions of the web may be obtained by using the effective area of the compression flange but the gross area of the web, see Figure 3.44.

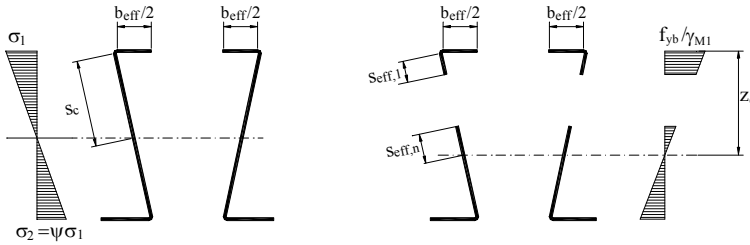


Figure 3.44 – Effective cross section for resistance to bending moments

If yielding occurs first at the compression edge of the cross section, unless the conditions given in §§3.8.4.2 are met the value of W_{eff} shall be based on a linear distribution of stress across the cross section.

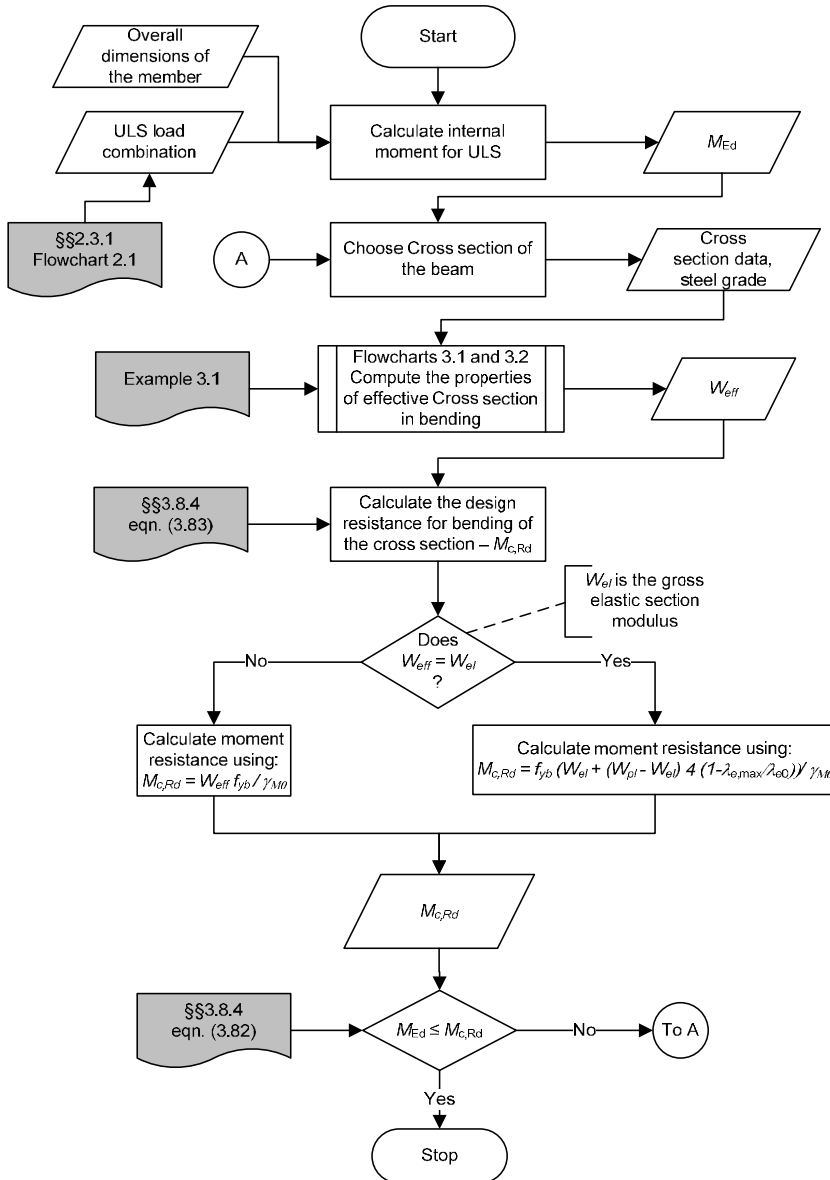
For biaxial bending the following criterion shall be satisfied:

$$\frac{M_{y,Ed}}{M_{cy,Rd}} + \frac{M_{z,Ed}}{M_{cz,Rd}} \leq 1 \quad (3.85)$$

where

- $M_{y,Ed}$ is the applied bending moment about the major axis;
- $M_{z,Ed}$ is the applied bending moment about the minor axis;
- $M_{cy,Rd}$ is the resistance of the cross section if subject only to moment about the y - y axis;
- $M_{cz,Rd}$ is the resistance of the cross section if subject only to moment about the z - z axis.

Flowchart 3.6 presents schematically the design procedure for determining the bending moment design resistance of a cold-formed steel beam. In §3.8.7, Flowchart 3.7 presents the general procedure for a simply supported member in bending, considering the presence of bending moment, shear force and reaction, while Example 3.5 presents a numerical example.



Flowchart 3.6 – Design resistance of a cold-formed steel cross section in bending

3.8.4.2 Elastic and elastoplastic resistance with yielding at the tension flange only

Provided that bending moment is applied only about one principal axis of the cross section, and provided that yielding occurs first at the tension edge, plastic reserves in the tension zone may be utilized without any strain limit until the maximum compressive stress $\sigma_{com,Ed}$ reaches f_{yb}/γ_{M0} . In this paragraph the pure bending case is considered. For combined axial load and bending the procedures described in §§3.8.8 and §§3.8.9 must be applied, as applicable.

When accounting for plastic reserve capacity, the effective partially plastic section modulus $W_{pp,eff}$ should be based on a stress distribution that is bilinear in the tension zone but linear in the compression zone. Figure 3.45 illustrates the bilinear stress distribution.

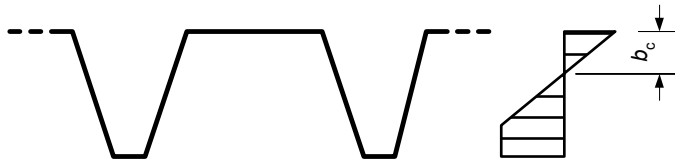


Figure 3.45 – Measure b_c for determination of effective width

In the absence of a more detailed analysis, the effective width b_{eff} of an element subject to stress gradient may be obtained using §§3.7.2 by basing b_c on a bilinear stress distribution, by assuming $\psi = -1$.

3.8.4.3 Effects of shear lag

Shear lag in flanges may be neglected if $b_0 < L_e/50$ where b_0 is taken as the flange outstand or half the width of an internal element (see Figure 3.46) and L_e is the length between points of zero bending moment, see Figure 3.47.

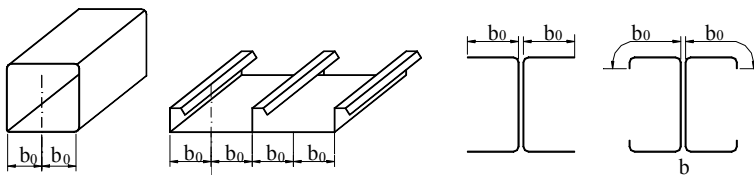


Figure 3.46 – Width b_0 contributing to shear lag

Where the above limit for b_0 is exceeded the effects due to shear lag in flanges should be considered at serviceability and fatigue limit state verifications by the use of an effective^s width as presented below and a stress distribution according to Figure 3.49. For the ultimate limit state verification an effective area may be used.

The effective^s width b_{eff} for shear lag under elastic conditions should be determined from:

$$b_{eff} = \beta b_0 \tag{3.86}$$

where the effective^s factor β is given in Table 3.7. This effective width may be relevant for serviceability and fatigue limit states.

Provided adjacent spans do not differ more than 50% and any cantilever span is not larger than half the adjacent span the effective lengths L_e may be determined from Figure 3.47. For all other cases L_e should be taken as the distance between adjacent points of zero bending moment.

Table 3.7 – Effective^s width factor β

κ	Verification	β – value
$\kappa \leq 0.02$		$\beta = 1.0$
	sagging bending	$\beta = \beta_1 = \frac{1}{1 + 6.4 \kappa^2}$
$0.02 < \kappa \leq 0.70$	hogging bending	$\beta = \beta_2 = \frac{1}{1 + 6.0 \left(\kappa - \frac{1}{2500 \kappa} \right) + 1.6 \kappa^2}$
	sagging bending	$\beta = \beta_1 = \frac{1}{5.9 \kappa}$
> 0.70	hogging bending	$\beta = \beta_2 = \frac{1}{8.6 \kappa}$
all κ	end support	$\beta_0 = (0.55 + 0.025 / \kappa) \beta_1$, but $\beta_0 < \beta_1$
all κ	Cantilever	$\beta = \beta_2$ at support and at the end

$$\kappa = \alpha_0 b_0 / L_e \quad \text{with} \quad \alpha_0 = \sqrt{1 + \frac{A_{st}}{b_0 t}}$$

in which A_{st} is the area of all longitudinal stiffeners within the width b_0 and other symbols are as defined in Figure 3.47 and Figure 3.48.

3. BEHAVIOUR AND RESISTANCE OF CROSS SECTION

The distribution of longitudinal stresses across the flange plate due to shear lag should be obtained from Figure 3.49.

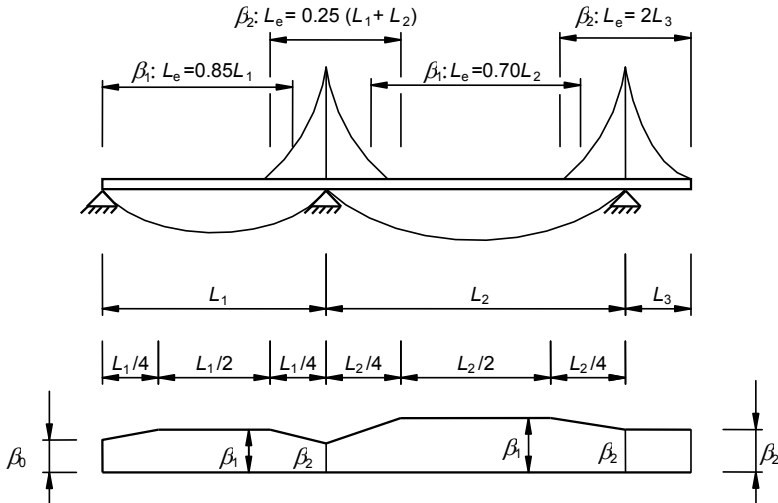


Figure 3.47 – Effective length L_e for continuous beam and distribution of effective^s width

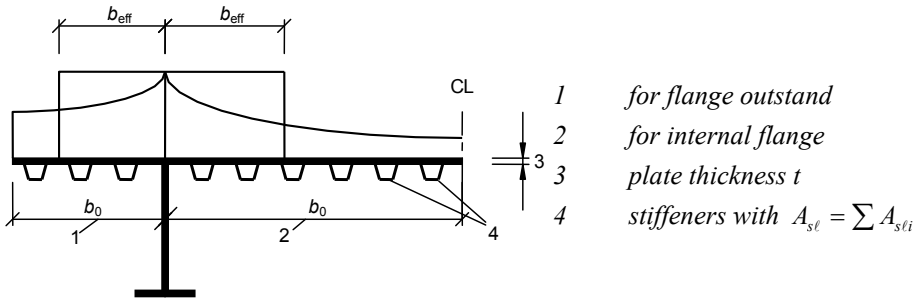


Figure 3.48 – Notations for shear lag

At the ultimate limit state shear lag effects may be determined as follows:

- a) elastic shear lag effects as determined for serviceability and fatigue limit states;
- b) combined effects of shear lag and of plate buckling;
- c) elastoplastic shear lag effects allowing for limited plastic strains.

The combined effects of plate buckling and shear lag may be taken into account by using A_{eff} as given by:

$$A_{eff} = A_{c,eff} \beta_{ult} \tag{3.87}$$

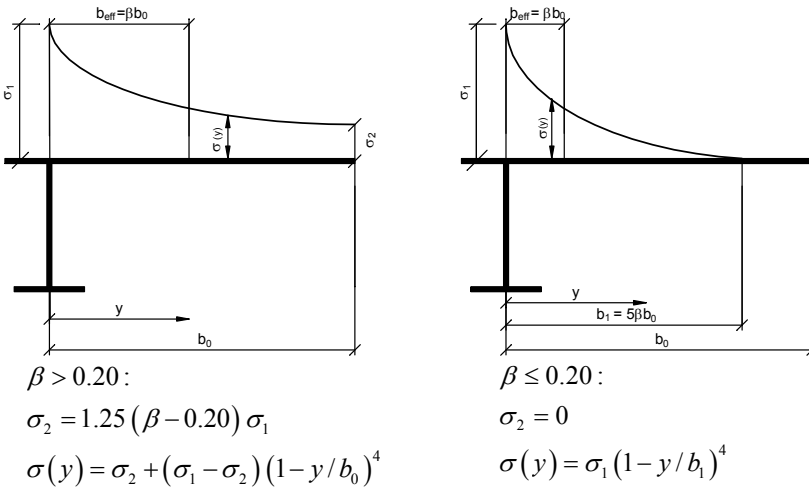
where

$A_{c,eff}$ is the effective^P area of the compression flange due to plate buckling;

β_{ult} is the effective^S width factor for the effect of shear lag at the ultimate limit state, which may be taken as β determined from Table 3.7 with α_0 replaced by

$$\alpha_0^* = \sqrt{\frac{A_{c,eff}}{b_0 t_f}} \tag{3.88}$$

t_f is the flange thickness.



σ_1 is calculated with the effective width of the flange b_{eff}

Figure 3.49 – Distribution of stresses due to shear lag

Elastoplastic shear lag effects allowing for limited plastic strains may be taken into account using A_{eff} as follows:

$$A_{eff} = A_{c,eff} \beta^\kappa \geq A_{c,eff} \beta \tag{3.89}$$

where β and κ are taken from Table 3.7.

The eqns. (3.87) and (3.89) may also be applied for flanges in tension in which case $A_{c,eff}$ should be replaced by the gross area of the tension flange.

3.8.5 Shear force

The design value of the shear force V_{Ed} at each cross section should satisfy:

$$\frac{V_{Ed}}{V_{b,Rd}} \leq 1 \tag{3.90}$$

where $V_{b,Rd}$ is the design shear resistance.

The design shear resistance $V_{b,Rd}$ shall be determined from:

$$V_{b,Rd} = \frac{\frac{h_w}{\sin \phi} \cdot t \cdot f_{bv}}{\gamma_{M0}} \tag{3.91}$$

where

- f_{bv} is the shear buckling strength considering buckling according to Table 3.8;
- h_w is the web height between the midlines of the flanges, see Figure 3.4c;
- ϕ is the slope of the web relative to the flanges, see Figure 3.50.

The shear buckling strength f_{bv} for the appropriate value of the relative web slenderness $\bar{\lambda}_w$ shall be obtained from Table 3.8.

Table 3.8 – Shear buckling strength f_{bv}

Relative web slenderness	Web without stiffening at the support	Web with stiffening at the support ¹⁾
$\bar{\lambda}_w \leq 0.83$	$0.58 f_{yb}$	$0.58 f_{yb}$
$0.83 < \bar{\lambda}_w < 1.40$	$0.48 f_{yb} / \bar{\lambda}_w$	$0.48 f_{yb} / \bar{\lambda}_w$
$\bar{\lambda}_w \geq 1.40$	$0.67 f_{yb} / \bar{\lambda}_w^2$	$0.48 f_{yb} / \bar{\lambda}_w$

¹⁾ Stiffening at the support, such as cleats, arranged to prevent distortion of the web and designed to resist the support reaction.

The relative web slenderness $\bar{\lambda}_w$ shall be obtained from the following:

$$\bar{\lambda}_w = \sqrt{\frac{f_{yb} / \sqrt{3}}{\tau_{cr}}} = \frac{s_w}{t} \sqrt{\frac{12 \cdot (1 - \nu^2) \cdot f_{yb}}{\sqrt{3} \cdot \pi^2 \cdot E \cdot k_\tau}} \tag{3.92a}$$

- for webs without longitudinal stiffeners:

$$\bar{\lambda}_w = 0.346 \frac{s_w}{t} \sqrt{\frac{f_{yb}}{E}} \quad (3.92b)$$

- for webs with longitudinal stiffeners, see Figure 3.50:

$$\bar{\lambda}_w = 0.346 \frac{s_d}{t} \sqrt{\frac{5.34 f_{yb}}{k_\tau E}} \quad \text{but} \quad \bar{\lambda}_w \geq 0.346 \frac{s_p}{t} \sqrt{\frac{f_{yb}}{E}} \quad (3.92c)$$

with:

$$k_\tau = 5.34 + \frac{2.10}{t} \left(\frac{\Sigma I_s}{s_d} \right)^{1/3} \quad (3.93)$$

where

- I_s is the second moment of area of the individual longitudinal stiffener as defined in §§3.7.3.4.3, about the axis $a-a$, see Figure 3.50;
- s_d is the total developed slant height of the web, see Figure 3.50;
- s_p is the slant height of the largest plane element in the web, see Figure 3.50;
- s_w is the total slant height of the web, as shown in Figure 3.50, between the midpoints of the corners, taken as the median points of the corners, see Figure 3.4c.

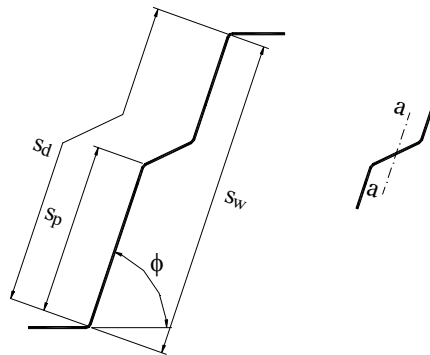


Figure 3.50 – Longitudinally stiffened web

Flowchart 3.7 presents schematically the general procedure for the design of a simply supported cold-formed steel beam, while Example 3.5 presents a numerical example.

3.8.6 Torsional moment

In light gauge steel sections, the role played by torsion is enhanced in comparison to stockier hot-rolled sections. There are three reasons why this is so (Davies, 1991):

1. Most cold-formed members have an open cross section and often have a shear centre which lies outside the section. It follows that application of the load through the shear centre is difficult to achieve and cold-formed beams are, in fact, subjected to an applied torsion so that twisting of the section occurs if it is not restrained against torsion;
2. For open cross sections, the torsional constant I_t , which is directly related to the resistance to twist, is proportional to the material thickness raised to the third power. It follows that thin walled cold-formed sections have less resistance to torsion than hot-rolled ones;
3. When torsion is restrained, for instance at the supports, longitudinal stresses appear which may be of the same order of magnitude as the bending stresses and should be accounted for. A section that is designed to be fully stressed in bending may therefore be overstressed when restrained torsion is taken into account.

Hence the load-bearing resistance may be reduced substantially by torsion and generally, torsional moment should be avoided in construction. However, in practice, light gauge steel beams are often loaded through the members that they support and these, in turn, provide torsional restraint. In many frequent applications (e.g. purlins, floor joists, wall studs) the loading and restraint are both continuous and to some extent self-equilibrating so that the tendency to twist is greatly reduced.

In design, the superposition of stresses due to axial force, bending moments and torsional moments must remain below the limit of yield stress. Additionally, the superposition of shear stresses has to be considered.

The elementary theory of torsion is usually known as St. Venant's theory. For a member under uniform torsion, the angle of rotation per unit length is related to the torsional moment through the following equation:

$$\frac{T_t}{GI_t} = \frac{d\varphi}{dx} \quad (3.94)$$

where

T_t = is the torsional moment;

I_t = is the torsion constant;

G = is the shear modulus;

φ = is the twist of the section;

x = is a variable with the direction of the longitudinal axis of the member.

The torsion constant I_t is given with sufficient accuracy for all engineering purposes for *an open cross section* of uniform thickness t by

$$I_t = \frac{l \cdot t^3}{3} \quad (3.95)$$

where l is the length of the middle line of the cross section.

For a closed cross section, the torsional constant I_t is:

$$I_t = \frac{4A^2t}{l} \quad (3.96)$$

where A is the area enclosed by the mid-thickness line.

Equation (3.94) is concerned solely with *shear stress* and this defines the restriction of the St. Venant theory as it is based on the fundamental assumption that *plane sections remain plane*. This assumption holds for circular sections only but is not applicable to both open and non-circular closed sections. The cross sections of light gauge steel members in torsion do not generally remain plane but undergo warping. It is convenient to illustrate the basic phenomenon with reference to a doubly symmetrical I-section as shown in Figure 3.51. However, warping is of more general occurrence in sections of all types.

Figure 3.51(a) shows a member subjected to uniform torsion with no restraint to warping. The member twists, as shown in plan in Figure 3.51(b), only the web deforms by pure twisting while the flanges rotate as rigid bodies. The section as a whole thus departs from its original plane cross section and this type of deformation is known as warping. If no restraint is provided to resist this deformation then no additional longitudinal stresses are developed.

If this warping is restrained, for instance in the case of a cantilever (see Figure 3.51(c)), the flanges are forced to bend in the horizontal direction. This in-plane bending of the flanges is clockwise for one flange and anti-clockwise for the other so that the effect is that of two equal and opposite moments. This type of behaviour was the subject of a classical investigation

by Vlaslov (1961) who termed this force system induced in the flanges by warping restraint a *bimoment*.

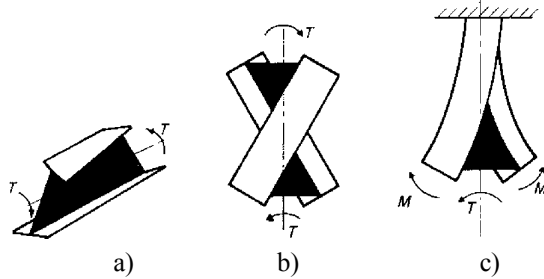


Figure 3.51 – Unrestrained and restrained warping: a) Member subject to uniform unrestrained torque, b) Plan view of unrestrained torque, c) Plan view of restrained torque showing components M of the bimoment (Davies, 1991)

The bimoment B has units of force \times distance² and for an I-section can be considered as a combination of the moments M and the depth h of the web as shown in Figure 3.51(c). Thus

$$B = M \cdot h \tag{3.97}$$

The presence of a bimoment causes longitudinal and shear stresses in the section. The longitudinal stresses act in the same sense as the ordinary flexural stresses and may be of the same order of magnitude. It follows that consideration of the combined longitudinal stresses due to both bending and warping is often necessary.

The longitudinal stress σ associated with a bimoment B is given by:

$$\sigma = \frac{B\omega}{I_w} \tag{3.98}$$

where I_w is a property of the cross section termed the warping constant and ω is the sectorial coordinate which varies around the section.

Values of I_w and ω for some common sections, together with I_t and the position of the shear centre are shown in Table 3.9.

Therefore, eqn. (3.98) makes possible the determination of the longitudinal stresses due to restrained torsion provided that the bimoment, warping constant and sectorial coordinates are known. The latter two quantities are properties of the cross section but the bimoment is a function

also of the loading and support conditions and must be evaluated separately for each given situation.

Table 3.9 – Torsional properties of some common cross sections

	Warping constant I_w	Torsion constant I_t	e for shear centre	Sectorial coordinate values ω
	$\frac{I_z b_w^2}{4}$ or $\frac{b_w^2 b_f^3 t_f}{24}$	$\frac{2b_f t_f^3 + b_w t_w^3}{3}$ or if $t_w = t_f$ $\frac{t^3}{3}(2b_f + b_w)$	0	
	$\frac{b_w^2 b_f^3 t}{12} \left[\frac{2 + \frac{3b_f}{b_w}}{1 + \frac{6b_f}{b_w}} \right]$	$\frac{t^3}{3}(2b_f + b_w)$	$\frac{3b_f^2}{6b_f + b_w}$	
	$\frac{b_f^2 t}{6} (4a^3 + 3b_w^2 a + 6b_w a^3 + b_f b_w^2) - I_y e^2$	$\frac{t^3}{3}(2b_f + 2a + b_w)$	$\frac{b_f b_w^2}{I_y} \cdot at \cdot \left[\frac{1}{2} + \frac{b_f}{4a} - \frac{2a^2}{3b_w^2} \right]$	
	$\frac{b_f^2 t}{12(2b_f + b_w + 2a)} \{ b_w^2 (b_f^2 + 2b_f b_w + 4b_f a + 6b_w a) + 4a^2 (3b_f b_w + 3b_w^2 + 4b_f a + 2b_w a + a^2) \}$	$\frac{t^3}{3}(2b_f + 2a + b_w)$	0	
	$\left(\frac{b_f^3 b_w^2 t}{12} \right) \left(\frac{b_f + 2b_w}{2b_f + b_w} \right)$	$\frac{t^3}{3}(2b_f + b_w)$	0	
	$\frac{t^3}{36}(b_f^3 + b_w^3)$	$\frac{t^3}{3}(b_w + b_f)$	0	Not relevant

Uniform torsion induces twisting of component elements that is caused by the rotation of the cross sections about the longitudinal axis. As a consequence, shear stresses appear which balance the applied torsional moment T . Under these circumstances, the resistance to the torsional moment T exclusively results from St. Venant's torsion, T_t . Although longitudinal warping displacements may exist, they do not introduce longitudinal stresses.

In non-uniform torsion, besides the St. Venant shear stresses, longitudinal strains also exist (because warping varies along the member). These longitudinal strains generate self-equilibrating normal stresses at the cross sectional level that, depending on the level of resistance to warping, vary along the member. The existence of varying normal stresses implies (by equilibrium in the longitudinal direction) the existence of additional shear stresses that also resist to torsional moments, leading to:

$$T = T_t + T_w \quad (3.99)$$

The applied torsional moment T is thus balanced by two terms, one due to the torsional rotation of the cross section, T_t , and the other caused by the restraint to warping, designated by warping torsion, T_w .

The equations relevant to this problem will be derived for a thin-walled I-section and then generalised. From eqn. (3.94) results:

198

$$T_t = GI_t \frac{d\phi}{dx} \quad (3.100)$$

The second part of the torque, T_w , is found by considering the bending of the flanges due to warping. When an I-section rotates about the x -axis as shown in Figure 3.52, the lateral deflection of the flanges v can, for small rotations, be obtained as:

$$v = \frac{\phi h}{2} \quad (3.101)$$

The lateral bending moment in each flange M_f will be:

$$M_f = EI_f \frac{d^2v}{dx^2} \quad (3.102)$$

where I_f is the second moment of area of the flange about the z -axis. Substituting for v gives

$$M_f = EI_f \frac{h}{2} \frac{d^2 \phi}{dx^2} \quad (3.103)$$

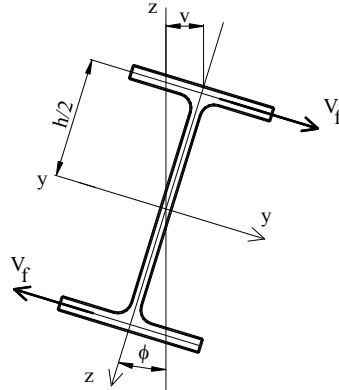


Figure 3.52 – Warping torsion of an I-section

The shear forces across the width of each flange V_f will be given by:

$$V_f = \frac{dM_f}{dx} = EI_f \frac{h}{2} \frac{d^3 \phi}{dx^3} \quad (3.104)$$

The couple produced by these two shear forces, provides the second part of the resistance to twist T_w . Thus

$$T_w = V_f h = EI_f \frac{h^2}{2} \frac{d^3 \phi}{dx^3} = EI_w \frac{d^3 \phi}{dx^3} \quad (3.105)$$

199

where, for a thin-walled I-section ($I_f \cong I_y/2$), $I_w = \frac{I_f h^2}{2} \cong \frac{I_y h^2}{4}$ is the warping constant and EI_w is the warping stiffness of the section.

Combining eqns. (3.99), (3.100) and (3.105) results in,

$$T = T_t + T_w = GI_t \frac{d\phi}{dx} - EI_w \frac{d^3 \phi}{dx^3} \quad (3.106)$$

This is the general equation for the torsion of a non-circular section. The evaluation of the longitudinal stresses and shear stresses due to an applied torque requires the solution of this equation with appropriate boundary conditions.

Alternatively, by differentiation,

3. BEHAVIOUR AND RESISTANCE OF CROSS SECTION

$$\frac{dT}{dx} = -EI_w \frac{d^4\varphi}{dx^4} + GI_t \frac{d^2\varphi}{dx^2} = -m \quad (3.107)$$

or

$$\frac{d^4\varphi}{dx^4} - k^2 \frac{d^2\varphi}{dx^2} = \frac{m}{EI_w} \quad (3.108)$$

where $k = \sqrt{\frac{GI_t}{EI_w}}$ and m is the intensity of a distributed torsional moment ($m = 0$ for a concentrated torsional moment).

It may be noted that it also follows from eqn. (3.103) that the bimoment is related to twist according to:

$$B = -EI_w \frac{d^2\varphi}{dx^2} \quad (3.109)$$

In order to calculate values of bimoment and then to evaluate the stresses arising from restrained warping, it is necessary to obtain solutions of the equation for torsion.

The general solution of eqn. (3.108) is,

$$\varphi = C_1 \cosh kx + C_2 \sinh kx + C_3 x + C_4 + \varphi_0 \quad (3.110)$$

where

C_1 to C_4 are constants;

φ_0 is the particular solution; $\varphi_0 = 0$ for $m = 0$, or $= \frac{mx^2}{2GI_t}$ for uniform

m .

The values of the constants C_1 to C_4 are determined by substituting known boundary conditions into eqn. (3.110).

The two most common idealised support conditions are:

- (1) Fixed end – one which is built in and can neither twist nor warp, i.e.

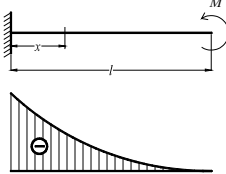
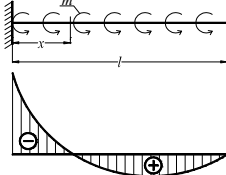
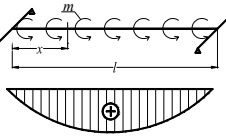
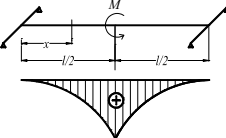
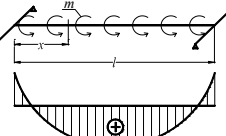
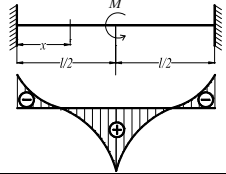
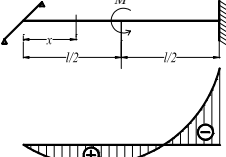
$$\varphi = 0, \quad \frac{d\varphi}{dx} = 0 \quad (3.111)$$

- (2) Simply supported end – one which cannot twist but is free to warp and is therefore free of longitudinal stresses due to torsion

$$\varphi = 0, \quad \frac{d^2\varphi}{dx^2} = 0 \quad (\text{i.e. } B = 0) \quad (3.112)$$

Although it is possible to obtain these idealised conditions in practice, the support conditions that are usually provided fall somewhere between the two so that accurate boundary conditions are difficult to specify. The values of bimoment for common boundary conditions are presented in Table 3.10.

Table 3.10 – Bimoment variation for common boundary conditions

Load condition	Bimoment equation	Maximum values	
	$B_{\omega} = -Ml \frac{\sinh k(l-x)}{kl \cdot \cosh kl}$	$x = 0$	$B_{\omega} = Mlb$
	$B_{\omega} = -\frac{m}{k^2 \cdot \cosh kl} \cdot [kl \cdot \sinh k(l-x) - \cosh kl + \cosh kx]$	$x = 0$	$B_{\omega} = ml^2 c$
	$B_{\omega} = \frac{m}{k^2} \cdot \left[1 - \frac{\cosh k\left(\frac{l}{2}-x\right)}{\cosh \frac{kl}{2}} \right]$	$x = \frac{l}{2}$	$B_{\omega} = ml^2 p$
	$B_{\omega} = \frac{M}{2k} \cdot \frac{\sinh kx}{\cosh \frac{kl}{2}}$	$x = \frac{l}{2}$	$B_{\omega} = \frac{Ml}{2} f$
	$B_{\omega} = \frac{m}{k^2} \cdot \left[1 - \frac{kl \cdot \cosh k\left(\frac{l}{2}-x\right)}{2 \cdot \sinh \frac{kl}{2}} \right]$	$x = 0$ $x = l$	$B_{\omega} = ml^2 g$ $B_{\omega} = ml^2 j$
	$B_{\omega} = \frac{M}{2k} \cdot \frac{\cosh kx - \cosh k\left(\frac{l}{2}-x\right)}{\sinh \frac{kl}{2}}$	$x = 0$ $x = \frac{l}{2}$ $x = l$	$B_{\omega} = \frac{Ml}{2} n$
	$B_{\omega} = \frac{m}{k^2} \cdot [1 - \cosh kx + \frac{1 + kl \cdot \sinh kl - \cosh kl - \frac{k^2 l^2}{2}}{kl \cdot \cosh kl - \sinh kl} \cdot \sinh kx]$	$x = l$	$B_{\omega} = \frac{ml}{2} w$

3. BEHAVIOUR AND RESISTANCE OF CROSS SECTION

	$B_{\omega 1} = \frac{M}{k} \cdot \frac{1}{kl \cdot \sinh kl - \sinh kl} \cdot \left(kl \cdot \cosh \frac{kl}{2} - \sinh \frac{kl}{2} - \frac{kl}{2} \right) \cdot \sinh kx$ $B_{\omega 2} = \frac{M}{k} \cdot \left[\frac{\text{sh} \cdot kx}{kl \cdot \text{ch} kl - \text{sh} kl} \cdot \left(kl \cdot \text{ch} \frac{kl}{2} - \text{sh} \frac{kl}{2} - \frac{kl}{2} \right) - \text{sh} k \left(x - \frac{l}{2} \right) \right]$	$x = \frac{l}{2}$ $x = l$	$B_{\omega} = \frac{Ml}{2} v$ $B_{\omega} = \frac{Ml}{2} u$
$b = \frac{\tanh kl}{kl}; c = \frac{kl \cdot \sinh kl - \cosh kl + 1}{k^2 l^2 \cosh kl}; p = \frac{\cosh \frac{kl}{2} - 1}{k^2 l^2 \cosh \frac{kl}{2}}; f = \frac{\cosh kl - 1}{kl \sinh kl}$ $g = \frac{kl}{2} \frac{(\cosh kl + 1) - \sinh kl}{k^2 l^2 \sinh kl}; j = \frac{\sinh kl - kl \cosh \frac{kl}{2}}{k^2 l^2 \sinh kl}; n = \frac{\sinh kl - 2 \sinh \frac{kl}{2}}{kl (\cosh kl - 1)}$ $v = \frac{kl \sinh kl - \cosh kl + 1 - kl \sinh \frac{kl}{2}}{kl (kl \cosh kl - \sinh kl)}; w = \frac{kl \sinh kl - 2 \cosh kl + 2}{kl (kl \cosh kl - \sinh kl)}; u = \frac{\sinh kl - 2 \sinh \frac{kl}{2}}{kl \cosh kl - \sinh kl}$			

In conclusion, where loads are applied eccentrically to the shear centre of the cross section, the effects of torsion shall be taken into account. As far as practicable, torsional moments should be avoided or reduced by restraints because they substantially reduce the load bearing capacity, especially in case of open sections.

In determining the effects of the torsional moment, the centroidal axis, shear centre and imposed rotation centre, should be taken as those of the gross cross section.

The longitudinal stresses due to the axial force N_{Sd} and the bending moments $M_{y,Sd}$ and $M_{z,Sd}$ should be based on the respective effective cross sections used in §§3.8.2 to §§3.8.4. The shear stresses due to transverse shear forces, the shear stress due to uniform (St. Venant) torsion, and the longitudinal stresses and shear stresses due to warping should all be based on the properties of the gross cross section.

In cross sections subject to torsion, the following conditions should be satisfied:

$$\sigma_{\text{tot},Ed} \leq f_y / \gamma_{M0} \quad (3.113)$$

$$\tau_{\text{tot},Ed} \leq \frac{f_y / \sqrt{3}}{\gamma_{M0}} \quad (3.114)$$

$$\sqrt{\sigma_{tot,Ed}^2 + 3 \cdot \tau_{tot,Ed}^2} \leq 1.1 \frac{f_y}{\gamma_{M0}} \quad (3.115)$$

where

$\sigma_{tot,Ed}$ is the total longitudinal stress, calculated on the relevant effective cross section;

$\tau_{tot,Ed}$ is the total shear stress, calculated on the gross cross section.

The total longitudinal stress $\sigma_{tot,Ed}$ and the total shear stress $\tau_{tot,Ed}$ should be obtained from:

$$\sigma_{tot,Ed} = \sigma_{N,Ed} + \sigma_{My,Ed} + \sigma_{Mz,Ed} + \sigma_{w,Ed} \quad (3.116a)$$

$$\tau_{tot,Ed} = \tau_{Vy,Ed} + \tau_{Vz,Ed} + \tau_{t,Ed} + \tau_{w,Ed} \quad (3.116b)$$

where

$\sigma_{My,Ed}$ is the direct stress due to the bending moment $M_{y,Sd}$;

$\sigma_{Mz,Ed}$ is the direct stress due to the bending moment $M_{z,Sd}$;

$\sigma_{N,Ed}$ is the direct stress due to the axial force N_{Sd} ;

$\sigma_{w,Ed}$ is the direct stress due to warping;

$\tau_{Vy,Ed}$ is the shear stress due to the transverse shear force $V_{y,Sd}$;

$\tau_{Vz,Ed}$ is the shear stress due to the transverse shear force $V_{z,Sd}$;

$\tau_{t,Ed}$ is the shear stress due to uniform (St. Venant) torsion;

$\tau_{w,Ed}$ is the shear stress due to warping.

3.8.7 Local transverse forces

3.8.7.1 General

To avoid crushing, crippling or buckling in a web subject to a support reaction or other local transverse force applied through the flange, the transverse force F_{Ed} shall satisfy:

$$F_{Ed} \leq R_{w,Rd} \quad (3.117)$$

where

$R_{w,Rd}$ is the local transverse resistance of the web.

The local transverse resistance of a web $R_{w,Rd}$ shall be obtained as follows:

- a) for an unstiffened web:
 - for a cross section with a single web: from §§3.8.7.2;
 - for any other case, including sheeting: from §§3.8.7.3;
- b) for a stiffened web: from §§3.8.7.4.

Where the local load or support reaction is applied through a cleat that is arranged to prevent distortion of the web and is designed to resist the local transverse force, the local resistance of the web to the transverse force need not be considered.

In beams with I-shaped cross sections built up from two channels, or with similar cross sections in which two components are interconnected through their webs, the connections between the webs should be located as close as practicable to the flanges of the beam.

3.8.7.2 Cross sections with a single unstiffened web

For a cross section with a single unstiffened web, see Figure 3.53, the local transverse resistance of the web may be determined as specified below, provided that the cross section satisfies the following criteria:

$$h_w / t \leq 200 \tag{3.118a}$$

$$r / t \leq 6 \tag{3.118b}$$

$$45^\circ \leq \phi \leq 90^\circ \tag{3.118c}$$

where

- h_w is the web height between the midlines of the flanges;
- r is the internal radius of the corners;
- ϕ is the slope of the web relative to the flanges [degrees].

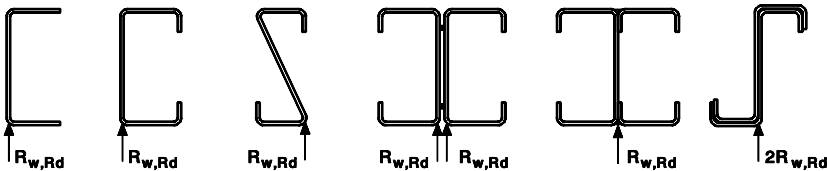


Figure 3.53 – Examples of cross sections with a single web

For cross sections that satisfy the criteria specified by eqns. (3.118), the local transverse resistance of a web $R_{w,Rd}$ may be determined as follows:

a) for a single local load or support reaction, see Figure 3.54(a):

i) $c \leq 1.5 h_w$ clear from a free end:

- for a cross section with stiffened flanges:

$$R_{w,Rd} = \frac{k_1 k_2 k_3 \left[9.04 - \frac{h_w/t}{60} \right] \left[1 + 0.01 \frac{s_s}{t} \right] \cdot t^2 \cdot f_{yb}}{\gamma_{M1}} \quad (3.119a)$$

- for a cross section with unstiffened flanges:

- if $s_s/t \leq 60$:

$$R_{w,Rd} = \frac{k_1 k_2 k_3 \left[5.92 - \frac{h_w/t}{132} \right] \left[1 + 0.01 \frac{s_s}{t} \right] \cdot t^2 \cdot f_{yb}}{\gamma_{M1}} \quad (3.119b)$$

- if $s_s/t > 60$:

$$R_{w,Rd} = \frac{k_1 k_2 k_3 \left[5.92 - \frac{h_w/t}{132} \right] \left[0.71 + 0.015 \frac{s_s}{t} \right] \cdot t^2 \cdot f_{yb}}{\gamma_{M1}} \quad (3.119c)$$

ii) $c > 1.5 h_w$ clear from a free end:

- if $s_s/t \leq 60$:

$$R_{w,Rd} = \frac{k_3 k_4 k_5 \left[14.7 - \frac{h_w/t}{49.5} \right] \left[1 + 0.007 \frac{s_s}{t} \right] \cdot t^2 \cdot f_{yb}}{\gamma_{M1}} \quad (3.119d)$$

- if $s_s/t > 60$:

$$R_{w,Rd} = \frac{k_3 k_4 k_5 \left[14.7 - \frac{h_w/t}{49.5} \right] \left[0.75 + 0.011 \frac{s_s}{t} \right] \cdot t^2 \cdot f_{yb}}{\gamma_{M1}} \quad (3.119e)$$

b) for two opposing local transverse forces closer together than $1.5 h_w$, see Figure 3.54(b):

i) $c \leq 1.5 h_w$ clear from a free end:

$$R_{w,Rd} = \frac{k_1 k_2 k_3 \left[6.66 - \frac{h_w/t}{64} \right] \left[1 + 0.01 \frac{s_s}{t} \right] \cdot t^2 \cdot f_{yb}}{\gamma_{M1}} \quad (3.119f)$$

3. BEHAVIOUR AND RESISTANCE OF CROSS SECTION

ii) $c > 1.5 h_w$ clear from a free end:

$$R_{w,Rd} = \frac{k_3 k_4 k_5 \left[21.0 - \frac{h_w/t}{16.3} \right] \left[1 + 0.0013 \frac{s_s}{t} \right] \cdot t^2 \cdot f_{yb}}{\gamma_{M1}} \quad (3.119g)$$

The values of the constants k_1 to k_5 should be determined as follows:

$$\begin{aligned} k_1 &= 1.33 - 0.33 k \\ k_2 &= 1.15 - 0.15 r/t \quad \text{but } k_2 \geq 0.50 \quad \text{and } k_2 \leq 1.0 \\ k_3 &= 0.7 + 0.3 (\phi / 90)^2 \\ k_4 &= 1.22 - 0.22 k \\ k_5 &= 1.06 - 0.06 r/t \quad \text{but } k_5 \leq 1.0 \end{aligned}$$

where

$$\begin{aligned} k &= f_{yb} / 228 \quad [\text{with } f_{yb} \text{ in N/mm}^2]; \\ s_s &\quad \text{is the nominal bearing length.} \end{aligned}$$

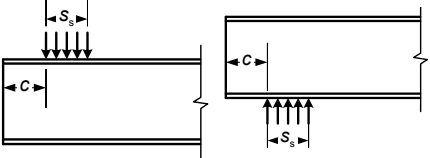
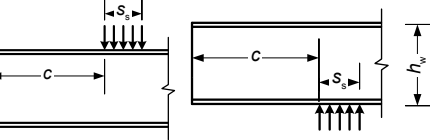
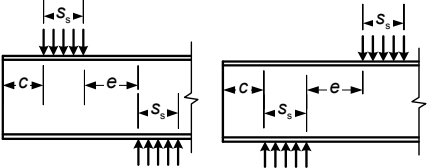
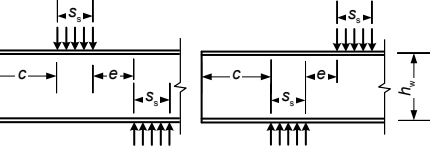
a) For a single local load or support reaction	
	i) $c \leq 1.5 h_w$ clear from a free end
	ii) $c > 1.5 h_w$ clear from a free end
b) For two opposing local transverse forces closer together than $1.5 h_w$	
	i) $c \leq 1.5 h_w$ clear from a free end
	ii) $c > 1.5 h_w$ clear from a free end

Figure 3.54 – Local loads and supports – cross sections with a single web

In the case of two equal and opposite local transverse forces distributed over unequal bearing lengths, the smaller value of s_s should be used.

If the web rotation is prevented either by suitable restraint or because of the section geometry (e.g. I-beams, see fourth and fifth cases from the left in the Figure 3.53) then the local transverse resistance of a web $R_{w,Rd}$ may be determined as follows:

a) for a single load or support reaction

i) $c < 1.5 h_w$ (near or at free end)

- for a cross section of stiffened and unstiffened flanges

$$R_{w,Rd} = \frac{k_7 \left[8.8 + 1.1 \sqrt{\frac{s_s}{t}} \right] \cdot t^2 \cdot f_{yb}}{\gamma_{M1}} \quad (3.120a)$$

ii) $c > 1.5 h_w$ (far from free end)

- for a cross section of stiffened and unstiffened flanges

$$R_{w,Rd} = \frac{k'_5 k_7 \left[13.2 + 2.87 \sqrt{\frac{s_s}{t}} \right] \cdot t^2 \cdot f_{yb}}{\gamma_{M1}} \quad (3.120b)$$

b) for opposite loads or reactions

i) $c < 1.5 h_w$ (near or at free end)

- for a cross section of stiffened and unstiffened flanges

$$R_{w,Rd} = \frac{k_{10} k_{11} \left[8.8 + 1.1 \sqrt{\frac{s_s}{t}} \right] \cdot t^2 \cdot f_{yb}}{\gamma_{M1}} \quad (3.120c)$$

ii) $c > 1.5 h_w$ (loads or reactions far from free end)

- for a cross section of stiffened and unstiffened flanges

$$R_{w,Rd} = \frac{k_8 k_9 \left[13.2 + 2.87 \sqrt{\frac{s_s}{t}} \right] \cdot t^2 \cdot f_{yb}}{\gamma_{M1}} \quad (3.120d)$$

3. BEHAVIOUR AND RESISTANCE OF CROSS SECTION

where the values of constants k'_5 to k_{11} and should be determined as follows:

$$k'_5 = 1.49 - 0.53 \cdot k \quad \text{but} \quad k'_5 \geq 0.6$$

$$k_6 = 0.88 - 0.12 t / 1.9$$

$$k_7 = 1 + h_w / t / 750 \quad \text{when} \quad h_w / t < 150 ; k_7 = 1.20 \quad \text{when} \quad h_w / t > 150$$

$$k_8 = 1/k \quad \text{when} \quad h_w / t < 66.5 ; k_8 = (1.10 - h_w / t / 665) / k \quad \text{when} \quad h_w / t > 66.5$$

$$k_9 = 0.82 + 0.15 t / 1.9$$

$$k_{10} = (0.98 - h_w / t / 865) / k$$

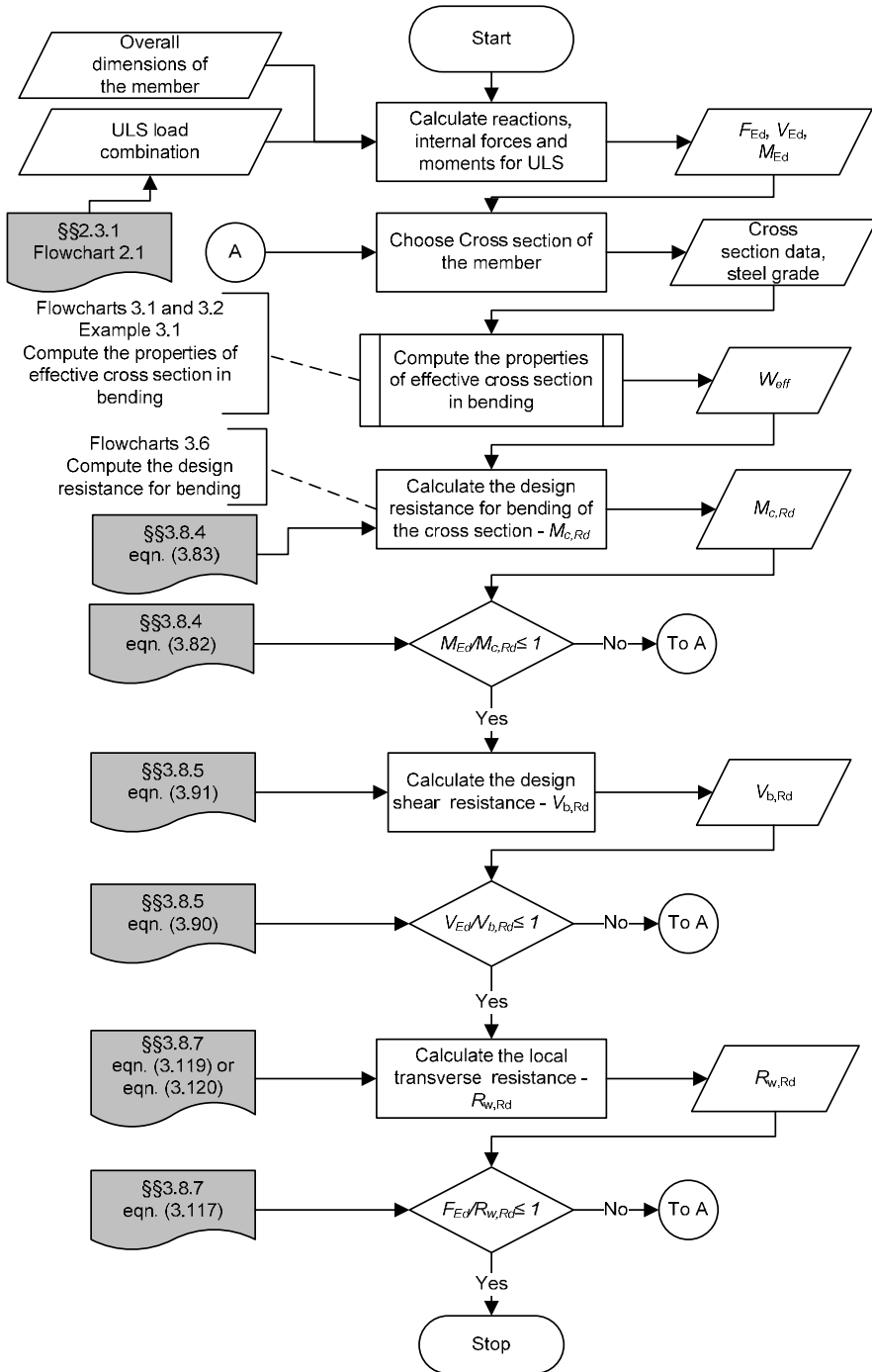
$$k_{11} = 0.64 + 0.31 t / 1.9$$

where

$$k = f_{yb} / 228 \quad [\text{with } f_{yb} \text{ in N/mm}^2];$$

s_s is the nominal bearing length.

Flowchart 3.7 presents the general procedure for a simply supported member in bending, considering the presence of bending moment, shear force and reaction (no interaction between them). Example 3.5 presents a numerical example.



Flowcharts 3.7 – Design of a cold-formed steel cross section in bending (SF041a-EN-EU, Access Steel 2006)

Example 3.5: Design of a cold-formed steel member in bending.

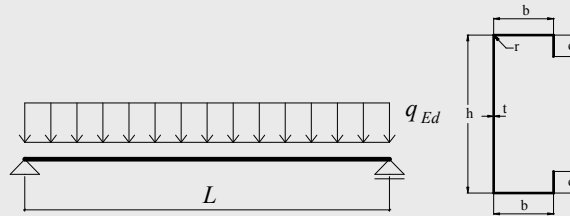
Basic Data

Span of joist $L = 5.5 \text{ m}$

Spacing between joists $S = 0.6 \text{ m}$

Distributed loads applied to the joist:

self-weight of the beam	$q_{G.beam} = 0.06 \text{ kN/m}$
lightweight slab	0.75 kN/m^2
	$q_{G.slab} = 0.75 \times 0.6 = 0.45 \text{ kN/m}$
dead load	$q_G = q_{G.beam} + q_{G.slab} = 0.51 \text{ kN/m}$
imposed load	2.50 kN/m^2
	$q_Q = 2.50 \times 0.6 = 1.50 \text{ kN/m}$



The dimensions of the cross section and the material properties are:

Total height	$h = 200 \text{ mm}$
Total width of flange in compression	$b_1 = 74 \text{ mm}$
Total width of flange in tension	$b_2 = 66 \text{ mm}$
Total width of edge fold	$c = 20.8 \text{ mm}$
Internal radius	$r = 3 \text{ mm}$
Nominal thickness	$t_{nom} = 2 \text{ mm}$
Steel core thickness	$t = 1.96 \text{ mm}$
Basic yield strength	$f_{yb} = 350 \text{ N/mm}^2$
Modulus of elasticity	$E = 210000 \text{ N/mm}^2$
Poisson's ratio	$\nu = 0.3$
Partial factors (§§2.3.1)	$\gamma_{M0} = 1.0$
	$\gamma_{M1} = 1.0$

$\gamma_G = 1.35$ – permanent loads

$\gamma_Q = 1.50$ – variable loads

Design of the joist for Ultimate Limit State (see Flowchart 3.7)

Effective section properties at the ULS (§§3.7.3, Flowcharts 3.1 and 3.2)

The properties of effective cross section in bending were calculated following the procedure presented in Example 3.1.

Second moment of area of cold-formed lipped channel section subjected to bending about its major axis: $I_{eff,y} = 4139861 \text{ mm}^4$

Position of the neutral axis:

- from the flange in compression: $z_c = 102.3 \text{ mm}$

- from the flange in tension: $z_t = 95.7 \text{ mm}$

Effective section modulus:

- with respect to the flange in compression:

$$W_{eff,y,c} = \frac{I_{eff,y}}{z_c} = \frac{4139861}{102.3} = 40463 \text{ mm}^3$$

- with respect to the flange in tension:

$$W_{eff,y,t} = \frac{I_{eff,y}}{z_t} = \frac{4139861}{95.7} = 43264 \text{ mm}^3$$

$$W_{eff,y} = \min(W_{eff,y,c}, W_{eff,y,t}) = 40463 \text{ mm}^3$$

Applied loading on the joist at the ULS (§§2.3.1, Flowchart 2.1)

$$q_d = \gamma_G q_G + \gamma_Q q_Q = 1.35 \times 0.51 + 1.50 \times 1.50 = 2.94 \text{ kN/m}$$

Maximum applied bending moment (at mid-span) about the major axis y-y:

$$M_{Ed} = q_d L^2 / 8 = 2.94 \times 5.5^2 / 8 = 11.12 \text{ kNm}$$

Check of bending resistance at ULS

Design moment resistance of the cross section for bending (§§3.8.4, eqn. (3.83)):

3. BEHAVIOUR AND RESISTANCE OF CROSS SECTION

$$M_{c,Rd} = W_{eff,y} f_{yb} / \gamma_{M0} = 40463 \times 10^{-9} \times 350 \times 10^3 / 1.0 = 14.16 \text{ kNm}$$

Verification of bending resistance (§§3.8.4, eqn. (3.83)):

$$\frac{M_{Ed}}{M_{c,Rd}} = \frac{11.12}{14.16} = 0.785 < 1 - \text{OK}$$

Check of shear resistance at the ULS

Design to shear force

Maximum applied shear force

$$V_{Ed} = q_d L / 2 = 2.94 \times 5.5 / 2 = 8.085 \text{ kN}$$

Design shear buckling resistance (§§3.8.5, eqn. (3.91))

$$V_{b,Rd} = \frac{\frac{h_w}{\sin \phi} t f_{bv}}{\gamma_{M0}}$$

where

f_{bv} is the shear strength, considering buckling

For a web with stiffening at the support:

$$f_{bv} = 0.58 f_{yb} \quad \text{if} \quad \bar{\lambda}_w \leq 0.83$$

$$f_{bv} = 0.48 f_{yb} / \bar{\lambda}_w \quad \text{if} \quad \bar{\lambda}_w > 0.83$$

The relative slenderness $\bar{\lambda}_w$ for webs without longitudinal stiffeners:

$$\begin{aligned} \bar{\lambda}_w &= 0.346 \frac{s_w}{t} \sqrt{\frac{f_{yb}}{E}} = 0.346 \frac{h - t_{nom}}{t} \sqrt{\frac{f_{yb}}{E}} = \\ &= 0.346 \times \frac{200 - 2}{1.96} \times \sqrt{\frac{350}{210000}} = 1.427 \end{aligned}$$

$$\bar{\lambda}_w = 1.427 > 0.83 \quad \text{so:}$$

$$f_{bv} = 0.48 f_{yb} / \bar{\lambda}_w = 0.48 \times 350 / 1.427 = 117.73 \text{ N/mm}^2$$

$$V_{b,Rd} = \frac{\frac{(200 - 2) \times 10^{-3}}{\sin 90^\circ} \times 1.96 \times 10^{-3} \times 117.73 \times 10^3}{1.0} = 45.7 \text{ kN}$$

Verification of shear resistance (§§3.8.5, eqn. (3.90))

$$\frac{V_{Ed}}{V_{c,Rd}} = \frac{8.085}{45.7} = 0.177 < 1 \quad \text{– OK}$$

Check of local transverse resistance at ULS

Support reaction:

$$F_{Ed} = q_d L/2 = 2.94 \times 5.5/2 = 8.085 \text{ kN}$$

To obtain the local transverse resistance of the web for a cross section with a single unstiffened web, the following criteria should be satisfied (§§3.8.7.2, eqn. (3.118)):

$$h_w/t \leq 200 \quad 198/1.96 = 101.02 < 200 \quad \text{– OK}$$

$$r/t \leq 6 \quad 3/1.96 = 1.53 < 6 \quad \text{– OK}$$

$$45^\circ \leq \phi \leq 90^\circ$$

where ϕ is the slope of the web relative to the flanges: $\phi = 90^\circ$ – OK

The local transverse resistance of the web (§§3.8.7, eqn. (3.120), Figure 3.53)

The bearing length is: $s_s = 110 \text{ mm}$

For $s_s/t = 80/1.96 = 40.816 < 60$ the local transverse resistance of the web

$R_{w,Rd}$ is:

$$R_{w,Rd} = \frac{k_1 k_2 k_3 \left[5.92 - \frac{h_w/t}{132} \right] \left[1 + 0.01 \frac{s_s}{t} \right] t^2 f_{yb}}{\gamma_{M1}}$$

where (§§3.8.7)

$$k_1 = 1.33 - 0.33k \quad \text{with} \quad k = f_{yb}/228 = 350/228 = 1.535$$

$$k_1 = 1.33 - 0.33 \times 1.535 = 0.823$$

$$k_2 = 1.15 - 0.15r/t = 1.15 - 0.15 \times 3/1.96 = 0.92$$

$$k_3 = 0.7 + 0.3(\phi/90)^\circ = 0.7 + 0.3 \times (90/90)^\circ = 1$$

$$R_{w,Rd} = \frac{0.823 \times 0.92 \times 1 \times \left[5.92 - \frac{198/1.96}{132} \right] \times \left[1 + 0.01 \times \frac{110}{1.96} \right] \times 1.96^2 \times 350}{1.0}$$

3. BEHAVIOUR AND RESISTANCE OF CROSS SECTION

$$= 8193 \text{ N} = 8.193 \text{ kN}$$

Verification of local transverse force (§§3.8.7.1, eqn. (3.117))

$$F_{Ed} = 8.085 \text{ kN} < R_{w,Rd} = 8.193 \text{ kN} \text{ – OK}$$

3.8.7.3 Cross sections with two or more unstiffened webs

In case of cross sections with two or more webs, including sheeting, see Figure 3.55, the local transverse resistance of an unstiffened web should be determined as specified below, provided that both of the following conditions are satisfied:

- the clear distance c from the actual bearing length for the support reaction or local load to a free end, see Figure 3.56, is at least 40 mm;
- the cross section satisfies the following criteria:

$$r/t \leq 10 \quad (3.121a)$$

$$h_w/t \leq 200 \sin \phi \quad (3.121b)$$

$$45^\circ \leq \phi \leq 90^\circ \quad (3.121c)$$

where

- h_w is the web height between the midlines of the flanges;
- r is the internal radius of the corners;
- ϕ is the slope of the web relative to the flanges [degrees].

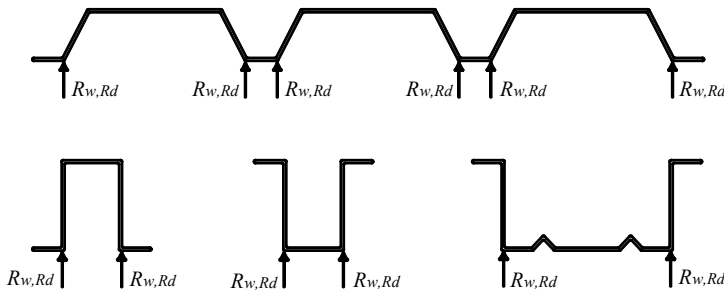


Figure 3.55 – Examples of cross sections with two or more webs

Where the conditions specified above are satisfied, the local transverse resistance $R_{w,Rd}$ per web of the cross section should be determined from:

$$R_{w,Rd} = \alpha \cdot t^2 \sqrt{f_{yb} E} \cdot \left(1 - 0.1 \sqrt{r/t}\right) \cdot \left[0.5 + \sqrt{0.02 \cdot l_a / t}\right] \cdot \left(2.4 + (\phi/90)^2\right) / \gamma_{M1} \quad (3.122)$$

where

- l_a is the effective bearing length for the relevant category;
 α is the coefficient for the relevant category.

The values of l_a and α should be obtained from eqns. (3.123) and (3.124) respectively. The maximum design value for l_a is 200 mm. When the support is a cold-formed section with one web or round tube, s_s should be taken as 10 mm. The relevant category (1 or 2) should be based on the clear distance e between the local load and the nearest support, or the clear distance c from the support reaction or local load to a free end, see Figure 3.56, as follows:

a) Category 1, see Figure 3.56(a):

- local load applied with $e \leq 1.5 h_w$ clear from the nearest support;
- local load applied with $c \leq 1.5 h_w$ clear from a free end;
- reaction at end support with $c \leq 1.5 h_w$ clear from a free end.

b) Category 2, see Figure 3.56(b):

- local load applied with $e > 1.5 h_w$ clear from the nearest support;
- local load applied with $c > 1.5 h_w$ clear from a free end;
- reaction at end support with $c > 1.5 h_w$ clear from a free end;
- reaction at internal support.

215

The value of the effective bearing length l_a should be obtained from the following

a) for Category 1: $l_a = 10 \text{ mm}$ (3.123a)

b) for Category 2:

- $\beta_V \leq 0.2$: $l_a = s_s$ (3.123b)

- $\beta_V \geq 0.3$: $l_a = 10 \text{ mm}$ (3.123c)

- $0.2 < \beta_V < 0.3$: Interpolate linearly between the values of l_a for 0.2 and 0.3, with:

$$\beta_V = \frac{|V_{Sd,1}| - |V_{Sd,2}|}{|V_{Sd,1}| + |V_{Sd,2}|}$$

3. BEHAVIOUR AND RESISTANCE OF CROSS SECTION

in which $|V_{sd,1}|$ and $|V_{sd,2}|$ are the absolute values of the transverse shear forces on each side of the local load or support reaction, and $|V_{sd,1}| \geq |V_{sd,2}|$ and s_s is the actual length of stiff bearing.

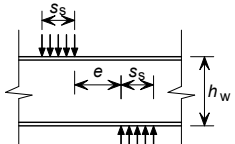
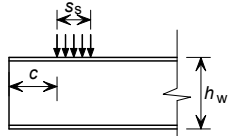
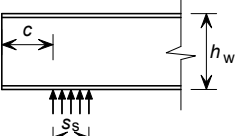
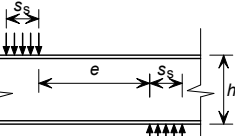
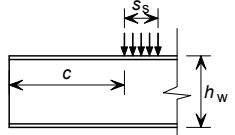
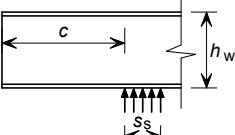
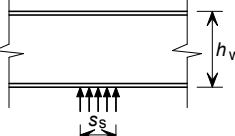
	<p>Category 1 - local load applied with $e \leq 1.5 h_w$ clear from the nearest support;</p>
	<p>Category 1 - local load applied with $c \leq 1.5 h_w$ clear from a free end;</p>
	<p>Category 1 - reaction at end support with $c \leq 1.5 h_w$ clear from a free end.</p>
	<p>Category 2 - local load applied with $e > 1.5 h_w$ clear from the nearest support;</p>
	<p>Category 2 - local load applied with $c > 1.5 h_w$ clear from a free end;</p>
	<p>Category 2 - reaction at end support with $c > 1.5 h_w$ clear from a free end;</p>
	<p>Category 2 - reaction at internal support.</p>

Figure 3.56 – Local loads and supports – cross sections with two or more webs

The value of the coefficient α should be obtained from the following:

a) for Category 1:

- for sheeting profiles: $\alpha = 0.075$ (3.124a)

- for liner trays and hat sections: $\alpha = 0.057$ (3.124b)

b) for Category 2:

- for sheeting profiles: $\alpha = 0.150$ (3.124c)

- for liner trays and hat sections: $\alpha = 0.115$ (3.124d)

3.8.7.4 Stiffened webs

The local transverse resistance of a stiffened web may be determined for cross sections with longitudinal web stiffeners folded in such a way that the two folds in the web are on opposite sides of the system line of the web joining the points of intersection of the midline of the web with the midlines of the flanges, see Figure 3.57, that satisfy the condition:

$$2 < \frac{e_{max}}{t} < 12 \quad (3.125)$$

where

e_{max} is the larger eccentricity of the folds relative to the system line of the web.

217

For cross sections with stiffened webs satisfying the condition specified in eqn. (3.125), the local transverse resistance of a stiffened web may be determined by multiplying the corresponding value for a similar unstiffened web, obtained from §§3.8.7.2 or §§3.8.7.3 as appropriate, by the factor $\kappa_{a,s}$ given by:

$$\kappa_{a,s} = 1.45 - 0.05 \cdot e_{max} / t \quad \text{but} \quad \kappa_{a,s} \leq 0.95 + 35000 \cdot t^2 \cdot e_{min} / (b_d^2 \cdot s_p) \quad (3.126)$$

where

b_d is the developed width of the loaded flange, see Figure 3.57;
 e_{min} is the smaller eccentricity of the folds relative to the system line of the web;
 s_p is the slant height of the plane web element nearest to the loaded flange, see Figure 3.57.

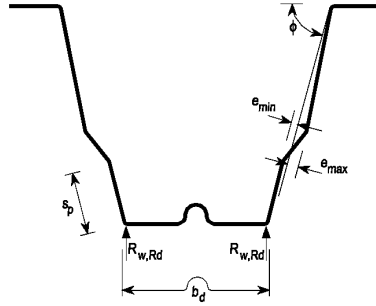


Figure 3.57 – Stiffened webs

3.8.8 Combined tension and bending

Cross sections subject to combined axial tension N_{Ed} and bending moments $M_{y,Ed}$ and $M_{z,Ed}$ should satisfy the criterion:

$$\frac{N_{Ed}}{N_{t,Rd}} + \frac{M_{y,Ed}}{M_{cy,Rd,ten}} + \frac{M_{z,Ed}}{M_{cz,Rd,ten}} \leq 1 \quad (3.127a)$$

where

$N_{t,Rd}$ is the design resistance of a cross section for uniform tension;

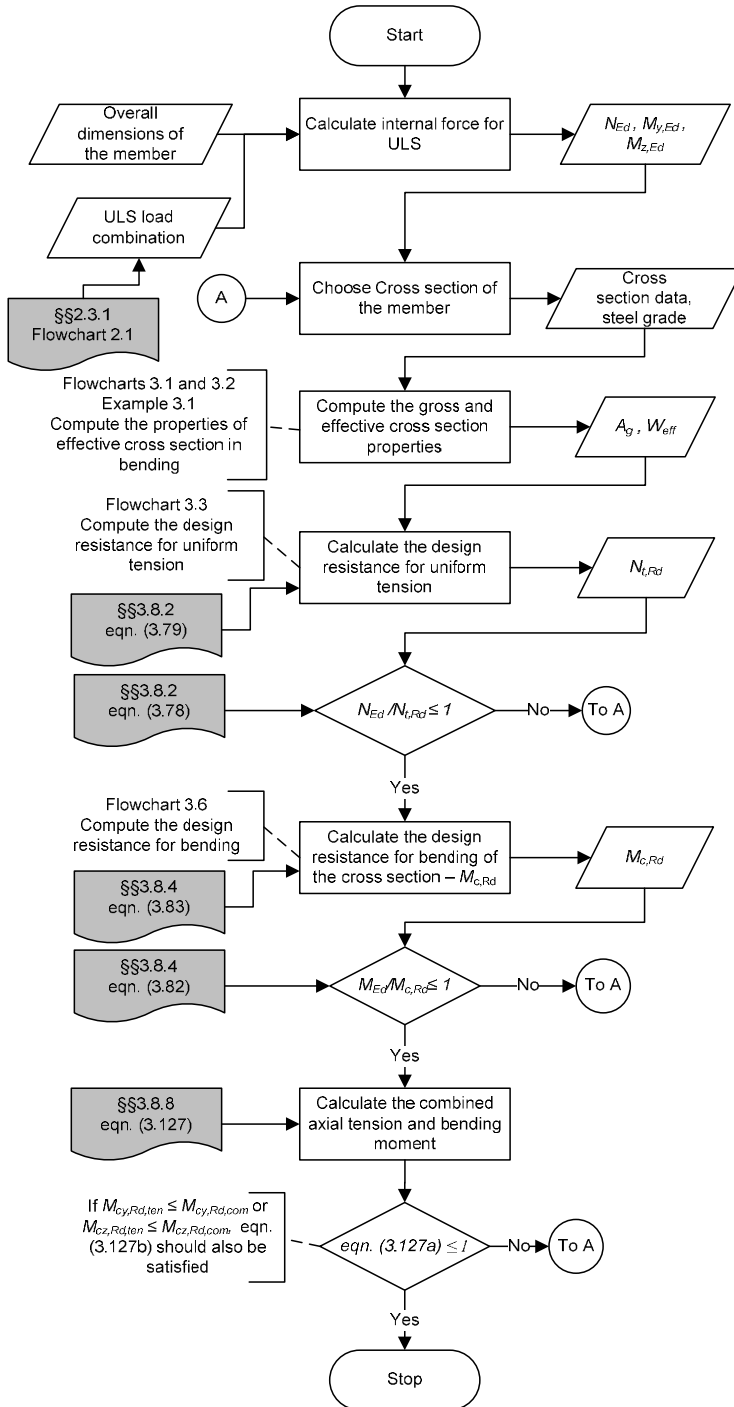
$M_{cy,Rd,ten}$ is the design moment resistance of a cross section for maximum tensile stress if subject only to moment about the y - y axis;

$M_{cz,Rd,ten}$ is the design moment resistance of a cross section for maximum tensile stress if subject only to moment about the z - z axis.

If $M_{cy,Rd,com} \leq M_{cy,Rd,ten}$ or $M_{cz,Rd,com} \leq M_{cz,Rd,ten}$ (where $M_{cy,Rd,com}$ and $M_{cz,Rd,com}$ are the moment resistances for the maximum compressive stress in a cross section that is subject only to moment about the relevant axis), the following criterion should also be satisfied:

$$\frac{M_{y,Ed}}{M_{cy,Rd,com}} + \frac{M_{z,Ed}}{M_{cz,Rd,com}} - \frac{N_{Ed}}{N_{t,Rd}} \leq 1 \quad (3.127b)$$

Flowchart 3.8 presents schematically the design of a cold-formed steel cross section in combined tension and bending.



Flowchart 3.8 – Cross section subjected to combined tension and bending

3.8.9 Combined compression and bending

Cross sections subject to combined axial compression N_{Ed} and bending moments $M_{y,Ed}$ and $M_{z,Ed}$ should satisfy the criterion:

$$\frac{N_{Ed}}{N_{c,Rd}} + \frac{M_{y,Ed} + \Delta M_{y,Ed}}{M_{cy,Rd,com}} + \frac{M_{z,Ed} + \Delta M_{z,Ed}}{M_{cz,Rd,com}} \leq 1 \quad (3.128a)$$

in which $N_{c,Rd}$ is as defined in §§3.8.3, $M_{cy,Rd,com}$ and $M_{cz,Rd,com}$ are as defined in §§3.8.3.

The additional moments $\Delta M_{y,Ed}$ and $\Delta M_{z,Ed}$ due to shifts of the effective centroidal axes should be taken as:

$$\Delta M_{y,Ed} = N_{Ed} \cdot e_{Ny}$$

$$\Delta M_{z,Ed} = N_{Ed} \cdot e_{Nz}$$

in which e_{Ny} and e_{Nz} are the shifts of y - y and z - z centroidal axis of the effective cross section relative to the gross cross section.

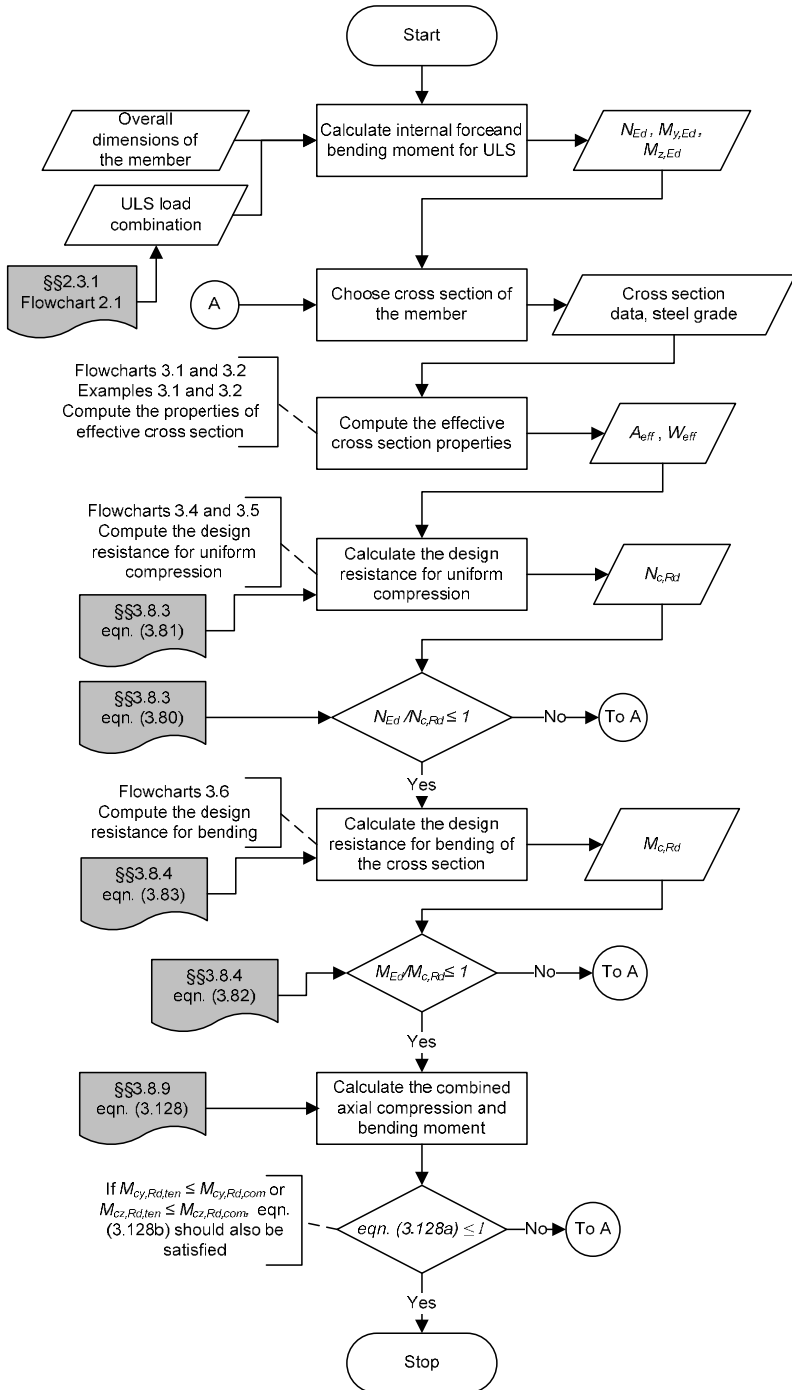
If $M_{cy,Rd,ten} \leq M_{cy,Rd,com}$ or $M_{cz,Rd,ten} \leq M_{cz,Rd,com}$ the following criterion should also be satisfied:

220

$$\frac{M_{y,Ed} + \Delta M_{y,Ed}}{M_{cy,Rd,ten}} + \frac{M_{z,Ed} + \Delta M_{z,Ed}}{M_{cz,Rd,ten}} - \frac{N_{Ed}}{N_{c,Rd}} \leq 1 \quad (3.128b)$$

in which $M_{cy,Rd,ten}$ and $M_{cz,Rd,ten}$ are as defined in §§3.8.4.

Flowchart 3.9 presents schematically the design of a cold-formed steel cross section in combined compression and bending. Example 3.6 presents a numerical example.



Flowchart 3.9 – Cross section subjected to combined compression and bending

Example 3.6: Design of a wall stud in compression and uniaxial bending.

This example presents the design of an external wall stud in compression and uniaxial bending. The stud has pinned end conditions and is composed of two thin-walled cold-formed lipped channel sections. The connection between the channels is assumed to be rigid (a welded connection, for example). Boards are attached to both flanges to prevent the buckling of the wall stud.

Basic Data

Height of wall stud $H = 3.5 \text{ m}$

The applied concentrated load on the external wall stud (compression) at the Ultimate Limit State is: $N_{Ed} = 17.4 \text{ kN}$

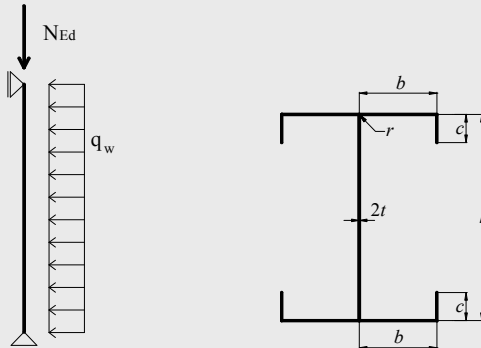
Uniform wind pressure: $q_w = 0.504 \text{ kN/m}$

The maximum applied bending moment:

$$M_{Ed} = \gamma_Q q_w H^2 / 8 = 1.5 \times 0.504 \times 3.50^2 / 8 = 1.16 \text{ kNm}$$

The dimensions of one lipped channel section and the material properties are:

222



Total height $h = 150 \text{ mm}$

Total width of flange $b = 40 \text{ mm}$

Total width of edge fold $c = 15 \text{ mm}$

Internal radius $r = 3 \text{ mm}$

Nominal thickness $t_{nom} = 1.2 \text{ mm}$

Steel core thickness	$t = 1.16 \text{ mm}$
Basic yield strength	$f_{yb} = 320 \text{ N/mm}^2$
Modulus of elasticity	$E = 210000 \text{ N/mm}^2$
Poisson's ratio	$\nu = 0.3$
Shear modulus	$G = \frac{E}{2(1+\nu)} = 81000 \text{ N/mm}^2$
Partial factors	$\gamma_{M0} = 1.0$ $\gamma_{M1} = 1.0$

Properties of the gross cross section

Area of gross cross section:	$A = 522 \text{ mm}^2$
Second moment of area about strong axis y - y :	$I_y = 1.143 \times 10^6 \text{ mm}^4$

Effective section properties of the cross section (§§3.7.3, Flowcharts 3.1 and 3.2)

The properties of effective cross section were calculated following the procedures presented in Examples 3.1 and 3.2.

Effective area of the cross section when subjected to compression only:

$$A_{eff,c} = 336.28 \text{ mm}^2$$

Effective section modulus in bending:

$$\text{with respect to the flange in compression: } W_{eff,y,c} = 18308 \text{ mm}^3$$

$$\text{with respect to the flange in tension: } W_{eff,y,t} = 19040 \text{ mm}^3$$

$$W_{eff,y,min} = \min(W_{eff,y,c}, W_{eff,y,t}) = 18308 \text{ mm}^3$$

Resistance check of the cross section

The following criterion should be met (§§3.8.9, eqn. (3.128a)):

$$\frac{N_{Ed}}{N_{c,Rd}} + \frac{M_{y,Ed} + \Delta M_{y,Ed}}{M_{cy,Rd,com}} \leq 1$$

where

$$N_{c,Rd} = A_{eff} f_{yb} / \gamma_{M0}$$

$$M_{cz,Rd,com} = W_{eff,com} f_{yb} / \gamma_{M0}$$

3. BEHAVIOUR AND RESISTANCE OF CROSS SECTION

$$\Delta M_{y,Ed} = N_{Ed} e_{Ny}$$

e_{Ny} – is the shift of the centroidal y - y axis; the cross section is doubly symmetric $\Rightarrow e_{Ny} = 0$.

The resistance check is:

$$\frac{17.4 \times 10^3}{336.28 \times 320/1.0} + \frac{1.16 \times 10^6 + 0}{18308 \times 320/1.0} = 0.360 < 1 \quad - \text{OK}$$

3.8.10 Combined shear force, axial force and bending moment

For cross sections subject to the combined action of an axial force N_{Ed} , a bending moment M_{Ed} and a shear force V_{Ed} no reduction due to shear force need not be done provided that $V_{Ed} \leq 0.5 V_{w,Rd}$. If the shear force is larger than half of the shear force resistance then following equations should be satisfied:

$$\frac{N_{Ed}}{N_{Rd}} + \frac{M_{y,Ed}}{M_{y,Rd}} + \left(1 - \frac{M_{f,Rd}}{M_{pl,Rd}}\right) \left(\frac{2V_{Ed}}{V_{w,Rd}} - 1\right)^2 \leq 1.0 \quad (3.129)$$

where

224

N_{Rd} is the design resistance of a cross section for uniform tension or compression given in §§3.8.2 or §§3.8.3;

$M_{y,Rd}$ is the design moment resistance of the cross section given in §§3.8.4;

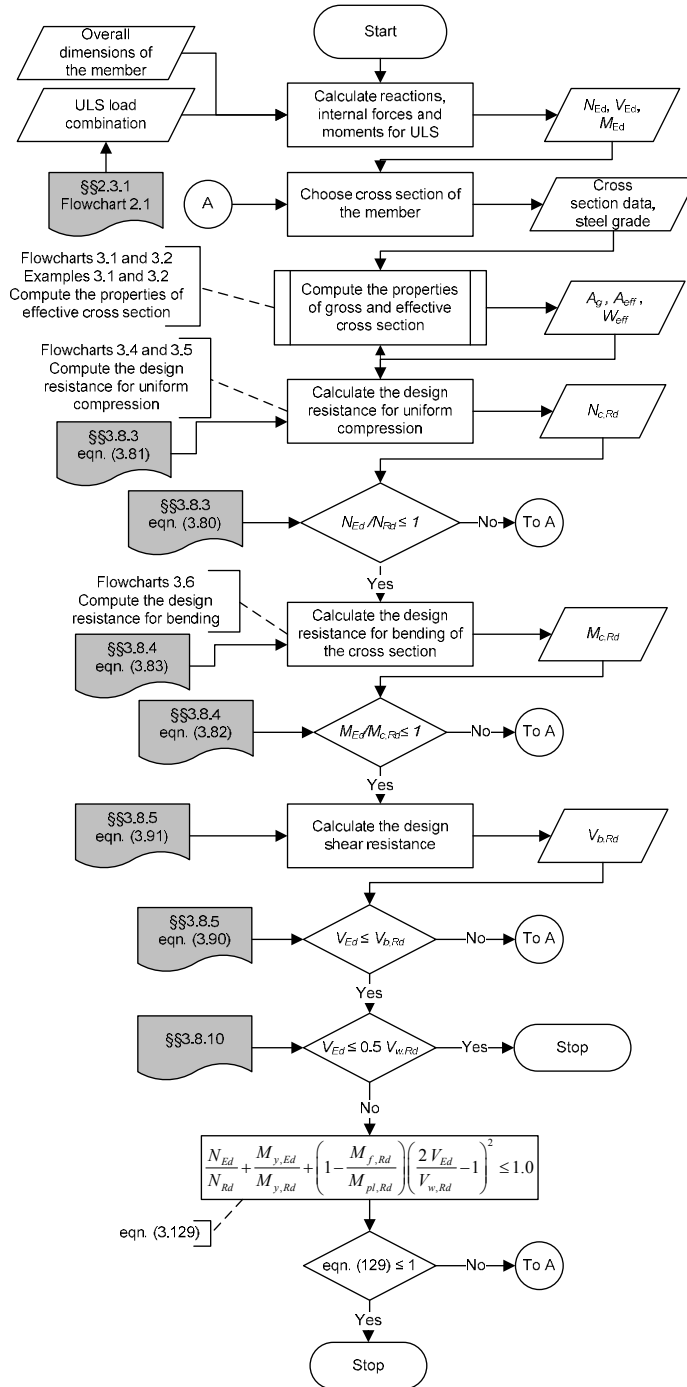
$V_{w,Rd}$ is the design shear resistance of the web given in §§3.8.8;

$M_{f,Rd}$ is the design plastic moment of resistance of the section consisting of the effective area of the flanges;

$M_{pl,Rd}$ is the design plastic resistance of the cross section consisting of the effective area of the flanges and the fully effective web irrespective of its section class.

For members and sheeting with more than one web $V_{w,Rd}$ is the sum of the resistances of the webs.

Flowchart 3.10 presents schematically the design of a cold-formed steel cross section in combined shear force, axial force and bending moment. Example 3.7 presents a numerical example.

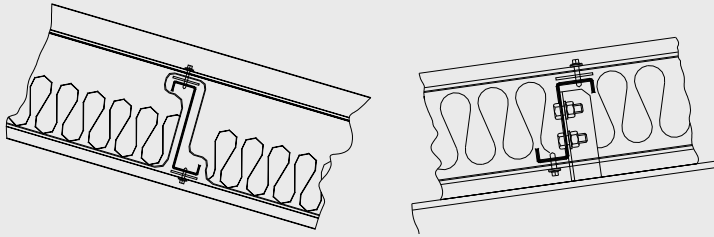


Flowchart 3.10 – Cross section in combined shear force, axial force and bending moment

3. BEHAVIOUR AND RESISTANCE OF CROSS SECTION

Example 3.7: Design of a two-span cold-formed steel Z-purlin with bolted lapped connections.

This example presents the design at ULS of a two-span cold-formed steel Z-purlin with bolted lapped connections under vertical loads. No check at the serviceability limit state is required. The roof has a slope of 8° . The roof system is made in such a way that buckling of the purlin is prevented, the purlin being connected at both flanges to corrugated sheets, fixed with self-drilling screws, as shown in figure below. No contribution of the corrugated sheets is considered. In order to avoid the web crippling under support reaction, the purlin is assumed to be suspended on the cleats.

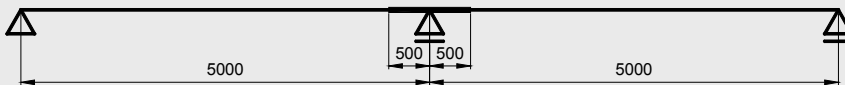


Basic Data

226

The static system is presented below.

The distance between purlins is $s_p = 1200\text{mm}$.



The dimensions of the cross section and the material properties are:

Total height	$h = 200\text{ mm}$
Total width of flange 1	$b_1 = 74\text{ mm}$
Total width of flange 2	$b_2 = 66\text{ mm}$
Total width of edge fold	$c = 21.2\text{ mm}$
Internal radius	$r = 3\text{ mm}$
Nominal thickness	$t_{nom} = 1.5\text{ mm}$
Steel core thickness	$t = 1.46\text{ mm}$

Basic yield strength	$f_{yb} = 350 \text{ N/mm}^2$
Modulus of elasticity	$E = 210000 \text{ N/mm}^2$
Poisson's ratio	$\nu = 0.3$

The loads applied to the purlin:

Dead loads (G)

- self-weight of the purlin	$0.043 \text{ kN/m} \Rightarrow 0.043/1.2 = 0.04 \text{ kN/m}^2$
- self-weight of the top and bottom sheeting	0.10 kN/m^2
- weight of the insulation	0.06 kN/m^2
Total dead load	$q_G = 0.20 \text{ kN/m}^2$

Variable load (Q)

snow load	$q_S = 2.00 \text{ kN/m}^2$
Partial factors	$\gamma_{M0} = 1.0 ; \gamma_{M1} = 1.0$ (§§2.3.1)
	$\gamma_G = 1.35$ – permanent loads (§§2.3.1, Table 2.3)
	$\gamma_Q = 1.50$ – variable loads

Applied loading on the joist at ULS (§§2.3.1, eqn. (2.2))

$$q_d = \gamma_G q_G + \gamma_Q q_S = 1.35 \times 0.20 \times 1.20 + 1.50 \times 2.00 \times 1.20 / \cos 8^\circ = 3.96 \text{ kN/m}$$

Load component normal to the roof:

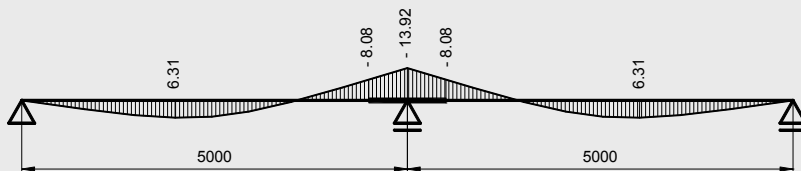
$$q_d \cdot \cos \alpha = 3.96 \cdot \cos 8^\circ = 3.92 \text{ kN/m}$$

Load component in the sheeting plane:

$$q_d \cdot \sin \alpha = 3.96 \cdot \sin 8^\circ = 0.551 \text{ kN/m}$$

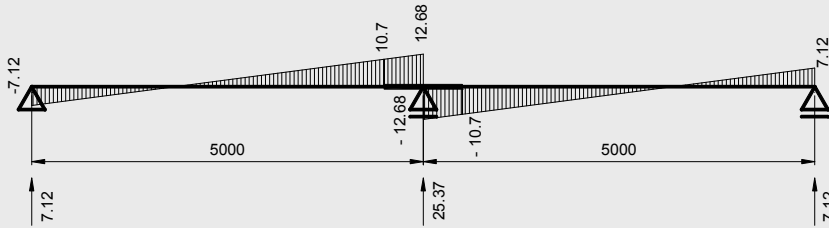
Internal forces

Bending moment diagram M_{Ed} [kNm]



3. BEHAVIOUR AND RESISTANCE OF CROSS SECTION

Shear force diagram V_{Ed} [kN] and reactions F_{Ed} [kN]



Effective section properties at the ultimate limit state (§§3.7.3, Flowcharts 3.1 and 3.2)

The properties of effective cross section were calculated following the procedures presented in Examples 3.1.

Second moment of area, for flange $b_1 = 74$ mm in compression:

$$I_{eff,y} = 2689910 \text{ mm}^4$$

- with respect to the flange in compression:

$$W_{eff,y,c} = \frac{I_{eff,y}}{z_c} = 23752 \text{ mm}^3$$

- with respect to the flange in tension:

$$W_{eff,y,t} = \frac{I_{eff,y}}{z_t} = 31553 \text{ mm}^3$$

228

Second moment of area, for flange $b_2 = 66$ mm in compression:

$$I_{eff,y} = 2786025 \text{ mm}^4$$

- with respect to the flange in compression:

$$W_{eff,y,c} = \frac{I_{eff,y}}{z_c} = 24169 \text{ mm}^3$$

- with respect to the flange in tension:

$$W_{eff,y,t} = \frac{I_{eff,y}}{z_t} = 33475 \text{ mm}^3$$

$$W_{eff,y} = \min(W_{eff,y,c}, W_{eff,y,t}) = 23752 \text{ mm}^3$$

Check of bending resistance at ULS

Design moment resistance for span (§§3.8.4, eqn. (3.83)):

$$M_{c,Rd} = W_{eff,y} f_{yb} / \gamma_{M0} = 23752 \times 350 / 1.0 = 8313200 \text{ Nmm} = 8.31 \text{ kNm}$$

Design moment resistance at the end of overlap – single section (§§3.8.4, eqn. (3.83)):

$$M_{c,Rd} = W_{eff,y} f_{yb} / \gamma_{M0} = 23752 \times 350 / 1.0 = 8313200 \text{ Nmm} = 8.31 \text{ kNm}$$

Design moment resistance for the intermediate support – double section (§§3.8.3, eqn. (3.82)):

$$\begin{aligned} M_{c,Rd} &= 2W_{eff,y} f_{yb} / \gamma_{M0} = 2 \times 23752 \times 350 / 1.0 = 16627400 \text{ Nmm} \\ &= 16.63 \text{ kNm} \end{aligned}$$

Verification of bending resistance (§§3.8.4, eqn. (3.82)):

- check of span	$\frac{M_{Ed1}}{M_{c,Rd}} = \frac{6.31}{8.31} = 0.759 < 1 \quad \text{– OK}$
- check at the end of overlap	$\frac{M_{Ed2}}{M_{c,Rd}} = \frac{8.08}{8.31} = 0.972 < 1 \quad \text{– OK}$
- check at the intermediate support	$\frac{M_{Ed3}}{M_{c,Rd}} = \frac{13.92}{16.63} = 0.837 < 1 \quad \text{– OK}$

Check of shear resistance at ULS

Design shear resistance (§§3.8.5, eqn. (3.91))

$$V_{b,Rd} = \frac{\frac{h_w}{\sin \phi} t f_{bv}}{\gamma_{M0}}$$

For a web without stiffening at the support:

$f_{bv} = 0.58 f_{yb}$	if	$\bar{\lambda}_w \leq 0.83$
$f_{bv} = 0.48 f_{yb} / \bar{\lambda}_w$	if	$0.83 < \bar{\lambda}_w < 1.40$
$f_{bv} = 0.67 f_{yb} / \bar{\lambda}_w^2$	if	$\bar{\lambda}_w \geq 1.40$

The relative slenderness $\bar{\lambda}_w$ for webs without longitudinal stiffeners:

3. BEHAVIOUR AND RESISTANCE OF CROSS SECTION

$$\bar{\lambda}_w = 0.346 \frac{s_w}{t} \sqrt{\frac{f_{yb}}{E}} = 0.346 \times \frac{(200-1.5)}{1.46} \times \sqrt{\frac{350}{210000}} = 1.92$$

$$\bar{\lambda}_w = 1.92 > 1.40 \quad \text{so:}$$

$$f_{bv} = 0.67 f_{yb} / \bar{\lambda}_w^2 = 0.67 \times 350 / 1.92^2 = 63.61 \text{ N/mm}^2$$

$$V_{b,Rd} = \frac{(200-1.5)}{\sin 90^\circ} \times 1.46 \times 63.61 = 18435 \text{ N} = 18.435 \text{ kN}$$

Verification of shear resistance (§§3.8.4, eqn. (3.90))

- check at the end of overlap $\frac{V_{Ed}}{V_{b,Rd}} = \frac{10.7}{18.435} = 0.580 < 1 \quad \text{-- OK}$

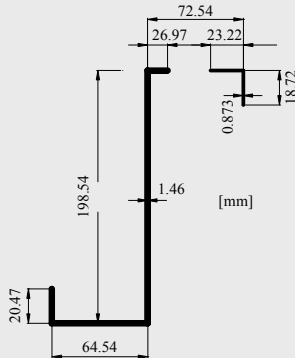
- check at the intermediate support $\frac{V_{Ed}}{2V_{b,Rd}} = \frac{12.68}{2 \times 18.435} = 0.344 < 1 \quad \text{-- OK}$

For cross sections subject to the combined actions of bending moment and shear force, where $V_{Ed} > 0.5 V_{b,Rd}$, the following equation should be satisfied (§§3.8.4, eqn. (3.129)):

$$\frac{M_{y,Ed}}{M_{y,Rd}} + \left(1 - \frac{M_{f,Rd}}{M_{pl,Rd}}\right) \left(\frac{2V_{Ed}}{V_{w,Rd}} - 1\right)^2 \leq 1.0$$

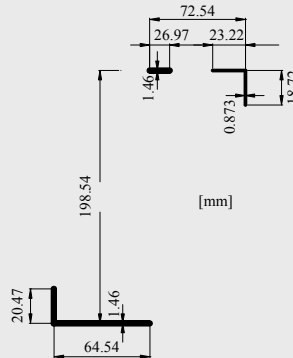
230

This situation is found at the cross section at the end of the overlap, where $V_{Ed} / V_{b,Rd} = 10.7 / 18.435 = 0.580 > 0.5$.



Cross section for $M_{pl,Rd}$
calculation

$$W_{pl} = 38296.1 \text{ mm}^3$$



Cross section for $M_{f,Rd}$
calculation

$$W_{pl,f} = 15484.1 \text{ mm}^3$$

W_{pl} is the plastic section modulus consisting of the effective area of the flanges and the fully effective area of the web;

$W_{pl,f}$ is the plastic section modulus consisting of the effective area of the flanges only.

$$M_{pl,Rd} = W_{pl} f_{yb} / \gamma_{M0} = 38296.1 \times 350 / 1.0 = 13403635 \text{ Nmm} = 13.40 \text{ kNm}$$

$$M_{f,Rd} = W_{pl,flange} f_{yb} / \gamma_{M0} = 15484.1 \times 350 / 1.0 = 5419435 \text{ Nmm} = 5.42 \text{ kNm}$$

$$\begin{aligned} \frac{M_{y,Ed}}{M_{y,Rd}} + \left(1 - \frac{M_{f,Rd}}{M_{pl,Rd}}\right) \left(\frac{2V_{Ed}}{V_{w,Rd}} - 1\right)^2 &= \\ &= \frac{8.08}{8.31} + \left(1 - \frac{5.42}{13.40}\right) \left(\frac{2 \times 10.7}{18.435} - 1\right)^2 = 0.988 \leq 1.0 \end{aligned} \quad \text{-- OK}$$

3.8.11 Combined bending moment and local load or support reaction

Cross sections subject to the combined action of a bending moment M_{Ed} and a transverse force due to a local load or support reaction F_{Ed} shall satisfy the following:

$$M_{Ed} / M_{c,Rd} \leq 1 \quad (3.130a)$$

$$F_{Ed} / R_{w,Rd} \leq 1 \quad (3.130b)$$

$$\frac{M_{Ed}}{M_{c,Rd}} + \frac{F_{Ed}}{R_{w,Rd}} \leq 1.25 \quad (3.130c)$$

where

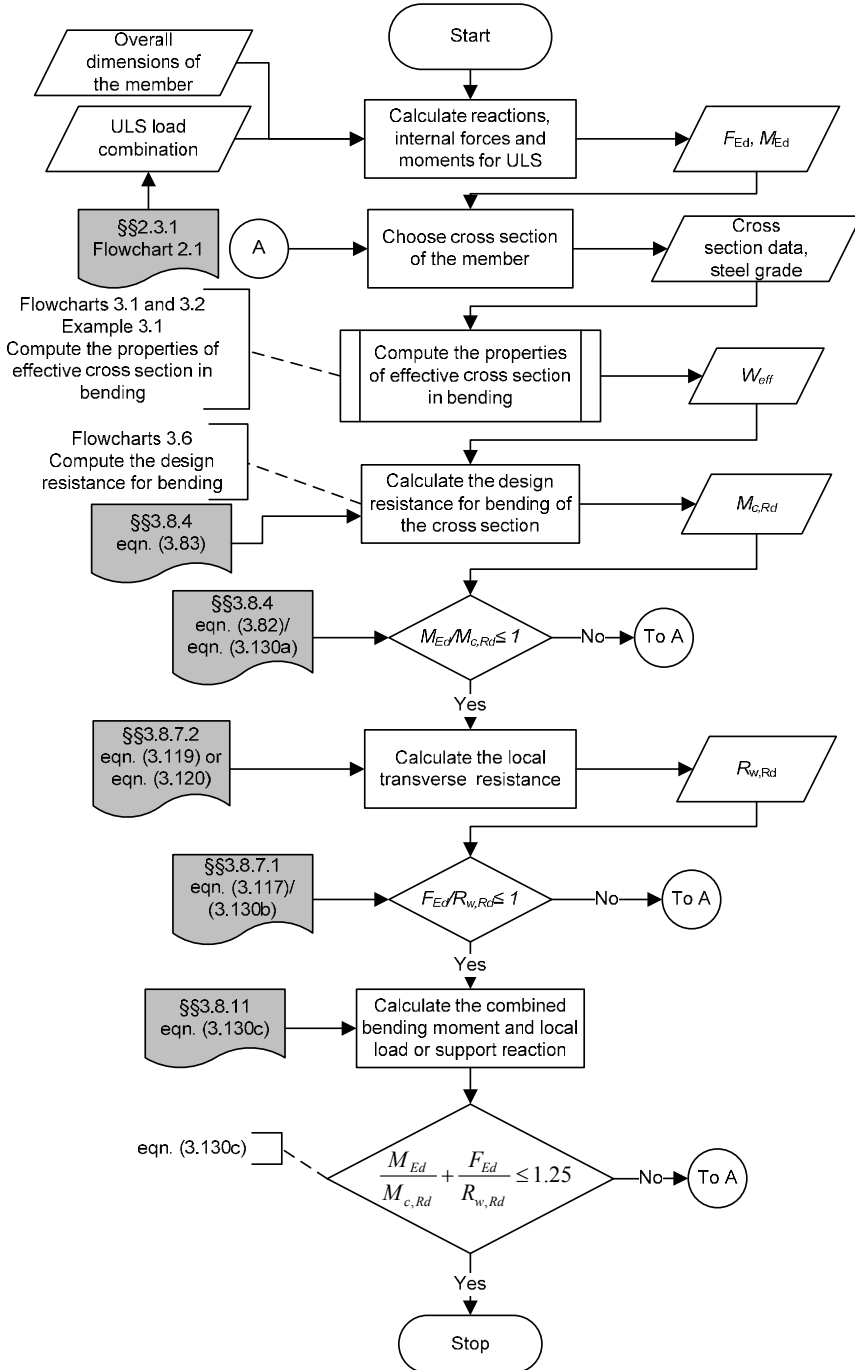
$M_{c,Rd}$ is the moment resistance of the cross section given in §§3.8.4.1;

$R_{w,Rd}$ is the appropriate value of the local transverse resistance of the web from §§3.8.7.

For members and sheeting with more than one web $R_{w,Rd}$ and F_{Sd} shall correspond to the same number of webs.

Flowchart 3.11 presents schematically the design of a cold-formed steel cross section in combined bending moment and local load or support reaction. Example 3.8 presents a numerical example.

3. BEHAVIOUR AND RESISTANCE OF CROSS SECTION



Flowchart 3.11 – Cross section in combined bending moment and local load or support reaction

Example 3.8: Design of a steel roof sheeting under vertical loads.

The roof is non-insulated and has a slope of 8° . The example is based on elastic behaviour of the sheeting and so no plastic reserve in the tension zone is taken into account. The roof sheeting is fixed with self-drilling screws to the purlins.

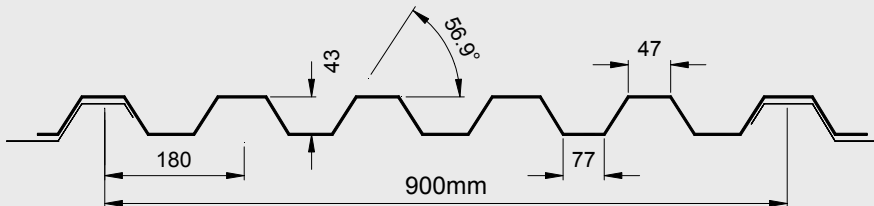
Basic Data

The static system of the sheeting is a five span static system as presented in the figure below.



The dimensions of the cross section sheeting profile and the material properties are:

Web height	$h_w = 43 \text{ mm}$
Bottom width	$b_b = 77 \text{ mm}$
Top width	$b_t = 47 \text{ mm}$
Internal radius	$r = 3 \text{ mm}$
Nominal thickness	$t_{nom} = 0.5 \text{ mm}$
Steel core thickness (§§2.4.2.1)	$t = 0.46 \text{ mm}$
Grade of steel	S250GD+Z
Basic yield strength	$f_{yb} = 250 \text{ N/mm}^2$
Ultimate tensile strength	$f_{yb} = 330 \text{ N/mm}^2$
Modulus of elasticity	$E = 210000 \text{ N/mm}^2$
Poisson's ratio	$\nu = 0.3$



3. BEHAVIOUR AND RESISTANCE OF CROSS SECTION

The loads applied to the roof sheeting:

self-weight of the sheeting	$q_G = 0.05 \text{ kN/m}^2$
snow load	$q_S = 2.00 \text{ kN/m}^2$

Partial factors $\gamma_{M0} = 1.0$ (§§2.3.1)

$$\gamma_{M1} = 1.0$$

$$\gamma_G = 1.35 \quad \text{– permanent loads (§§2.3.1, Table 2.3)}$$

$$\gamma_Q = 1.50 \quad \text{– variable loads}$$

Design for Ultimate Limit State

The effective section properties at the ultimate limit state were calculated according to §3.7.2, for effective widths of plate elements without longitudinal stiffeners - sheeting subjected to bending.

Second moment of area and section modulus of the effective cross section calculated for the case with bottom flanges in tension – in the span:

$$I_{eff,y} = 110.37 \text{ mm}^4/\text{mm}$$

- with respect to the flange in compression:

$$W_{eff,y,c} = \frac{I_{eff,y}}{z_c} = 3.77 \text{ mm}^3/\text{mm}$$

- with respect to the flange in tension:

$$W_{eff,y,t} = \frac{I_{eff,y}}{z_t} = 8.04 \text{ mm}^3/\text{mm}$$

Second moment of area and section modulus of the effective cross section calculated for the case with bottom flanges in compression – at the intermediate support:

$$I_{eff,y} = 98.38 \text{ mm}^4/\text{mm}$$

- with respect to the flange in compression:

$$W_{eff,y,c} = \frac{I_{eff,y}}{z_c} = 3.81 \text{ mm}^3/\text{mm}$$

- with respect to the flange in tension:

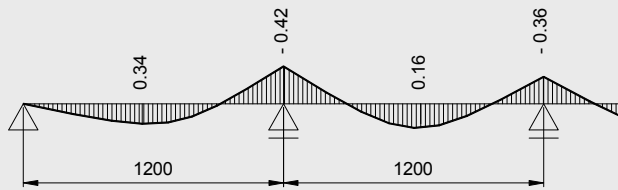
$$W_{eff,y,t} = \frac{I_{eff,y}}{z_t} = 5.73 \text{ mm}^3/\text{mm}$$

Applied loading on the joist at ULS (§§2.3.1, eqn. (2.2))

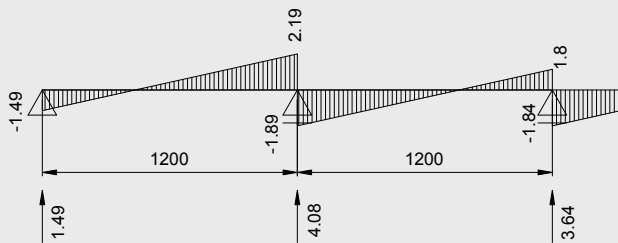
$$q_d = \gamma_G q_G + \gamma_Q q_S = 1.35 \times 0.05 + 1.50 \times 2.00 = 3.07 \text{ kN/m}^2$$

Internal forces

Bending moment diagram M_{Ed} [kNm]



Shear force diagram V_{Ed} [kN] and reactions F_{Ed} [kN]



Maximum span bending moment:

$$M_{Ed1} = 0.34 \text{ kNm/m}$$

First intermediate support:

$$M_{Ed2} = 0.42 \text{ kNm/m}$$

$$F_{Ed} = 4.08 \text{ kN/m}$$

$$V_{Ed} = 2.19 \text{ kN/m}$$

Check of bending resistance at ULS

Design moment resistance for span (§§3.8.4, eqn. (3.83)):

$$M_{c,Rd} = W_{eff,y,c} f_{yb} / \gamma_{M0} = 3.77 \times 250 / 1.0 = 925 \text{ Nmm/mm} = 0.925 \text{ kNm/m}$$

3. BEHAVIOUR AND RESISTANCE OF CROSS SECTION

Design moment resistance for the intermediate support (§§3.8.4, eqn. (3.83)):

$$M_{c,Rd} = W_{eff,y,c} f_{yb} / \gamma_{M0} = 3.81 \times 250 / 1.0 = 953 \text{ Nmm/mm} = 0.953 \text{ kNm/m}$$

Verification of bending resistance (§§3.8.11, eqn. (3.130a)):

- check of span	$\frac{M_{Ed1}}{M_{c,Rd}} = \frac{0.34}{0.925} = 0.368 < 1$ – OK
- check of intermediate support	$\frac{M_{Ed2}}{M_{c,Rd}} = \frac{0.42}{0.953} = 0.441 < 1$ – OK

Check of shear resistance at ULS

Design shear resistance (§§3.8.5, eqn. (3.91))

$$V_{b,Rd} = \frac{\frac{h_w}{\sin \phi} t f_{bv}}{\gamma_{M0}}$$

For a web without stiffening at the support:

$$f_{bv} = 0.58 f_{yb} \quad \text{if} \quad \bar{\lambda}_w \leq 0.83$$

$$f_{bv} = 0.48 f_{yb} / \bar{\lambda}_w \quad \text{if} \quad 0.83 < \bar{\lambda}_w < 1.40$$

$$f_{bv} = 0.67 f_{yb} / \bar{\lambda}_w^2 \quad \text{if} \quad \bar{\lambda}_w \geq 1.40$$

The relative slenderness $\bar{\lambda}_w$ for webs without longitudinal stiffeners:

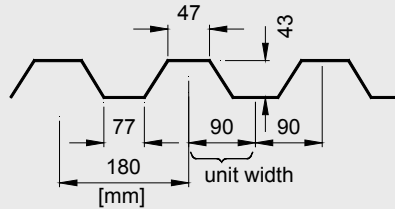
$$\bar{\lambda}_w = 0.346 \frac{s_w}{t} \sqrt{\frac{f_{yb}}{E}} = 0.346 \times \frac{50.83}{0.46} \times \sqrt{\frac{250}{210000}} = 1.32$$

$$0.83 < \bar{\lambda}_w = 1.32 < 1.40 \quad \text{so:}$$

$$f_{bv} = 0.48 f_{yb} / \bar{\lambda}_w = 0.48 \times 250 / 1.32 = 90.91 \text{ N/mm}^2$$

$$V_{b,Rd} = \frac{\frac{(43 - 0.5) \times 10^{-3}}{\sin 56.9^\circ} \times 0.46 \times 10^{-3} \times 90.91 \times 10^3}{1.0} = 2.12 \text{ kN/web}$$

Per unit width of the sheeting: 2.12 kN / 0.09 m = 23.56 kN/m



Verification of shear resistance (§§3.8.5, eqn. (3.90))

$$\frac{V_{Ed}}{V_{b,Rd}} = \frac{2.19}{23.56} = 0.093 < 1 \text{ – OK}$$

Due to the fact that $V_{Ed} \leq 0.5 V_{w,Rd}$ there is no reduction due to combined action.

Check of local transverse resistance at ULS

To obtain the local transverse resistance of an unstiffened web, the following criteria should be satisfied (§§3.8.7.3, eqn. (3.121)):

- the clear distance c from the actual bearing length for the support reaction to a free end, is 100 mm;

$$h_w/t \leq 200 \sin \phi \quad 42.5/0.46 = 92.4 < 200 \cdot \sin 56.9 = 167.5 \text{ – OK}$$

$$r/t \leq 10 \quad 3/0.46 = 6.52 < 10 \text{ – OK}$$

$$45^\circ \leq \phi \leq 90^\circ \quad \phi = 56.9^\circ \text{ – OK}$$

where ϕ is the slope of the web relative to the flanges.

The local transverse resistance of the web (§§3.8.7.3, eqn. (3.122))

$$R_{w,Rd} = \alpha \cdot t^2 \sqrt{f_{yb} E} \cdot (1 - 0.1 \sqrt{r/t}) \cdot [0.5 + \sqrt{0.02 \cdot l_a / t}] \cdot (2.4 + (\phi/90)^2) / \gamma_{M1}$$

According to §§3.8.7.3, when the support is a cold-formed section with one web or round tube, for s_s should be taken as 10 mm $\Rightarrow l_a = 10$ mm and for Category 2 the coefficient α is 0.15.

$$R_{w,Rd} = 0.15 \cdot 0.46^2 \sqrt{250 \cdot 210000} \cdot (1 - 0.1 \sqrt{3/0.46}) \cdot [0.5 + \sqrt{0.02 \cdot 10/0.46}] \cdot (2.4 + (56.9/90)^2) / 1 = 55.85 \text{ N/web} = 0.56 \text{ kN/web}$$

3. BEHAVIOUR AND RESISTANCE OF CROSS SECTION

Per unit width of the sheeting: $0.56 \text{ kN} / 0.09 \text{ m} = 6.22 \text{ kN/m}$

Verification of local transverse force (§§3.8.11, eqn. (3.130b))

$$F_{Ed} = 4.08 \text{ kN/m} < R_{w,Rd} = 6.22 \text{ kN/m} - \text{OK}$$

Check of combination of bending moment and support reaction (§§3.8.11, eqn. (3.130c))

$$\frac{M_{Sd}}{M_{c,Rd}} + \frac{F_{Sd}}{R_{w,Rd}} = \frac{0.39}{0.953} + \frac{4.03}{6.22} = 1.057 \leq 1.25$$

Chapter 4

BEHAVIOUR AND DESIGN RESISTANCE OF BAR MEMBERS

4.1 GENERAL

In the previous chapter, i.e. Chapter 3, the behaviour and resistance of cross sections of thin-walled cold-formed steel members under different stress states have been presented and discussed. Therefore, in the present chapter, the problems in which the length and end-supports or other structural links and restraints of bar members become additional parameters to those characterising the resistance of the cross sections, particularly the design against instability and for serviceability conditions.

In §§1.3.1 of Chapter 1, *Buckling strength of cold-formed members*, a qualitative discussion on the single and interactive buckling modes was presented, and the general approach used to account for the effect of coupling between a local and an overall mode was displayed in Figure 1.18.

The instability behaviour of bar members is generally characterised by stable post-critical modes. However the interaction of two stable symmetric post-critical modes may generate an unstable coupled asymmetric mode, rendering the member highly sensitive to imperfections. In such cases significant erosion of critical load occurs. Examining the cases of coupled instability, we find that two very different types exist (Gioncu, 1994):

- (a) *naturally* coupled instabilities, which result in garland curves. Two forms of instability are possible at the intersection points of these curves. The post-critical curves can be stable for uncoupled modes, but by coupling, they become unstable. This phenomenon of the change in

buckling patterns in plates and shells due to this mode interaction is very well known and may appear in the case of local buckling of the component walls of thin-walled cold-formed sections. The flexural-torsional buckling of bars with mono-symmetric open section in compression could be, in general, considered also a natural coupling between torsional and flexural buckling;

- (b) *coupling due to design*; implying that the geometric dimensions of a structure are chosen such that two or more buckling modes are simultaneously possible (see Figure 4.1). For this case, the optimisation based on the simultaneous mode design principle plays a very important role and the attitude of the designer towards this principle is decisive. This type of coupling is the most interesting in practice.

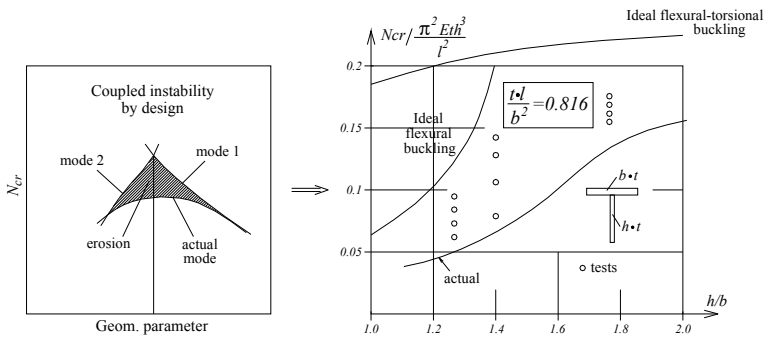


Figure 4.1 – Coupled instability by design: Flexural buckling (mode 1) + Flexural-torsional buckling (mode 2) in case of a compressed T-section (Gioncu *et al*, 1992)

Due to imperfections, the *interaction erosion* of the critical bifurcation load (e.g. the load which corresponds to the coupling point of instability modes) occurs. This erosion is *maximum* in the vicinity of the coupling point. For bar members, an interactive slenderness range, in which sensitivity to imperfections is increased, may be identified. Classes of interaction types, separated by specific levels of erosion intensity, may be defined.

For a given compression member, one may assume that two simultaneous buckling modes occur. If N_u is the critical ultimate load, and N_{cr} the ideal critical load at the coupling point, the following relation may be written:

$$N_u = (1 - \psi)N_{cr} \tag{4.1}$$

The *erosion factor* ψ was introduced as a *measure* of erosion of critical load. Gioncu (1994) has classified the interaction types by means of this erosion factor, as follows:

- class I: weak interaction (W), $\psi \leq 0.1$;
- class II: moderate interaction (M), $0.1 < \psi \leq 0.3$;
- class III: strong interaction (S), $0.3 < \psi \leq 0.5$;
- class IV: very strong interaction (VS), $\psi > 0.5$.

Cold-formed sections are, usually thin-walled, being of class 4, according to EN1993-1-1, EN1993-1-3 and also of EN1993-1-5. For such sections, the most frequent interaction occurs between a local or distortional buckling mode (i.e. sectional buckling) and an overall mode (bar member buckling) which can be flexural or flexural-torsional for compression members, or lateral-torsional for bending members.

Obviously, an appropriate classification of each coupled instability mode into the relevant erosion class is very important because the methods of analysis used for design are different from one class to another. In the case of weak or moderate interaction, structural reliability will be provided by simply using current design code methods with the relevant partial coefficients, while in the case of strong interaction, special methods are needed.

In the following, the specific instability problems of class 4 cold-formed bar members are addressed. Class 1 to 3 members, even when produced by cold-forming, may be treated according to the general provision of EN1993-1-1, and the reader is advised to use the book *Design of Steel Structures. Eurocode 3: Design of steel structures. Part 1-1: General rules and rules for buildings* (da Silva *et al*, 2010) for technical support.

4.2 COMPRESSION MEMBERS

4.2.1 Theoretical background

4.2.1.1 Ideal elastic members

The theoretical model applied in EN1993-1-1 for the design against buckling of bars in compression is based on the so called *divergence model*,

which considers the imperfect pinned bar (see Figure 4.2) and takes into account the 2nd order effect of the axial force N which, due to the eccentricity represented by the initial imperfection e_0 , generates a bending moment M , and transform the compression problem into a combined compression – bending problem.

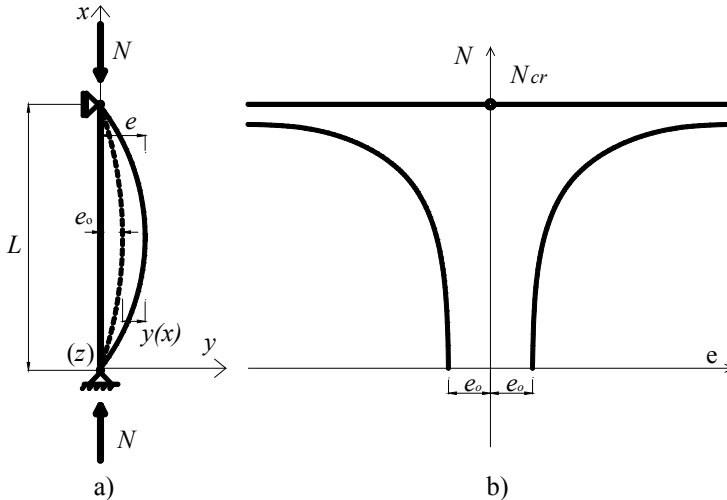


Figure 4.2 – a) Imperfect bar member in compression; b) load – deflection path

To understand the problem, one starts with the ideal straight bar shown in Figure 4.3 and applies the classic theory of elastic stability to obtain the critical bifurcation load. On this purpose, some simplifying assumptions are needed to complete the physical model of Figure 4.3, i.e.:

- material with linear elastic behaviour;
- member free from geometric imperfections and residual stresses;
- perfectly centred load;
- small displacement theory.

Accordingly, the equation of equilibrium in terms of moments can be written as:

$$(\Sigma M)_z = EI \frac{d^2 y}{dx^2} + N \cdot y = 0 \tag{4.2}$$

where E is the modulus of elasticity of the material and I is the second moment of area with respect to the $z-z$ axis, perpendicular to the plane of

buckling. Equation (4.2) is a linear homogeneous differential equation with constant coefficients, which has the general:

$$y(x) = C_1 \sin(kx) + C_2 \cos(kx) \quad (4.3)$$

with $k^2 = N/(EI)$.

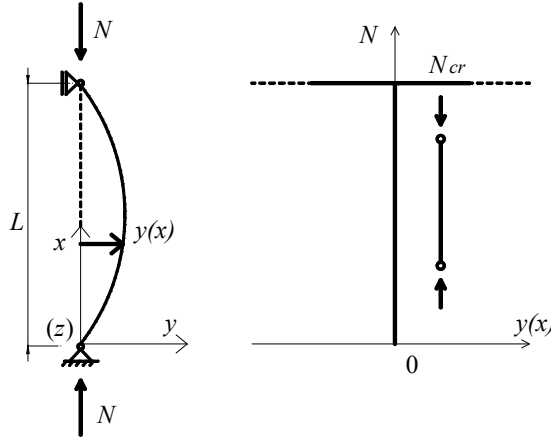


Figure 4.3 – Model of ideal pinned bar member under pure compression (Euler's column)

The constants C_1 and C_2 results from the support conditions:

$$y(x=0) = 0 \Rightarrow C_2 = 0 \quad (4.4)$$

$$y(x=L) = 0 \Rightarrow C_1 \sin(kL) = 0 \Rightarrow C_1 = 0 \text{ or } kL = n\pi \quad (4.5)$$

The critical load is obtained from:

$$kL = n\pi \Rightarrow k^2 = \frac{n^2 \pi^2}{L^2} = \frac{N}{EI} \quad (4.6)$$

and $N_{cr} = n^2 \pi^2 EI / L^2$ (with $n = 1, 2, \dots$). The reference critical load (i.e. 1st buckling load) is the lowest of the series ($n = 1$) and corresponds to the deformed configuration illustrated in Figure 4.3. It is given by the well-known formula of Euler:

$$N_{cr} = \frac{\pi^2 EI}{L^2} \quad (4.7)$$

The shape of the buckling mode is characterised by the equation:

$$y(x) = C_1 \sin\left(\frac{n\pi}{L}x\right) \tag{4.8}$$

which is indeterminate in amplitude, C_1 , and for $n = 1$ becomes:

$$y(x) = C_1 \sin\left(\frac{\pi}{L}x\right) \tag{4.9}$$

which features a half-wave over the length of column (see Figure 4.3). Thus, in the case of an ideal bar (i.e. no imperfections), the resistance to buckling depends on the bending stiffness of the cross section, on its length and on the support conditions.

For other support conditions, the critical load can be obtained in a similar way by solving the differential equation of equilibrium. Alternatively, the critical load may be obtained directly from eqn. (4.7), replacing the real length L by the buckling length L_{cr} . The buckling length L_{cr} of a member is defined as the length of a fictitious equivalent pinned member with the same critical load. Figure 4.4 illustrates the buckling lengths for isolated members, for several support conditions, considered as fundamental cases.

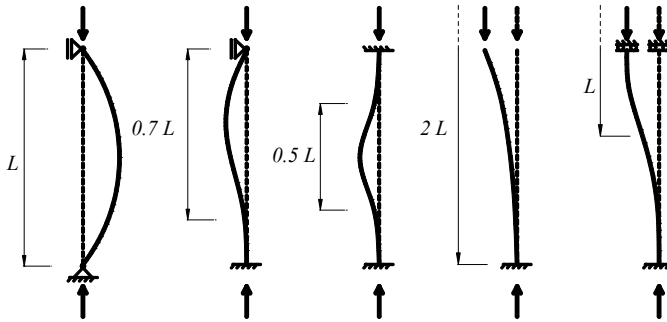


Figure 4.4 – Buckling length L_{cr} as a function of the real length L of the column

To generalize, one can use L_{cr} in the Euler’s formula (4.7), and write

$$L_{cr} = \mu L \tag{4.10}$$

where μ is the buckling length multiplier, which takes the values corresponding to the fundamental cases presented in Figure 4.4, or other values.

$$N_{cr} = \frac{\pi^2 EI}{L_{cr}^2} \quad (4.7')$$

By dividing Euler's critical load by the area of the cross section, A , the critical stress is obtained:

$$\sigma_{cr} = \frac{\pi^2 EI}{A L_{cr}^2} = \frac{\pi^2 E}{\lambda^2} \quad (4.11)$$

where, $\lambda = L_{cr}/i$ is the slenderness coefficient and $i = \sqrt{I/A}$ is the radius of gyration of the section.

In a member without imperfections, composed of a material with elastic-perfectly plastic behaviour (i.e. mild steel), failure will only occur by buckling in the elastic range if Euler's critical stress is lower than the yield stress f_y . For a short member (with a low slenderness coefficient λ), failure occurs by yielding of the cross section, when the applied stress equals the yield stress, that is, when $\sigma = N/A = f_y$. The limit between the two types of behaviour is defined by a value of the slenderness coefficient, denoted as λ_1 , given by:

$$\sigma_{cr} = \frac{\pi^2 E}{\lambda_1^2} = f_y \Rightarrow \lambda_1 = \pi \sqrt{\frac{E}{f_y}} \quad (4.12)$$

Based on the slenderness coefficient λ_1 , the non-dimensional slenderness coefficient $\bar{\lambda}$ is defined as:

$$\bar{\lambda} = \frac{\lambda}{\lambda_1} = \pi \sqrt{\frac{A f_y}{N_{cr}}} \quad (4.13)$$

The behaviour of a compressed bar member, without imperfections, for the full slenderness range, is represented in Figure 4.5.

The solution represented by Euler's formula (4.7) corresponds to flexural buckling, according to which the instability is caused by a pure deflection and no twist rotation occurs. The lowest value of critical load corresponds to the buckling plane characterised by the largest slenderness of the bar.

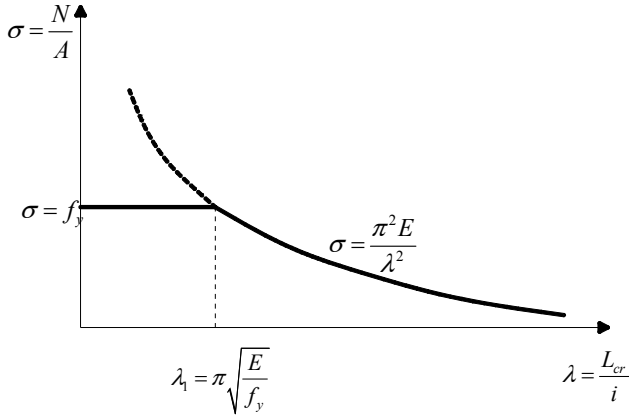
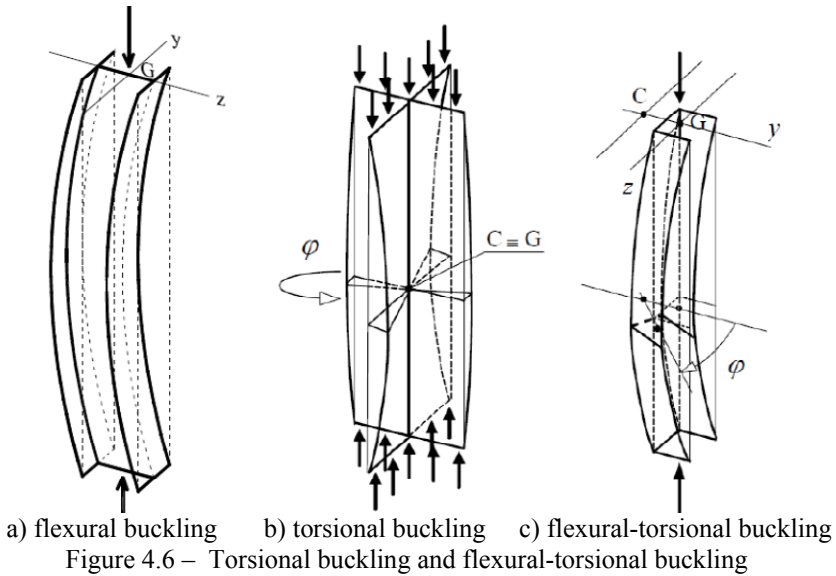


Figure 4.5 – $\sigma - \lambda$ relationship of a compressed ideal member

However, in case of members in compression of thin-walled open cross section (and hence low torsional stiffness), not only flexural buckling may occur (see Figure 4.6a) but also torsional buckling or flexural-torsional buckling may occur (Trahair, 1993; Hirt *et al*, 2006). Torsional buckling is due to the rotation of cross sections around the shear centre axis of the member, as illustrated in Figure 4.6b; flexural-torsional buckling consists of the simultaneous occurrence of torsional and flexural deformations along the axis of the member (see Figure 4.6c).



The instability modes illustrated in Figure 4.6 are characteristic of thin-walled open cross sections, such as channels, angles or cruciform cross sections. The torsional mode is considered, in general, a theoretical one, mainly important as component of the naturally coupled flexural-torsional (FT) buckling mode.

For members of symmetric cross section with respect to the y axis, the torsional buckling critical load is given by:

$$N_{cr,T} = \frac{1}{i_o^2} \left(GI_t + \frac{\pi^2 EI_w}{L_{cr,T}^2} \right) \quad (4.14)$$

For the same type of cross sections, the flexural-torsional (FT) buckling critical load is given by:

$$N_{cr,FT} = \frac{N_{cr,y}}{2\beta} \left[1 + \frac{N_{cr,T}}{N_{cr,y}} - \sqrt{\left(1 + \frac{N_{cr,T}}{N_{cr,y}} \right)^2 - 4\beta \frac{N_{cr,T}}{N_{cr,y}}} \right] \quad (4.15)$$

where

- G is the shear modulus;
- I_t is the torsion constant of the gross cross section;
- I_w is the warping constant of the gross cross section;
- i_y is the radius of gyration of the gross cross section about the y -axis;
- i_z is the radius of gyration of the gross cross section about the z -axis;

- $L_{cr,T}$ is the buckling length of the member for torsional buckling;
- y_o, z_o are the shear centre co-ordinates with respect to the centroid of the gross cross section ($z_o = 0$ for a cross section symmetric with respect to the y -axis);

- i_o is the polar radius of gyration given by

$$i_o^2 = i_y^2 + i_z^2 + y_o^2 + z_o^2 \quad (4.16)$$

- $N_{cr,y}$ is the critical load for flexural buckling about the y -axis;

$$\beta \text{ is a factor given by } \beta = 1 - (y_o/i_o)^2 \quad (4.17)$$

4.2.1.2 Imperfect member

In real structures, imperfections are unavoidable and cause different column behaviour from the theoretical behaviour described in §§4.2.1.1. The theoretical critical load is, in general, not reached in the presence of imperfections. Imperfections can be divided into two types: (i) geometrical imperfections (initial bowing, warping, twisting, local deviations characterised by dents and regular undulations in component walls, eccentricity of the loads) and (ii) material imperfections (variations of yield strength, residual stresses). For further details, see §§2.6.

To obtain the real column behaviour one considers the imperfect bar shown in Figure 4.2, which is affected by an equivalent geometrical imperfection of amplitude e_o , and takes as model of that, a sine shape affine with the 1st buckling mode of the perfect bar (see eqn. 4.9), represented by the following equation:

$$y_o = e_o \sin\left(\frac{\pi x}{L}\right) \quad (4.18)$$

The differential equation for equilibrium of a pinned imperfect member is:

$$EI \frac{d^2 y}{dx^2} + N(y + y_o) = 0 \quad (4.19)$$

Introducing eqn. (4.18) in eqn. (4.19) and considering the same boundary conditions as for the ideal pin-ended bar, the following solution is obtained:

$$y(x) = \frac{e_o}{\frac{N_{cr}}{N} - 1} \sin\left(\frac{\pi}{L} x\right) \quad (4.20)$$

where N_{cr} is the Euler critical load given by eqn. (4.7). The total deformation of the member is $y_t(x) = y_o(x) + y(x)$ and results as a function of the applied axial force N :

$$y_t(x) = \frac{e_o}{1 - \frac{N}{N_{cr}}} \sin\left(\frac{\pi x}{L}\right) \quad (4.21)$$

Its maximum amplitude, denoted by e , is obtained for $x = L/2$:

$$e = \frac{e_o}{1 - \frac{N}{N_{cr}}} \quad (4.22)$$

The existence of an initial deformation, $y_o(x)$, even for low values of the axial force N , generates a 2nd order bending moment given by:

$$M(x) = N(y + y_o) = N \frac{e_o}{1 - \frac{N}{N_{cr}}} \sin\left(\frac{\pi x}{L}\right) \quad (4.23)$$

which causes a progressive increase of the lateral displacements, and the behaviour and failure mode displayed in Figure 1.16. The relation between the maximum lateral displacement e and the applied axial force N , introduced by eqn. (4.22), is represented in Figure 4.2b.

Figure 4.7 illustrates the results of experimental tests on axially compressed members with several slenderness coefficients $\bar{\lambda}$ and compares the test strengths with the theoretical ideal strength (ECCS, 1976). It can be observed that for low values of $\bar{\lambda}$, failure occurs essentially by plastification of the section (this is the case (a) in Figure 1.16) and values of σ/f_y higher than 1.0 are obtained experimentally due to strain-hardening. For slender bars, of high values of $\bar{\lambda}$, failure occurs essentially by buckling in the elastic range, the imperfections not having much influence. For intermediate values of $\bar{\lambda}$, failure occurs by elastoplastic instability, and it is in this slenderness domain that imperfections have most influence (the experimental results deviate most from the bounding theoretical curve comprised of yielding and elastic Euler buckling).

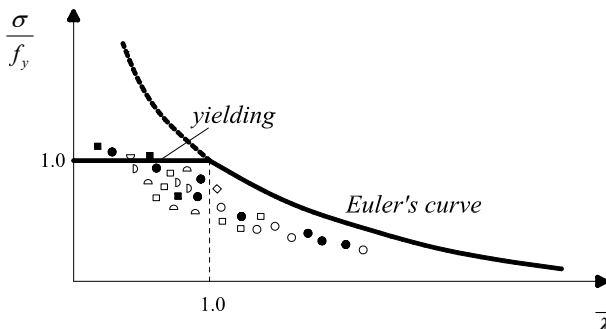


Figure 4.7 – Results of experimental tests in real members

The resistance of compressed members is based on the “European design buckling curves” (ECCS, 1978) that relate the ratio $\chi = \sigma / f_y$ to the non-dimensional slenderness $\bar{\lambda}$. These (five) curves (see Figure 4.8) were the result of an extensive experimental and numerical research programme (ECCS, 1976), conducted on hot-rolled and welded sections, that accounted for all imperfections in real compressed members (initial out-of-straightness, eccentricity of the applied loads, residual stresses).

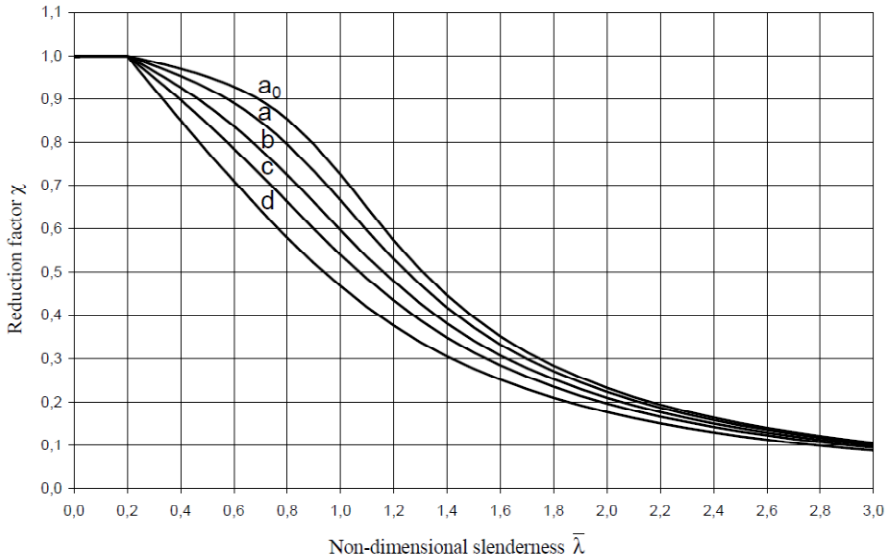


Figure 4.8 – European design buckling curves

The analytical formulation of the buckling curves was derived by Maquoi & Rondal (1978), and is based on the Ayrton-Perry formula, considering an initial sinusoidal deformed configuration corresponding to an “*equivalent initial deformed configuration*” where the amplitude was calibrated in order to reproduce the effect of all imperfections.

Considering the model of a compressed column as presented in Figure 4.2a, with a sinusoidal initial deformation according to eqn. (4.18), and assuming that the column is free from residual stresses, the plastification in outer fibres of cross section is attained when the following condition is met:

$$\frac{N}{A} + \frac{N e}{W_{el}} = f_y \tag{4.24}$$

where

- N is the value of axial compression N ($N \leq N_{cr}$);
 e is the maximum lateral deformation;
 A is the area;
 W_{el} is the elastic section modulus.

Equation (4.24) can be written in a non-dimensional form, by replacing e with the expression given by eqn. (4.22) and dividing all terms by f_y :

$$\frac{N}{N_{pl}} + \frac{N e_o A}{W_{el} \left(1 - \frac{N}{N_{pl}} \frac{N_{pl}}{N_{cr}} \right) N_{pl}} = 1 \quad (4.25)$$

Defining $\chi = N / N_{pl} = \bar{N}$ yields:

$$\chi + \frac{\chi}{\left(1 - \chi \bar{\lambda}^2 \right)} \frac{e_o A}{W_{el}} = 1 \quad (4.26)$$

or

$$(1 - \chi) \left(1 - \chi \bar{\lambda}^2 \right) = \frac{e_o A}{W_{el}} \chi = \eta \chi \quad (4.27)$$

which constitutes the basic form of the Ayrton-Perry equation. η represents the generalized initial imperfection and can be used to account for the effects on the buckling strength of initial imperfections such as geometrical, material or mechanical. Because the influence of some of these initial imperfections is linked to the length of the member, it has been chosen to express η as follows (Maquoi & Rondal, 1978):

$$\eta = \alpha (\bar{\lambda} - 0.2) \quad (4.28)$$

where the imperfection factor α depends on the shape of the cross section, buckling plane, etc. and offset 0.2 defines the length of the plateau along which $\chi = 1.0$. Based on the previous relations, the Ayrton-Perry eqn. (4.27) can be written in the form:

$$\left(1 - \chi \bar{\lambda}^2 \right) (1 - \chi) = \eta \chi = \alpha \chi (\bar{\lambda} - 0.2) \quad (4.29a)$$

or, in terms of normalised or non-dimensional axial force, $\bar{N} = N / N_{pl}$, as:

$$(1 - \bar{N})(1 - \bar{N} \bar{\lambda}^2) = \alpha \bar{N}(\bar{\lambda} - 0.2) \tag{4.29b}$$

Equation (4.29) is a quadratic equation in χ , from which the minimum solution only is relevant:

$$\chi = \frac{\phi - \sqrt{\phi^2 - \bar{\lambda}^2}}{\bar{\lambda}^2} \tag{4.30}$$

with

$$\phi = 0.5 \left[1 + \alpha(\bar{\lambda} - 0.2) + \bar{\lambda}^2 \right] \tag{4.31}$$

By multiplying the numerator and the denominator of the eqn. (4.30) by the conjugated term $\phi + \sqrt{\phi^2 - \bar{\lambda}^2}$, the expression from EN1993-1-1 is obtained, which gives the χ factor (reduction factor accounting for the potential of flexural buckling) as a function of the non-dimensional slenderness coefficient $\bar{\lambda}$ and the imperfection factor α :

$$\chi = \frac{1}{\phi + \sqrt{\phi^2 - \bar{\lambda}^2}} \tag{4.32}$$

The European buckling curves, modelled by eqns. (4.28), (4.31) and (4.32) are displayed in Figure 4.8. The corresponding values of the imperfection factor α are shown in Table 4.1.

Table 4.1 – Imperfection factors for buckling curves

Buckling curve	a_0	a	b	c	d
Imperfection factor α	0.13	0.21	0.34	0.49	0.76

This design approach is applicable to class 1 to 3 cross sections. For class 4, the case of thin-walled sections, interaction between local or distortional buckling with overall buckling occurs and is accounted for in EN1993-1-1.

4.2.1.3 Class 4 sections: local-global interactive buckling

To take into account the interaction between local and global buckling of thin-walled sections (class 4), the calculation of the load bearing capacity is based upon the effective cross section, calculated for uniform compression. For practical reasons, the same approach is applied in EN1993-1-3 for thin-walled cold-formed sections. In fact, the same buckling curves, based on hot-rolled section tests are used for cold-formed sections too, even though the behaviour of cold-formed sections is different due to the different fabrication process, which affects the nature and influence of imperfections (see §§1.2.3 and §§2.7.4.1).

A member is subjected to concentric compression if the line of action of the applied load goes through the neutral axis of the effective cross section. If this line does not coincide with the centroid of the gross cross section, bending moments corresponding to the shift of the centroidal axes (see Figure 4.9) should be taken into account.

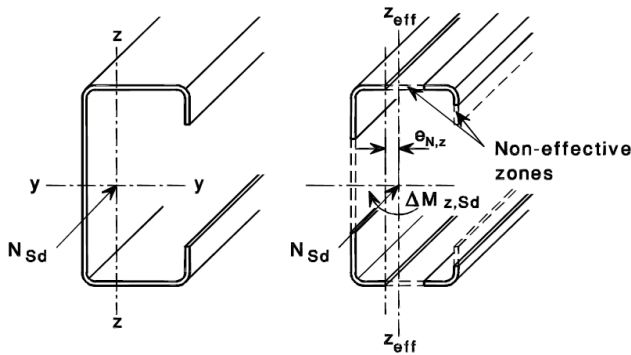


Figure 4.9 – Shift of neutral axis due to effective cross section

To take the effect of local buckling into account, the strength of the cross section is expressed as:

$$N = A_{eff} f_y \quad (4.33)$$

where A_{eff} is the effective area of cross section, calculated using the effective width approach.

Introducing $A_{eff} = QA$, where A is the area of the gross cross section and Q is a reduction factor calculated on the basis of the effective width

principle, the strength of the *effective* or *reduced* cross section can be written as:

$$N = A_{eff} f_y = Q A f_y \quad (4.34)$$

and, as a consequence, eqn. (4.29b) becomes:

$$(Q - \bar{N})(1 - \bar{\lambda}^2 \bar{N}) = \alpha(\bar{\lambda} - 0.2)\bar{N} \quad (4.35)$$

with $\bar{N} = N / Q A f_y$ and

$$\bar{\lambda} = \sqrt{\frac{A_{eff} f_y}{N_{cr}}} = \frac{\lambda}{\lambda_1} \sqrt{Q} \quad (4.36)$$

Equation (4.35) represents the Ayrton-Perry formula for *Local-Overall Interactive Buckling*.

There are also other approaches available to account for the interactive buckling of thin-walled members which, in some way, are replicating better the nature of the interactive phenomenon. Two of these approaches are summarised in the following.

Direct Strength Method

254

Schafer & Peköz (1998) have proposed a new procedure which works only with the gross properties of the cross section of a member and can take into account the interaction between local and global buckling and also the interaction between distortional and global buckling.

The Direct Strength Method is an extension of the column design approach to other modes such as local and distortion buckling modes, developed both for columns and beams, as proposed by Schafer (2001). The method was adopted in 2004 as Appendix 1 of the *North American Specification for the Design of Cold-Formed Steel Structural Members (AISI, 2004)* and in 2005 by the *Australian/New Zealand Standard for Cold-formed steel structures (AS/NZS4600:2005)*.

In the following only the method for columns is presented.

The nominal axial strength, P_{ne} , for *flexural, torsional, or flexural-torsional buckling* is:

$$\lambda_c \leq 1.5 \quad P_{ne} = (0.658^{\lambda_c^2}) P_y \quad (4.37a)$$

$$\lambda_c > 1.5 \quad P_{ne} = \left(\frac{0.877}{\lambda_c^2} \right) P_y \quad (4.37b)$$

where

$$\lambda_c = \sqrt{P_y / P_{cre}}$$

$$P_y = A f_y$$

P_{cre} = minimum of the critical elastic column buckling load for flexural, torsional or flexural-torsional buckling.

The nominal axial strength, P_{nl} , for *local buckling* is:

$$\lambda_l \leq 0.776 \quad P_{nl} = P_{ne} \quad (4.38a)$$

$$\lambda_l > 0.776 \quad P_{nl} = \left[1 - 0.15 \left(\frac{P_{crl}}{P_{ne}} \right)^{0.4} \right] \left(\frac{P_{crl}}{P_{ne}} \right)^{0.4} P_{ne} \quad (4.38b)$$

where

$$\lambda_l = \sqrt{P_{ne} / P_{crl}}$$

P_{crl} = critical elastic local buckling load

The nominal axial strength, P_{nd} , for *distortional buckling* is:

$$\lambda_d \leq 0.561 \quad P_{nd} = P_y \quad (4.39a)$$

$$\lambda_d > 0.561 \quad P_{nd} = \left[1 - 0.25 \left(\frac{P_{crd}}{P_y} \right)^{0.6} \right] \left(\frac{P_{crd}}{P_y} \right)^{0.6} P_y \quad (4.39b)$$

where

$$\lambda_d = \sqrt{P_y / P_{crd}}$$

$$P_y = A f_y$$

P_{crd} = critical elastic distortional buckling load.

Erosion of Critical Bifurcation Load (ECBL) approach

On the basis of the Erosion of Critical Bifurcation Load (ECBL) concept (Dubina, 2001), a new approach was proposed to evaluate the ultimate strength for local – overall interactive buckling. Even, perhaps, not

so successful for practical application, it enhances the understanding of the coupled instability phenomenon.

Assuming the two instability modes are the Euler bar instability mode, $\bar{N}_E = 1/\bar{\lambda}^2$, and the local instability mode, $\bar{N}_L = Q$ (see Figure 4.10), then the maximum erosion of the critical load, due both to imperfections and coupling effects, occurs in the coupling point $\bar{\lambda}_C = 1/\sqrt{Q}$.

The interactive buckling load, $\bar{N}(\bar{\lambda}, Q, \psi)$, passes through this point and the corresponding value of relative ultimate buckling load is $\bar{N}_E = (1 - \psi)\bar{N}_L$, where ψ is the erosion factor.

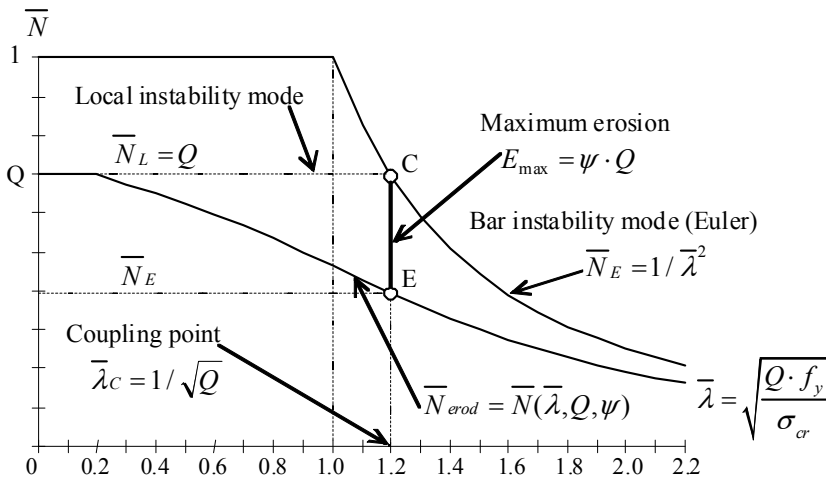


Figure 4.10 – The interactive buckling model based on the ECBL theory

It should be notice that $\bar{N}_L = Q$ does not represent rigorously the theoretical local buckling curve, but it can be assumed (in a simplified way) as a *level* of the cross section local buckling strength, and, on the basis of this assumption, it is possible to evaluate the ultimate strength of a short length of column.

It is easy to show the relation between the imperfection and erosion factors. The *negative sign* solution of eqn. (4.29b), at the particular point $\bar{\lambda} = 1$ has to be taken equal to $(1 - \psi)$, because it corresponds to the maximum erosion of the Euler curve when no local buckling occurs (see Figure 4.11), i.e.

$$\bar{N}(\bar{\lambda} = 1, \alpha) = \frac{1}{2} [2 + 0.8\alpha - \sqrt{(2 + 0.8\alpha)^2 - 4}] = 1 - \psi \quad (4.40)$$

which gives:

$$\alpha = \frac{\psi^2}{0.8(1-\psi)} \tag{4.41}$$

or

$$\psi = 0.4(\sqrt{5\alpha + \alpha^2} - \alpha) \tag{4.42}$$

In this case the *erosion* can be related to the plastic-elastic interaction between the *rigid plastic mode* (plastic strength) of a stub column and the overall elastic buckling strength of the bar, given by the Euler formula.

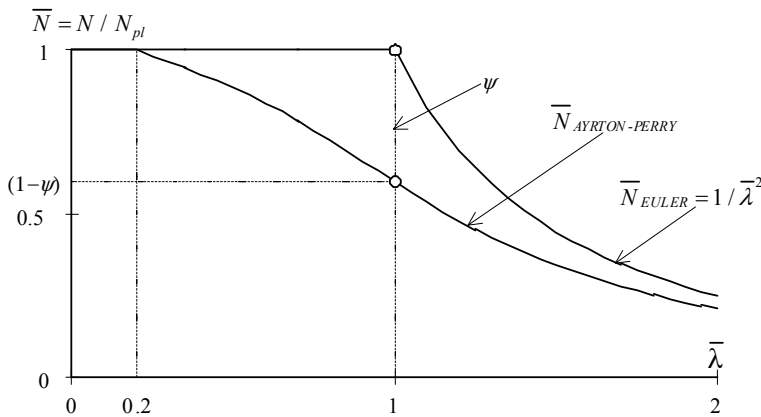


Figure 4.11 – The erosion of bar buckling curve

Figure 4.12 shows the change of ψ erosion factor as a function of the imperfection coefficient α .

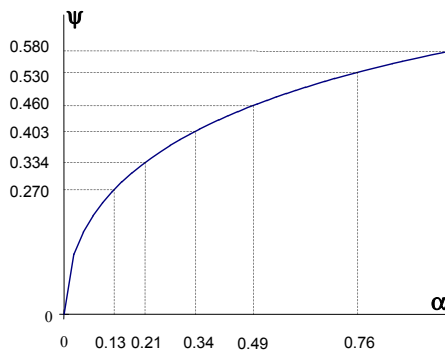


Figure 4.12 – Relation between erosion factor ψ and imperfection coefficient α

When local buckling occurs prior to bar buckling, the corresponding solution of eqn. (4.35), at the coupling point, E (see Figure 4.10) is:

$$\bar{N} = \frac{1 + \alpha(\bar{\lambda} - 0.2) + Q\bar{\lambda}^2}{2\bar{\lambda}^2} - \frac{1}{2\bar{\lambda}^2} \sqrt{[1 + \alpha(\bar{\lambda} - 0.2) + Q\bar{\lambda}^2]^2 - 4Q\bar{\lambda}^2} = (1 - \psi)Q \tag{4.43}$$

which leads to

$$\alpha = \frac{\psi^2}{1 - \psi} \cdot \frac{\sqrt{Q}}{1 - 0.2\sqrt{Q}} \tag{4.44}$$

This represents a new formula for the imperfection coefficient, α , which could be introduced in the European buckling curves in order to adapt these to more accurately account for local – overall buckling interaction effects. Figure 4.13 (a and b) show the change of α as a function of ψ and Q .

When one speaks about the erosion of theoretical buckling strength at the coupling point, distinction should be made between the *erosion* expressed by ψ , which refers to the effect of both imperfections and coupling, and the reduced ultimate strength of member due to local buckling, which is represented by the Q factor.

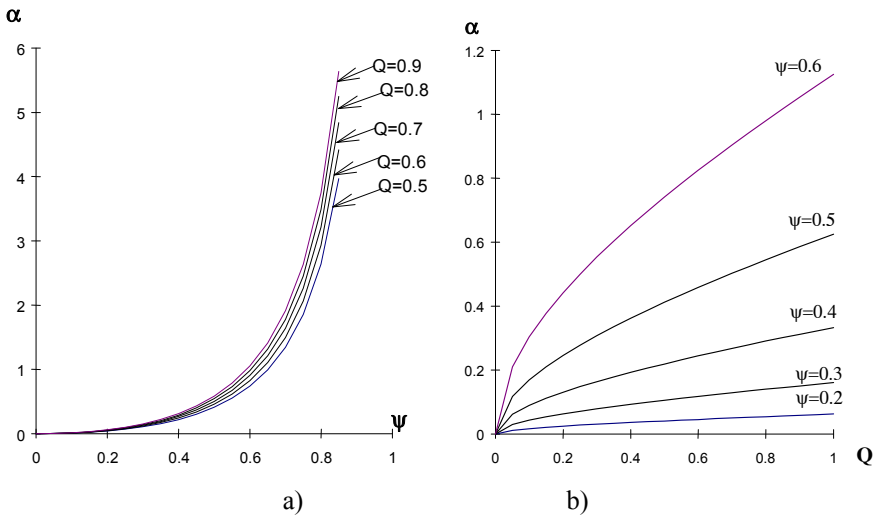


Figure 4.13 – Relation between α , Q and ψ

Compared to the large experimental campaign developed to obtain the European buckling curves (Sfintesco, 1970), it appears easier to evaluate experimentally and/or numerically the ψ erosion factors for specific types of cold-formed steel sections and, on this basis, to calibrate appropriate imperfection coefficients α , for these to be implemented in the Eurocode 3 approach. Examples of calibration of the imperfection coefficients α are presented by Dubina & Ungureanu (2002) and Dubina (2008).

4.2.2 Buckling resistance of uniform members in compression. Design according to EN1993-1-3

The provisions in EN1993-1-1 (§§6.3.1 of the code) for buckling resistance of uniform members with cross sections of Class 4 in compression have to be combined with the relevant provisions of §§6.2.1 of EN1993-1-3.

A member in compression should be verified against buckling using the following equation:

$$\frac{N_{Ed}}{N_{b,Rd}} \leq 1 \quad (4.45)$$

where

N_{Ed} is the design value of the compression force;

$N_{b,Rd}$ is the design buckling resistance of the compression member.

 259

The design buckling resistance of a compression member with Class 4 cross section should be taken as:

$$N_{b,Rd} = \frac{\chi A_{eff} f_y}{\gamma_{M1}} \quad (4.46)$$

where χ is the reduction factor for the relevant buckling mode.

For members with non-symmetric class 4 sections, the additional moment ΔM_{Ed} should be taken into account due to the eccentricity of the centroidal axis of the effective section, as shown in Figure 3.42 of §§3.8.3 of this book (see also §§6.2.2.5(4) of EN1993-1-1 and the interaction should be carried out according to §§6.3.3 of EN1993-1-1).

For axial compression members, the value of χ for the appropriate non-dimensional slenderness $\bar{\lambda}$ should be determined from the relevant buckling curve according to:

$$\chi = \frac{1}{\phi + \sqrt{\phi^2 - \bar{\lambda}^2}} \quad \text{but} \quad \chi \leq 1 \quad (4.47)$$

where

$$\phi = 0.5 \left[1 + \alpha (\bar{\lambda} - 0.2) + \bar{\lambda}^2 \right]$$

and $\bar{\lambda} = \sqrt{\frac{A_{eff} f_y}{N_{cr}}}$ for class 4 cross sections.

α is the imperfection factor;

N_{cr} is the elastic critical force for the relevant buckling mode based on the gross cross sectional properties.

The imperfection factor α corresponding to the appropriate buckling curve should be obtained from Table 4.1 and Table 4.2.

For slenderness $\bar{\lambda} \leq 0.2$ or for $N_{Ed} / N_{cr} \leq 0.04$, the buckling effects may be ignored and only cross sectional strength checks are required.

4.2.2.1 Flexural buckling

The design buckling resistance $N_{b,Rd}$ for flexural buckling should be obtained from EN1993-1-1 using the appropriate buckling curve according to the type of cross section, axis of buckling and yield strength used.

For flexural buckling the appropriate buckling curve should be obtained from Table 4.2. The buckling curve for a cross section not included in Table 4.2 may be obtained by analogy.

The buckling resistance of a closed built-up cross section should be determined using either:

- buckling curve *b* in association with the basic yield strength f_{yb} of the flat sheet material out of which the member is made by cold-forming;
- buckling curve *c* in association with the average yield strength f_{ya} of the member after cold forming, provided that $A_{eff} = A$.

The appropriate non-dimensional slenderness $\bar{\lambda}$ could be written as:

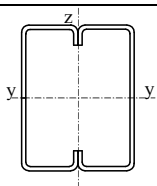
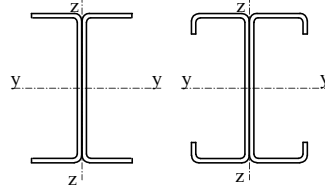
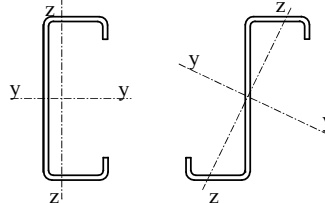
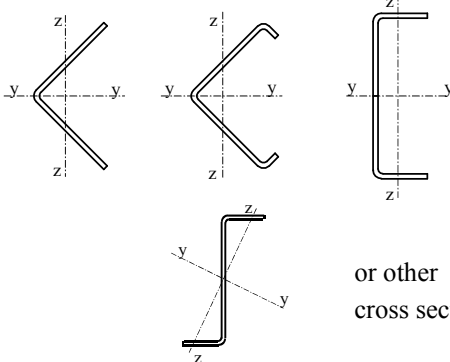
$$\bar{\lambda} = \sqrt{\frac{A_{eff} f_y}{N_{cr}}} = \frac{L_{cr}}{i} \sqrt{\frac{A_{eff}}{A}} \lambda_1 \quad (4.48)$$

where

- L_{cr} is the buckling length in the buckling plane considered;
- I is the radius of gyration about the relevant axis, determined using the properties of the gross cross section;

$$\lambda_1 = \pi \sqrt{\frac{E}{f_y}}$$

Table 4.2 – Appropriate buckling curve for various types of cross section

Type of cross section	Buckling about axis	Buckling curve
	if f_{yb} is used	b
	if f_{ya} is used *)	c
	y-y	a
	z-z	b
	any	b
 or other cross section	any	c
*) The average yield strength f_{ya} should not be used unless $A_{eff} = A_g$		

4.2.2.2 Torsional buckling and flexural-torsional buckling

For members with point-symmetric open cross sections (e.g. cruciform section or Z-purlin with equal flanges), account should be taken of the possibility that the resistance of the member to torsional buckling might be less than its resistance to flexural buckling.

For members with mono-symmetric open cross sections, as shown Figure 4.14, account should be taken of the possibility that the resistance of the member to flexural-torsional buckling might be less than its resistance to flexural buckling. For members with non-symmetric open cross sections the problem, even more complex, is quite similar.

The design buckling resistance $N_{b,Rd}$ for torsional or flexural-torsional buckling should be obtained using eqn. (4.46) and the relevant buckling curve for buckling about the $z-z$ axis obtained from Table 4.2; however, the $y-y$ axis is relevant for determining the flexural buckling strength of plain and lipped angles.

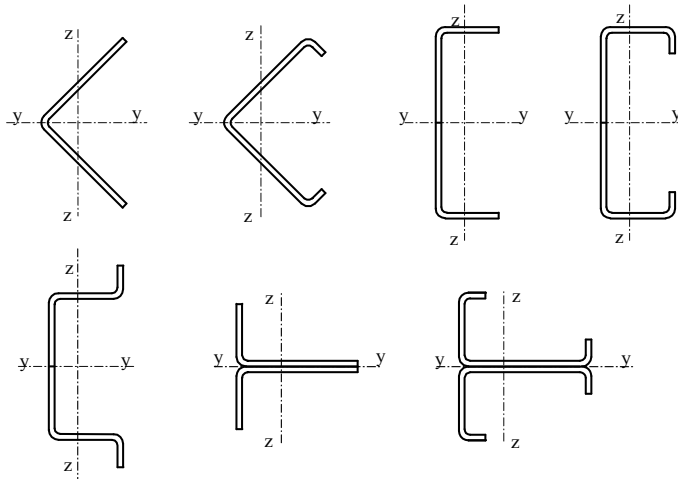


Figure 4.14 – Mono-symmetric cross sections susceptible to torsional-flexural buckling

The elastic critical force $N_{cr,T}$ for torsional buckling of a simply supported column should be determined using eqn. (4.14).

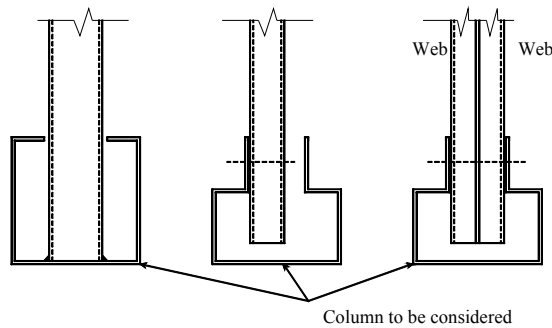
In case of doubly symmetric cross sections (i.e. $y_0 = z_0 = 0$), there are no flexural-torsional modes, so, all modes, i.e. $N_{cr,y}$, $N_{cr,z}$ and $N_{cr,T}$ are uncoupled and will be calculated appropriately.

For cross sections that are symmetrical about the y - y axis (e.g. $z_o = 0$), the elastic critical force $N_{cr,FT}$ for flexural-torsional buckling should be determined using eqn. (4.15).

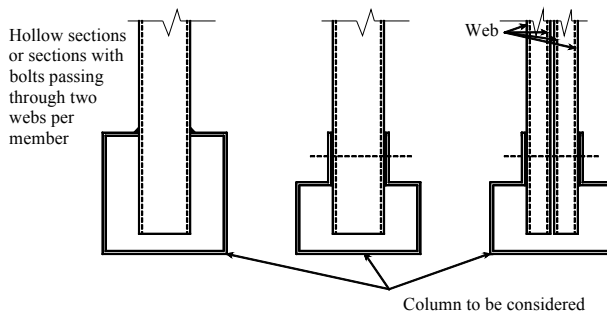
The buckling length l_T for torsional or flexural-torsional buckling should be determined taking into account the degree of torsional and warping restraint at each end of the member length L_T .

For practical connections at each end, the value of l_T / L_T may be taken as follows:

- 1.0 for connections that provide partial restraint against torsion and warping, see Figure 4.15(a);
- 0.7 for connections that provide significant restraint against torsion and warping, see Figure 4.15(b).



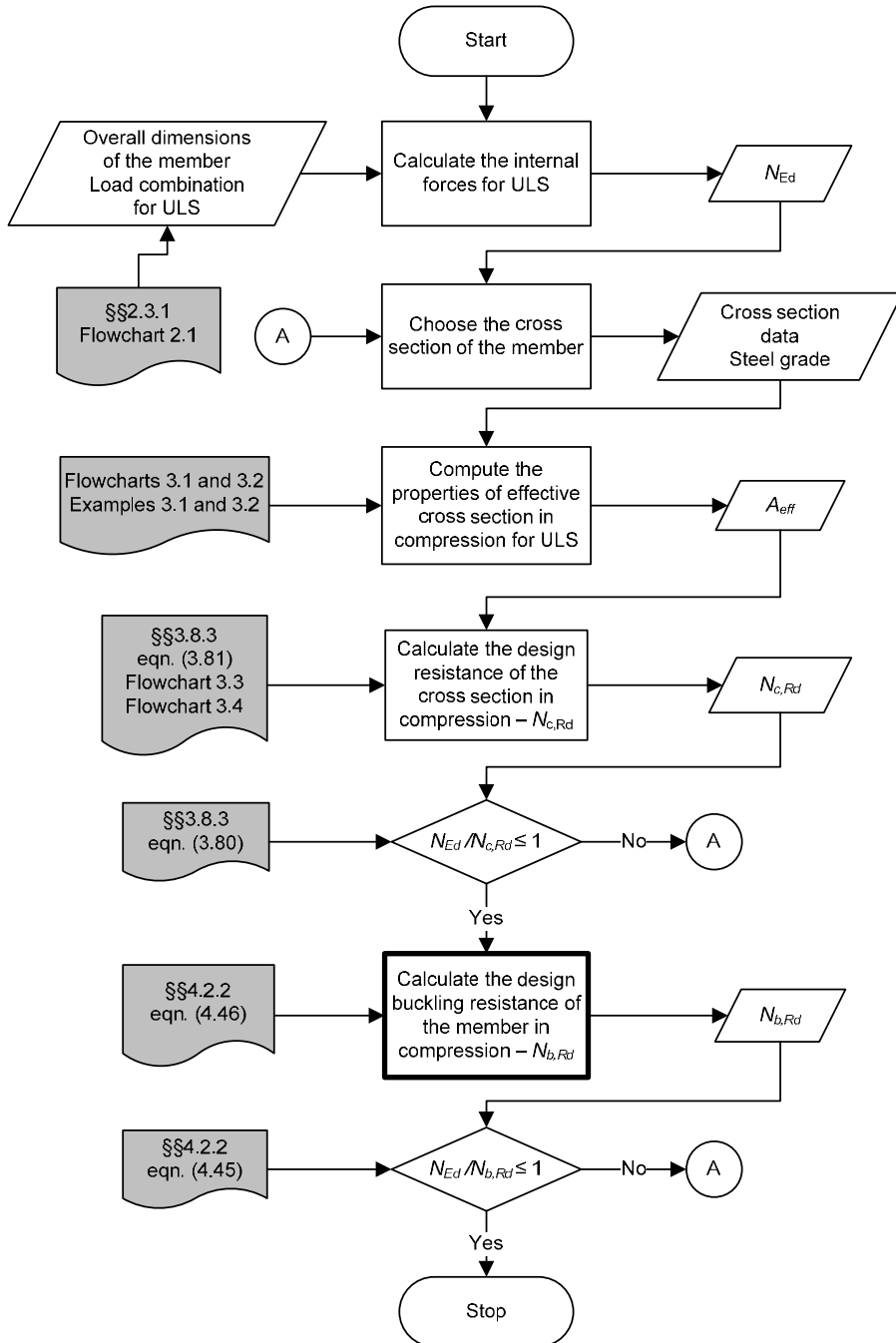
a) Connections capable of giving partial torsional and warping restraint



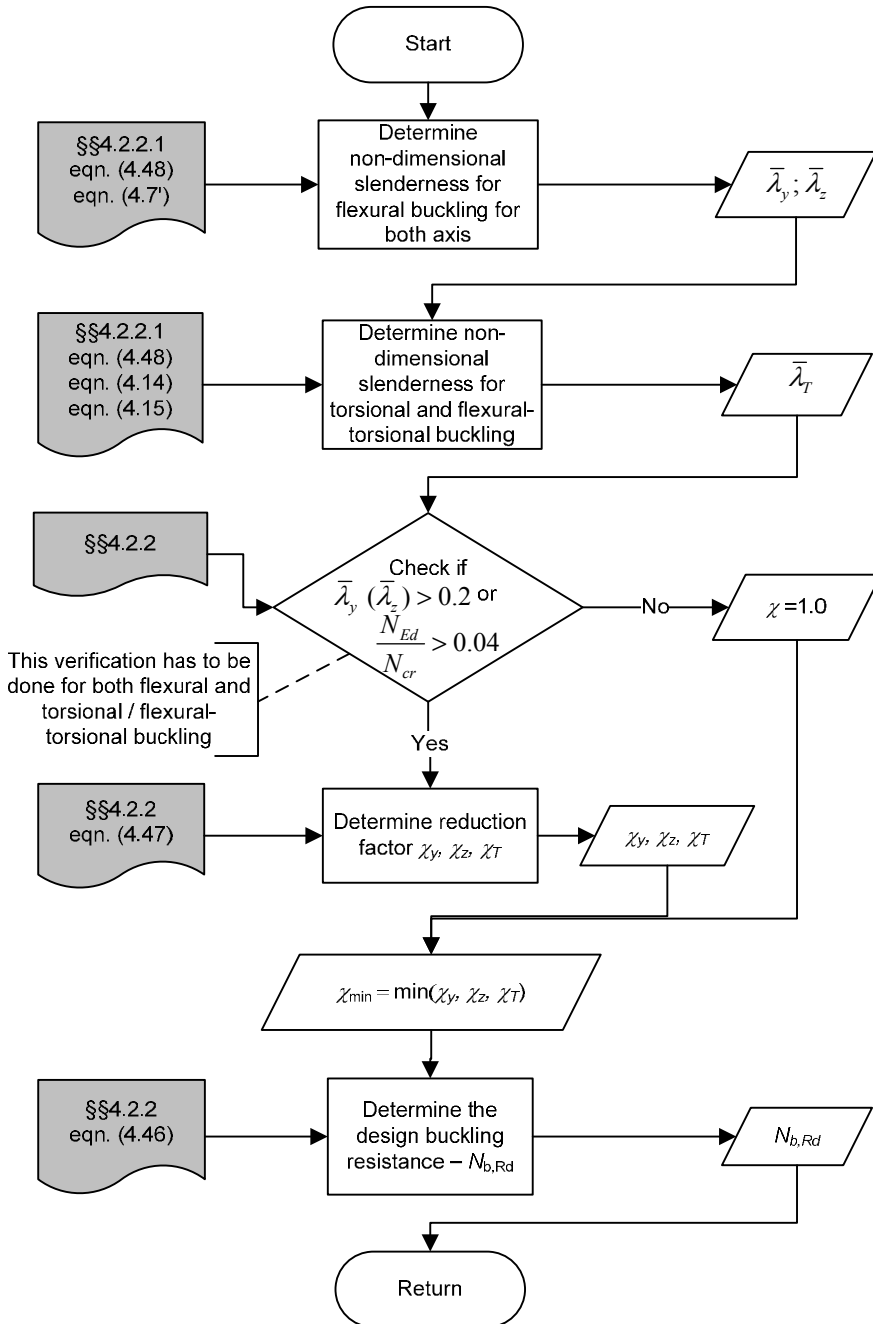
b) Connections capable of giving significant torsional and warping restraint

Figure 4.15 – Torsional and warping restraint for practical connections

Flowcharts 4.1 and 4.2 present schematically the design of a cold-formed steel member in compression. Examples 4.1 and 4.2 present numerical examples.



Flowchart 4.1 – Design of a cold-formed steel member in compression (SF039a-EN-EU, Access Steel 2006)



Flowchart 4.2 – Calculate the design buckling resistance of a member in compression – $N_{b,Rd}$ (SF039a-EN-EU, Access Steel 2006)

Example 4.1: This example deals with the design of an internal wall stud in compression. The stud has pinned end conditions and is composed of two thin-walled cold-formed back-to-back lipped channel sections. The connection between the channels is assumed to be rigid (a welded connection, for example). No restraints against buckling are applied between the ends.

Basic Data

Height of column $H = 3.00 \text{ m}$

Span of floor $L = 6.00 \text{ m}$

Spacing between floor joists $S = 0.6 \text{ m}$

Distributed loads applied to the floor:

- dead load – lightweight slab: 1.5 kN/m^2
 $q_G = 1.5 \times 0.6 = 0.9 \text{ kN/m}$

- imposed load: 3.00 kN/m^2
 $q_Q = 3.00 \times 0.6 = 1.80 \text{ kN/m}$

Ultimate Limit State concentrated load from upper level and roof:

$$Q = 7.0 \text{ kN}$$

266

The dimensions of a lipped channel section and the material properties are:

Total height $h = 150 \text{ mm}$

Total width of flange $b = 40 \text{ mm}$

Total width of edge fold $c = 15 \text{ mm}$

Internal radius $r = 3 \text{ mm}$

Nominal thickness $t_{nom} = 1.2 \text{ mm}$

Steel core thickness (§§2.4.2.3) $t = 1.16 \text{ mm}$

Steel grade S350GD+Z

Basic yield strength $f_{yb} = 350 \text{ N/mm}^2$

Modulus of elasticity $E = 210000 \text{ N/mm}^2$

Poisson's ratio $\nu = 0.3$

Shear modulus $G = \frac{E}{2(1+\nu)} = 81000 \text{ N/mm}^2$

Partial factors $\gamma_{M0} = 1.0$ (§§2.3.1)

$$\gamma_{M1} = 1.0$$

$$\gamma_G = 1.35, \text{ – permanent loads (§§2.3.1)}$$

$$\gamma_Q = 1.50 \text{ – variable loads}$$

The applied concentrated load on the external column (compression) at the Ultimate Limit State is (§§2.3.1, Flowchart 2.1):

$$N_{Ed} = (\gamma_G q_G + \gamma_Q q_Q) L / 2 + Q = (1.35 \times 0.9 + 1.50 \times 1.80) \times 5 / 2 + 7 = 16.79 \text{ kN}$$

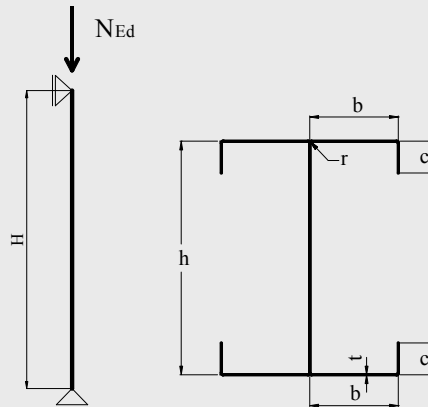


Figure 4.16 – Overall dimensions of internal wall stud and cross section

Properties of the gross cross section

Area of gross cross section:	$A = 592 \text{ mm}^2$
Radii of gyration:	$i_y = 57.2 \text{ mm} ; i_z = 18 \text{ mm}$
Second moment of area about strong axis y - y :	$I_y = 1.936 \times 10^6 \text{ mm}^4$
Second moment of area about weak axis z - z :	$I_z = 19.13 \times 10^4 \text{ mm}^4$
Warping constant:	$I_w = 4.931 \times 10^8 \text{ mm}^6$
Torsion constant:	$I_t = 266 \text{ mm}^4$

Effective section properties of the cross section (§§3.7.3, Flowchart 3.1 and Flowchart 3.2)

The properties of effective cross section were calculated following the procedures presented in Example 3.2 in Chapter 3.

Effective area of the cross section when subjected to compression only:

$$A_{eff} = 322 \text{ mm}^2$$

Resistance check of the cross section

The following criterion should be met (§§3.8.3, eqn. (3.80), Flowchart 3.4):

$$\frac{N_{Ed}}{N_{c,Rd}} \leq 1$$

where

$$N_{c,Rd} = A_{eff} f_{yb} / \gamma_{M0} \quad (\text{§§3.8.3, eqn. (3.81), Flowchart 3.5})$$

The cross section is doubly symmetric and so the shift of the centroidal *y*-*y* axis is $e_{Ny} = 0$ (§§3.8.3, Figure 3.43).

The resistance check is:

$$\frac{16.79 \times 10^3}{322 \times 350 / 1.0} = 0.149 < 1 - \text{OK}$$

Buckling resistance check

Members which are subjected to axial compression should satisfy (§§4.2.2, eqn. (4.45), Flowchart 4.1):

$$\frac{N_{Ed}}{N_{b,Rd}} \leq 1$$

$$N_{b,Rd} = \frac{\chi A_{eff} f_y}{\gamma_{M1}}, \text{ where } \chi \text{ is the reduction factor for the relevant}$$

buckling mode.

$$\chi = \frac{1}{\phi + \sqrt{\phi^2 - \bar{\lambda}^2}} \quad \text{but} \quad \chi \leq 1.0 \quad (\text{§§4.2.2, eqn. (4.47)})$$

$$\phi = 0.5 \left[1 + \alpha (\bar{\lambda} - 0.2) + \bar{\lambda}^2 \right]$$

α – imperfection factor

The non-dimensional slenderness is:

$$\bar{\lambda} = \sqrt{\frac{A_{eff} f_{yb}}{N_{cr}}}$$

N_{cr} – the elastic critical force for the relevant buckling mode.

Determination of the reduction factors χ_y , χ_z , χ_T

Flexural buckling (§§4.2.2.1, eqn. (4.48), Flowchart 4.2)

$$\bar{\lambda}_F = \sqrt{\frac{A_{eff} f_{yb}}{N_{cr}}} = \frac{L_{cr}}{i} \frac{\sqrt{A_{eff}/A}}{\lambda_1}$$

The buckling length:

$$L_{cr,y} = L_{cr,z} = H = 3000 \text{ mm}$$

$$\lambda_1 = \pi \sqrt{\frac{E}{f_{yb}}} = \pi \times \sqrt{\frac{210000}{350}} = 76.95$$

Buckling about y - y axis (§§4.2.2.1, Table 4.2):

$$\bar{\lambda}_y = \frac{L_{cr,y}}{i_y} \frac{\sqrt{A_{eff}/A}}{\lambda_1} = \frac{3000}{57.2} \times \frac{\sqrt{322/592}}{76.95} = 0.503$$

$\alpha_y = 0.21$ – buckling curve a (§§4.2.1.2, Table 4.1)

$$\begin{aligned} \phi_y &= 0.5 \left[1 + \alpha_y (\bar{\lambda}_y - 0.2) + \bar{\lambda}_y^2 \right] = \\ &= 0.5 \times \left[1 + 0.21 \times (0.503 - 0.2) + 0.503^2 \right] = 0.658 \end{aligned}$$

$$\chi_y = \frac{1}{\phi_y + \sqrt{\phi_y^2 - \bar{\lambda}_y^2}} = \frac{1}{0.658 + \sqrt{0.658^2 - 0.503^2}} = 0.924$$

Buckling about z - z axis (§§4.2.2.1, Table 4.2):

$$\bar{\lambda}_z = \frac{L_{cr,z}}{i_z} \frac{\sqrt{A_{eff}/A}}{\lambda_1} = \frac{3000}{18} \times \frac{\sqrt{322/592}}{76.95} = 1.597$$

$\alpha_z = 0.34$ – buckling curve b (§§4.2.1.2, Table 4.1)

$$\phi_z = 0.5 \left[1 + \alpha_z (\bar{\lambda}_z - 0.2) + \bar{\lambda}_z^2 \right] =$$

$$= 0.5 \times [1 + 0.34 \times (1.597 - 0.2) + 1.597^2] = 2.013$$

$$\chi_z = \frac{1}{\phi_z + \sqrt{\phi_z^2 - \bar{\lambda}_z^2}} = \frac{1}{2.013 + \sqrt{2.013^2 - 1.597^2}} = 0.309$$

Torsional buckling (§§4.2.1.1, eqn. (4.14))

$$N_{cr,T} = \frac{1}{i_o^2} \left(GI_t + \frac{\pi^2 EI_w}{l_T^2} \right)$$

where

$$i_o^2 = i_y^2 + i_z^2 + y_o^2 + z_o^2$$

y_o, z_o – the shear centre coordinates with respect to the centroid of the gross cross section: $y_o = z_o = 0$

$$i_o^2 = 57.2^2 + 18^2 + 0 + 0 = 3594 \text{ mm}^2$$

$$l_T = H = 3000 \text{ mm}$$

The elastic critical force for torsional buckling is:

$$N_{cr,T} = \frac{1}{3594} \times \left(81000 \times 266 + \frac{\pi^2 \times 210000 \times 4.931 \times 10^8}{3000^2} \right) = 37.59 \times 10^3 \text{ N}$$

270

The elastic critical force will be:

$$N_{cr} = N_{cr,T} = 37.59 \text{ kN}$$

The non-dimensional slenderness is:

$$\bar{\lambda}_T = \sqrt{\frac{A_{eff} f_{yb}}{N_{cr}}} = \sqrt{\frac{322 \times 350}{37.59 \times 10^3}} = 1.731$$

$\alpha_T = 0.34$ – buckling curve *b* (§§4.2.2.1, Table 4.2, §§4.2.1.2, Table 4.1)

$$\begin{aligned} \phi_T &= 0.5 \left[1 + \alpha_T (\bar{\lambda}_T - 0.2) + \bar{\lambda}_T^2 \right] = \\ &= 0.5 \times [1 + 0.34 \times (1.731 - 0.2) + 1.731^2] = 2.258 \end{aligned}$$

The reduction factor for torsional buckling is:

$$\chi_T = \frac{1}{\phi_T + \sqrt{\phi_T^2 - \bar{\lambda}_T^2}} = \frac{1}{2.258 + \sqrt{2.258^2 - 1.731^2}} = 0.270$$

$$\chi = \min(\chi_y, \chi_z, \chi_T) = \min(0.924, 0.309, 0.270) = 0.270$$

$$N_{b,Rd} = \frac{\chi A_{eff} f_y}{\gamma_{M1}} = \frac{0.270 \times 322 \times 350}{1.00} = 30429 \text{ N} = 30.429 \text{ kN}$$

$$\frac{N_{Ed}}{N_{b,Rd}} = \frac{16.79}{30.429} = 0.552 \leq 1 - \text{OK}$$

Example 4.2: Consider the truss girder shown in Figure 4.17, made of cold-formed steel square hollow sections (SHS), supporting a roof structure. The most compressed chord member and the most compressed diagonal have to be designed.

The members comprise square hollow sections with welded connections. Assuming that the centreline axes of the members intersect at each node, there is no reduction of the resistance due to eccentricities in the connections.

The following cross sections have been chosen: a SHS160×160×4 mm cross section for the upper and bottom chord and a SHS120×120×3 mm cross section for the diagonal members. The steel grade used is S355.

The span of the truss is 18.00 m and the distance between two consecutive trusses is 7.00 m. The loading, applied on the roof and transmitted to the truss as concentrated loads applied at the nodes (purlins are connected at each node of the top chord of the truss), is defined by the following distributed loads:

- Permanent action of the roof = 1.00 kN/m² ($\gamma_G = 1.35$); the loading already includes the self-weight of the steel truss;
- Snow load on the roof = 2.50 kN/m² ($\gamma_Q = 1.50$).

The applied concentrated load in each node of the truss, according to §2.3.1, at the Ultimate Limit State is:

$$P = (1.35 \times 1.00 + 1.50 \times 2.50) \times 7 \times 1.8 = 64.26 \text{ kN}$$

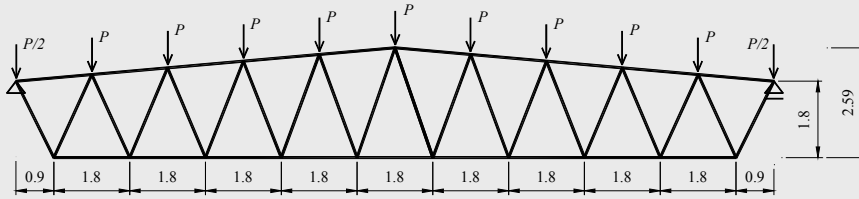


Figure 4.17 – Truss girder and actions

The truss girder and the internal forces are represented in Figure 4.18. Based on the axial force diagrams, the most compressed chord member supports an axial force of -566.46 kN with the length of the member of $L = 1.81$ m. For the diagonals, the most compressed member, with a length $L = 2.15$ m, supports an axial force of -304.88 kN. For the definition of the buckling lengths of the members, it is assumed that all the nodes of the truss are braced in the direction perpendicular to the plane of the structure.

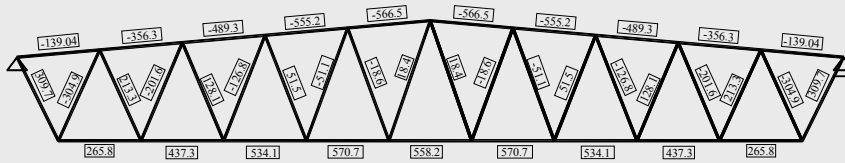


Figure 4.18 – Internal forces on the structure

Properties of the gross cross section

272

Upper chord SHS 160×160×4

Area of gross cross section: $A = 24.55 \times 10^2 \text{ mm}^2$

Radii of gyration: $i_y = i_z = 63.4 \text{ mm}$

Compressed diagonal SHS 120×120×3

Area of gross cross section: $A = 13.81 \times 10^2 \text{ mm}^2$

Radii of gyration: $i_y = i_z = 47.6 \text{ mm}$

Cross section classification

Upper chord SHS 160×160×4

According to EN1993-1-1, Table 5.2(1)

$$\frac{c}{t} = \frac{h-3 \cdot t}{t} = \frac{160-3 \cdot 4}{4} = 37 > 42 \cdot \varepsilon = 42 \cdot 0.81 = 34 \Rightarrow \text{Class 4 cross section}$$

Compressed diagonal SHS 120×120×3

According to EN1993-1-1, Table 5.2(1)

$$\frac{c}{t} = \frac{h-3 \cdot t}{t} = \frac{120-3 \cdot 3}{3} = 37 > 42 \cdot \varepsilon = 34 \Rightarrow \text{Class 4 cross section}$$

where

$$\varepsilon = \sqrt{\frac{235}{f_y [N/mm^2]}} = \sqrt{\frac{235}{355}} = 0.81$$

Checking of geometrical proportions

The design method of EN1993-1-3 can be applied if the following conditions are satisfied (§§3.2.3, Table 3.1):

Upper chord SHS 160×160×4

$$b/t \leq 500 \quad b/t = 160/4 = 40 < 60 \quad - \text{OK}$$

Compressed diagonal SHS 120×120×3

$$b/t \leq 500 \quad b/t = 120/3 = 40 < 60 \quad - \text{OK}$$

The influence of rounding of the corners is neglected if (§§3.2.1, eqns. (3.2)):

Upper chord SHS 160×160×4

$$r/t \leq 5 \quad r/t = 8/4 = 2 < 5 \quad - \text{OK}$$

$$r/b_p \leq 0.10 \quad r/b_p = 8/160 = 0.05 < 0.10 \quad - \text{OK}$$

Compressed diagonal SHS 120×120×3

$$r/t \leq 5 \quad r/t = 6/3 = 2 < 5 \quad - \text{OK}$$

$$r/b_p \leq 0.10 \quad r/b_p = 6/120 = 0.05 < 0.10 \quad - \text{OK}$$

ffective section properties of the cross section (§§3.7.3, Flowchart 3.1 and Flowchart 3.2, Figure 4.19)

The properties of effective cross section were calculated following the procedures presented in Example 3.2 in Chapter 3.

The stress ratio: $\psi = 1$ (uniform compression), so the buckling factor is $k_\sigma = 4$ for internal compression element (§§3.7.2, Table 3.5) and $\varepsilon = \sqrt{235/f_{yb}}$.

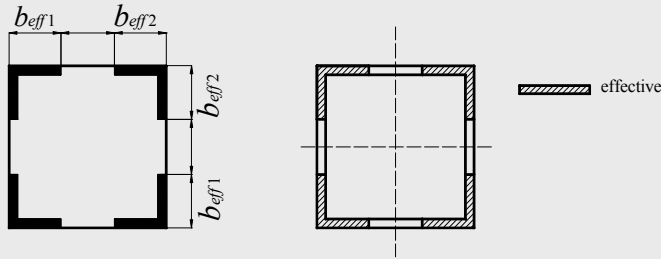


Figure 4.19 – Effective area

Upper chord SHS 160×160×4

The relative slenderness (§§3.7.2, eqn. (3.38)):

274

$$\bar{\lambda}_{p,b} = \frac{b_p/t}{28.4 \varepsilon \sqrt{k_\sigma}} = \frac{(160-4)/4}{28.4 \cdot 0.81 \cdot \sqrt{4}} = 0.848$$

The width reduction factor is (§§3.7.2, eqn. (3.36)):

$$\rho = \frac{\bar{\lambda}_{p,b} - 0.055(3 + \psi)}{\bar{\lambda}_{p,b}^2} = \frac{0.848 - 0.055 \cdot (3 + 1)}{0.848^2} = 0.873 < 1$$

The effective width is:

$$b_{eff} = \rho b_p = 0.873 \times (160 - 4) = 136.2 \text{ mm}$$

$$b_{e1} = b_{e2} = 0.5 b_{eff} = 0.5 \times 136.2 = 68.1 \text{ mm}$$

The effective area of the cross section subjected to compression only:

$$A_{eff} = 4 \cdot t \cdot b_{eff} = 4 \cdot 4 \cdot 136.2 = 2179.2 \text{ mm}^2$$

Compressed diagonal SHS 120×120×3

The relative slenderness (§§3.7.2, eqn. (3.38)):

$$\bar{\lambda}_{p,b} = \frac{b_p/t}{28.4 \varepsilon \sqrt{k_\sigma}} = \frac{(120-3)/3}{28.4 \cdot 0.81 \cdot \sqrt{4}} = 0.851$$

The width reduction factor is (§§3.7.2, eqn. (3.36)):

$$\rho = \frac{\bar{\lambda}_{p,b} - 0.055(3 + \psi)}{\bar{\lambda}_{p,b}^2} = \frac{0.851 - 0.055 \cdot (3 + 1)}{0.851^2} = 0.871 < 1$$

The effective width is:

$$b_{eff} = \rho b_p = 0.871 \times (120 - 3) = 101.91 \text{ mm}$$

$$b_{e1} = b_{e2} = 0.5 b_{eff} = 0.5 \times 101.91 = 50.95 \text{ mm}$$

The effective area of the cross section subjected to compression only:

$$A_{eff} = 4 \cdot t \cdot b_{eff} = 4 \cdot 3 \cdot 101.91 = 1222.92 \text{ mm}^2$$

Resistance check of the cross section

The following criterion should be met (§§3.8.3, eqn. (3.80), Flowchart 3.4):

$$\frac{N_{Ed}}{N_{c,Rd}} \leq 1$$

where

$$N_{c,Rd} = A_{eff} f_{yb} / \gamma_{M0} \quad (\text{§§3.8.3, eqn. (3.81), Flowchart 3.5})$$

The resistance check is:

Upper chord SHS 160×160×4

$$\frac{566.46 \times 10^3}{2179.2 \times 355 / 1.0} = 0.732 < 1 \quad - \text{OK}$$

Compressed diagonal SHS 120×120×3

$$\frac{304.88 \times 10^3}{1222.92 \times 355 / 1.0} = 0.702 < 1 \quad - \text{OK}$$

Buckling resistance check

Members which are subjected to axial compression should satisfy (§§4.2.2, eqn. (4.45), Flowcharts 4.1 and 4.2): $\frac{N_{Ed}}{N_{b,Rd}} \leq 1$

$N_{b,Rd} = \frac{\chi A_{eff} f_y}{\gamma_{M1}}$, where χ is the reduction factor for the relevant buckling mode.

$$\chi = \frac{1}{\phi + \sqrt{\phi^2 - \bar{\lambda}^2}} \quad \text{but} \quad \chi \leq 1.0 \quad (\text{§§4.2.2, eqn. (4.47)})$$

$$\phi = 0.5 \left[1 + \alpha (\bar{\lambda} - 0.2) + \bar{\lambda}^2 \right]$$

α – imperfection factor

The non-dimensional slenderness is (§§4.2.2.1, eqn. (4.48)):

$$\bar{\lambda} = \sqrt{\frac{A_{eff} f_{yb}}{N_{cr}}}$$

N_{cr} – the elastic critical force for the relevant buckling mode.

Upper chord SHS 160×160×4

The buckling length according to Annex BB.1.3(1) of EN1993-1-1:

$$L_{cr,y} = L_{cr,z} = 0.9 \cdot 1.81\text{m} = 1.63\text{m}$$

$$\lambda_1 = \pi \sqrt{\frac{E}{f_{yb}}} = \pi \times \sqrt{\frac{210000}{355}} = 76.41$$

$$\bar{\lambda} = \frac{L_{cr}}{i} \frac{\sqrt{A_{eff}/A}}{\lambda_1} = \frac{1630}{63.4} \frac{\sqrt{2179.2/2455}}{76.41} = 0.317$$

For cold-formed square hollow section \Rightarrow *Buckling curve c*, so $\alpha = 0.49$;

$$\phi = 0.5 \left[1 + \alpha (\bar{\lambda} - 0.2) + \bar{\lambda}^2 \right] =$$

$$= 0.5 \times \left[1 + 0.49 \times (0.317 - 0.2) + 0.317^2 \right] = 0.579$$

$$\chi = \frac{1}{\phi + \sqrt{\phi^2 - \bar{\lambda}^2}} = \frac{1}{0.579 + \sqrt{0.579^2 - 0.317^2}} = 0.940$$

$$N_{b,Rd} = \frac{\chi A_{eff} f_y}{\gamma_{M1}} = \frac{0.940 \times 2179.2 \times 355}{1.00} \cdot 10^{-3} = 727.2 \text{ kN}$$

$$\frac{N_{Ed}}{N_{b,Rd}} = \frac{566.46}{727.2} = 0.779 \leq 1 \quad - \text{OK}$$

Compressed diagonal SHS 120×120×3

The buckling length according to Annex BB.1.3(1) of EN1993-1-1:

$$L_{cr,y} = L_{cr,z} = 0.9 \cdot 2.151 \text{ m} = 1.935 \text{ m}$$

$$\lambda_1 = \pi \sqrt{\frac{E}{f_{yb}}} = \pi \times \sqrt{\frac{210000}{355}} = 76.41$$

$$\bar{\lambda} = \frac{L_{cr}}{i} \frac{\sqrt{A_{eff}/A}}{\lambda_1} = \frac{1935}{47.6} \frac{\sqrt{1222.92/1381}}{76.41} = 0.501$$

For cold-formed square hollow section \Rightarrow *Buckling curve c*, so $\alpha = 0.49$;

$$\begin{aligned} \phi &= 0.5 \left[1 + \alpha (\bar{\lambda} - 0.2) + \bar{\lambda}^2 \right] = \\ &= 0.5 \times \left[1 + 0.49 \times (0.501 - 0.2) + 0.501^2 \right] = 0.699 \end{aligned}$$

$$\chi = \frac{1}{\phi + \sqrt{\phi^2 - \bar{\lambda}^2}} = \frac{1}{0.699 + \sqrt{0.699^2 - 0.501^2}} = 0.843$$

$$N_{b,Rd} = \frac{\chi A_{eff} f_y}{\gamma_{M1}} = \frac{0.843 \times 1222.92 \times 355}{1.00} \cdot 10^{-3} = 365.91 \text{ kN}$$

$$\frac{N_{Ed}}{N_{b,Rd}} = \frac{304.88}{365.91} = 0.833 \leq 1 \quad - \text{OK}$$

4.3 BUCKLING STRENGTH OF BENDING MEMBERS

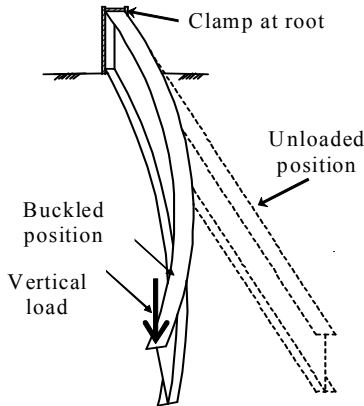
4.3.1 Theoretical background

The problems related to restrained beams (i.e. when out-of-plane deformation under in-plane bending is prevented) have been discussed and

illustrated by examples in Chapter 3. In the case of laterally restrained beams, either in *pure bending*, which is mostly a *theoretical* case, or in interactive situations (e.g. in-plane bending with axial compression, in-plane bending with shear, in-plane bending with local transverse force, in-plane bending with shear and torsion) the member resistance is given by the cross section resistance. Thin-walled sections, which are usually the case for cold-formed steel profiles, may be prone to local instability, too.

In the case of unrestrained beams, out-of-plane lateral-torsional (LT) buckling may affect the beam capacity. Since, particularly in the case of open-section thin-walled slender beams, LT buckling can be very dangerous, a proper design – calculation and preventive constructional measures – must be able to guard against this phenomenon.

If a slender member is loaded in bending in its stiff plane (bending about the stronger axis), there is always a tendency for it to fail by buckling in the flexible plane (about the weak axis). In the case of a beam bent about its major axis, failure may occur by a form of buckling which involves both lateral deflection and twisting – the lateral-torsional buckling mode. Figure 4.20 (a, b) illustrates this phenomenon for a slender cantilever beam loaded by a vertical end-load.



a) LT buckling of a slender cantilever beam (SSEDTA, Lecture 12) b) LT buckling of a slender cantilever beam in testing (da Silva *et al*, 2010)

Figure 4.20 – Lateral-torsional buckling of a slender cantilever beam

Most applications involving cold-formed steel open sections in bending – purlins, wall rails, slab joists – use mono-symmetric sections – lipped channels, or point symmetric sections – zees, of which sensitivity to

LT buckling is significantly higher than for members with doubly symmetric section. However, for such types of applications, the beams are frequently laterally restrained by the roofing or wall cladding or, in the case of joists, by the floor deck. Even in such cases, the attached sheeting does not necessarily eliminate the LT problem. For roof purlins with cladding connected to the top flanges only, the out-of-plane deflection at the level of the upper flange is generally restrained by the cladding, but uplift loads from wind may induce lateral buckling because, in this load case, the lower flange, which is in compression, is not restrained against lateral displacement.

Consider a perfect elastic, initially straight, doubly symmetric I-section beam, loaded by equal and opposite end-moments about its major axis (i.e. pure bending). The beam is unrestrained along its length except at its ends, where it has end-fork (simple) supports, which prevent twisting and lateral deflection, but allow for free warping and free rotations both in the planes of the web and flanges. The compressed flange (with a part of the adjacent web, which is in fact a T-section of some elastic restraint from the tension part of the beam section) might be prone to LT buckling. The buckled shape and resultant deformation are schematically displayed in Figure 4.21. The behaviour of such a beam can be described, according to elastic 2nd order theory by three differential equations of equilibrium, two for bending about axes y - y and z - z , and the third for torsion around axis x - x (Timoshenko & Gere, 1961; Kirby & Nethercot, 1979; Allen & Bulson 1980; Trahair & Bradford, 1988; da Silva *et al*, 2010).

Since the equations for bending about the major axis, y - y , and torsion can be coupled, the system of governing equations reduces at two equations only, i.e.

- bending about minor axis, z - z

$$EI_z \frac{d^2 v(x)}{dx^2} + \varphi(x) M_y = 0 \quad (4.49)$$

- torsion around x - x axis

$$EI_w \frac{d^3 \varphi(x)}{dx^3} - GI_T \frac{d\varphi(x)}{dx} + M_y \frac{dv(x)}{dx} = 0 \quad (4.50)$$

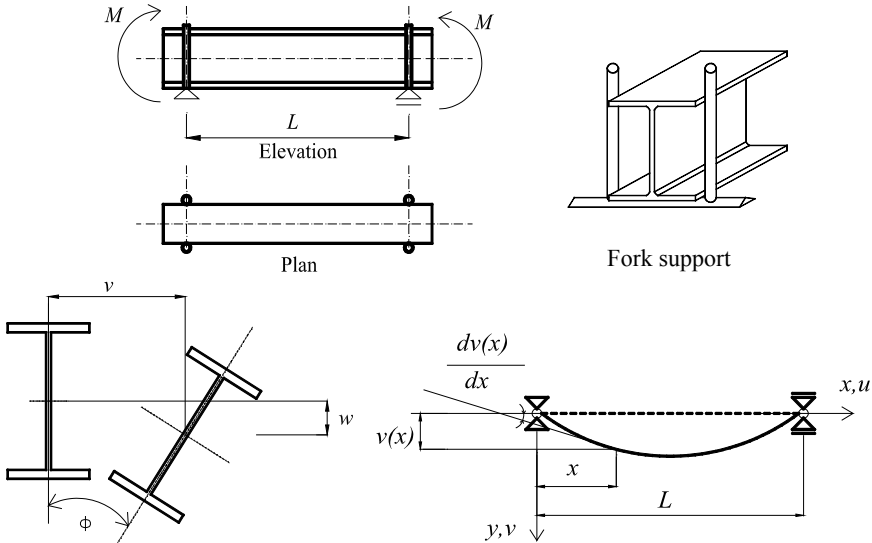


Figure 4.21 – Lateral-torsional buckling of a simple I beam under uniform bending moment (SSEDTA, Lecture 12)

The common unknown, e.g. lateral displacement, v , can be eliminated by combining eqns. (4.49) and (4.50) which results in:

$$EI_w \frac{d^4 \varphi(x)}{dx^4} - GI_T \frac{d^2 \varphi(x)}{dx^2} - \frac{M_y^2}{EI_z} \varphi(x) = 0 \tag{4.51}$$

280

For the stated boundary conditions, the solution to this equation is a sine function, similar to the one for compression, with amplitude φ_0 at mid-span,

$$\varphi = \varphi_0 \sin \frac{\pi x}{L} \tag{4.52}$$

Substitution of the solution (4.52) into eqn. (4.51), results in the critical moment

$$M_{cr} = \frac{\pi EI_z}{L^2} \sqrt{\frac{I_w}{I_T} + \frac{L^2 GI_T}{\pi^2 EI_z}} \tag{4.53}$$

or

$$M_{cr} = \frac{\pi \sqrt{EI_z GI_T}}{L} \sqrt{1 + \frac{\pi^2 EI_w}{L^2 GI_T}} \tag{4.53'}$$

where

- I_T is the torsion constant;
- I_w is the warping constant;
- I_z is the second moment of area about the minor axis;
- L is the unrestrained length of beam.

Equation (4.53) applies to simply supported beams with doubly symmetric cross sections in pure bending only.

For the case of mono-symmetric cross sections (the symmetry is usually related to the minor axis of inertia), for different types of loading, the expression of critical moment becomes more complex (da Silva *et al*, 2010), i.e.:

$$M_{cr} = C_1 \frac{\pi^2 EI_z}{(k_z L)^2} \left\{ \left[\left(\frac{k_z}{k_w} \right)^2 \frac{I_w}{I_z} + \frac{(k_z L)^2 GI_T}{\pi^2 EI_z} + (C_2 z_g - C_3 z_j)^2 \right]^{0.5} - (C_2 z_g - C_3 z_j) \right\} \quad (4.54)$$





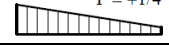
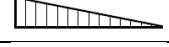
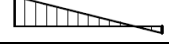
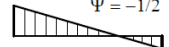
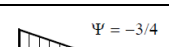
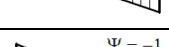
where

- C_1 , C_2 and C_3 are coefficients depending on the loading conditions (i.e. the shape of the bending moment diagram), and on the support conditions, given in Tables 4.3 and 4.4 for some usual situations (Boissonnade *et al*, 2006). In Tables 4.3 and 4.4 the support conditions are those for a simply supported beam, however, lateral bending restraints and warping restraints may be taken into account through the parameters k_z and k_w , described below;
- k_z and k_w are effective length factors that depend on the support conditions at the end sections. The factor k_z is related to rotations at the end sections about the weak axis $z-z$, and k_w refers to warping restraint of the same cross sections. These factors vary between 0.5 (restrained deformations) and 1.0 (free deformations), and are equal to 0.7 in the case of free deformations at one end and restrained deformations at the other. Since in most practical situations restraint is only partial, conservatively value of $k_z = k_w = 1.0$ may be adopted;
- $z_g = (z_a - z_s)$, where z_a and z_s are the z - coordinates of the point of application of the load and of the shear centre. These coordinates are positive if located in the compressed part and negative if located in the tension part;

4. BEHAVIOUR AND DESIGN RESISTANCE OF BAR MEMBERS

- $z_j = z_s - [0.5 \int_A (y^2 + z^2)(z/I_y)dA]$ is a parameter that reflects the degree of asymmetry of the cross section in relation to the y - y axis. It is zero for beams with doubly symmetric cross section and takes positive values when the flange with the largest second moment of area about z is the compressed flange, at the cross section with maximum bending moment.

Table 4.3 – Coefficients C_1 and C_3 for beams with end moments

Loading and support conditions	Diagram of moments	k_z	C_1	C_3	
				$\psi_f \leq 0$	$\psi_f > 0$
	$\Psi = +1$ 	1.0 0.5	1.00 1.05	1.000 1.019	
	$\Psi = +3/4$ 	1.0 0.5	1.14 1.19	1.000 1.017	
	$\Psi = +1/2$ 	1.0 0.5	1.31 1.37	1.000 1.000	
	$\Psi = +1/4$ 	1.0 0.5	1.52 1.60	1.000 1.000	
	$\Psi = 0$ 	1.0 0.5	1.77 1.86	1.000 1.000	
	$\Psi = -1/4$ 	1.0 0.5	2.06 2.15	1.000 1.000	0.850 0.650
	$\Psi = -1/2$ 	1.0 0.5	2.35 2.42	1.000 0.950	$1.3 - 1.2\psi_f$ $0.77\psi_f$
	$\Psi = -3/4$ 	1.0 0.5	2.60 2.45	1.000 0.850	$0.55\psi_f$ $0.35\psi_f$
	$\Psi = -1$ 	1.0 0.5	2.60 2.45	$-\psi_f$ $-0.125 - 0.7\psi_f$	$-\psi_f$ $-0.125 - 0.7\psi_f$
	<p>- In beams subjected to end moments, by definition $C_2 z_g = 0$;</p> <p>- $\psi_f = \frac{I_{fc} - I_{ft}}{I_{fc} + I_{ft}}$, where I_{fc} and I_{ft} are the second moments of area of the compression and tension flanges respectively, relative to the weak axis of the section ($z - z$ axis);</p> <p>- C_1 must be divided by 1.05 when $\frac{\pi}{k_w L} \sqrt{\frac{EI_w}{GI_T}} \leq 1.0$, but $C_1 \geq 1.0$.</p>				

Equation (4.54) also allows the elastic critical moment of beams with other support conditions (including cantilever beams – the upper flange of

the beam is in tension) and other loading conditions to be determine than those shown in Table 4.3 and 4.4, such as combinations of end moments with transverse loads, taking the parameters C_1 , C_2 , C_3 , k_z and k_w from Boissonnade *et al* (2006).

Table 4.4 – Coefficients C_1 , C_2 and C_3 for beams with transverse loads

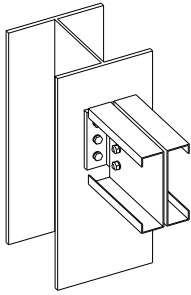
Loading and support conditions	Diagram of moments	k_z	C_1	C_2	C_3
		1.0 0.5	1.127 0.97	0.454 0.36	0.525 0.478
		1.0 0.5	1.348 1.05	0.630 0.48	0.411 0.338
		1.0 0.5	1.04 0.95	0.42 0.31	0.562 0.539

In the case of mono-symmetric I and H shape cross sections, Tables 4.3 and 4.4 must only be used if the following condition is verified: $-0.9 \leq \psi \leq 0.9$, where ψ is the gradient of the bending moment diagram.

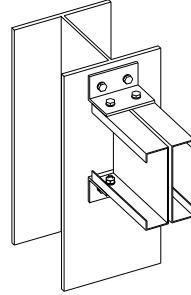
Figure 4.22 shows schematic examples of various end-restraints (Galambos, 1998), while in Figure 4.23 examples of practical end-support details are presented.

I		$u = \phi = u'' = \phi'' = 0$ Simply supported
II		$u = \phi = u'' = \phi' = 0$ Warping prevented
III		$u = \phi = u' = \phi'' = 0$ Lateral bending prevented
IV		$u = \phi = u' = \phi' = 0$ Fixed end
V		Lateral supports at centre. Restraint: equal at both ends

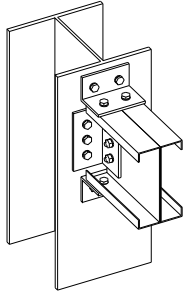
Figure 4.22 – Idealised end-restraints (Galambos, 1998)



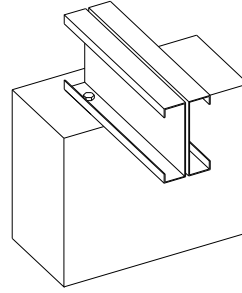
Beam compression flange free to rotate on plan
a) Web cleats bolted to beam



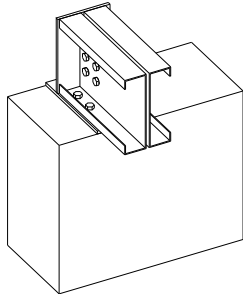
Full torsional end restraint to beam
b) Upper and bottom bolted flange cleats



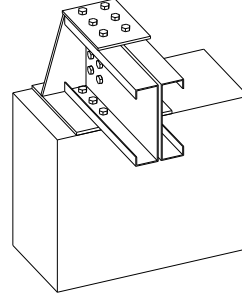
Full torsional end restraint to beam
c) Upper and bottom bolted flange cleats + web cleats bolted to beam



Compression flange free to rotate. No torsional restraint
d) Bottom flange bolted to a wall



Compression flange rotation reduced. Torsional end partially restraint
e) Bottom flange bolted to a wall and web bolted to a stiffener



Full torsional restraint. No rotation of compression flange
f) Bottom flange bolted to a wall and full end stiffener

Figure 4.23 – Practical end-support details

Similarly, Figure 4.24 shows schematic restraint conditions for cantilever beams (Galambos, 1998) and Figure 4.25 gives examples of practical cantilever solutions (adapted version Source: BS 5950 Part 1:2000).

The presence of the flexural, torsional and warping stiffness in the equation for M_{cr} emphasises the importance of the shape of cross section of a given beam (see Figure 4.26).

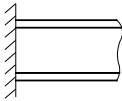
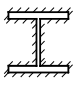
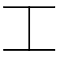
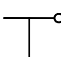
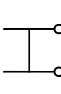
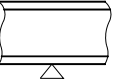
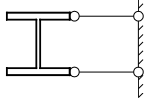
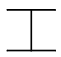
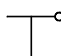
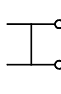
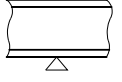
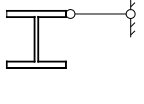
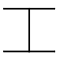
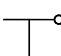
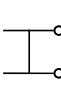
Restraint conditions		Effective length	
At root	At tip	Top flange loading	All other cases
 		1.4L	0.8L
		1.4L	0.7L
		1.6L	0.6L
 		2.5L	1.0L
		2.5L	0.9L
		1.5L	0.8L
 		7.5L	3.0L
		7.5L	2.7L
		4.5L	2.4L

Figure 4.24 – Idealised restraint conditions and effective length factors for cantilevers (Galambos, 1998)

Summarising, the critical moment of a member under bending depends on several factors, such as:

- loading (shape of the bending moment diagram);
- support conditions;
- length of the member between laterally braced cross sections;
- lateral bending stiffness;
- torsion stiffness;
- warping stiffness.

4. BEHAVIOUR AND DESIGN RESISTANCE OF BAR MEMBERS

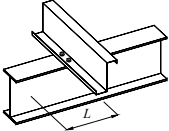
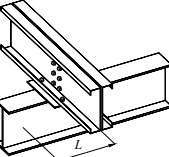
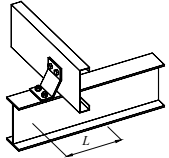
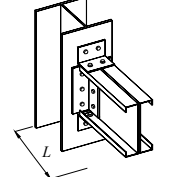
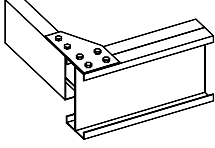
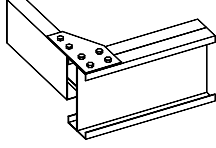
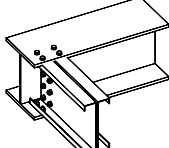
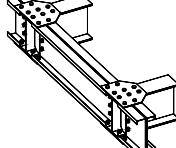
Restraint conditions		Loading conditions	
At support	At tip	Normal	Top flange (destabilizing)
(a) Continuous, with lateral restraint to top flange 	(1) Free (2) Lateral restraint to top flange (3) Torsional restraint (4) Lateral and torsional restraint	3.0L 2.7L 2.4L 2.1L	7.5L 7.5L 4.5L 3.6L
(b) Continuous, with partial torsional restraint 	(1) Free (2) Lateral restraint to top flange (3) Torsional restraint (4) Lateral and torsional restraint	2.0L 1.8L 1.6L 1.4L	5.0L 5.0L 3.0L 2.4L
(c) Continuous, with lateral and torsional restraint 	(1) Free (2) Lateral restraint to top flange (3) Torsional restraint (4) Lateral and torsional restraint	1.0L 0.9L 0.8L 0.7L	2.5L 2.5L 1.5L 1.2L
(d) Restrained laterally, torsionally and against rotation on plan 	(1) Free (2) Lateral restraint to top flange (3) Torsional restraint (4) Lateral and torsional restraint	0.8L 0.7L 0.6L 0.5L	1.4L 1.4L 0.6L 0.5L
Tip restraint conditions			
(1) Free	(2) Lateral restraint to top flange	(3) Torsional restraint	(4) Lateral and torsional restraint
			
(not braced on plan)	(braced on plan in at least one bay)	(not braced on plan)	(braced on plan in at least one bay)

Figure 4.25 – Examples of practical details and corresponding effective lengths for cantilever beams without intermediate restraints
(adapted version Source: BS5950 Part 1:2000)

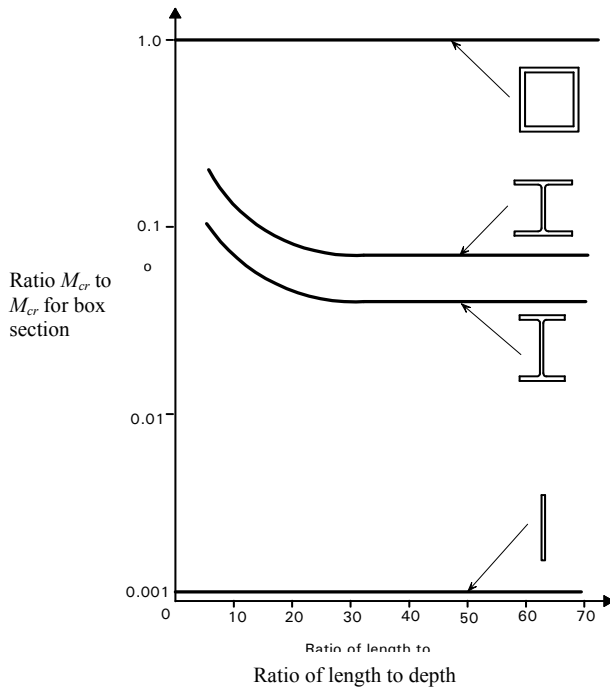


Figure 4.26 – Effect of cross section shape on theoretical elastic critical moment (SSEDTA, Lecture 12)

Besides these factors, the point of application of the loading also has a direct influence on the elastic critical moment of a beam. A gravity load applied below the shear centre C (that coincides with the centroid in case of doubly symmetric sections) has a stabilizing effect, whereas the same load applied above the shear centre has a destabilizing effect (see Figure 4.27). So, the calculation of the critical moment for design of a beam must also incorporate this effect, as shown in Figure 4.27.

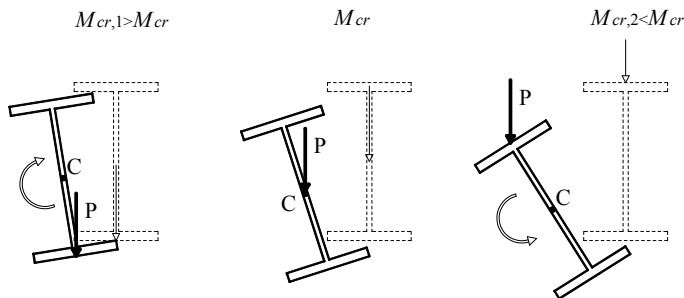


Figure 4.27 – Influence of the location of load application point (da Silva *et al*, 2010)

Beams used in practice, usually, cannot reach the full elastic buckling strength given by equation (4.53), except for very slender beams. For *compact* sections (of class 1 and 2), the attainment of the elastic critical moment can be limited by the plastic capacity of the given section, while for *slender* sections (of class 3 and 4), the limitation is due to attainment of elastic strength in the outer fibres of the section or the occurrence of local buckling of compressed plate elements. Considering the analogy between a bar in compression and a bar in bending, i.e. between N_{cr} and M_{cr} respectively, the lateral-torsional behaviour of a beam is similar to the one of a column. So, in comparing the behaviour of a compact section beam with a class 4 section beam, Figure 1.16 is also representative for beams when replacing the axial force N by the bending moment M .

In case of real beams, the reduction of buckling capacity is caused also by imperfections – geometric and residual ones. The generic buckling curve of a beam, with upper and lower bounds is shown in Figure 4.28.

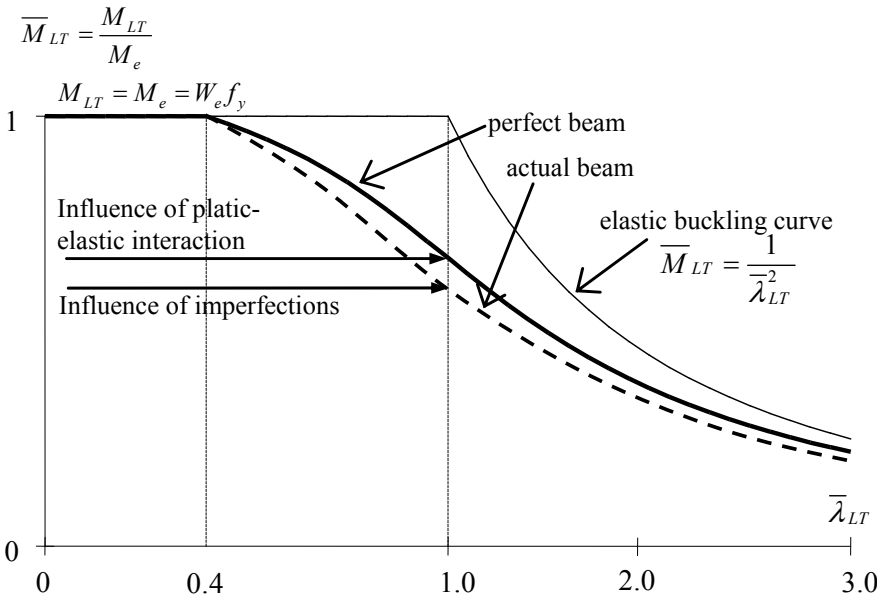


Figure 4.28 – Lateral-torsional buckling curve of an unrestrained beam

In case of class 4 cross sections, interaction between local or sectional buckling modes with lateral-torsional buckling might occur. Figure 4.29 shows the theoretical uncoupled buckling modes of a lipped channel section beam in bending obtained using CUFSM 3.12 (www.ce.jhu.edu/)

bschafer/cufsm). To take local buckling into account, the effective cross section of the beam will be considered, and the lateral-torsional buckling curve takes the shape shown in Figure 4.30.

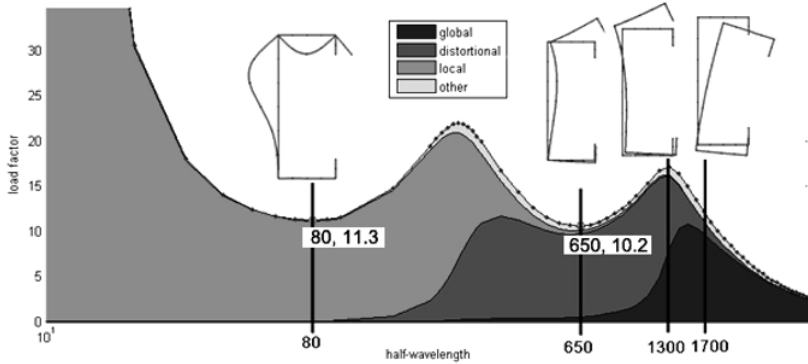


Figure 4.29 – Lateral-torsional buckling curve for a class 4 cross section beam (interaction local – LT buckling) – CUFSM 3.12 (www.ce.jhu.edu/bschafer/cufsm)

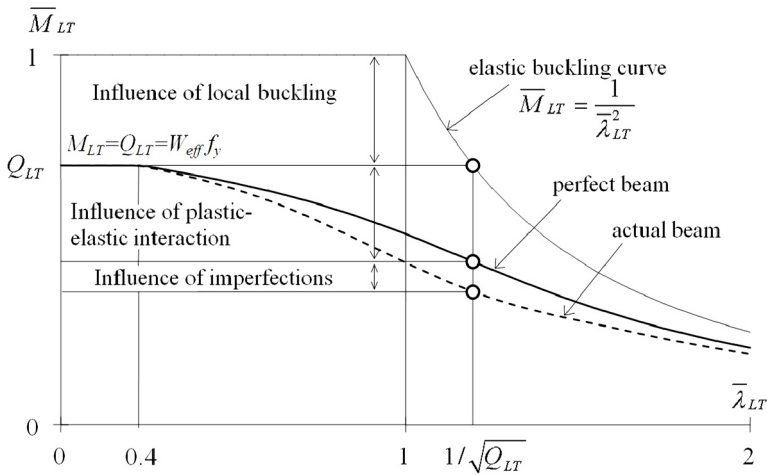


Figure 4.30 – Buckling modes for a lipped channel beam

4.3.2 Design according to EN1993-1-3

4.3.2.1 Lateral-torsional buckling of members subject to bending

The design buckling resistance moment of a member that is susceptible to lateral-torsional buckling should be determined according to EN 1993-1-1, §§6.3.2.2 using the lateral buckling curve *b*.

This method should not be used for sections that have a significant angle between the principal axes of the effective cross section, compared to those of the gross cross section.

A laterally unrestrained member subject to major axis bending should be verified against lateral-torsional buckling as follows:

$$\frac{M_{Ed}}{M_{b,Rd}} \leq 1.0 \quad (4.55)$$

where

- M_{Ed} is the design value of the moment;
- $M_{b,Rd}$ is the design buckling resistance moment.

Beams with sufficient restraint to the compression flange are not susceptible to lateral-torsional buckling. In addition, beams with certain types of cross sections, such as square or circular hollow sections, fabricated circular tubes or square box sections are generally not susceptible to lateral-torsional buckling, because of their high torsion rigidity GI_T .

The design buckling resistance moment of a laterally unrestrained beam should be taken as:

$$M_{b,Rd} = \chi_{LT} W_y f_y / \gamma_{M1} \quad (4.56)$$

where

- W_y is the appropriate section modulus as follows:
 - $W_y = W_{el,y}$ is for class 3 cross section;
 - $W_y = W_{eff,y}$ is for class 4 cross section;

In determining W_y , holes for fasteners at the beam ends need not to be taken into account.

- χ_{LT} is the reduction factor for lateral-torsional buckling,

$$\chi_{LT} = \frac{1}{\phi_{LT} + \left(\phi_{LT}^2 - \bar{\lambda}_{LT}^2 \right)^{0.5}}, \text{ but } \chi_{LT} \leq 1 \quad (4.57)$$

with: $\phi_{LT} = 0.5 \left[1 + \alpha_{LT} (\bar{\lambda}_{LT} - 0.2) + \bar{\lambda}_{LT}^2 \right]$;

α_{LT} is the imperfection factor corresponding to buckling curve b ,
 $\alpha_{LT} = 0.34$;

$$\bar{\lambda}_{LT} = \sqrt{\frac{W_y f_y}{M_{cr}}};$$

M_{cr} is the elastic critical moment for lateral-torsional buckling. M_{cr} is based on gross cross sectional properties and takes into account the loading conditions, the real moment distribution and the lateral restraints, as presented in eqn. (4.54) and Tables 4.3 and 4.4;

For slenderness $\bar{\lambda}_{LT} \leq 0.4$ or for $M_{Ed}/M_{cr} \leq 0.16$, lateral-torsional buckling effects may be ignored and only cross sectional checks are required.

4.3.2.2 Simplified assessment methods for beams with restraints in building

Members with discrete lateral restraint to the compression flange (see Figure 4.31) are not susceptible to lateral-torsional buckling if the length L_c between restraints or the resulting slenderness $\bar{\lambda}_f$ of the equivalent compression flange satisfies:

$$\bar{\lambda}_f = \frac{k_c L_c}{i_{f,z} \lambda_1} \leq \bar{\lambda}_{c0} \frac{M_{c,Rd}}{M_{y,Ed}} \quad (4.58)$$

where

$M_{y,Ed}$ is the maximum design value of the bending moment within the restraint spacing;

$$M_{c,Rd} = W_y \frac{f_y}{\gamma_{M0}}$$

W_y is the appropriate section modulus corresponding to the compression flange;

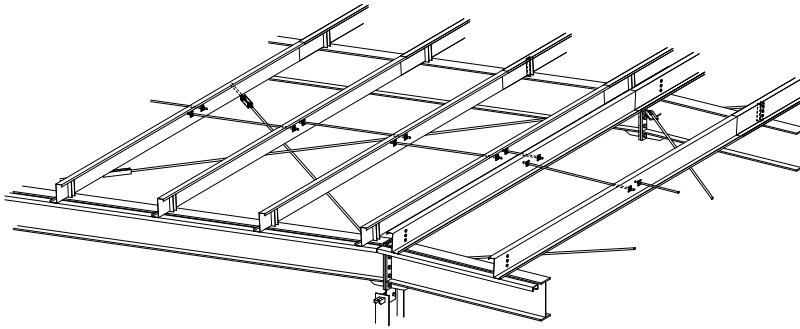
k_c is a slenderness correction factor for moment distribution between restraints, as shown in Table 4.5;

$i_{f,z}$ is the radius of gyration of the equivalent compression flange composed of the compression flange plus 1/3 of the compressed part of the web area, about the minor axis of the section;

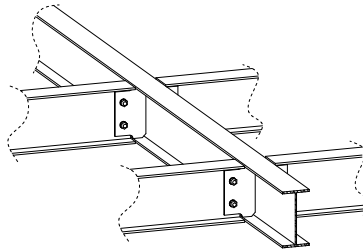
$\bar{\lambda}_{c,0}$ is a slenderness limit for the equivalent compression flange defined above. A recommended value is $\bar{\lambda}_{c,0} = \bar{\lambda}_{LT,0} + 0.1$, where $\bar{\lambda}_{LT,0} = 0.4$;

$$\lambda_1 = \pi \sqrt{\frac{E}{f_y}} = 93.9\varepsilon; \quad \varepsilon = \sqrt{\frac{235}{f_y}} \quad (f_y \text{ in N/mm}^2).$$

Also, purlins and side rails acting as secondary beams are often restrained by the building envelope (e.g. trapezoidal sheeting, sandwich panels, OSB panels, etc.), and may be considered as members with discrete lateral restraint to the compression flange. Aspects related to design of these members are presented in §§4.5.



a) anti-sag bars for Z-purlins and Z-purlins for roof beams



b) secondary beams

Figure 4.31 – Members with discrete lateral restraint

For class 4 cross sections $i_{f,z}$ may be taken as:


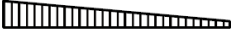


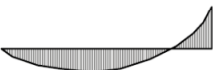
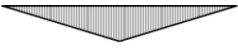

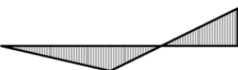
$$i_{f,z} = \sqrt{\frac{I_{eff,f}}{A_{eff,f} + \frac{1}{3}A_{eff,w,c}}} \quad (4.59)$$

where

$I_{eff,f}$ is the effective second moment of area of the compression flange about the minor axis of the section;

$A_{eff,f}$ is the effective area of the compression flange;
 $A_{eff,w,c}$ is the effective area of the compressed part of the web.

Table 4.5 – Correction factor k_c

Moment distribution	k_c
 <p style="text-align: center;">$\psi = 1$</p>	1.0
 <p style="text-align: center;">$-1 \leq \psi \leq 1$</p>	$\frac{1}{1.33 - 0.33\psi}$
	0.94
	0.90
	0.91
	0.86
	0.77
	0.82

If the slenderness of the compression flange $\bar{\lambda}_f$ exceeds the limit $\bar{\lambda}_{c,0} = \bar{\lambda}_{LT,0} + 0.1$, the design buckling resistance moment may be taken as:

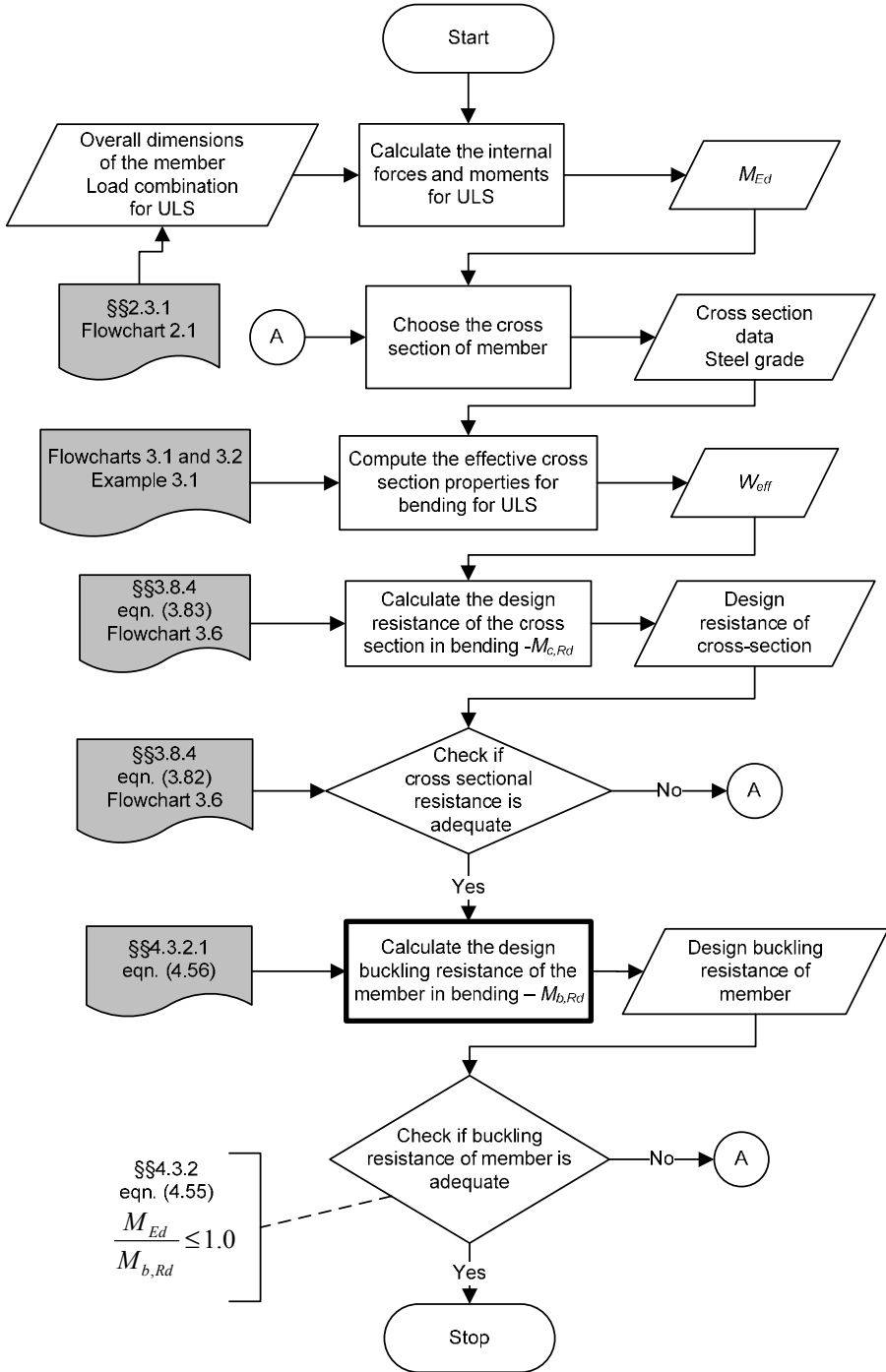
$$M_{b,Rd} = k_{fl} \chi M_{c,Rd} \quad \text{but} \quad M_{b,Rd} \leq M_{c,Rd} \quad (4.60)$$

where

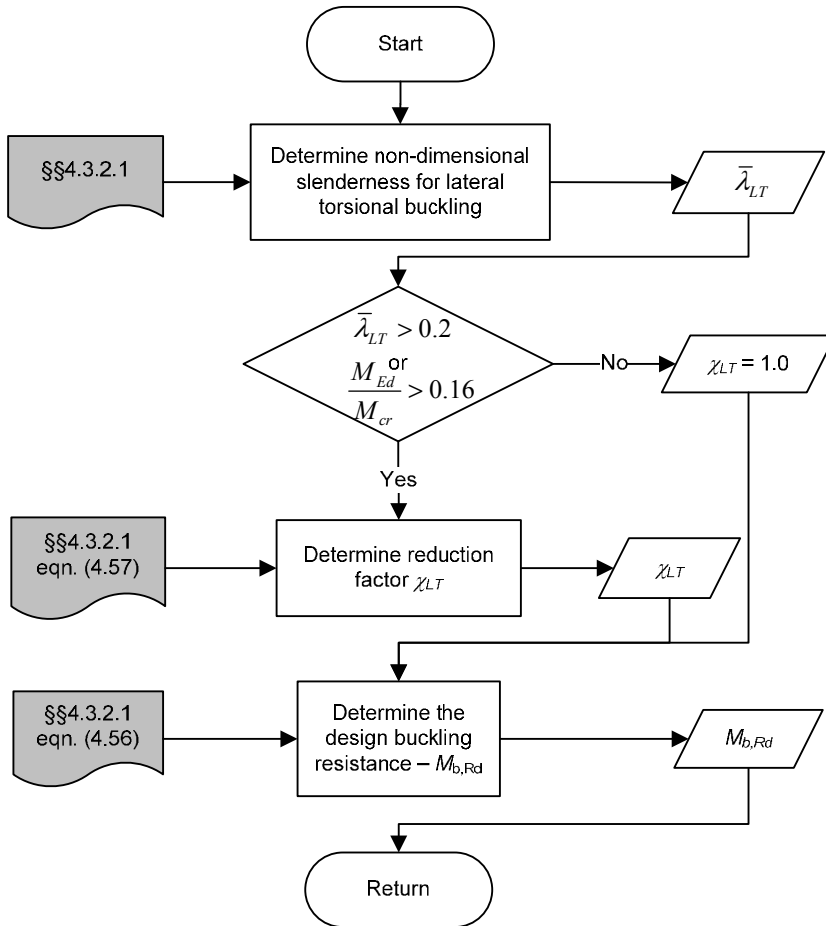
- χ is the reduction factor of the equivalent compression flange determined with $\bar{\lambda}_f$;
- k_{fl} is the modification factor accounting for the conservatism of the equivalent compression flange method. The value $k_{fl} = 1.10$ is recommended.

The buckling curves to be used to calculate the design buckling resistance moment using eqn. (4.60) should be taken as curve *c*.

Flowcharts 4.3 and 4.4 present schematically the design of a cold-formed steel member in bending. Example 4.3 presents a numerical example.



Flowchart 4.3 – Design of a cold-formed steel member in bending



Flowchart 4.4 – Calculate the design buckling resistance of a member in bending – $M_{b,Rd}$

Example 4.3: Design of an unrestrained cold-formed steel beam in bending at the Ultimate Limit State (see Figure 4.32). The beam has pinned end conditions and is composed of two thin-walled cold-formed steel back-to-back lipped channel sections. The connection between the channels is assumed to be rigid.

Basic Data

Span of beam	$L = 4.5$ m
Spacing between beams	$S = 3.0$ m

Distributed loads applied to the joist:

self-weight of the beam	$q_{G,beam} = 0.14 \text{ kN/m}$
weight of the floor and finishing	0.6 kN/m^2
	$q_{G,slab} = 0.55 \times 3.0 = 1.65 \text{ kN/m}$
total dead load	$q_G = q_{G,beam} + q_{G,slab} = 1.79 \text{ kN/m}$
imposed load	1.50 kN/m^2
	$q_Q = 1.50 \times 3.0 = 4.50 \text{ kN/m}$

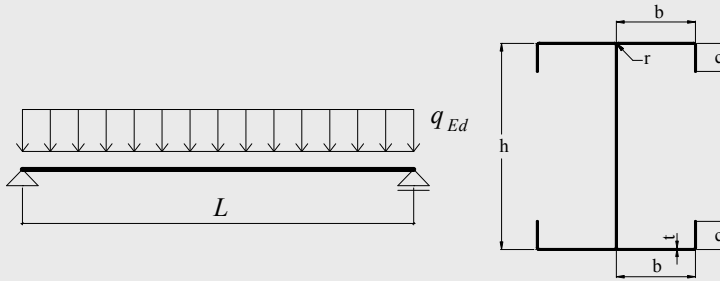


Figure 4.32 – Overall dimensions of beam and of the cross section

The dimensions of the cross section and the material properties are:

Total height	$h = 250 \text{ mm}$
Total width of flanges	$b = 70 \text{ mm}$
Total width of edge fold	$c = 25 \text{ mm}$
Internal radius	$r = 3 \text{ mm}$
Nominal thickness	$t_{nom} = 3.0 \text{ mm}$
Steel core thickness (§§2.4.2.3)	$t = 2.96 \text{ mm}$
Steel grade	S350GD+Z
Basic yield strength	$f_{yb} = 350 \text{ N/mm}^2$
Modulus of elasticity	$E = 210000 \text{ N/mm}^2$
Poisson's ratio	$\nu = 0.3$

Partial factors	$\gamma_{M0} = 1.0$ (§§2.3.1)
	$\gamma_{M1} = 1.0$
	$\gamma_G = 1.35$ – permanent loads (§§2.3.1, Table 2.3)
	$\gamma_Q = 1.50$ – variable loads

Design of the beam for Ultimate Limit State

Properties of the gross cross section

Second moment of area about strong axis y - y : $I_y = 2302.15 \times 10^4 \text{ mm}^4$

Second moment of area about weak axis z - z : $I_z = 244.24 \times 10^4 \text{ mm}^4$

Radii of gyration: $i_y = 95.3 \text{ mm}$; $i_z = 31 \text{ mm}$

Warping constant: $I_w = 17692.78 \times 10^6 \text{ mm}^6$

Torsion constant: $I_t = 7400 \text{ mm}^4$

Effective section properties at the ultimate limit state (§§3.7.3, Flowchart 3.1 and Flowchart 3.2)

The properties of effective cross section were calculated following the procedures presented in Example 3.1 in Chapter 3.

Second moment of area of cold-formed lipped channel section subjected to bending about its major axis: $I_{eff,y} = 22688890 \text{ mm}^4$

Position of the neutral axis:

- from the flange in compression: $z_c = 124.6 \text{ mm}$

- from the flange in tension: $z_t = 122.4 \text{ mm}$

Effective section modulus:

- with respect to the flange in compression:

$$W_{eff,y,c} = \frac{I_{eff,y}}{z_c} = \frac{22688890}{124.6} = 182094 \text{ mm}^3$$

- with respect to the flange in tension:

$$W_{eff,y,t} = \frac{I_{eff,y}}{z_t} = \frac{22688890}{122.4} = 185367 \text{ mm}^3$$

$$W_{eff,y} = \min(W_{eff,y,c}, W_{eff,y,t}) = 182094 \text{ mm}^3$$

Applied loading on the beam at ULS (§§2.3.1, Flowchart 2.1)

$$q_d = \gamma_G q_G + \gamma_Q q_Q = 1.35 \times 1.79 + 1.50 \times 4.5 = 9.17 \text{ kN/m}$$

Maximum applied bending moment (at mid-span) about the major axis y - y :

$$M_{Ed} = q_d L^2 / 8 = 9.17 \times 4.5^2 / 8 = 23.21 \text{ kNm}$$

Check of bending resistance at ULS

Design moment resistance of the cross section for bending (§§3.8.4, eqn. (3.83), Flowchart 3.6):

$$M_{c,Rd} = W_{eff,y} f_{yb} / \gamma_{M0} = 182094 \times 10^{-9} \times 350 \times 10^3 / 1.0 = 63.73 \text{ kNm}$$

Verification of bending resistance (§§3.8.4, eqn. (3.82), Flowchart 3.6):

$$\frac{M_{Ed}}{M_{c,Rd}} = \frac{23.21}{63.73} = 0.364 < 1 \text{ – OK}$$

Determination of the reduction factor χ_{LT}

Lateral-torsional buckling (§§4.3.2.1, eqn. (4.57), Flowchart 4.4)

$$\chi_{LT} = \frac{1}{\phi_{LT} + \sqrt{\phi_{LT}^2 - \bar{\lambda}_{LT}^2}} \text{ but } \chi_{LT} \leq 1.0$$

$$\phi_{LT} = 0.5 \left[1 + \alpha_{LT} (\bar{\lambda}_{LT} - 0.2) + \bar{\lambda}_{LT}^2 \right]$$

$$\alpha_{LT} = 0.34 \text{ – buckling curve } b$$

The non-dimensional slenderness is (§§4.3.2.1):

$$\bar{\lambda}_{LT} = \sqrt{\frac{W_{eff,y,min} f_{yb}}{M_{cr}}}$$

M_{cr} – the elastic critical moment for lateral-torsional buckling

$$M_{cr} = C_1 \frac{\pi^2 EI_z}{L^2} \sqrt{\frac{I_w}{I_z} + \frac{L^2 GI_t}{\pi^2 EI_z}}$$

where $C_1 = 1.127$ for a simply supported beam under uniform loading

$$M_{cr} = 1.127 \times \frac{\pi^2 \times 210000 \times 244.24 \times 10^4}{4500^2} \times \sqrt{\frac{17692.78 \times 10^6}{244.24 \times 10^4} + \frac{4500^2 \times 81000 \times 7400}{\pi^2 \times 210000 \times 244.24 \times 10^4}}$$

$$M_{cr} = 27.66 \text{ kNm}$$

$$\bar{\lambda}_{LT} = \sqrt{\frac{W_{eff,y,min} f_{yb}}{M_{cr}}} = \sqrt{\frac{182094 \times 350}{27.66 \times 10^6}} = 1.518$$

$$\begin{aligned} \phi_{LT} &= 0.5 \left[1 + \alpha_{LT} (\bar{\lambda}_{LT} - 0.2) + \bar{\lambda}_{LT}^2 \right] = \\ &= 0.5 \left[1 + 0.34 \times (1.437 - 0.2) + 1.437^2 \right] = 1.743 \end{aligned}$$

$$\chi_{LT} = \frac{1}{\phi_{LT} + \sqrt{\phi_{LT}^2 - \bar{\lambda}_{LT}^2}} = \frac{1}{1.743 + \sqrt{1.734^2 - 1.437^2}} = 0.369$$

Check of buckling resistance at ULS

Design moment resistance of the cross section for bending (§§4.3.2.1, eqn. (4.56), Flowchart 4.4):

$$M_{b,Rd} = \chi_{LT} W_{eff,y} f_{yb} / \gamma_{M1} = 0.369 \times 182091 \times 10^{-9} \times 350 \times 10^3 / 1.0 = 23.52 \text{ kNm}$$

Verification of buckling resistance (§§4.3.2.1, eqn. (4.55), Flowchart 4.4):

$$\frac{M_{Ed}}{M_{b,Rd}} = \frac{23.21}{23.52} = 0.987 < 1 \text{ - OK}$$

4.4 BUCKLING OF MEMBERS IN BENDING AND AXIAL COMPRESSION

4.4.1 Theoretical background

In practical situations axial compression forces in columns are accompanied by bending moments acting about the major and minor axes of the cross section. Usually, members in such loading conditions are called *beam-columns*. The design for axial compression force and bending moment varying along the length of the member through an exact analysis is complicated. For class 1 to 3 sections the overall buckling modes, e.g. flexural (F) and lateral – torsional (LT) buckling, can interact. In case of members in compression it is more likely that the interaction F + FT to be a problem of unsymmetrical and mono-symmetric cross sections. In case of

eccentric compression or members in bending and compression, when no lateral restrains are provided, such a coupled buckling mode can often occur due to inherent imperfections, even for symmetrical sections. Additionally, for the case of class 4 cross sections, where wall/thickness ratios are large, prone to local (L) buckling (e.g. local and/or distortional), the interaction could be even more complex (e.g. L+F+LT or D+F+LT).

Bending generally results from three sources, depending on the nature of beam-column application. These sources are shown in Figure 4.33 and described as follows (Hancock, 1998; Yu, 2000):

1. Eccentric axial load. A typical case is the pinned connection of the beam to the column when the connection is centred at the face of column (e.g. on the flange);
2. Distributed transverse loading on a beam in compression. It could be the case of the upper chord of a truss under gravity loads when the sheathing is directly supported on the chord; similarly, is the case of cladded walls stud panels under the wind action;
3. End moments, shear and axial forces in moment resisting framings such as portal frames.

Since, in principle, due to the effect of imperfections, there is no pure compression or pure bending in the members of framed structures, all members are beam-columns. The beams ($N = 0$) and columns ($M = 0$) are, in fact, particular cases representing the boundaries of the *beam-column domain*.

300

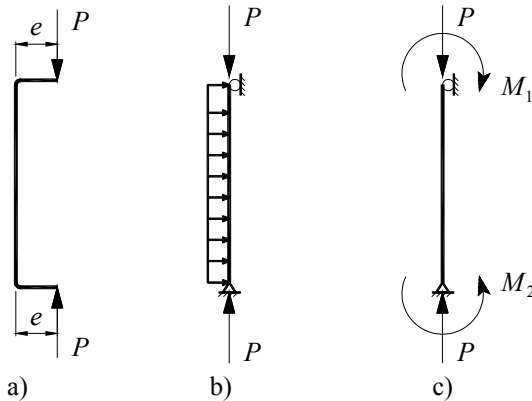


Figure 4.33 – Beam-columns (a) subjected to eccentric loads; (b) subjected to axial and transverse loads; (c) subjected to axial load and end moments

The simplest case to analyse for understanding the compression-bending interaction is case of a slender column subjected to axial compression and bending about major axis $y-y$, laterally restraint about minor axis $z-z$, as shown in Figure 4.34a. When the deformation of an isolated beam-column is confined to the plane of bending, its behaviour can be regarded as a coupling between bending (laterally restrained *beam*) and compression (*column* flexural buckling), as indicated in Figure 4.34b (SSEDTA, Lecture 14). Curve 1 of this figure shows the linear behaviour of the *elastic beam*, while curve 6 shows the limiting behaviour of a *rigid-plastic beam* at the full plastic moment M_{pl} . Curve 2 shows the transition of real elastoplastic beams from curve 1 to curve 6. The elastic buckling of an axially compression member (e.g. *the column*) at its elastic critical load N_{cr} is shown by curve 4. Curve 3 shows the interaction between bending and buckling, and takes into account for the 2nd order effects due to the bending moment $N-w$, exerted by the axial load. Curve 7 shows the interaction between bending moment and axial force. There is a distinction to make between the *primary bending* effect, which is due to the action of the loads directly applied on the beam when it is not yet deflected, those loads being transverse forces and/or moments, and the *secondary bending* effect due to the additional moment generated by the axial load acting on the beam already deflected. The *secondary bending* amplifies the deflection induced by *primary bending*. In terms of moment capacity, *secondary bending* reduces the capacity corresponding to primary bending, which follows the path described by curve 7 in Figure 4.34b.

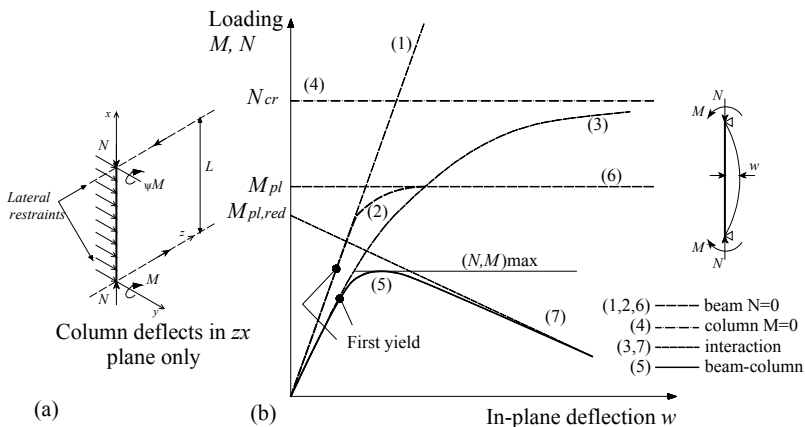


Figure 4.34 – In-plane behaviour of beam-columns (SSEDTA, Lecture 14)

The full plastic moment M_{pl} is reduced to $M_{pl,red}$ due do *second order bending action* of the axial load, i.e. $N \cdot w$. The actual elastoplastic non-linear behaviour of a beam-column is shown by curve 5 which provides a transition from curve 3 for elastic members to curve 7 for rigid plastic behaviour.

In the case of members of class 4 cross section, local or distortional buckling may occur in the compressed part of the cross section (usually a flange), before reaching first yield (see Figure 1.16). Such sectional buckling will reduce both the axial and bending stiffness of the member, and also the ultimate strength, as shown in Figure 4.35.

The ultimate capacity of a class 4 cross section of beam-columns can be satisfactorily evaluated when the maximum longitudinal stress $\sigma_{x,Ed}$ is calculated for the coupled effects of compression and bending using the effective widths of elements in compression (see §§3.8.6, together with §§3.8.3 and §§3.8.4).

At the end, it is important to emphasise that cold-formed sections are, usually, of class 3 or class 4, consequently they are not able to develop plastic bending moments and form plastic hinges. The previous discussion has to be interpreted in these terms.

In Figure 4.35 interaction (9) additionally to (3) and (7) considers the local and overall buckling interaction (as in Figures 1.16 and 3.2).

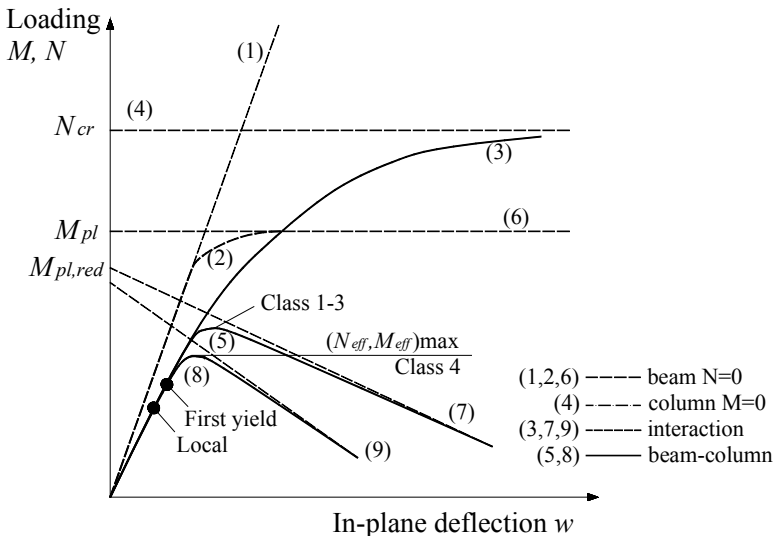


Figure 4.35 – In-plane behaviour of beam-columns of class 4 cross section

4.4.2 Design of beam-columns according to EN1993-1-1 and EN1993-1-3

Two different formats of the interaction formulae are provided in EN 1993-1-1, called Method 1 and Method 2. The main difference between them is the presentation of the different structural effects, either by specific coefficients in Method 1 or by one compact interaction factor in Method 2. This makes Method 1 more adaptable to identifying and accounting for the structural effects, while Method 2 is mainly focussed on the direct design of standard cases (Boissonade *et al*, 2006).

Method 1 (Annex A of EN 1993-1-1) contains a set of formulae that favours transparency and provides a wide range of applicability together with a high level of accuracy and consistency.

Method 2 (Annex B of EN 1993-1-1) is based on the concept of global factors, in which simplicity prevails against transparency. This approach appears to be the more straightforward in terms of a general format.

Both methods use the same basis of numerically calculated limit load results and test data for calibration and validation of the different coefficients. In this respect, the new interaction equations follow the format of those in the previous Eurocode 3 in principle. Both methods follow similar paths, namely the adaptation of the flexural-buckling formulae to lateral-torsional buckling by modified interaction factors calibrated using the limit-load results.

This leads to a design concept which differentiates between the two cases of buckling behaviour of members, firstly those which are susceptible to torsional deformations, and secondly those which are not. Members not susceptible to torsional deformations fail in flexural buckling, by in-plane or spatial deflection. These are closed sections, e.g. RHS, or open sections appropriately restrained against torsional deformations, as frequently found in building structures. Members susceptible to torsional deformations fail by lateral-torsional buckling, such as slender open sections. Accordingly, two sets of design formulae are provided, each covering a specified field of practical design situations.

As explained before, both sets of formulae are based on a second-order in-plane theory. Therefore, they rely on several common concepts, such as the equivalent moment concept, the definition of buckling length and the amplification concept.

4. BEHAVIOUR AND DESIGN RESISTANCE OF BAR MEMBERS

Members which are subjected to combined bending and axial compression should satisfy:

$$\frac{N_{Ed}}{\chi_y N_{Rk} / \gamma_{M1}} + k_{yy} \frac{M_{y,Ed} + \Delta M_{y,Ed}}{\chi_{LT} M_{y,Rk} / \gamma_{M1}} + k_{yz} \frac{M_{z,Ed} + \Delta M_{z,Ed}}{M_{z,Rk} / \gamma_{M1}} \leq 1.0 \quad (4.61a)$$

$$\frac{N_{Ed}}{\chi_z N_{Rk} / \gamma_{M1}} + k_{zy} \frac{M_{y,Ed} + \Delta M_{y,Ed}}{\chi_{LT} M_{y,Rk} / \gamma_{M1}} + k_{zz} \frac{M_{z,Ed} + \Delta M_{z,Ed}}{M_{z,Rk} / \gamma_{M1}} \leq 1.0 \quad (4.61b)$$

where

N_{Ed} , $M_{y,Ed}$ and $M_{z,Ed}$ are the first order design values of the compression force and the maximum moments about the y - y and z - z axis along the member, respectively.

$\Delta M_{y,Ed}$, $\Delta M_{z,Ed}$ are the moments due to the shift of the centroidal axis for class 4 sections (see Table 4.6 and Figure 4.9);

χ_y and χ_z are the reduction factors due to flexural buckling from §§4.2.2;

χ_{LT} is the reduction factor due to lateral torsional buckling from §§4.3.2. For members not susceptible to torsional deformation $\chi_{LT} = 1.0$;

k_{yy} , k_{yz} , k_{zy} , k_{zz} are interaction factors.

304

Table 4.6 – Values for $N_{Rk} = f_y A_i$, $M_{i,Rk} = f_y W_i$ and $\Delta M_{i,Ed}$

Class	1	2	3	4
A_i	A	A	A	A_{eff}
W_y	$W_{pl,y}$	$W_{pl,y}$	$W_{el,y}$	$W_{eff,y}$
W_z	$W_{pl,z}$	$W_{pl,z}$	$W_{el,z}$	$W_{eff,z}$
$\Delta M_{y,Ed}$	0	0	0	$e_{N,y} N_{Ed}$
$\Delta M_{z,Ed}$	0	0	0	$e_{N,z} N_{Ed}$

The interaction factors k_{yy} , k_{yz} , k_{zy} , k_{zz} depend on the method which is chosen, being derived from two alternative approaches: (1) Alternative method 1 – see Tables 4.7 and 4.8 (Annex A of EN1993-1-1) and (2) Alternative method 2 – see Tables 4.9, 4.10 and 4.11 (Annex B of EN1993-1-1). In the following, for both methods, the factors k_{ij} for class 3 and 4 will be presented only.

Table 4.7 – Method 1 – Interaction factors k_{ij}

Interaction factors	Elastic cross sectional properties – class 3, class 4
k_{yy}	$C_{my} C_{mLT} \frac{\mu_y}{1 - \frac{N_{Ed}}{N_{cr,y}}}$
k_{yz}	$C_{mz} \frac{\mu_y}{1 - \frac{N_{Ed}}{N_{cr,z}}}$
k_{zy}	$C_{my} C_{mLT} \frac{\mu_z}{1 - \frac{N_{Ed}}{N_{cr,y}}}$
k_{zz}	$C_{mz} \frac{\mu_z}{1 - \frac{N_{Ed}}{N_{cr,z}}}$
Auxiliary terms	
$C_{yy} = 1 + (w_y - 1) \left[\left(2 - \frac{1.6}{w_y} C_{my}^2 \bar{\lambda}_{max} - \frac{1.6}{w_y} C_{my}^2 \bar{\lambda}_{max}^2 \right) n_{pl} - b_{LT} \right] \geq \frac{W_{el,y}}{W_{pl,y}}$ $\mu_y = \frac{1 - \frac{N_{Ed}}{N_{cr,y}}}{1 - \chi_y \frac{N_{Ed}}{N_{cr,y}}}$ $\mu_z = \frac{1 - \frac{N_{Ed}}{N_{cr,z}}}{1 - \chi_z \frac{N_{Ed}}{N_{cr,z}}}$ $w_y = \frac{W_{pl,y}}{W_{el,y}} \leq 1.5$ $w_z = \frac{W_{pl,z}}{W_{el,z}} \leq 1.5$ $n_{pl} = \frac{N_{Ed}}{N_{Rk} / \gamma_{M0}}$ $a_{LT} = 1 - \frac{I_T}{I_y} \geq 0$ C_{my}, C_{mz} are presented in Table 4.8.	$\text{with } b_{LT} = 0.5 a_{LT} \bar{\lambda}_0^2 \frac{M_{y,Ed}}{\chi_{LT} M_{pl,y,Rd}} \frac{M_{z,Ed}}{M_{pl,z,Rd}}$ $C_{yz} = 1 + (w_z - 1) \left[\left(2 - 14 \frac{C_{mz}^2 \bar{\lambda}_{max}^2}{w_z^5} \right) n_{pl} - c_{LT} \right] \geq 0.6 \sqrt{\frac{w_z}{w_y}} \frac{W_{el,z}}{W_{pl,z}}$ $\text{with } c_{LT} = 10 a_{LT} \frac{\bar{\lambda}_0^2}{5 + \bar{\lambda}_z^4} \frac{M_{y,Ed}}{C_{my} \chi_{LT} M_{pl,y,Rd}}$ $C_{zy} = 1 + (w_y - 1) \left[\left(2 - 14 \frac{C_{my}^2 \bar{\lambda}_{max}^2}{w_y^5} \right) n_{pl} - d_{LT} \right] \geq 0.6 \sqrt{\frac{w_y}{w_z}} \frac{W_{el,y}}{W_{pl,y}}$ $\text{with } d_{LT} = 2 a_{LT} \frac{\bar{\lambda}_0}{0.1 + \bar{\lambda}_z^4} \frac{M_{y,Ed}}{C_{my} \chi_{LT} M_{pl,y,Rd}} + \frac{M_{z,Ed}}{C_{mz} M_{pl,z,Rd}}$ $C_{zz} = 1 + (w_z - 1) \left[\left(2 - \frac{1.6}{w_z} C_{mz}^2 \bar{\lambda}_{max} - \frac{1.6}{w_z} C_{mz}^2 \bar{\lambda}_{max}^2 \right) - e_{LT} \right] n_{pl} \geq \frac{W_{el,z}}{W_{pl,z}}$ $\text{with } e_{LT} = 1.7 a_{LT} \frac{\bar{\lambda}_0}{0.1 + \bar{\lambda}_z^4} \frac{M_{y,Ed}}{C_{my} \chi_{LT} M_{pl,y,Rd}}$ For class 3 and 4 $w_y = w_z = 1.0$. $\bar{\lambda}_{max} = \max(\bar{\lambda}_y, \bar{\lambda}_z)$ $\bar{\lambda}_0$ = non-dimensional slenderness for lateral-torsional buckling due to uniform bending moment, i.e. $\psi_y = 1.0$ in Table 4.8.

4. BEHAVIOUR AND DESIGN RESISTANCE OF BAR MEMBERS

<p>$\bar{\lambda}_{LT}$ = non-dimensional slenderness for lateral-torsional buckling.</p> <p>If</p> $\bar{\lambda}_0 \leq 0.2\sqrt{C_1} \sqrt{\left(1 - \frac{N_{Ed}}{N_{cr,z}}\right) \left(1 - \frac{N_{Ed}}{N_{cr,T}}\right)} : C_{my} = C_{my,0}; C_{mz} = C_{mz,0}; C_{mLT} = 1.0$ <p>If</p> $\bar{\lambda}_0 > 0.2\sqrt{C_1} \sqrt{\left(1 - \frac{N_{Ed}}{N_{cr,z}}\right) \left(1 - \frac{N_{Ed}}{N_{cr,T}}\right)} : C_{my} = C_{my,0} + (1 - C_{my,0}) \frac{\sqrt{\varepsilon_y} a_{LT}}{1 + \sqrt{\varepsilon_y} a_{LT}}$ $C_{mz} = C_{mz,0}; C_{mLT} = C_{my}^2 \frac{a_{LT}}{\sqrt{\left(1 - \frac{N_{Ed}}{N_{cr,z}}\right) \left(1 - \frac{N_{Ed}}{N_{cr,T}}\right)}} \geq 1;$ <p>$C_{mi,0}$ see Table 4.8</p> <p>$\varepsilon_y = \frac{M_{y,Ed}}{N_{Ed}} \frac{A}{W_{el,y}}$ for class 3; $\varepsilon_y = \frac{M_{y,Ed}}{N_{Ed}} \frac{A_{eff}}{W_{eff,y}}$ for class 4;</p> <p>$N_{cr,y}$ = elastic flexural buckling force about the y-y axis; $N_{cr,z}$ = elastic flexural buckling force about the z-z axis; $N_{cr,T}$ = elastic torsional buckling force; I_T = St. Venant torsional constant; I_y = second moment of area about y-y axis; C_1 is a factor depending on the loading and end conditions and may be taken as $C_1 = k_c^{-2}$ where k_c is correction factor from Table 4.5.</p>

Table 4.8 – Equivalent uniform moment factors $C_{mi,0}$

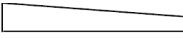
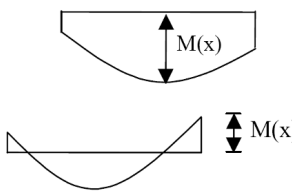
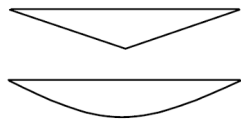
Moment diagram	$C_{mi,0}$
<p>M_1  ψM_1</p> <p>$-1 \leq \psi \leq 1$</p>	$C_{mi,0} = 0.79 + 0.21\psi_i + 0.36(\psi_i - 0.33) \frac{N_{Ed}}{N_{cr,i}}$
 <p>$M(x)$</p> <p>$M(x)$</p>	$C_{mi,0} = 1 + \left(\frac{\pi^2 EI_i \delta_x }{L^2 M_{i,Ed}(x) } - 1 \right) \frac{N_{Ed}}{N_{cr,i}}$ <p>$M_{i,Ed}(x)$ is the maximum moment $M_{y,Ed}$ or $M_{z,Ed}$ according to the first order analyses δ_x is the maximum member deflection along the member δ_z (due to $M_{y,Ed}$) or δ_y (due to $M_{z,Ed}$)</p>
	$C_{mi,0} = 1 - 0.18 \frac{N_{Ed}}{N_{cr,i}}$ $C_{mi,0} = 1 - 0.03 \frac{N_{Ed}}{N_{cr,i}}$

Table 4.9 – Method 2 – Interaction factors k_{ij} for members not susceptible to torsional deformations


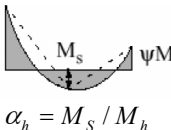
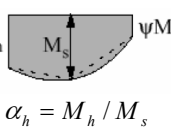
Interaction factors	Type of sections	Elastic cross sectional properties class 3, class 4
k_{yy}	I-sections RHS-sections	$C_{my} \left(1 + 0.6 \bar{\lambda}_y \frac{N_{Ed}}{\chi_y N_{Rk} / \gamma_{M1}} \right) \leq$ $\leq C_{my} \left(1 + 0.6 \frac{N_{Ed}}{\chi_y N_{Rk} / \gamma_{M1}} \right)$
k_{yz}	I-sections RHS-sections	k_{zz}
k_{zy}	I-sections RHS-sections	$0.8k_{yy}$
k_{zz}	I-sections RHS-sections	$C_{mz} \left(1 + 0.6 \bar{\lambda}_z \frac{N_{Ed}}{\chi_z N_{Rk} / \gamma_{M1}} \right) \leq$ $\leq C_{mz} \left(1 + 0.6 \frac{N_{Ed}}{\chi_z N_{Rk} / \gamma_{M1}} \right)$

Table 4.10 – Method 2 – Interaction factors k_{ij} for members susceptible to torsional deformations

Interaction factors	elastic cross sectional properties class 3, class 4
k_{yy}	k_{yy} from Table 4.9
k_{yz}	k_{yz} from Table 4.9
k_{zy}	$\left[1 - \frac{0.05 \bar{\lambda}_z}{(C_{mLT} - 0.25)} \frac{N_{Ed}}{\chi_z N_{Rk} / \gamma_{M1}} \right]$ $\geq \left[1 - \frac{0.05}{(C_{mLT} - 0.25)} \frac{N_{Ed}}{\chi_z N_{Rk} / \gamma_{M1}} \right]$
k_{zz}	k_{zz} from Table 4.9

4. BEHAVIOUR AND DESIGN RESISTANCE OF BAR MEMBERS

Table 4.11 – Equivalent uniform moment factors C_{mi} in Tables 4.9 and 4.10

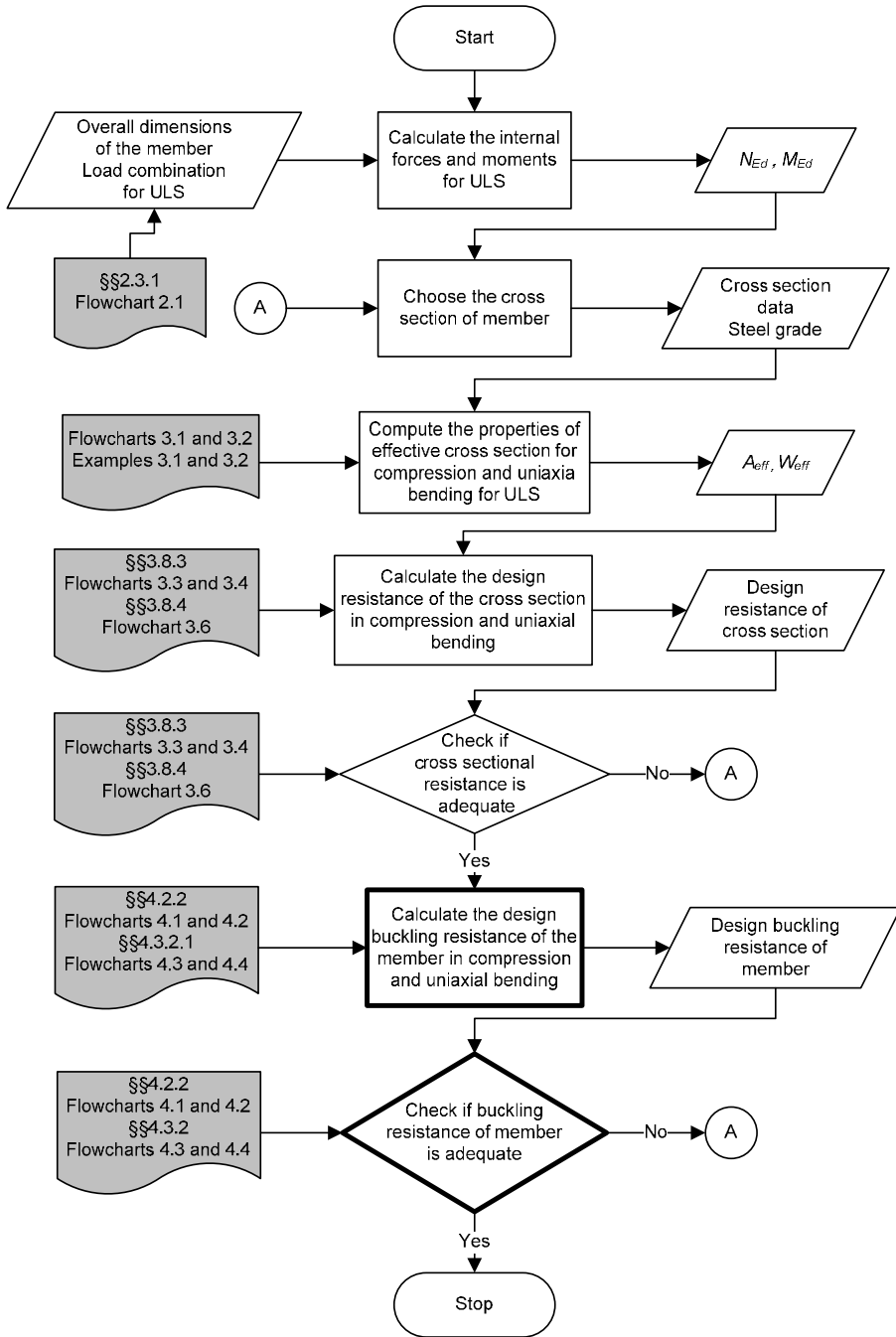
Moment diagram	Range		C_{my}, C_{mz} and C_{mLT}	
			Uniform loading	Concentrated load
	$-1 \leq \psi \leq 1$		$0.6 + 0.4\psi \geq 0.4$	
 $\alpha_h = M_s / M_h$	$0 \leq \alpha_s \leq 1$	$-1 \leq \psi \leq 1$	$0.2 + 0.8\alpha_s \geq 0.4$	$0.2 + 0.8\alpha_s \geq 0.4$
	$-1 \leq \alpha_s < 1$	$0 \leq \psi \leq 1$	$0.1 - 0.8\alpha_s \geq 0.4$	$-0.8\alpha_s \geq 0.4$
$-1 \leq \psi < 0$		$0.1(1 - \psi) - 0.8\alpha_s \geq 0.4$	$0.2(-\psi) - 0.8\alpha_s \geq 0.4$	
 $\alpha_h = M_h / M_s$	$0 \leq \alpha_h \leq 1$	$-1 \leq \psi \leq 1$	$0.95 + 0.05\alpha_h$	$0.90 + 0.10\alpha_h$
	$-1 \leq \alpha_h < 1$	$0 \leq \psi \leq 1$	$0.95 + 0.05\alpha_h$	$0.90 + 0.10\alpha_h$
		$-1 \leq \psi < 0$	$0.95 + 0.05\alpha_h(1 + 2\psi)$	$0.90 + 0.10\alpha_h(1 + 2\psi)$
In the calculation of α_h and α_s , a hogging moment should be taken as negative and a sagging moment should be taken as positive.				
For members susceptible to sway buckling the equivalent uniform moment factors should be taken $C_{my} = 0.9$ and $C_{mz} = 0.9$.				
C_{my}, C_{mz} and C_{mLT} should be obtained according to the bending moment diagram between the relevant braced points as follows:				
moment factor	bending axis	point braced direction		
C_{my}	y-y	z-z		
C_{mz}	z-z	y-y		
C_{mLT}	y-y	y-y		

As an alternative, the interaction formula may be used

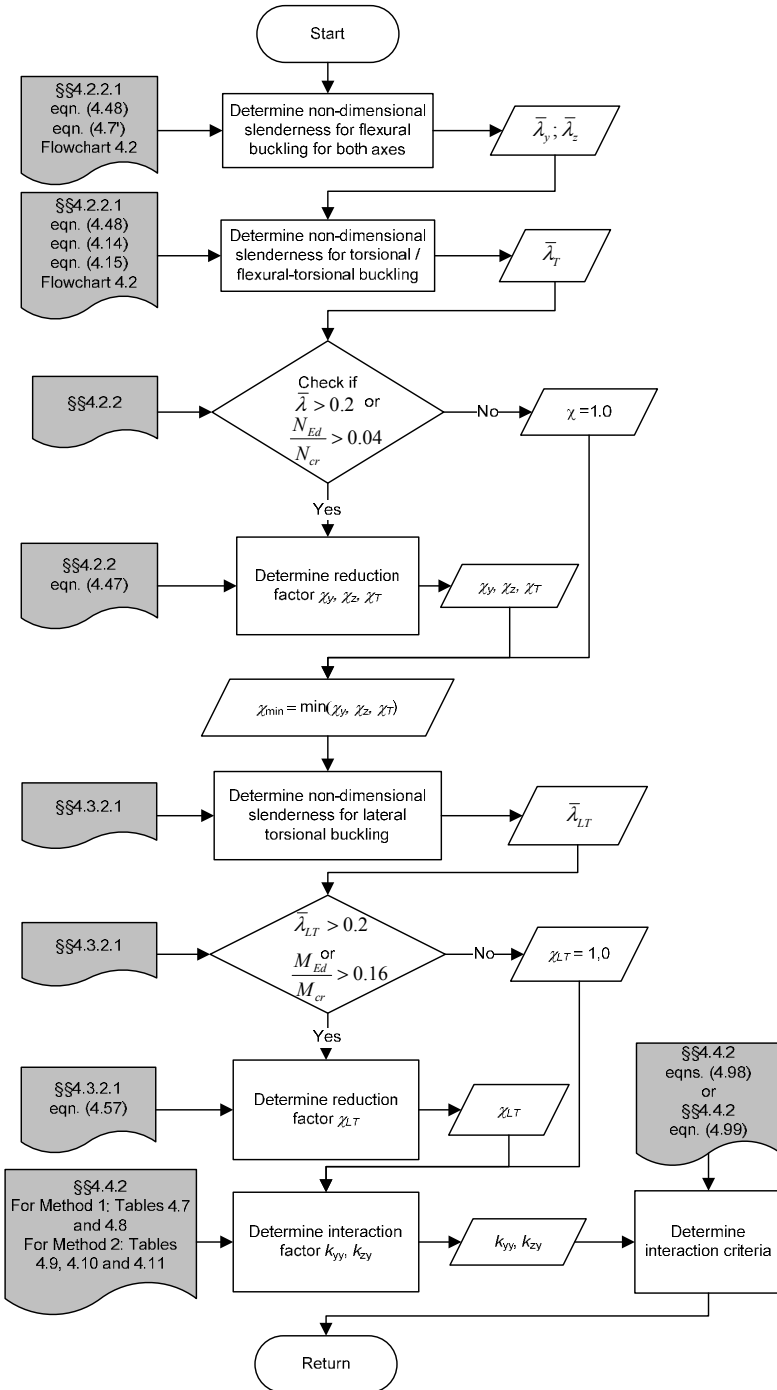
$$\left(\frac{N_{Ed}}{N_{b,Rd}} \right)^{0.8} + \left(\frac{M_{Ed}}{M_{b,Rd}} \right)^{0.8} \leq 1.0 \tag{4.62}$$

where $N_{b,Rd}$ is the design buckling resistance of a compression member according to §§4.2.2 (flexural, torsional or flexural-torsional buckling), $M_{b,Rd}$ is the design bending moment resistance according to §§4.3.2 and M_{Ed} is the second order moment, including the effects of the shift of the neutral axis, if relevant.

Flowcharts 4.5 and 4.6 present schematically the design of a cold-formed steel member in combined compression and uniaxial bending. Example 4.4 presents a numerical example.



Flowchart 4.5 – Design of a cold-formed steel member in combined compression and uniaxial bending (SF042a-EN-EU, Access Steel 2006)



Flowchart 4.6 – Calculate the design buckling resistance of the member in compression and uniaxial bending (SF042a-EN-EU, Access Steel 2006)

4.4.2.1 General method for lateral and lateral-torsional buckling of structural components

The following method may be used where the classical methods do not apply. It allows the verification of the resistance to lateral and lateral-torsional buckling for structural components such as:

- single members with mono-symmetric cross sections, built-up or not, uniform or not, with complex support conditions or not, or
 - plane frames or subframes composed of such members,
- which are subject to compression and/or mono-axial bending in the plane, but which do not contain rotative plastic hinges.

The method requires the main following steps (SN032a-EN-EU):

- ***In-plane analysis of the structural component.*** The objective is to determine the design effects in the structural component under the design loading and then to assess the magnitude of the effects in relation to the characteristic resistance at the most critical cross section, considering only the in-plane behaviour. The ratio between characteristic resistance and design effects is expressed as the load amplifier, $\alpha_{ult,k}$;
- ***Out-of-plane buckling analysis of the structural component.*** The objective is to determine the magnitude of the loading, as a multiple of the design loading, at which the structural component fails by out-of-plane elastic buckling. The magnitude is expressed as the amplifier $\alpha_{cr,op}$;
- ***Check of the overall resistance of the structural component.*** The objective is to verify the adequacy of the structural component, considering the interaction between the in-plane behaviour of the structural component and the out-of-plane behaviour.

The overall resistance to out-of-plane buckling for any structural component conforming to the scope presented above can be verified by ensuring that:

$$\frac{\chi_{op} \alpha_{ult,k}}{\gamma_{M1}} \geq 1.0 \quad (4.63)$$

where

$\alpha_{ult,k}$ is the minimum load amplifier of the design loads to reach the characteristic resistance of the most critical cross section of

the structural component considering its in-plane behaviour without taking lateral or lateral-torsional buckling into account however accounting for all effects due to in plane geometrical deformation and imperfections, global and local, where relevant;

χ_{op} is the reduction factor for the non-dimensional slenderness $\bar{\lambda}_{op}$, to take account of lateral and lateral-torsional buckling;

γ_{M1} is the safety coefficient ($\gamma_{M1} = 1$).

The global non-dimensional slenderness $\bar{\lambda}_{op}$ for the structural component should be determined from:

$$\bar{\lambda}_{op} = \sqrt{\frac{\alpha_{ult,k}}{\alpha_{cr,op}}} \quad (4.64)$$

where

$\alpha_{cr,op}$ is the minimum amplifier for the in-plane design loads to reach the elastic critical load of the structural component with regards to lateral or lateral-torsional buckling without accounting for in plane flexural buckling. In determining $\alpha_{cr,op}$ and $\alpha_{ult,k}$ Finite Element analysis may be used.

The reduction factor χ_{op} may be determined from either of the following methods:

a) the minimum value of

χ_z for lateral buckling according to §§4.2.2;

χ_{LT} for lateral torsional-buckling according to §§4.3.2;

each calculated for the global non-dimensional slenderness $\bar{\lambda}_{op}$.

b) a value interpolated between the values χ_z and χ_{LT} as determined in a) by using the formula for $\alpha_{ult,k}$ corresponding to the critical cross section.

Examples where a linear cross section resistance criterion governs $\alpha_{ult,k}$ (SN032a-EN-EU)

N_{Ed} and $M_{y,Ed}$ are the maximum compression force and bending moment determined from the in-plane analysis accounting for all relevant in-plane second order effects (global for the frame and local for the structural component) and all relevant in-plane imperfections (sway imperfection for the frame and bow imperfection for the structural component). So,

considering for example Class 3 cross sections for the structural component, $\alpha_{ult,k}$ may be determined using the following cross section check:

$$\frac{N_{Ed}}{N_{Rk}} + \frac{M_{y,Ed}}{M_{y,Rk}} \leq 1 \quad (4.65)$$

It follows that:

$$\alpha_{ult,k} = \frac{1}{\frac{N_{Ed}}{N_{Rk}} + \frac{M_{y,Ed}}{M_{y,Rk}}} \quad (4.66)$$

and this general method leads to check:

$$\frac{\chi_{op} \alpha_{ult,k}}{\gamma_{M1}} = \frac{\chi_{op}}{\gamma_{M1} \left(\frac{N_{Ed}}{N_{Rk}} + \frac{M_{y,Ed}}{M_{y,Rk}} \right)} \geq 1.0 \quad (4.67)$$

that is:

$$\frac{N_{Ed}}{N_{Rk} / \gamma_{M1}} + \frac{M_{y,Ed}}{M_{y,Rk} / \gamma_{M1}} \leq \chi_{op} \quad (4.68)$$

(This is the expression given in the Note to EN1993-1-1, §§6.3.4(4)a).

Moreover, for this case, if χ_{op} is to be determined using the “interpolated value” method, it follows:

313

$$\chi_{op} = \frac{\left(\frac{N_{Ed}}{N_{Rk}} + \frac{M_{y,Ed}}{M_{y,Rk}} \right)}{\left(\frac{N_{Ed}}{\chi_z N_{Rk}} + \frac{M_{y,Ed}}{\chi_{LT} M_{y,Rk}} \right)} \geq 1.0 \quad (4.69)$$

and one is led to check:

$$\frac{\chi_{op} \alpha_{ult,k}}{\gamma_{M1}} = \frac{\left(\frac{N_{Ed}}{N_{Rk}} + \frac{M_{y,Ed}}{M_{y,Rk}} \right)}{\left(\frac{N_{Ed}}{\chi_z N_{Rk}} + \frac{M_{y,Ed}}{\chi_{LT} M_{y,Rk}} \right) \gamma_{M1} \left(\frac{N_{Ed}}{N_{Rk}} + \frac{M_{y,Ed}}{M_{y,Rk}} \right)} \geq 1.0 \quad (4.70)$$

4. BEHAVIOUR AND DESIGN RESISTANCE OF BAR MEMBERS

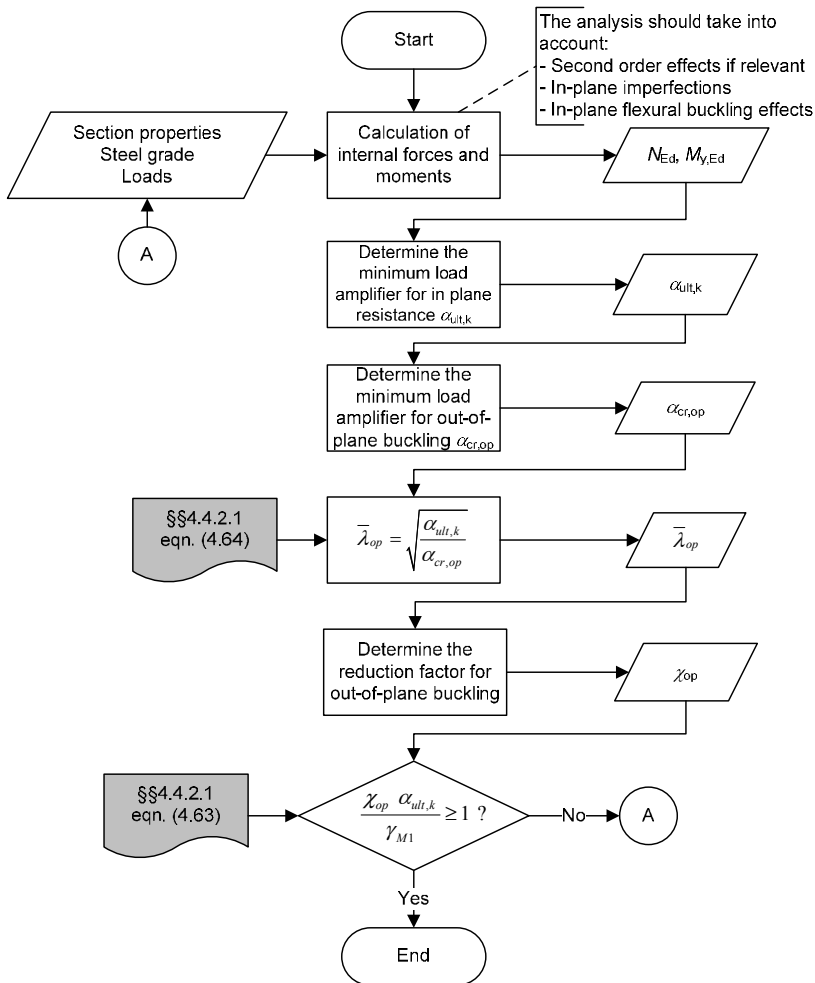
that is:

$$\frac{N_{Ed}}{\chi_z N_{Rk} / \gamma_{M1}} + \frac{M_{y,Ed}}{\chi_{LT} M_{y,Rk} / \gamma_{M1}} \leq 1 \quad (4.71)$$

(This is the expression given in the Note to EN1993-1-1 §6.3.4(4)b).

One can see that it is not necessary to calculate χ_{op} explicitly when using the “interpolated value” method.

Flowchart 4.7 presents schematically the buckling verification of non-uniform members in portal frames using *General method*.



Flowchart 4.7 – Buckling verification of non-uniform members in portal frames (SF044a-EN-EU, Access Steel 2006)

Example 4.4: Design of a cold-formed steel built-up column in compression and bending, as component of a pitched roof cold-formed steel portal frame consisting of back-to-back lipped channel sections and bolted joints. Pinned supports are considered at the column bases. The ridge and eave connections are assumed to be rigid (see Figure 4.36).

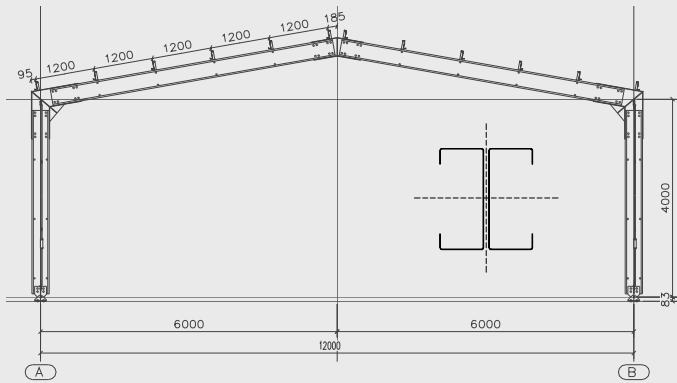


Figure 4.36 – Overall dimensions of the frame and the cross section

Basic Data

Height of column:	$H = 4.00 \text{ m}$
Span:	$L = 12.00 \text{ m}$
Bay:	$T = 4.00 \text{ m}$
Roof angle:	10°

The dimensions of one lipped channel section and the material properties are:

Total height	$h = 350 \text{ mm}$
Total width of flange	$b = 96 \text{ mm}$
Total width of edge fold	$c = 32 \text{ mm}$
Internal radius	$r = 3 \text{ mm}$
Nominal thickness	$t_{nom} = 3 \text{ mm}$
Steel core thickness (§§2.4.2.3)	$t = 2.96 \text{ mm}$
Basic yield strength (S350GD+Z)	$f_{yb} = 350 \text{ N/mm}^2$
Modulus of elasticity	$E = 210000 \text{ N/mm}^2$

Poisson's ratio	$\nu = 0.3$
Shear modulus	$G = 81000 \text{ N/mm}^2$
Partial factors (§§2.3.1)	$\gamma_{M0} = 1.0; \gamma_{M1} = 1.0$
	$\gamma_G = 1.35$ – permanent loads
	$\gamma_Q = 1.50$ – variable loads

Distributed loads applied to the frame:

- self-weight of the structure (applied by the static computer program)
- dead load – the roof structure: 0.20 kN/m^2
 $q_G = 0.2 \times 4.0 = 0.8 \text{ kN/m}$
- snow load: 1.00 kN/m^2
 $q_S = 1.00 \times 4.00 = 4.00 \text{ kN/m}$

Only one load combination at the Ultimate Limit State was considered in the analysis. The uniform distributed load on the frame, according to §§2.3.1 (see Flowchart 2.1) is:

$$(\gamma_G q_G + \gamma_Q q_Q) T = (1.35 \times 0.2 + 1.50 \times 1.00 \times \cos 10^\circ) \times 4 \cong 7.00 \text{ kN/m}$$

Properties of the gross cross section

316

Area of gross cross section:	$A = 3502 \text{ mm}^2$
Radii of gyration:	$i_y = 133.5 \text{ mm}; i_z = 45.9 \text{ mm}$
Second moment of area about strong axis y-y:	$I_y = 6240.4 \times 10^4 \text{ mm}^4$
Second moment of area about weak axis z-z:	$I_z = 737.24 \times 10^4 \text{ mm}^4$
Warping constant:	$I_w = 179274 \times 10^6 \text{ mm}^6$
Torsion constant:	$I_t = 10254.8 \text{ mm}^4$

Effective section properties of the cross section (§§3.7.3, Flowchart 3.1 and Flowchart 3.2)

The properties of effective cross section were calculated following the procedures presented in Examples 3.1 and 3.2 in Chapter 3.

Effective area of the cross section when subjected to compression only:

$$A_{eff,c} = 1982.26 \text{ mm}^2$$

Second moment of area of effective cross section about strong axis y - y :

$$I_{eff,y} = 5850.85 \times 10^4 \text{ mm}^4$$

Effective section modulus in bending:

$$\text{with respect to the flange in compression: } W_{eff,y,c} = 319968 \text{ mm}^3$$

$$\text{with respect to the flange in tension: } W_{eff,y,t} = 356448 \text{ mm}^3$$

$$W_{eff,y,min} = \min(W_{eff,y,c}, W_{eff,y,t}) = 319968 \text{ mm}^3$$

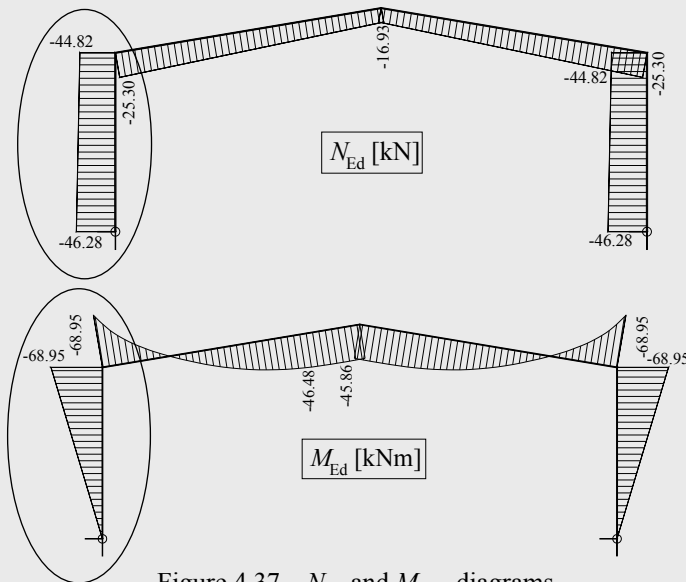


Figure 4.37 – N_{Ed} and $M_{y,Ed}$ diagrams

The built-up column has to be designed to:

- the axial force (compression): $N_{Ed} = -44.82 \text{ kN}$;
- the maximum bending moment: $M_{y,Ed} = -68.95 \text{ kNm}$.

Resistance check of the cross section

The following criterion should be met (§§3.8.9, eqn. (3.128a)):

$$\frac{N_{Ed}}{N_{c,Rd}} + \frac{M_{y,Ed} + \Delta M_{y,Ed}}{M_{cy,Rd,com}} \leq 1$$

where

$$N_{c,Rd} = A_{eff} f_{yb} / \gamma_{M0} \quad (\S\S 3.8.3, \text{ eqn. (3.81), Flowcharts 3.4 and 3.5})$$

$$M_{cz,Rd,com} = W_{eff,com} f_{yb} / \gamma_{M0} \quad (\S\S 3.8.4, \text{ eqn. (3.83), Flowchart 3.6})$$

$$\Delta M_{y,Ed} = N_{Ed} e_{Ny}$$

e_{Ny} – is the shift of the centroidal y - y axis; but as the cross section is doubly symmetric: $e_{Ny} = 0$ (§§3.8.9)

The resistance check is:

$$\frac{44.82 \times 10^3}{1982 \times 350 / 1.0} + \frac{68.95 \times 10^6 + 0}{319968 \times 350 / 1.0} = 0.680 < 1 \quad - \text{OK}$$

Buckling resistance check

Members which are subjected to combined axial compression and uniaxial bending should satisfy (§§4.4.2, eqn. (4.61)):

$$\frac{N_{Ed}}{\chi_y \frac{N_{Rk}}{\gamma_{M1}}} + k_{yy} \frac{M_{y,Ed} + \Delta M_{y,Ed}}{\chi_{LT} \frac{M_{y,Rk}}{\gamma_{M1}}} \leq 1$$

$$\frac{N_{Ed}}{\chi_z \frac{N_{Rk}}{\gamma_{M1}}} + k_{zy} \frac{M_{y,Ed} + \Delta M_{y,Ed}}{\chi_{LT} \frac{M_{y,Rk}}{\gamma_{M1}}} \leq 1$$

where

$$N_{Rk} = f_{yb} A_{eff} = 350 \times 1982 = 693.7 \times 10^3 \text{ N} = 693.7 \text{ kN}$$

$$M_{y,Rk} = f_{yb} W_{eff,y,min} = 350 \times 319968 = 112 \times 10^6 \text{ Nmm} = 112 \text{ kNm}$$

$\Delta M_{y,Ed}$ – additional moment due to the shift of the centroidal axes;

$$\Delta M_{y,Ed} = 0$$

$$\chi = \frac{1}{\phi + \sqrt{\phi^2 - \bar{\lambda}^2}} \quad \text{but } \chi \leq 1.0 \quad (\S\S 4.2.2, \text{ eqn. (4.47)})$$

$$\phi = 0.5 \left[1 + \alpha (\bar{\lambda} - 0.2) + \bar{\lambda}^2 \right]$$

α – imperfection factor

The non-dimensional slenderness is:

$$\bar{\lambda} = \sqrt{\frac{A_{eff} f_{yb}}{N_{cr}}}$$

N_{cr} – the elastic critical force for the relevant buckling mode

Determination of the reduction factors χ_y , χ_z , χ_T

Flexural buckling (§§4.2.2.1, eqn. (4.48), Flowchart 4.2)

$$\bar{\lambda}_F = \sqrt{\frac{A_{eff} f_{yb}}{N_{cr}}} = \frac{L_{cr}}{i} \frac{\sqrt{A_{eff}/A}}{\lambda_1}$$

The buckling length:

$$L_{cr,y} = L_{cr,z} = H = 4000 \text{ mm}$$

$$\lambda_1 = \pi \sqrt{\frac{E}{f_{yb}}} = \pi \times \sqrt{\frac{210000}{350}} = 76.95$$

Buckling about y - y axis (§§4.2.2.1, Table 4.2):

$$\bar{\lambda}_y = \frac{L_{cr,y}}{i_y} \frac{\sqrt{A_{eff}/A}}{\lambda_1} = \frac{4000}{133.5} \times \frac{\sqrt{1982.26/3502}}{76.95} = 0.293$$

$\alpha_y = 0.21$ – buckling curve a (§§4.2.1.2, Table 4.1)

$$\begin{aligned} \phi_y &= 0.5 \left[1 + \alpha_y (\bar{\lambda}_y - 0.2) + \bar{\lambda}_y^2 \right] = \\ &= 0.5 \times \left[1 + 0.21 \times (0.293 - 0.2) + 0.293^2 \right] = 0.553 \end{aligned}$$

$$\chi_y = \frac{1}{\phi_y + \sqrt{\phi_y^2 - \bar{\lambda}_y^2}} = \frac{1}{0.553 + \sqrt{0.553^2 - 0.293^2}} = 0.978$$

Buckling about z - z axis (§§4.2.2.1, Table 4.2):

$$\bar{\lambda}_z = \frac{L_{cr,z}}{i_z} \frac{\sqrt{A_{eff}/A}}{\lambda_1} = \frac{4000}{45.9} \times \frac{\sqrt{1982.26/3502}}{76.95} = 0.852$$

$\alpha_z = 0.34$ – buckling curve b (§§4.2.1.2, Table 4.1)

$$\begin{aligned}\phi_z &= 0.5 \left[1 + \alpha_z (\bar{\lambda}_z - 0.2) + \bar{\lambda}_z^2 \right] = \\ &= 0.5 \times \left[1 + 0.34 \times (0.852 - 0.2) + 0.852^2 \right] = 0.974\end{aligned}$$

$$\chi_z = \frac{1}{\phi_z + \sqrt{\phi_z^2 - \bar{\lambda}_z^2}} = \frac{1}{0.974 + \sqrt{0.974^2 - 0.852^2}} = 0.692$$

Torsional buckling (§§4.2.1.1, eqn. (4.14))

$$N_{cr,T} = \frac{1}{i_o^2} \left(GI_t + \frac{\pi^2 EI_w}{l_T^2} \right)$$

where

$$i_o^2 = i_y^2 + i_z^2 + y_o^2 + z_o^2$$

y_o, z_o – the shear centre coordinates with respect to the centroid of the gross cross section: $y_o = z_o = 0$

$$i_o^2 = 133.5^2 + 45.9^2 + 0 + 0 = 19929.1 \text{ mm}^2$$

$$l_T = H = 4000 \text{ mm}$$

The elastic critical force for torsional buckling is:

$$\begin{aligned}N_{cr,T} &= \frac{1}{19929.1} \times \left(81000 \times 10254.8 + \frac{\pi^2 \times 210000 \times 179274 \times 10^6}{4000^2} \right) = \\ &= 1206.96 \times 10^3 \text{ N}\end{aligned}$$

The non-dimensional slenderness is:

$$\bar{\lambda}_T = \sqrt{\frac{A_{eff} f_{yb}}{N_{cr}}} = \sqrt{\frac{1982.26 \times 350}{1206.96 \times 10^3}} = 0.758$$

$\alpha_T = 0.34$ – buckling curve b (§§4.2.2.1, Table 4.2, §§4.2.1.2, Table 4.1)

$$\begin{aligned}\phi_T &= 0.5 \left[1 + \alpha_T (\bar{\lambda}_T - 0.2) + \bar{\lambda}_T^2 \right] = \\ &= 0.5 \times \left[1 + 0.34 \times (0.758 - 0.2) + 0.758^2 \right] = 0.882\end{aligned}$$

The reduction factor for torsional and flexural-torsional buckling is:

$$\chi_T = \frac{1}{\phi_T + \sqrt{\phi_T^2 - \bar{\lambda}_T^2}} = \frac{1}{0.882 + \sqrt{0.882^2 - 0.758^2}} = 0.750$$

Determination of the reduction factor χ_{LT}

Lateral-torsional buckling (§§4.3.2.1, eqn. (4.57), Flowchart 4.4)

$$\chi_{LT} = \frac{1}{\phi_{LT} + \sqrt{\phi_{LT}^2 - \bar{\lambda}_{LT}^2}} \quad \text{but} \quad \chi_{LT} \leq 1.0$$

$$\phi_{LT} = 0.5 \left[1 + \alpha_{LT} (\bar{\lambda}_{LT} - 0.2) + \bar{\lambda}_{LT}^2 \right]$$

$$\alpha_{LT} = 0.34 - \text{buckling curve } b \text{ (§§4.2.1.2, Table 4.1)}$$

The non-dimensional slenderness is (§§4.3.2.1):

$$\bar{\lambda}_{LT} = \sqrt{\frac{W_{eff,y,min} f_{yb}}{M_{cr}}}$$

M_{cr} – the elastic critical moment for lateral-torsional buckling

$$M_{cr} = C_1 \frac{\pi^2 EI_z}{L^2} \sqrt{\frac{I_w}{I_z} + \frac{L^2 GI_t}{\pi^2 EI_z}}$$

where $C_1 = 1.77$ for a simply supported beam under uniform loading

$$M_{cr} = 1.77 \times \frac{\pi^2 \times 210000 \times 737.24 \times 10^4}{4000^2} \times \sqrt{\frac{179274 \times 10^6}{737.24 \times 10^4} + \frac{4000^2 \times 81000 \times 10254.8}{\pi^2 \times 210000 \times 737.24 \times 10^4}}$$

$$M_{cr} = 282.27 \text{ kNm}$$

$$\bar{\lambda}_{LT} = \sqrt{\frac{W_{eff,y,min} f_{yb}}{M_{cr}}} = \sqrt{\frac{319968 \times 350}{268.27 \times 10^6}} = 0.646$$

$$\begin{aligned} \phi_{LT} &= 0.5 \left[1 + \alpha_{LT} (\bar{\lambda}_{LT} - 0.2) + \bar{\lambda}_{LT}^2 \right] = \\ &= 0.5 \left[1 + 0.34 \times (0.646 - 0.2) + 0.646^2 \right] = 0.784 \end{aligned}$$

$$\chi_{LT} = \frac{1}{\phi_{LT} + \sqrt{\phi_{LT}^2 - \bar{\lambda}_{LT}^2}} = \frac{1}{0.784 + \sqrt{0.784^2 - 0.646^2}} = 0.814$$

Determination of interaction factors k_{yy} and k_{zy} – Method 1 (§§4.4.2, Tables 4.7 and 4.8)

$$k_{yy} = C_{my} C_{mLT} \frac{\mu_y}{1 - \frac{N_{Ed}}{N_{cr,y}}}; \quad k_{zy} = C_{my} C_{mLT} \frac{\mu_z}{1 - \frac{N_{Ed}}{N_{cr,y}}}$$

where

$$\mu_y = \frac{1 - \frac{N_{Ed}}{N_{cr,y}}}{1 - \chi_y \frac{N_{Ed}}{N_{cr,y}}}; \quad \mu_z = \frac{1 - \frac{N_{Ed}}{N_{cr,z}}}{1 - \chi_z \frac{N_{Ed}}{N_{cr,z}}}$$

$$N_{cr,y} = \frac{\pi^2 EI_y}{L_{cr,y}^2} = \frac{\pi^2 \times 210000 \times 6240.4 \times 10^4}{4000^2} = 8083.72 \times 10^3 \text{ N} = 8083.72 \text{ kN}$$

$$N_{cr,z} = \frac{\pi^2 EI_z}{L_{cr,z}^2} = \frac{\pi^2 \times 210000 \times 737.24 \times 10^4}{4000^2} = 955 \times 10^3 \text{ N} = 955 \text{ kN}$$

$$\mu_y = \frac{1 - \frac{N_{Ed}}{N_{cr,y}}}{1 - \chi_y \frac{N_{Ed}}{N_{cr,y}}} = \frac{1 - \frac{44.82}{8083.72}}{1 - 0.978 \times \frac{44.82}{8083.72}} = 1.00$$

$$\mu_z = \frac{1 - \frac{N_{Ed}}{N_{cr,z}}}{1 - \chi_z \frac{N_{Ed}}{N_{cr,z}}} = \frac{1 - \frac{44.82}{955}}{1 - 0.692 \times \frac{44.82}{955}} = 0.985$$

$$C_{my} = C_{my,0} + (1 - C_{my,0}) \frac{\sqrt{\varepsilon_y} a_{LT}}{1 + \sqrt{\varepsilon_y} a_{LT}};$$

$$C_{mLT} = C_{my}^2 \frac{a_{LT}}{\sqrt{\left(1 - \frac{N_{Ed}}{N_{cr,z}}\right) \left(1 - \frac{N_{Ed}}{N_{cr,T}}\right)}}$$

$$C_{my,0} = 1 + 0.03 \frac{N_{Ed}}{N_{cr,y}} = 1 + 0.03 \times \frac{44.82}{8083.72} = 1.0002$$

$$\varepsilon_y = \frac{M_{y,Ed}}{N_{Ed}} \frac{A_{eff}}{W_{eff,y,min}} = \frac{68.95 \times 10^6}{44.82 \times 10^3} \times \frac{1982.26}{319968} = 9.53$$

$$a_{LT} = 1 - \frac{I_t}{I_y} = 1 - \frac{10254.8}{6240.4 \times 10^4} = 1$$

$$C_{my} = 1.0002 + (1 - 1.0002) \times \frac{\sqrt{9.53} \times 1}{1 + \sqrt{9.53} \times 1} = 1$$

$$C_{mLT} = 1^2 \times \frac{1}{\sqrt{\left(1 - \frac{44.82}{955}\right) \times \left(1 - \frac{44.82}{1206.96}\right)}} = 1.090$$

The interaction factors are:

$$k_{yy} = C_{my} C_{mLT} \frac{\mu_y}{1 - \frac{N_{Ed}}{N_{cr,y}}} = 1 \times 1.090 \times \frac{1}{1 - \frac{44.82}{8083.72}} = 1.096$$

$$k_{zy} = C_{my} C_{mLT} \frac{\mu_z}{1 - \frac{N_{Ed}}{N_{cr,y}}} = 1 \times 1.090 \times \frac{0.985}{1 - \frac{44.82}{8083.72}} = 1.080$$

Buckling resistance check

$$\begin{aligned} \frac{N_{Ed}}{\chi_y \frac{N_{Rk}}{\gamma_{M1}}} + k_{yy} \frac{M_{y,Ed} + \Delta M_{y,Ed}}{\chi_{LT} \frac{M_{y,Rk}}{\gamma_{M1}}} &= \\ = \frac{44.82}{0.978 \times \frac{693.7}{1.0}} + 1.096 \times \frac{68.95 + 0}{0.814 \times \frac{112}{1.0}} &= 0.895 < 1 \end{aligned} \quad \text{-- OK}$$

$$\begin{aligned} \frac{N_{Ed}}{\chi_z \frac{N_{Rk}}{\gamma_{M1}}} + k_{zy} \frac{M_{y,Ed} + \Delta M_{y,Ed}}{\chi_{LT} \frac{M_{y,Rk}}{\gamma_{M1}}} &= \\ = \frac{44.82}{0.692 \times \frac{693.7}{1.0}} + 1.080 \times \frac{68.95 + 0}{0.814 \times \frac{112}{1.0}} &= 0.910 < 1 \end{aligned} \quad \text{-- OK}$$

As an alternative, the interaction formula (4.99) may be used:

$$\left(\frac{N_{Ed}}{N_{b,Rd}} \right)^{0.8} + \left(\frac{M_{Ed}}{M_{b,Rd}} \right)^{0.8} \leq 1.0$$

$$\chi = \min(\chi_y, \chi_z, \chi_T) = \min(0.978; 0.692; 0.750) = 0.692$$

$$N_{b,Rd} = \frac{\chi A_{eff} f_y}{\gamma_{M1}} = \frac{0.692 \times 1982.26 \times 350}{1.00} = 480.10 \times 10^3 \text{ N} = 480.10 \text{ kN}$$

$$M_{b,Rd} = \chi_{LT} W_{eff,y} f_{yb} / \gamma_{M1} = 0.814 \times 319968 \times 10^{-9} \times 350 \times 10^3 / 1.0 = 91.16 \text{ kNm}$$

$$\left(\frac{N_{Ed}}{N_{b,Rd}} \right)^{0.8} + \left(\frac{M_{Ed}}{M_{b,Rd}} \right)^{0.8} = \left(\frac{44.82}{480.1} \right)^{0.8} + \left(\frac{68.95}{91.16} \right)^{0.8} = 0.950 \leq 1.0$$

4.5 BEAMS RESTRAINED BY SHEETING

4.5.1 General. Constructional detailing and static system

Purlins and side rails acting as secondary beams supported by primary beams (e.g. rafters) or columns are often restrained by the building envelope (e.g. trapezoidal sheeting, cassettes, sandwich panels, OSB panels, etc.). Similarly, floor joists are restrained by the dry floor deck or the reinforced concrete slab.

Currently, Z- and C-sections are used as purlins or rails which, due to their shapes can be sensitive to lateral-torsional buckling, so it is important to take advantage of sheeting, if effective. Figure 4.38 shows, schematically, the position of a Z-section purlin on a sloped roof, while Figure 4.49 presents the composition of a roof panel.

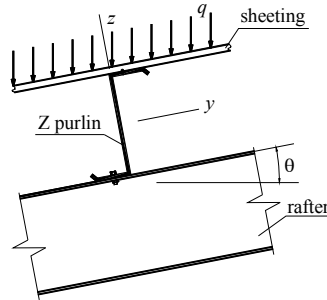


Figure 4.38 – Sloped Z-section roof system

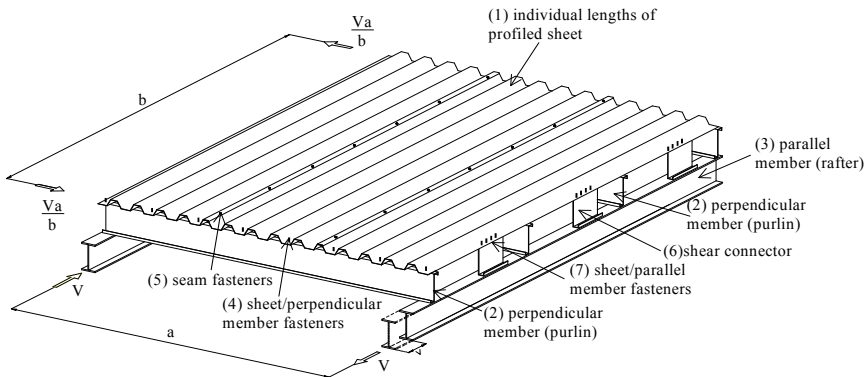


Figure 4.39 – Arrangement of an individual shear panel (ECCS, 1995)

Purlins can be connected to the rafter to restrain lateral-torsional and bearing deformations at the fixing point. Figure 4.40 (a, b, c) displays such connecting details.

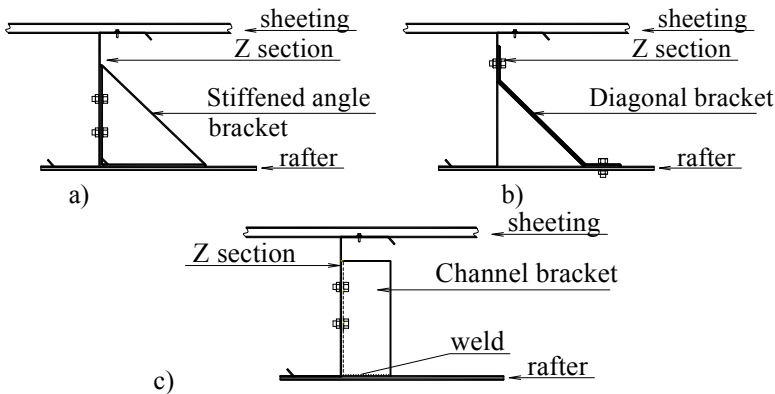


Figure 4.40 – Connecting details providing lateral-torsional restraint (details a) and b) from Seeka & Murray (2008))

In special cases, purlins can be fixed only through the bottom flange without supporting elements, as already shown in Figure 4.40. In such cases, the position of the purlins over the support (top flange of primary beam) shall be retained by placing steel bars as shown in Figure 4.41.

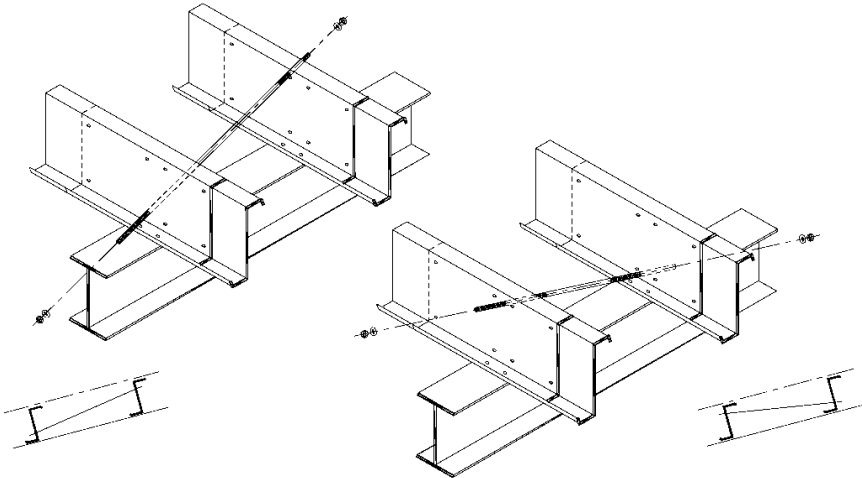


Figure 4.41 – Purlin directly fastened onto the top of primary beam (Lindab Systemline)

Sheeting is usually installed on the upper flange of purlins, and restrains the upper flange laterally (see Figure 4.42b). Since such a system can be subjected either to gravity or uplift loading, then either the upper or bottom flange can be in compression. The lateral-torsional buckling of purlins will be restrained for the case when the upper flange is in compression, only. Nevertheless, there are also cladding systems in which corrugated sheeting are installed on both upper and lower flanges of the purlins, and in that case, both lateral and torsional displacements can be prevented by sheeting, for both gravity and uplift loading (see Figure 4.42a).

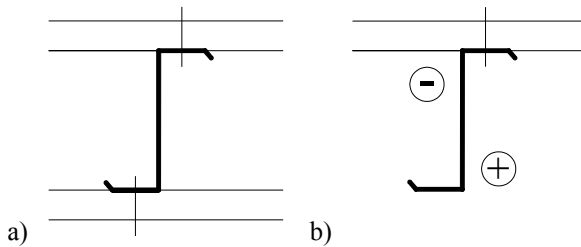


Figure 4.42 – Position of sheeting on purlin

The shape and sign of the bending moment diagram is depending not only on the type of loading, gravity or uplift, but also on the support conditions of the purlin, which can be simply supported or continuous over two or more spans. When it is continuous, the purlin may have uniform cross section in the span and over the support, or stepped cross sections, by overlapping the profiles over the supports. In the latter case, the Z-sections can be selected to adapt the purlin capacity to the moment variation along the member, and also to the transverse load demand at the supports.

Figure 4.43 shows typical support and overlapping arrangements for purlins. Z- and C- section fabricators usually offer design tables for such arrangements for various loading cases.

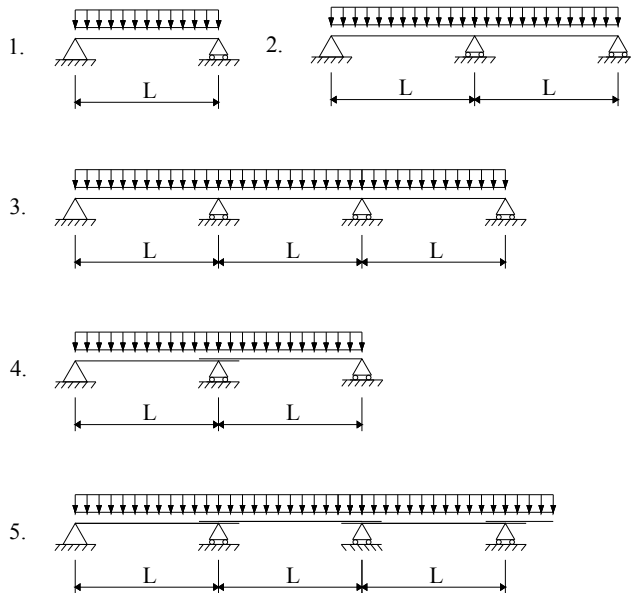


Figure 4.43 – Support and overlap arrangements for purlins

For an effective design, when spans are around 6.0 m to 7.0 m, continuous purlins are usually made with sections lapped and bolted at intermediate supports. Alternatively, double-sections can be used for strengthening the purlin at intermediate supports (see Figure 4.44).

As seen, sheeting itself can be used as a continuous restraint system to prevent lateral and torsional deformations of purlins. To be effective, such restraint systems must possess sufficient translational and rotational stiffness.

4. BEHAVIOUR AND DESIGN RESISTANCE OF BAR MEMBERS

When the restraint by sheeting is not fully effective, non-continuous or discrete lateral bracing devices, spaced along the purlins can be used. Figure 4.45 shows examples of such solutions, realised with tying rods. The distance between them will be obtained to limit, or avoid, the lateral-torsional buckling ($\bar{\lambda}_{LT} \leq 0.4$) of the purlin.

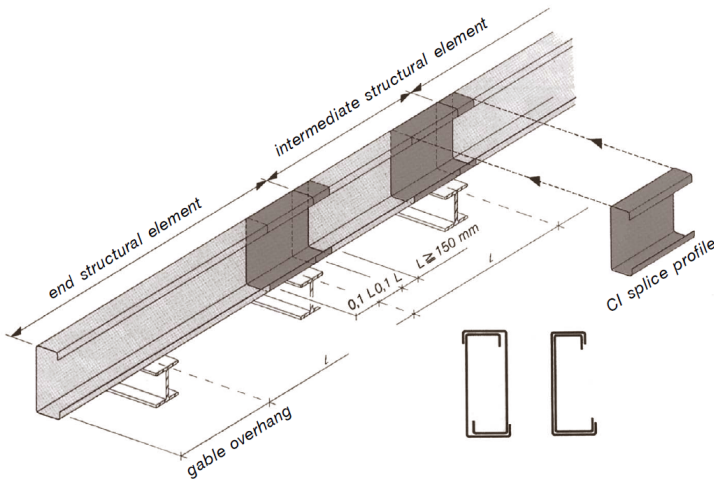
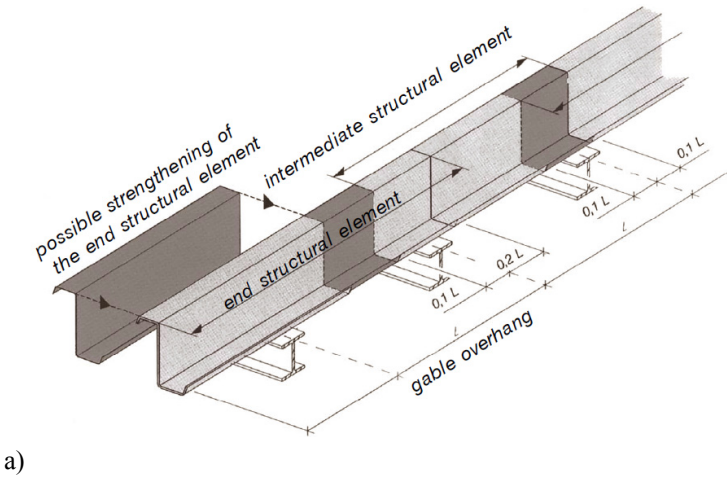


Figure 4.44 – Double-sections or splices of Z- and C-purlins or rails (Lindab Systemline)

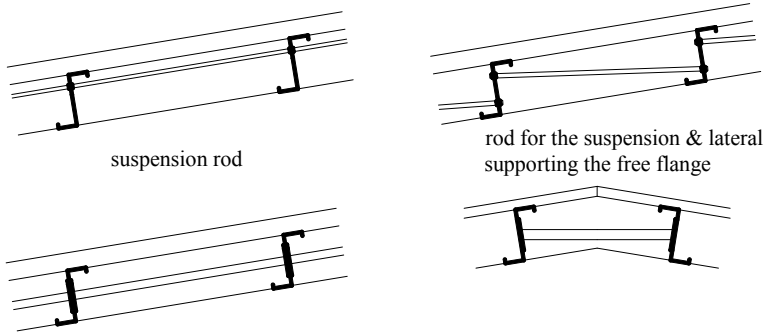


Figure 4.45 – Discrete tie-bracing system (Lindab Systemline)

4.5.2 Modelling of beam-sheeting interaction

The restraining effect of sheeting has to be considered for an effective design of purlin-sheeting systems. It is generally assumed that the sheeting can provide the necessary in-plane stiffness and capacity to carry the component of the load in the plane of the sheeting (see Figure 4.46), while the purlin resists to normal component. In fact, the sheeting may provide not only lateral restraint but can also partially restrain the twisting of purlins, taking account of the flexural stiffness of the sheeting if substantial (e.g. as for trapezoidal sheeting) and properly connected to the purlin.

According to EN1993-1-3, if trapezoidal sheeting is connected to a purlin and the condition expressed by the eqn. (4.71) is met, the purlin at the connection may be regarded as being laterally restrained in the plane of the sheeting:

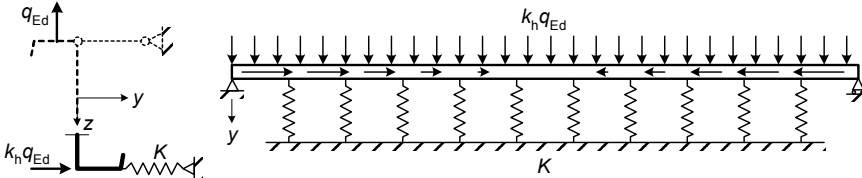
$$S \geq \left(EI_w \frac{\pi^2}{L^2} + GI_t + EI_z \frac{\pi^2}{L^2} 0.25 h^2 \right) \frac{70}{h^2} \quad (4.72)$$

where

- S is the portion of the shear stiffness provided by the sheeting for the examined member connected to the sheeting at each rib. If the sheeting is connected to a purlin every second rib only, then S should be replaced by $0.20 S$;
- I_w is the warping constant of the purlin;
- I_t is the torsion constant of the purlin;
- I_z is the second moment of area of the cross section about the minor axis of the cross section of the purlin;

4. BEHAVIOUR AND DESIGN RESISTANCE OF BAR MEMBERS

- L is the span of the purlin;
- h is the height of the purlin.



As a simplification replace the rotational spring C_D by a lateral spring of stiffness K

Free flange of purlin modelled as a beam on an elastic foundation. Model representing effect of torsion and lateral bending (including cross section distortion) on single span under with uplift loading

Figure 4.46 – Modelling laterally braced purlins rotationally restrained by sheeting

To evaluate the restraining effect of sheeting, in EN1993-1-3 the free flange is considered as a beam on an elastic foundation, as shown in Figure 4.46, where q_{Ed} is the vertical load, K is the stiffness of an equivalent lateral linear spring and k_h is the equivalent lateral load factor.

The equivalent lateral spring stiffness for the strength and stability check is obtained by a combination of:

1. Rotational stiffness of the connection between the sheeting and the purlin C_D , (see Figure 4.47);

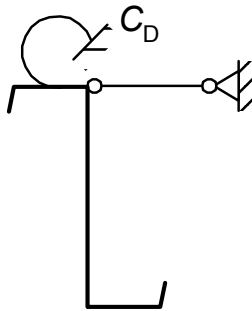


Figure 4.47 – Torsional and lateral restraining of purlin by sheeting

2. Distortion of the cross section of the purlin, K_B , as shown in Figure 4.48;
3. Bending stiffness of the sheeting, $C_{D,C}$, perpendicular to the span of the purlin (see Figure 4.49).

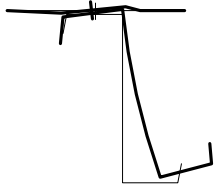


Figure 4.48 – Distortion of purlin

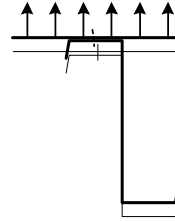


Figure 4.49 – Bending of the purlin

The composed distortion-torsion-bending effect is shown in Figure 4.50.

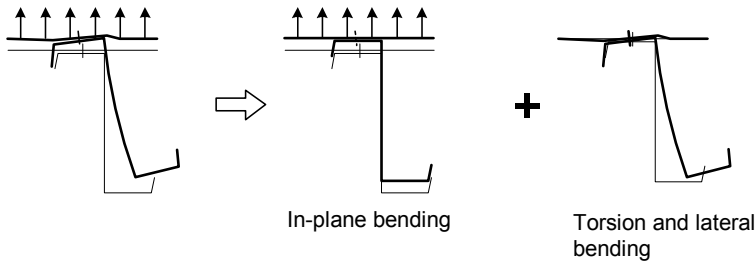


Figure 4.50 – Deformation of purlin restrained by sheeting

According to EN1993-1-3, the partial torsional restraint may be represented by a rotational spring with a spring stiffness C_D , which can be calculated based on the stiffness of the sheeting and the connection between the sheeting and the purlin, as follows,

$$\frac{1}{C_D} = \frac{1}{C_{D,A}} + \frac{1}{C_{D,C}} \quad (4.73)$$

where

$C_{D,A}$ is the rotational stiffness of the connection between the sheeting and the purlin;

$C_{D,C}$ is the rotational stiffness corresponding to the flexural stiffness of the sheeting.

Both $C_{D,A}$ and $C_{D,C}$ are specified in Section 10.1.5 of EN1993-1-3. Alternatively, the $C_{D,A}$ stiffness and $C_{D,C}$ stiffness values can be obtained experimentally applying the recommendation in Annex A5 of EN1993-1-3.

The model presented above can be also used for other types of claddings. For instance, Figure 4.51 shows the model adopted to represent the sandwich panel-purlin interaction.

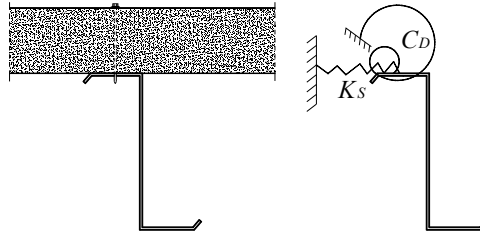


Figure 4.51 – Model adopted for sandwich panel – purlin interaction (Davies, 2001)

The restraints of the sheeting to the purlin have important influence on the buckling behaviour of the purlin. Figure 4.52 shows the buckling curves of a simply supported Z-purlin beam ($h=202$ mm, $b=75$ mm, $c=20$ mm and $t=2.3$ mm) with various different lateral restraints applied at the junction between the web and the compression flange when subjected to pure bending (Martin & Purkiss, 2008). One observes that, when the translational displacement of the compression flange is restrained, the purlin does not buckle lateral-torsionally, while when the rotation of the compression flange is restrained, the critical stresses of the local buckling and distortional buckling modes are increased significantly.

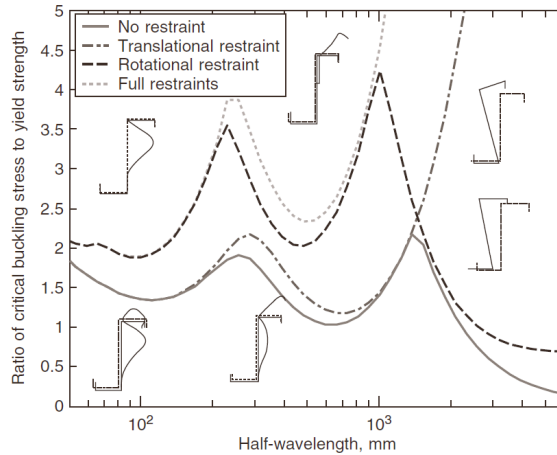


Figure 4.52 – Buckling curves of a simply supported zed section beam with different restraint applied at the junction between web and compression flange subjected to pure bending ($h=202$ mm, $b=75$ mm, $c=20$ mm, $t=2.3$ mm) (Martin & Purkiss, 2008)

However, when the restraints are applied at the junction between the web and the tension flange, it is only the rotational restraint that influences the lateral–torsional buckling of the purlin (see Figure 4.53).

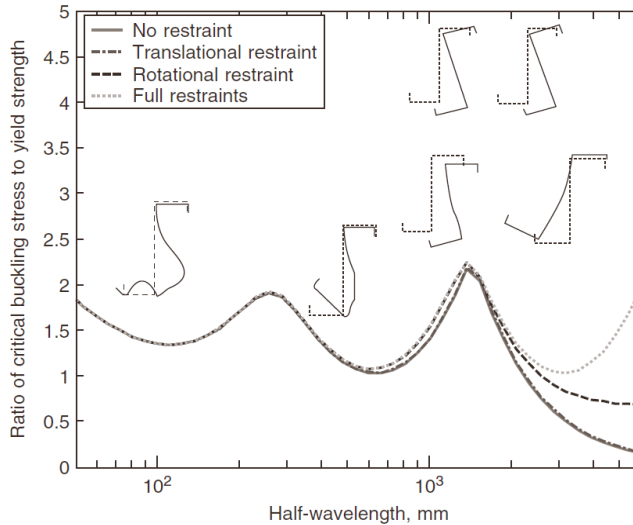


Figure 4.53 – Buckling curves of a simply supported zed section beam with different restraint applied at the junction between web and tension flange subjected to pure bending ($h=202$ mm, $b=75$ mm, $c=20$ mm, $t=2.3$ mm) (Martin & Purkiss, 2008)

4.5.3 Design of beams restrained by sheeting according to EN1993-1-3

The provisions given in this paragraph (and Section 10.1 of EN1993-1-3) may be applied to purlins of Z , C , Σ , U and Hat cross section with $h/t < 233$, $c/t \leq 20$ for single fold lips and $d/t \leq 20$ for double edge fold lips. Other limits are possible if verified by testing according to Annex A of EN1993-1-3.

These provisions may be used for structural systems of purlins with anti-sag bars, continuous, sleeved and overlapped systems. These provisions may also be applied to cold-formed members used as side rails, floor beams and other similar types of beam that are similarly restrained by sheeting.

Full continuous lateral restraint may be supplied by trapezoidal steel sheeting or other profiled steel sheeting with sufficient stiffness, continuously connected to the flange of the purlin through the troughs of the

sheets. The purlin at the connection to trapezoidal sheeting may be regarded as laterally restrained, if eqn. (4.72) is fulfilled. In other cases (for example, fastening through the crests of the sheets) the degree of restraint should either be validated by experience, or determined from tests.

The connection of the purlin to the sheeting may be assumed to partially restrain the twisting of the purlin. This partial torsional restraint may be represented by a rotational spring with a spring stiffness C_D (see Figure 4.47). The stresses in the free flange, not directly connected to the sheeting, should then be calculated by superposing the effects of in-plane bending and the effects of torsion, including lateral bending due to cross sectional distortion.

In order to take into account of the tendency of the free flange to move laterally, which induces additional stresses, the method given in §§4.5.3.1 and §§4.5.3.2 should be used, by treating the lateral movement as a beam subject to a lateral load $q_{h,Ed}$ (see Figure 4.46). In this method the rotational spring should be replaced by an equivalent lateral linear spring of stiffness K . In determining K , the effects of cross sectional distortion should also be considered. For this purpose, the free flange may be treated as a compression member subject to a non-uniform axial force, with a continuous lateral spring support of stiffness K .

4.5.3.1 Design criteria

334

In case of single span purlins, under gravity loading, the criteria for cross section resistance should be satisfied. If subject to axial compression, the purlin should also satisfy the criteria for stability of the free flange. For uplift loading, the purlin should satisfy the criteria for cross section resistance and the criteria for stability of the free flange.

In case of two-span continuous purlins, which are continuous over two spans without overlaps or sleeves, under gravity loads, the moments may either be obtained by calculation or based on the results of tests. If the moments are calculated they should be determined using elastic global analysis. The purlin should satisfy the criteria for cross section resistance. For the moment at the internal support, the criteria for buckling of the free flange should also be satisfied. At internal supports, the purlins should be checked for combined bending moment and support reaction (web crippling

if cleats are not used) and for combined bending moment and shear force depending on the case under consideration.

The moments due to uplift loading in a purlin that is continuous over two spans without overlaps or sleeves should be determined using elastic global analysis. The moment over the internal support should satisfy the criteria for cross section resistance. Because the support reaction is a tensile force, no account need be taken of its interaction with the support moment. The internal support should also be checked for interaction of bending moment and shear forces. The moments in the spans should satisfy the criteria for stability of the free flange.

In case of purlins with semi-continuity given by overlaps or sleeves, the moments should be determined taking into account the effective section properties of the cross section and the effects of overlaps or sleeves. Tests may be carried out to determine:

- the flexural stiffness of the overlapped or sleeved part;
- the moment-rotation characteristic for the overlapped or sleeved part;
- the resistance of the overlapped or sleeved part to combined support reaction and moment;
- the resistance of the non-overlapped unsleeved part to combined shear force and bending moment.

Figure 4.54 presents an analysis model that accounts for the flexural stiffness of overlaps.

For gravity loading, the purlin should satisfy the following criteria:

- at internal supports, the resistance to combined support reaction and moment;
- near supports, the resistance to combined shear force and bending moment;
- in the spans, the criteria for cross section resistance;
- if the purlin is subject to axial compression, the criteria for stability of the free flange.

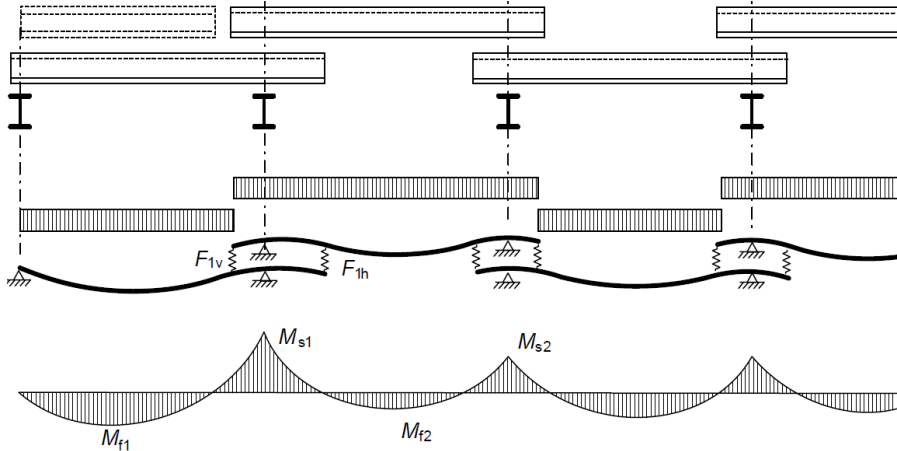


Figure 4.54 – Purlins with overlaps – model to consider the flexural stiffness of lapped joints

For uplift loading, the purlin should satisfy the following criteria:

- at internal supports, the resistance to combined support reaction and moment, taking into account the fact that the support reaction is a tensile force in this case;
- near supports, the resistance to combined shear force and bending moment;
- in the spans, the criteria for stability of the free flange;
- if the purlin is subjected to axial compression, the criteria for stability of the free flange.

The serviceability criteria relevant to purlins should also be satisfied.

4.5.3.2 Design resistance

Resistance of cross sections

For a purlin subjected to axial force and transverse load the resistance of the cross section should be verified as shown in Figure 4.55 by superposing the stresses due to:

- the in-plane bending moment $M_{y,Ed}$;
- the axial force N_{Ed} ;
- an equivalent lateral load $q_{h,Ed}$ acting on the free flange, due to torsion and lateral bending.

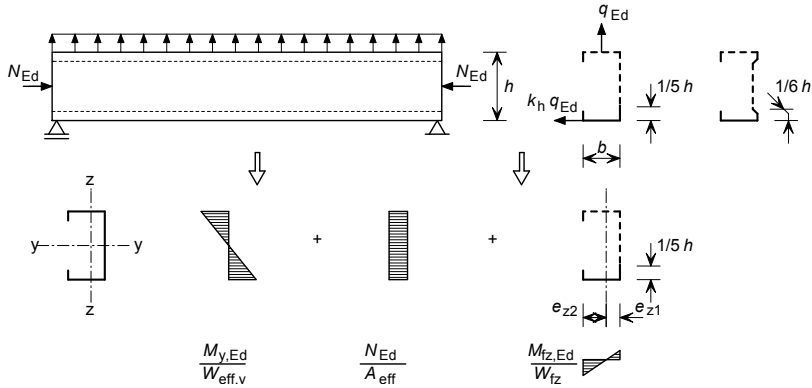


Figure 4.55 – Superposition of stresses

The maximum stresses in the cross section should satisfy the following:

- restrained flange:
$$\sigma_{max,Ed} = \frac{M_{y,Ed}}{W_{eff,y}} + \frac{N_{Ed}}{A_{eff}} \leq f_y / \gamma_M \quad (4.74)$$

- free flange:
$$\sigma_{max,Ed} = \frac{M_{y,Ed}}{W_{eff,y}} + \frac{N_{Ed}}{A_{eff}} + \frac{M_{fz,Ed}}{W_{fz}} \leq f_y / \gamma_M \quad (4.75)$$

where

A_{eff} is the effective area of the cross section for uniform compression;

f_y is the yield strength;

$M_{fz,Ed}$ is the bending moment in the free flange due to the lateral load $q_{h,Ed}$;

$W_{eff,y}$ is the effective section modulus of the cross section for bending about the y - y axis;

W_{fz} is the gross elastic section modulus of the free flange plus the contributing part of the web for bending about the z - z axis; the contributing part of the web may be taken equal to 1/5 of the web height from the point of web-flange intersection in case of C- and Z-sections and 1/6 of the web height in case of Σ -section, as shown in Figure 4.55;

and $\gamma_M = \gamma_{M0}$ if $A_{eff} = A_g$ or if $W_{eff,y} = W_{el,y}$ and $N_{Ed} = 0$, otherwise $\gamma_M = \gamma_{M1}$.

4. BEHAVIOUR AND DESIGN RESISTANCE OF BAR MEMBERS

The equivalent lateral load $q_{h,Ed}$ acting on the free flange, due to torsion and lateral bending, should be obtained from:

$$q_{h,Ed} = k_h q_{Ed} \tag{4.76}$$

The coefficient k_h should be obtained as shown in Figure 4.56, for common types of cross section.

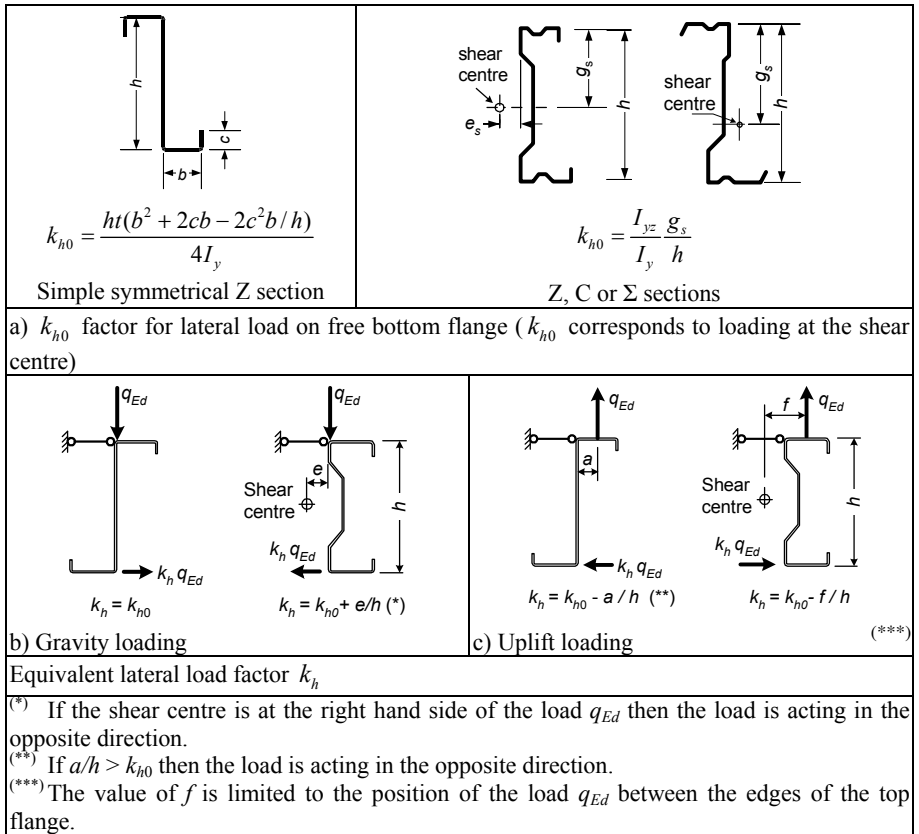


Figure 4.56 – Conversion of torsion and lateral bending into an equivalent lateral load

The lateral bending moment $M_{fz,Ed}$ may be determined from eqn. (4.77) except for a beam with the free flange in tension, where, due to positive influence of flange curling and second order effects, the moment $M_{fz,Ed}$ may be taken equal to zero:

$$M_{fz,Ed} = \kappa_R M_{0,fz,Ed} \tag{4.77}$$

where

$M_{0,fz,Ed}$ is the initial lateral bending moment in the free flange without any spring support;

κ_R is a correction factor for the effective spring support.

The initial lateral bending moment in the free flange $M_{0,fz,Ed}$ may be determined from Table 4.12 for the critical locations in the span, at supports, at anti-sag bars and between anti-sag bars. The validity of the Table 4.12 is limited to the range $R \leq 40$, where the value of the coefficient R of the spring supports is given by:

$$R = \frac{K L_a^4}{\pi^4 E I_{fz}} \tag{4.78}$$

where

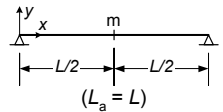
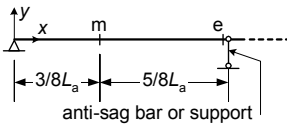
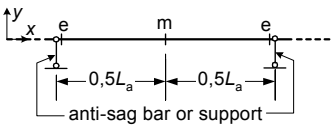
I_{fz} is the second moment of area of the gross cross section of the free flange plus the contributing part of the web for bending about the $z-z$ axis (see Figure 4.55);

K is the lateral spring stiffness per unit length;

L_a is the distance between anti-sag bars, or if none are present, the span L of the purlin.

The correction factor κ_R for the relevant location and boundary conditions, may be determined also from Table 4.12.

Table 4.12 – Values of initial moment $M_{0,fz,Ed}$ and correction factor κ_R

System	Location	$M_{0,fz,Ed}$	κ_R
	m	$\frac{1}{8} q_{h,Ed} L_a^2$	$\kappa_R = \frac{1 - 0.0225R}{1 + 1.013R}$
	m	$\frac{9}{128} q_{h,Ed} L_a^2$	$\kappa_R = \frac{1 - 0.0141R}{1 + 0.416R}$
	e	$-\frac{1}{8} q_{h,Ed} L_a^2$	$\kappa_R = \frac{1 + 0.0314R}{1 + 0.396R}$
	m	$\frac{1}{24} q_{h,Ed} L_a^2$	$\kappa_R = \frac{1 - 0.0125R}{1 + 0.198R}$
	e	$-\frac{1}{12} q_{h,Ed} L_a^2$	$\kappa_R = \frac{1 + 0.0178R}{1 + 0.191R}$

Buckling resistance of free flange

If the free flange is in compression, its buckling resistance should be verified using:

$$\frac{1}{\chi_{LT}} \left(\frac{M_{y,Ed}}{W_{eff,y}} + \frac{N_{Ed}}{A_{eff}} \right) + \frac{M_{fz,Ed}}{W_{fz}} \leq f_{yb} / \gamma_{M1} \quad (4.79)$$

in which χ_{LT} is the reduction factor for lateral-torsional buckling (flexural buckling of the free flange), using buckling curve *b* ($\alpha_{LT} = 0.34$; $\bar{\lambda}_{LT,0} = 0.4$; $\beta = 0.75$ according to §§6.3.2.3 of EN1993-1-1) for the relative slenderness $\bar{\lambda}_{fz}$.

The relative slenderness $\bar{\lambda}_{fz}$ for flexural buckling of the free flange should be determined from:

$$\bar{\lambda}_{fz} = \frac{l_{fz} / i_{fz}}{\lambda_1} \quad (4.80)$$

with $\lambda_1 = \pi \left[E / f_{yb} \right]^{0.5}$,

where

- l_{fz} is the buckling length for the free flange;
- i_{fz} is the radius of gyration of the gross cross section of the free flange plus the contributing part of the web for bending about the *z-z* axis.

340

For gravity loading, provided that $0 \leq R \leq 200$, the buckling length of the free flange for a variation of the compressive stress over the length *L* as shown in Figure 4.57 may be obtained from:

$$l_{fz} = \eta_1 L_a \left(1 + \eta_2 R^{\eta_3} \right)^{\eta_4} \quad (4.81)$$

where

- L_a is the distance between anti-sag bars or, if none are present, the span *L* of the purlin;
- R is as given by eqn. (4.78);

and η_1 to η_4 are coefficients that depend on the number of anti-sag bars, as given in Table 4.13. Tables 4.13a and 4.13b are valid only for equal-span uniformly loaded beam systems without overlap or sleeve and with anti-sag bars that provide lateral rigid support for the free flange. The tables may be used for systems with sleeves and overlaps provided that the connection

system may be considered as fully continuous. In other cases the buckling length should be determined by more appropriate calculations.

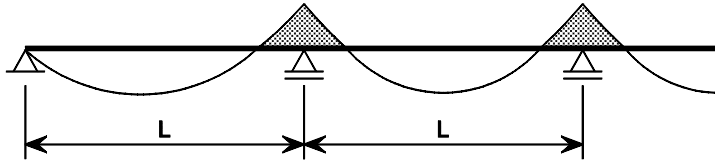


Figure 4.57 – Varying compressive stress in free flange for gravity load cases

Table 4.13a – Coefficients η_i for down load with 0, 1, 2, 3, 4 anti-sag bars

Situation	Anti-sag bar Number	η_1	η_2	η_3	η_4
End span	0	0.414	1.72	1.11	-0.178
Intermediate span		0.657	8.17	2.22	-0.107
End span	1	0.515	1.26	0.868	-0.242
Intermediate span		0.596	2.33	1.15	-0.192
End and intermediate span	2	0.596	2.33	1.15	-0.192
End and intermediate span	3 and 4	0.694	5.45	1.27	-0.168

Table 4.13b – Coefficients η_i for uplift load with 0, 1, 2, 3, 4 anti-sag bars

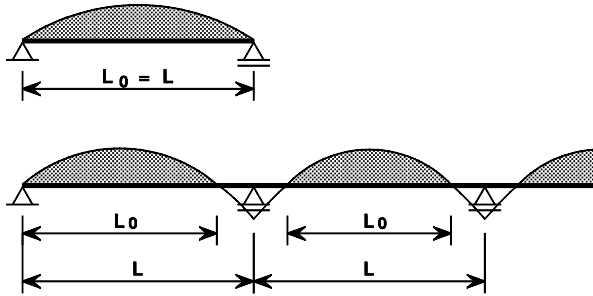
Situation	Anti-sag bar Number	η_1	η_2	η_3	η_4
Simple span	0	0.694	5.45	1.27	-0.168
End span		0.515	1.26	0.868	-0.242
Intermediate span	1	0.306	0.232	0.742	-0.279
Simple and end spans		0.800	6.75	1.49	-0.155
Intermediate span	2	0.515	1.26	0.868	-0.242
Simple span		0.902	8.55	2.18	-0.111
End and intermediate spans	3 and 4	0.800	6.75	1.49	-0.155
Simple and end spans		0.902	8.55	2.18	-0.111
Intermediate span		0.800	6.75	1.49	-0.155

For uplift loading, when anti-sag bars are not used, provided that $0 \leq R_0 \leq 200$, the buckling length of the free flange for variations of the compressive stress over the length L_0 as shown in Figure 4.58, may be obtained from:

$$l_{fc} = 0.7L_0 \left(1 + 13.1R_0^{1.6}\right)^{-0.125} \quad (4.82)$$

with:

$$R_0 = \frac{KL_0^4}{\pi^4 EI_{\bar{x}}} \tag{4.83}$$



[Dotted areas show regions in compression]

Figure 4.58 – Varying compressive stress in free flange for uplift cases

4.5.3.3 Rotational restraint given by the sheeting

The lateral spring support given to the free flange of the purlin by the sheeting should be modelled as a lateral spring acting at the free flange (see Figure 4.46). The total lateral spring stiffness K per unit length should be determined from:

$$\frac{1}{K} = \frac{1}{K_A} + \frac{1}{K_B} + \frac{1}{K_C} \tag{4.84}$$

where

- K_A is the lateral stiffness corresponding to the rotational stiffness of the joint between the sheeting and the purlin;
- K_B is the lateral stiffness due to distortion of the cross section of the purlin;
- K_C is the lateral stiffness due to the flexural stiffness of the sheeting.

Normally it may be assumed to be safe as well as acceptable to neglect $1/K_C$ because K_C is very large compared to K_A and K_B . The value of K should then be obtained from:

$$K = \frac{1}{\frac{1}{K_A} + \frac{1}{K_B}} \quad (4.85)$$

The value of $(1/K_A + 1/K_B)$ may be obtained either by testing or by calculation. Appropriate testing procedures are given in Annex A of EN1993-1-3.

The lateral spring stiffness K per unit length may be determined by calculation using:

$$\frac{1}{K} = \frac{4(1-\nu^2)h^2(h_d + b_{mod})}{Et^3} + \frac{h^2}{C_D} \quad (4.86)$$

in which the dimension b_{mod} is determined as follows:

- for cases where the equivalent lateral force $q_{h,Ed}$ brings the purlin into contact with the sheeting at the purlin web: $b_{mod} = a$;
- for cases where the equivalent lateral force $q_{h,Ed}$ brings the purlin into contact with the sheeting at the tip of the purlin flange: $b_{mod} = 2a + b$

where

- t is the thickness of the purlin;
- a is the distance from the sheet-to-purlin fastener to the purlin web as shown in Figure 4.59;
- b is the width of the purlin flange connected to the sheeting (see Figure 4.59);
- C_D is the total rotational spring stiffness;
- h is the overall height of the purlin;
- h_d is the developed height of the purlin web, see Figure 4.59.

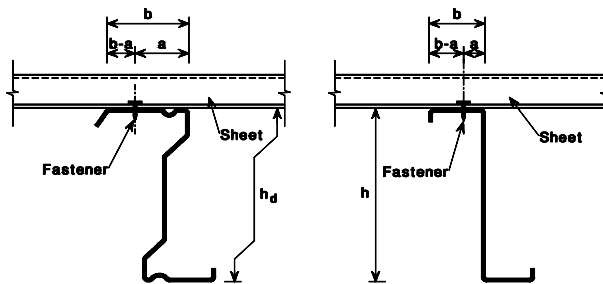
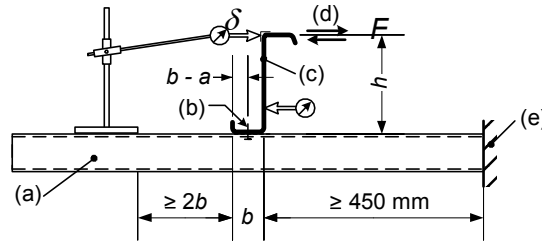


Figure 4.59 – Purlin and attached sheeting

The test set-up to determine $(1/K_A + 1/K_B)$, the amount of torsional restraint given by adequately fastened sheeting or by another member perpendicular to the span of the beam, is shown in Figure 4.60 (see also Annex A.5.3 of EN1993-1-3). This test set-up covers two different contributions to the total amount of restraint as follows:

- a) The lateral stiffness K_A per unit length corresponding to the rotational stiffness of the connection between the sheeting and the beam;
- b) The lateral stiffness K_B per unit length due to distortion of the cross section of the purlin.



a) sheeting, b) fastener, c) profile, d) load, e) clamped support

Figure 4.60 – Experimental determination of spring stiffness K_A and K_B

The combined restraint per unit length may be determined from:

$$(1/K_A + 1/K_B) = \delta / F \quad (4.87)$$

344

where

- F is the load per unit length of the test specimen to produce a lateral deflection of $h/10$;
- h is the overall depth of the specimen;
- δ is the lateral displacement of the top flange in the direction of the load F .

The rotational restraint given to the purlin by the sheeting should be modelled as a rotational spring acting at the top flange of the purlin (see Figure 4.47). The total rotational spring stiffness C_D should be determined from:

$$C_D = \frac{1}{(1/C_{D,A} + 1/C_{D,C})} \quad (4.88)$$

where

- $C_{D,A}$ is the rotational stiffness of the connection between the sheeting and the purlin;
- $C_{D,C}$ is the rotational stiffness corresponding to the flexural stiffness of the sheeting.

The value of $C_{D,C}$ may be taken as the minimum value obtained from calculation models of the type shown in Figure 4.61, taking account of the rotations of the adjacent purlins and the degree of continuity of the sheeting, using:

$$C_{D,C} = m / \theta \quad (4.89)$$

where

- m is the applied moment per unit width of sheeting, applied as indicated in Figure 4.61;
- θ is the resulting rotation, as indicated in Figure 4.61 [radians].

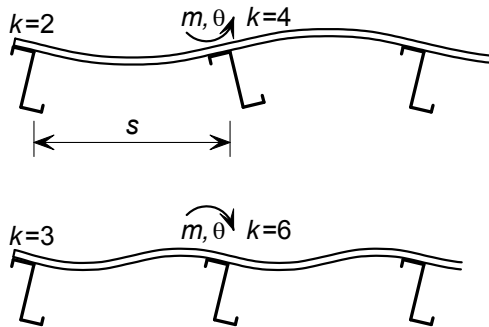


Figure 4.61 – Model for calculating $C_{D,C}$

Alternatively a conservative value of $C_{D,C}$ may be obtained from:

$$C_{D,C} = \frac{k E I_{eff}}{s} \quad (4.90)$$

in which k is a numerical coefficient, with values as follows:

- end, upper case of Figure 4.61 $k = 2$;
- end, lower case of Figure 4.61 $k = 3$;
- mid, upper case of Figure 4.61 $k = 4$;
- mid, lower case of Figure 4.61 $k = 6$;

where

- I_{eff} is the effective second moment of area per unit width of sheeting;
- s is the spacing of the purlins.

Generally $C_{D,A}$ may be calculated provided that the sheet-to-purlin fasteners are positioned centrally on the flange of the purlin. The value of $C_{D,A}$ for trapezoidal sheeting connected to the top flange of the purlin may be determined using clause 10.1.5.2(5) and Table 10.3 of EN1993-1-3.

Alternatively $C_{D,A}$ may be taken as equal to $130p$ [Nm/m/rad], where p is the number of sheet-to-purlin fasteners per metre length of purlin (but not more than one per rib of sheeting), provided that:

- the flange width b of the sheeting through which it is fastened does not exceed 120 mm;
- the nominal thickness t of the sheeting is at least 0.66 mm;
- the distance a or $b - a$ between the centreline of the fastener and the centre of rotation of the purlin (depending on the direction of rotation), as shown in Figure 4.59, is at least 25 mm.

If the effects of cross section distortion have to be taken into account it may be assumed to be realistic to neglect $C_{D,C}$, because the spring stiffness is mainly influenced by the value of $C_{D,A}$ and the cross section distortion.

346

Alternatively, values of $C_{D,A}$ may be obtained from a combination of testing and calculation. If the value of $(1/K_A + 1/K_B)$ is obtained by testing according to Annex A of EN1993-1-3 (in mm/N), the values of $C_{D,A}$ for gravity loading and for uplift loading should be determined from:

$$C_{D,A} = \frac{h^2 / l_A}{(1/K_A + 1/K_B) - 4(1 - \nu^2)h^2 (h_d + b_{mod}) / Et^3 l_B} \quad (4.91)$$

in which b_{mod} , h and h_d are as defined in eqn. (4.85) and l_A is the modular width of tested sheeting and l_B is the length of tested beam.

4.5.4 Simplified design of purlins

This method was proposed by Lindner (2003) and was included as an alternative design method in Annex E of EN1993-1-3.

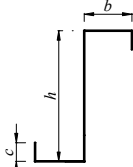
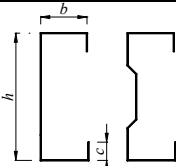
Purlins with C-, Z- and Σ -cross sections with or without additional stiffeners in web or flange may be designed as described in this clause if the following conditions are fulfilled:

- the cross section dimensions are within the range of Table 4.14;
- the purlins are horizontally restrained by trapezoidal sheeting where the horizontal restraint fulfils the condition of eqn. (4.72);
- the purlins are restrained rotationally by trapezoidal sheeting and the conditions of Table 4.14 are met;
- the purlins have equal spans and uniform loading.

This method should not be used:

- for systems using anti-sag bars;
- for sleeve or overlapping systems;
- for purlins subjected to axial forces N_{Ed} .

Table 4.14 – Limitations to be fulfilled if the simplified design method is used

Purlins	t [mm]	b/t	h/t	h/b	c/t	b/c	L/h
	≥ 1.25	≤ 55	≤ 160	≤ 3.43	≤ 20	≤ 4.0	≥ 15
	≥ 1.25	≤ 55	≤ 160	≤ 3.43	≤ 20	≤ 4.0	≥ 15

The design value of the bending moment M_{Ed} should satisfy:

$$\frac{M_{Ed}}{M_{LT,Rd}} \leq 1 \tag{4.92}$$

where

$$M_{LT,Rd} = \left(\frac{f_y}{\gamma_{M1}} \right) W_{eff,y} \frac{\chi_{LT}}{k_d} \tag{4.93}$$

and

$W_{eff,y}$ is the section modulus of the effective cross section with regard to the y - y axis;

χ_{LT} is the reduction factor for lateral-torsional buckling in terms of $\bar{\lambda}_{LT}$, where α_{LT} is substituted by $\alpha_{LT,eff}$;

and

$$\bar{\lambda}_{LT} = \sqrt{\frac{W_{eff,y} f_y}{M_{cr}}} \tag{4.94}$$

$$\alpha_{LT,eff} = \alpha_{LT} \sqrt{\frac{W_{el,y}}{W_{eff,y}}} \tag{4.95}$$

and

α_{LT} is the imperfection factor;
 $W_{el,y}$ is the section modulus of the gross cross section with regard to the y-y axis;
 k_d is a coefficient for consideration of the non-restrained part of the purlin;

$$k_d = \left(a_1 - a_2 \frac{L}{h} \right), \text{ but } k_d \geq 1 \tag{4.96}$$

a_1, a_2 coefficients defined in Table 4.15;
 L span of the purlin;
 h overall depth of the purlin.

Table 4.15 – Coefficients a_1, a_2 for eqn. (4.96)

System	Z-purlins		C-purlins		Σ-purlins	
	a_1	a_2	a_1	a_2	a_1	a_2
single span beam gravity load	1.0	0	1.1	0.002	1.1	0.002
single span beam uplift load	1.3	0	3.5	0.050	1.9	0.020
continuous beam gravity load	1.0	0	1.6	0.020	1.6	0.020
continuous beam uplift load	1.4	0.010	2.7	0.040	1.0	0

The reduction factor χ_{LT} may be determined from eqn. (4.97) for a single span purlins under gravity load or if eqn. (4.98) is met.

$$\chi_{LT} = 1.0 \tag{4.97}$$

$$C_D \geq \frac{M_{el,u}^2}{EI_v} k_\theta \tag{4.98}$$

where

$M_{el,u}$ is the elastic moment of the gross cross section with regard to the major u - u axis (see Figure 4.62);

$$M_{el,u} = W_{el,u} f_y \tag{4.99}$$

I_v is the moment of inertia of the gross cross section with regard to the minor v - v axis (see Figure 4.62);

k_θ is a factor for considering the static system of the purlin as per Table 4.16.

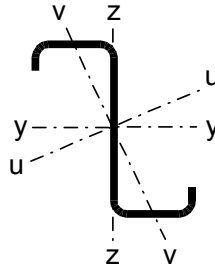


Figure 4.62 – Conventions used for cross section axes

For equal flanged C-purlins and Σ -purlins $I_v = I_z$, $W_u = W_z$, and $M_{el,u} = M_{el,y}$.

Table 4.16 – Factors k_θ

Static system	Gravity load	Uplift load
	-	0.210
	0.07	0.029
	0.15	0.066
	0.10	0.053

4. BEHAVIOUR AND DESIGN RESISTANCE OF BAR MEMBERS

In cases where eqns. (4.97) and (4.98) are not met, the reduction factor χ_{LT} should be calculated according to §§4.3.2.1 using $\bar{\lambda}_{LT}$ and $\alpha_{LT,eff}$. The elastic critical moment for lateral-torsional buckling M_{cr} may be calculated as follows:

$$M_{cr} = \frac{k}{L} \sqrt{G I_t^* E I_v} \tag{4.100}$$

where

I_t^* is the fictitious St. Venant torsion constant considering the effective rotational restraint by equation (4.101) and (4.102):

$$I_t^* = I_t + C_D \frac{L^2}{\pi^2 G} \tag{4.101}$$

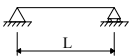

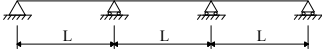
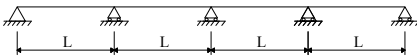
I_t is the St. Venant torsion constant of the purlin;

$$\frac{1}{C_D} = \frac{1}{C_{D,A}} + \frac{1}{C_{D,B}} + \frac{1}{C_{D,C}} \tag{4.102}$$

where

- $C_{D,A}, C_{D,C}$ rotational stiffnesses according to §§4.5.3.3;
- $C_{D,B}$ rotational stiffness due to distortion of the cross section of the purlin, $C_{D,B} = K_B h^2$, where h = depth of the purlin and K_B according to §§4.5.3.3;
- k lateral torsional buckling coefficient presented in Table 4.17.

Table 4.17 – Lateral-torsional buckling coefficients k for purlins restrained horizontally at the upper flange

Static system	Gravity load	Uplift load
	∞	10.3
	17.7	27.7
	12.2	18.3
	14.6	20.5
≥ 4 spans		

Example 4.5: This example presents the design at ULS of a two-span cold-formed steel Z-purlin with bolted lapped connections under vertical loads. The roof has a slope of 8° . The purlin is connected at the top flange by corrugated sheets, fixed with self-drilling screws, as shown in Figure 4.63. No contribution of the corrugated sheets was considered. In order to avoid the web crippling under support reaction, the purlin is assumed to be suspended on the cleats. Anti-sag bars are used in the middle of each span.

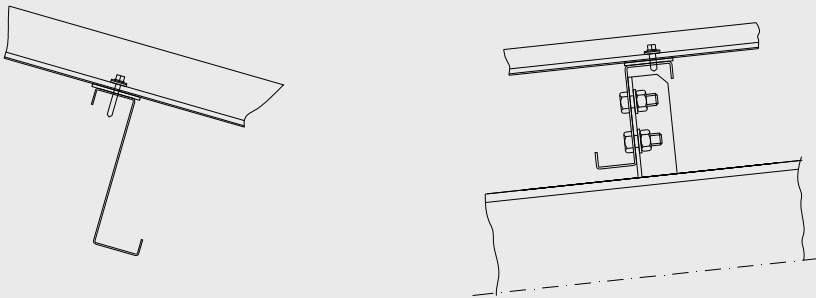


Figure 4.63 – Connection of corrugated sheets to the purlin using self-drilling screws

Basic Data

The static system is presented in Figure 4.64.

The distance between purlins is $s_p = 1200\text{mm}$.

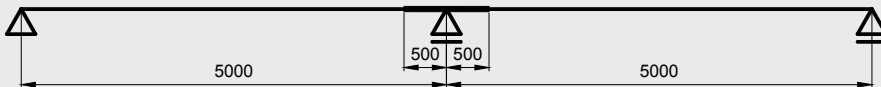


Figure 4.64 – Static system

The dimensions of the cross section and the material properties are:

Total height	$h = 200\text{ mm}$
Total width of flange 1	$b_1 = 74\text{ mm}$
Total width of flange 2	$b_2 = 66\text{ mm}$
Total width of edge fold	$c = 21.2\text{ mm}$
Internal radius	$r = 3\text{ mm}$
Nominal thickness	$t_{nom} = 1.5\text{ mm}$

Steel core thickness (§§2.4.2.3)	$t = 1.46 \text{ mm}$
Steel grade	S350GD+Z
Basic yield strength	$f_{yb} = 350 \text{ N/mm}^2$
Modulus of elasticity	$E = 210000 \text{ N/mm}^2$
Poisson's ratio	$\nu = 0.3$

The loads applied to the purlin:

Dead loads (G)

- self-weight of the purlin	0.05 kN/m^2
- self-weight of the top sheeting	0.05 kN/m^2
Total dead load	$q_G = 0.10 \text{ kN/m}^2$

Variable load

- snow load	$q_S = 1.2 \text{ kN/m}^2$
- wind load	$q_w = 0.3 \text{ kN/m}^2$

Partial factors $\gamma_{M0} = 1.0$ (§§2.3.1)

$$\gamma_{M1} = 1.0$$

$\gamma_G = 1.35$ – permanent loads (§§2.3.1, Table 2.3)

$\gamma_Q = 1.50$ – variable loads

Applied loading on the purlin at ULS (§§2.3.1, Flowchart 2.1)

Gravity loading

$$q_d = \gamma_G q_G + \gamma_q q_S = 1.35 \cdot 0.1 \cdot 1.2 + 1.5 \cdot 1.2 \cdot 1.2 \cos 8^\circ = 2.3 \text{ kN/m}$$

Load component normal to the roof:

$$q_d \cdot \cos \alpha = 2.3 \cdot \cos 8^\circ = 2.28 \text{ kN/m}$$

Load component in the sheeting plane:

$$q_d \cdot \sin \alpha = 2.3 \cdot \sin 8^\circ = 0.32 \text{ kN/m}$$

Uplift loading

Normal to the roof:

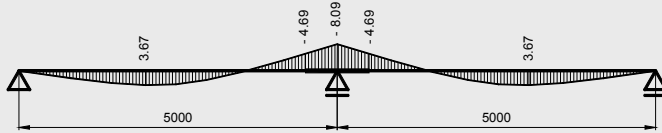
$$q_w = \gamma_G q_G + \gamma_w q_w = 1.35 \cdot 0.1 \cdot 1.20 \cdot \cos 8^\circ - 1.5 \cdot 0.3 \cdot 1.20 = -0.38 \text{ kN/m}$$

Load in the sheeting plane:

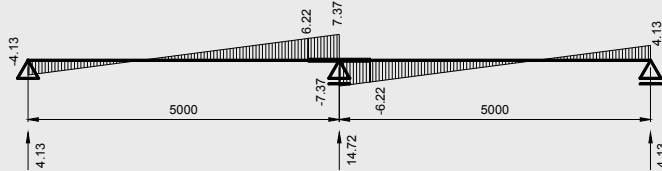
$$q_w = \gamma_G q_G \cos \alpha = 1.35 \cdot 0.1 \cdot 1.20 \cdot \sin 8^\circ = 0.023 \text{ kN/m}$$

Internal forces for gravity loading

Bending moment diagram M_{Ed} [kNm]

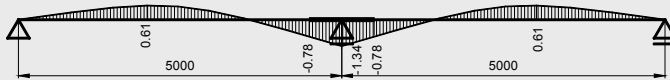


Shear force diagram V_{Ed} [kN]

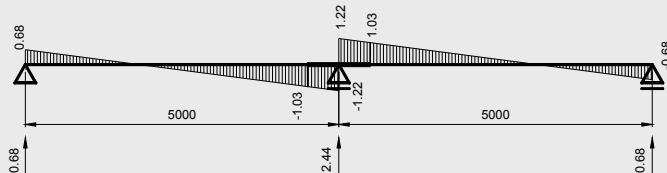


Internal forces for uplift loading

Bending moment diagram M_{Ed} [kNm]



Shear force diagram V_{Ed} [kN]



Effective section properties at the ultimate limit state (§§3.7.3, Flowchart 3.1 and Flowchart 3.2)

The properties of effective cross section were calculated following the procedures presented in Example 3.1 in Chapter 3.

Second moment of area, for flange $b_1 = 74$ mm in compression:

$$I_{eff,y} = 2689910 \text{ mm}^4$$

- with respect to the flange in compression:

$$W_{eff,y,c} = \frac{I_{eff,y}}{z_c} = 23752 \text{ mm}^3$$

- with respect to the flange in tension:

$$W_{eff,y,t} = \frac{I_{eff,y}}{z_t} = 31553 \text{ mm}^3$$

Second moment of area, for flange $b_2 = 66$ mm in compression:

$$I_{eff,y} = 2786025 \text{ mm}^4$$

- with respect to the flange in compression:

$$W_{eff,y,c} = \frac{I_{eff,y}}{z_c} = 24169 \text{ mm}^3$$

- with respect to the flange in tension:

$$W_{eff,y,t} = \frac{I_{eff,y}}{z_t} = 33475 \text{ mm}^3$$

$$W_{eff,y} = \min(W_{eff,y,c}, W_{eff,y,t}) = 23752 \text{ mm}^3$$

Gravity loading

For gravity loading, the purlin should satisfy the following criteria:

- in the spans, the criteria for cross section resistance;
- near supports, the resistance to combined shear force and bending moment;
- at internal supports, the resistance to combined support reaction and moment.

Check of bending resistance at ULS

Design moment resistance for span (§§3.8.4, eqn. (3.83), Flowchart 3.6):

$$M_{c,Rd} = W_{eff,y} f_{yb} / \gamma_{M0} = 23752 \times 350 / 1.0 = 8313200 \text{ Nmm} = 8.31 \text{ kNm}$$

Verification of bending resistance (§§3.8.4, eqn. (3.82), Flowchart 3.6):

- check of span $\frac{M_{Ed1}}{M_{c,Rd}} = \frac{3.67}{8.31} = 0.442 < 1 - \text{OK}$

Stability check for the gravity loading case

Gross properties of the free flange (a $1/5^{\text{th}}$ part of the purlin web is considered according to (§§4.5.3.2, Figure 4.55).

At the end of overlap

$$A_{fz} = \left(\frac{h}{5} + b_2 + c \right) t = \left(\frac{200}{5} + 66 + 21.2 \right) 1.46 = 185.71 \text{ mm}^2$$

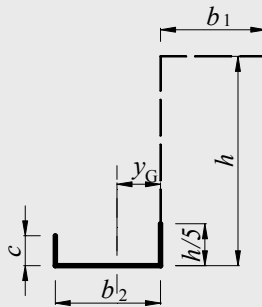
$$y_G = 28.12 \text{ mm}; \quad b_2 - y_G = 66 - 28.12 = 37.88 \text{ mm}$$

$$I_{fz} = \frac{h/5 \cdot t^3}{12} + \frac{t \cdot b_2^3}{12} + \frac{c \cdot t^3}{12} + y_G^2 \left(\frac{h}{5} t \right) + \left(\frac{b_2}{2} - y_G \right)^2 (b_2 t) + (b_2 - y_G)^2 (c \cdot t)$$

$$I_{fz} = 127881.05 \text{ mm}^4$$

$$W_{fz} = \frac{I_{fz}}{b_2 - y_G} = 3375.2 \text{ mm}^3$$

$$i_{fz} = \sqrt{\frac{I_{fz}}{A_{fz}}} = 26.24 \text{ mm}$$



Free flange identification

At the intermediate support

$$A_{fz} = \left(\frac{h}{5} + b_2 + c\right)t + \left(\frac{h}{5} + b_1 + c\right)t =$$

$$= \left(\frac{200}{5} + 66 + 21.2\right)1.46 + \left(\frac{200}{5} + 74 + 21.2\right)1.46 = 383.104\text{mm}^2$$

$$y_G = 31.4\text{mm}, \quad b_2 - y_G = 74 - 31.4 = 42.6\text{mm}$$

$$I_{fz} = 294296.95\text{mm}^4$$

$$W_{fz} = 6908.4\text{mm}^3$$

$$i_{fz} = 27.72\text{mm}$$

Lateral bending

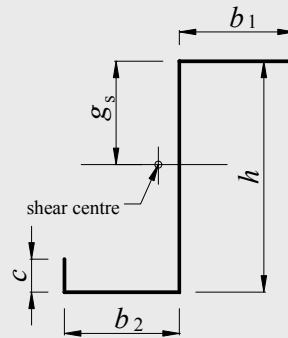
Lateral load

$$k_{h0} = \frac{I_{yz}}{I_y} \frac{g_s}{h} = \frac{1101451.60}{3307851} \cdot \frac{97.89}{200} = 0.163$$

(see Figure 4.56, where $b_1 \neq b_2$)

$$k_h = k_{h0}$$

$$q_{h,d} = k_h q_d = 0.163 \cdot 2.279 = 0.371\text{N/mm}$$



Spring support coefficient

At the end of overlap

$$\frac{1}{K} = \frac{4(1-\nu^2)h^2(h_d + b_{mod})}{Et^3} + \frac{h^2}{C_D} \Rightarrow K = 0.0091\text{N/mm/mm}$$

where

C_D is a rotational spring stiffness determined by testing:

$C_D = 700\text{ Nmm/mm}$ (determined by experimental tests according to clause A.5.3)

$$b_{mod} = a = 74/2 = 37\text{ mm.}$$

$$t = 1.46\text{mm}$$

$L_a = 2500$ mm (anti-sag bars are used in the middle of each span)

$$R = \frac{KL_a^4}{\pi^4 EI_{fz}} = \frac{0.0091 \cdot 2500^4}{\pi^4 \cdot 210000 \cdot 127881.05} = 0.136$$

$$k_R = \frac{1 + 0.0178 \cdot R}{1 + 0.191 \cdot R} = 0.977$$

$$M_{0fz,Ed} = -\frac{1}{12} q_{h,d} L_a^2 = -\frac{1}{12} \cdot 0.371 \cdot 2500^2 = -193229.2 \text{ Nmm}$$

$$M_{fzEd} = k_R M_{0fz,Ed} = -188785 \text{ Nmm}$$

Buckling length of the free flange in compression

$$l_{fz} = \eta_1 L_a \left(1 + \eta_2 R^{n_3}\right)^{\eta_4} = 0.515 \cdot 2500 \left(1 + 1.26 \cdot 0.136^{0.868}\right)^{-0.242}$$

$$= 1226 \text{ mm}$$

$$\lambda_1 = \pi \left(\frac{E}{f_{yb}}\right)^{0.5} = 76.95$$

Relative slenderness

$$\lambda_{fz} = \frac{l_{fz}/i_{fz}}{\lambda_1} = \frac{1226/26.24}{76.95} = 0.607$$

Buckling curve b: $\alpha_{LT} = 0.34$, $\lambda_{LT,0} = 0.4$, $\beta = 0.75$, $\lambda_{LT} = \lambda_{fz}$

$$\phi_{LT} = 0.5 \left[1 + \alpha_{LT} (\lambda_{LT} - \lambda_{LT,0}) + \beta \lambda_{LT}^2\right] =$$

$$= 0.5 \left[1 + 0.34 (0.607 - 0.4) + 0.75 \cdot 0.607^2\right] = 0.673$$

$$\chi_{LT} = \frac{1}{\phi_{LT} + \sqrt{\phi_{LT}^2 - \beta \lambda_{LT}^2}} = \frac{1}{0.673 + \sqrt{0.673^2 - 0.75 \cdot 0.607^2}} = 0.915$$

$$\frac{1}{\chi_{LT}} \frac{M_{yEd}}{W_{eff}} + \frac{M_{fz,Ed}}{W_{fz}} = \frac{1}{0.915} \frac{4.69 \cdot 10^6}{23752} + \frac{188785}{3375.95} =$$

$$= 271.72 \frac{\text{N}}{\text{mm}^2} < f_{yb} / \gamma_{M1} \quad \text{--- OK}$$

At intermediate support

$$\frac{1}{K} = \frac{4(1-\nu^2)h^2(h_d + b_{mod})}{Et^3} + \frac{h^2}{C_D} \Rightarrow K = 0.016 \text{ N/mm/mm}$$

where

$$C_D = 700 \text{ Nmm/mm}$$

$$b_{mod} = a = 74/2 = 37 \text{ mm.}$$

$$t = 2 \times 1.46 \text{ mm} = 2.92 \text{ mm}$$

$$L_a = 2500 \text{ mm}$$

$$R = \frac{KL_a^4}{\pi^4 EI_{fz}} = \frac{0.016 \cdot 2500^4}{\pi^4 \cdot 210000 \cdot 294296.95} = 0.104$$

$$k_R = \frac{1 + 0.0178 \cdot R}{1 + 0.191 \cdot R} = 0.982$$

$$M_{0fz,Ed} = -\frac{1}{12} q_{h,d} L_a^2 = -\frac{1}{12} \cdot 0.371 \cdot 2500^2 = -193229.2 \text{ Nmm}$$

$$M_{fz,Ed} = k_R M_{0fz,Ed} = -189751 \text{ Nmm}$$

$k_h = k_{h0} = 0.163$ (the same value at the intermediate support for the double cross section).

358

Buckling length of the free flange in compression

$$l_{fz} = \eta_1 L_a (1 + \eta_2 R^{\eta_3})^{\eta_4} = 0.515 \cdot 2500 (1 + 1.26 \cdot 0.104^{0.868})^{-0.242} = 1238 \text{ mm}$$

$$\lambda_1 = \pi \left(\frac{E}{f_{yb}} \right)^{0.5} = 76.95$$

Relative slenderness

$$\lambda_{fz} = \frac{l_{fz}/i_{fz}}{\lambda_1} = \frac{1238/27.72}{76.95} = 0.580$$

Buckling curve b: $\alpha_{LT} = 0.34$, $\lambda_{LT,0} = 0.4$, $\beta = 0.75$, $\lambda_{LT} = \lambda_{fz}$

$$\phi_{LT} = 0.5 \left[1 + \alpha_{LT} (\lambda_{LT} - \lambda_{LT,0}) + \beta \lambda_{LT}^2 \right] =$$

$$= 0.5 \left[1 + 0.34(0.580 - 0.4) + 0.75 \cdot 0.580^2 \right] = 0.657$$

$$\chi_{LT} = \frac{1}{\phi_{LT} + \sqrt{\phi_{LT}^2 - \beta \lambda_{LT}^2}} = \frac{1}{0.657 + \sqrt{0.657^2 - 0.75 \cdot 0.580^2}} = 0.926$$

$$\frac{1}{\chi_{LT}} \frac{M_{yEd}}{2W_{eff}} + \frac{M_{fz,Ed}}{W_{fz}} = \frac{1}{0.926} \frac{8.09 \cdot 10^6}{2 \cdot 23752} + \frac{189751}{6908.4} =$$

$$= 229.8 \frac{N}{mm^2} < f_{yb} / \gamma_{M1} \quad \text{— OK}$$

Check of shear resistance

Design shear resistance (§§3.8.5, eqn. (3.91))

$$V_{b,Rd} = \frac{\frac{h_w}{\sin \phi} f_{bv}}{\gamma_{M0}}$$

For a web without stiffening at the support:

$$f_{bv} = 0.58 f_{yb} \quad \text{if} \quad \bar{\lambda}_w \leq 0.83$$

$$f_{bv} = 0.48 f_{yb} / \bar{\lambda}_w \quad \text{if} \quad 0.83 < \bar{\lambda}_w < 1.40$$

$$f_{bv} = 0.67 f_{yb} / \bar{\lambda}_w^2 \quad \text{if} \quad \bar{\lambda}_w \geq 1.40$$

The relative slenderness $\bar{\lambda}_w$ for webs without longitudinal stiffeners:

$$\bar{\lambda}_w = 0.346 \frac{s_w}{t} \sqrt{\frac{f_{yb}}{E}} = 0.346 \times \frac{(200 - 1.5)}{1.46} \times \sqrt{\frac{350}{210000}} = 1.92$$

$$\bar{\lambda}_w = 1.92 > 1.40 \quad \text{so:}$$

$$f_{bv} = 0.67 f_{yb} / \bar{\lambda}_w^2 = 0.67 \times 350 / 1.92^2 = 63.61 \text{ N/mm}^2$$

$$V_{b,Rd} = \frac{\frac{(200 - 1.5)}{\sin 90^\circ} \times 1.46 \times 63.61}{1.0} = 18435 \text{ N} = 18.435 \text{ kN}$$

Verification of shear resistance (§§3.8.5, eqn. (3.90))

$$\text{— check at the end of overlap } \frac{V_{Ed1}}{V_{b,Rd}} = \frac{6.22}{18.435} = 0.337 < 1 \quad \text{— OK}$$

- check at the intermediate support $\frac{V_{Ed2}}{2V_{b,Rd}} = \frac{7.37}{2 \cdot 18.435} = 0.200 < 1$ – OK

Due to the fact that the shear force $V_{Ed} < 0.5 V_{b,Rd}$ no reduction due to shear force need be done.

Uplift loading

For uplift loading, the purlin should satisfy the following criteria:

- at internal supports, the resistance to combined support reaction and moment, taking into account the fact that the support reaction is a tensile force in this case;
- near supports, the resistance to combined shear force and bending moment;
- in the spans, the criteria for stability of the free flange.

Check of bending resistance at ULS

Design moment resistance at the end of overlap – single section (§§3.8.4, eqn. (3.83), Flowchart 3.6):

$$M_{c,Rd} = W_{eff,y} f_{yb} / \gamma_{M0} = 23752 \times 350 / 1.0 = 8313200 \text{ Nmm} = 8.31 \text{ kNm}$$

Design moment resistance for the intermediate support (§§3.8.4, eqn. (3.83), Flowchart 3.6):

$$M_{c,Rd} = 2W_{eff,y} f_{yb} / \gamma_{M0} = 2 \times 23752 \times 350 / 1.0 = 16627400 \text{ Nmm} = 16.63 \text{ kNm}$$

Verification of bending resistance (§§3.8.4, eqn. (3.82), Flowchart 3.6):

- check at the end of overlap $\frac{M_{Ed2}}{M_{c,Rd}} = \frac{0.78}{8.31} = 0.094 < 1$ – OK

- check at the intermediate support $\frac{M_{Ed3}}{M_{c,Rd}} = \frac{1.34}{16.63} = 0.081 < 1$ – OK

Verification of shear resistance (EN1993-1-1, §6.2.6(1))

- check at the end of overlap $\frac{V_{Ed1}}{V_{b,Rd}} = \frac{1.03}{18.435} = 0.06 < 1$ – OK

- check at the intermediate support $\frac{V_{Ed2}}{2V_{b,Rd}} = \frac{1.22}{2 \cdot 18.435} = 0.033 < 1$ – OK

Due to the fact that the shear force $V_{Ed} < 0.5 V_{b,Rd}$ no reduction due to shear force need be done.

Stability for the uplift loading case

Gross properties of the free flange (a 1/5th part of the purlin web is considered (§§4.5.3.2, Figure 4.55)

At the span

$$A_{fz} = \left(\frac{h}{5} + b_2 + c \right) t = \left(\frac{200}{5} + 66 + 21.2 \right) 1.46 = 185.71 \text{mm}^2$$

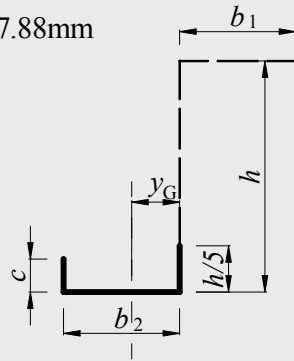
$$y_G = 28.12 \text{mm}; \quad b_2 - y_G = 66 - 28.12 = 37.88 \text{mm}$$

$$I_{fz} = \frac{h/5 \cdot t^3}{12} + \frac{t \cdot b_2^3}{12} + \frac{c \cdot t^3}{12} + y_G^2 \left(\frac{h}{5} t \right) + \left(\frac{b_2}{2} - y_G \right)^2 (b_2 t) + (b_2 - y_G)^2 (c \cdot t)$$

$$I_{fz} = 127881.05 \text{mm}^4$$

$$W_{fz} = \frac{I_{fz}}{b_2 - y_G} = 3375.2 \text{mm}^3$$

$$i_{fz} = \sqrt{\frac{I_{fz}}{A_{fz}}} = 26.24 \text{mm}$$



Free flange identification

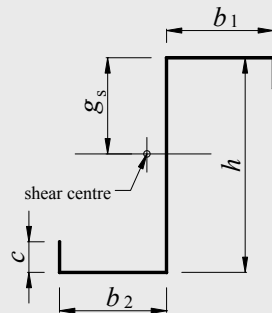
Lateral bending

Lateral load

$$k_{h0} = \frac{I_{yz}}{I_y} \frac{g_s}{h} = \frac{1101451.60}{3307851} \cdot \frac{97.89}{200} = 0.163$$

$$k_h = k_{h0} - a/h = 0.163 - 37/200 = 0.163 - 0.185 = -0.022$$

$$q_{h,d} = k_h q_d = -0.022 \cdot (-0.38) = 0.00836 \text{N/mm}$$



Spring support coefficient

$$\frac{1}{K} = \frac{4(1-\nu^2)h^2(h_d + b_{mod})}{Et^3} + \frac{h^2}{C_D} \Rightarrow K = 0.0074 \text{ N/mm/mm}$$

where

$$C_D = 700 \text{ Nmm/mm}$$

$$b_{mod} = 2a + b = 2 \times 74/2 + 74 = 148 \text{ mm.}$$

$$t = 1.46 \text{ mm}$$

$$R_0 = \frac{KL_a^4}{\pi^4 EI_{fz}} = \frac{0.0074 \cdot 2500^4}{\pi^4 \cdot 210000 \cdot 127881.05} = 0.111$$

$$k_R = \frac{1 + 0.0178R}{1 + 0.191R} = 0.981$$

$$M_{0fz,Ed} = \frac{1}{12} q_{h,w} L_a^2 = \frac{1}{12} \cdot 0.00836 \cdot 2500^2 = 4354 \text{ Nmm}$$

$$M_{fzEd} = k_R M_{0fz,Ed} = 0.981 \cdot 4354 = 4271 \text{ Nmm}$$

Buckling length of the free flange in compression

$$l_{fz} = 0.7L_0 \left(1 + 13.1R_0^{1.6}\right)^{-0.125} = 0.7 \cdot 2500 \left(1 + 13.1 \cdot 0.111^{1.6}\right)^{-0.125} = 1680 \text{ mm}$$

where $L_0 = 2500 \text{ mm}$.

$$\lambda_1 = \pi \left(\frac{E}{f_{yb}} \right)^{0.5} = 76.95$$

Relative slenderness

$$\lambda_{fz} = \frac{l_{fz}/i_{fz}}{\lambda_1} = \frac{1680/26.24}{76.95} = 0.832$$

Buckling curve b: $\alpha_{LT} = 0.34$, $\lambda_{LT,0} = 0.4$, $\beta = 0.75$, $\lambda_{LT} = \lambda_{fz}$

$$\begin{aligned} \phi_{LT} &= 0.5 \left[1 + \alpha_{LT} (\lambda_{LT} - \lambda_{LT,0}) + \beta \lambda_{LT}^2 \right] = \\ &= 0.5 \left[1 + 0.34 (0.832 - 0.4) + 0.75 \cdot 0.832^2 \right] = 0.833 \end{aligned}$$

$$\chi_{LT} = \frac{1}{\phi_{LT} + \sqrt{\phi_{LT}^2 - \beta \lambda_{LT}^2}} = \frac{1}{0.833 + \sqrt{0.833^2 - 0.75 \cdot 0.832^2}} = 0.799$$

$$\frac{1}{\chi_{LT}} \frac{M_{yEd}}{W_{eff}} + \frac{M_{fz,Ed}}{W_{fz}} = \frac{1}{0.799} \frac{0.61 \cdot 10^6}{23752} + \frac{4271}{3375.95} = 33.4 \frac{\text{N}}{\text{mm}^2} < f_{yb} / \gamma_{M1} \text{ -OK}$$

4.6 DESIGN OF BEAMS AT SERVICEABILITY LIMIT STATES

The rules for serviceability limit states given in Section 7 of EN1993-1-1 should also be applied to cold-formed members and sheeting.

The properties of the effective cross section for serviceability limit states should be used in all serviceability limit state calculations for cold-formed members and sheeting.

The second moment of area may be calculated alternatively by interpolation of gross cross section and effective cross section using the expression

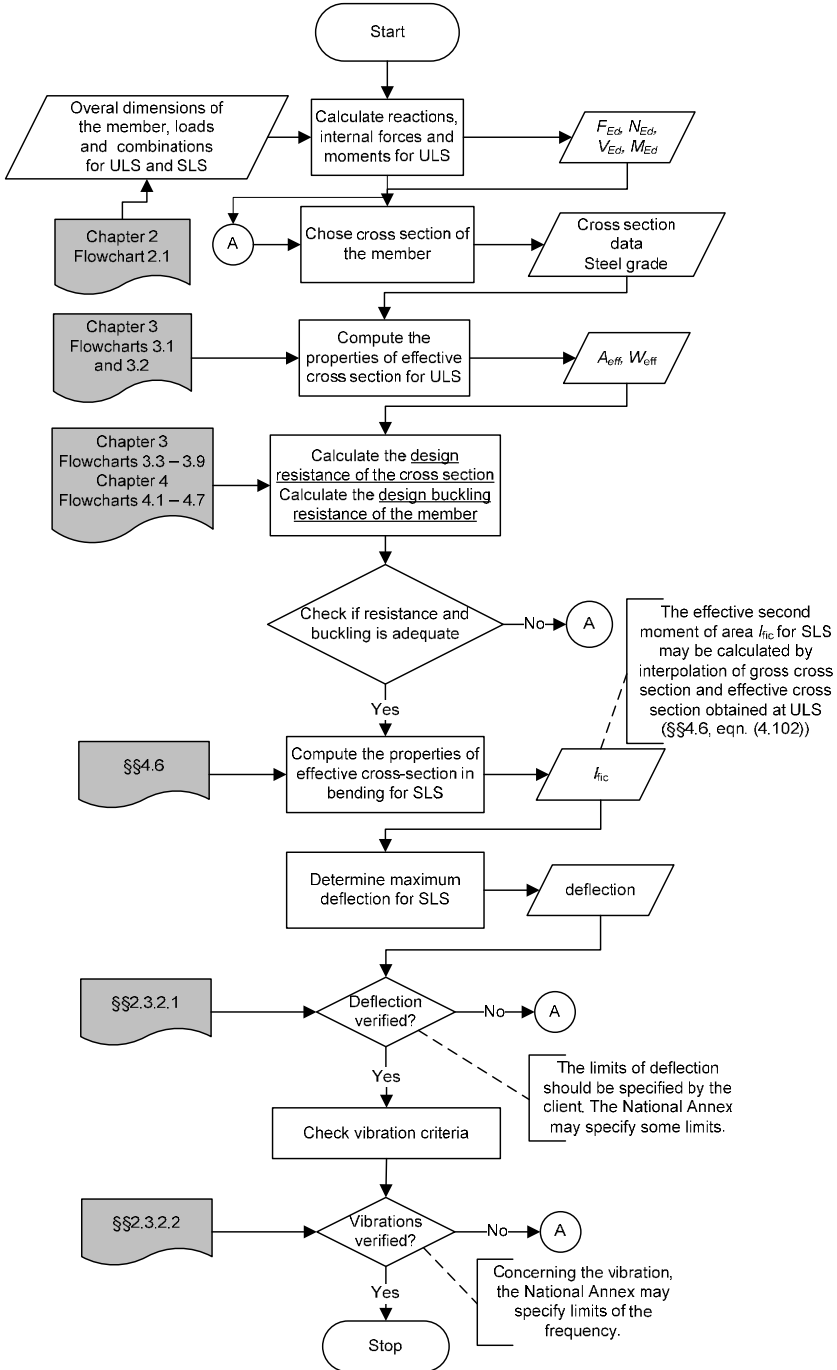
$$I_{fic} = I_{gr} - \frac{\sigma_{gr}}{\sigma} (I_{gr} - I(\sigma)_{eff}) \quad (4.103)$$

where

- I_{gr} is second moment of area of the gross cross section;
- σ_{gr} is maximum compressive bending stress in the serviceability limit state, based on the gross cross section (positive in formula);
- $I(\sigma)_{eff}$ is the second moment of area of the effective cross section with allowance for local buckling calculated for a maximum stress $\sigma \geq \sigma_{gr}$, in which the maximum stress is the largest absolute value of stress within the calculation length considered.

The effective second moment of area I_{eff} (or I_{fic}) may be taken as variable along the span. Alternatively a uniform value may be used, based on the maximum absolute span moment due to serviceability loading.

Flowchart 4.8 presents schematically the serviceability limit state design of a cold-formed steel member in bending.



Flowcharts 4.8 – Serviceability limit state check of a cold-formed steel member (SF041a-EN-EU, Access Steel 2006)

Example 4.6: This example continues *Example 4.3* with the serviceability limit state check of a cold-formed steel member in bending. The beam has pinned end conditions and is composed of two thin-walled cold-formed steel back-to-back lipped channel sections, with a span $L = 4.5$ m. Loadings and cross section dimensions and properties are presented in *Example 4.3*.

Verification for Serviceability Limit State

Applied loading on the joist at SLS (frequent combination) according to §2.3.2:

$$q_{d,ser} = q_G + q_Q = 1.79 + 4.50 = 6.29 \text{ kN/m}$$

The maximum applied bending moment:

$$M_{Ed,ser} = q_{d,ser} L^2 / 8 = 6.29 \times 4.5^2 / 8 = 15.92 \text{ kNm}$$

Effective section properties at the serviceability limit state

Second moment of area for SLS (§§4.6, eqn. (4.103)):

$$I_{fic} = I_{gr} - \frac{\sigma_{gr}}{\sigma} \left(I_{gr} - I(\sigma)_{eff} \right)$$

with:

$I_{gr} = 2302.15 \times 10^4 \text{ mm}^4$ – is the second moment of area of the gross cross section

σ_{gr} – maximum compressive bending stress in SLS

$z_{c,gr} = 125 \text{ mm}$ – distance from the centroidal axis to the compressed flange

$$\sigma_{gr} = \frac{M_{Ed,ser}}{W_{gr}} = \frac{M_{Ed,ser}}{I_{gr} / z_{c,gr}} = \frac{15.92 \times 10^6}{2302.15 \times 10^4 / 125} = 86.45 \text{ N/mm}^2$$

$$\sigma = f_{yb} = 350 \text{ N/mm}^2$$

$I(\sigma)_{eff} = I_{eff,y} = 2268.89 \times 10^4 \text{ mm}^4$ (is the effective second moment of area of cold-formed lipped channel section subjected to bending about major axis from *Example 4.3*)

4. BEHAVIOUR AND DESIGN RESISTANCE OF BAR MEMBERS

$$I_{fic} = 2302.15 \times 10^4 - \frac{96.45}{350} \times (2302.15 - 2269.89) \times 10^4 =$$
$$= 2293.26 \times 10^4 \text{ mm}^4$$

Deflection check

Deflection at the centre of the joist:

$$\delta = \frac{5}{384} \frac{q_{d,ser} L^4}{EI_{fic}} = \frac{5}{384} \times \frac{6.29 \times 4500^4}{210000 \times 2293.26 \times 10^6} = 5.36 \text{ mm}$$

The deflection is $L/840$ – OK

Chapter 5

SHEETING ACTING AS A DIAPHRAGM (STRESSED SKIN DESIGN)

5.1 INTRODUCTION

It has long been recognised that the building framework is considerably strengthened and stiffened once the roof, floors and walls have been added. Frame stresses and deflections calculated on the basis of the frame are usually quite different from the real values. By taking the cladding into account, the actual behaviour of the building can be predicted and usually worthwhile savings may be made in the costs of the frame.

The contribution that panels of roofing, flooring and side cladding make to the resistance and stiffness of frameworks is by virtue of their resistance and stiffness in shear, i.e. the resistance of rectangular panels to being deformed into parallelograms. Hence such panels are known as "shear diaphragms" or simply "diaphragms". In the United States, the design method which takes this effect into account is called "diaphragm design" whereas in Europe it is called "stressed skin design".

Profiled steel sheeting used as roof sheeting or decking, floor decking or side cladding, is very effective as a shear diaphragm. Provided it is effectively attached to the secondary members and main frames by mechanical fasteners or welding, it is extremely reliable and predictable and may be confidently used as a structural component. This has been verified by many full scale tests and proven by practical experience of many building designs.

5. SHEETING ACTING AS A DIAPHRAGM (STRESSED SKIN DESIGN)

Stressed skin action was originally discovered in the context of industrial buildings with pitched roof portal frames. As shown in Figure 5.1, under vertical load, the frames try to spread and this action is resisted by the roof sheeting and purlins which, together, act rather in the manner of a very deep (and, therefore stiff) plate girder. Because of the proportions, considerations of shear predominate over bending. Notwithstanding this origin, most practical applications of stressed skin design have been concerned with flat roof construction, as shown in Figure 5.2.

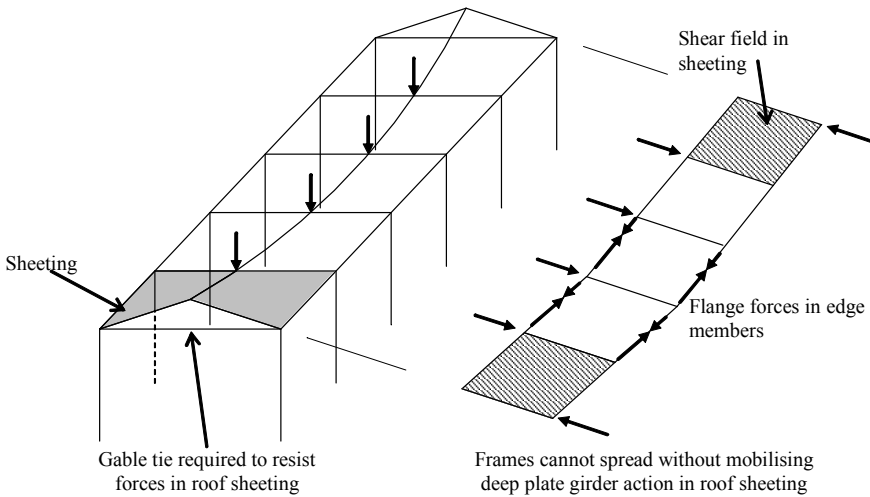


Figure 5.1 – Stressed skin action in a pitched roof portal frame structure, carrying vertical loads (ECCS, 1995)

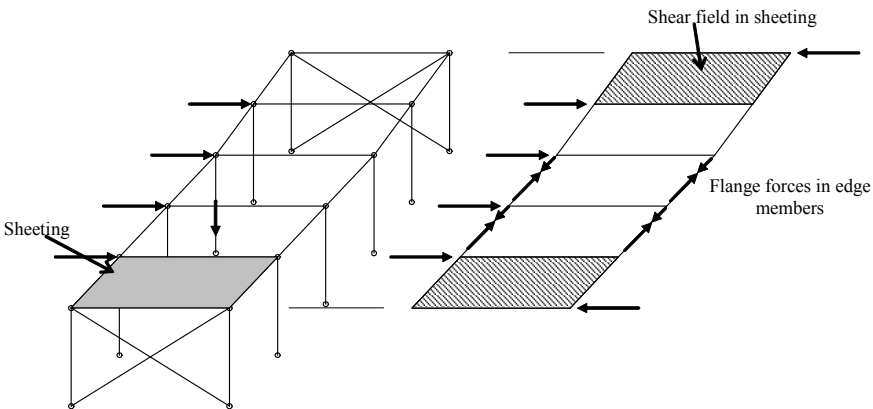


Figure 5.2 – Stressed skin action in a flat-roofed structure with non-rigid frames (ECCS, 1995)

The diaphragm action of the roof sheeting and its supporting members can be used to replace wind (or seismic) bracing in the plane of the roof with both a saving in material and a simplification of the detailing. In Figure 5.2 the gables of the building are shown braced in order to provide a path to the foundations for the diaphragm forces. This gable may itself be sheeted and act as a stressed skin diaphragm, in which case the gable bracing may be also omitted.

Early research into diaphragm action was concerned with buildings clad with a single skin or trapezoidal profiled metal sheeting. Shear diaphragms and shell roof structures, including folded plate (see Figure 5.3) and hyperbolic parabolic roofs (see Figure 5.4) are also examples of the steel shear diaphragm systems studied in the past. Summary of research on these two subjects are reported by Yu (2000).

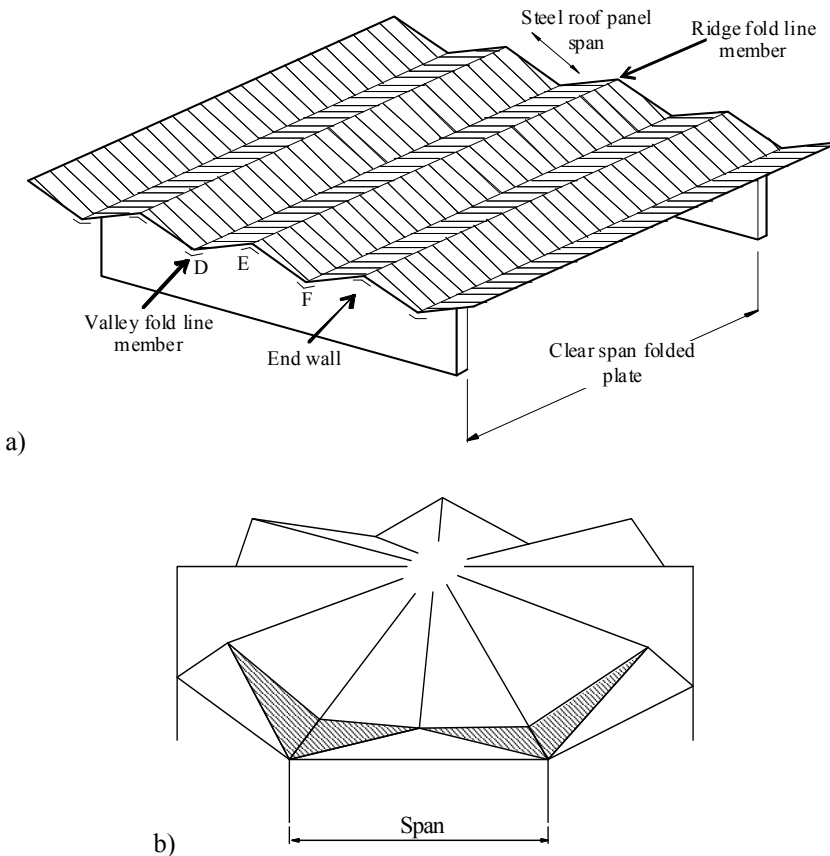


Figure 5.3 – Folded-plate structure (Yu, 2000)

5. SHEETING ACTING AS A DIAPHRAGM (STRESSED SKIN DESIGN)

Multi-storey framed buildings can also take advantage of sheeting diaphragm action in roof, wall and floor decking panels (with or without concrete fill, e.g. composite decks) to resist horizontal loads, provided they are adequately connected to each other and to the supporting frame (see Figure 5.5). Additionally, steel sheeting panels used in floor, roof, and wall construction can be used to prevent the lateral buckling of beams and the overall buckling of columns.

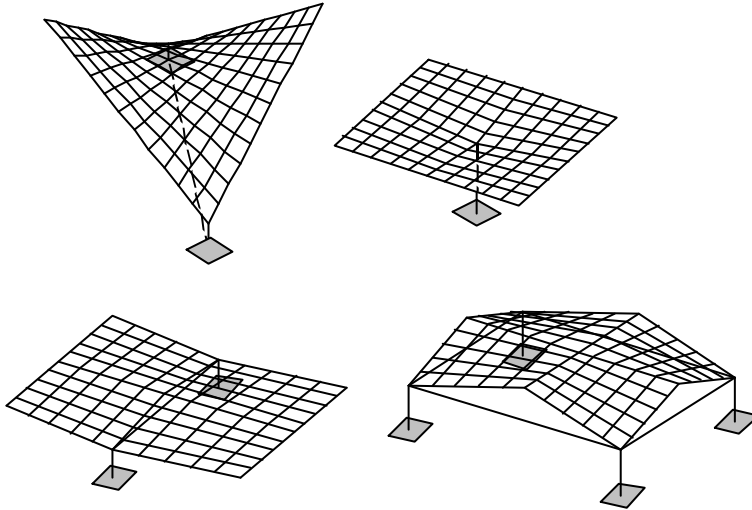


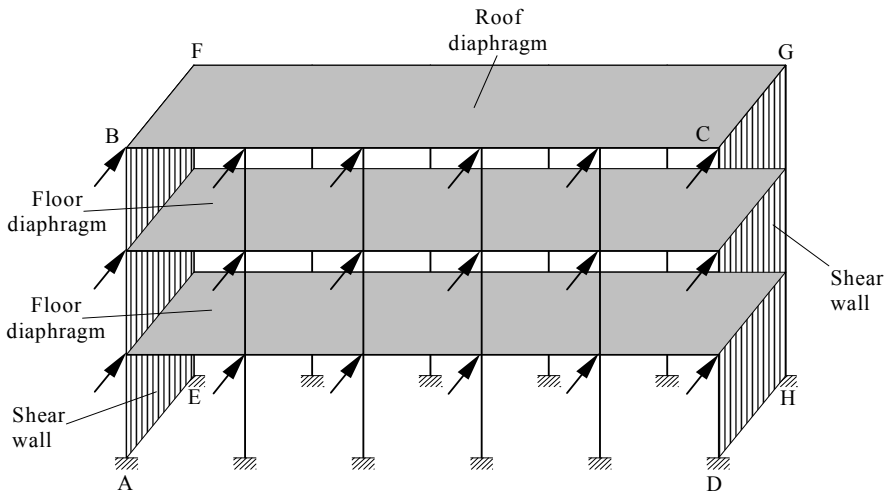
Figure 5.4 – Types of hyperbolic paraboloid shells (ECCS, 1995)

The stiffening effect of sheeting panels is always present and influences the behaviour of structures, even if it is generally ignored due to the difficulties of taking it correctly into account, both with respect to the building type and the connections between panels and framing.

The inherent stiffness of panels, however, can always be considered as adding to the building's strength and stiffness, provided it does not essentially affect the behavioural model assumed for the analysis. In the case of buildings in seismic areas, on the contrary, the cladding panels may have a decisive contribution to the dynamic response of the framed structure subjected to horizontal quakes. Even under a non-destructive earthquake, wall panels can suffer considerably damage, thus contributing to the absorption and damping of the seismic energy. The computation of this contribution seems, therefore, very important whether to preserve the panels

themselves from damage, or to know the actual load carrying capacity of the "skin-frame" system as a whole, with consistent savings in structural steel.

A seismic resistant "all-steel" structure, therefore must be designed and analysed taking into consideration the presence of the infill panels by means of a reliable technology and on the basis of suitable design criteria (Mazzolani & Sylos Labini, 1984).



Note: Wall panels or other bracing system in planes ABCD and EFGH are not shown

Figure 5.5 – Shear diaphragms in multi-storey framed buildings (Yu, 2000)

At the present time a number of methods and design guides exist to calculate the shear capacity and stiffness of sheeting diaphragms. Among them, the well-known manual by Davies & Bryan (1982) and the *European Recommendations for the Application of Metal Sheeting acting as a Diaphragm* (ECCS, 1995) in Europe and that of the Steel Deck Institute (2004) in USA, provide the background of stressed skin design.

The Third Edition, DDMO3, of the SDI Diaphragm Design Manual continues the evolution of building shear resistance presented in the First and Second Editions of this manual. The Third Edition is based on the 2004 Supplement of the 2001 North American Specification for the Design of Cold-Formed Steel Structural Members. The manual explains the method developed to calculate the capacity of diaphragms using steel roof decks or composite steel floor decks and the use of the diaphragm load tables.

In Europe, provisions for stress skin design are presented in Section 10.3 of EN1993-1-3:2006. These provisions are based on the generic design document *European Recommendations for the Application of Metal Sheeting acting as a Diaphragm* (ECCS, 1995). The first edition of this document was published in 1977, by ECCS and edited in 1995.

Relevant references concerning early contributions to this problem have been presented by Davies (1978). Recent research has extended the scope to a wide range of modern cladding such as two-skin built-up systems (Davies & Lawson, 1999; Davies, 2006). Also, remarkable progress has been made in utilising stressed skin effects in seismic resistant structures. The main aim of this chapter is to summaries the European Recommendations (ECCS, 1995) and to present some relevant examples.

5.2 GENERAL DESIGN CONSIDERATIONS FOR DIAPHRAGM ACTION

5.2.1 Conditions and restrictions for the use of stressed skin design

In stressed skin design, advantage may be taken of the contribution that diaphragms of sheeting used as roofing, flooring or wall cladding make to the overall stiffness and strength of the structural frame, by means of their stiffness and strength in shear.

Roofs and floors may be treated as deep plate girders extending throughout the length of the building, resisting transverse in-plane loads and transmitting loads to the end gables, or to intermediate stiffened frames. The panel of sheeting may be treated as a web that resists in-plane transverse loads in shear, with the edge members acting as flanges resisting axial tension and compression forces as shown in Figures 5.1 and 5.2.

According to EN1993-1-3 (CEN, 2006a), the method of stressed skin design that utilizes sheeting as an integral part of a structure may be used only under the following conditions:

- the use made of the sheeting, in addition to its primary purpose, is limited to the formation of shear diaphragms to resist structural displacement in the plane of that sheeting;

- the diaphragms have longitudinal edge members to carry flange forces arising from the diaphragm action;
- the diaphragm forces in the plane of a roof or floor are transmitted to the foundations by means of braced frames, further stressed skin diaphragms, or other methods of sway resistance;
- suitable structural connections are used to transmit diaphragm forces to the main steel framework and to join the sheeting to edge members acting as flanges;
- the sheeting is treated as a structural component that cannot be removed without proper consideration;
- the project specification, including the calculations and drawings, draws attention to the fact that the building is designed to utilize stressed skin action;
- in sheeting with the corrugation oriented in longitudinal direction of the roof, the flange forces due to the diaphragm action may be taken up by the sheeting.

Stressed skin design shall be used predominantly in low-rise buildings, or in the floors or facades of high-rise buildings.

Stressed skin diaphragms shall be used predominantly to resist wind loads, snow loads and other loads that are applied through the sheeting itself. They may also be used to resist small transient loads, such as surges from light overhead cranes or hoists on runaway beams, but may not be used to resist permanent external loads.

373

In a profiled steel sheet diaphragm, both ends of the sheet shall be attached to the supporting members by means of self-tapping screws, cartridge fired pins, welding, bolts or other fasteners of a type that will not work loose in service, pull out, or fail in shear before causing tearing of the sheeting. All such fasteners shall be fixed directly through the sheeting into the supporting member, for example through the troughs of profiled sheets, unless special measures are taken to ensure that the connections effectively transmit the forces assumed in the design.

Figure 4.39 (§§4.5, Beams restrained by sheeting) is reused in this chapter as Figure 5.6 to present a typical arrangement for an individual shear panel (ECCS, 1995). It is composed of:

- (1) Individual lengths of profiled steel sheeting or decking;

5. SHEETING ACTING AS A DIAPHRAGM (STRESSED SKIN DESIGN)

- (2) Purlins or secondary members perpendicular to the direction of span of the sheeting;
- (3) Rafters or main beams parallel to the direction of span of the sheeting;
- (4) Sheet / purlin fasteners;
- (5) Seam fasteners between adjacent sheets;
- (6) Shear connectors to provide attachment between the rafters and sheeting;
- (7) Sheet / shear connector fasteners;
- (8) Purlin / rafter connections, e.g. cleats.

The seam between adjacent sheets shall be fastened by rivets, self-drilling screws, welds, or other fasteners of a type that will not work loose in service, pull out, or fail in shear before causing tearing of the sheeting. The spacing of such fasteners shall not exceed 500 mm, and the distances from all fasteners to the edge and ends of the sheets shall be adequate to prevent premature tearing of the sheets.

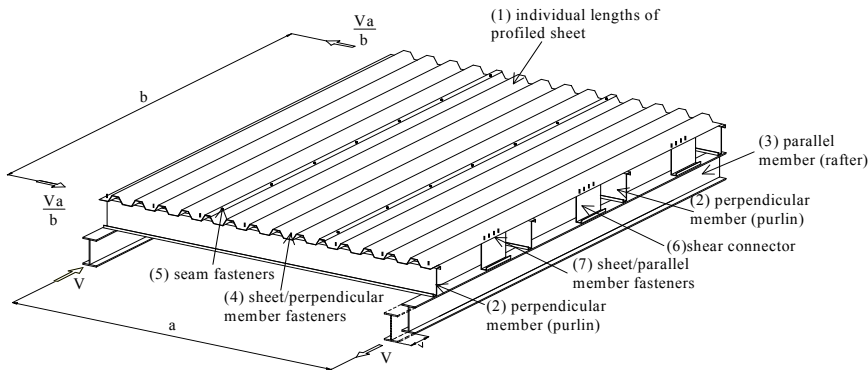


Figure 5.6 – Arrangement of an individual shear panel (ECCS, 1995)

Small randomly arranged openings, up to 3% of the relevant area, may be introduced without special calculation, provided that the total number of fasteners is not reduced. Openings up to 15% of the relevant area (the area of the surface of the diaphragm taken into account for the calculations) may be introduced if justified by detailed calculations. Areas that contain larger openings should be split into smaller areas, each with full diaphragm action. Detailed provisions concerning diaphragms with openings are given in §§5.3.3.

All sheeting that also forms part of a stressed skin diaphragm shall first be designed for its primary purpose in bending. To ensure that any deterioration of the sheeting would be apparent in bending before the resistance to stressed skin action is affected, it shall then be verified that the shear stress due to diaphragm action does not exceed $0.25f_y/\gamma_{M1}$, where f_y is the yield strength of sheet based material and $\gamma_{M1}=1.0$.

The shear resistance of a stressed skin diaphragm shall be based on the least tearing strength of the seam fasteners or the sheet-to-member fasteners parallel to the corrugations, or for diaphragms fastened only to longitudinal edge members, the end sheet-to-member fasteners. The calculated shear resistance for any other type of failure shall exceed this minimum value by at least the following:

- for failure of sheet-to-purlin fastener under combined shear and wind uplift, by at least 40%;
- for any other type of failure, by at least 25%.

The design rules presented in this chapter apply to trapezoidal sheeting. However, they can be also used for sinusoidal sheeting except for the case when the sheeting is connected to the substructure by fastenings in the crest of the corrugation, and when testing is required.

5.2.2 Types of diaphragms

There are two fundamental types of stressed skin diaphragms, i.e.:

- (1) Diaphragm beams, identified by Figures 5.1 and 5.2, in which the diaphragm spans between two gable frames;
- (2) Cantilever diaphragms, identified in Figure 5.6, in which a rectangular shear panel is loaded on one side and restrained on the other three.

Diaphragm beams arise more frequently in practice although cantilever diaphragms may be important in special situations. The great majority of the tests used to establish current stress skin design theory have been carried out using cantilever diaphragms.

For both types of diaphragms, there are two subtypes. Figure 5.7 shows the case of the sheeting or decking spanning at right angles to the span of the diaphragm whereas Figure 5.8 shows the alternative arrangement

5. SHEETING ACTING AS A DIAPHRAGM (STRESSED SKIN DESIGN)

in which the sheeting or decking spans in the same direction as the span of the diaphragm. From the practical point of view, the arrangements give rise to similar levels of strength and stiffness, although they have to be analysed differently.

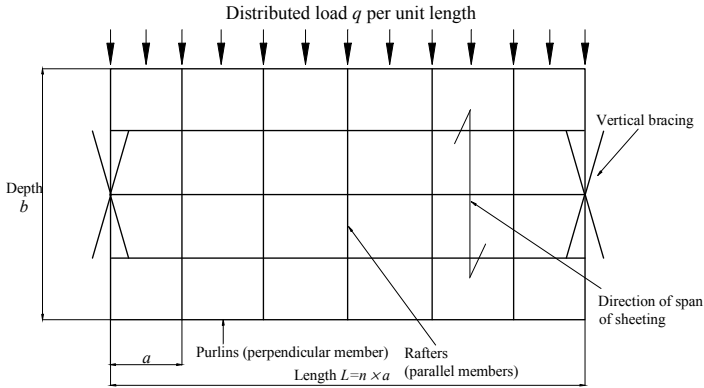


Figure 5.7 – Sheeting spanning perpendicular to the length of the building (ECCS, 1995)

Another sub-grouping of diaphragms is illustrated in Figure 5.9. This concerns the fastenings to the supporting structure. The normal procedure for fixing sheeting and decking result in diaphragms fastened on two sides only (indirect shear connection). Four side fastening (direct shear connection) is advantageous but usually requires special measures to be taken. One possibility is to provide “shear connectors” in the form of purlins offcuts, as shown in Figure 5.6.

376

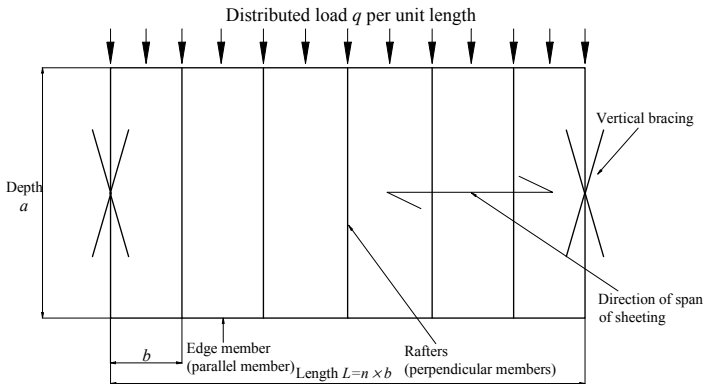


Figure 5.8 – Sheeting spanning parallel to the length of the building (ECCS, 1995)

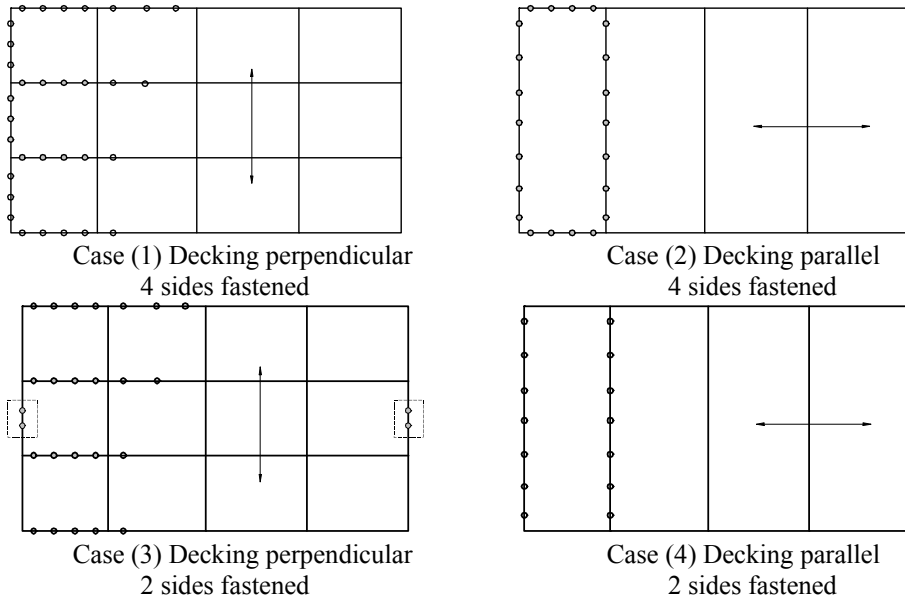


Figure 5.9 – Arrangements of diaphragms of either 2 or 4 sides fastened to the supporting structure (ECCS, 1995)

With all these arrangements, it is necessary to provide a path to ground of the forces in the diaphragms. With diaphragm beams, the path usually takes the form of the end gables of the building which are cross-braced or otherwise stiffened, as illustrated in Figures 5.1 and 5.2. With a cantilever diaphragm, three reaction forces must be provided, as shown in Figure 5.6.

5.2.3 Irregular roof shape

Many buildings have an irregular plan form, as illustrated in Figure 5.10. In such cases, it is necessary to divide the roof into a number of rectangular diaphragms and to ensure that each individual diaphragm has the required load path to the ground for the relevant forces. In providing this path to the ground, it has to be appreciated that wind can blow from all sides.

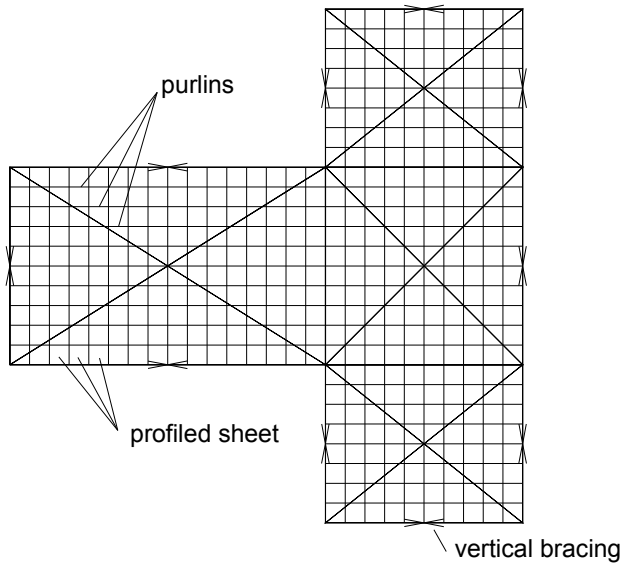


Figure 5.10 – Irregular roof division into diaphragm area

5.2.4 Design criteria

5.2.4.1 Diaphragm flexibility

Although structural engineers usually think in terms of stiffness, it is logistically simpler to work in terms of flexibility, the reciprocal of stiffness, and this section briefly summarises the main factors governing the flexibility of a complete diaphragm assembly such as those shown in previous figures. The relevant design expressions (ECCS, 1995) embrace both beam and cantilever diaphragms and all sub-types.

The diaphragm flexibility c is defined as the shear deflection per unit shear load in a direction parallel to the corrugation in the sheeting (Figure 5.11). For simple diaphragms (which embrace the majority of the cases) this flexibility may be calculated by summing the following component flexibilities (e.g. design criteria for flexibility):

- $c_{1,1}$ = flexibility due to distortion of the corrugation;
- $c_{1,2}$ = flexibility due to shear strain in the sheeting;
- $c_{2,1}$ = flexibility due to movement in sheet to purlin fasteners;
- $c_{2,2}$ = flexibility due to movement in seam fasteners;

- $c_{2,3}$ = flexibility due to movement in shear connectors (in purlin to rafter connection in the case of direct shear transfer);
- c_3 = flexibility due to the axial strain in the purlins (secondary framing members).

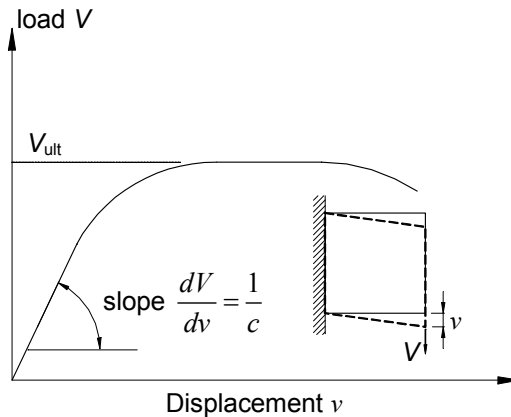


Figure 5.11 – Typical load-deflection curve of a shear panel (Davies, 2005)

Simple expressions for each of these flexibilities are given in the ECCS Recommendations (ECCS, 1995) and will be summarised in the subsequent sections.

Evidently, flexibility due to movement at the fasteners plays an important role. The design expressions require that the flexibility of the individual fasteners is known and this can be determined by a simple test on a lapped connection. Alternatively, conservative design expressions are available for the majority of the usual fastener types such as self-drilling, self-tapping screws, blind rivets and fired pins.

The major component of the total flexibility is $c_{1,1}$, the flexibility due to distortion of the corrugation. Profile distortion is influenced greatly by the sheet thickness, size of profiles and especially whether the sheeting is fastened in every corrugation or alternate corrugations; the latter case is much more flexible than the former. This complex issue has been subject to a good deal of research. Design expressions were first obtained empirically and later justified by a sounder theoretical basis as a result of the research described by Davies (1986). The design expressions require a constant K which is a property of the cross-section. Appropriate K -values to calculate $c_{1,1}$ flexibility are provided by Davies & Bryan (1982), or improved values

by Davies (1986). Values of this constant have been tabulated for trapezoidal and similar profiles fastened in either every, or alternate corrugation troughs. Slip in the seam fastener is often also an important component of flexibility.

5.2.4.2 Diaphragm strength

The diaphragm strength V_{ult} , is defined as the ultimate capacity of the diaphragm under shear load as shown in Figure 5.11. Failure of an individual diaphragm may occur in any one of a number of alternative modes, as follows:

1. Failure at seam fasteners between individual sheet lengths;
2. Failure at sheet-to-shear connector fasteners (direct shear transfer only);
3. Failure at sheet-to-purlin fasteners;
4. Failure at the sheet ends due to the collapse of the profile. This is relatively rare but can influence the design when long span decking profiles are used (Davies & Fisher, 1987);
5. Failure by buckling of sheeting in shear. This is unlikely in panels of sheeting of conventional gauge and typical fastener spacing;
6. Buckling of the apex purlin. Unlike 1-5, this will not occur in the end panel of the building but at the centre owing to bending forces as the sheeting panels from a deep plate girder spanning between the gables.

380

The strength of the diaphragm is given by the lowest failure load obtained when each of the above modes is considered. Again, fastener performance dominates the considerations with seam failure being the most common failure mode.

When designing diaphragms, it is always good practice to aim for ductile failure. This means that the diaphragm should be designed to fail in one of the modes shown in Table 5.1.

It is recommended that other failure modes should show a 25% reserve of safety relative to the lowest load associated with the above modes. Simple expressions for the calculation of failure loads are available in the literature.

Table 5.1 – Failure modes of diaphragm depending of their side fastening

Type of diaphragm	Failure mode
Diaphragm fastened on four sides (direct shear transfer)	- failure at seam fasteners or - failure at shear connector fasteners
Diaphragms fastened on two sides (indirect shear transfer)	- failure at seam fasteners, or - failure at end sheet to purlin fastener

5.2.5 Interaction of diaphragm action and rigid-jointed frames

As mentioned in the Introduction (§§5.1), stressed skin action was first discovered in the context of pitched roof portal frame structures as exemplified in Figure 5.1 and much of the early research was aimed at understanding the behaviour of this type of structure. It was found that stressed skin action relieved the frames of some of their load so that the measured stresses and deflections were smaller than the values calculated by a conventional plane frame analysis. The applied load, e.g. wind or snow, is carried partly by frame action and partly by stressed skin action according to the relative stiffness of the two alternative load bearing mechanism.

Nowadays, the roof slopes of pitched roof portal frames are rather low, typically of the order of 5° , and in such cases it is found that the contribution of stressed skin action to the overall behaviour under vertical (snow) load is rather small. As this load case tends to govern the design of the majority of pitched frames, interest in stressed skin designed has waned. Conversely, however, stressed skin action is much more effective in helping to control sway under wind blowing from the side. Indeed, in tall sway frames a high proportion of side loads is likely to be carried by stressed skin action, whether or not the designer takes account of this. These considerations have a strong influence on the practical usage of stressed skin design.

5.2.6 The danger of ignoring stressed skin action in conventional construction

Regardless of whether the design of clad building is elastic or plastic and whether the design takes into account the stiffening effects or cladding

or not, it is likely that the relative strength and stiffness of the frames and sheeting panels are such that, under increasing load, first yield will take place in the sheeting panels. This is particularly the case in relatively tall, steel framed structures where a major design factor is lateral loading due to wind or earthquake and where the relative displacements between the end gable frames can seriously damage the cladding. In such structures, yield or even failure of the sheeting panels can occur at the working loads. As has been pointed out earlier, stressed skin action is present whether the designer acknowledges it or not. The methods of stressed skin design allow the forces induced by horizontal actions, such as wind or earthquake, into the sheeting to be checked. This is the correct way to proceed whether or not it is intended to take account of stressed skin action in the design of the frame (Davies, 2005).

A number of tall rectangular buildings have been analysed in order to investigate the condition of typical roof sheeting panels at the working loads. It is shown that tearing of the sheeting at the fasteners may be predicted at wind loads well below the working values. As the structure was designed as a simple sway frame, this does not suggest total failure but it could well indicate difficulty in keeping the building watertight. This is a typical pattern of behaviour in tall rectangular framed buildings and is particularly critical when the cladding is fastened to the supporting members on two sides only, which is invariably the case when no considerations of stressed skin effects is included in the design. In such structures calculated sway moments and deflections are likely to be inaccurate and the forces in the cladding panels large enough to require serious consideration.

5.3 DESIGN PROCEDURES FOR SHEETING ACTING AS DIAPHRAGM (ECCS, 1995)

5.3.1 Design expressions for shear flexibility of diaphragm

5.3.1.1 *Sheeting spanning perpendicular to length of diaphragm*

The total shear flexibility of a shear panel is the sum of the component shear flexibilities mentioned in §5.2.4.1. For shear panel assemblies of the type shown in Figure 5.12 (beam type diaphragm), the calculation process

for flexibility components and deflection are presented in Flowchart 5.1 and Table 5.2(1).

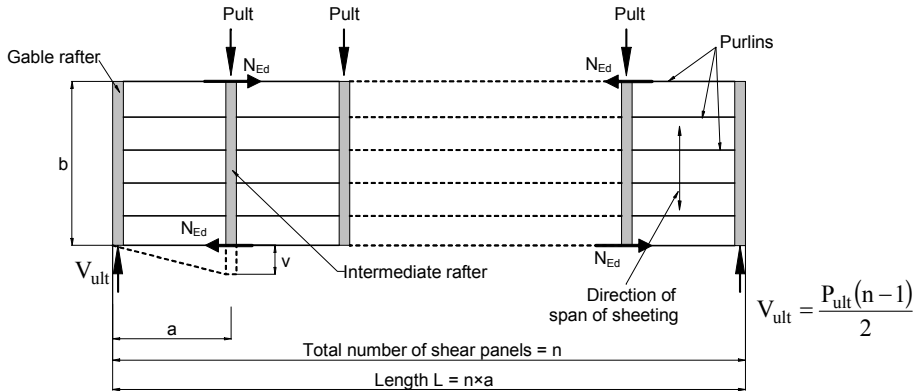


Figure 5.12 – Shear panel assembly: sheeting spanning perpendicular to length of diaphragm (e.g. length of building)

For a cantilever diaphragm, as shown in Figure 5.13, the same flow chart can be used but with formulas given in Table 5.2(2).

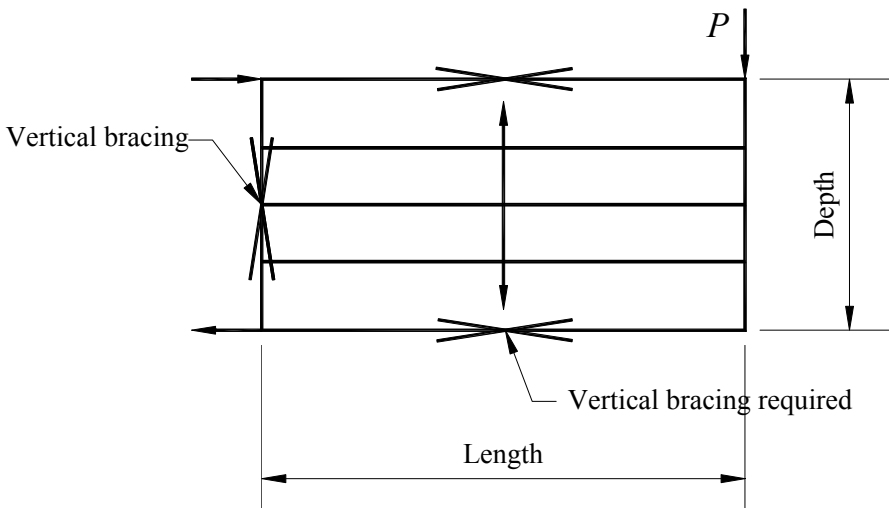
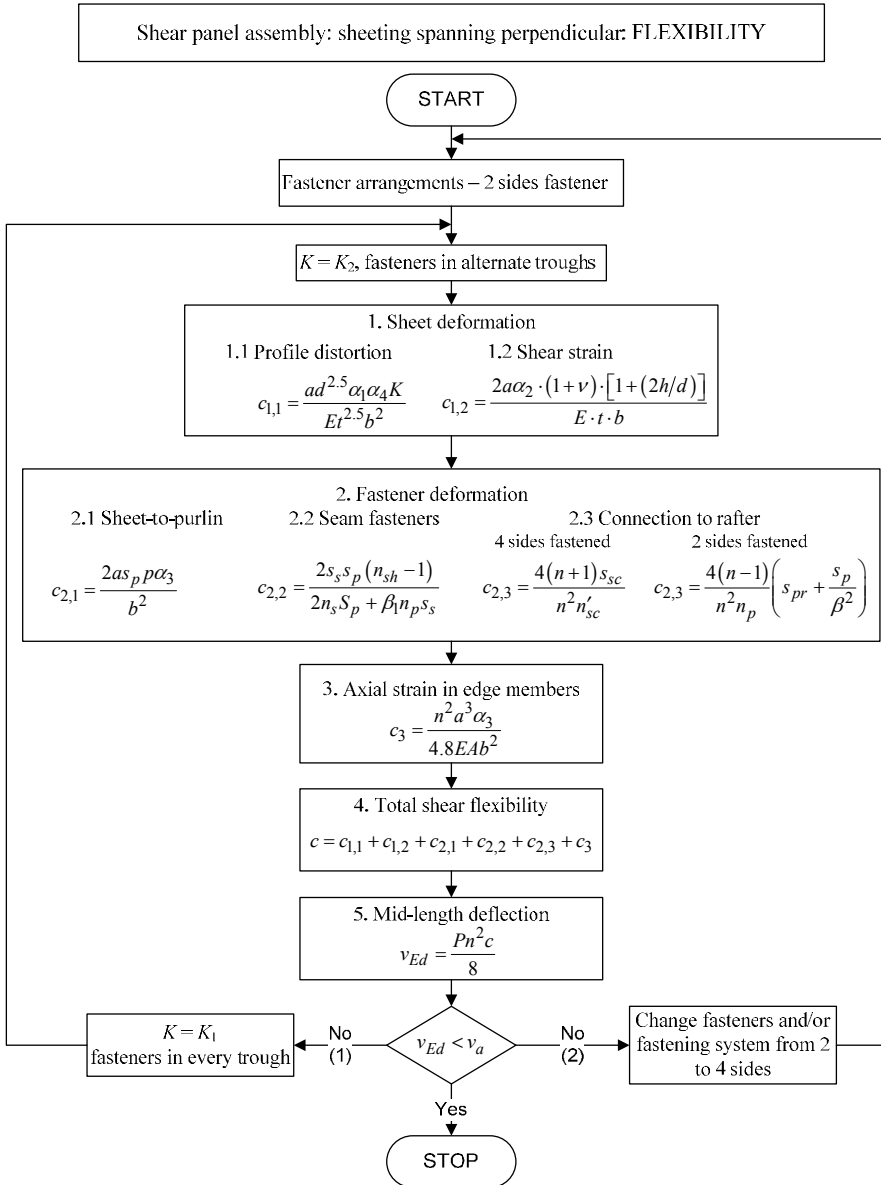


Figure 5.13 – Cantilever diaphragm with sheeting spanning perpendicular to length of diaphragm

5. SHEETING ACTING AS A DIAPHRAGM (STRESSED SKIN DESIGN)



Flowchart 5.1 – Flowchart for flexibility and deflection calculation of a shear panel assembly with sheeting spanning perpendicular to length (Vayas & Dubina, 2004)

Table 5.2 – Components of shear flexibility: sheeting spanning perpendicular to length of diaphragm (ECCS, 1995)

Shear flexibility due to:		(1) panel assemblies	(2) cantilevered diaphragm
		Shear flexibility mm/kN	Shear flexibility mm/kN
Sheet deformation	Profile distortion	$c_{1.1} = \frac{ad^{2.5}\alpha_1\alpha_4K}{Et^{2.5}b^2}$	$c_{1.1} = \frac{ad^{2.5}\alpha_1\alpha_4K}{Et^{2.5}b^2}$
	Shear strains	$c_{1.2} = \frac{2a\alpha_2(1+\nu)[1+(2h/d)]}{Etb}$	$c_{1.2} = \frac{2a(1+\nu)[1+(2h/d)]}{Etb}$
Fastener deformation	Sheet to purlin fastener	$c_{2.1} = \frac{2as_p p \alpha_3}{b^2}$	$c_{2.1} = \frac{2as_p p}{b^2}$
	Seam fasteners	$c_{2.2} = \frac{2s_s s_p (n_{sh} - 1)}{2n_s s_p + \beta_1 n_p s_s}$	$c_{2.2} = \frac{2s_s s_p (n_{sh} - 1)}{2n_s s_p + \beta_1 n_p s_s}$
	Connections to rafters	4 sides fastened $c_{2.3} = \frac{4(n+1)s_{sc}}{n^2 n_{sc}}$ or 2 sides only fastened with gable shear connection $c_{2.3} = \frac{4(n-1)}{n^2 n_p} (s_{pr} + \frac{s_p}{\beta_2})$	4 sides fastened $c_{2.3} = \frac{2s_{sc}}{n_{sc}}$ or 2 sides only fastened $c_{2.3} = \frac{2}{n_p} (s_{pr} + \frac{s_p}{\beta_2})$
Total flexibility in true shear		$c' = (c_{1.1} + c_{1.2} + c_{2.1} + c_{2.2} + c_{2.3})$	
Flange forces	Axial strains in purlins	$c_3 = \frac{n^2 a^3 \alpha_3}{4.8EAb^2}$	$c_3 = \frac{2a^3}{3EAb^2}$
Total shear flexibility		$c = c' + c^3$	$c = c' + c^3$

* The expression for $c_{1.1}$ applies for $b/d \geq 10$

In Flowchart 5.1 and Table 5.2 the following notations have been used:

- a is the width of a shear panel in a direction perpendicular to the corrugations (see Figure 5.12);
- A is the cross sectional area of a longitudinal edge member;
- b is the depth of a shear panel in the direction parallel to the corrugations (see Figure 5.12);

5. SHEETING ACTING AS A DIAPHRAGM (STRESSED SKIN DESIGN)

- c is the total shear flexibility of a shear panel;
- $c_{i,j}$ are the component shear flexibilities (see §§5.2.4.1);
- d is the pitch of the corrugations (see Figure 5.14);
- E is the modulus of elasticity of steel;
- h is the height of the sheeting profile (see Figure 5.14);
- K is a sheeting constant which can take values K_1 or K_2 as given in Tables 5.3 and 5.4;
- n is the number of shear panels in the length of the diaphragm assembly (see Figure 5.12);
- n_p is the number of purlin (edge + intermediate);
- n_s is the number of seam fasteners per slide lap (excluding those which pass through both sheets and the supporting purlin);
- n_{sc} is the number of sheet to shear connector fasteners per end rafter;
- n'_{sc} is the number of sheet to shear connector fasteners per internal rafter;
- n_{sh} is the number of sheet widths per shear panel;
- p is the pitch of sheet / purlin fasteners;
- s_p is the slip per sheet / purlin fastener per unit load (see Table 5.5);
- s_{sc} is the slip per sheet / shear connector fastener per unit load. Values are given in Table 5.5;
- t is the net sheet thickness, excluding metallic and other coatings;
- α_1 to α_4 are factors to allow for intermediate purlins and number of sheet lengths. Values are given in Table 5.7;
- β_1, β_2 are factors to allow for the number of sheet / purlin fasteners per sheet width. Values are given in Table 5.8;
- ν is Poisson's ratio (for steel 0.3).

386

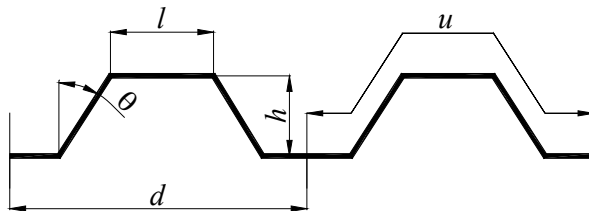


Figure 5.14 – Geometry of a single corrugation

In order to use correctly the formulas of Flowchart 5.1 and Table 5.2 the calculation of the shear flexibility is explained in the following:

a) Profile distortion

In the expression for $c_{1,1}$, K can take values K_1 or K_2 given in Tables 5.3 and 5.4 depending on whether the sheeting is fastened in every corrugation or alternate corrugation. The factor α_1 takes account of the effect of fasteners to intermediate purlins and is given in Table 5.7. The factor α_4 takes account of the effect of the number of sheet lengths in the depth of the diaphragm and is given in Table 5.9 for various fasteners arrangements.

b) Shear strain in the sheet

In the expression for $c_{1,2}$ if there are intermediate purlins present, the shear across the depth of the shear panel is not uniform. The factor α_2 takes account of this effect and is given in Table 5.7.

c) Slip in the sheet/purlin fasteners

The flexibility due to slip in the sheet/purlin fasteners, $c_{2,1}$, depends on the slip value (see Table 5.5) and the spacing of fasteners. The factor α_3 given in Table 5.7 allows for the effect of fasteners at intermediate purlins.

d) Slip in the seam fasteners

In the case of roof sheeting and side cladding, the seams are usually fastened in the crests by seam fasteners only. In the case of roof decking, the seams are usually fastened in the troughs by seam fasteners and sheet to purlin fasteners which pass through both sheet thicknesses at the overlaps. The expressions for $c_{2,2}$ takes account of this difference by means of the values of β_1 (see Table 5.8) and by allowing for the relative values of slip (see Table 5.5) at the seam and the adjacent sheet/purlin fasteners.

e) Slip in the sheet to shear connector fasteners

If four sides of the shear panel are fastened and if $n_{sc} = \frac{1}{2}(n-1)n'_{sc}$ the expression given in Table 5.2 for the shear flexibility $c_{2,3}$ due to slip in the sheet to shear connector fasteners is the same at the end shear panels and internal shear panels.

f) Movement in the purlin to rafter connections

For the case of a shear panel with only two sides fastened (plus sheet / shear connector fasteners at the end gable), the expression given for $c_{2,3}$ ignores the small movement at the end rafters in comparison with the movement of the purlin / rafter connections at the internal rafters.

g) Axial strain in the edge members

The flexibility due to this cause is strictly a bending effect but for convenience it is replaced by an equivalent shear flexibility. The expression given for c_3 is an average value over the length of the shear panel assembly. The factor α_3 given in Table 5.7 allows for the effect of intermediate purlins.

h) Deflection

The sum of component shear flexibilities gives the total shear flexibility c of the shear panel. The mid length deflection of the typical shear panel assembly, shown in Figure 5.12 is given by:

$$v_{Ed} = P(n^2 / 8)c \quad (5.1)$$

where

- P is the shear panel point load on the diaphragm, calculated with unfactored side loads;
- n is the number of shear panels in the length of the diaphragm assembly;
- c is the total shear flexibility of a shear panel as given in Table 5.2.

The value obtained for v_{Ed} has to be compared with v_a (e.g. $v_{Ed} \leq v_a$) where v_a is the permitted or allowable deflection established by code specifications. In case $v_{Ed} > v_a$ the components of flexibility must be increased (firstly by modifying the fastening in alternate troughs in every trough, in order to increase the $c_{1,1}$ component which is the dominant flexibility term).

5.3 DESIGN PROCEDURES FOR SHEETING ACTING AS DIAPHRAGM

Table 5.3 – Value of K_1 for fasteners in every trough (ECCS, 1995)

θ	h/d	h/d																		
		0.1	0.2	0.3	0.4	0.5	0.6	0.7	0.8	0.9	0.1	0.2	0.3	0.4	0.5	0.6	0.7	0.8	0.9	
0°	0.1	0.013	0.030	0.041	0.041	0.046	0.050	0.066	0.103	0.193	0.1	0.019	0.032	0.038	0.038	0.038	0.045	0.068	0.126	0.313
	0.2	0.042	0.096	0.131	0.142	0.142	0.153	0.199	0.311	0.602	0.2	0.072	0.099	0.103	0.095	0.095	0.129	0.236	0.513	
	0.3	0.086	0.194	0.264	0.285	0.283	0.302	0.388	0.601	1.188	0.3	0.151	0.178	0.166	0.144	0.160	0.268	0.557		
	0.4	0.144	0.323	0.438	0.473	0.468	0.494	0.629	0.972	1.935	0.4	0.238	0.244	0.204	0.176	0.247	0.494			
	0.5	0.216	0.438	0.654	0.703	0.695	0.729	0.922	1.420	2.837	0.5	0.306	0.272	0.203	0.204	0.376				
	0.6	0.302	0.638	0.911	0.980	0.965	1.008	1.266	1.938	3.892	0.6	0.333	0.248	0.172	0.241					
	0.7	0.402	0.895	1.208	1.300	1.277	1.329	1.661	2.536	5.098	0.7	0.300	0.174	0.142						
	0.8	0.516	1.146	1.546	1.662	1.631	1.692	2.107	3.208	6.453	0.8	0.204	0.081							
5°	0.1	0.014	0.031	0.041	0.044	0.044	0.049	0.066	0.107	0.205	0.1	0.020	0.032	0.037	0.036	0.036	0.044	0.070	0.133	
	0.2	0.050	0.099	0.128	0.134	0.132	0.146	0.198	0.336	0.652	0.2	0.075	0.095	0.094	0.084	0.087	0.132	0.256		
	0.3	0.107	0.202	0.253	0.260	0.254	0.280	0.386	0.681	1.548	0.3	0.148	0.157	0.135	0.116	0.152	0.291			
	0.4	0.188	0.338	0.413	0.417	0.404	0.448	0.629	1.158	2.639	0.4	0.208	0.186	0.139	0.139	0.253				
	0.5	0.295	0.507	0.604	0.601	0.578	0.648	0.934	1.783		0.5	0.226	0.161	0.112	0.176					
	0.6	0.429	0.706	0.823	0.826	0.772	0.877	1.306	2.586		0.6	0.180	0.089	0.093						
	0.7	0.591	0.935	1.066	1.028	0.983	1.385	1.756	3.605		0.7	0.077								
	0.8	0.780	1.191	1.328	1.264	1.208	1.423	2.990	4.838											
10°	0.1	0.016	0.031	0.040	0.042	0.042	0.048	0.065	0.111	0.221	0.1	0.021	0.032	0.036	0.034	0.034	0.043	0.072	0.142	
	0.2	0.056	0.101	0.123	0.125	0.123	0.139	0.200	0.366	0.873	0.2	0.076	0.089	0.083	0.072	0.082	0.137	0.281		
	0.3	0.125	0.204	0.238	0.233	0.260	0.264	0.402	0.786		0.3	0.137	0.130	0.102	0.093	0.151				
	0.4	0.222	0.338	0.375	0.356	0.345	0.418	0.689	1.445		0.4	0.162	0.119	0.082	0.120					
	0.5	0.349	0.494	0.526	0.486	0.473	0.605	1.082	2.428		0.5	0.123	0.059							
	0.6	0.502	0.668	0.682	0.615	0.608	0.837	1.607			0.6	0.032								
	0.7	0.677	0.851	0.834	0.736	0.752	1.128	2.308												
	0.8	0.869	1.035	0.975	0.844	0.907	1.494	3.200												
15°	0.1	0.017	0.031	0.040	0.041	0.041	0.047	0.066	0.115	0.241	0.1	0.023	0.032	0.034	0.032	0.032	0.043	0.075		
	0.2	0.062	0.102	0.118	0.115	0.113	0.134	0.209	0.403		0.2	0.075	0.081	0.070	0.060	0.077	0.146			
	0.3	0.139	0.202	0.218	0.204	0.200	0.254	0.440	0.945		0.3	0.116	0.096	0.068	0.078					
	0.4	0.244	0.321	0.325	0.293	0.294	0.414	0.796			0.4	0.100	0.053	0.048						
	0.5	0.370	0.448	0.426	0.371	0.396	0.636	1.329			0.5	0.024								
	0.6	0.508	0.568	0.508	0.434	0.513	0.941													
	0.7	0.646	0.668	0.561	0.483	0.664	1.349													
	0.8	0.768	0.735	0.578	0.527	0.861														
20°	0.1	0.018	0.032	0.039	0.039	0.039	0.046	0.066	0.111	0.276	0.1	0.024	0.031	0.032	0.029	0.030	0.043	0.079		
	0.2	0.068	0.101	0.111	0.106	0.104	0.131	0.221	0.452		0.2	0.071	0.069	0.056	0.050	0.073				
	0.3	0.148	0.193	0.194	0.174	0.177	0.255	0.492			0.3	0.086	0.057	0.041						
	0.4	0.249	0.289	0.267	0.230	0.259	0.444	0.931			0.4	0.032								
	0.5	0.356	0.372	0.315	0.270	0.364	0.725													
	0.6	0.448	0.420	0.326	0.303	0.512														
	0.7	0.509	0.423	0.301	0.346															
	0.8	0.521	0.372	0.259	0.413															

5. SHEETING ACTING AS A DIAPHRAGM (STRESSED SKIN DESIGN)

Table 5.4 – Value of K_2 for fasteners in alternate trough (ECCS, 1995)

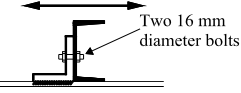
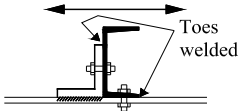
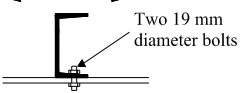
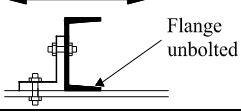
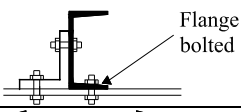
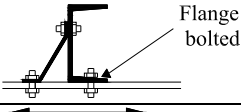

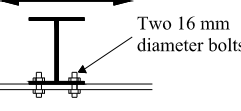
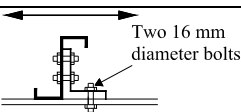
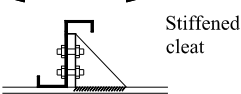
θ	h/d	l/d									
		0.1	0.2	0.3	0.4	0.5	0.6	0.7	0.8	0.9	
0°	0.1	0.014	0.025	0.036	0.046	0.054	0.061	0.070	0.108	0.211	
	0.2	0.031	0.065	0.099	0.129	0.151	0.169	0.206	0.318	0.649	
	0.3	0.054	0.123	0.192	0.252	0.294	0.328	0.402	0.608	1.269	
	0.4	0.084	0.202	0.316	0.414	0.482	0.535	0.653	0.968	2.056	
	0.5	0.123	0.299	0.468	0.614	0.712	0.790	0.958	1.410	3.006	
	0.6	0.169	0.415	0.649	0.846	0.982	1.090	1.318	1.928	4.113	
	0.7	0.222	0.549	0.855	1.108	1.286	1.433	1.730	2.525	5.383	
	0.8	0.284	0.699	1.086	1.398	1.623	1.818	2.196	3.198	6.811	
5°	0.1	0.089	0.138	0.184	0.228	0.269	0.311	0.359	0.432	0.590	
	0.2	0.300	0.433	0.564	0.690	0.810	0.934	1.091	1.338	2.046	
	0.3	0.627	0.872	1.113	1.345	1.569	1.806	2.125	2.710	4.441	
	0.4	1.076	1.453	1.826	2.187	2.535	2.910	3.446	4.498	8.057	
	0.5	1.644	2.171	2.694	3.205	3.703	4.244	5.058	6.761	12.94	
	0.6	2.280	2.961	3.639	4.313	4.999	5.797	6.971	9.571		
	0.7	2.961	3.803	4.620	5.443	6.347	7.479	9.206	13.01		
	0.8	3.802	4.838	5.788	6.612	7.701	9.257	11.76	17.20		
10°	0.1	0.091	0.140	0.186	0.229	0.270	0.312	0.362	0.440	0.627	
	0.2	0.312	0.446	0.575	0.699	0.817	0.943	1.112	1.425	2.472	
	0.3	0.665	0.907	1.144	1.370	1.589	1.835	2.204	2.979		
	0.4	1.156	1.529	1.891	2.239	2.578	2.984	3.655	5.251		
	0.5	1.793	2.313	2.819	3.305	3.782	4.397	5.519	7.872		
	0.6	2.533	3.206	3.858	4.509	5.192	6.096	7.875			
	0.7	3.334	4.148	4.949	5.780	6.737	8.112	10.82			
	0.8	4.236	5.170	6.051	7.066	8.404	10.47	12.59			
15°	0.1	0.093	0.142	0.188	0.231	0.271	0.313	0.364	0.448	0.682	
	0.2	0.325	0.458	0.586	0.707	0.824	0.953	1.140	1.523		
	0.3	0.703	0.942	1.174	1.393	1.610	1.874	2.316	3.411		
	0.4	1.237	1.602	1.953	2.285	2.624	3.089	3.981			
	0.5	1.937	2.443	2.926	3.379	3.869	4.640	6.256			
	0.6	2.778	3.428	4.058	4.664	5.366	6.581				
	0.7	3.692	4.488	5.273	6.081	7.138	8.902				
	0.8	4.648	5.570	6.516	7.628	9.910					
20°	0.1	0.096	0.144	0.190	0.232	0.273	0.315	0.368	0.459	0.680	
	0.2	0.339	0.472	0.597	0.716	0.832	0.966	1.177	1.659		
	0.3	0.743	0.978	1.204	1.416	1.633	1.927	2.481			
	0.4	1.317	1.673	2.009	2.325	2.679	3.246	3.840			
	0.5	2.075	2.559	3.011	3.436	3.993	4.969				
	0.6	3.006	3.625	4.197	4.752	5.588					
	0.7	4.042	4.789	5.494	6.272						
	0.8	5.122	6.013	6.883	7.861						
25°	0.1	0.101	0.150	0.194	0.236	0.276	0.319	0.378	0.495		
	0.2	0.372	0.500	0.621	0.734	0.850	1.005	1.298			
	0.3	0.827	1.051	1.260	1.456	1.697	2.098				
	0.4	1.477	1.801	2.092	2.393	2.830					
	0.5	2.319	2.727	3.075	3.499						
	0.6	3.320	3.738	4.041							
	0.7	4.378									
	0.8	5.487									
30°	0.1	0.105	0.153	0.197	0.238	0.278	0.322	0.385	0.525		
	0.2	0.390	0.516	0.634	0.744	0.862	1.035	1.329			
	0.3	0.872	1.088	1.284	1.476	1.741					
	0.4	1.553	1.849	2.105	2.412						
	0.5	2.400	2.713								
	0.6	3.278									
	0.7	4.378									
	0.8	5.487									
35°	0.1	0.109	0.156	0.200	0.241	0.280	0.325	0.394	0.569		
	0.2	0.411	0.538	0.647	0.753	0.878	1.077				
	0.3	0.919	1.122	1.301	1.496						
	0.4	1.614	1.859	2.085							
	0.5	2.376									
	0.6										
	0.7										
	0.8										
40°	0.1	0.114	0.160	0.203	0.243	0.282	0.329	0.409			
	0.2	0.434	0.553	0.661	0.764	0.899					
	0.3	0.965	1.148	1.306							
	0.4	1.634									
	0.5										
	0.6										
	0.7										
	0.8										
45°	0.1	0.114	0.160	0.203	0.243	0.282	0.329	0.409			
	0.2	0.434	0.553	0.661	0.764	0.899					
	0.3	0.965	1.148	1.306							
	0.4	1.634									
	0.5										
	0.6										
	0.7										
	0.8										

Table 5.5 – Design strengths and slip values for fastener (ECCS, 1995)

(1) Sheet/purlin and sheet/shear connector fasteners					
	Washer type	Overall diam. (mm)	Design shear strength F_p and F_{sc}		Slip s_p and s_{sc} (mm/kN)
			Design formula	Design values kN per mm thickness of sheet	
Screws	Collar head	5.5	$1.9f_u dt$	6.5	0.15
		6.3	$1.9f_u dt$	8.0	
	Collar head + Neoprene washer	5.5	$1.9f_u dt$	6.5	0.35
		6.3	$1.9f_u dt$	8.0	
Fired pins	φ23 mm steel washer	3.7 to 4.8	$2.9f_u dt$	8.0	0.10
(2) Seam fasteners (no washers)					
		Overall diam. (mm)	Design shear strength F_s		Slip s_s (mm/kN)
			Design formula	Design values kN per mm thickness of sheet	
Screws		4.1 to 4.8	$2.9(t/d)^{1/2} f_u dt$	2.5	0.25
Steel or monel blind rivets		4.8	$3.2(t/d)^{1/2} f_u dt$	2.8	0.30
Notes:					
<p>(1) In the above table, f_u is the specified ultimate tensile strength of the steel sheet (kN/mm²), d is the nominal diameter of the fastener (mm) and t is the net sheet thickness (mm).</p> <p>(2) The design strengths and slip values in this table apply to the range of fasteners, number of fasteners, sheet thickness and material strengths typically found in stressed skin panels. For other conditions, lap joint test should be made, in accordance with recommendations given in Chapter 7, to determine the resistance and slip values and to ensure that failure occurs by tearing of the sheeting. Strength formulas from above are in fact the bearing resistances for edge or end fasteners, and they have been obtained by using the relevant formulae of Chapter 7, Tables 7.8, 7.13 and 7.14, using for γ_{M2} the value of 1.1 instead of 1.25 (due to large number of fasteners in panel). For sheet-to-purlin and sheet-to-shear connector fasteners, it is assumed that the two material thickness, t_1 or $t_{sup} > 2.5t$, where t is the sheet thickness. For seam fasteners it assumed that the sheet thicknesses, which overlap, are equal. Alternatively the full calculation procedures, according to Tables 7.8 and 7.13 may be used. However end distance, edge distance and spacing limits for fasteners must be rigorously respected, and it is essential that the absolute limits on design strengths given in Table 5.5 to be not exceeded.</p> <p>(3) Shear strength and slip values in this table are based on the following assumptions:</p> <ul style="list-style-type: none"> - the net sheet thickness is between 0.5 mm and 1.2 mm; - the nominal yield and ultimate tensile strength of steel sheet do not exceed 355N/mm² and 480N/mm² respectively. 					

5. SHEETING ACTING AS A DIAPHRAGM (STRESSED SKIN DESIGN)

Table 5.6 – Design strengths and flexibilities of purlin/rafter connections (ECCS, 1995)

Connection number	Type of purlin (and cleat)	Connection detail	Design resistance F_{pr} [kN]	Flexibility s_{pr} [mm/kN]
1	102 × 51 rolled steel channel	 Two 16 mm diameter bolts	4.9	0.84
2	(89 × 64 × 7.8 angle cleat × 89 mm long)	 Toes welded	20.0	0.11
3	152 × 76 rolled steel channel	 Two 19 mm diameter bolts	14.4	0.60
4	(76 × 64 × 6.2 angle cleat × 127 mm long)	 Flange unbolted	7.2	1.20
5		 Flange bolted	19.6	0.35
6		 Flange bolted	25.0	0.13
7		 Stiffened cleat	25.0	0.05
8	254 × 102 × 22 kg/m Universal beam	 Two 16 mm diameter bolts	10.0	2.60
9	203 × 51 × 2.0 zed	 Two 16 mm diameter bolts	4.4	1.40
10	(178 × 89 × 9.4 angle cleat × 127 mm long)	 Stiffened cleat	7.2	0.38

NOTE: The strength and flexibility of other types and sizes of purlin/rafter connections may be estimated from the values given above or may be obtained by test.

Table 5.7 – Factors to allow for the effect of intermediate purlins (ECCS, 1995)

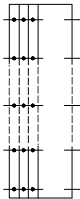
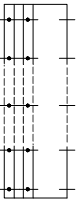
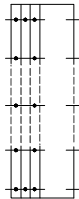
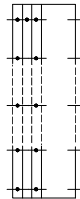

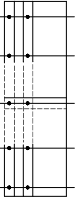

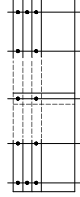
Total number of purlins per panel (or per sheet length for α_1) n_p	Factors		
	α_1	α_2	α_3
2	1.00	1.00	1.00
3	1.00	1.00	1.00
4	0.85	0.75	0.90
5	0.70	0.67	0.80
6	0.60	0.55	0.71
7	0.60	0.50	0.64
8	0.60	0.44	0.58
9	0.60	0.40	0.53
10	0.60	0.36	0.49
11	0.60	0.33	0.45
12	0.60	0.30	0.42
13	0.60	0.29	0.39
14	0.60	0.27	0.37
15	0.60	0.25	0.35
16	0.60	0.23	0.33
17	0.60	0.22	0.31
18	0.60	0.21	0.30
19	0.60	0.20	0.28
20	0.60	0.19	0.27

Table 5.8 – Factors to allow for the number of sheet/purlin fasteners per sheet width (ECCS, 1995)

Total number of fasteners per sheet width n_f	Factor β_1		Factor β_2
	Case 1 – sheeting	Case 2 – decking	
2	0.13	1.00	1.00
3	0.30	1.00	1.00
4	0.44	1.04	1.11
5	0.58	1.13	1.25
6	0.71	1.22	1.40
7	0.84	1.33	1.56
8	0.97	1.45	1.71
9	1.10	1.56	1.88
10	1.23	1.68	2.04

5. SHEETING ACTING AS A DIAPHRAGM (STRESSED SKIN DESIGN)

Table 5.9 – Factor α_4 to allow for the member of sheet lengths in the depth of the diaphragms (ECCS, 1995)

	Fastener positions			
	every corrugation	alternate corrugation	every corrugation at both sheet ends	every corrugation at one sheet end
one sheet length for full depth of diaphragm	 $K=K_1$ α_4 from Table 5.7 $\alpha_4=1$ (1)	 $K=K_2$ α_4 from Table 5.7 $\alpha_4=1$ (2)	 $K=K_1$ $\alpha_4=1$ $\alpha_4=1$ (3)	 $K=K_2$ $\alpha_4=0.5$ $\alpha_4=1$ (4)
n_b sheet lengths in depth of diaphragm	 $K=K_1$ α_4 from Table 5.7 for a number of purlins per sheet length $\alpha_4=(1+0.3n_b)$ (5)	 $K=K_2$ α_4 from Table 5.7 for a number of purlins per sheet length $\alpha_4=(1+0.3n_b)$ (6)	 $K=K_1$ $\alpha_4=1$ $\alpha_4=(1+0.3n_b)$ (7)	 $K=K_2$ α_4 from Table 5.7 for a number of purlins per sheet length $\alpha_4 = (1 + 0.3n_b) \left(1 - \frac{1}{n_b}\right)$ (8)

5.3.1.2 Sheeting spanning parallel to length of diaphragm

For shear panel assemblies (beam type) and cantilevered diaphragms, as shown in Figures 5.15 and 5.16 respectively, the related flexibility formulas are given in Table 5.10 and can be introduced in a similar manner as Flowchart 5.1.

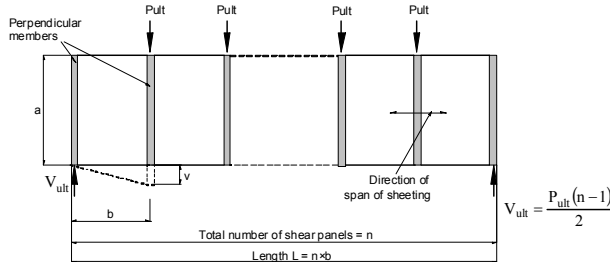


Figure 5.15 – Shear panel assembly: sheeting spanning parallel to length of diaphragm

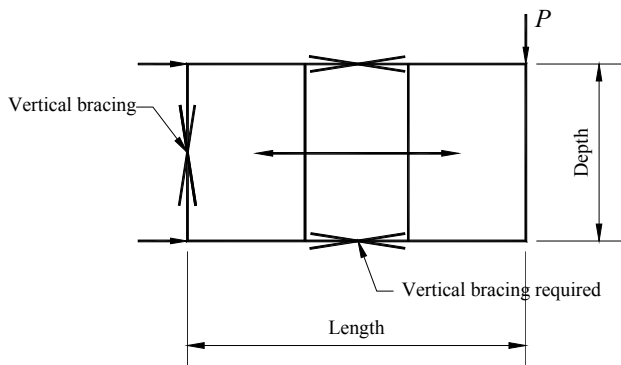


Figure 5.16 – Cantilevered diaphragm: sheeting spanning parallel to length of diaphragm

Table 5.10 – Components of shear flexibility: sheeting spanning parallel to length of diaphragm (ECCS, 1995)

Shear flexibility due to:		(1) panel assemblies Shear flexibility mm/kN	(2) cantilevered diaphragm Shear flexibility mm/kN
Sheet deformation	Profile distortion	$c_{1.1} = \frac{ad^{2.5}\alpha_3 K}{Et^{2.5}b^2}$	$c_{1.1} = \frac{ad^{2.5}\alpha_1\alpha_4 K}{Et^{2.5}b^2}$
	Shear strain	$c_{1.2} = \frac{2a(1+\nu)[1+(2h/d)]}{Etb}$	$c_{1.2} = \frac{2a(1+\nu)[1+(2h/d)]}{Etb}$
Fastener deformation	Sheet to perpendicular member fastener	$c_{2.1} = \frac{2as_p p}{b^2}$	$c_{2.1} = \frac{2as_p p}{b^2}$
	Seam fasteners	$c_{2.2} = \frac{s_s s_p (n_{sh} - 1)}{n_s s_p + \beta_1 s_s}$	$c_{2.2} = \frac{2s_s s_p (n_{sh} - 1)}{2n_s s_p + \beta_1 n_p s_s}$
	Connections to edge members	4 sides fastened $c_{2.3} = \frac{2s_{sc}}{n_{sc}}$ or 2 sides only fastened $c_{2.3} = s_{pr} + \frac{s_p}{\beta_2}$	4 sides fastened $c_{2.3} = \frac{2s_{sc}}{n_{sc}}$ or 2 sides only fastened $c_{2.3} = \frac{2}{n_p} (s_{pr} + \frac{s_p}{\beta_2})$
Total flexibility in true shear		$c' = \frac{b^2}{a^2} (c_{1.1} + c_{1.2} + c_{2.1} + c_{2.2} + c_{2.3})$	
Flange forces	Axial strain in edge members	$c_3 = \frac{n^2 b^3}{4.8EAa^2}$	$c_3 = \frac{2b^3}{3EAa^2}$
Total shear flexibility		$c = c' + c_3$	$c = c' + c_3$

The expression for $c_{1.1}$ applies for $b/d \geq 10$.

Note: here s_p is the slip in the fastening between sheeting and rafter and d is the pitch of the sheet corrugations (see Figure 5.14).

5. SHEETING ACTING AS A DIAPHRAGM (STRESSED SKIN DESIGN)

All the notations and symbols used in Table 5.10 have been specified previously, except the α_5 factor in the expression of $c_{1,1}$, which takes account of the effect of the sheeting continuity over two or more spans as illustrated in Table 5.11, and has the value of Table 5.12.

Table 5.11 – Influence of sheet length for sheeting spanning parallel to length of diaphragm (ECCS, 1995)

Separate sheet length per panel	
	$\alpha_5 = 1$
Overlapping separate sheets	
	α_5 is given by Table 5.12
Overlapping continuous sheets	
	α_5 is given by values in Table 5.12 divided by m
m	is the number of shear panels within a sheet length;
n	is the number of shear panels in the length of the diaphragm assembly;
n_1	is the number of sheet lengths in the length of the diaphragm assembly (i.e. $m \cdot n_1 = n$).

Table 5.12 – Factor α_5 to allow for sheet continuity

Number of sheet lengths n_1	α_5
2	1.0
3	0.9
4	0.8
5 or more	0.7

The mid-length deflection, v_{Ed} , of the typical panel assembly shown in Figure 5.15 can be calculated with eqn. (5.1) provided the total shear flexibility, c , is determined according to Table 5.10.

5.3.2 Design expression for shear strength of diaphragms

5.3.2.1 Sheeting spanning perpendicular to length of diaphragm

With reference to Figure 5.12, the shear strength of the shear panel assembly should normally be checked by considering failure (see §§5.2.4.2) in the end-bays panels which, in principle, are the most loaded (see Figures 5.1 and 5.2).

The ultimate shear strength of the panel, V_{ult} , associated with these failure modes, may be obtained as given in the following:

a) Seam capacity

$$V_{ult} = n_s F_s + \frac{\beta_1}{\beta_3} n_p F_p \quad (5.2)$$

where all symbols have been previously defined except:

- F_s is the design resistance (shear resistance $F_{v,Rd}$) of an individual seam fastener (e.g. bearing resistance $F_{b,Rd}$ not considered as relevant). Values are given in Table 5.5;
- F_p is the design resistance (shear resistance $F_{v,Rd}$) of an individual sheet-to-purlin fastener (e.g. bearing resistance $F_{b,Rd}$ not considered as relevant). Values are given in Table 5.5;
- $\beta_3 = 1.0$ for decking (seam fasteners in the troughs);
- $\beta_3 = (n_f - 1) / n_f$ for sheeting (seam fasteners in the crests);
- n_f is the number of sheet / purlin fasteners per sheet width (including those at the overlaps).

b) Shear connector fastener capacity (at end gables).

$$V_{ult} = n_{sc} F_{sc} \quad (5.3)$$

where F_{sc} = is the design strength of an individual sheet to shear connector (see Figure 5.6) fastener. Values are given in Table 5.5.

c) Shear connector fastener capacity (at internal rafters)

$$P_{ult} = n'_{sc} F_{sc} \quad (5.4)$$

where P_{ult} is the ultimate load at a shear panel point, i.e. $P_{ult} = a q_{ult}$, as shown in Figure 5.12, and q_{ult} is the ultimate uniformly distributed horizontal load at the level of the eaves, along the bay, a (Davies & Bryan, 1982).

With reference to Figure 5.12, the force in the end rafters is $1/2(n-1)$ times the force in the internal rafters, so the corresponding numbers of the shear connector fasteners should normally be in the same ratio, i.e. $n_{sc} = 1/2(n-1)n'_{sc}$.

d) Two sides of the shear panels fastened

For sheeting attached to the purlins only and the end rafters (see Figure 5.9 case 3):

(1) capacity of end fasteners in an internal shear panel

$$P_{ult} = \beta_2 \cdot n_p \cdot F_p \quad (5.5)$$

(2) capacity of purlin to rafter connections

$$P_{ult} = n_p \cdot F_{pr} \quad (5.6)$$

where F_{pr} is the design strength of a purlin to rafter connection for which values are given in Table 5.6.

398

e) Design shear capacity

The design shear capacity of a shear panel, V_{Rd} , may be taken as the lesser of the values of V_{ult} given by eqn. (5.2) and eqn. (5.3), and the value of V_{ult} given by:

$$V_{ult} = \frac{1}{2} P_{ult} (n-1) \quad (5.7)$$

with P_{ult} obtained from eqns. (5.4) and (5.5) or (5.6), as appropriate to the case considered.

f) Non permissible mode

The sheeting has to be checked for the following clause which refers to non permissible or non accepted failure modes in the design process. They are:

1. Sheet/purlin strength

In order to take account of the effect of combined shear and prying action by sheeting, the capacity of the sheet to purlin fasteners in shear is reduced by 40%. Hence it should be checked that:

$$V_{Rd} \leq \frac{0.6 \cdot b \cdot F_p}{p \cdot \alpha_3} \quad (5.8)$$

where p is the pitch of the sheet/purlin fasteners and α_3 can be taken obtained from Table 5.7.

2. End collapse of sheeting profile

In order to prevent collapse or gross distortions of the profile at the end of the sheeting, the following limitations on shear force should be observed:

- Every corrugation fastened at the end of the sheeting:

$$V_{Rd} \leq 0.9 \cdot f_y \cdot b \sqrt{\frac{t^3}{d}} \quad (5.9a)$$

- Alternate corrugation fastened at the end of the sheeting

$$V_{Rd} \leq 0.3 \cdot f_y \cdot b \sqrt{\frac{t^3}{d}} \quad (5.9b)$$

 399

where

- t is the net sheet thickness, excluding metallic or other coating;
- b is the depth of a shear panel in a direction parallel to the corrugations (see Figure 5.12);
- f_y is the nominal yield strength of the steel sheet;
- d is the pitch of the sheet corrugations (see Figure 5.18).

3. Shear buckling

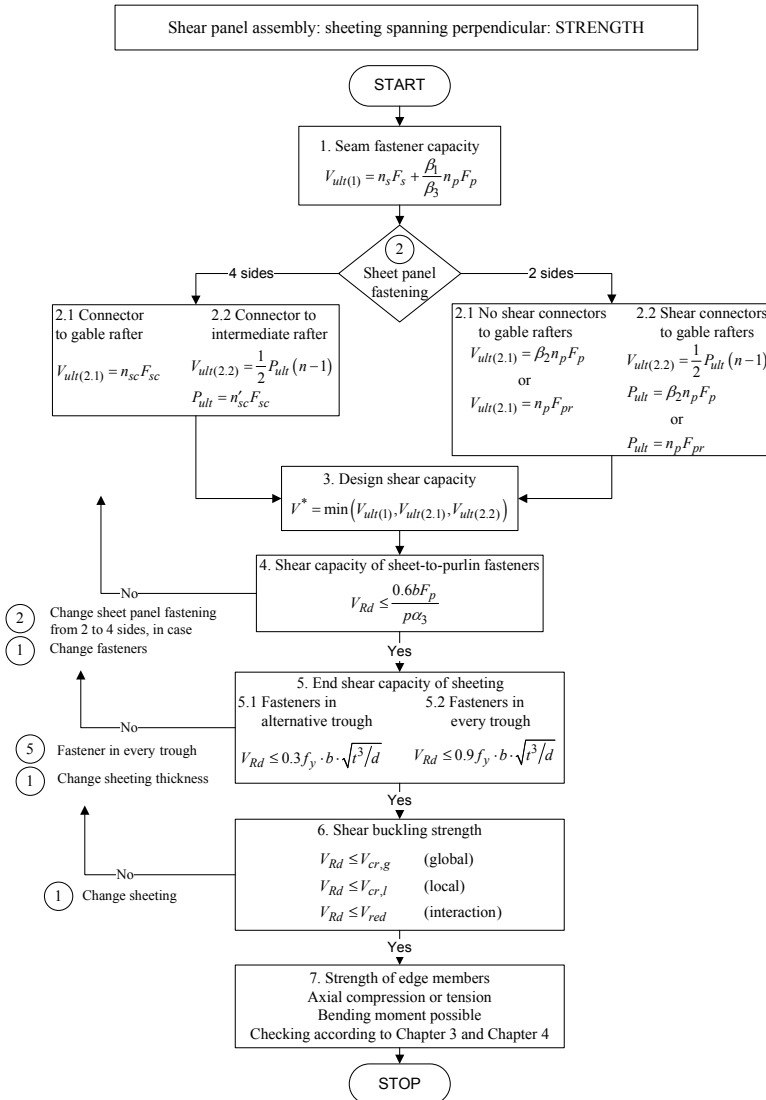
As stated in §§5.2.4.2 failure by buckling of sheeting in shear is unlikely in profiled sheets correctly fastened on supporting framing. Therefore this is the reason why buckling of sheeting in shear is considered a “non permissible” failure mode.

Flowchart 5.2 shows the design checking process for the shear strength of a panel assembly, spanning perpendicular to the length.

5. SHEETING ACTING AS A DIAPHRAGM (STRESSED SKIN DESIGN)

Shear stresses may cause (1) local buckling of wide flanges and webs of the trapezoidal sheeting and (2) global buckling of the diaphragm as a whole.

The influence of local buckling on the load bearing capacity of the sheeting under transverse loadings as well as on the diaphragm flexibility is normally negligible.



Flowchart 5.2 – Flowchart for checking the shear strength of a panel assembly, spanning perpendicular to the length (Vayas & Dubina, 2004)

The interaction of global and local shear buckling can be neglected if:

$$\frac{l}{t} \leq 2.9 \sqrt{\left(\frac{E}{f_y}\right)} \quad (5.10)$$

If $\frac{l}{t} > 2.9 \sqrt{\left(\frac{E}{f_y}\right)}$ the interaction has to be taken into account by a reduction of the global buckling strength as follows:

$$V_{red} = \frac{V_{cr,g} \cdot V_{cr,l}}{V_{cr,g} + V_{cr,l}} \quad (5.11)$$

and the design checking condition is

$$V_{Rd} \leq V_{red} \quad (5.12)$$

In the above expressions the following terms have been used:

- l is the width of the top or bottom flange of the sheeting, whichever is wider (see Figure 5.17);
- t is the net sheet thickness excluding metallic and other coating;
- E is the modulus of elasticity of steel;
- f_y is the design yield strength of steel;
- $V_{cr,g}$ is the design value of the global shear buckling strength of the diaphragm;
- $V_{cr,l}$ is the design value of the local shear buckling strength of the diaphragm;
- V_{Rd} is the design shear capacity of the diaphragm;
- V_{red} is the design value of the reduced shear buckling strength of the diaphragm under combined local and global buckling.

Calculation procedures for $V_{cr,g}$ and $V_{cr,l}$ specific to corrugated sheet diaphragms will be presented in §§5.3.2.3.

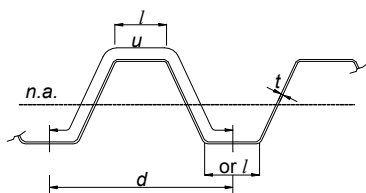


Figure 5.17 – Geometry of a single corrugation

4. Edge members

The capacity of the edge members and their connections to carry the flange forces arising from diaphragm action should be checked for an additional axial load of 25%, for the reason to avoid such a failure mode. The maximum axial load of edge purlins (see Figure 5.12), may be calculated as:

$$N_{Ed} = \frac{q \cdot L^2 \cdot \alpha_3}{8b} \quad (5.13)$$

where

- q is the distributed in-plane line load carried by the diaphragm;
- L is the length of the diaphragm assembly between braced frames;
- α_3 is a factor to allow for intermediate purlins (see Table 5.7);
- b is the depth of a shear panel in a direction parallel to the corrugations.

The purlin, either in tension or in compression, and its connections have to be checked for an axial load equal to $1.25N_{Ed}$. Bending of the purlin also has to be considered.

5.3.2.2 Sheeting spanning parallel to length of diaphragm

402

With reference to Figure 5.15, the shear strength of the shear panel assembly should normally be checked by considering failure modes in the end shear panels and at the internal rafters. The ultimate strengths V_{ult} associated with these failure modes may be obtained as follow:

a) Seam strength

$$V_{ult} = \frac{a}{b} \left(n_s F_s + \frac{\beta_1 F_p}{\beta_3} \right) \quad (5.14)$$

b) Edge member fastener strength

$$V_{ult} = \frac{a}{b} (n_{sc} F_{sc}) \quad (5.15)$$

c) Two sides of a shear panel fastened

Although not normally recommended (see Figure 5.9 case 4) this case applies to the sheeting attached to the rafters only (not to the edge members). At the end rafter:

$$V_{ult} = \frac{a}{b}(1.5 \cdot \beta_2 \cdot F_p) \quad (5.16)$$

If the value of V_{ult} given by this expression is not sufficient, shear connectors may be added to the edge members in the end shear panels. In this case the design criterion for the end shear panel is given by eqn. (5.15), and the design criterion for an internal panel is:

$$P_{ult} = \frac{a}{b}(1.5\beta_2 F_p) \quad (5.17)$$

All symbols in the above formulas have been already defined.

- d) The design shear capacity, V_{Rd} may be taken as the lower of the values of V_{ult} , given by eqn. (5.14) and eqn. (5.15) (or eqn. (5.16)). It should be checked that the capacity in other failure modes is greater than V_{Rd} as specified by eqn. (5.18) and eqn. (5.20).
- e) Non permissible modes.

1. Sheet to rafter fasteners strength

It should be checked that

$$V_{Rd} \leq \frac{0.6 \cdot a \cdot F_p}{p} \quad (5.18)$$

where a is the width of the shear panel in the direction perpendicular to the corrugations, as shown in Figure 5.15 and the other symbols are as previously defined.

2. End collapse of sheeting

The following limitations on the shear force in a shear panel should be observed:

- Every corrugation fastened at the end of the sheeting

$$V_{Rd} \leq 0.9 \cdot f_y \cdot a \sqrt{\frac{t^3}{d}} \quad (5.19)$$

- Alternate corrugations fastened at the end of the sheeting:

$$V_{Rd} \leq 0.3 \cdot f_y \cdot a \sqrt{\frac{t^3}{d}} \quad (5.20)$$

3. Shear buckling

It should be checked that the design shear capacity, V_{Rd} , is less than the reduced shear buckling strength of the sheeting, V_{red} , according to eqn. (5.12). Care should be taken to calculate correctly the global shear buckling strength, $V_{cr,g}$, which is different to that for the case of sheeting spanning perpendicular to the length of the diaphragm.

4. Edge member

The edge member and its connections should be designed in accordance with EN 1993-1-3 (CEN, 2006a) (see also Chapter 3 and 4 in this book) to carry their designated loads (e.g. the axial load coming from diaphragm action) multiplied by 1.25. The maximum axial load, N_{Ed} , for an edge member, may be taken as:

$$N_{Ed} = \frac{q \cdot L^2}{8a} \quad (5.21)$$

404

where the symbols have been defined in Figures 5.8 and 5.15. The flowchart of design process is similar to that shown in Flowchart 5.2.

5.3.2.3 Bucking strength of sheeting in shear

5.3.2.3.1 General

Design formulae for the shear buckling strength of transverse loaded webs of steel beams, stiffened and unstiffened longitudinally, have been presented in Chapter 3, §§3.8.9.

However, due to sheet-purlin interaction and the different edge conditions the specific design procedures presented in the ECCS Recommendations (ECCS, 1995) are strongly recommended for checking the shear buckling strength of diaphragm sheeting. As specified in §§5.3.2.1 shear stress may cause, in a trapezoidal sheeting acting as a diaphragm,

either the local buckling of wide flanges and webs, $V_{cr,l}$, or the global buckling of sheeting as a whole, $V_{cr,g}$. In some geometrical and mechanical conditions, with reference to the criterion related to eqn. (5.10), the interaction of global and local buckling modes may occur. The effect of these interactions is the reduction of buckling strength of the diaphragm panel, as shown in eqn. (5.11).

5.3.2.3.2 Global shear buckling

The design value of the global shear buckling strength of the sheeting spanning perpendicular to diaphragm length may be calculated from:

$$V_{cr,g} = 14.4 \cdot \frac{(n_p - 1)^3}{b} \cdot \sqrt[4]{D_x \cdot D_y^3} \quad (5.22)$$

where D_x and D_y are the orthogonal bending stiffness given by:

$$D_x = \frac{E \cdot t^3 \cdot d}{12 \cdot (1 - \nu^2) \cdot u} \quad (5.23)$$

$$D_y = \frac{E \cdot I}{d} \quad (5.24)$$

where

- E is the modulus of elasticity of steel;
- t is the net sheet thickness;
- d is the pitch of the corrugation (see Figure 5.17);
- ν is the Poisson's ratio for steel (0.3);
- u is the perimeter length of a complete single corrugation of pitch d (see Figure 5.17);
- I is the second moment of area of a single corrugation about its neutral axis (see Figure 5.17);
- b is the depth of a shear panel in a direction parallel to the corrugations;
- n_p is the number of the purlins (edge + intermediate).

In the case of sheeting spanning parallel to diaphragm length, the following relation must be used:

- for fasteners in every corrugation:

$$V_{cr,g} = 28.8 \cdot \frac{a}{b^2} \cdot \sqrt[4]{D_x \cdot D_y^3} \quad (5.25a)$$

- for fastener in alternate corrugations:

$$V_{cr,g} = 14.4 \cdot \frac{a}{b^2} \cdot \sqrt[4]{D_x \cdot D_y^3} \quad (5.25b)$$

where a is the width of a shear panel in direction perpendicular to the corrugations.

5.3.2.3.3 Local shear buckling

Certain sheeting profiles have a relatively wide trough (flange) which may or may not be stiffened as shown in Figure 5.18. When the trough element is unstiffened (or not sufficiently stiffened) the failure of the diaphragm may be initiated by local shear buckling of the trough element, and the corresponding design value of the local shear buckling strength may be calculated from:

$$V_{cr,l} = 4.83 \cdot b \cdot t \cdot E \cdot \left(\frac{t}{l}\right)^2 \quad (5.26)$$

where the notations are specified in Figures 5.17 and 5.18.

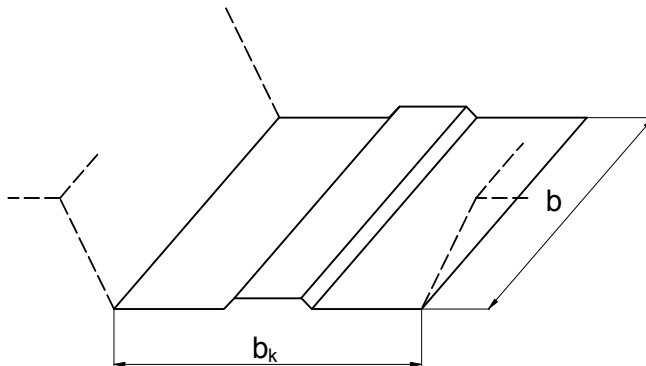


Figure 5.18 – Trough element which may be subjected to load shear buckling

If the trough element is stiffened, the design values of the local shear buckling may be conservatively taken as:

$$V_{cr,l} = 36 \cdot \frac{b}{b_k^2} \sqrt[4]{D_x \cdot D_y^3} \quad (5.27)$$

where, in addition to the terms defined above:

b_k is the width of the trough element (see Figure 5.18);

$$D_x = \frac{E \cdot I_f}{b_k};$$

$$D_y = \frac{E \cdot t^3}{10.92};$$

I_f is the second moment of area of the trough element about its horizontal axis.

5.3.2.4 Effect of combined loads

As stated in §§5.2.1, all sheeting that also forms a part of stressed skin diaphragm shall first be designed for its primary purpose in bending under transverse loading. To ensure that any deterioration of the sheeting would be apparent in bending, due to the fact the stressed skin action is activated, it should be verified that the shear stress due to diaphragm action does not exceed $0.25f_y/\gamma_{M1}$, where f_y is the yield strength of base material of sheeting, and $\gamma_{M1}=1.1$.

To simplify the design process, it may be assumed that the effect of normal loads, both downward (e.g. dead and imposed load) and upward (e.g. wind suction load), should not be taken into account in calculating the diaphragm shear flexibility or strength.

When fasteners are subjected to combined shear and prying action by diaphragm action in the sheeting, and to direct tensile load by transverse loading of the sheeting (e.g. wind suction), the fasteners must be checked according to the related interaction eqn. (7.2) given in §§7.4.2.1.

5.3.3 Diaphragms with openings

Small openings, totalling no more than 3% of the area in each shear panel, may be ignored for the purpose of calculating the diaphragm strength and stiffness. Larger openings may be of two types:

- (a) discrete openings (Figure 5.19a);

(b) strip openings (Figure 5.19b).

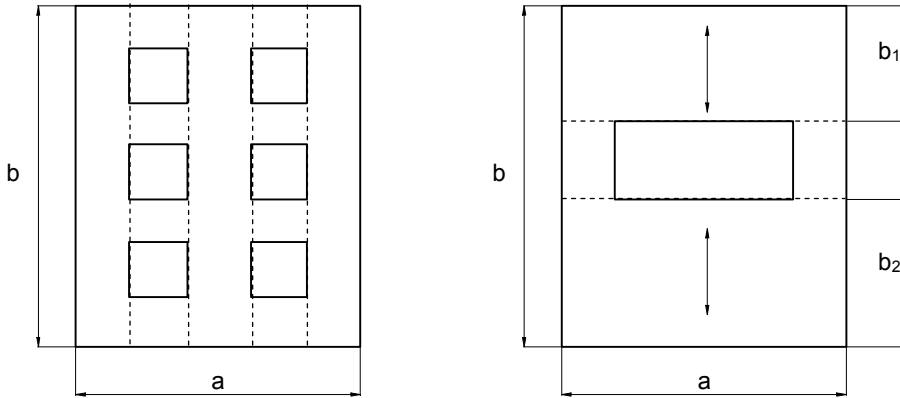


Figure 5.19 – Openings in diaphragm: a) discrete openings; b) strip openings

5.3.3.1 Discrete openings

5.3.3.1.1 Requirements for discrete openings

For discrete openings in diaphragms the following requirements should be fulfilled:

- (a) Openings should be bounded on all four sides by steel trimmers attached to the supporting structure;
- (b) The sheeting should be fixed in every trough to trimmers running perpendicular to the corrugation and at the spacing not greater than 300 mm to trimmers running parallel to the corrugations;
- (c) In the direction perpendicular to the corrugations, the adjacent sheet widths between openings should be equal to or greater than the width of the opening;
- (d) In the direction parallel to the corrugations, the total openings should not exceed 25% of the depths of the diaphragm;
- (e) The requirements (c) and (d) result in a maximum area of openings of 12.5 % of the area in each shear panel. Openings up to 15% of the area may be allowed if further detailed calculations are made in accordance with reference (Davies & Bryan, 1982).

For a diaphragm assembly in which some shear panels contain openings and others do not, the expression for deflection calculated

according to eqn. (5.1) is not applicable. In such cases the mid-length deflection should be calculated as sum of the product of the shear force in each shear panel and the shear flexibility of the panel, considering half the length of the diaphragm.

5.3.3.1.2 Flexibility of diaphragms with discrete openings

The increase in the flexibility of a diaphragm due to the presence of openings may be taken into account by applying a multiplying factor, μ , to the value of shear flexibility, c , obtained using Tables 5.2 and 5.10. The value of this multiplying factor is:

- Fasteners in every corrugation

$$\mu = \frac{1}{1 - 4 \cdot \left(\frac{h}{50}\right)^{0.5} \cdot \left(\frac{A_d}{a \cdot b}\right)} \quad (5.28a)$$

- Fasteners in alternate corrugation

$$\mu = \frac{1}{1 - 2.5 \cdot \left(\frac{h}{50}\right)^{0.5} \cdot \left(\frac{A_d}{a \cdot b}\right)} \quad (5.28b)$$

where

- h is the height of the profile [mm] (e.g. the depth of corrugation);
- A_d is the total area of openings in a shear panel;
- a is the width of the shear panel;
- b is the depth of the shear panel.

5.3.3.1.3 Strength of diaphragms with discrete openings

For diaphragms with openings conforming to §§5.3.3.1.1 and a uniform spacing of seam fasteners throughout, the maximum reduction in diaphragm strength may be taken as 50%. To avoid a reduction in diaphragm strength, the number of seam fasteners on a seam interrupted by an opening should be doubled, or openings should be precluded from the end 25% of the length of the building.

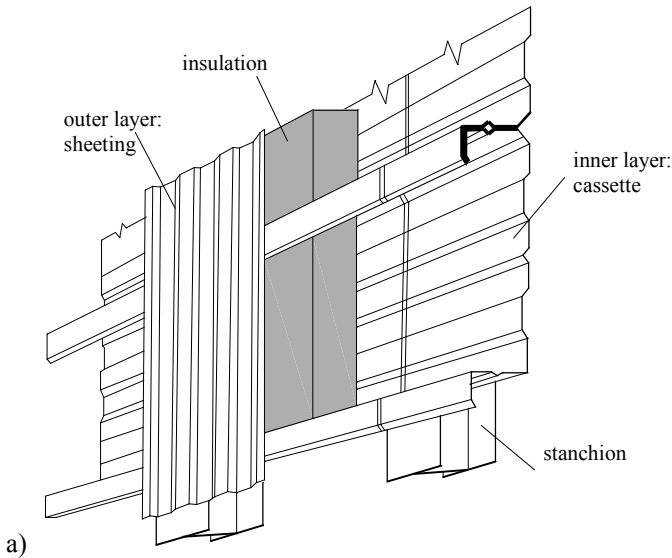
5.3.3.2 Strip openings

Diaphragms with strip openings should comply with the requirements of §5.3.3.1.1(c). Provided b_1 and b_2 (see Figure 5.19b) do not differ more than 20% of the effective depth may be taken as the sum of b_1 and b_2 . In other cases the diaphragm may be conservatively designed by taking the effective depth as the greater of b_1 and b_2 .

5.3.4 Two skin envelopes

This section is concerned with the form of construction which consists of two layers of metal sheeting with loose insulation placed between them. The two layers are connected together either directly, if for example one of the layers is a cassette (see Figure 5.20a), or sheeting is fixed on both sides of the purlins (see Figure 5.20c), or indirectly through spacing elements (see Figure 5.21b).

Testing has demonstrated that the outer skin can provide a significant increase in strength even when the flexibility of the spacing system results in little additional stiffness in the elastic range of loading.



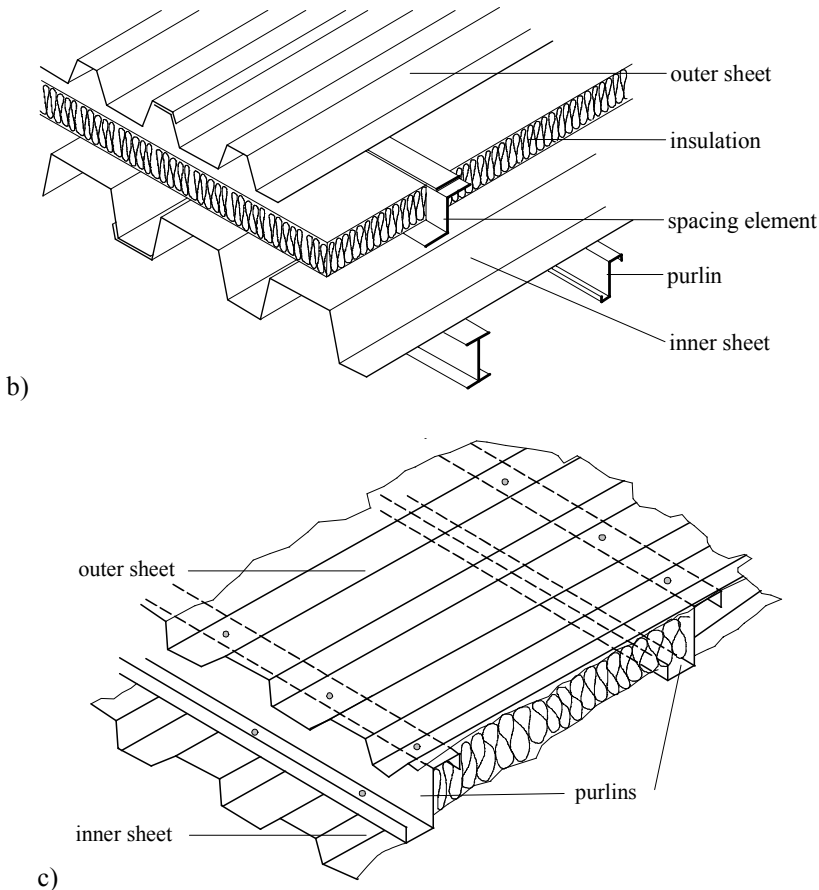


Figure 5.20 – Two skin envelope examples

In regard to the case illustrated in Figure 5.20b it should be noticed that conventional liner tray systems with a thin inner skin generally perform poorly with regard to in-plane shear because the in-plane shear buckling strength of elements with large b/t ratios is relatively low. If it is required to take advantage of the in-plane stiffness of such systems, careful design is required in order to avoid slender web or flange elements in the profile of the inner skin.

In fact both flexibility and strength of each of the two skins can be determined following the rules given in this chapter independently of each other.

In general, one skin (usually the inner) will be connected directly to the supporting members. In such cases it is safe to ignore the contribution of

the other skin and to base the stressed skin design on the connected skin only.

If the spacing system provides a connection between the two skins, then it is permissible to share the in-plane loads between the two skins according to their relative flexibilities taking into account the flexibility of the spacer system. This is the case of the system of Figure 5.20b, for which is necessary to determine the flexibility of the spacer system by testing, while for the case from Figure 5.20c, the sharing in-plan loads can be done directly.

5.4 INTERACTION OF THE SHEAR DIAPHRAGMS WITH SUPPORTING FRAMING

5.4.1 General

If the frames shown in Figures 5.1 and 5.2 are pin jointed, the roof diaphragm carries all the side loads. The diaphragm shear panel arrangements are as shown in Figures 5.7 and 5.8, and the design criteria for strength apply to the end panels, while the deflection is checked at midspan, if necessary, additional bracing can be added, but the two systems coupled to work together.

412

In case of moment resisting frames, stressed skin action in the sheeting envelopes of the building should be considered as tending to restrain joint movements of the supporting frames, with a consequent reduction in the associated forces and moments. Stressed skin action should not be assumed to resist forces and moments out of the plane of the sheeting.

With reference to Figure 5.21, stressed skin action may be seen to have no effect on the non-sway or non-spread moments in a structure, but it may have considerable effect on the sway or spread moments. The effect may be shown to depend on the in-plane flexibility of the shear panel relative to the frame flexibility.

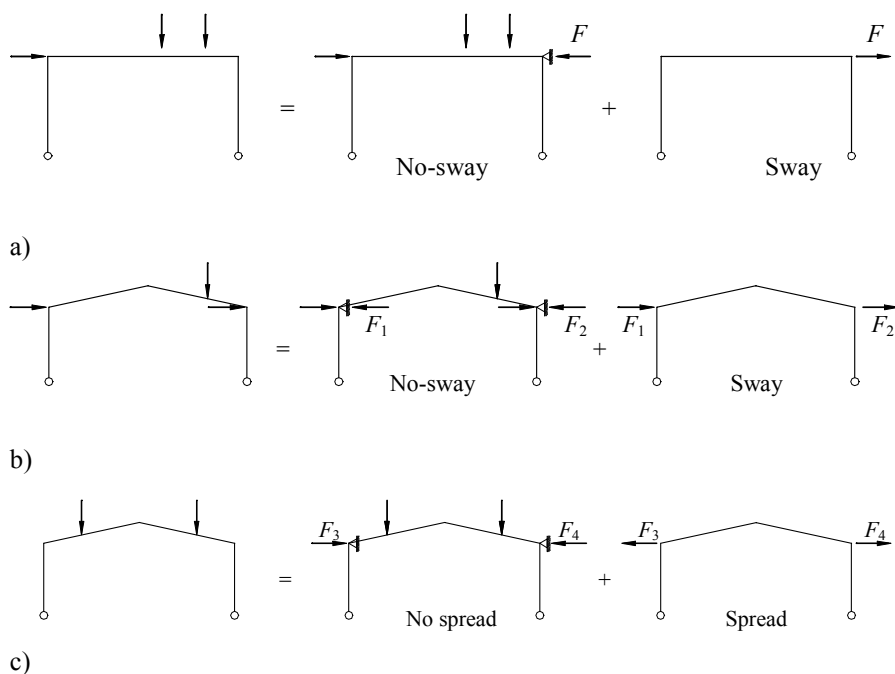


Figure 5.21 – Portal moment resisting frames: a) Sway in a rectangular frame; b) Sway in pitched roof frame; c) Spread in pitched roof frame

The treatment given in this section applies only to single-bay flat roof frames and to symmetrical single bay pitched roof frames. It assumes that all bays in a building are similar, that all shear panels are similar and that all foundations and other conditions are similar. Both elastic and plastic design of framing can be considered in accordance with EN1993-1-1 (CEN, 2005a) criteria. For multi-bay frames, or for cases where the above conditions are not met, computer methods should be employed.

5.4.2 Elastic design of framing

5.4.2.1 Rectangular frames: all frames loaded

The shear flexibility c of a shear panel of sheeting is defined as the shear deflection per unit load (see Figure 5.22a) and may be calculated according to §§5.3.1. The frame flexibility k of a rectangular frame is the eaves deflection per unit horizontal eaves load (see Figure 5.22b) and may be calculated by normal elastic methods. The relative flexibility is defined as

5. SHEETING ACTING AS A DIAPHRAGM (STRESSED SKIN DESIGN)

$r = c/k$. If r is large (flexible sheeting or stiff frames) then the sheeting will have a small stiffening effect; if r is small (stiff sheeting or flexible frames) then the sheeting will have a large stiffening effect.

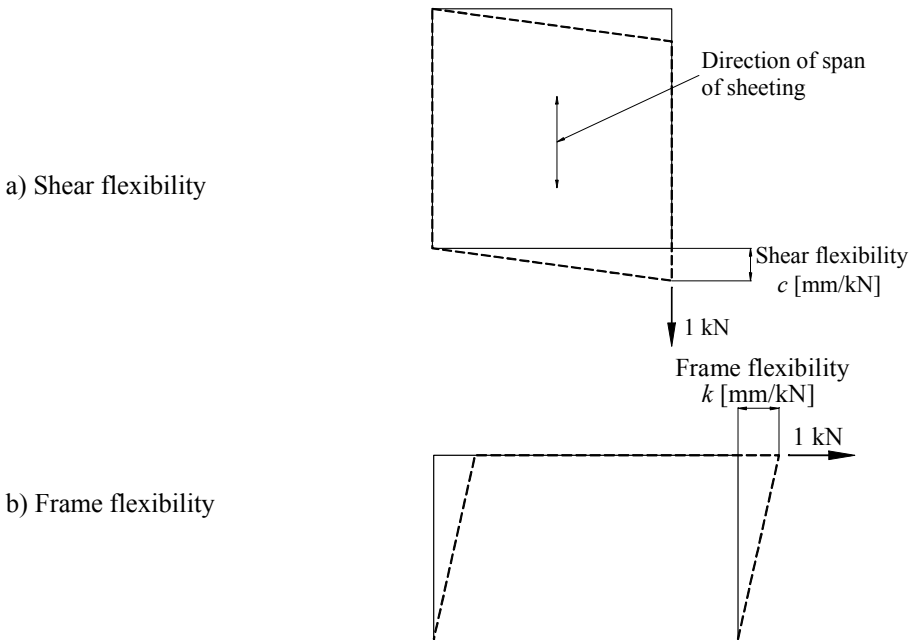


Figure 5.22 – Definition of shear and sway frame flexibility

The distribution of load between the diaphragms and the frames depends on r , or the number of panels in the length of the building, and the position of the plane in the building (see Figure 5.23a). Table 5.13 gives the reduction factor, η , to be applied to the sideway for a small value of r . The full range values of η in terms of r ($r = 0.01$ to 2.00) are given in (Davies & Bryan, 1982), while the related mathematical expression can be found in (ECCS, 1995).

The bending moment in a clad rectangular frame, M_c may be expressed as:

$$M_c = M_{n-sw} + \eta \cdot M_{sw} \tag{5.28}$$

where

- M_{n-sw} is the non-sway bending moment in current frame;
- M_{sw} is the sway bending moment in current frame.

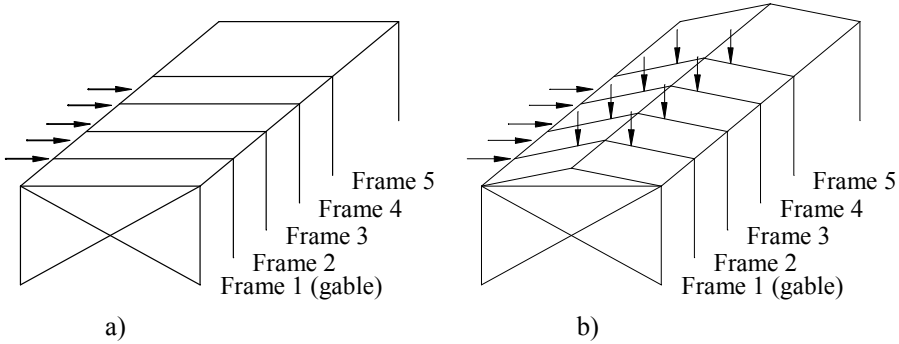


Figure 5.23 – Numbering of frames in clad building

The sway force on the clad frame is $\eta \times$ (sway force on the current frame), and the sway force on the sheeting is $(1-\eta) \times$ (sway force on the current frame).

5.4.2.2 Pitched roof frames: all frames loaded

The in-plane shear flexibility of a shear panel of sheeting, c , may be calculated according to §§5.3.1, taking the depth of the shear panel as the length of one roof slope. If θ is the angle of the rafter to the horizontal, the horizontal shear flexibility, c_h , is given by $c_h = c \cdot \sec^2 \theta$.

The general sway of the frame may be divided into sway and spread. The frame flexibility due to sway, k_{sw} , is defined in Figure 5.24a and the frame flexibility due to spread, k_{sp} , is defined in Figure 5.24b. The corresponding relative flexibilities are $r_{sw} = c_h/k_{sw}$ and $r_{sp} = c_h/k_{sp}$. The reduction factors, η_{sw} and η_{sp} , may be obtained for each frame in a building (see Figure 5.23b) from Table 5.13.

The moments in a clad pitched roof portal frame, M_c , may be expressed as:

$$M_c = M_{n-sw} + \eta_{sw} \cdot M_{sw} + \eta_{sp} \cdot M_{sp} \tag{5.30}$$

where

- M_{n-sw} is the non-sway bending moment in current frame;
- M_{sw} is the sway bending moment in current frame;
- M_{sp} is the spread bending moment in current frame.

5. SHEETING ACTING AS A DIAPHRAGM (STRESSED SKIN DESIGN)

Table 5.13 – Values of the reduction factor $\eta = \eta(r)$

No. of frames in building	Frame number (Fig. 5.23)	Values of relative flexibility $r = c/k$														
		0.25	0.30	0.35	0.40	0.45	0.50	0.60	0.70	0.80	0.90	1.00	1.50			
3	2	0.111	0.130	0.149	0.167	0.184	0.200	0.231	0.259	0.286	0.310	0.333	0.129			
	4	0.200	0.231	0.259	0.286	0.310	0.333	0.375	0.412	0.444	0.474	0.500	0.600			
5	2	0.265	0.301	0.333	0.362	0.388	0.412	0.454	0.490	0.521	0.548	0.571	0.659			
	3	0.347	0.392	0.432	0.468	0.500	0.529	0.580	0.622	0.658	0.688	0.714	0.805			
6	2	0.310	0.347	0.379	0.407	0.432	0.455	0.494	0.526	0.554	0.579	0.600	0.677			
	3	0.448	0.497	0.540	0.576	0.608	0.636	0.684	0.721	0.752	0.778	0.800	0.871			
7	2	0.340	0.375	0.406	0.432	0.456	0.477	0.513	0.543	0.569	0.591	0.611	0.683			
	3	0.515	0.563	0.604	0.638	0.667	0.692	0.734	0.767	0.793	0.815	0.833	0.892			
8	4	0.569	0.620	0.663	0.698	0.728	0.754	0.795	0.827	0.852	0.873	0.889	0.938			
	2	0.359	0.393	0.421	0.447	0.469	0.488	0.522	0.551	0.575	0.597	0.615	0.685			
9	3	0.558	0.603	0.641	0.672	0.698	0.721	0.758	0.787	0.811	0.830	0.846	0.898			
	4	0.646	0.695	0.734	0.765	0.792	0.814	0.849	0.875	0.895	0.911	0.923	0.959			
10	2	0.371	0.403	0.430	0.454	0.475	0.494	0.527	0.554	0.578	0.599	0.617	0.686			
	3	0.585	0.627	0.662	0.690	0.715	0.733	0.770	0.796	0.818	0.836	0.851	0.901			
10	4	0.695	0.739	0.774	0.802	0.825	0.844	0.874	0.896	0.913	0.926	0.936	0.966			
	5	0.729	0.773	0.808	0.835	0.857	0.875	0.903	0.923	0.938	0.949	0.957	0.981			
10	2	0.379	0.409	0.436	0.458	0.479	0.497	0.529	0.556	0.579	0.599	0.618	0.686			
	3	0.602	0.641	0.673	0.700	0.723	0.743	0.775	0.800	0.821	0.838	0.853	0.901			
10	4	0.725	0.766	0.797	0.822	0.843	0.860	0.886	0.906	0.920	0.932	0.941	0.968			
	5	0.780	0.820	0.850	0.873	0.891	0.904	0.929	0.944	0.956	0.964	0.971	0.987			

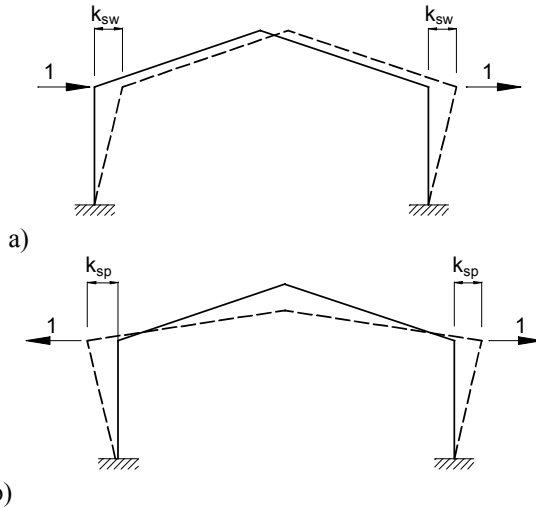


Figure 5.24 – Frame flexibilities for a pitched roof portal frames

The procedures described by eqn. (5.29) and eqn. (5.30) may be applied only to symmetrical frames. For other cases it is necessary to use computer analysis.

5.4.2.3 One frame loaded

Stressed skin action in a sheeted building may be shown to be especially effective if only one frame is loaded. The effect of sheeting is to distribute the load to a number of frames. Table 5.14 gives the factor by which the values η in Table 5.13 should be divided, if only one frame is loaded. The procedure given may be applied only to symmetrical frames.

Table 5.14 – Factors by which η (see Table 5.13) should be divided for central frame only loaded

Value of r	Number of frames in building									
	3	4	5	6	7	8	9	10	11	12
0.00	1.00	1.50	2.00	2.50	3.00	3.50	4.00	4.50	5.00	5.50
0.01	1.00	1.50	2.00	2.49	2.98	3.47	3.95	4.43	4.90	5.37
0.02	1.00	1.50	1.99	2.48	2.96	3.43	3.90	4.36	4.81	5.24
0.03	1.00	1.49	1.99	2.46	2.94	3.40	3.86	4.29	4.72	5.12
0.04	1.00	1.49	1.98	2.45	2.92	3.37	3.81	4.23	4.64	5.01
0.06	1.00	1.49	1.97	2.43	2.89	3.31	3.73	4.10	4.48	4.81
0.08	1.00	1.48	1.96	2.41	2.85	3.25	3.65	3.99	4.34	4.63
0.10	1.00	1.48	1.95	2.39	2.82	3.20	3.57	3.89	4.21	4.46
0.12	1.00	1.47	1.94	2.36	2.79	3.14	3.50	3.79	4.08	4.31

5. SHEETING ACTING AS A DIAPHRAGM (STRESSED SKIN DESIGN)

0.14	1.00	1.47	1.93	2.34	2.75	3.09	3.43	3.70	3.97	4.18
0.16	1.00	1.46	1.93	2.33	2.72	3.05	3.37	3.62	3.87	4.05
0.18	1.00	1.46	1.92	2.31	2.69	3.00	3.31	3.54	3.77	3.94
0.20	1.00	1.45	1.91	2.29	2.67	2.96	3.25	3.47	3.68	3.83
0.25	1.00	1.44	1.89	2.24	2.60	2.86	3.12	3.30	3.48	3.60
0.30	1.00	1.43	1.87	2.20	2.54	2.77	3.01	3.16	3.31	3.41
0.35	1.00	1.43	1.85	2.17	2.48	2.69	2.90	3.03	3.16	3.24
0.40	1.00	1.42	1.83	2.13	2.43	2.62	2.81	2.92	3.03	3.10
0.45	1.00	1.41	1.82	2.10	2.38	2.55	2.72	2.82	2.92	2.97
0.50	1.00	1.40	1.80	2.07	2.33	2.49	2.65	2.73	2.82	2.86
0.60	1.00	1.38	1.77	2.01	2.25	2.38	2.51	2.58	2.65	2.68
0.70	1.00	1.37	1.74	1.96	2.18	2.29	2.40	2.45	2.50	2.53
0.80	1.00	1.36	1.71	1.91	2.11	2.21	2.30	2.34	2.39	2.40
0.90	1.00	1.34	1.69	1.87	2.05	2.13	2.22	2.25	2.29	2.30
1.00	1.00	1.33	1.67	1.83	2.00	2.07	2.14	2.17	2.20	2.21
1.50	1.00	1.29	1.57	1.69	1.80	1.84	1.88	1.89	1.90	1.91
2.00	1.00	1.25	1.50	1.58	1.67	1.69	1.71	1.72	1.73	1.73

Note: The full table (e.g. for $r=0.00$ to 2.00) can be found in (Davies & Bryan, 1982), while the related mathematical expression are given in (ECCS, 1995).

5.4.3 Plastic design of framing

Plastic design of the substructure should be in accordance with EN1993-1-1:2005, except that it should be assumed that the effect of stressed skin diaphragm is to modify the actions in frames of a clad building as shown in §§5.4.2.1 and §§5.4.2.2. The designer should satisfy himself that second order effects are not significant or should carry out a rational analysis taking second order effects into account.

Provided that the criterion for the least shear strength of the panel of sheeting is by tearing at the seam fastener or sheet / shear connector fasteners then the shear panel will generally be able to sustain large shear deformations at the design shear capacity. In this case, at the ultimate load of a building, collapse will occur in all intermediate frames simultaneously and at this stage the force on each frame will be the same.

5.4.3.1 Rectangular frames

For a clad flat roof building (see Figure 5.25a) the restraining force R provided by the sheeting is the same at each intermediate frame at collapse (see Figure 5.25b) and is given by:

$$R = \frac{2 \cdot V_{Rd}}{n - 1} \quad (5.31)$$

where

V_{Rd} is the design shear capacity of a shear panel (see Figure 5.25b);

n is the number of shear panels in the length of the building.

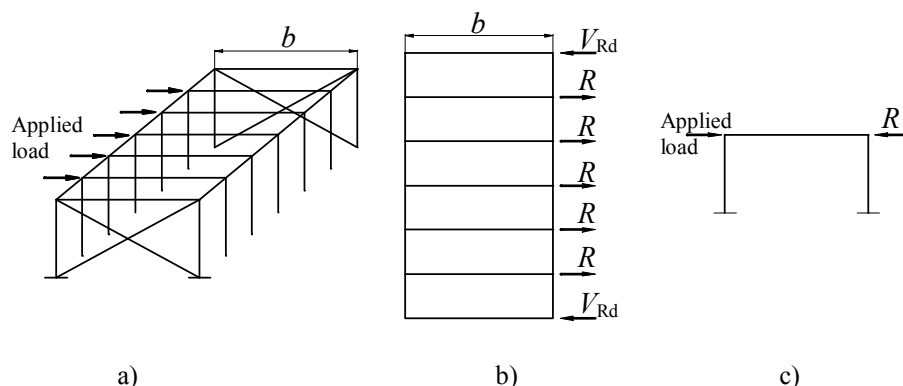


Figure 5.25 – Distribution of horizontal (side) loads for plastic design of clad rectangular portal frames

Each frame should then be plastically designed under a net sideways force of (applied load R) as shown in Figure 5.25c.

5.4.3.2 Pitched roof frames

For a clad pitched roof building under side load (see Figure 5.26a) or vertical load (see Figure 5.27a) the in-plane restraining force R provided by the sheeting on each roof slope is the same at each intermediate frame at collapse (see Figure 5.26b and 5.26c) and is given by:

$$R = \frac{2 \cdot V_{Rd}}{n - 1} \quad (5.32)$$

The horizontal component of the restraining force R_h is given by:

$$R_h = R \cdot \cos \theta \quad (5.33)$$

where θ is the angle of the rafter with the horizontal.

5. SHEETING ACTING AS A DIAPHRAGM (STRESSED SKIN DESIGN)

For a clad building under side load, each frame should be plastically designed under the net sideway force of (applied load – R_h), as shown in Figure 5.26c.

For a clad building under vertical load, each frame should be plastically designed under the action of a vertical applied load and the horizontal restraining force at eaves, as shown in Figure 5.27c.

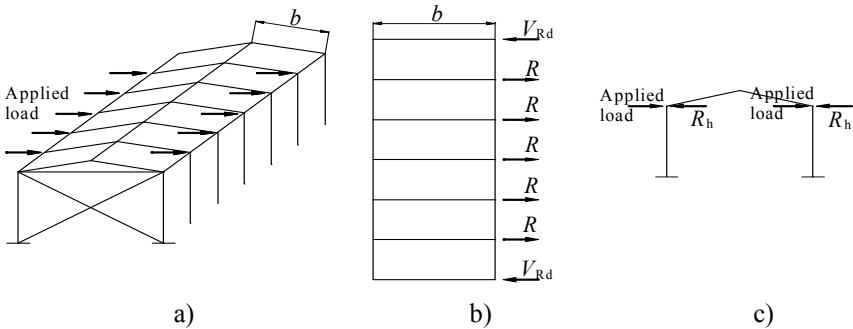


Figure 5.26 – Distribution of horizontal (side) loads for plastic design of clad pitched roof portal frames

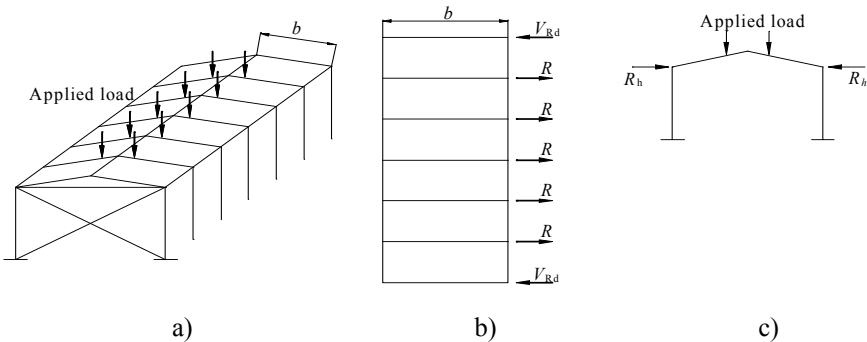


Figure 5.27 – Distribution of vertical loads for plastic design of clad pitched roof portal frames

5.4.4 Modelling of diaphragm effect for frame analysis

The analysis of clad frames given in (Davies & Bryan, 1982) may only be applied to single-bay flat roof frames and to symmetrical single-bay pitched roof frames. For other cases, it is necessary to use computer analysis. Any program suitable for the analysis of plane frames may be used. The procedure is given with reference to Figure 5.28.

Each intermediate frame is assumed to be a plane rigid-jointed frame pinned or fixed at the base. The individual frames are connected together by sheeting panels, the shear flexibility for each is given by the single quantity c . The computer analysis consist of moving the individual frames close together and replacing the sheeting panels with an equivalent tensile spring (or tie) of the same flexibility c , as shown in Figure 5.28a.

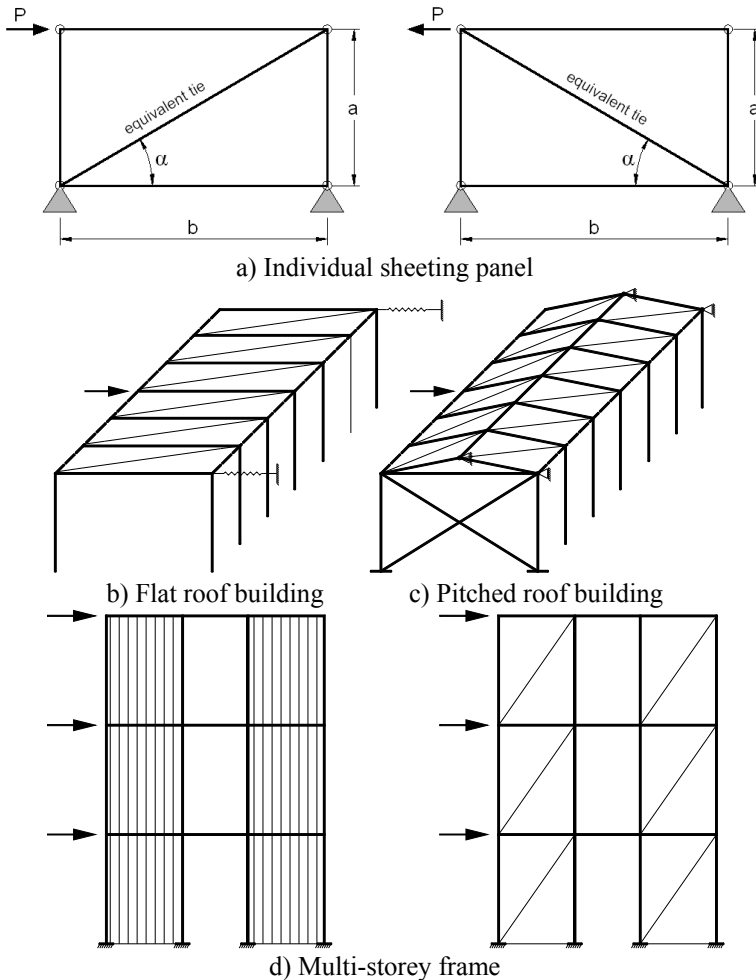


Figure 5.28 – Modelling of diaphragms for frame analysis

The equivalent spring may be modelled as a member of length $L = \sqrt{a^2 + b^2}$, modulus of elasticity E and equivalent cross section area A given by:

$$A = \frac{1}{\cos^3 \theta} \cdot \left(\frac{b}{c \cdot E} \right) = \frac{L^3}{c \cdot b^2 \cdot E} \quad (5.34)$$

Both roof and wall panels can be modelled in such a way.

Flexible end gables can be modelled as shown in Figure 5.28b, and rigid end gables may be modelled as shown in Figure 5.28c.

Figures 5.28b and 5.28c show the individual frames slightly apart for illustrative purpose, but computationally there is no reason why they cannot be coincident. If the frames are considered to be coincident, the complete three-dimensional structure reduces to a plane frame in which there are a number of joints with the same coordinates and a number of members in the same position. This simplification does not invalidate the use of a plane frame program to analyse the clad structure.

A multi-storey frame with in-filled sheeting panels can be modelled as shown in Figure 5.28d. A similar procedure can be applied to floor decks.

5.5 DIAPHRAGM ACTION OF SANDWICH PANELS

A sandwich panel is, according to the definition given in the European Recommendations for Sandwich Panels (ECCS, 2001), a composite construction of layered materials which comprises outer facings of rigid material (usually sheet metal) and an adhesively bonded lightweight core material(s) which provides the insulation and other mechanical properties. This enables panels to achieve large span/weight ratios with a high level of thermal insulation. The facings may be of colour coated steel, aluminium or wood, or they may be non-metallic such as plywood particle board or glass reinforced concrete. The core may be made of cork, balsa wood, rubber, solid plastic material (polyethylene), rigid foam material (polyurethane, polystyrene, phenolic foam), mineral wool slabs or from honeycombs of metal or even paper.

This possibility of combining materials to form composite panels enables optimum designs to be produced by particular applications. In composite panels, the positive properties of the individual materials can be combined and the negative properties can be eliminated.

Sandwich panels with thin steel or aluminium facings with low density plastic or mineral wool cores have a particular combination of properties that make them ideal for use as walls and roofs.

Figure 5.29 shows a typical roof panel. The shape with strongly profiled outer face is essentially because, until recently, it was necessary to consider that the loads, particularly the long term loads due to self-weight and snow, are carried entirely by the profiled face. Now, flat or lightly profiled panel can also be used in roof constructions, provided that the effect of creep of the core can be calculated (Davies, 2001). As shown in Figure 5.29, the longitudinal joints are usually lapped in a similar manner to conventional trapezoidally profiled sheeting. Side laps are usually fastened by either screws or blind rivets through the overlapping sheets at 0.5-1.0 meter centres. The panels are fastened to the supporting structure by means of self-tapping or self-drilling screws which usually pass through the top flange of the ribs. More recently, bottom flange fixing, using screws with scaling washers is becoming increasingly common.

As background documents for designing sandwich panel structures, the text book prepared by the International Council for Building Research, Studies and Documentations (CIB), Commission W58, titled "Lightweight Sandwich Construction" (Ed. Davies JM, 2001) and the recent European Recommendations for Sandwich Panels (ECCS, 2001), edited by a Joint Working Group composed of the ECCS Technical Committee TC 7.9 and CIB working commission W56, are recommended.

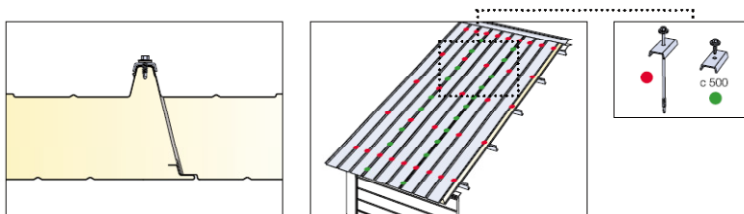


Figure 5.29 – Typical roof panel

A series of sandwich panels fixed continuously together and to the supporting structure constitutes a very rigid sheet that has the potential to carry large shear loads in the plane of the sheet with small deformations. This physical function of a series of sandwich panels is called 'diaphragm' or 'stressed skin' action. The shear stiffness and the shear resistance in the plane of the sandwich panels can be utilized in stabilising the frames of buildings against either horizontal or vertical loads. They may also be utilised in stabilising structural elements such as cold-formed purlins against the different buckling failure modes. This in-plane shear stiffness may also be

activated in certain types of shell structures and in folded plate roof construction. Depending primarily on the connections between adjacent sandwich panels and between the panels and the supporting structure, the in-plane shear stiffness of walls and roofs may take part in stabilising the frame of a building regardless of whether or not the sandwich panels have been designed for that function. Therefore, the in-plane shear stiffness and the resistance are important characteristics of sandwich panels mounted in large continuous areas in the walls and roofs of buildings.

Sandwich wall panels are usually only fastened to the supporting structure and are not connected to each other along the longitudinal joints. It follows that wall panels have a relatively low strength and a rather large flexibility with respect to in-plane shear forces (see Figure 5.30). An in-plane shear wall becomes much more rigid if the adjacent sandwich panels can be connected together along the longitudinal joints. This is especially true if the span of the sandwich panels is large.

In roof panels, the typical seam fasteners in the external faces connect the adjacent panels lightly together. The in-plane shear rigidity is dependent on the location, number and type of the fasteners in the longitudinal joints between the adjacent sandwich panels and in the joints between the panels and the supporting structure.

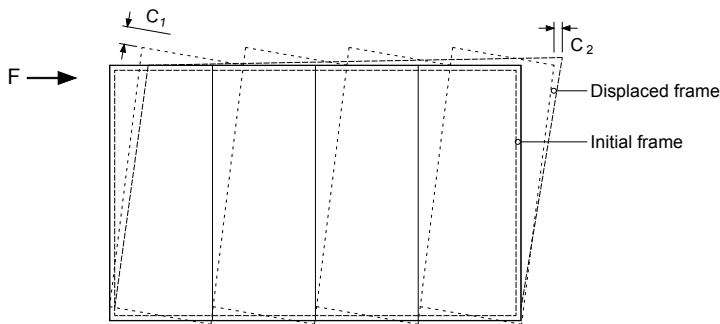


Figure 5.30 – In-plane shear deformations in the longitudinal joints between sandwich panels, C_1 and in the edge joints between the sandwich panels and the supporting structure, C_2 (Davies, 2001)

If the sandwich panels are fixed to the supporting structure with screws passing through the full thickness of the panel, it is usually the shear strength of the shafts of the screws in the lower face which determines the in-plane stiffness and the resistance. If, as is usually the case, the lower face

is relatively thin, the panel assembly is likely to have a low shear resistance. The in-plane shear stiffness and the resistance can be increased by fixing both the faces together and, furthermore, fixing them directly to the supporting structure. This generally requires additional load-bearing components in the longitudinal seams as shown in Figure 5.31.

In order to analyse the stresses in the faces and in the fastenings of sandwich panels in shear, the displacements of each single sandwich panel relative to the supporting structure must be determined. The in-plane displacements and rotations depend mainly on the shear flexibility of the fastenings in the longitudinal joints between the adjacent sandwich panels and in the joints between the sandwich panels and the supporting structure as shown in Figure 5.30. The flexibilities of the fastenings have to be determined experimentally. From the experimental, and usually non-linear, shear load-deformation curves, tangent modulus values are determined to represent the shear flexibilities of the fastenings. In the analyses, the shear deformations have to be limited in order to avoid plastic deformations at the serviceability limit state. In some rare cases, the shear flexibility of the sandwich panel itself and the deformations in the supporting structure may also have an influence on the stresses in the face layers and in the fastenings. Useful guidelines for the analysis of the shear rigidity and the resistance of sandwich panels are also given in the European Recommendations for the application of metal sheeting acting as a diaphragm (ECCS, 1995).

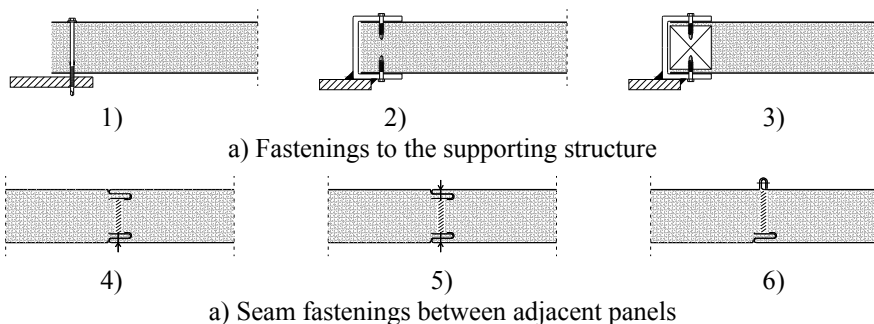


Figure 5.3 – In-plane shear stiffness and the resistance depend on the fastening in the edges of the sandwich panels. 1) Fastening with screws through the complete panel; 2) fastening of both faces through an additional edge joint profile; 3) strengthening of the edge joint by timber rails which have been glued between the face sheets together with fastening in the longitudinal seams; 4) fasteners in one face layer only; 5) fasteners in both face layers; 6) fasteners in the standing seam of the external face of a roof panel (Davies, 2001)

5. SHEETING ACTING AS A DIAPHRAGM (STRESSED SKIN DESIGN)

The in-plane shear resistance of a sandwich panel wall or roof is typically determined by a shear failure in a fastening as a result of local tearing of one of the face sheets or shear failure of the fastener itself. If the longitudinal joints have been strengthened and connected together with a large number of screws, the shear resistance may, in rare cases, also be limited either by global shear buckling of the complete sandwich panel assembly or by a local shear buckling failure mode in one of the face sheets. The possibilities to increase the in-plane shear stiffness and the resistance of a panel assembly by placing fasteners in the longitudinal seams, by adding fasteners in the edge joints and by additional strengthening of the joints depends in practice not only on using appropriate technical solutions but often also on the architectural requirements.

Example 5.1: Roof diaphragm

Given the flat roofed building shown in Figure 5.32, of portal frames of 12m span, at 5m centres and purlins at 1.5m centres. The roof sheeting spans perpendicular to the length of the building.

426

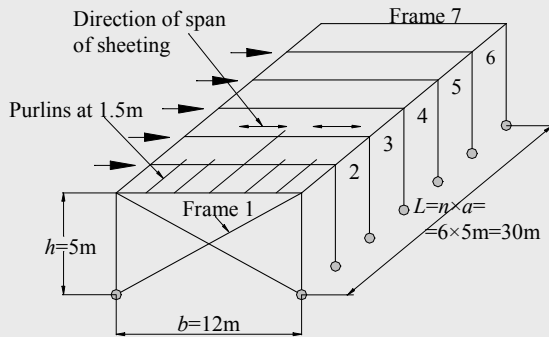


Figure 5.32 – Flat roof building with roof sheeting spanning perpendicular to the length of the building

Data of structural components

Main frames: Universal beam IPE330, Steel grade S355 ($h=330$ mm; $b=160$ mm; $t_w=7.5$ mm; $t_f=11.5$ mm; $A=62.6$ cm²; $I_y=11770$ cm⁴; $G=49.1$ kg/m);

Purlins:	Z150×2.5, Steel grade S350GD+Z ($h=150$ mm; $b=44$ mm; $c=20.9$ mm; $t_{nom}=2.5$ mm; $t=2.46$ mm ; $A=6.56$ cm ² ; $I_y=210.12$ cm ⁴ ; $G=5.15$ kg/m);
Roof profile:	Trapezoidal sheeting (see Figure 5.33) of steel grade S320GD+Z with $f_y=320$ N/mm ² and $f_u=390$ N/mm ² ; $E=210000$ N/mm ² , $G=5$ kg/m ² ;
Roof arrangement:	The roof is fastened on all four sides (tops of purlins level and tops of main frames using shear connectors);
Fasteners:	a) Sheet-to-purlin (see Table 5.5): 5.5 mm self-drilling screws in alternate corrugations of purlins; b) Sheet-to-shear connector fasteners (see Table 5.5): 5.5 mm self-drilling screws at 250 mm centre along frames; c) Seam fasteners (see Table 5.5): 4.8 mm self-drilling screws at 250 mm centre;
Wind action:	Wind load on side of building, $q_w = 1.2$ kN/m ² ;
Load factor:	$\gamma_Q=1.50$;
Sway:	Available sway deflection of frames under unfactored load, $v_d=h/300 = 5000/300 = 16.7$ mm.

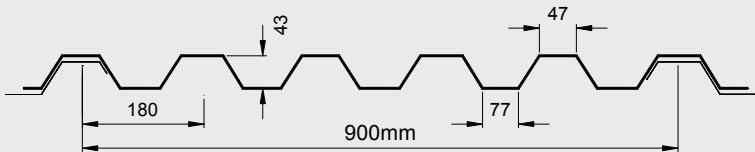


Figure 5.33 – Trapezoidal sheeting ($t_{nom}=0.5$ mm; $t = 0.46$ mm)

Side loads on roof: The unfactored wind load per panel is:

$$P = q_w \cdot a \cdot \frac{h}{2} = 1.2 \text{ kN/m}^2 \cdot 5 \text{ m} \cdot 2.5 \text{ m} = 15 \text{ kN}$$

and is shown in Figure 5.32.

The factored value is:

$$\gamma_Q P = 1.50 \cdot 15 \text{ kN} = 22.5 \text{ kN}.$$

5. SHEETING ACTING AS A DIAPHRAGM (STRESSED SKIN DESIGN)

It is required to check the strength and deflection of the frames under horizontal wind load, allowing for stressed skin action in the roof sheeting considering three different cases i.e.:

Case (a): The frames are pin jointed so that all the horizontal load is carried by the roof diaphragm spanning from gable to gable.

Case (b): The frames are of rigid beam-to-column joints (moment resisting MR frames) and carry all the horizontal wind load by themselves.

Case (c): The frames are rigid as in Case (b), and act in conjunction with roof diaphragm as in Case (a).

Case (a): Pin jointed frames: roof diaphragms carrying all the wind load

Data to calculate flexibility and strength properties of roof diaphragms are:

a : length of diaphragm in a direction perpendicular to the corrugations = 5000 mm;

A : cross-section area of longitudinal edge member (eaves purlin) = 656 mm²;

b : depth of diaphragm in the direction parallel to the corrugations = 12000 mm;

d : pitch of corrugations = 180 mm;

F_p : design shear of individual sheet-to-purlin fastener (see Table 5.5) = $1.9 \times 0.390 \text{ kN/mm}^2 \times 5.5 \text{ mm} \times 0.46 \text{ mm} = 1.87 \text{ kN}$;

F_s : design shear resistance of individual seam fastener (see Table 5.5) = $2.9 \times (0.5 \text{ mm}/4.8 \text{ mm})^{0.5} \times 0.390 \text{ kN/mm}^2 \times 4.8 \text{ mm} \times 0.46 \text{ mm} = 0.81 \text{ kN}$;

F_{sc} : design shear resistance of individual sheet-to-shear connector fastener (see Table 5.5) = $F_p = 1.87 \text{ kN}$;

K : sheeting constant (see Table 5.4, K_2 for alternate corrugations, for $l/d = 77 \text{ mm}/180 \text{ mm} = 0.43$; $h/d = 43 \text{ mm}/180 \text{ mm} = 0.24$; and $\theta = 33^\circ$, by interpolating) $K = K_2 = 1.083$;

L : span of diaphragm between braced frames = $30 \times 10^3 \text{ mm}$;

n : number of shear panels in the length of the diaphragm assembly = 6;

n_b : number of sheet lengths within the lengths of diaphragm = 1;

n_f : is the number of sheet-to-purlin fasteners per sheet width (alternate corrugations) = 4;

- n_p : number of purlins (edge + intermediate) = 9;
 n_s : number of seam fasteners per side lap (excluding those which pass through both sheets and the supporting purlin) = $(1500/250 - 1) \times 8 = 40$;
 n_{sc} : number of sheet-to-shear connector fasteners per end rafter = $5 \times 8 + 9 = 49$;
 n'_{sc} : number of sheet-to-shear connector fasteners per intermediate rafter = $n_{sc} = 49$;
 n_{sh} : number of sheet widths per panel = 6;
 p : $2 \times 180 \text{ mm} = 360 \text{ mm}$ (alternate troughs fastened);
 s_p = 0.15 mm/kN (see Table 5.5);
 s_s = 0.25 mm/kN (see Table 5.5);
 s_{sc} = 0.15 mm/kN (see Table 5.5);
 α_1 = 0.60 (see Table 5.7, for $n_p = 9$);
 α_2 = 0.40 (see Table 5.7, for $n_p = 9$);
 α_3 = 0.53 (see Table 5.7, for $n_p = 9$);
 α_4 = 1 (factor to allow for number of sheet lengths, see Table 5.8);
 β_1 = 0.44 (see Table 5.9);
 β_2 = 1.11 (see Table 5.9);
 β_3 = $(n_f - 1)/n_f = (4 - 1)/4 = 0.75$ seam fasteners in the crest (see 5.3.2.1).

Calculation of diaphragm flexibility and deflection using the formulas of Table 5.2 one can calculate the components of flexibility (fasteners in alternate corrugation trough) as follows:

$$c_{1,1} = \frac{ad^{2.5}\alpha_1\alpha_4K}{Et^{2.5}b^2} = \frac{5000 \times 180^{2.5} \times 0.6 \times 1 \times 1.083}{210 \times 0.46^{2.5} \times (12000)^2} = 0.325 \text{ mm/kN}$$

$$c_{1,2} = \frac{2a\alpha_2(1+\nu)[1+(2h/d)]}{Etb} = \frac{2 \times 5000 \times 0.4 \times (1+0.3) \times [1+(2 \times 43/180)]}{210 \times 0.46 \times 12000} = 0.007 \text{ mm/kN}$$

$$c_{2,1} = \frac{2as_p p \alpha_3}{b^2} = \frac{2 \times 5000 \times 0.15 \times 360 \times 0.53}{(12000)^2} = 0.002 \text{ mm/kN}$$

$$c_{2,2} = \frac{2s_s s_p (n_{sh} - 1)}{2n_s s_p + \beta_1 n_p s_s} =$$

$$= \frac{2 \times 0.25 \times 0.15 \times (6-1)}{2 \times 40 \times 0.15 + 0.44 \times 9 \times 0.25} = 0.029 \text{ mm/kN}$$

$$c_{2,3} = \frac{4(n+1)s_{sc}}{n^2 n'_{sc}} = \frac{4 \times (6+1) \times 0.15}{6^2 \times 49} = 0.002 \text{ mm/kN}$$

$$c_3 = \frac{n^2 a^3 \alpha_3}{4.8 E A b^2} = \frac{6^2 \times (5000)^3 \times 0.53}{4.8 \times 210 \times 656 \times (12000)^2} = 0.025 \text{ mm/kN}$$

Total flexibility:

$$c = c_{1,1} + c_{1,2} + c_{2,1} + c_{2,2} + c_{2,3} + c_3 = 0.39 \text{ mm/kN}$$

Maximum deflection at mid-length of diaphragm, v_{max} , will be calculated with eqn. (5.1)

$$v_{Ed} = v_{max} = \left(\frac{n^2}{8} \right) \cdot c \cdot P = \left(\frac{6^2}{8} \right) \cdot 0.39 \cdot 15 = 26.3 \text{ mm}$$

at unfactored load.

The maximum deflection is then $v_{max} = 26.3 \text{ mm}$ which is greater than the permissible deflection $v_a = \frac{5000}{300} = 16.7 \text{ mm}$, but will not be reached in practice due to the end of panel being fastened in every corrugation.

430

Calculation of diaphragm strength

Design formulae are given in §§5.3.2.1. One obtains the following results for panel assembly:

Seam strength:

$$V_{ult(1)} = n_s \cdot F_s + \frac{\beta_1}{\beta_3} \cdot n_p \cdot F_p = 40 \cdot 0.81 + \frac{0.44}{0.75} \cdot 9 \cdot 1.87 = 42.27 \text{ kN}$$

Shear connector strength:

$$V_{ult(2.1)} = n_{sc} \cdot F_{sc} = 49 \cdot 1.87 = 91.63 \text{ kN}$$

Hence design shear capacity:

$$V_{Rd} = \min(V_{ult(1)}, V_{ult(2.1)}) = 42.27 \text{ kN}$$

Checking for non-permissible failure modes

1) Sheet-to-purlin fasteners: check if $\frac{0.6 \cdot b \cdot F_p}{p \cdot \alpha_3} > V_{Rd}$

$$\frac{0.6 \times 12000 \times 1.87}{360 \times 0.53} = 70.6 \text{ kN} > V_{Rd}, \text{ this is satisfactory.}$$

2) The shear buckling strength

From the manufacturer's data, the second moment of area of the sheeting profile about its neutral axis is given as $163.77 \text{ mm}^4/\text{mm}$. For a single corrugation (see Figure 5.17)

$$I = 163.77 \text{ mm}^4/\text{mm} \times 180 \text{ mm} = 29478.6 \text{ mm}^4$$

The perimeter length, u , of a single corrugation is obtained by calculation from the sheeting profile shown in Figure 5.33 in shown in Figure 5.17. Thus $u = 226 \text{ mm}$.

Hence bending stiffness:

$$D_x = \frac{E \cdot t^3 \cdot d}{12 \cdot (1 - \nu^2) \cdot u} = \frac{210 \times 0.46^3 \times 180}{12 \times (1 - 0.3^2) \times 226} = 1.491 \text{ kNmm}$$

$$\text{and bending stiffness } D_y = \frac{E \cdot I}{d} = \frac{210 \times 29478.6}{180} = 34391.7 \text{ kNmm}$$

431

Shear buckling capacity:

$$\begin{aligned} V_{cr,g} &= 14.4 \cdot \frac{(n_p - 1)^3}{b} \cdot \sqrt[4]{D_x \cdot D_y^3} = 14.4 \cdot \frac{(9 - 1)^3}{12000} \sqrt[4]{1.491 \cdot 34391.7^3} = \\ &= 1784.47 \text{ kN} > V_{Rd} = 42.27 \text{ kN} \end{aligned}$$

This is satisfactory.

Local shear buckling:

$$\begin{aligned} V_{cr,l} &= 4.83 \cdot b \cdot t \cdot E \cdot \left(\frac{t}{l}\right)^2 = 4.83 \times 12000 \times 0.46 \times 210 \times \left(\frac{0.46}{77}\right)^2 = \\ &= 199.82 \text{ kN} > V_{Rd} = 42.27 \text{ kN} \end{aligned}$$

This is satisfactory.

5. SHEETING ACTING AS A DIAPHRAGM (STRESSED SKIN DESIGN)

The interaction of global and local shear buckling:

$$V_{red} = \frac{V_{cr,g} \cdot V_{cr,l}}{V_{cr,g} + V_{cr,l}} = \frac{1784.47 \cdot 199.82}{1784.47 + 199.82} = 179.7 \text{ kN} > V_{Rd} = 42.27 \text{ kN}$$

This is satisfactory.

3) End collapse of profile: Check if $0.3 \cdot f_y \cdot b \cdot \sqrt{\frac{t^3}{d}} > V_{Rd}$

$$0.3 \times 0.320 \times 12000 \times \sqrt{\frac{0.46^3}{180}} = 26.8 \text{ kN}$$

End collapse is not permissible mode. This is not satisfactory hence use fasteners in every corrugation in end panel only

$$(0.9 \cdot f_y \cdot b \cdot \sqrt{\frac{t^3}{d}} = 80.4 \text{ kN} > V_{Rd} > 42.27 \text{ kN}).$$

Finally, the design shear capacity of a panel, 42.27 kN, is less than the maximum shear force in a panel, 56.25 kN (see Figure 5.34). To increase the design shear capacity, a solution is to decrease the distance between seam fasteners from 250 mm to 200 mm.

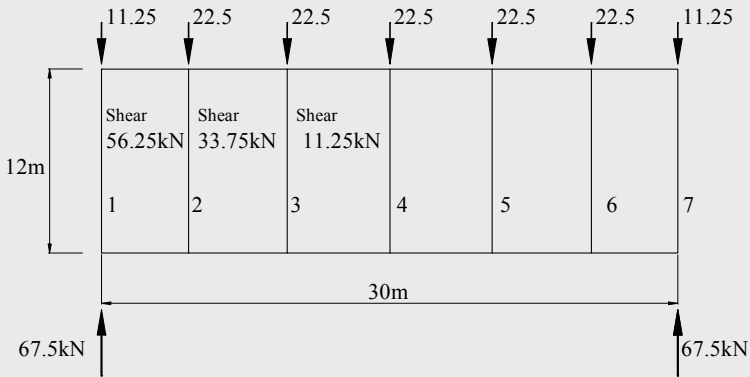


Figure 5.34 – Distribution of shear forces

Important notes

- (1) If the sheeting have been fastened in every corrugation throughout, the value of K would have been $K_1 = 0.0942$ (see Table 5.3), the shear flexibility would have been $c = 0.09 \text{ mm/kN}$ and the value of v_{max} at unfactored load would have been 6.1 mm which is satisfactory.

- (2) For sheeting fastened in every corrugation in the end panels and in alternate corrugations in the interior panels, the value of v_{max} may be calculated as the sum of the shear force times shear flexibility over half the length of the diaphragm (see Figure 3.34), i.e.

$$v_{max} = \frac{1}{1.5} [56.25 \times 0.09 + 33.75 \times 0.39 + 11.25 \times 0.39] = 15.1 \text{ mm}$$

at unfactored load

which is lower than the permissible deflection $v_a = 16.7 \text{ mm}$. This is satisfactory.

Case (b): MR frames: frames alone carrying all wind loads

It is easy to show that the deflection, v , of the MR frames alone at the unfactored load is of 23.18 mm (see Figure 5.35) which is greater than $v_a = 16.7 \text{ mm}$.

Thus, the frame alone, even with rigid beam-to-column joints, is not adequate.

Note, that the frame flexibility (see Figure 5.21b) is $k = v/P = 23.18 \text{ mm}/15 \text{ kN} = 1.545 \text{ mm/kN}$.

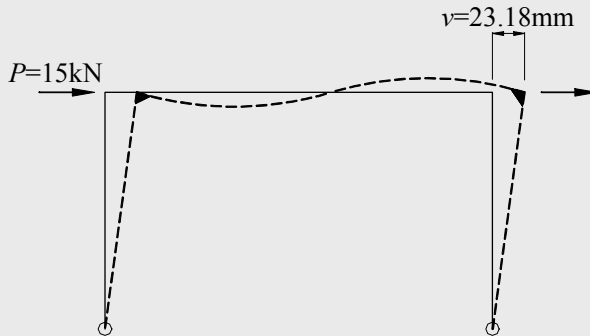


Figure 5.35 – Sway behaviour of MR frame carrying alone the wind load

Case (c): Rigid frames: frames acting in conjunction with roof diaphragm

According to §§5.4.2.1, the relative flexibility is defined as $r = c/k$. From Case (a) for fasteners in alternate corrugations throughout, $c = 0.39 \text{ mm/kN}$ and from Case (b), for the frame, $k = 1.545 \text{ mm/kN}$.

5. SHEETING ACTING AS A DIAPHRAGM (STRESSED SKIN DESIGN)

For a value of $r = c/k = 0.39/1.545 = 0.252$ and for a building of 7 frames, it is found from Table 5.13 that the reduction factor, η , on sway forces and moments are (interpolated values):

- For frame 2, $\eta_2 = 0.341$;
- frame 3, $\eta_3 = 0.517$;
- frame 4, $\eta_4 = 0.571$;

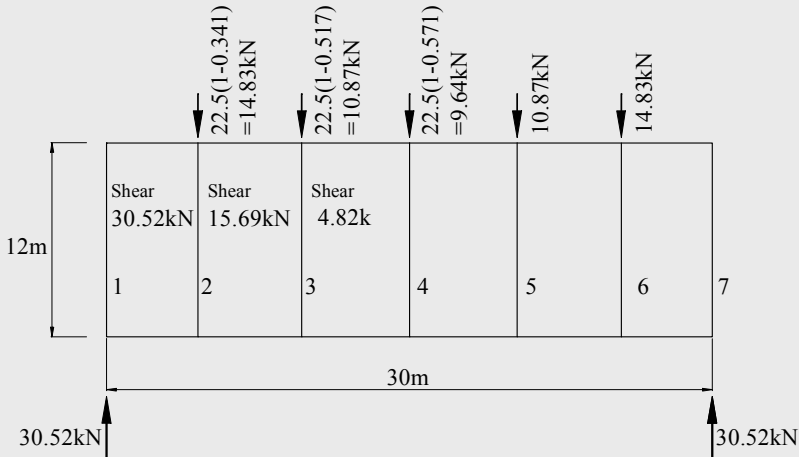


Figure – 5.36: Side forces on the roof diaphragm in case when it cooperates with MR frames

434

The maximum deflection (frame 4) is then $v_{max} = 0.571 \times 23.18 \text{ mm} = 13.24 \text{ mm}$ which is less than $v_a = 16.7 \text{ mm}$.

The unfactored forces on the roof diaphragm are as shown in Figure 5.36. It is noted that the maximum shear in the end panel, 30.52 kN, is less than when the diaphragms acts alone (56.25 kN, see Figure 5.34) and it is also less than the design shear capacity of the diaphragm (42.27 kN). Hence, this design is amply safe even with fasteners in alternate corrugation in the end panels.

Conclusions

Case (a): Roof diaphragm only

The calculation shows that, for fasteners in alternate corrugations, end collapse of the profile can occur in the end panels of the diaphragm. More,

the fastener strength is not adequate. To avoid this, fasteners should be used in every corrugation in the end panels and alternate corrugations elsewhere. Also, to increase the design shear capacity, a solution is to decrease the distance between seam fasteners from 250 mm to 200 mm.

In conclusion, to satisfy the criteria for both strength and deflection, it is therefore necessary to use fasteners in every corrugation throughout.

Case (b): Rigid frames only

The deflection of a rigid frame, without assistance from the roof diaphragm, is excessive.

Case (c): Rigid frames and roof diaphragms

The calculation shows that, for fasteners in alternate corrugations throughout, the shear in the end panels when the frames and diaphragms act in conjunction, is only 30.52 kN. This is less than the shear required to cause end collapse of the profile, 42.27 kN. The maximum deflection of the diaphragm is also within the specified limit ($13.24 \text{ mm} < v_a = 16.7 \text{ mm}$).

The use of diaphragm, with fasteners in alternate corrugation throughout, in conjunction with rigid frames, satisfies the criteria for both strength and deflection. This is therefore the most economical design.

Chapter 6

STRUCTURAL LINER TRAYS

6.1 INTRODUCTION

Light gauge steel cassettes, also known as structural liner trays offer an alternative form of wall assembly for use in low rise steel frame buildings. Figure 6.1 shows the architectural appearance of Citroen Showroom in Bucharest, Romania, for which a cassette wall system promoted by Ruukki has been used, while Figure 6.2 presents an example of using cassettes as wall members.



Figure 6.1 – Citroen Showroom built by Ruukki cassette wall system

However, while the main application of cassettes are the structural walls, they also can be used for roof envelopes.

Cassettes are made of cold-formed C-shaped steel sections of typical geometry shown in Figure 6.3.



Figure 6.2 – Use of cassette as wall members

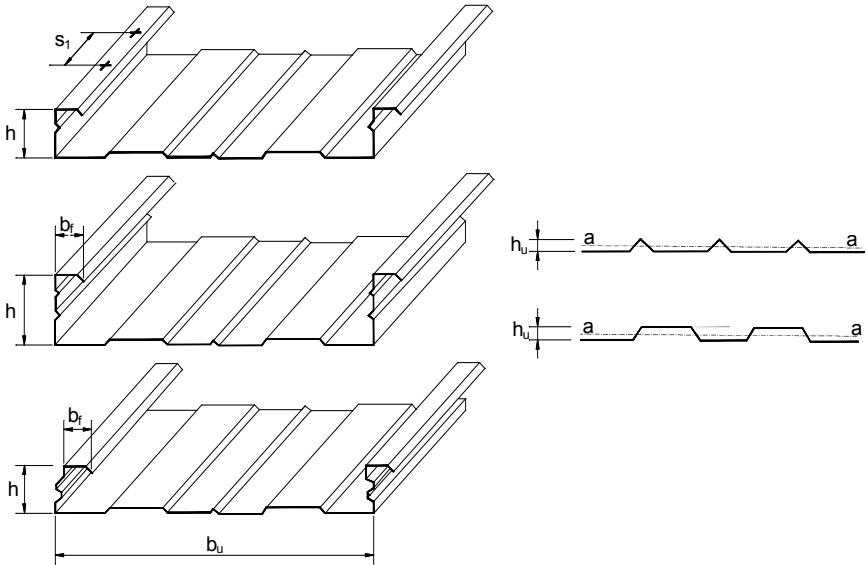


Figure 6.3 – Typical geometry for cassette sections (CEN, 2006a)

The cassette wall system has been pioneered in France by the company “Produits Acier Batiment” (PAB) under the name “CIBBAP”. Cassettes may be used either as outer or inner sheet for insulated double wall cladding. The basic arrangement for cassette wall construction is shown in

Figure 6.4, where the cassettes spanning vertically form the outer layer of the walls.

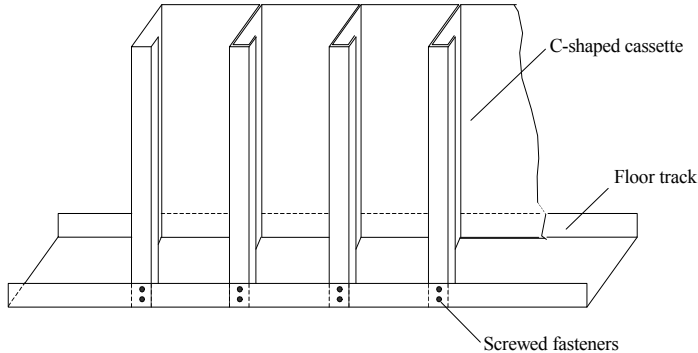


Figure 6.4 – Cassettes spanning vertically in a wall panel (Davies, 2005)

To prevent distortion the two narrow flanges of cassettes should be laterally restrained by attached profile steel sheeting, or other appropriate inner panels (OSB-Oriented Strand Board, Plywood etc.). The core of this sandwich system is formed by insulating material like rigid foam or mineral fibres. The foamed plastic core may be polyurethane, polyisocyanurate, polystyrene or phenolic foam and can also contribute, if bonded to the metal sheet, to increase the buckling and bending strengths of the cassettes, in conjunction with the insulation requirements with regard to temperature, sound and humidity.

439

Cassette construction may be viewed as being similar to conventional light gauge wall stud system integrally combined with a metal lining sheet to provide a metal frame together with a flat steel wall. Its main advantages in comparison with the alternative wall stud construction may be summarised as follows:

- Simple details and rapid construction;
- The wall structure is immediately water tight;
- The stability problems of thin slender studs are avoided;
- A rational provision for wind or earthquake shear, can be made without additional bracing;
- In shear, the walls are extremely robust and ductile;
- The seam fastening of adjacent cassettes can be realised by using the clinching (press joining) techniques which enables for a very rapid and efficient erection.

6. STRUCTURAL LINER TRAYS

The idea of cassette wall construction appears to originate from Baehre in Stockholm in the late 1960's (Davies, 2002). He envisaged the steel cassettes as the primary structural elements in modular construction as illustrated in Figures 6.5.

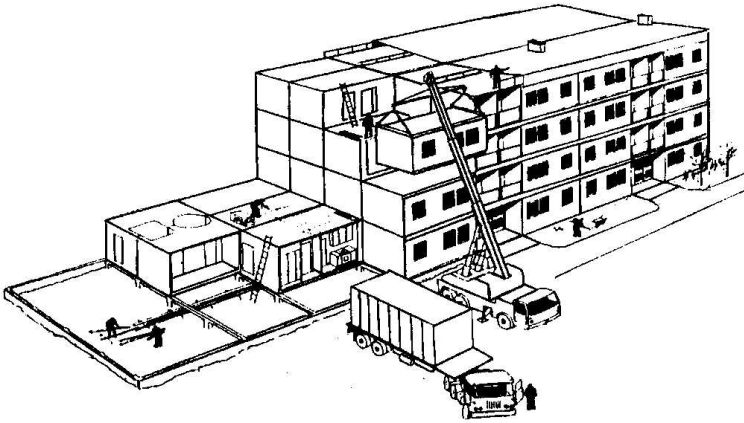


Figure 6.5 – Modular cassettes construction (Davies, 2002)

When used in this way, as shown in Figures 6.4 and 6.6, cassette walls are subjected to the three primary load systems of axial compression (from the storeys above), bending (from wind pressure and suction) and shear (from wind or earthquake induced diaphragm action).

440

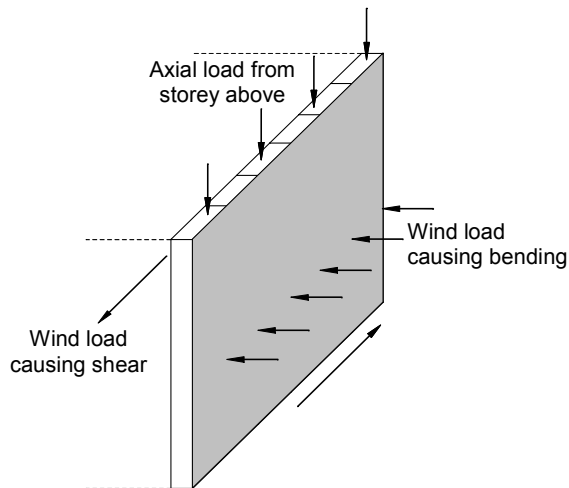


Figure 6.6 – Primary loading cases for cassettes walls (Davies, 2006b)

Baehre's research team in Karlsruhe, Germany, investigated the behaviour of cassette sections when subjected to each of these three actions individually (Thomasson, 1978; König, 1978; Vyberg, 1976).

In recent years, cassettes sections have been widely used, mainly for industrial buildings, in an alternative wall construction in which they span horizontally between structural frames. Here the cassettes interact with and are stabilised by a relatively high trapezoidal profiled metal outer skin which spans at right angles to the span of the cassette. When used in this way to form a two-layer, built-up cladding system, cassettes are often termed "structural liner trays". Typical construction of this type is shown in Figure 6.7. A similar arrangement to Figure 6.7 is also used in roof construction.

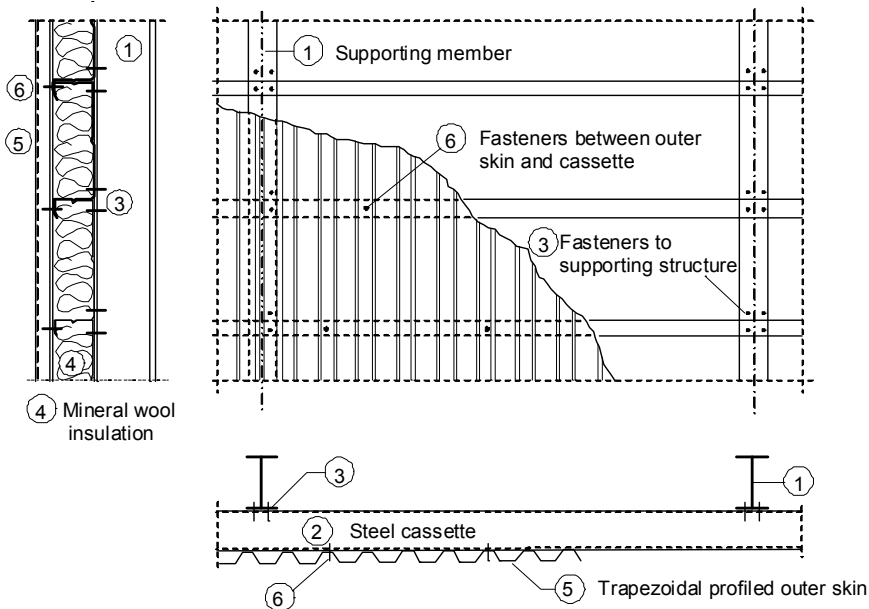


Figure 6.7 – Two layer built-up wall cladding system for industrial buildings

Figures 6.8a and 6.8b show two examples of liner tray walls. The roof arrangement is similar.

The Baehre test-based approach (Baehre & Buca, 1986; Baehre, 1987; Baehre, Buca & Egner, 1990) was completed by the studies carried out in the last decade by Davies' team at the University of Manchester (Davies & Dewhurst, 1997; Davies & Fragos, 2002, 2004; Davies, 2002; Voutay & Davies, 2002). These results formed the basis of the design clauses in

6. STRUCTURAL LINER TRAYS

Eurocode 3 – Part 1.3. As these design procedures are based on tests results, the code imposes geometric restrictions on cassettes that appears to reflect the limits of Baehre’s tests rather than the limits of the structural system (Davies, 2005).

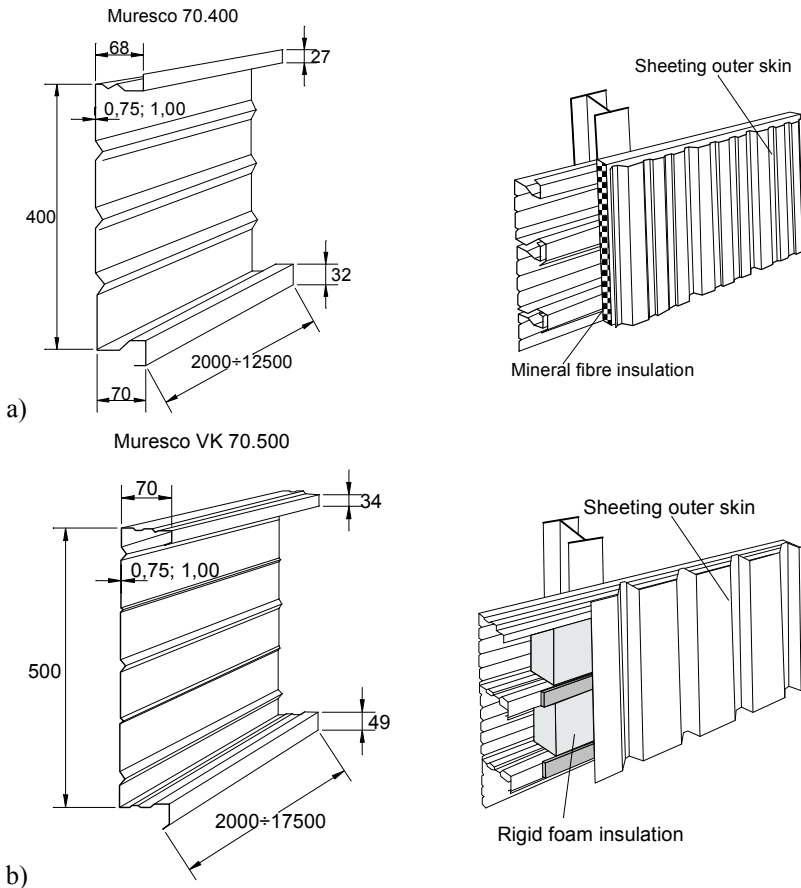


Figure 6.8 – Two examples of using PAB liner trays in “Two layer built-up wall cladding construction”

6.2 DESIGN PROCEDURES FOR CASSETTE SECTIONS

6.2.1 General

The elements of a cassette section are the wide flange, the webs, the narrow flanges and the lips (see Figure 6.3).

The range of validity of the design procedures in EN1993-1-3 (CEN, 2006a) is as follows (see Figure 6.3):

$$\begin{array}{rcl}
 0.75 \text{ mm} < & t_{nom} < & 1.5 \text{ mm} \\
 30 \text{ mm} < & b_f < & 60 \text{ mm} \\
 60 \text{ mm} < & h < & 200 \text{ mm} \\
 300\text{mm} < & b_u < & 600 \text{ mm} \\
 & I_a/b_u < & 10 \text{ mm}^4/\text{mm} \\
 & h_u < & h/8 \\
 & s_1 < & 1000 \text{ mm}
 \end{array}$$

where I_a is the second moment of area of the wide flange about its own centroid axis $a-a$ as shown in the right hand side of Figure 6.3.

It may be noted here that, primarily because of “flange curling” which was discussed in Section 3.3, there is more scatter in the comparison of test results with theory than is customary with cold-formed sections in bending. The EN1993-1-3 therefore requires a material factor of $\gamma_{M2}=1.25$ for bending strength in contrast to the more usual value of $\gamma_{M0(1)}=1.0$. It is implicit therefore, that significantly higher bending strength is likely to be obtained by test than by calculation.

As the clauses in EN1993-1-3 (CEN, 2006a) explicitly require the stabilising effect of the second metal skin, it is necessary to reconsider their applicability to cassette wall construction where this second skin is unlikely to be present (or may be replaced by a much weaker material such as plasterboard).

The resistance of cassettes sections in bending, including the resistance of webs to shear forces and to local transverse forces should be obtained using the relevant paragraphs of Chapter 3.

6.2.2 Axial compression

This case is not explicitly considered in EN 1993-1-3 (CEN, 2006a) However, the cross section properties can be evaluated according to the procedures given in §§3.8.3. For the wide flange and web, the effective width approach will be applied, while for the narrow flange and the adjacent edge stiffener the iterative procedure presented in paragraph §§3.7.3.2.2 has to be used (see Figure 6.9 and, also, Example 3.2). In fact, this part of the

design procedure for axially loaded cassettes is similar to that for bending with narrow flanges in compression, which is presented in detail in §§6.2.3.1.

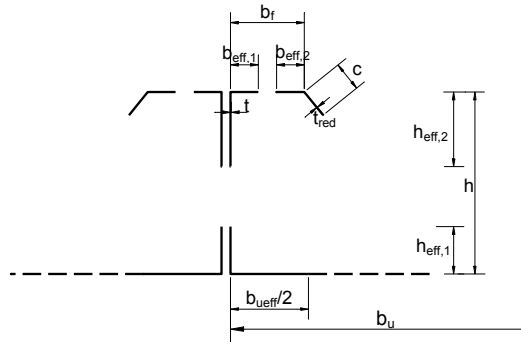


Figure 6.9 – Design model for a cassette section subjected to axial compression

The design procedure then follows that for any thin-walled column, bearing in mind that the column is stable with respect to buckling in the plane of the wall. If the narrow flanges are not properly restrained, distortional buckling must be also considered.

6.2.3 Moment resistance

444

The moment resistance $M_{c,Rd}$ of a liner tray may be obtained using §§6.2.3.1 and §§6.2.3.2 provided that:

- the geometrical properties are within the range given in §§6.2.1;
- the depth h_u of the corrugations of the wide flange does not exceed $h/8$, where h is the overall height of the liner tray (see Figure 6.3).

Alternatively the moment resistance of a liner tray may be determined by testing provided that it is ensured that the local behaviour of the liner tray is not affected by the testing equipment, as described in Annex A of EN 1993-1-3 (CEN, 2006a).

6.2.3.1 Bending with the narrow flange in compression (wide flange in tension)

The behaviour of a cassette section in bending is characterised by the usual considerations of thin-walled cold-formed section construction with

the addition that the wide flange tends to curl towards the neutral axis, as illustrating by Figure 6.10, whether this flange is in tension or compression (see also Section 3.3).

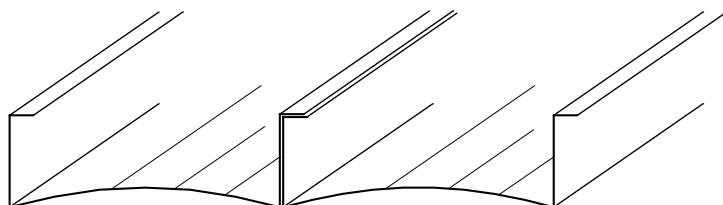


Figure 6.10 – Flange curling of cassette sections

The design for bending with the narrow flange in compression is a particularly complicated design problem because there are three effects to be considered:

- local buckling of the web and narrow flanges;
- distortional buckling (tripping) of the narrow flange/lip assembly;
- “flange curling” of the wide flange (which is in tension).

According to the EN 1993-1-3 provisions, the moment resistance of a cassette section (liner tray) with its narrow flange in compression (wide flange in tension), should be determined using the step-by-step procedure outlined in Figure 6.11 as follows:

Step 1: Locate the centroid of the cross section;

Step 2: Obtain the effective width of the wide flange $b_{u,eff}$, allowing for possible flange curling, from:

$$b_{u,eff} = \frac{53.3 \cdot 10^{10} \cdot e_o^2 \cdot t^3 \cdot t_{eq}}{h \cdot L \cdot b_u^3} \quad (6.1)$$

where

- b_u is the overall width of the wide flange;
- e_o is the distance from the centroidal axis of the gross cross section to the centroidal axis of the narrow flanges;
- h is the overall depth of the liner tray;
- L is the span of the liner tray;
- t_{eq} is the equivalent thickness of the wide flange, given by:

$$t_{eq} = (12 \cdot I_a / b_u)^{1/3}$$

I_a is the second moment of area of the wide flange, about its own centroid (see Figure 6.3).

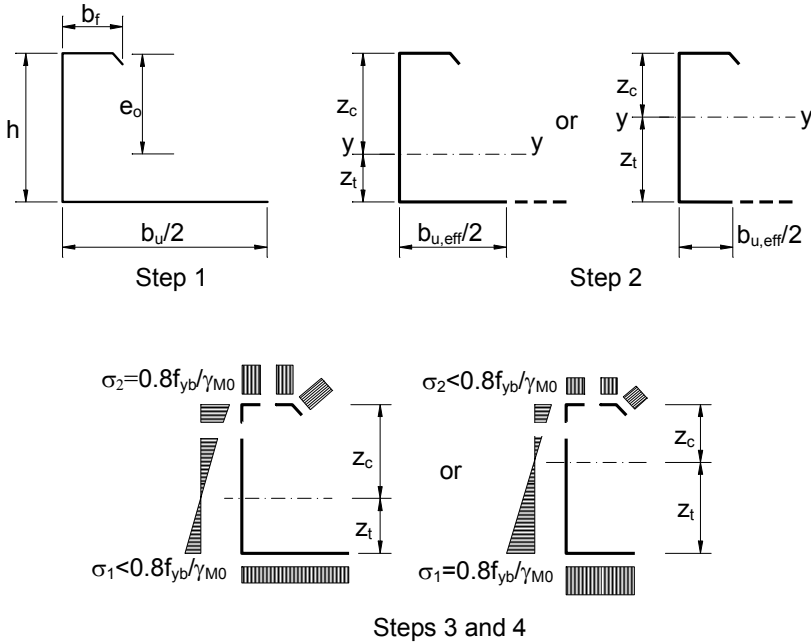


Figure 6.11 – Determination of moment resistance – narrow flange in compression and wide flange in tension (CEN, 2006a)

Step 3: Determine the effective area of all compression elements, based on values of the strain ratio $\psi = \sigma_2 / \sigma_1$ obtained using the effective widths of the flanges but the gross area of the webs;

Step 4: Find the centroid of the effective cross section, then obtain the buckling resistance moment $M_{b,Rd}$ using:

$$M_{b,Rd} = 0.8 \cdot \beta_b W_{eff,com} \cdot f_{yb} / \gamma_{M0} \quad (6.2)$$

but $M_{b,Rd} \leq 0.8 \cdot W_{eff,t} \cdot f_{yb} / \gamma_{M0}$

with

$$W_{eff,com} = I_{y,eff} / z_c \quad \text{and} \quad W_{eff,t} = I_{y,eff} / z_t$$

in which the correlation factor β_b is given by the following:

- if $s_1 \leq 300\text{mm}$: $\beta_b = 1.0$
 - if $300\text{mm} \leq s_1 \leq 1000\text{mm}$: $\beta_b = 1.15 - s_1/2000$

where

s_1 is the longitudinal spacing of fasteners supplying lateral restraint to the narrow flanges, see Figure 6.3.

In what concerns distortional buckling, the minimum fastener spacing (e.g. $s_1 \leq 1000\text{mm}$) in EN1993-1-3 (see §§6.2.1) are clearly intended to prevent this phenomenon. We may note, however, that the requirements are very simplistic and presumably reflect the observation that distortional buckling was not critical in any of Baehre's test panels when this fastener spacing was present (Davies, 2005). It does not automatically follow that fasteners to an auxiliary bracing system are always necessary. It may also be observed that the web connections between adjacent cassettes, which are usually necessary in the cassette wall construction, will also inhibit distortional buckling.

The effects of shear lag need not be considered if $L/b_{u,eff} \geq 25$. Otherwise a reduced value of ρ should be determined as specified in §§3.8.4.3.

Flange curling need not be taken into account in determining deflections at serviceability limit states.

As a simplified alternative, the moment resistance of a liner tray with an unstiffened wide flange may be approximated by taking the same effective area for the wide flange in tension as for the two narrow flanges in compression combined.

6.2.3.2 Bending with the wide flange in compression

In this case the more complex narrow flange and lip (e.g. edge stiffener) assembly is in tension and does not buckle. Therefore, the bending behaviour is dominated by the local buckling of the wide flange. However, flange curling occurs for the wide flange in compression and interacts with local buckling.

EN1993-1-3 (CEN, 2006a) does not propose any rigorous treatment of this interaction and, indeed, this would appear to be extremely difficult. Instead, it suggests that the beneficial effect of intermediate stiffeners should

be neglected and the conventional effective width procedure should be used through with the material factor γ_M increased to 1.25 (e.g. γ_{M2}) in order to deal with the additional uncertainty caused by flange curvature. The absence of the second skin clearly has no influence when the narrow flange is in tension.

According to the code provisions, the moment resistance of a cassette section with its wide flange in compression should be determined using the step-by-step procedure outlined in Figure 6.12, as follows:

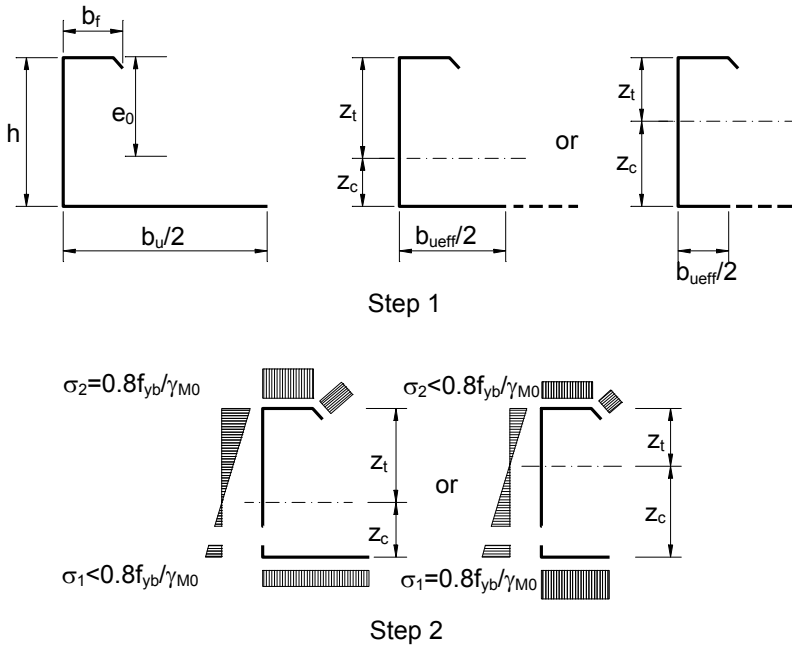


Figure 6.12 – Determination of moment resistance – wide flange in compression (CEN, 2006a)

Step 1: Determine the effective areas of all compression elements of the cross section, based on values of the strain ratio $\psi = \sigma_2 / \sigma_1$ obtained using the effective widths of the compression flanges but the gross areas of the webs;

Step 2: Find the centroid of the effective cross section, then obtain the moment resistance $M_{c,Rd}$ from:

$$M_{c,Rd} = 0.8 \cdot W_{eff,min} \cdot f_{yb} / \gamma_{M0} \tag{6.3}$$

with

$$W_{eff,min} = I_{y,eff} / z_c \quad \text{but} \quad W_{eff,min} \leq I_{y,eff} / z_t$$

where z_c and z_t are as indicated in Figure 6.12.

6.2.4 Behaviour in shear

A cassette sub-assembly is also a ready-made shear panel or “diaphragm” for stressed skin construction as discussed in Chapter 5. Stressed skin design is explicitly allowed in EN1993-1-3 and appropriate enabling clauses are included in Section 10.3 of the code. The code includes some provisions for cassettes acting as shear panels. These make it clear that the behaviour of cassette wall panels in shear is not significantly different from that of the conventional shear panels comprising trapezoidal steel sheeting framed by appropriate edge members, so that the procedures described in Chapter 5 of this book may generally be applied.

There are three main differences between cassette and liner tray systems and trapezoidally profiled roof sheeting and decking for which the calculation procedures were originally devised (Davies, 2005):

- (1) There is negligible flexibility due to shear distortion of the profile. This removes a design equation which tends to dominate the deflection calculation for trapezoidal profiles. Here it is possible to make a simplified estimate of deflections based on the assumption that the flexibility arises mainly from the fastenings;
- (2) The strength calculation tends to be dominated by the tendency of the wide flange to buckle locally in shear before any of the more usual diaphragm failure modes (fastener failure, profile and failure or global shear buckling) are mobilised;
- (3) There is often no separate edge member parallel to the cassettes. This means that there are no longitudinal edge fasteners to check the web and the narrow flange of the outermost cassette act as their own edge member which should be checked for the induced compressive force.

The first two of these considerations lead to two equation given in EN1993-1-3 for the ultimate and serviceability limit states design.

For the case of a single cassette section (see Figure 6.3), considered as a component of a shear panel, Baehre (1987) has shown that the simplified Easley equation is valid for the determination of the shear flow $T_{V,Rd}$ to cause local buckling:

$$T_{V,Rd} = \frac{36}{b_u^2} \cdot \sqrt[4]{D_x \cdot D_y^3} \quad (6.4)$$

where

D_x is the bending stiffness across the wide flange;

$$D_x = \frac{E \cdot I_a}{b_u} \quad (6.5)$$

D_y is the bending stiffness along the wide flange;

$$D_y = \frac{E \cdot t^3}{12(1-\nu^2)} = \frac{E \cdot t^3}{10.96} \quad (6.6)$$

I_a is the second moment of area of the wide flange about its own centroid (see Figure 6.3).

Thus¹,

$$T_{V,Rd} = \frac{36 \cdot E}{\sqrt[4]{10.96^3}} \cdot \sqrt[4]{\frac{I_a \cdot t^9}{b_u^9}} = 6 \cdot E \cdot \sqrt[4]{I_a \left(\frac{t}{b_u}\right)^9} \quad (6.7)$$

For the calculation of deflection, the following four components of shear flexibility have to be considered (ECCS, 1995), i.e.:

$c_{1,2}$ shear strain;

¹ Davies (2006b) has shown that the numerical coefficient in this clause has had a chequered history. Mathematically, it works out to be close to 6.0, as was corrected in the Corrigenda to ENV1993-1-3 dated 1997-02-25. However, based on Baehre's original paper (Baehre, 1987), the ENV1993-1-3(CEN, 1996) version of the Eurocode gave the value as 0.2! By 2001, this had increased to 0.6. The present value in EN1993-1-3 (CEN, 2006a), of 8.43, is based on a comparison of the Easley equation with the "exact" value given by the theoretical equation for the shear buckling of a simply-supported flat plate. This is logical because, in many cases, the degree of orthotropy is not great and there is some continuity of the webs so that the simply-supported solution is conservative.

- $c_{2,1}$ flexibility of the sheet end fasteners;
- $c_{2,2}$ flexibility of the seam fasteners;
- $c_{2,3}$ flexibility of the “shear connector”(longitudinal edge) fasteners.

To calculate these components, formulas in Table 5.10 and the Flowchart 5.1 in Chapter 5 of this book can be used.

These flexibility components are of similar magnitude and, correspondingly the resultant stiffness of the shear panel can be approximated by:

$$S_v = \frac{\alpha \cdot L \cdot b_u}{e_s \cdot (b - b_u)} \tag{6.8}$$

where

- L is the overall length of the shear diaphragm (in the direction of the span of the liner tray);
- b is the overall width of the shear diaphragm; $b = \sum b_u$;
- e_s is the spacing between seam fasteners through the web, $e_s \leq 300$ mm (see Figure 6.13)
- α is the stiffness factor, which may be derived from tests, or in absence of tests results, α may conservatively taken as equal to 2000 N/mm.

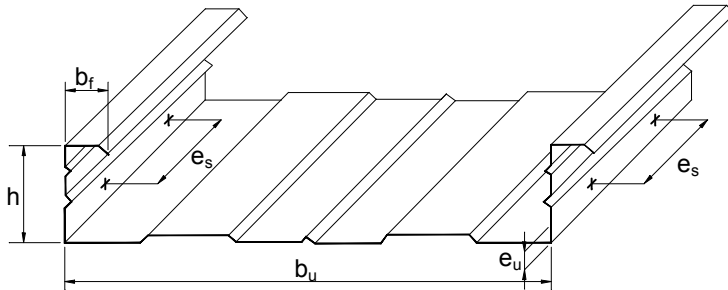


Figure 6.13 – Location of the seam fasteners

This rather crude approach to stiffness appears to be justified because, in the absence of distortion term, the deflections tend to be small and because cassettes tend to be of fairly similar proportions and to have similar fastening systems, the individual fasteners have similar flexibilities. However, this simplification is not essential and, if the deflections are at all

critical, the more rigorous approach to the calculation of deflections is given in ECCS Recommendations (Davies & Fragos, 2003).

More importantly, the wording of the clauses in EN1993-1-3 (CEN, 2006a), and the above equation for the shear stiffness to cause local buckling, may lead designers to overlook that fastener strength may also be critical. In addition to considering local buckling of the wide flange, it is essential also to consider the possibility of failure in each of the fastener failure modes considered in conventional stressed skin design, namely:

- a) failure in the seam fasteners between adjacent cassettes;
- b) failure in the fasteners connecting the ends of the cassettes to the foundation or the primary structure;
- c) failure in the shear connector (longitudinal edge fastener).

The design provisions included in EN1993-1-3 (CEN, 2006a) for checking the shear capacity of a cassette section (liner tray), belonging to a shear wall panel, can be summarised as follows:

- (1) Liner trays used to form shear diaphragms should have stiffened wide flanges;
- (2) Liner trays in shear diaphragms should be inter-connected by seam fasteners through the web at a spacing e_s of not more than 300 mm and by seam fasteners (normally blind rivets) located at a distance e_u from the wide flange of not more than 30 mm, as shown in Figure 6.13;
- (3) An accurate evaluation of deflections due to the flexibility of fasteners may be made using a similar procedure to that for trapezoidal profiled sheeting;
- (4) The shear flow $T_{V,Ed}$ due to ultimate limit state design loads should not exceed $T_{V,Rd}$ given by:

$$T_{V,Rd} = 8.43 \cdot E \cdot \sqrt[4]{I_a (t/b_u)^9} \quad (6.9)$$

One observes that compared to eqn. (6.7), the above formula significantly increases the local shear buckling resistance of the wide flange.

- (5) The shear flow $T_{v,ser}$ due to serviceability design loads should not exceed $T_{v,Cd}$ given by:
-

$$T_{V,cd} = S_v / 375 \quad (6.10)$$

where

S_v is the shear stiffness of the diaphragm, per unit length of the span of the liner trays, and is given by the eqn. (6.8).

6.3 DESIGN PROCEDURES FOR CASSETTE PANELS ACTING AS DIAPHRAGM

6.3.1 Cassettes spanning horizontal to the length of diaphragm (liner tray shear panels)

Following the ECCS Recommendations (ECCS, 1995), the design shear capacity of a liner tray shear panel, $V_{b,Rd}$ has to be taken as minimum from the capacity of the seam fasteners in the web, V_{ult} , and the shear buckling strength, V_{cr} . The ultimate limit states requirement is that the shear force in the diaphragm, caused by the design value of the load (e.g. T in Figure 6.14) should be smaller than both V_{ult} and V_{cr} , where:

$$V_{ult} = n_s \cdot F_s + \beta_1 \cdot F_p \quad (6.11)$$

$$V_{cr} = \frac{8.43}{b_u^2} \cdot E \cdot \sqrt[4]{I_a' \cdot t^9} \cdot L \quad (6.12)$$

453

where

n_s is the number of seam fasteners (fasteners in the web) per seam;

F_s is the design strength of an individual seam fastener;

β_1 is the factor to allow for the number of sheet/column fasteners per cassette. Values are given in Table 5.9 for case 1 and n_f are the number of sheet/column fasteners per cassette;

F_p is the design strength of an individual cassette/column fastener;

V_{cr} is the design shear capacity of a diaphragm when shear buckling of the wide flange governs;

6. STRUCTURAL LINER TRAYS

- I_a' is the moment of inertia of the wide flange in mm^4/mm width of diaphragm, e.g. $I_a' = \frac{I_a}{b_u}$;
- b_u is the width of the wide flange;
- t is the core thickness of the cassette material;
- E is the modulus of elasticity;
- L is the length of the diaphragm in the span direction of the cassettes.

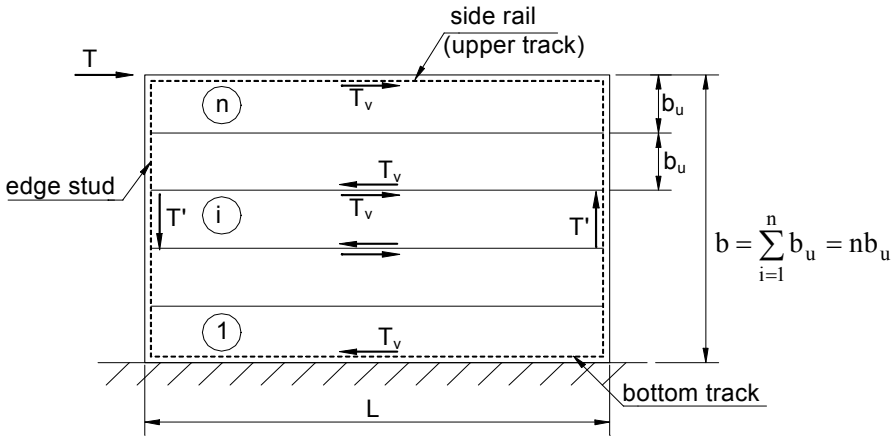


Figure 6.14 – Liner trays diaphragm cassette spanning horizontally

454

Comparison of eqn. (6.12) and eqn. (6.9), shows that:

$$\frac{V_{cr}}{L} = T_{V,Rd} \tag{6.13}$$

Consequently, the design criterion becomes:

$$T_{V,Ed} \leq \min\left(T_{V,Rd}, \frac{V_{ult}}{L}\right) \tag{6.14}$$

where

$T_{V,Ed}$ is the design shear flow, calculated using the design loads corresponding to the ultimate limit state, and with reference to Figure 6.14 is given by:

$$T_{V,Ed} = \frac{T_{Ed}}{L} \quad (6.15)$$

The design stiffness of the shear panel, S , should be determined from:

$$S = S_v \cdot b \quad (6.16)$$

where S_v is given by eqn. (6.8).

The serviceability limit state requirement for shear panel assemblies composed of cassettes is:

$$T_{V,Ed} \leq T_{V,Cd} \quad (6.17)$$

where

- $T_{V,Ed}$ is the shear flow in the cassettes of the shear panel caused by the serviceability limit state load;
- $T_{V,Cd}$ is given by eqn. (6.10);
- L is the length of the diaphragm in the span direction of the cassette.

6.3.2 Some peculiar problems for design of wall panels of cassettes spanning vertically to the length of diaphragm

455

For a typical vertically-spanning cassette wall, at first sight, it might be thought that providing a continuous connection to the foundations at every seam line might reduce the forces in the vertical edge members and thus avoid high local uplift forces at the ends of the diaphragms. However, the following simple calculation carried out for an individual cassette with reference to Figure 6.15 demonstrates that this is not the case (Davies, 2005):

$$T_v = \frac{T'_v \cdot H}{b_u} = \frac{T \cdot H}{\sum b_u} = \frac{T \cdot H}{b} \quad (6.18)$$

It follows that continuous connection to the foundations merely has the potential to reduce the forces in the seam fasteners between adjacent cassettes but has no influence at all on the critical forces at the ends of the diaphragm. Indeed, resisting the uplift forces at the ends of the diaphragm

6. STRUCTURAL LINER TRAYS

walls is one of the more troublesome aspects of cassette wall design and there is scope for some ingenuity in achieving good practical details.

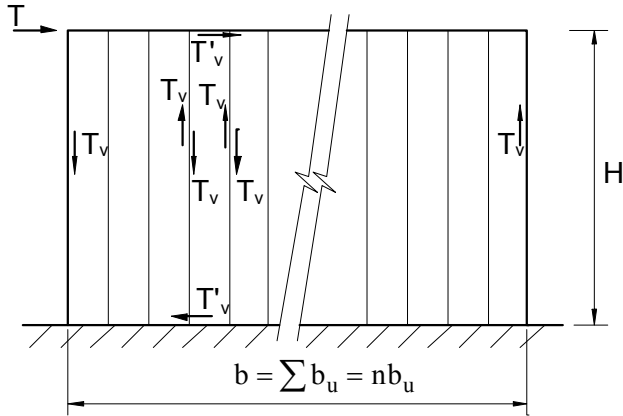


Figure 6.15 – Diaphragm forces in cassette wall constructions (Davies, 2005)

It is expedient to space the holding down points as far apart as possible in order to reduce the shear forces in the wall and, at the same time, to reduce the holding down forces into the foundations. This has implications for the architectural design so that early interaction between the architect and the engineer is required. The design of the holding down detail itself is another critical point in the structural design.

456

Figure 6.16 shows an elevation of a cassette wall as used in a typical house facade. The lines $x-x$ shows the division into prefabricated sub-panels for factory construction. The wind-shear diaphragms are indicated by cross-hatching.

More recently, it has become clear that it is often better to treat the cassette wall with openings as a whole, as shown in Figure 6.17 (Davies, 2005), and to provide holding down points at the corners only. This reduces both the in-plane shear forces and the uplift forces on the foundations. Shear transfer across the window and door openings is via the roof and floor edge beams and the (concrete) ground beam.

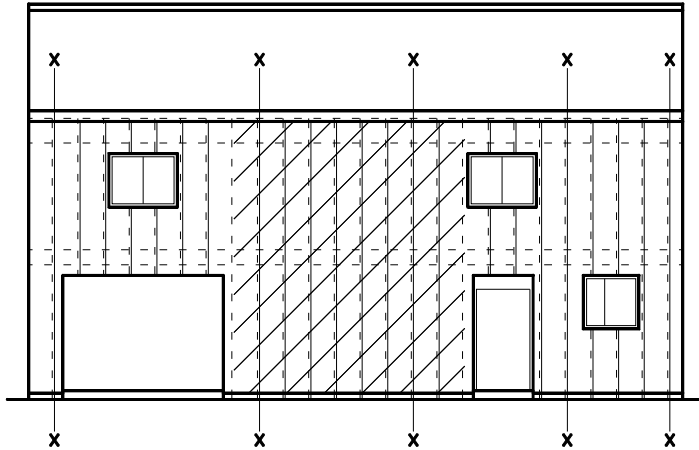


Figure 6.16 – Typical cassette wall in house construction (Davies, 2005)

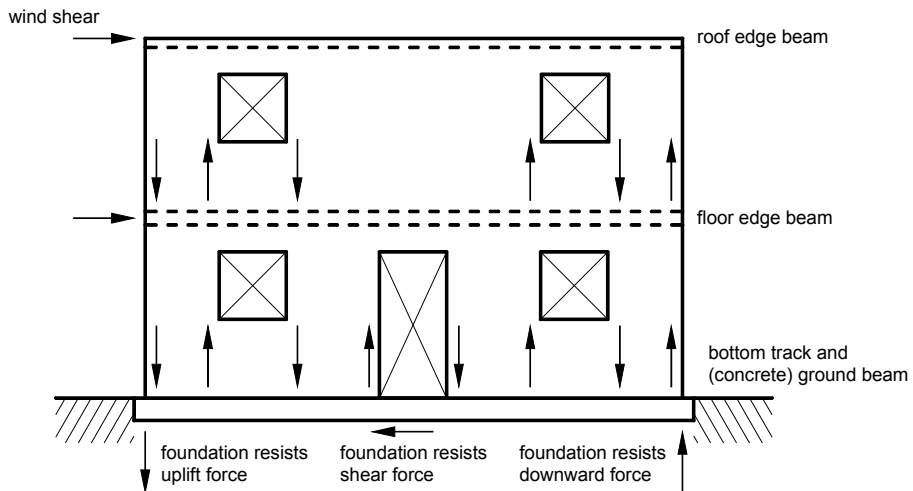


Figure 6.17 – Improved treatment of diaphragm action in a cassette wall (Davies, 2005)

6.4 COMBINED EFFECTS

Although considered separately in §§6.2.2 to §§6.2.4 of this Chapter, axial load, bending and shear effects may evidently interact. Noting that there is no major axis bending or buckling, minor axis bending and axial load can be readily combined. The shear stresses in stressed skin action are very low and it is usual to neglect interaction between in-plane shear and

primary axial load and bending. However, the axial compressive force arising from stressed skin action in the edge of a diaphragm (see Figure 6.14) must be combined with the axial force arising from load from the floors and roofs above. This will usually be of major design significance.

Cassette wall panels can, therefore, be readily designed on the basis of design procedures presented in Chapters 3 and 4, which are in accordance with EN1993-1-3, together with the established procedures for stressed skin design given in Chapter 5 and Section 6.3. It is found that, for most low-rise construction, a standard panel and fastener specification is sufficient to carry the wind shear without any special provisions other than for holding down forces at the end of the diaphragm.

Example 6.1: The purpose of this design example is to provide evidence of the effectiveness of the diaphragm capacity (e.g. shear strength) of cassette walls.

Given an industrial pitch roof portal frame building for which plan and gable frame are shown in Figure 6.18. The cassette gable walls are designed to work as diaphragms to resist horizontal wind load.

458

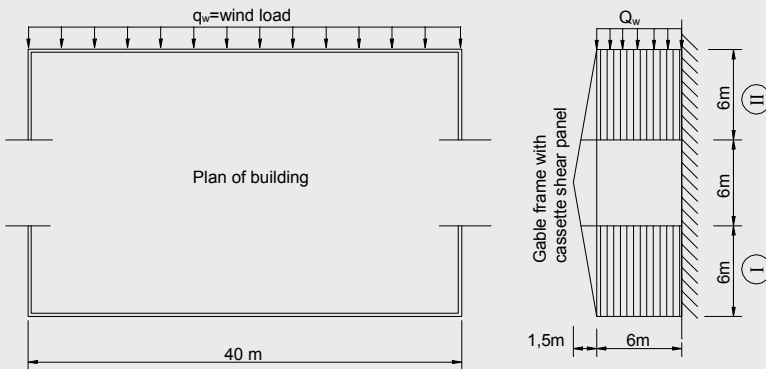


Figure 6.18 – Pitch roof industrial building: plan and gable frame

Figure 6.19 shows the cassette sections used, connected to supporting members with 6.3 mm diameter collar head screws – three per cassette – and seam fasteners of 4.8 mm diameter monel metal blind rivets at 300 mm centres.

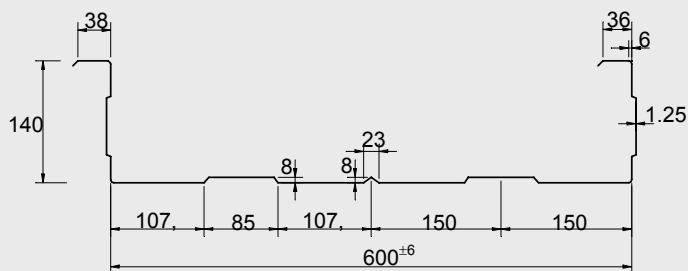


Figure 6.19 – Cassette section

Input data*Wind load*

$$q_w = 0.5 \text{ kN/m}^2 \text{ with load factor, } \gamma_Q = 1.5$$

$$q_{w,d} = 1.5 \cdot 0.5 = 0.75 \text{ kN/m}^2$$

The wind load will be supported by the gable frames stiffened by cassette walls (two shear panels for each gable frame) and will be transferred to the panels as reaction forces at the level of the eaves and basement (see Figure 6.20).

$$Q_{w,d} = (q_{w,d} \cdot 40 \text{ m}) / 2 = (0.75 \text{ kN/m}^2 \cdot 40 \text{ m}) / 2 = 15 \text{ kN/m}$$

$$T_{Ed} = \left(Q_{w,d} \cdot \frac{H}{2} \right) / 2 = \left(15 \cdot \frac{6}{2} \right) / 2 = 22.5 \text{ kN / shear panel (I or II)}$$

The shear flow in cassettes due to the wind loading at ultimate limit state is $T_{v,Ed} = 22.5 \text{ kN} / 6 \text{ m} = 3.75 \text{ kN/m}$

Cassette properties

Cassette type (see Figure 6.19)

$$t_{nom} = 1.25 \text{ mm}; t_{core} = 1.21 \text{ mm};$$

$$I'_a = \frac{I_a}{b_u} = 16 \text{ mm}^4 / \text{mm};$$

Steel grade: S320GD with $f_{yb} = 320 \text{ N/mm}^2$; $f_u = 390 \text{ N/mm}^2$;

$$E = 210000 \text{ N/mm}^2.$$

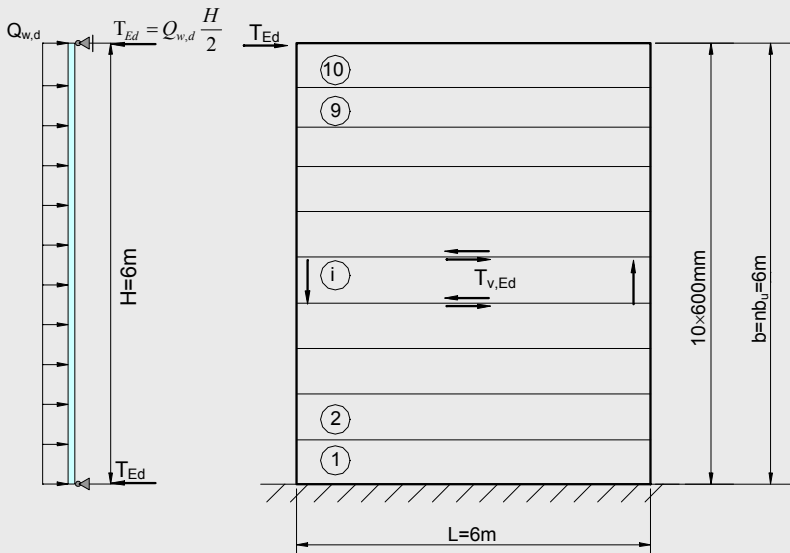


Figure 6.20 – Shear flow in cassettes due to the wind loading

Checking at the Ultimate Limit State (eqn. 6.14)

Design shear capacity of cassettes

$$T_{V,Rd} = \frac{8.43 \cdot E^4}{b_u^2} \cdot \sqrt[4]{I_a \cdot t^9} = \frac{8.43 \cdot 2.1 \cdot 10^5}{600^2} \cdot \sqrt[4]{16 \cdot 1.21^9} = 9.1 \text{ N/mm (kN/m)}$$

Thus, $T_{V,Ed} = 3.75 \text{ N/mm} < T_{V,Rd} = 9.1 \text{ N/mm}$.

Design strength of fasteners

Fasteners to supporting members:

$$F_p = 1.9 \cdot f_u \cdot d \cdot t \quad (\text{see Table 5.5})$$

$$F_p = 1.9 \cdot 0.39 \cdot 6.3 \cdot 1.21 = 5.65 \text{ kN}$$

Seam fasteners:

$$F_s = 3.2 \cdot (t/d)^{1/2} \cdot f_u \cdot d \cdot t \quad (\text{see Table 5.5})$$

$$F_s = 3.2 \cdot (1.21/4.8)^{1/2} \cdot 0.39 \cdot 4.8 \cdot 1.21 = 3.64 \text{ kN}$$

$$V_{ult} = n_s \cdot F_s + \beta_1 \cdot F_p$$

$$n_s = 6000 / 300 = 20 \text{ fasteners in web per seam}$$

$$\beta_1 = 0.30 \text{ (from Table 5.9 for } n_f = 3)$$

$$V_{ult} = 20 \cdot 3.64 + 0.30 \cdot 5.65 = 74.5 \text{ kN}$$

$$V_{ult} / L = 74.5 / 6 = 12.4 \text{ kN/m} > T_{V,Ed} = 3.75 \text{ kN/m}$$

Thus the design criteria given by eqn. (6.14) is verified.

Checking the Serviceability Limit State

Limitation of shear flow according to eqn. (6.17):

$$T_{V,Cd} = \frac{2000 \cdot L \cdot b_u}{375 \cdot e_s \cdot (b - b_u)}$$

$$T_{V,Cd} = \frac{2000 \cdot 6000 \cdot 600}{375 \cdot 300 \cdot (6000 - 600)} = 11.85 \text{ N/mm (kN/m)} > T_{V,Ed} = 3.75 \text{ kN/m}$$

Thus the design criteria given by eqn. (6.17) is verified.

Deflection calculation

Deflection (sway displacement) will be calculated for cantilever diaphragm with cassettes spanning perpendicular to the span of diaphragm (Table 5.10 and the Flowchart 5.1) using the following formulas:

$$c_{1,2} = \frac{2 \cdot a \cdot (1 + \nu) \cdot [1 + (2 \cdot h / d)]}{E \cdot t \cdot b} = \frac{2 \cdot 6000 \cdot (1 - 0.3) \cdot [1 + (2 \cdot 140 / 600)]}{210 \cdot 1.21 \cdot 6000} = 0.011 \text{ mm/kN}$$

$$c_{2,1} = \frac{2 \cdot a \cdot s_p \cdot p}{b^2} = \frac{2 \cdot 6000 \cdot 0.15 \cdot 200}{6000^2} = 0.01 \text{ mm/kN}$$

$$c_{2,2} = \frac{2 \cdot s_s \cdot s_p \cdot (n_{sh} - 1)}{2 \cdot n_s \cdot s_p + \beta_1 \cdot n_p \cdot s_s} = \frac{2 \cdot 0.30 \cdot 0.15 \cdot (10 - 1)}{2 \cdot 20 \cdot 0.15 + 0.30 \cdot 2 \cdot 0.30} = 0.11 \text{ mm/kN}$$

$$c_{2,3} = \frac{2 \cdot s_{sc}}{n_{sc}} = \frac{2 \cdot 0.15}{20} = 0.015 \text{ mm/kN}$$

6. STRUCTURAL LINER TRAYS

in which

$$a = L = 6000\text{mm} ; b = \sum b_u = 6000\text{mm} ; d = b_u = 600\text{mm} ;$$

$$h = 140\text{mm} ; t = 1.21\text{mm} ; E = 210 \text{ kN/mm}^2 ;$$

$$s_p = 0.15\text{mm/kN} ; p = 200\text{mm} ; s_s = 0.30\text{mm/kN} ; s_{sc} = 0.15\text{mm/kN} ;$$

$$n_s = 6000/300=20 ; n_{sc} = 6000/300=20 ; n_{sh} = 10 ; n_p = 2 ; \beta_1 = 0.30.$$

The total flexibility in shear of a shear panel is:

$$c' = c_{1,2} + c_{2,1} + c_{2,2} + c_{2,3} = 0.011 + 0.01 + 0.11 + 0.015 = 0.146\text{mm/kN}$$

and the corresponding deflection, for the two shear panels, will be:

$$\begin{aligned} v_1 &= 2 \cdot T_{Ed} \cdot c' = 2 \cdot 22.5 \cdot 0.146 = 6.57 \text{ mm} < \\ &< 0.008 H = 0.008 \cdot 6000 = 48\text{mm} \end{aligned}$$

which is largely satisfactory.

Chapter 7

CONNECTIONS

7.1 INTRODUCTION

Connections are an important part of every structure, not only from the point of view of structural behaviour, but also in relation to the method of production. It has been shown that, for a structure made of hot-rolled sections, the connections account for a minimum of 50% of the total value of constructional steelwork (Fenster *et al*, 1992). There is no reason to believe that the percentage will be much lower for cold-formed steel structures (Yu *et al*, 1993). Connections in cold-formed steel structures are used for:

1. connecting steel sheets to supporting structure (thin-to-thick), e.g. roof sheeting to purlins, cladding sheeting to side-rails etc.;
2. interconnecting two or more sheets (thin-to-thin), e.g. seam fastening of sheeting;
3. assembling bar members (thin-to-thin or thick-to-thick), e.g. for framed structures, trusses etc.

In comparison with hot-rolled sections, the behaviour of connections in cold-formed steel elements is influenced by the reduced stiffness of thin walls. Therefore, additional effects are, for example, the tilting of the fastener in hole bearing failure under the shear distortion of the sheet when the fastener is loaded in tension and the sheet is pulled over the head of the fastener. This is the reason why specific technologies and related design procedures, either by calculation or calculation assisted by testing, have been developed for cold-formed steel structures.

A variety of joining methods is available for these structures. They can be classified as follows (Toma *et al*, 1993; Yu, 2000):

- fastenings with mechanical fasteners;
- fastenings based on welding;
- fastenings based on adhesive bonding.

Fasteners for light gauge steelwork can be also classified into three main groups depending on the thickness of the parts being connected. These groupings and some typical types of fasteners within each group are shown in Table 7.1.

Table 7.1 – Some typical application of different type of fasteners

Thin-to-thin	Thin-to-thick or thin-to-hot rolled	Thick-to-thick or thick-to-hot rolled
- self-drilling, self-tapping screws;	- self-drilling, self-tapping screws;	- bolts;
- blind rivets;	- fired pins;	- arc welds.
- press-joints;	- bolts;	
- single-flare V welds;	- arc spot puddle welds;	
- spot welds;	- adhesive bonding.	
- seam welding;		
- adhesive bonding.		

The selection of the most suitable types of fastener for a given application is governed by several factors (Davies, 1991):

- Load-bearing requirements
 - Strength;
 - Stiffness;
 - Ductility (deformation capacity);
- Economic requirements
 - Number of fasteners required;
 - Cost of labour and materials;
 - Skill required in fabrication;
 - Design life;
 - Maintenance;
 - Ability to be dismantled;
- Durability
 - Resistance to aggressive environments
- Water tightness
- Appearance (architectural aspect).

Although the structural engineers tend to be primarily concerned with the most economical way of meeting the load-bearing requirements, in many applications other factors may be equally important.

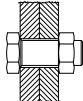
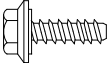
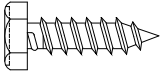
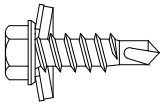

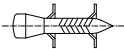
In the first part, this chapter surveys the most frequently used mechanical fasteners and provides information on welding and adhesive bonding. Subsequently, general design considerations and the design procedures from EN1993-1-3 (CEN, 2006a) will be presented, accompanied by design examples. At the end of this chapter an example of design assisted by testing for connections with self-tapping screws is presented.

7.2 FASTENING TECHNIQUES OF COLD-FORMED STEEL CONSTRUCTIONS

7.2.1 Mechanical fasteners

Fasteners for sheets of sections and sandwich panels are discussed separately. Most fasteners can be used in almost all kinds of cold-formed steel applications (like screws), others are appropriate for specific applications, only. Table 7.2 gives a general overview of the application of different mechanical fasteners in cold-formed steel sections.

Table 7.2 – Usual mechanical fasteners for common applications (Yu *et al*, 1993)

Thin-to-thick	Steel-to-wood	Thin-to-thin	Fasteners	Remark
X		X		Bolts M5-M16
X				Self-tapping screw $\phi 6.3$ with washer ≥ 16 mm, 1 mm thick with elastomer
	X	X		Hexagon head screw $\phi 6.3$ or $\phi 6.5$ with washer ≥ 16 mm, 1 mm thick with elastomer
X		X		Self-drilling screws with diameters: - $\phi 4.22$ or $\phi 4.8$ mm - $\phi 5.5$ mm - $\phi 6.3$ mm
		X		Blind rivets with diameters: - $\phi 4.0$ mm - $\phi 4.8$ mm - $\phi 6.4$ mm
X				Shot (fired) pins
X				Nuts

In recent years, the press-joining technology (Predeschi *et al*, 1997), originating from the automotive industry, and the “Rosette” system (Makelainen & Kesti, 1999) have augmented the family of mechanical fasteners for thin-walled steel constructions.

7.2.1.1 Mechanical fasteners for sections

Bolts with nuts

Bolts with nuts are threaded fasteners which are assembled in drilled holes through the material elements to be joined. Thin members will necessitate the use of bolts threaded close to the head. Head shapes may be hexagonal, cup, countersunk, or hexagonal flanged (see Figure 7.1). The nuts should normally be hexagonal. For thin-walled sections bolt diameters are usually M5 to M16. The preferred property classes are 8.8 or 10.9.

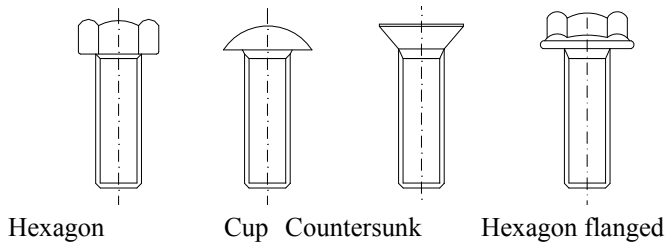


Figure 7.1 – Head shapes

Bolts with nuts are used for connections in cold-formed steel framed and truss structures, and for purlin-to-rafter or purlin-to-purlin attachment by sleeved or overlapping purlin (see Figure 7.2).

Tests have revealed the following basic types of failure for thin steel bolted connections working in shear and tension:

- a) Failure modes in shear:
 1. Shearing of the bolt: rupture (Figure 7.3a) or crushing (Figure 7.3b);
 2. Bearing (yield) and/or piling of thinner material (Figure 7.3c). When both materials are thin, yielding of both sheets may occur together with bolt tilting (Figure 7.3d);
 3. Tearing of the sheet in the net sections (Figure 7.3e);
 4. End failure by shearing of thin material (Figure 7.3f);

b) Failure modes in tension:

1. Tension failure or rupture of bolt (Figure 7.4a);
2. Pull-through failure (Figure 7.4b).

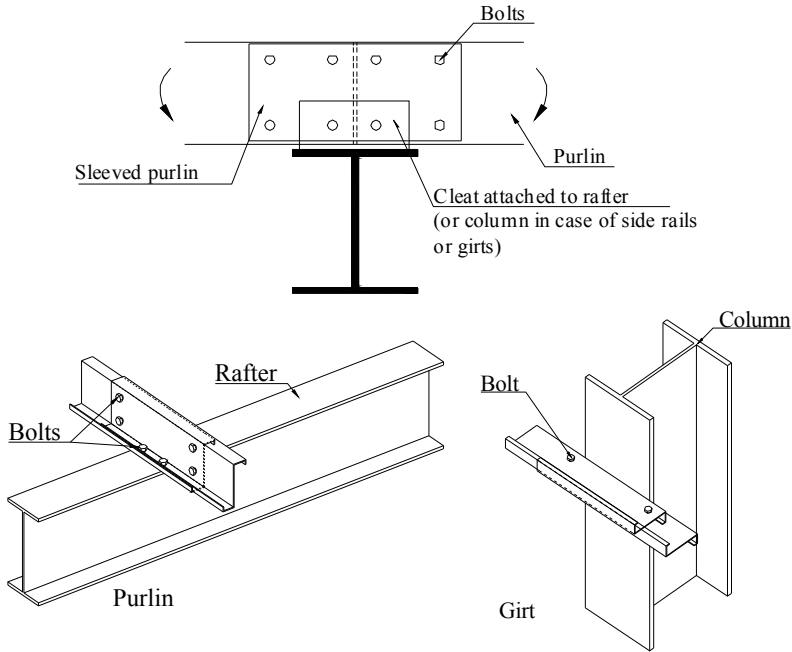


Figure 7.2 – Bolted lapped connections for purlins and side rails

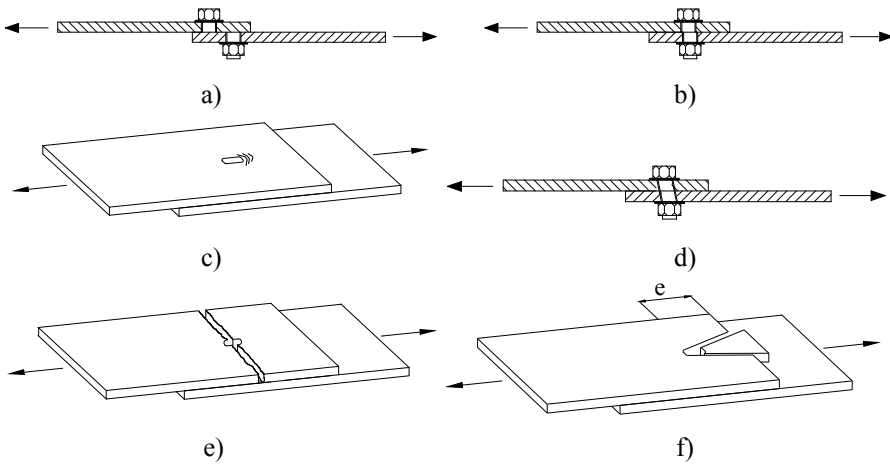


Figure 7.3 – Failure modes of bolted connections in shear

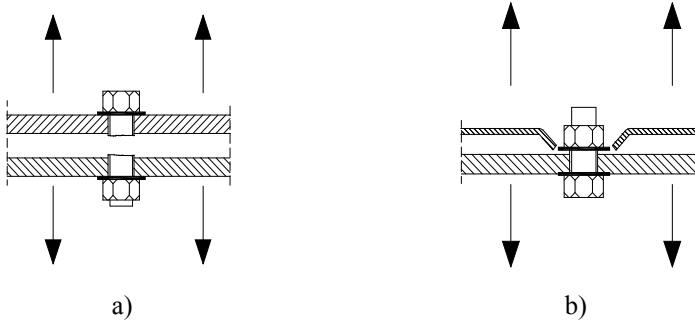


Figure 7.4 – Failure modes for bolted connections in tension

Screws

The two main types of screws are self-tapping and self-drilling screws. Most screws will be combined with washers to improve the load-bearing capacity of the fastening or to make the fastening self-sealing. Some types have plastic heads or plastic caps, which are available for additional corrosion resistance and/or colour matching.

Self-tapping screws. Self-tapping screws tap their counterthread in a prepared hole. They can be classified as thread-forming and thread-cutting.

Figure 7.5 shows the thread types for thread-forming screws (Yu *et al*, 1993). Type A is used for fastening thin sheets to thin sheets. Type B is used for fixing to steel bases of thicknesses greater than 2 mm. Type C is generally used for fixing to thin steel bases up to 4 mm thick.

Thread-forming screws normally are fabricated from carbon steel (plated with zinc for corrosion protection and lubrication) or stainless steel (plated with zinc for lubrication).

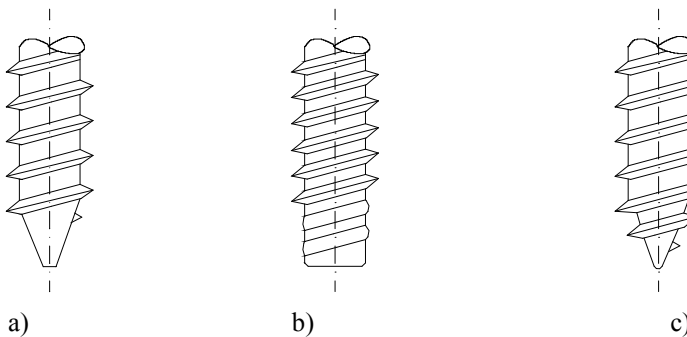


Figure 7.5 – Thread types for thread-forming screws

Figure 7.6 shows examples of threads and points of thread-cutting screws. Thread-cutting screws have treads of machine screw diameter pitch combinations with blunt points and tapered entering threads having one or more cutting edges and chip cavities. They are used for fastening to thicker metal bases. Resistance to loosening is normally not as high for thread-cutting screws as for thread-forming screws.

Thread-cutting screws are fabricated from case-hardened carbon steel and normally plated with zinc for corrosion protection and lubrication.

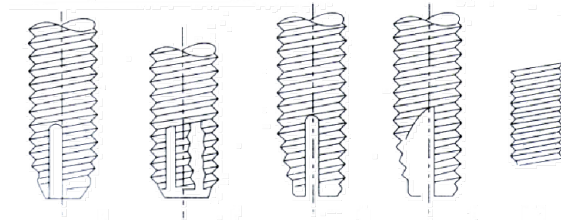


Figure 7.6 – Threads and points of thread-cutting screws

Self-drilling screws. Self-drilling screws drill their own holes and form their mating threads in one operation. Figure 7.7 shows two examples of self-drilling screws. The screw in Figure 7.7b serves to fasten thin sheets to thin sheets.

Self-drilling screws are normally fabricated from heat-treated carbon steel (plated with zinc for corrosion protection and lubrication) or from stainless steel (with carbon-steel drill point and plated with zinc for lubrication).

469

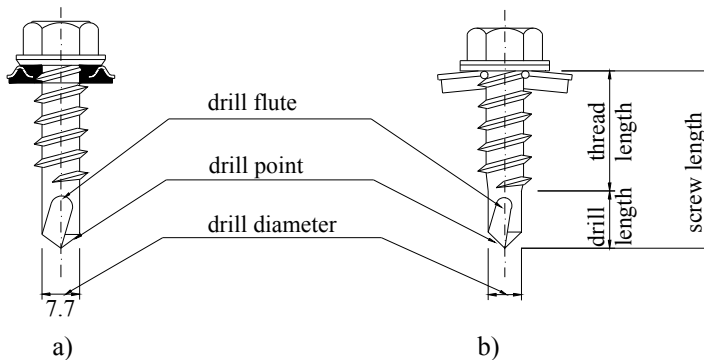


Figure 7.7 – Self-drilling screws: a) drill diameter equal to body diameter for thin-to-thick connections; b) drill diameter smaller than body diameter for thin-to-thin connections

Self-tapping and self-drilling screws are usually combined with washers as shown in Figure 7.8. The washers increase the load-bearing capacity and/or the sealing ability. Elastomeric or combined metal-elastomeric washers cause a marked reduction in the strength and stiffness of the connections (Davies, 1991).

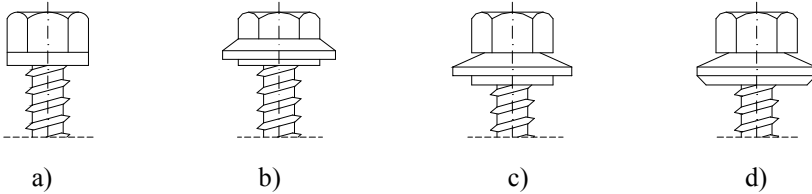


Figure 7.8 – Washers for self-tapping/self-drilling screws: a) metal washers; b) elastomeric washers; c), d) elastomeric bonded or vulcanised to metal washers

With all types of screwed fasteners, it is important to adhere closely to the manufacturers’ instructions regarding such matters as the diameter of the pre drilled hole, the thickness of the elements to be fastened in relation to the type of fastener, and the tightening torque. Examples of applications of screwed fastenings are shown in Figure 7.9 according to SFS Intec AG catalogue (<http://www.sfsintec.biz>).

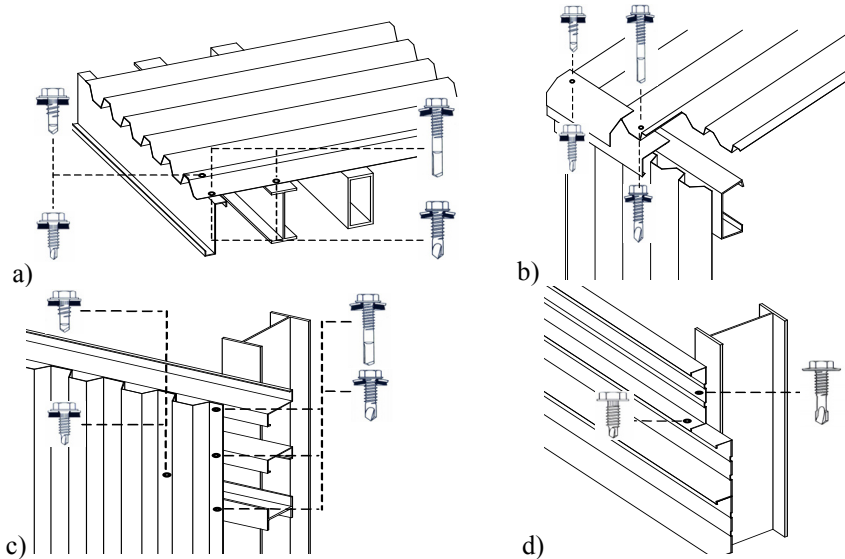


Figure 7.9 – Application examples of self-drilling screws: (a) fastenings of roof sheeting on purlins; (b) fastening of sheeting at an eave detail; (c) fastening of wall sheeting on side rails; (d) fastenings of wall cassettes on stanchions

The failure modes of screwed connections in shear are generally similar to those of bolted connections. However, due to the fact that the connected materials are usually thin (or at least one of the connected parts is thin), usually does not fail in shear. Bearing, pulling, tearing and/or shearing of the material connected by screws and working in shear are possible failure modes. Also, the tilting and pulling out of the fastener may occur (see Figure 7.10).



Figure 7.10 – Tilting and pull-out of fastener (inclination failure)

In what concerns the behaviour in tension, compared with bolted connections, there are three supplementary failure modes characteristic for screwed connections, i.e. (1) pull-out (see Figure 7.11a); (2) pull-over (see Figure 7.11b) and distortion of thinner material (see Figure 7.11c).

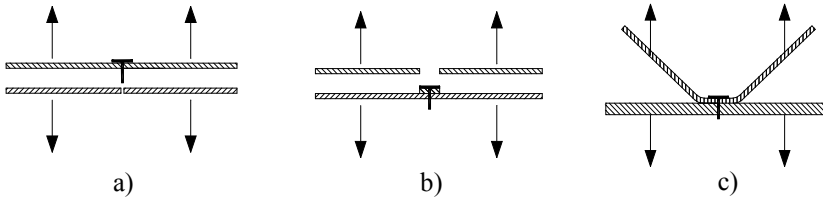


Figure 7.11 – Supplementary failure modes for screwed fastening in tension:
a) pull-out; b) pull-over; c) gross distortion of sheeting

Failure modes of mechanical fastener in tension are not easy to understand. Usually, failure occurs in combinations of two or even three modes. The following supplementary comments may be helpful to the reader:

- (a) Tensile failure of the fastener itself. This failure mode is only likely to occur when the sheeting is excessively thick or when an unsuitable or faulty fastener is used;
- (b) Pull-out of the fastener. This failure mode may occur when the support member is insufficiently thick or when there is insufficient thread engagement;
- (c) Pull-over of the sheeting. In this mode, the sheeting tears around the fastener head of the washer;
- (d) Pull-through of the sheeting. Here, the sheeting distorts sufficiently to pull through from under the head of the fastener and its washer. This is

7. CONNECTIONS

the most frequent mode of failure and is always accompanied by a significant amount of sheet distortion and possibly also distortion of the washer. It is with this and the next mode of failure that the profile geometry starts to become important;

- (e) Gross distortion of the sheeting. This mode of failure is almost entirely a function of the profile geometry rather than the fastener and to some extent, this mode is present in almost all tests of fasteners in tension. It is not at all clear how to define a serviceability or failure limit for this case. This assessment is largely the discretion of the person carrying out the tests.

Figure 7.12 provide test evidence for some of the above mentioned failure modes.

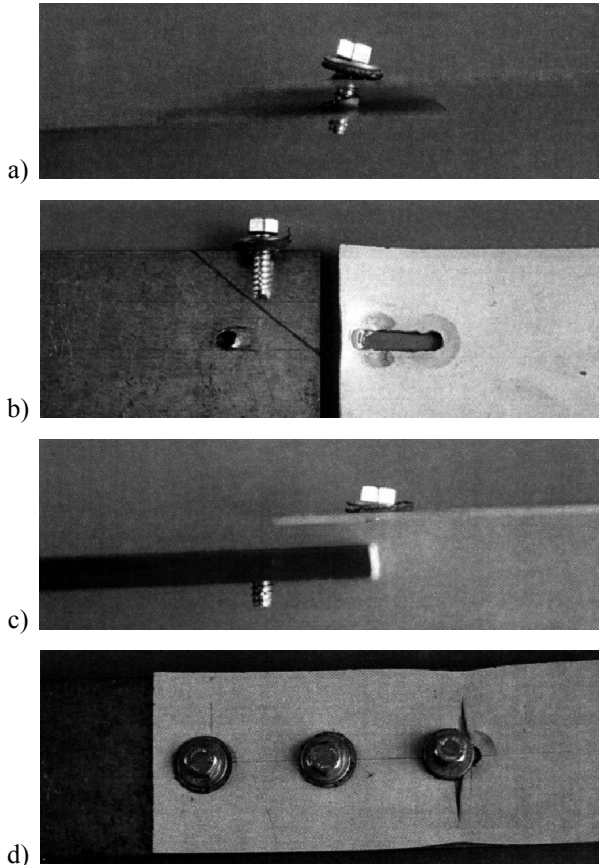


Figure 7.12 – Test evidence for failure of screwed connections: a) Tilling and pull-out of screw; b) Tearing of upper sheet; c) Shearing of screw; d) Net section failure

Rivets

Blind rivets and tubular rivets are often used in cold-formed steel constructions by extension of their applications in automotive and aircraft industries. A blind rivet is a mechanical fastener capable of joining work pieces together where access is limited to one side only. Typically, blind rivets are installed using a locking mechanism which expands the rivet shank. The rivets are installed in predrilled holes. They are used for thin-to-thin fastenings.

Based on the locking method, blind rivets can be classified into pull-stem rivets, explosive rivets and drive-pin rivets (Yu, 2000):

1. *Pull-stem Rivets*. As shown in Figure 7.13(a), pull-stem rivets can be classified into three types:
 - (a) Self-plugging rivets. The stem is pulled into but not through the rivet body and the projecting end is removed in a separate operation;
 - (b) Pull-through rivets. A mandrel or stem is pulled completely out, leaving a hollow rivet;
 - (c) Crimped-mandrel rivets. A part of the mandrel remains as a plug in the rivet body. There are two alternatives: open end (Pull through) and closed end (Pull break);
2. *Explosive Rivets*. (Figure 7.13b) Explosive rivets have a chemical charge in the body. The blind end is expanded by applying heat to the rivet head.
3. *Drive-pin Rivets*. (Figure 7.13c) Drive-pin rivets are two piece rivets consisting of a rivet body and a separate pin installed from the head side of the rivet. The pin, which can be driven into the rivet body by a hammer, flares out of the slotted ends on the blind side.

Tubular rivets are also often used to fasten sheet metal. The strength in shear or compression is comparable to that of solid rivets. Nominally body diameter range from 0.8 to 7.9 mm. The corresponding minimum lengths range from 0.8 to 6.4 mm. When tubular rivets are used to join heavy and thin-gauge stock, the rivet head should be on the side of thin sheet.

Failure of riveted connections is similar to those of screwed connections. Generally speaking, for all kinds of mechanical fasteners it is desirable that the mode of failure of a connection is ductile. It follows that

shear failure of the fastener itself is undesirable and should be avoided. In general, this mode will only occur if the diameter of the fastener is thin compared to the thickness of connected sheets. Aluminium blind rivets are particularly prone to shear failure and are only suitable for load-bearing applications in relatively thin material ($t < 0.7$ mm approx.) (Davies, 1991).

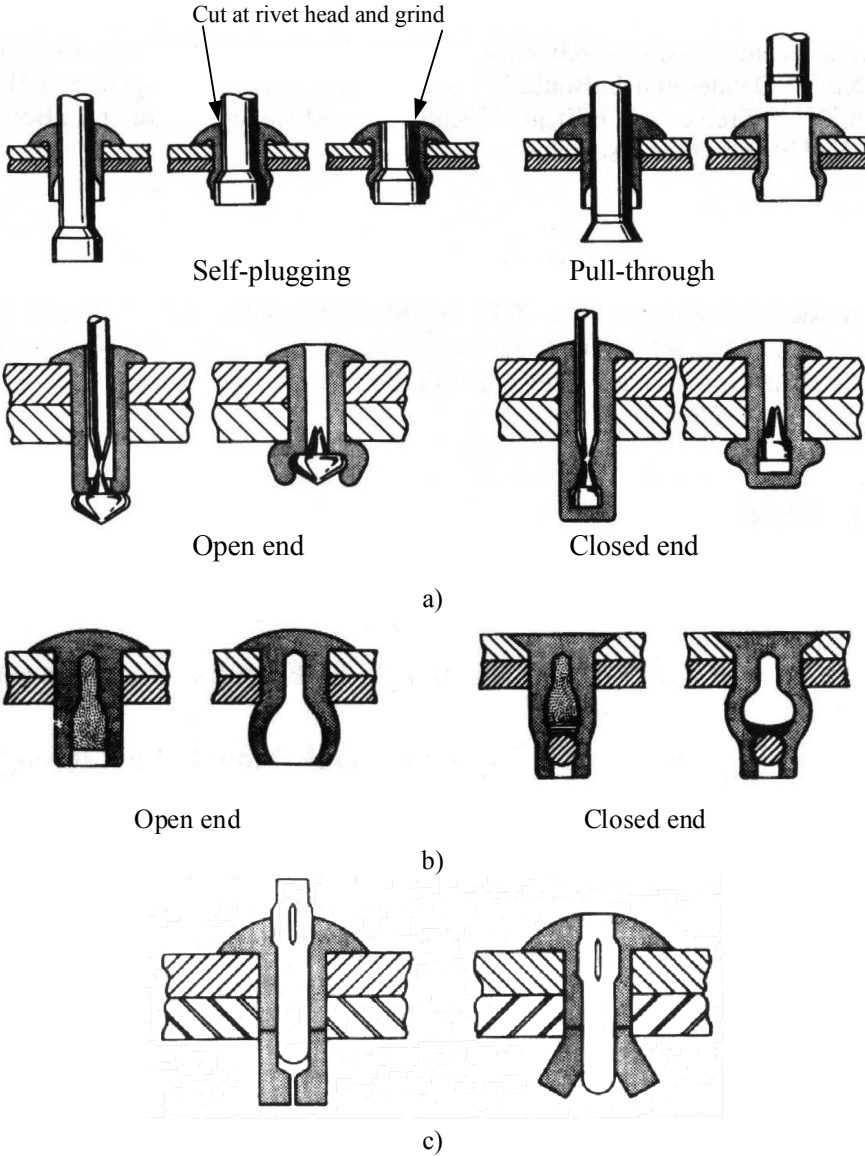


Figure 7.13 – Different types of blind rivets (Yu, 2000)

For other modes of failure, as a very rough guide, adequate deformation capacity of connections may be taken to be (Davies, 1991):

- for seam fasteners between adjacent cladding elements: 0.5 mm;
- for all other connections: 3.0 mm.

Special Mechanical Fastenings

a) Nuts

A number of systems is available where a nut will be fastened to one of the connected parts. Such systems can be used when loose nuts cannot be applied or when it is not possible to make a sufficiently strong fastening with screws. The thickness of the parts to be fastened will not limit the application. Figure 7.14 shows a number of examples featuring loose nuts (Yu *et al*, 1993).

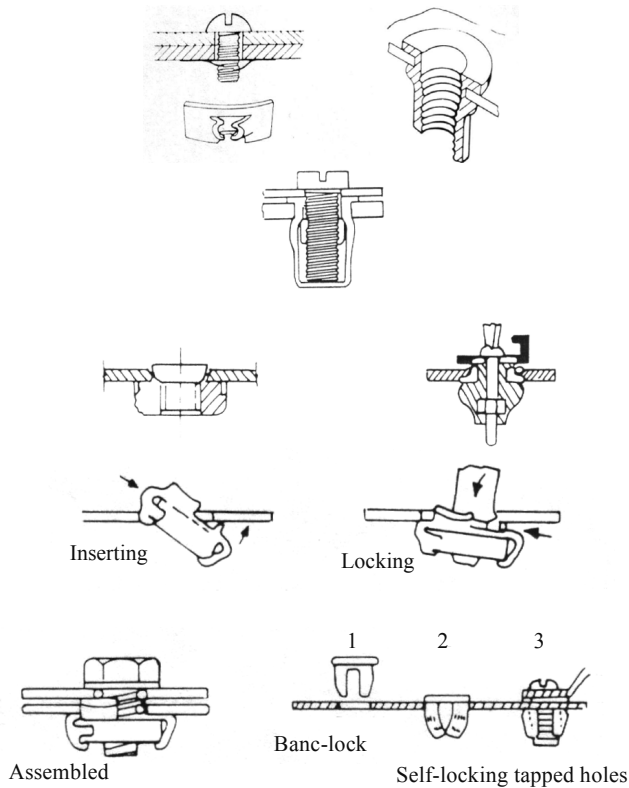


Figure 7.14 – Nut systems (Yu *et al*, 1993)

b) Press joints (Clinched connections)

Press joining is a relatively new technique for joining cold-formed steel sections (Predeschi *et al*, 1997). Press joining is a single-step process which requires a tool consisting of a punch and expanding die as shown in Figure 7.15. The tool parts have a rectangular profile and the punch tapers along the line of cut. The die has a fixed anvil with spring plates on either side. Although the process is a single action, it consists of two phases. In the first phase, the punch moves towards the die and forms a double cut in the two steel sheets. In the second phase, the pressed sheets are flattened against an anvil in order to spread the sheets laterally and form a permanent connection.

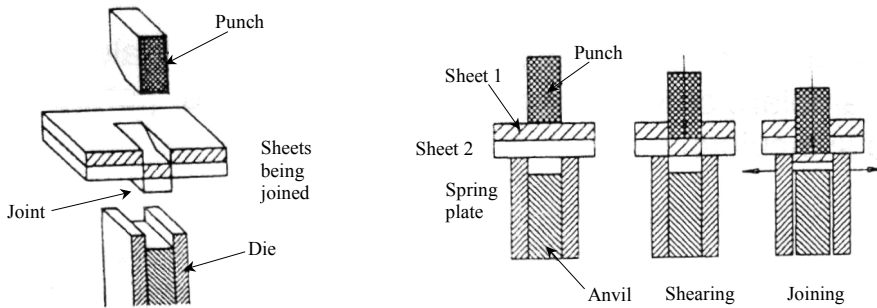


Figure 7.15 – Press joining

The advantages of press joining in the context of construction are (Davies *et al*, 1996):

- the joint is formed using the material of the sheets to be connected and no additional items are required;
- it does not destroy protective coatings such as galvanising;
- it is very rapid, taking less than one second to form a joint;
- it is very efficient, requiring about 10% of the energy for spot welding;
- multipoint joining tools can produce several joints simultaneously;
- the joint can be made air and water tight.

Press joining can be used for fabrication of beams, studs, trusses and other structural systems. Davies *et al* (1996) have discussed the strength and stiffness of press joints and shown that these are entirely suitable for structural purposes. Helenius (2000) has given a detailed discussion of their

mechanical strength and Davies *et al* (1996) have described their successful application in modular construction. Joins of this type have been extensively used in a number of buildings, including the “CIBBAP” cassettes wall project in France (Davies, 2005). Evidently, this is a technique that should have a prominent place in the panel or modular construction of steel framed houses.

c) “Rosette” system

The “Rosette” is another joining method which is particularly suited to the fabrication of light gauge steel frames (Makelainen & Kesti, 1999). A Rosette joint is made between a preformed hole in one of the parts to be joined and a collared hole in the other. The parts are snapped together and then a special hydraulic tool is used to pull back the collar and crimp it over the non-collared part of the connection, as shown in Figure 7.16. A Rosette typically has a nominal diameter of 20 mm and a strength several times that of a press joint or conventional mechanical connection such as screw or blind rivet.

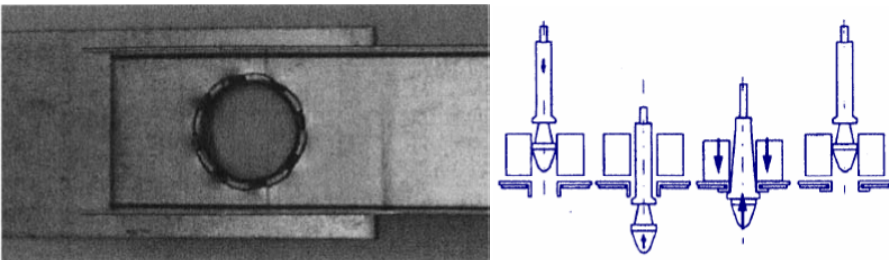


Figure 7.16 – Rosette-joint and rosette-joining process (Makelainen & Kesti, 1999)

Design codes do not contain provisions for special fasteners. Their design is mainly based on testing and guidelines offered by fabricators.

7.2.1.2 Mechanical fasteners for sheeting

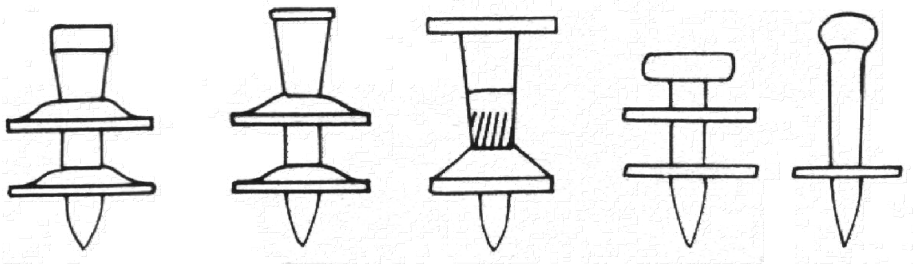
In sheeting applications, screws are used for fastening to the substructure, and screws and blind rivets are used for fastening at the seams (see Figure 7.9). Furthermore shot pins and seam locking are also used.

Shot (Fired) Pins. Shot pins are fasteners driven through the material to be fastened into the base metal structure. Depending on the type of the driving energy, there are:

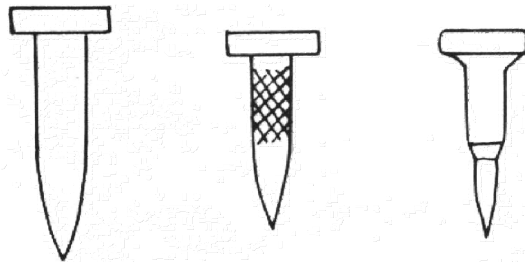
- Powder actuated fasteners, which are installed with tools containing cartridges filled with propellant that is ignited (minimum thickness of substructure 4 mm);
- Air-driven fasteners, which are installed with tools powered by compressed air (minimum thickness of substructure 3 mm).

Figure 7.17 shows examples of shot fired pins. The failure modes and design of shot pin connections are similar to those of screwed connections.

Seam locking. Seam locking is used in structural applications as longitudinal connections between adjacent (flat) sheets. Single or double fold locking can be used.



Five types of powder actuated fasteners



Three types of air driven fasteners

Figure 7.17 – Shot fired pins

7.2.1.3 Mechanical fasteners for sandwich panels

Sandwich panels are usually fastened to the building frame with long screws going through the panel or with special connectors placed in the

longitudinal joints between the panels. Figure 7.18 shows examples of screws used to fasten sandwich panels, both for roof and wall cladding are shown (SFS Intec AG, <http://www.sfsintec.biz>). For flashing and covers of seams, blind rivets or screws are often being used.

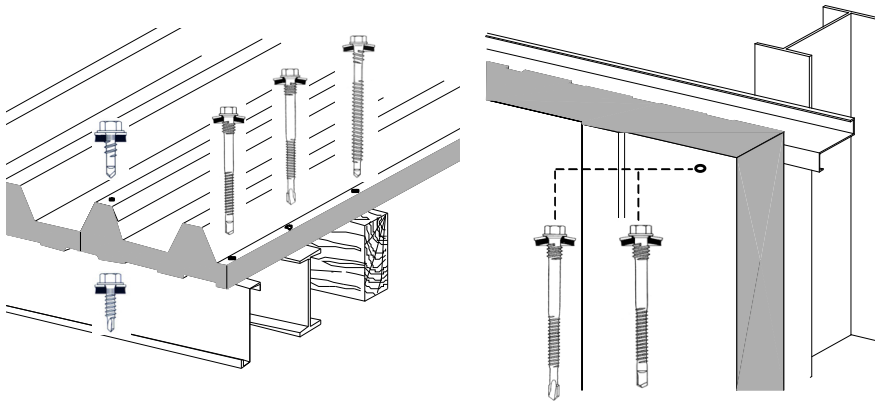


Figure 7.18 – Screws used to fastening sandwich panels (SFS Intec AG, <http://www.sfsintec.biz>)

Fasteners between the panel and the supporting structure are loaded by tensile and shear forces. Tensile forces are caused by wind suction and temperature loads and shear forces by temperature expansion of the faces, by diaphragm (stress skin) action and sometime also by the self-weight of the panel. The characteristic strength of connections loaded in tension and shear by either static or repeated loads may be determine by testing according to the procedure given in ECCS no. 127/CIB no. 320 Recommendations (ECCS, 2009).

The failure modes and the flexibility of screw connections in sandwich panels differ from those in trapezoidal sheeting as illustrated in Figure 7.19. In tension, the screws which pass right through the sandwich panel fix the external face to the supporting structure. The presence of the elastic core between the head of the screw and the supporting structure increases the flexibility and changes the failure mode. Conversely, in shear, the through fixing screws effectively only transfer the shear force between the inner face of the panel and the supporting structure.

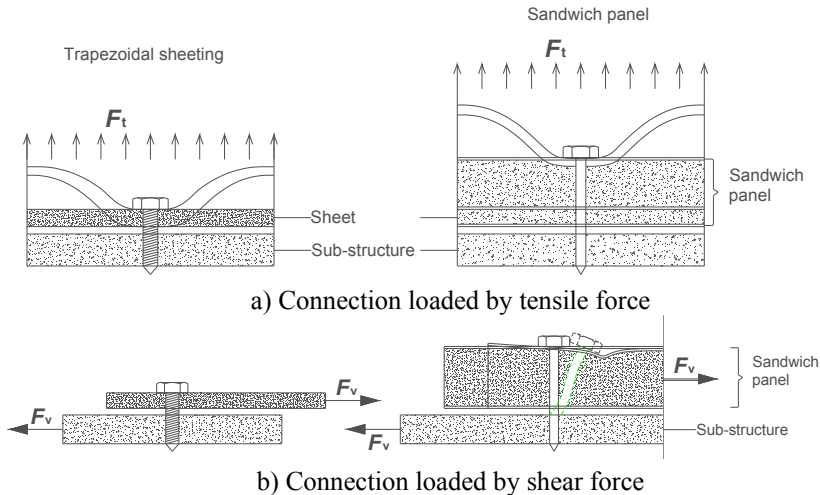


Figure 7.19 – Local deformations of screw connections in trapezoidal sheeting and sandwich panels when loaded by a) tensile and b) shear forces (Davies, 2001)

In principle, the design expressions for screw connections similar to those for two metal sheets can be used to provide very approximate expressions for the common screw connections used in the erection of sandwich panels. These expressions should only be used in the preliminary phases of the design (Davies, 2001).

480

For a reliable design it is recommended to evaluate experimentally both tension and shear strengths of crews connections following the provisions of ECCS no. 127/CIB no. 320 Recommendations (ECCS, 2009).

7.2.2 Welding

Welds to connect cold-formed steel may be either arc welds or resistance welds. In building construction, however, welds are generally made using the arc welding process. Resistance welds are commonly used for connecting thin sheet steels in the automotive industry. Arc welding is the process of fusing material together by an electric arc and the addition of weld filler material.

EN1993-1-3 (CEN, 2006a) contains provisions for the design of welds for cold-formed steel construction. All welding consumables must conform to the requirements of EN1993-1-8 (CEN, 2005e). The code contains

requirements for the following types of welds: (1) spot welds (2) fillet welds and (3) arch spot welds. Both resistance welds and fusion arc welds are permitted.

7.2.2.1 Fusion arc welding

The principle of open arc welding is a heat input by an electrical open arc struck between an electrode and a workpiece. Either covered electrodes or welding wires are used as welding consumables. During the welding process, the molten pool is protected against harmful environmental influences by slag gas.

The following welding procedures are normally used for thin-walled sections (Yu, 2000; Toma *et al*, 1993): SMA – Shield Metal Arc Welding; FCA – Flux Cored Arc Welding; SA – Submerged Arc Welding; GMA – Gas Metal Arc Welding; GTA – Gas Tungsten Arc, or TIG – Tungsten Inert Gas Welding and Plasma Welding.

The most common weld type to connect sheet-to-sheet or cross section-to-cross section is the fillet weld. Groove (or butt) welds are commonly used during the roll-forming process to connect flat sheet of one coil to the subsequent coil. Arc spot welds, commonly called puddle welds, are used extensively to attach deck and panels to bar joists or hot-rolled shapes.

Welding electrodes should appropriately match the strength of the base metals. The following welding processes may be used for cold-formed steel construction: shielded metal arc welding (SMA); gas metal arc welding (GMA); flux cored arc welding (FCA); gas tungsten arc welding (GTA) also known as tungsten-inert gas welding (TIG) and submerged arc welding (SA).

Shield metal arc welding (SMA), commonly known as stick electrode welding or manual welding, is the oldest of the arc welding processes. It is characterised by versatility, simplicity and flexibility. The SMA process is commonly used for tack welding, fabrication of miscellaneous components, and repair welding. SMA has earned a reputation for depositing high quality welds. It is, however, slower and more costly than other methods of welding, and is more dependent on operator skill for high quality welds.

The flux cored arc welding (FCA) process offers two distinct advantages over shield metal arc welding. First, the electrode is continuous. This eliminates the starts and stops (welding discontinuities) that are inevitable with shielded metal arc welding. Another advantage is that increased amperages can be used with flux cored arc welding, with a corresponding increase in deposition rate and productivity.

Submerged arc welding (SA) differs from other arc welding processes in that a layer of fusible granular material called flux is used for shielding the arc and the molten metal. The arc is struck between the workpiece and a bare wire electrode, the tip of which is submerged in the flux. Since the arc is completely covered by the flux, it is not visible and the weld is made without the flash, spatter, and sparks that characterise the open-arc processes. The nature of the flux is such that very little smoke or visible fumes are released to the air.

Gas metal arc welding (GMA) utilizes equipment much that like used in flux cored arc welding. Indeed, the two processes are very similar, except the GMA uses a solid or metal cored electrode and leaves no appreciable amount of residual slag. Gas metal arc has not been a popular method of welding in the fabrication shop. A variety of shielding gases or gas mixtures may be used for GMA. Carbon dioxide (CO_2) is the lowest cost gas, and while acceptable for welding carbon steel, the gas is not inert but active at elevated temperatures. This has given rise to the term MAG (metal active gas) for the process when (CO_2) is used, and MIG (metal inert gas) when predominantly argon-based mixtures are used.

Gas tungsten arc welding (GTA) or tungsten inert gas (TIG) is a process where fusion is produced by heating with an arc between a tungsten electrode and the base metal. The hot tungsten electrode, arc, and weld pool are shielded by an inert gas or mixture of the inert gases. Filler metal may be added, if needed, by feeding a filler rod into the weld pool either manually or automatically.

An alternative to the GTA (TIG) process is plasma welding. Plasma is produced between a tungsten electrode and the base material. In comparison with the GTA (TIG) process, the energy input during the welding procedure is more concentrated.

The usual types of arc welds used to connect steel members are shown in Figure 7.20. Groove or butt welds may be difficult to produce in thin sheet

and are therefore not as common as fillet, spot and slot welds. Arc spot and slot welds are commonly used for welding cold-formed steel decks and panels to their supporting frames. Flare bevel grooved welds and flare V-grove welds are used to produce built-up sections.

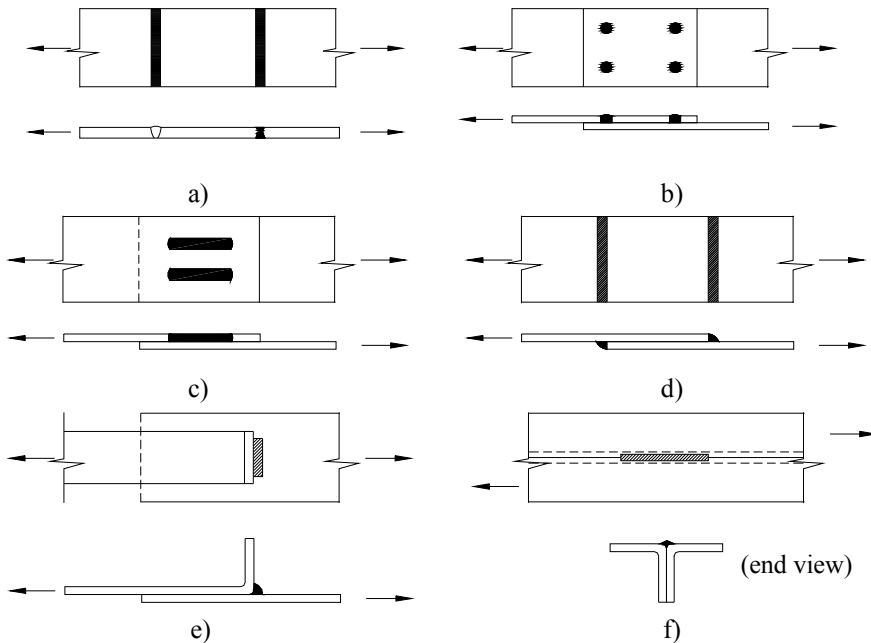


Figure 7.20 – Types of arc (fusion) welds (Yu, 2000): a) Groove welds in butt joints; b) Arc spot weld (puddle weld); c) Plug and slot welds; d) Fillet welds; e) Flare bevel groove weld; f) Flare V-grove weld

7.2.2.2 Resistance welding

Resistance welding is done without open arc. In contrary to the open arc welding process there is no need of protection of the molten metal by shielding gas slag.

During this procedure, special electrodes led the welding current locally with high density to the base material. The workpiece is being so strongly heated that it turns into plastic condition and starts to melt. In this condition a pressure transferred by the electrodes to the workpiece leads to a local connection of the construction pieces. Figure 7.21 shows the available resistance welding procedures.

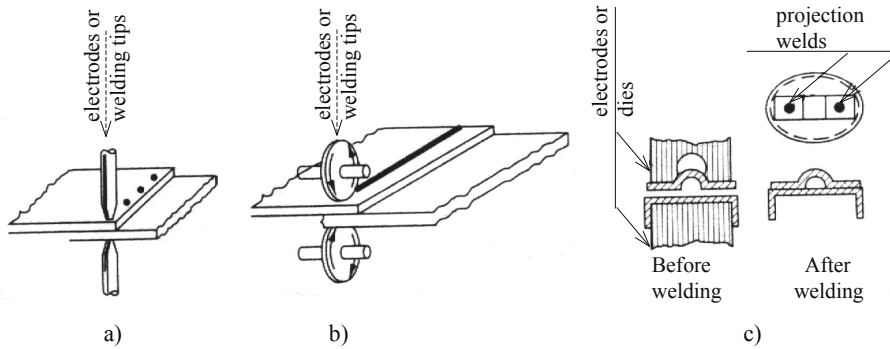


Figure 7.21 – Resistance welding procedures: a) spot welding; b) seam welding; c) projection welding

7.2.2.3 Behaviour of cold-formed steel welds

As previously shown, thin-walled sections and sheeting are normally welded with conventional equipment and electrodes. However, the design of cold-formed steel connections is usually different from that of hot-rolled sections and plates for the following reasons (Yu, 2000):

- Stress resisting areas are more difficult to define;
- Welds such as spot and slot welds are made through the welded sheet without any preparation;
- Galvanising and paint are not normally removed prior to welding;
- Failure modes are complex and difficult to categorise.

Concerning the last point, failure modes in welded thin steel often involve a combination of basic modes, such as base steel (sheet) tearing and weld shear, as well as large amount of out-of-plane distortion of the welded sheet.

In general, fillet welds in thin sheet steel are detailed such that the leg length on the sheet edge is equal to the sheet thickness and the other leg is often two to three times longer. The throat thickness a (see Figure 7.22a1) is commonly larger than the thickness t of the sheet steel and hence ultimate failure is usually found to occur by tearing of the plate adjacent to the weld or along the weld contour (see Figure 7.22). In most cases, yielding is poorly defined (e.g. no ductility) and rupture rather than yielding is a more reliable criterion of failure.

Figure 7.22 shows comparatively the failure modes of transverse and longitudinal fillet welds.

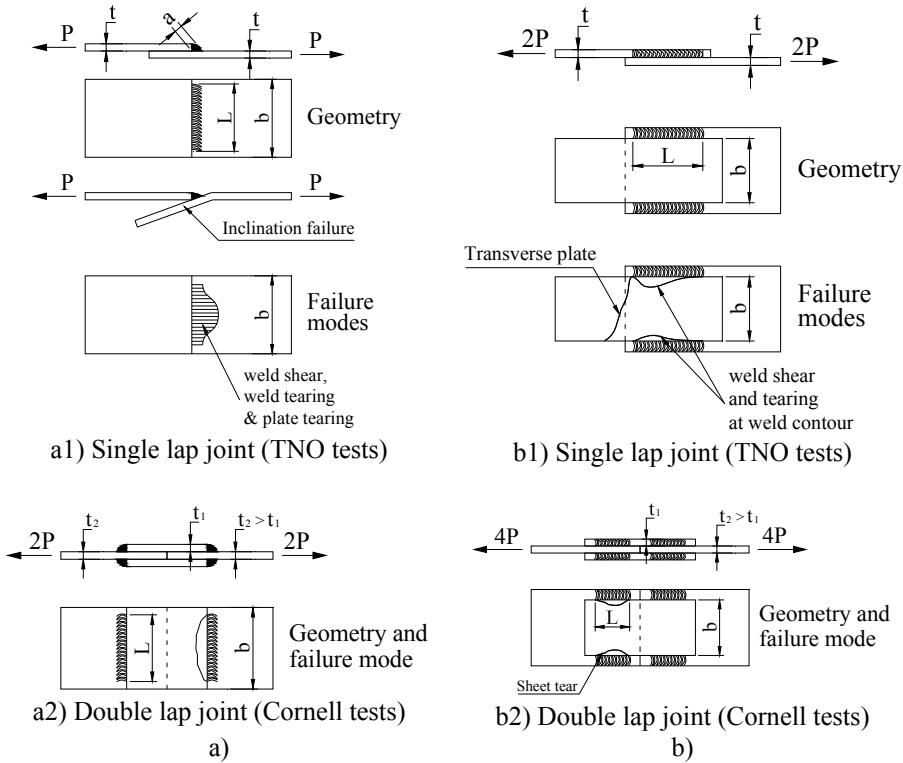


Figure 7.22 – Failure modes in fillet welds: a) transverse weld action; b) longitudinal weld action (Stark & Soetens, 1980)

The failure modes of spot welds are similar to those of lap bolted joints, as shown in Figure 7.23.

EN1993-1-8 (CEN, 2005e) states that assembly and welding shall be carried out in such a way that the final dimensions are within the appropriate tolerance. In accordance with the code, the project specifications must stipulate details pertaining to welded connections that require special welding procedures, special levels of quality control, special inspections procedures, or special test procedures.

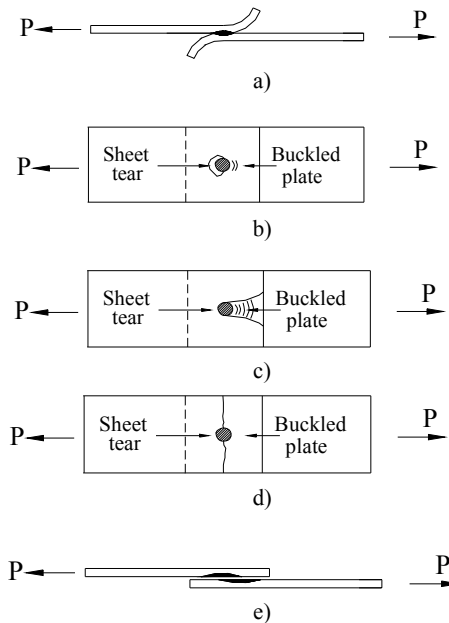


Figure 7.23 – Failure modes in spot welds (Stark & Soetens, 1980): a) Inclusion failure; b) tearing and bearing at weld contour; c) Edge failure; d) Net section failure; e) Weld shear failure

7.2.3 Fastening based on adhesive bonding

486

For fastening by means of bonding it is important to realise that a bonded connection possesses good shear resistance and mostly poor peeling resistance (see Figure 7.24). For that reason, a combination of bonding and mechanical fastening is occasionally chosen. Adhesives used for thin-walled steels are as follows:

- epoxy adhesive types – best hardening will appear under elevated temperature (typically 80-120°C);
- acrylic adhesive types – more flexible than the epoxy types.

Two advantages of bonded connections are a uniform distribution of forces over the connection and a high resistance to repeated loading. Some disadvantages are that the surface should be flat and clean and there is a hardening time.

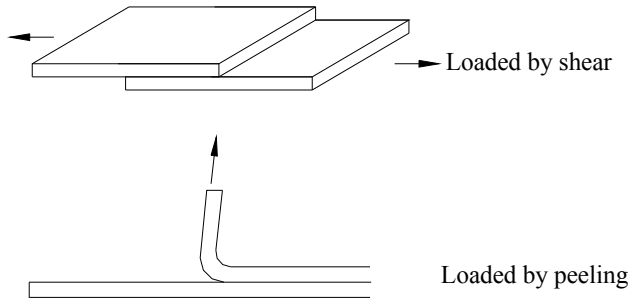


Figure 7.24 – Shear and peeling of connections by means of adhesive bonding

7.3 MECHANICAL PROPERTIES OF CONNECTIONS

The important mechanical properties of connections are strength (capacity), rigidity, and deformation capacity or ductility (see Figure 7.25).

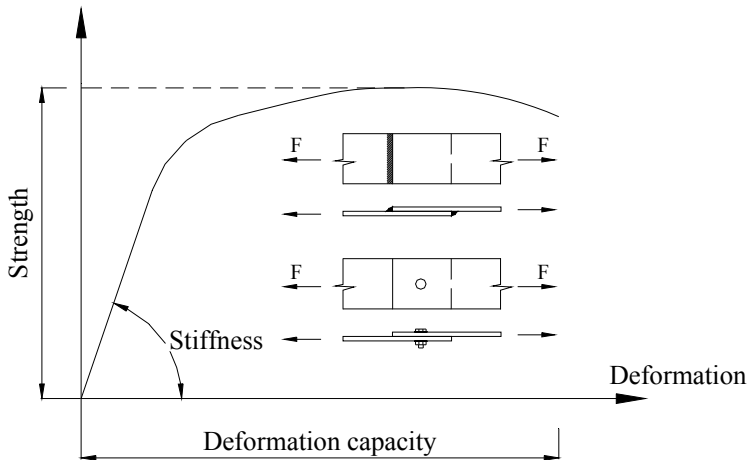


Figure 7.25 – Main feature of connection response

Strength

Connection must possess the necessary strength to ensures the reliable transfer of internal forces, in Ultimate Limit State stage, in between connected elements.

The strength of the connections mainly depends on:

- the type of the fastener, and

- the properties of the connected elements e.g. thickness and yield stress.

The most reliable strength values are determined by testing. However, design codes, like EN1993-1-3 (CEN, 2006a), for instance, but also the North American Specifications AISI S100-07 and AS/NZS 4600:2005 provide formulas to determine the shear and tension resistance of most common fastener types together with their range of application.

In case of special fasteners techniques, like press joining, “Rosette” or loose nuts, design procedures are provided by fabricators.

Stiffness

The stiffness of a connection is important because it determines the overall stiffness of the structures or its components. Moreover, the stiffness of the connections will influence the force distribution within the structure. Especially when the connection is a part of a bracing structure, the stiffer the connection the lower the bracing force will be (Yu *et al.*, 1993).

Traditionally, bolted and screwed connections in cold-formed steel framing and trusses are considered either rigid (continuous framing) or pinned. Experimental research and numerical studies performed in last decade have provided evidence of the semi-rigid character of the behaviour of these connections (Zandanfarrokh & Bryan, 1992; Zaharia & Dubina, 2000; Lim, 2001, Wong & Chung, 2002). As direct consequence of semi-rigidity, these connections have partial moment resistance or semi-continuous.

In case of thin-walled steel structures the real behaviour of connections should be taken into account because, if neglected, it could lead either to unsafe or uneconomic design.

For the purpose of evaluation of the rigidity of bolted connections in cold-formed steel joints, Zandanfarroch & Bryan (1992) and Zaharia & Dubina (2000) proposed basic formulas for single bolt lap joints. For the cases not covered by such formulas, testing procedures are available (Annex A: Testing procedures of EN1993-1-3(CEN, 2006a)).

Special systems are available where cold-formed sections interlock to form a connection with a good bending and shear rigidity. This is particularly the case for pallet rack frames.

Deformation capacity

Deformation capacity or ductile behaviour of connections is required in order to allow local redistribution of forces without detrimental effects. Otherwise brittle fracture might be caused by local overloading. A proper detailing and fastener selection is vital in order to ensure sufficient deformation capacity of the connection, particularly in seismic actions.

7.4 DESIGN OF CONNECTIONS

In this section, design procedures according to EN1993-1-3 (CEN, 2006a) and EN 1993-1-8 (CEN, 2005e) will be presented, accompanied by design examples.

7.4.1 General design considerations

EN1993-1-8:2005 distinguishes between connections and joints. For this reason the following basic definitions must be considered:

Connection: location at which two or more elements meet. For design purposes it is the assembly of the basic components required to represent the behaviour during the transfer of the relevant internal forces and moments at the connection.

Joint: zone where two or more members are interconnected. For design purposes it is the assembly of the basic components required to represent the behaviour during the transfer of the relevant internal forces and moments between the connected members.

Joint configuration: type or layout of the joint or joints in a zone within which the axes of two or more inter-connected members intersect.

However, in case of cold-formed steel framing, generally no significant distinction can be made between joint and connection.

The resistance of a joint shall be determined on the basis of the resistance of the individual fasteners, welds and other components of the joint. For cold-formed steel structures, elastic analysis is recommended for

the design of joints. Alternatively, for special cases, elastoplastic analysis of the joint may be used provided it takes account of the load-deformation characteristics of the components of the joint.

Where fasteners with different stiffness are used to carry a shear load, the fastener with the highest stiffness should be designed to carry the design load.

Design of connections for cold-formed steel may be based on calculation procedures and specific test results. Testing procedures to produce experimental results to be used in the design procedure presented in this book will be based on the provisions of Chapter 9 and Annex A of EN1993-1-3. Alternatively, design data provided by fabricators for specific type of fasteners may also be used.

The following general design assumptions have to be considered when designing structural connections in cold-formed steel constructions:

- 1) Joints shall be designed on the basis of a realistic assumption of the distribution of internal forces and moments, having regard to relative stiffness within the joint. This distribution shall be representative of the load paths through the elements of the joint. It shall be ensured that equilibrium is maintained with the applied external forces and moments;
- 2) Allowance may be made for the ductility of steel in facilitating the redistribution of internal forces generated within a joint. Accordingly, residual stresses and stresses due to tightening of fasteners and normal accuracy of fit-up need not be considered;
- 3) Ease of fabrication and erection shall be taken into account in the detailing of connections and splices. Attention shall be paid to the clearance necessary for tightening the fasteners, the requirements of welding procedures, and the need for subsequent inspection, surface treatment and maintenance;
- 4) The determination of any structural property of fastener or joint shall be based on design assisted by testing; e.g. a design model should be calibrated/validated by relevant tests according to Annex D of EN1990 (CEN, 2002a).

Usually, members connecting in a joint shall be arranged so that their centroidal axes meet in a point. If there is an eccentricity at the intersection of connected members, the members and connections shall be designed accounting for the resulting moments.

In the case of joints of angles or tees attached by either a single line of

bolts or two lines of bolts, possible eccentricities should be taken into account. In-plane and out-of-plane eccentricities should be determined by considering the relative positions of the centroidal axes of the members and of the setting out lines in the plane of the connection (see Figure 7.26).

Where a connection is subjected to impact or vibration, either preloaded bolts, bolts with locking devices or welding shall be used.

When a connection loaded in shear is subjected to reversal of stresses (unless such stresses are due solely to wind) or where for some special reasons slipping of bolts is not acceptable, either preloaded bolts, fit bolts or welding should be used. However, while available, preloaded bolts are not widely used in cold-formed steel framing.

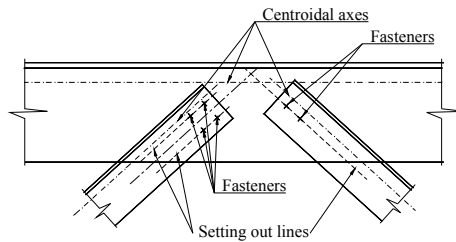


Figure 7.26 – Setting out lines

7.4.2 Design of connections with mechanical fasteners

Standard design procedures, accordingly to EN1993-1-3 (CEN, 2006a) and EN1993-1-8 (CEN, 2005e), for connections with bolts, self-tapping screws, blind rivets and cartridge fired pins will be presented in this section.

The checking formula to be used in the connection design process compares the design resistance of the fastener with the design action induced in the fastener as a result of the design actions on the structure.

The general format for the design checking is:

$$F_{i,Ed} \leq F_{i,Rd} \quad (7.1)$$

where

$F_{i,Ed}$ is the design stress for the fastener, corresponding to failure mode i ;

$F_{i,Rd}$ is the design strength for the fastener, corresponding to failure mode i .

7.4.2.1 General rules

Connections with mechanical fasteners should be compact in shape. The positions of the fasteners (e.g. bolts, screws, rivets, spot welds) should be such as to prevent corrosion and local buckling and to facilitate their installation. Maximum and minimum spacing and end edge distances are given in Table 7.3 with reference to Figure 7.27 (see EN1993-1-8 (CEN, 2005e)).

The minimum spacing values in Table 7.3 are expressed in terms of the nominal diameter of the fastener hole, d_0 , and apply when the thickness of the connected part, t , is greater than 3mm. Therefore, for $t < 3\text{mm}$, and depending the type of mechanical fastener, the minimum spacing values specified in the design procedures given in EN1993-1-3 are a little greater than those of Table 7.3, see §§7.4.3.2 to §§7.4.3.5 for details.

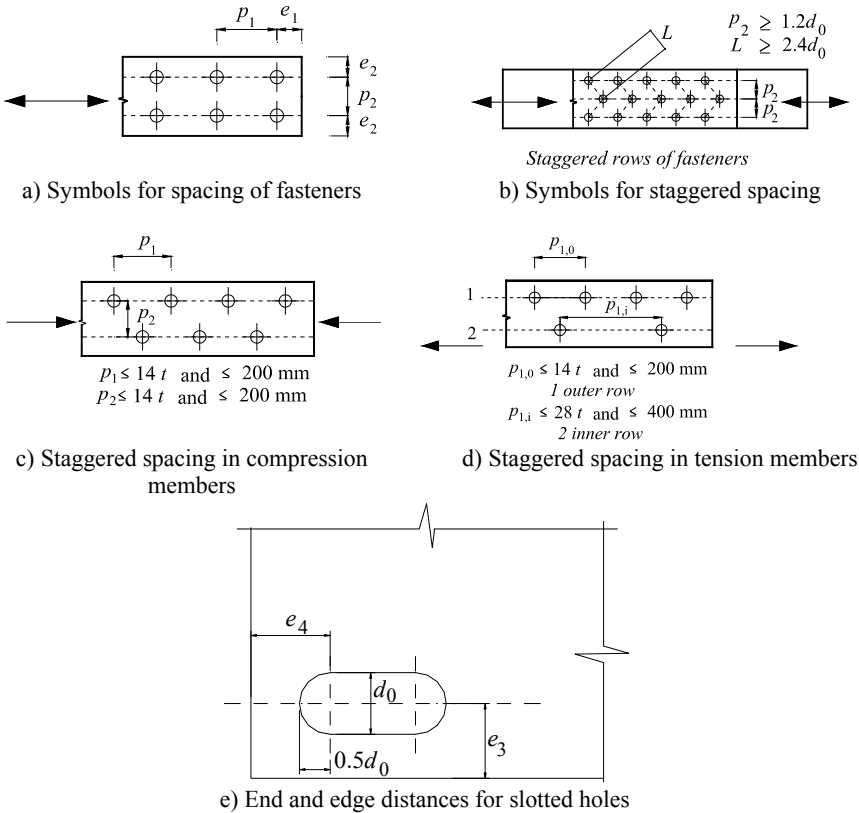


Figure 7.27 – Symbols for end and edge distances and spacing of fasteners (CEN, 2005e)

The shear forces on individual mechanical fasteners in a connection may be assumed to be equal, provided that:

- the fasteners have sufficient ductility;
- shear is not the critical failure mode.

Table 7.3 – Minimum and maximum spacing and end and edge distances (CEN, 2005e), $t > 3$ mm

Distances and spacings, see Figure 7.27	Minimum	Maximum ^{1) 2) 3)}		
		Structures made of steels according to EN 10025 except steels acc. to EN 10025-5		Structures made of steels according to EN 10025-5
		Steel exposed to the weather or other corrosive influences	Steel not exposed to the weather or other corrosive influences	Steel used unprotected
End distance e_1	$1.2d_0$	$4t + 40$ mm		The larger of $8t$ or 125 mm
Edge distance e_2	$1.2d_0$	$4t + 40$ mm		The larger of $8t$ or 125 mm
Distance e_3 in slotted holes	$1.5d_0$ ⁴⁾			
Distance e_4 in slotted holes	$1.5d_0$ ⁴⁾			
Spacing p_1	$2.2d_0$	The smaller of $14t$ or 200 mm	The smaller of $14t$ or 200 mm	The smaller of $14t_{\min}$ or 175 mm
Spacing $p_{1,0}$		The smaller of $14t$ or 200 mm		
Spacing $p_{1,i}$		The smaller of $28t$ or 400 mm		
Spacing p_2 ⁵⁾	$2.4d_0$	The smaller of $14t$ or 200 mm	The smaller of $14t$ or 200 mm	The smaller of $14t_{\min}$ or 175 mm

¹⁾ Maximum values for spacings, edge and end distances are unlimited, except in the following cases:

- for compression members in order to avoid local buckling and to prevent corrosion in exposed members and;
- for exposed tension members to prevent corrosion.

²⁾ The local buckling resistance of the plate in compression between the fasteners should be calculated as a column by using $0.6 p_i$ as buckling length. Local buckling between the fasteners need not to be checked if p_i/t is smaller than 9ε . The edge distance should not exceed the maximum to satisfy local buckling requirements for an outstand element in the compression members. The end distance is not affected by this requirement.

³⁾ t is the thickness of the thinner outer connected part.

⁴⁾ The limits for slotted holes, see execution standards (e.g. EN1090:2008)

⁵⁾ For staggered rows of fasteners a minimum line spacing $p_2 = 1.2d_0$ may be used, if the minimum distance between any two fasteners in a staggered row $L \geq 2.4d_0$, see Figure 7.27b.

7. CONNECTIONS

The resistance of individual mechanical fasteners is specified by relevant standards or can be determined by tests. For bolts, the nominal values of the yield strength, f_{yb} and the ultimate strength f_{ub} are given in Table 7.4 and they should be adopted as characteristic values in design calculations.

Table 7.4: Nominal values of the yield strength f_{yb} and the ultimate tensile strength f_{ub} for bolts

Bolt grade	4.6	4.8	5.6	5.8	6.8	8.8	10
f_{yb} (N/mm ²)	240	320	300	400	480	640	90
f_{ub} (N/mm ²)	400	400	500	500	600	800	10

As the characteristic minimum shear resistance $F_{v,Rk}$ of self-tapping screws, the values given in Table 7.5 can be used. As the characteristic minimum tension resistance $F_{t,Rk}$ of self-tapping screws the value $1.2 F_{v,Rk}$ can be used.

Table 7.5 – Characteristic shear resistance $F_{v,Rk}$ of self-tapping screws (N/screw)

The outside diameter of the thread (mm)	The material of the screw	
	Hardened steel	Stainless steel
4.8	5200	4600
5.5	7200	6500
6.3	9800	8500
8.0	16300	14300

As the characteristic minimum shear resistance $F_{v,Rk}$ of blind rivets, the value given in Table 7.6 can be used. As the characteristic minimum tension resistance $F_{t,Rk}$ of blind rivets the value $1.2 F_{v,Rk}$ can be used.

Table 7.6 – Characteristic shear resistance $F_{v,Rk}$ of blind rivets (N/blind rivet)

The diameter of the shank (mm)	The material of the blind rivet			
	Steel	Stainless steel	Monel	Aluminium
4.0	1600	2800	2400	800
4.8	2400	4200	3500	1100
5.0	2600	4600	-	-
6.4	4400		6200	2000

The values given in Tables 7.5 and 7.6 can be used if a certified product clarification approved by competent authority is available. It shall be stated in the certified products clarification that the values given in Tables 7.5 and 7.6 can be achieved. Larger characteristic values can be used if they are proved by tests according to Section 9 of EN1993-1-3.

If the pull-out resistance of a fastener, $F_{o,Rd}$ is smaller than its pull-through resistance, $F_{p,Rd}$, the deformation capacity should be determined by tests.

The pull-through resistance calculated for self-tapping screws and cartridge fired pins, according to the design procedures given in EN1993-1-3 and presented in the following paragraphs of this book, should be reduced if the fasteners are not located centrally in the troughs of the sheeting. If attachment is at a quarter point, the design resistance should be reduced to $0.9F_{p,Rd}$ and if there are fasteners at both quarter points, the resistance should be taken $0.7F_{p,Rd}$ per fastener (see Figure 7.28).

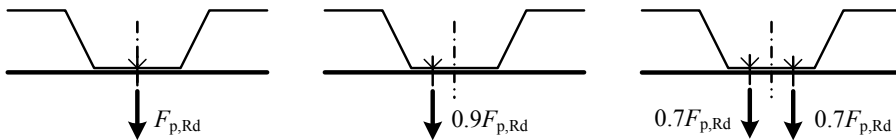


Figure 7.28 – Reduction of pull-through resistance, $F_{p,Rd}$, due to the position of the fasteners

For a fastener loaded in combined shear and tension, if either the shear resistance, $F_{v,Rd}$ or the tension resistance, $F_{t,Rd}$ have been determined by testing, the resistance of the fastener to the combined effect of shear and tension should also be verified on the basis of tests. Provided that both $F_{t,Rd}$ and $F_{v,Rd}$ are determined by calculation, then the following interactive equation must be verified using:

$$\frac{F_{t,Ed}}{\min(F_{p,Rd}, F_{o,Rd})} + \frac{F_{v,Ed}}{\min(F_{b,Rd}, F_{n,Rd})} \leq 1 \quad (7.2)$$

where $F_{t,Ed}$ and $F_{v,Ed}$ are tension and shear design stresses acting on the fastener.

The limit state of gross section distortion may be assumed to be implicitly satisfied if the design resistance of a fastener is verified by calculation, provided that the fastening is through a flange not more than 150 mm wide.

The diameter of the holes for screws should be in accordance with the manufacturer’s guidelines. These guidelines should be based on the following criteria:

1. the applied torque should be just higher than the threading torque;
2. the applied torque should be lower than the thread stripping torque or head-shearing torque;
3. the threading torque should be smaller than 2/3 of the head-shearing torque.

For long joints, characterised by the distance L_j between the centre of the end fasteners, measured in the direction of the load transfer (see Figure 7.29), being larger than $15d$, the design shear resistance $F_{v,Rd}$ of all fasteners should be reduced by multiplying the resistance by a reduction factor β_{Lf} , given by:

$$\beta_{Lf} = 1 - \frac{L_j - 15 \cdot d}{200 \cdot d} \tag{7.3}$$

but $0.75 \leq \beta_{Lf} \leq 1.0$, where d is the diameter of the fastener.

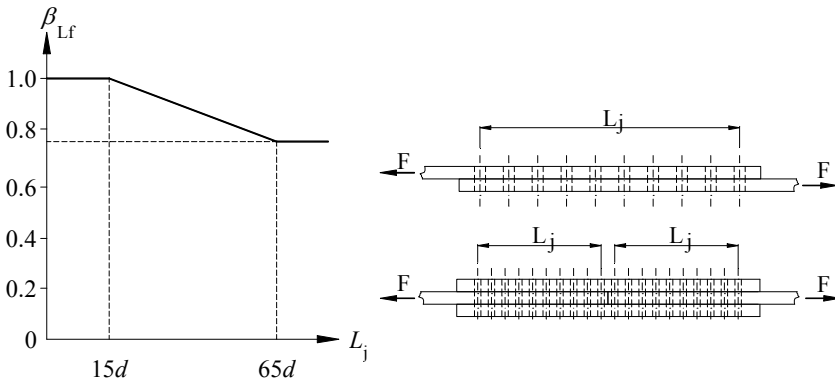


Figure 7.29 – Long joints

This provision does not apply when there is an uniform distribution of

the force transfer over the length of the joint, e.g. the transfer of the shear force between the web and the flange of a section.

The design rules for blind rivets are valid only if the diameter of the hole is not more than 0.1 mm larger than the diameter of the rivet.

Bolts M12 and M14, for which the normal clearance is of 1 mm, may also be used in 2 mm clearance holes provided that for bolts of strength grade 4.8 to 10.9 the design shear resistance $F_{v,Rd}$ is taken as 0.85 times the value corresponding to normal clearance. This application should be applied only when $F_{b,Rd} \geq F_{v,Rd}$.

In single lap joints with only one bolt row (see Figure 7.30), the bolts should be provided with washers under both the head and the nut. The bearing resistance $F_{b,Rd}$ for each bolt should be limited to:

$$F_{t,Rd} \leq 1.5 \cdot f_u \cdot d \cdot t / \gamma_{M2}; t = \min(t_1, t_2); \gamma_{M2} = 1.25 \quad (7.4)$$

Single rivets should not be used in single lap joints.

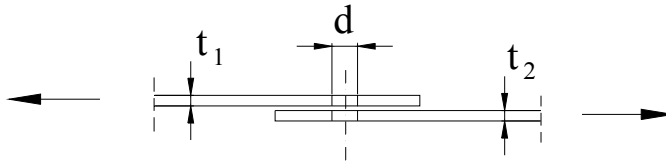


Figure 7.30 – Single lap joint with one row of bolts

In this chapter the following notations will be used:

- A is the gross cross sectional area of a fastener;
- A_s is the tensile stress area of a fastener;
- A_{net} is the net cross sectional area of the connected part;
- β_{lf} is the reduction factor for long joints according to EN1993-1-8;
- d is the nominal diameter of the fastener;
- d_o is the nominal diameter of the hole;
- d_w is the diameter of the washer or the head of the fastener;
- e_1 is the end distance from the centre of the fastener to the adjacent end of the connected part, in the direction of the load transfer;
- e_2 is the edge distance from the centre of the fastener to the

	adjacent edge of the connected part, in the direction perpendicular to the direction of the load transfer;
f_{ub}	is the ultimate tensile strength of the fastener material;
$f_{u,sup}$	is the ultimate tensile strength of the supporting member into which a screw is fixed;
n	is the number of sheets that are fixed to the supporting member by the same screw or pin;
n_f	is the number of mechanical fasteners in one connection;
p_1	is the spacing centre-to-centre of fasteners in the direction of the load transfer;
p_2	is the spacing centre-to-centre of fasteners in the direction perpendicular to the direction of load transfer;
t	is the thickness of the thinner connected part or sheet;
t_1	is the thickness of the thicker connected part or sheet;
t_{sup}	is the thickness of the supporting member into which a screw or a pin is fixed.

The following paragraphs present the EN1993-1-3 (CEN, 2006a) design procedures for connections with bolts, screws, rivets and fired pins. The format of presentation is kept as in the code. The partial factor γ_{M2} for calculating the design resistance of mechanical fasteners shall be taken as $\gamma_{M2} = 1.25$. For connections with bolts and screws, relevant design examples are presented to the reader.

7.4.2.2 Design of bolted connections

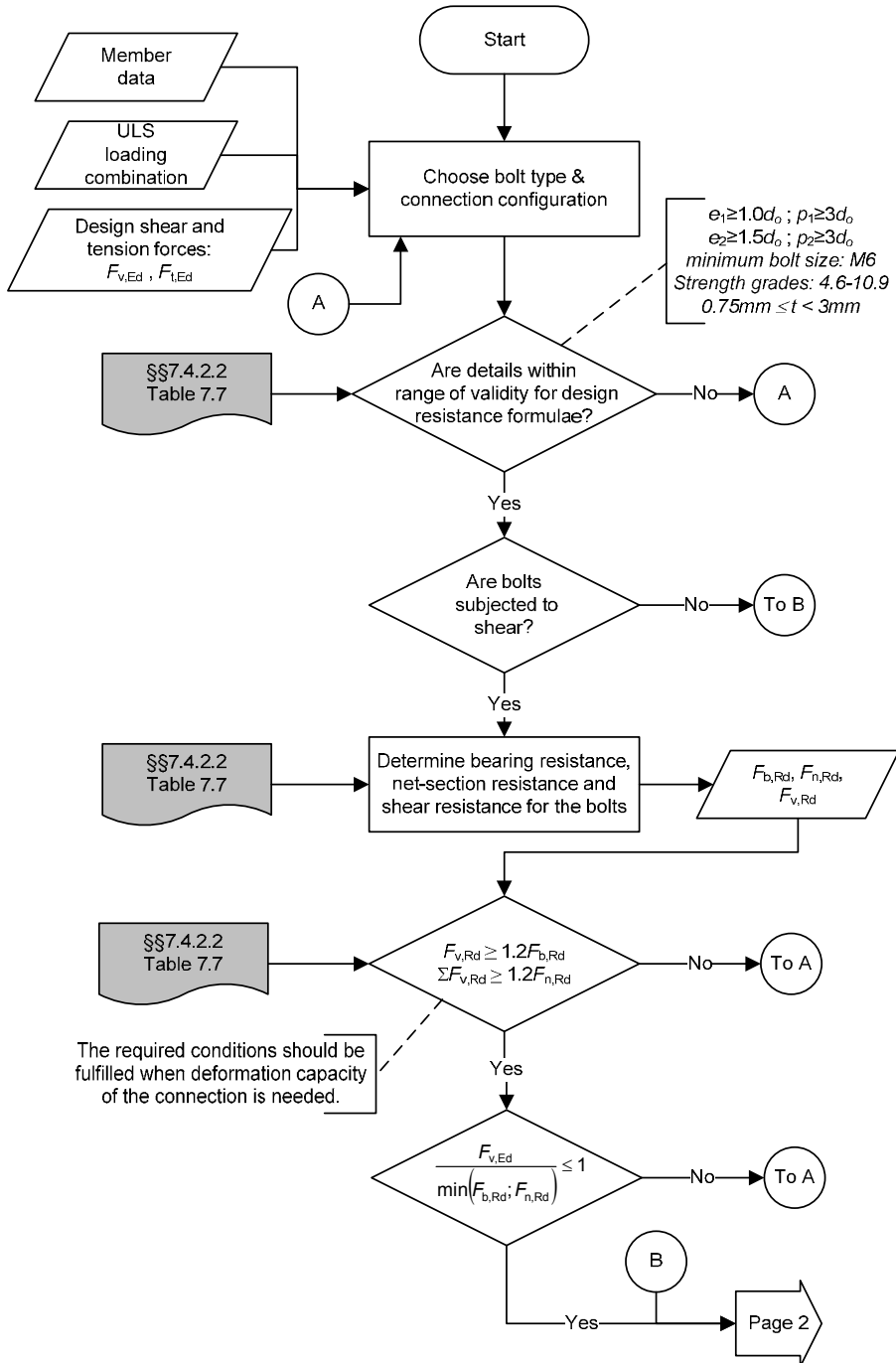
Bolted connections are normally used as shear, tension or moment resistant connections in cold-formed steel framing.

Design of bolted connections can be done on the basis of the general formula (7.1), in which the design resistances given in Table 7.7 must be used and the partial factor $\gamma_{M2} = 1.25$.

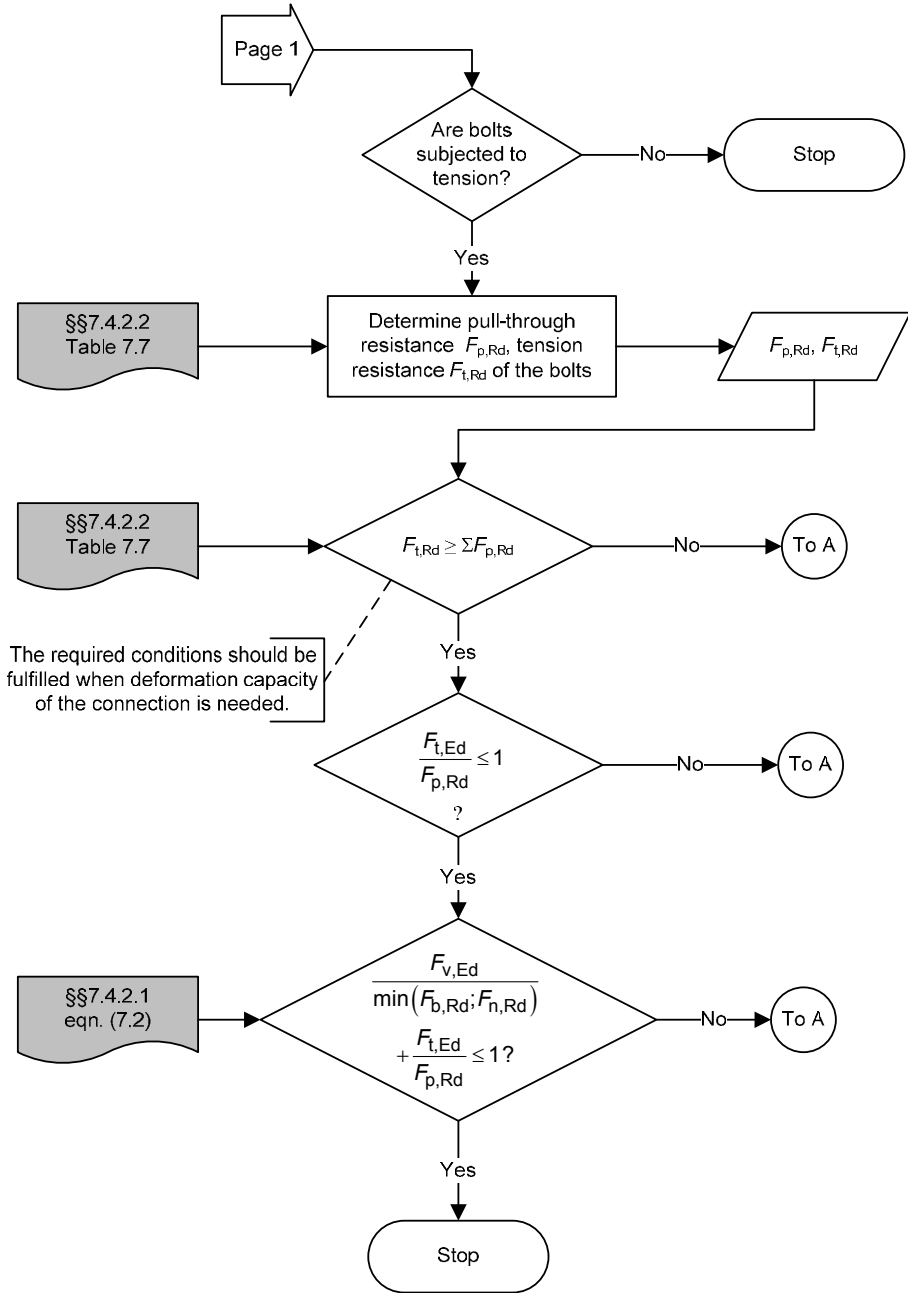
Flowchart 7.1 presents schematically the calculation procedure for pinned bolted connections of cold-formed steel members.

Table 7.7 – Design resistances for bolts according to EN1993-1-3

Bolts loaded in shear:	
<u>Bearing resistance:</u> ²⁾	
$F_{b,Rd} = 2.5 \cdot \alpha_b \cdot k_t \cdot f_u \cdot d \cdot t / \gamma_{M2}$	
with α_b is the smallest of 1.0 or $e_1/(3d)$ and	
$k_t = (0.8t + 1.5)/2.5$ for $0.75 \text{ mm} \leq t \leq 1.25 \text{ mm}$; $k_t = 1.0$ for $t > 1.25 \text{ mm}$	
<u>Net-section resistance:</u>	
$F_{n,Rd} = (1 + 3 \cdot r \cdot (d_o / u - 0.3)) \cdot A_{net} \cdot f_u / \gamma_{M2}$ but $F_{n,Rd} \leq A_{net} \cdot f_u / \gamma_{M2}$	
with:	
$r = [\text{number of the bolts at the cross section}] / [\text{total number of the bolts in the connection}]$	
$u = 2 \cdot e_2$ but $u \leq p_2$	
<u>Shear resistance:</u>	
- for strength grades 4.6, 5.6 and 8.8:	$F_{v,Rd} = 0.6 \cdot f_{ub} \cdot A_s / \gamma_{M2}$
- for strength grades 4.8, 5.8, 6.8 and 10.9:	$F_{v,Rd} = 0.5 \cdot f_{ub} \cdot A_s / \gamma_{M2}$
<u>Conditions:</u> ³⁾ $F_{v,Rd} \geq 1.2 F_{b,Rd}$ or $\sum F_{v,Rd} \geq 1.2 \cdot F_{n,Rd}$	
Bolts loaded in tension:	
<u>Pull-through resistance:</u> Pull through resistance $F_{p,Rd}$ to be determined by testing.	
<u>Pull-out resistance:</u> Not relevant for bolts.	
<u>Tension resistance:</u> $F_{t,Rd} = 0.9 \cdot f_{ub} \cdot A_s / \gamma_{M2}$	
<u>Conditions:</u> ³⁾ $F_{t,Rd} \geq \sum F_{p,Rd}$	
Range of validity: ¹⁾	
$e_1 \geq 1.0 \cdot d_o$	$p_1 \geq 3 \cdot d_o$ $3 \text{ mm} > t \geq 0.75 \text{ mm}$ Minimum bolt size: M6
$e_2 \geq 1.5 \cdot d_o$	$p_2 \geq 3 \cdot d_o$ Strength grades: 4.6-10.9
$f_u \leq 550 \text{ N/mm}^2$	
¹⁾ Bolts may be used beyond this range of validity if the resistance is determined from the results of tests.	
²⁾ For thickness larger or equal to 3 mm the rules for bolts in EN1993-1-8 are valid:	
$F_{b,Rd} = \frac{k_1 \cdot \alpha_b \cdot f_u \cdot d \cdot t}{\gamma_{M2}}$	
where α_b is the smallest of $\frac{e_1}{3 \cdot d_o}$; $\frac{p_1}{3 \cdot d_o} - \frac{1}{4}$; $\frac{f_{ub}}{f_u}$ or 1.0;	
k_t is the smallest of $2.8 \cdot \frac{e_2}{d_o} - 1.7$; $1.4 \cdot \frac{p_2}{d_o} - 1.7$ or 2.5.	
³⁾ The required conditions should be fulfilled when deformation capacity of the connection is needed. When the conditions are not fulfilled it should be proven that the required deformation capacity will be provided by other parts of the structure.	



Flowchart 7.1 – Calculation procedure for pinned bolted connections of cold-formed steel members (continues)



Flowchart 7.1 – Calculation procedure for pinned bolted connections of cold-formed steel members

Example 7.1: Bolted lap joint. Determine the design resistance of the lap bolted connection in tension shown in Figure 7.31.

Given: Steel grade S350GD+Z

Connected part: $f_{yb}=350 \text{ N/mm}^2$, $f_u=420 \text{ N/mm}^2$

Bolt grade 8.8 with a bolt diameter $d=12 \text{ mm}$; $d_o=13 \text{ mm}$, $f_{ub}=800 \text{ N/mm}^2$; $A_s=84.3 \text{ mm}^2$.

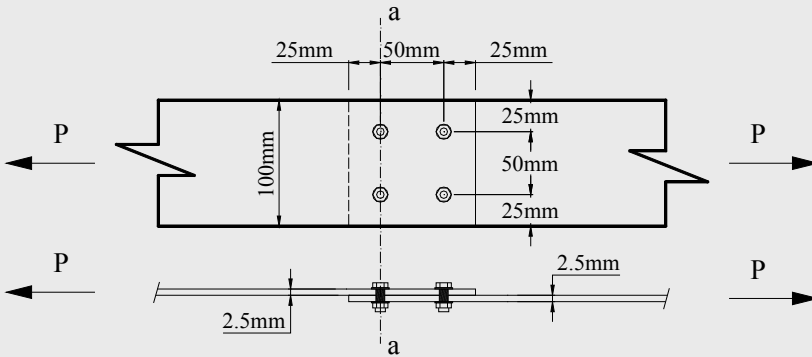


Figure 7.31 – Lap bolted connection in tension

Bolt position:

Bolt pitch distance between centre of the holes:

$$p_1 = p_2 = 50 \text{ mm} > 3d = 36 \text{ mm};$$

Distance from the centre of the hole to the end of part:

$$e_1 = 25 \text{ mm} > 1.5d = 18 \text{ mm}.$$

Tension resistance of connected parts:

$$\begin{aligned} N_{t,Rd} &= f_y \cdot A_g / \gamma_{M0}; \quad \gamma_{M0} = 1.0 \\ &= 350 \text{ N/mm}^2 \times 100 \text{ mm} \times 2.5 \text{ mm} / 1.0 / 1000 = 87.5 \text{ kN} \end{aligned}$$

Evaluate the net section resistance of the connection at line a-a.

$$\begin{aligned} F_{n,Rd} &= (1 + 3 \cdot r \cdot (d_o / u - 0.3)) \cdot A_{net} \cdot f_u / \gamma_{M2}; \quad \gamma_{M2} = 1.25 \\ &= (1 + 3 \times 0.5 \times (13 \text{ mm} / 50 \text{ mm} - 0.3)) \times 185 \text{ mm}^2 \times 420 \text{ N/mm}^2 / 1.25 / 1000 \\ &= 58.4 \text{ kN} \end{aligned}$$

$$A_{net} \cdot f_u / \gamma_{M2} = 185 \text{ mm}^2 \times 420 \text{ N/mm}^2 / 1.25 / 1000 = 62.6 \text{ kN}$$

$$F_{n,Rd} = 58.4 \text{ kN} < 62.6 \text{ kN}$$

The tension resistance of the connected part is governed by the net section resistance of connection.

Bearing resistance:

$$F_{b,Rd} = 2.5 \cdot \alpha_b \cdot k_t \cdot f_u \cdot d \cdot t / \gamma_{M2}$$

$$= 2.5 \times 0.694 \times 1 \times 420 \text{ N/mm}^2 \times 12 \text{ mm} \times 2.5 \text{ mm} / 1.25 / 1000 = 17.5 \text{ kN/bolt}$$

where

$$k_t = 1.0 \text{ for } t > 1.25 \text{ mm}$$

$$\alpha_b = \min(1, e_1 / (3d)) = \min(1, 25 / (3 \cdot 12)) = \min(1, 0.694) = 0.694$$

$$\text{Total bearing resistance} = 4 \text{ bolts} \times 17.5 \text{ kN/bolt} = 70 \text{ kN.}$$

Shear resistance of bolts:

$$F_{u,Rd} = 0.6 \cdot f_{ub} \cdot A_s / \gamma_{M2}$$

$$= 0.6 \times 800 \text{ N/mm}^2 \times 84.3 \text{ mm}^2 / 1.25 / 1000 = 32.4 \text{ kN/bolt}$$

Total bolt shear resistance = 4 bolts \times 32.4 kN/bolt = 129.6 kN > 70 kN

Conclusions: The net section resistance of the connection governs the connection resistance, $F_{n,Rd} = 58.4 \text{ kN}$.

Example 7.2: Purlin-to-rafter cleat bolted connection

Determine the design resistance of a purlin-to-rafter cleat bolted connection, shown in Figure 7.32, under longitudinal and transversal wind.

a) Longitudinal action of wind

A metal building roof system consists of cold-formed steel Z-sections. When a longitudinal wind load is applied to the end wall of a building, a common structural system to resist the wind load is to assume that the wind load is transferred longitudinally in the framing system to a braced bay. If the purlins are single span members, cleats are required over the rafter to

provide the force transfer. Figure 7.32 shows a typical simple span purlin connection at a rafter.

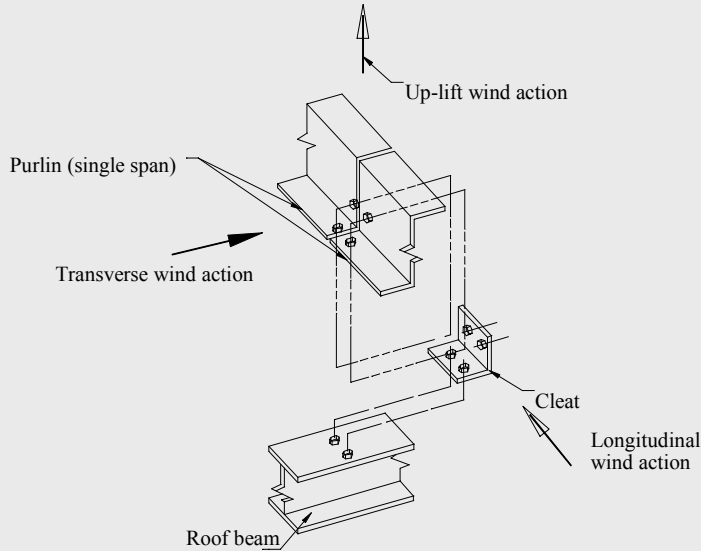


Figure 7.32 – Cleat bolted connection of a single span purlin

In this case the purlin-to-rafter connection is working in shear under a longitudinal wind force.

504

Given:

Connected part: Steel grade S320GD+Z

$$f_{yb}=320 \text{ N/mm}^2, f_u=390 \text{ N/mm}^2$$

Purlin thickness=1.5 mm

Cleat thickness=2.0 mm

Bolt grade 8.8 with a bolt diameter $d=12$ mm; $A_s=84.3 \text{ mm}^2$, $f_{ub}=800 \text{ N/mm}^2$.

Bolt position:

Minimum distance from centre of hole to end of part $e_1=1.5d=18$ mm.

Bearing resistance:

$$F_{b,Rd} = 2.5 \cdot \alpha_b \cdot k_t \cdot f_u \cdot d \cdot t / \gamma_{M2}$$

$$= 2.5 \times 0.5 \times 1 \times 390 \text{ N/mm}^2 \times 12 \text{ mm} \times 1.5 \text{ mm} / 1.25 / 1000 = 7.02 \text{ kN/bolt}$$

where

$$k_t = 1.0 \text{ for } t > 1.25 \text{ mm}$$

$$\alpha_b = \min(1, e_1/(3d)) = \min(1, 18/(3 \cdot 12)) = \min(1, 0.5) = 0.5$$

$$\text{Total bearing resistance} = 2 \text{ bolts} \times 7.02 \text{ kN/bolt} = 14.04 \text{ kN}$$

Shear resistance of bolts:

$$F_{u,Rd} = 0.6 \cdot f_{ub} \cdot A_s / \gamma_{M2}$$

$$= 0.6 \times 800 \text{ N/mm}^2 \times 84.3 \text{ mm}^2 / 1.25 = 32.4 \text{ kN/bolt}$$

Total bolt shear resistance = 2 bolts \times 32.4 kN per bolt = 64.8 kN

Conclusion: The bearing resistance governs the connection shear resistance.

Note: The up-lift wind action is also loading the connection in shear. The calculations for this case are practically the same as those for longitudinal wind action.

b) Transverse action of wind

When a transverse wind load is applied to the roof panel of a building, a common structural system to resist the wind load is to assume that the wind load is transferred to the purlin, and the purlin transfers the wind to the framing rafter. If the purlins are simple span members, the bolt that connects the purlin to the rafter working in tension must have adequate resistance to transfer the force from the purlin to the rafter.

Tension resistance of bolts:

$$F_{u,Rd} = 0.9 \cdot f_{ub} \cdot A_s / \gamma_{M2}$$

$$= 0.9 \times 800 \text{ N/mm}^2 \times 84.3 \text{ mm}^2 / 1.25 = 48.6 \text{ kN/bolt}$$

The connection contains only one bolt per purlin, therefore, the connection tension resistance = 48.6 kN

EN1993-1-3 also stipulates that the tension capacity is to be limited by the pull-through resistance. That is, the strength of the bolted connection to resist the purlin bottom flange from pulling over the head of the bolt. The pull-through resistance, $F_{p,Rd}$, cannot be computed and must be determined

by tests. Thus, before it can be concluded that the tension resistance is 48.6 kN, a test for pull-through resistance is required.

Example 7.3: Continuous span purlin connection

a) Longitudinal action

A metal building roof system consists of cold-formed steel Z-sections. When wind load is applied to the end wall of a building, a common structural system for resisting the wind load is to assume that the wind load is transferred longitudinally in the framing system to a braced bay. If the purlins are continuous span members and nested over the rafter, they will provide both the axial wind force transfer, and a transfer of moment through the connection. Figure 7.33 shows a typical continuous span purlin connection at a rafter.

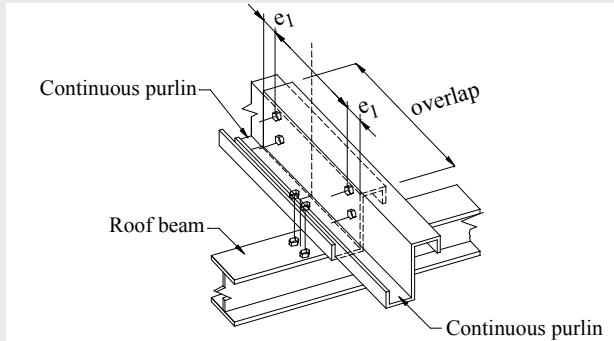


Figure 7.33 – Continuous span purlin bolted connection

Given:

Connected part: Steel grade S350GD+Z;

$$f_{yb} = 350 \text{ N/mm}^2, f_u = 420 \text{ N/mm}^2;$$

Purlin thickness=1.2 mm;

Bolt grade 8.8 with a bolt diameter $d=12$ mm; $A_s=84.3 \text{ mm}^2$, $f_{ub}=800 \text{ N/mm}^2$.

Bolt position:

Minimum distance from centre of hole to end part $e_1 = 1.5d = 18$ mm. For the present detail the distance $e_1 = 50$ mm will be used in order to avoid

premature end-shearing.

Bearing resistance:

$$F_{b,Rd} = 2.5 \cdot \alpha_b \cdot k_t \cdot f_u \cdot d \cdot t / \gamma_{M2}$$

$$= 2.5 \times 1 \times 1 \times 420 \text{ N/mm}^2 \times 12 \text{ mm} \times 1.2 \text{ mm} / 1.25 / 1000 = 12.1 \text{ kN/bolt}$$

where

$$k_t = 1.0 \text{ for } t > 1.25 \text{ mm}$$

$$\alpha_b = \min(1, e_1 / (3d)) = \min(1, 50 / (3 \cdot 12)) = \min(1, 1.39) = 1.0$$

The purlin longitudinal continuity is assumed to be done by 2×2 bolts installed on the webs of sections, as shown in Figure 7.33. Providing these bolts also ensure the fastening of two Z-sections to work as a built-up section on the rafter, the bearing resistance of the purlin-to-rafter connection, realized with two bolts only must be calculated considering a double section thickness e.g.:

$$F_{b,Rd} = 2.5 \cdot \alpha_b \cdot k_t \cdot f_u \cdot d \cdot 2t / \gamma_{M2}$$

$$= 2.5 \times 1 \times 1 \times 420 \text{ N/mm}^2 \times 12 \text{ mm} \times (2 \times 1.2 \text{ mm}) / 1.25 / 1000 = 24.2 \text{ kN/bolt}$$

Thus it follows:

Total bearing resistance purlin-to-purlin connection:

$$4 \text{ bolts} \times 12.1 \text{ kN/bolt} = 48.4 \text{ kN}$$

Total bearing resistance of purlin-to-rafter connection

$$2 \text{ bolt} \times 24.2 \text{ kN/bolt} = 48.4 \text{ kN}$$

Shear resistance of bolts:

$$F_{u,Rd} = 0.6 \cdot f_{ub} \cdot A_s / \gamma_{M2}$$

$$= 0.6 \times 800 \text{ N/mm}^2 \times 84.3 \text{ mm}^2 / 1.25 / 1000 = 32.4 \text{ kN/bolt}$$

Total bolt shear resistance of purlin-to-purlin connection:

$$4 \text{ bolts} \times 32.4 \text{ kN/bolt} = 129.6 \text{ kN}$$

Total bolt shear resistance of purlin-to-rafter connection:

$$2 \text{ bolts} \times 32.4 \text{ kN/bolt} = 64.8 \text{ kN}$$

Conclusion: The connection resistance is governed by the bearing resistance.

b) Transverse action

Bearing resistance:

The same as for longitudinal action

$$F_{b,Rd} = 24.2 \text{ kN/bolt}$$

Total bearing resistance = 2 bolts \times 24.2 kN/bolt = 48.4 kN

Shear resistance of bolts:

$$F_{u,Rd} = 32.4 \text{ kN/bolt}$$

Total bolt shear resistance = 2 bolts \times 32.4 kN/bolt = 64.8 kN > 48.4 kN

Conclusion: The connection resistance is governed by the bearing resistance.

c) Up-lift action

Tension resistance of bolts:

$$\begin{aligned} F_{u,Rd} &= 0.9 \cdot f_{ub} \cdot A_s / \gamma_{M_2} \\ &= 0.9 \times 800 \text{ N/mm}^2 \times 84.3 \text{ mm}^2 / 1.25 = 48.6 \text{ kN/bolt} \end{aligned}$$

The connection contains two bolts therefore the connection shear resistance = 97.2 kN

508

EN1993-1-3 also stipulates that the tension capacity is to be limited by the pull-through resistance. That is, the strength of the bolted connection to resist the purlin bottom flange from pulling over the head of the bolt. The pull-through resistance cannot be computed and must be defined by tests. Thus, before it can be concluded that the tension resistance is 97.2 kN, a test is required.

7.4.2.3 Design of connections with self-tapping screws

Screws are used for thin-to-thin and thin-to-moderate thick connections (see Table 7.1) to fasten sheeting to sheeting as seam connectors, sheeting to purlins or side rails, or to rafters if the rafter sections are not too thick, and also to connect sections in light gauge framing.

The basic relations for fastener resistance are presented in Table 7.8.

Table 7.8 – Design resistance for self-tapping screws¹⁾ according to EN1993-1-3

Screws loaded in shear:
Bearing resistance: $F_{b,Rd} = \alpha \cdot f_u \cdot d \cdot t / \gamma_{M2}$ In which α is given by the following: - if $t = t_1$ $\alpha = 3.2 \cdot \sqrt{t/d}$ but $\alpha \leq 2.1$ - if $t_1 \geq 2.5 \cdot t$ and $t < 1.0$ mm: $\alpha = 3.2 \cdot \sqrt{t/d}$ but $\alpha \leq 2.1$ - if $t_1 \geq 2.5 \cdot t$ and $t \geq 1.0$ mm: $\alpha = 2.1$ - if $t < t_1 < 2.5 \cdot t$ obtain α by linear interpolation.
Net-section resistance: $F_{n,Rd} = A_{net} \cdot f_u / \gamma_{M2}$
Shear resistance: Shear resistance $F_{v,Rd}$ to be determined by testing and $F_{v,Rd} = F_{v,Rk} / \gamma_{M2}$
Conditions: ⁴⁾ $F_{v,Rd} \geq 1.2 F_{b,Rd}$ or $\Sigma F_{v,Rd} \geq 1.2 F_{n,Rd}$
Screws loaded in tension:
Pull-through resistance: ²⁾ - for static loads: $F_{p,Rd} = d_w \cdot t \cdot f_u / \gamma_{M2}$ - for screws subjected to wind loads and combination of wind loads and static loads: $F_{p,Rd} = 0.5 \cdot d_w \cdot t \cdot f_u / \gamma_{M2}$
Pull-out resistance: If $t_{sup} / s < 1$: $F_{o,Rd} = 0.45 \cdot d \cdot t_{sup} \cdot f_{u,sup} / \gamma_{M2}$ (s is the thread pitch) If $t_{sup} / s \geq 1$: $F_{o,Rd} = 0.65 \cdot d \cdot t_{sup} \cdot f_{u,sup} / \gamma_{M2}$
Tension resistance: Tension resistance $F_{t,Rd}$ to be determined by testing.
Conditions: ⁴⁾ $F_{t,Rd} \geq \Sigma F_{p,Rd}$ or $F_{t,Rd} \geq F_{o,Rd}$
Range of validity: ³⁾
Generally: $e_1 \geq 3 \cdot d$ $p_1 \geq 3 \cdot d$; $3 \text{ mm} \leq d \leq 8 \text{ mm}$; $e_2 \geq 1.5 \cdot d$; $p_2 \geq 3 \cdot d$ For tension: $0.5 \text{ mm} \leq t \leq 1.5 \text{ mm}$ and $t_1 \geq 0.9 \text{ mm}$ $f_u \leq 550 \text{ N/mm}^2$
¹⁾ In this table it is assumed that the thinnest sheet is next to the head of the screw. ²⁾ These values assume that the washer has sufficient rigidity to prevent it from being deformed appreciably or pulled over the head of the fastener. ³⁾ Self-tapping screws may be use beyond this range of validity if the resistance is determined from the results of tests. ⁴⁾ The required conditions should be fulfilled when the deformation capacity of the connection is needed. When these conditions are not fulfilled it should be proved that the required deformation capacity will be provided by other parts of the structure.

7. CONNECTIONS

In Table 7.8, t has to be considered as the thickness of the member in contact with the screw head, while t_l the thickness of the supporting member. Usually fabricators provide data for the design resistance of their products. As an example, Tables 7.9 and 7.10 present the resistance values corresponding to pull-through and pull-out resistance for SFS Intec self-tapping screws.

Table 7.9– Pull-through resistance, $F_{p,Rd}$ (kN) for SFS Intec screws

f_y (N/mm ²)	Thickness of the fastened plate, t , in mm									
	0.40	0.50	0.60	0.65	0.70	0.80	0.90	1.00	1.25	1.50
250	1.50	1.88	2.25	2.44	2.63	3.00	3.38	3.75	4.69	5.63
280	1.68	2.10	2.52	2.73	2.94	3.36	3.78	4.20	5.25	6.30
350	2.10	2.63	3.15	3.41	3.68	4.20	4.73	5.25	6.56	7.88

Note: The diameter of washers is $d_w=14$ mm.

Table 7.10 – Pull-out resistance, $F_{o,Rd}$ (kN) for $d=5.5$ mm SFS Intec screws

f_y (N/mm ²)	t (mm)												
	0.60	0.65	0.70	0.80	0.90	1.00	1.25	1.50	2.00	2.50	3.00	4.00	5.00
270	0.38	0.42	0.47	0.58	0.69	0.81	1.13	1.49	2.29	3.21	4.21	6.49	9.07
320	0.45	0.50	0.56	0.69	0.82	0.96	1.34	1.77	2.72	3.80	4.99	7.69	10.75
350	0.49	0.55	0.62	0.75	0.9	1.05	1.47	1.93	2.97	4.16	5.46	8.41	11.75

Usually, the resistance of screws in tension, $F_{t,Rd}$, is greater than the values in Tables 7.9 and 7.10. This is demonstrated in the following calculations of the pull-through and pull-out resistances of SFS Intec screws:

Pull-through resistance

Assume a sheet of steel grade S280GD+Z with $f_y = 320$ N/mm² and $f_u = 360$ N/mm² and consider five different thicknesses i.e. 1) $t = 0.4$ mm; 2) $t = 0.5$ mm; 3) $t = 0.7$ mm; 4) $t = 1.0$ mm; and 5) $t = 1.5$ mm. The washer diameter is as specified in Table 7.10, $d_w = 14$ mm. The results are compared in Table 7.11, for static loads only.

Table 7.11 – Comparative values for $F_{p,Rd}$

t (mm)	$F_{p,Rd}$ (kN)	
	$F_{p,Rd} = d_w \cdot t \cdot f_u / \gamma_{M2}$	Table 7.10
0.40	1.61	1.68
0.50	2.02	2.10
0.70	2.82	2.94
1.00	4.03	4.20
1.50	6.05	6.30

It appears that the calculated values and those offered by producers fit very well. However for wind loading, the producer values overestimate the resistance if those calculated with formula of Table 7.9 are taken as reference.

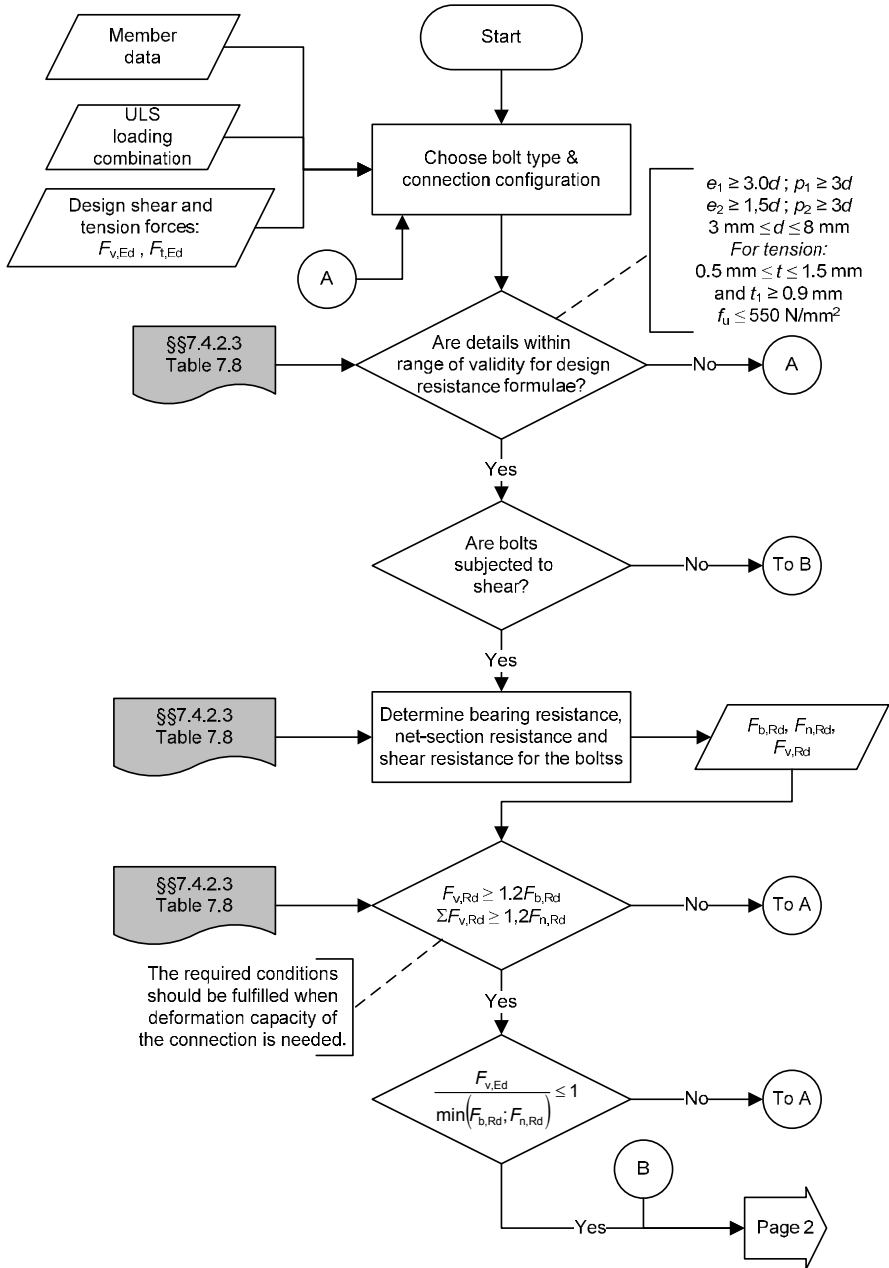
Pull-out resistance

Assume a supporting member of steel grade S350GD+Z with $f_y = 350$ N/mm² and $f_u = 420$ N/mm², and consider five different thicknesses, i.e. 1) $t = 0.6$ mm; 2) $t = 1.0$ mm; 3) $t = 1.25$ mm; 4) $t = 1.5$ mm and 5) $t = 2.5$ mm. The nominal diameter of the screw is $d = 5.5$ mm. The results are compared in Table 7.12.

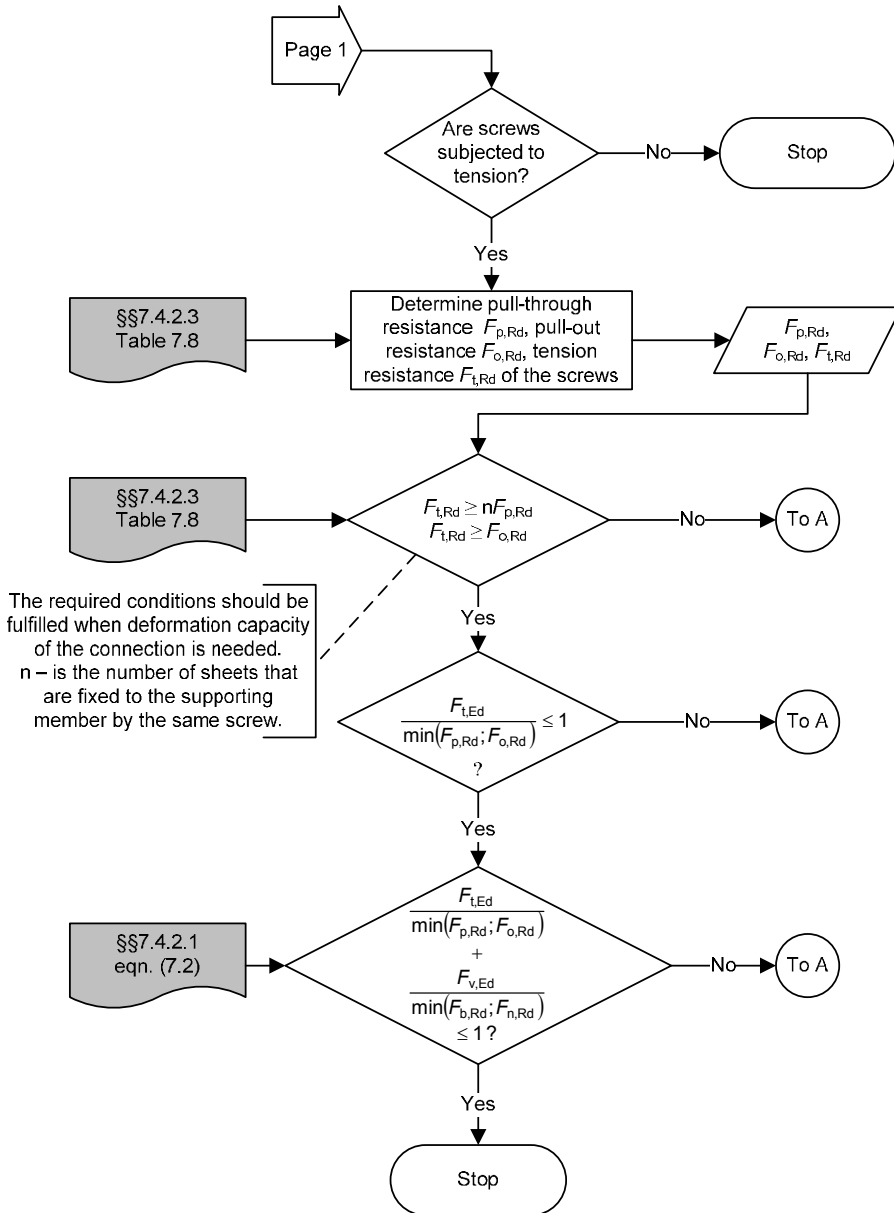
Table 7.12 – Comparative results for $F_{o,Rd}$

t (mm)	$F_{o,Rd}$ (kN)	
	$F_{o,Rd} = 0.45 \cdot d \cdot t_{\text{sup}} \cdot f_{u,\text{sup}} / \gamma_{M2}$	Table 7.11
0.60	0.49	0.49
1.00	0.83	1.05
1.25	1.04	1.47
1.50	1.25	1.93
2.50	2.08	4.16

Flowchart 7.2 presents schematically the calculation procedure for screwed connections of cold-formed steel members.



Flowchart 7.2 – Design resistance of screwed connections of cold-formed members (SF043a-EN-EU, AccessSteel 2006) (continues)



Flowchart 7.2 – Design resistance of screwed connections of cold-formed members (SF043a-EN-EU, AccessSteel 2006)

Example 7.4: Sheeting-to-purlin connection

Determine the design resistance of the screwed connection of the sheeting on the purlin as shown in Figure 7.34.

Given:

Sheet material, $t = 0.6$ mm, S250GD+Z: $f_y = 250$ N/mm², $f_u = 330$ N/mm²;

Base material, $t = 2.5$ mm, S350GD+Z: $f_y = 350$ N/mm², $f_u = 420$ N/mm².

Screw $d = 4.8$ mm, washer $d_w = 16$ mm and $F_{v,Rk} = 5.2$ kN, $F_{t,Rd} = 5.0$ kN.

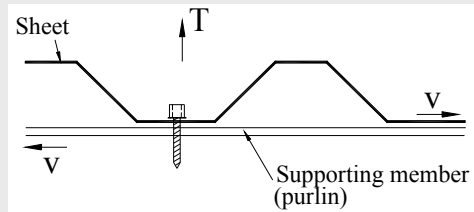


Figure 7.34 – Screwed connection of sheeting on the purlin

Screw position (see Figure 7.27):

Distance between centres of fastener: $p_1 = 36$ mm $> 3d$

Distance from centre of fastener to the end of part: $e_1 = 36$ mm $> 3d$

Tension Resistance: Tension resistance must be evaluated for pull-through, pull-out, and screw tension resistance.

514

a) Pull-through resistance (screws subjected to wind load)

$$\begin{aligned} F_{p,Rd} &= 0.5 \cdot d_w \cdot t \cdot f_u / \gamma_{M2} \\ &= 0.5 \times 16 \text{ mm} \times 0.6 \text{ mm} \times 330 \text{ N/mm}^2 / 1.25 = 1.27 \text{ kN} \end{aligned}$$

b) Pull-out

$$\begin{aligned} F_{o,Rd} &= 0.65 \cdot d \cdot t_{sup} \cdot f_{u,sup} / \gamma_{M2} \\ &= 0.65 \times 4.8 \text{ mm} \times 2.5 \text{ mm} \times 420 \text{ N/mm}^2 / 1.25 = 2.62 \text{ kN} \end{aligned}$$

c) Tension resistance of screw

Consider that one sheet is fixed on the supporting member with the screw

$$F_{t,Rd} \geq F_{p,Rd}$$

The manufacturers tested tension resistance of screw $F_{t,Rd} = 5.0 \text{ kN} > F_{p,Rd} = 1.27 \text{ kN}$, therefore the screw is adequate. Tension resistance is governed by the pull-through of the fastener in the connection.

Bearing resistance:

$$t=0.6 \text{ mm}, t_1=2.5 \text{ mm}$$

$$t_1/t=4.17, \text{ therefore linear interpolation must be used to determine } \alpha.$$

Because $t_1 \geq 2.5 \cdot t$ and $t < 1.0 \text{ mm}$: $\alpha = 3.2 \cdot \sqrt{t/d}$ but $\alpha \leq 2.1$

$$t_1=2.5 \text{ mm} > 2.5 \times 0.6 \text{ mm} = 1.5 \text{ mm}, t = 0.6 \text{ mm} < 1.0 \text{ mm}$$

$$\Rightarrow \alpha = 3.2 \cdot \sqrt{t/d} = 3.2 \sqrt{0.6/4.8} = 1.13 \leq 2.1, \text{ use } \alpha = 1.13$$

$$\begin{aligned} F_{b,Rd} &= \alpha \cdot f_u \cdot d \cdot t / \gamma_{M2} \\ &= 1.13 \times 330 \text{ N/mm}^2 \times 4.8 \text{ mm} \times 0.6 \text{ mm} / 1.25 = 0.86 \text{ kN/screw} \end{aligned}$$

Shear resistance of screw:

$$F_{v,Rd} = F_{v,Rk} / \gamma_{M2} = 5.2 \text{ kN} / 1.25 = 4.16 \text{ kN}$$

$$F_{v,Rd} > 1.2 \cdot F_{b,Rd} = 1.2 \times 0.86 \text{ kN} = 1.03 \text{ kN/screw}$$

The manufacturers tested shear resistance of screw is $F_{v,Rd} = 4.16 \text{ kN} > 1.03 \text{ kN}$, therefore the screw is adequate.

Conclusion: The shear resistance of the connection is governed by the bearing resistance = 1.03 kN. The tension resistance of the connection is governed by the pull-through resistance = 1.27 kN.

Example 7.5: Sheeting-to-sheeting seam connection in shear

When sheeting is acting as a diaphragm, the seam connectors are working in shear. The shear performance of the diaphragm is strongly dependent on the seam fastening performance, which usually is the weakest component of the system. Figure 7.35 shows a decking system with seam and edge connections. The floor decking system is assumed to be covered with corrugated sheet of 0.7 mm thickness and with a steel grade of S350GD+Z ($f_y = 350 \text{ N/mm}^2$ and $f_u = 420 \text{ N/mm}^2$). Seam fastening is realized with

$d = 4.8$ mm self-tapping screws, $d_w = 16$ mm, $F_{v,Rd} = 4.2$ kN, $F_{t,Rd} = 5.0$ kN. Four seam fasteners are installed per meter along the seam line.

Determine the shear resistance capacity of 1m length seam fastener line.

Bearing resistance (shear of sheeting and fastener tilting)

$$t = t_f = 0.7 \text{ mm}$$

$$t/t_f = 1.0; \alpha = 3.2 \cdot \sqrt{t/d} = 3.2 \cdot \sqrt{0.7/4.8} = 1.22 < 2.1$$

$$F_{b,Rd} = \alpha \cdot f_u \cdot d \cdot t / \gamma_{M2}$$

$$= 1.22 \times 420 \text{ N/mm}^2 \times 4.8 \text{ mm} \times 0.7 \text{ mm} / 1.25 = 1.38 \text{ kN/screw} < 4.2 \text{ kN}$$

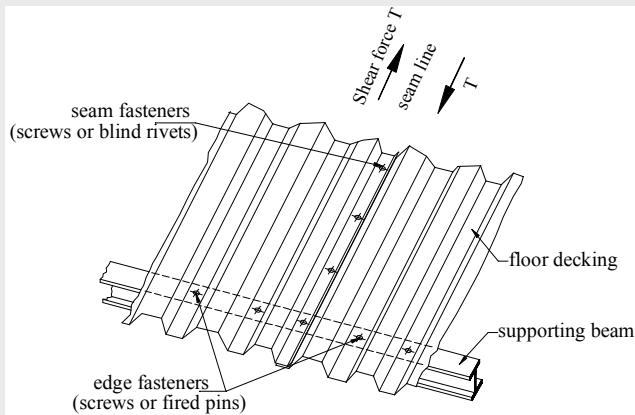


Figure 7.35 – Fastening of floor decking

The shear resistance capacity of one meter length of seam fastener line is:

$$4 \text{ screws/m} \times 1.38 \text{ kN/screw} = 5.52 \text{ kN/m.}$$

Example 7.6: Design resistance of a screwed connection of cold-formed members

This example describes the design of a pinned screwed connection of a lipped channel section wall stud. The stud is connected to a plain channel section bottom rail by means of self-tapping screws installed at both flanges of the stud, as shown in Figure 7.36.

Basic Data

Nominal diameter of the screw	$d = 6.3 \text{ mm}$
Total number of screws	$n_f = 4$
End and edge distance for screw	$e_1 = 20 \text{ mm} ; e_2 = 25 \text{ mm}$
Spacing of screws	$p_1 = 25 \text{ mm}$
The dimensions of the stud cross section are:	
Total height	$h_1 = 150 \text{ mm}$
Total width of flange	$b_1 = 50 \text{ mm}$
Total width of edge fold	$c_1 = 17.5 \text{ mm}$
Nominal thickness	$t_{1,nom} = 2.0 \text{ mm}$
Steel core thickness	$t_1 = 1.96 \text{ mm}$
Gross area of the stud cross section:	$A_1 = 543 \text{ mm}^2$
The dimensions of the rail cross section:	
Total height	$h = 155 \text{ mm}$
Total width of flange	$b = 70 \text{ mm}$
Nominal thickness	$t_{nom} = 1.5 \text{ mm}$
Steel core thickness	$t = 1.46 \text{ mm}$

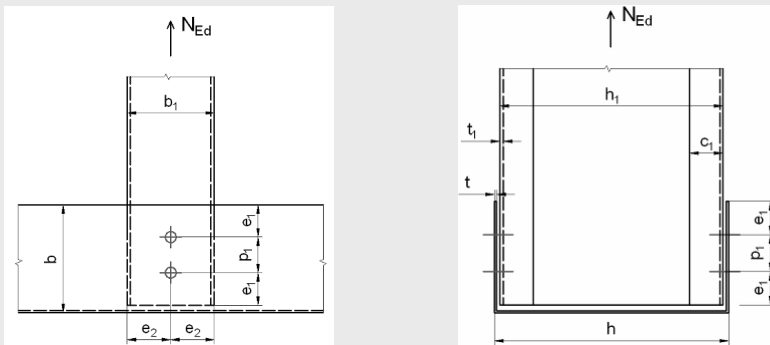


Figure 7.36 – Pinned screwed connection of a lipped channel section wall stud

The material properties are (S320GD+Z):

Basic yield strength	$f_{yb} = 320 \text{ N/mm}^2$
Ultimate strength	$f_u = 390 \text{ N/mm}^2$
Modulus of elasticity	$E = 210000 \text{ N/mm}^2$
Poisson's ratio	$\nu = 0.3$

Shear modulus $G = \frac{E}{2(1+\nu)} = 81000 \text{ N/mm}^2$

Partial factor $\gamma_{M2} = 1.25$

The design force on the connection is: $N_{Ed} = 17.6 \text{ kN}$.

The design shear force per screw in the ultimate limit state is:
 $F_{v,Ed} = N_{Ed}/n_f = 17.6/4 = 4.4 \text{ kN}$.

Check the range of validity for design resistance formulas

The following conditions should be satisfied:

$$e_1 \geq 3d \quad ; \quad p_1 \geq 3d \quad ; \quad e_2 \geq 1.5d \quad ; \quad 3.0 \text{ mm} \leq d \leq 8.0 \text{ mm}$$

$$e_1 = 20 \text{ mm} > 3d = 3 \times 6.3 = 18.9 \text{ mm} \quad \text{– OK}$$

$$e_2 = 25 \text{ mm} > 1.5d = 1.5 \times 6.3 = 9.45 \text{ mm} \quad \text{– OK}$$

$$p_1 = 25 \text{ mm} > 3d = 3 \times 6.3 = 18.9 \text{ mm} \quad \text{– OK}$$

$$3.0 \text{ mm} < d = 6.3 \text{ mm} < 8.0 \text{ mm} \quad \text{– OK}$$

Resistance check for self-tapping screws loaded in shear

Bearing resistance

$$F_{b,Rd} = \frac{\alpha f_u dt}{\gamma_{M2}}$$

where:

$t < t_1 < 2.5t$ so α is obtained by linear interpolation:

$$\text{for } t_1 = t: \quad \alpha = 3.2\sqrt{t/d} = 3.2 \times \sqrt{1.16/6.3} = 1.54$$

$$\text{for } t_1 \geq 2.5t \text{ and } t \geq 1.0 \text{ mm}: \quad \alpha = 2.1$$

$$\Rightarrow \text{for } t_1/t = 1.96/1.46 = 1.342, \text{ by linear interpolation: } \alpha = 1.683$$

The bearing resistance of one screw is:

$$F_{b,Rd} = \frac{\alpha f_u dt}{\gamma_{M2}} = \frac{1.683 \times 390 \times 6.3 \times 1.46}{1.25} = 4830 \text{ N} = 4.83 \text{ kN}$$

Net-section resistance:

$$F_{n,Rd} = \frac{A_{net} f_u}{\gamma_{M2}}$$

where the net cross sectional area is:

$$A_{net} = A_1 - 2dt_1 = 543 - 2 \times 6.3 \times 1.96 = 518.3 \text{ mm}^2$$

The net-section resistance is:

$$F_{n,Rd} = \frac{A_{net} f_u}{\gamma_{M2}} = \frac{518.3 \times 390}{1.25} = 161711 \text{ N} = 161.71 \text{ kN}$$

Shear resistance

$$F_{v,Rd} = F_{v,Rk} / \gamma_{M2}$$

$$F_{v,Rk} = 13500 \text{ N (according to manufacturer catalogue)}$$

$$F_{v,Rd} = F_{v,Rk} / \gamma_{M2} = 13500 / 1.25 = 10800 \text{ N} = 10.8 \text{ kN}$$

When deformation capacity of the connection is needed, the shear resistance should satisfy the following conditions (not required for this example): $F_{n,Rd}$

$$F_{v,Rd} \geq 1.2 F_{b,Rd} \text{ or } \sum F_{v,Rd} \geq 1.2 F_{n,Rd}$$

The resistance of a fastener in shear may be verified using:

$$\frac{F_{v,Ed}}{\min(F_{b,Rd}; F_{n,Rd} / n_f; F_{v,Rd})} \leq 1$$

$$\frac{4.40}{\min(4.83; 161.71; 10.8)} = \frac{4.40}{4.83} = 0.911 < 1 \quad \text{– OK}$$

7.4.2.4 Design of connections with blind rivets

Blind rivets are used for thin-to-thin connections (see Table 7.1), mainly as seam fasteners for sheeting panels. They are working in shear and/or tension. Figure 7.35 shows an example of dry floor decking with blind rivets seam fasteners. The design formulas are presented in Table 7.13.

Table 7.13 – Design resistance for blind rivets¹⁾ according to EN1993-1-3

Rivets loaded in shear:		
<u>Baring resistance:</u>		
$F_{b,Rd} = \alpha \cdot f_u \cdot d \cdot t / \gamma_{M2}$	but	$F_{b,Rd} \leq f_u \cdot e_1 \cdot t / (1.2 \cdot \gamma_{M2})$
In which α is given by the following:		
- if $t = t_1$	$\alpha = 3.6 \cdot \sqrt{t/d}$	but $\alpha \leq 2.1$
- if $t_1 \geq 2.5 \cdot t$	$\alpha = 2.1$	
- if $t < t_1 < 2.5 \cdot t$ obtain α by linear interpolation		
<u>Net-section resistance:</u> $F_{n,Rd} = A_{net} \cdot f_u / \gamma_{M2}$		
<u>Shear resistance:</u>		
Shear resistance $F_{v,Rd}$ to be determined by testing and $F_{v,Rd} = F_{v,Rk} / \gamma_{M2}$		
<u>Conditions:</u> ⁴⁾ $F_{v,Rd} \geq 1.2 \cdot F_{b,Rd} / (n_f \cdot \beta_{Lf})$ or $F_{v,Rd} \geq 1.2 \cdot F_{n,Rd}$		
Rivets loaded in tension: ²⁾		
<u>Pull-through resistance:</u> Pull-through resistance $F_{p,Rd}$ to be determined by testing		
<u>Pull-out resistance:</u> Not relevant for rivets		
<u>Tension resistance:</u> Tension resistance $F_{t,Rd}$ to be determined by testing.		
<u>Conditions:</u> $F_{t,Rd} \geq \sum F_{p,Rd}$		
Range of validity: ³⁾		
$e_1 \geq 1.5 \cdot d$	$p_1 \geq 3 \cdot d$	$2.6 \text{ mm} \leq d \leq 6.4 \text{ mm}$
$e_2 \geq 1.5 \cdot d$	$p_2 \geq 3 \cdot d$	$f_u \leq 550 \text{ N/mm}^2$
¹⁾ In this table it is assumed that the thinnest sheet is next to the preformed head of the blind rivets.		
²⁾ Blind rivets are not usually used in tension.		
³⁾ Blind rivets may be used beyond this range of validity if the resistance is determined from the results of tests.		
⁴⁾ The required condition should be fulfilled when the deformation capacity of the connection is needed. When these conditions are not fulfilled it should be proved that the required deformation capacity will be provided by other parts of the structure.		

One can see that, excepting the fact that in the case of rivets no pull-out resistance needs to be calculated, the design procedures for connections with blind rivets is very similar with those for self-tapping screws (see Table 7.8). Thus the worked examples presented in the previous paragraph can be also taken as a guideline for rivets.

7.4.2.5 Design of connections with fired pins

Fired pins are used for thin-to-thick connections (see Table 7.1), usually to fasten roof and floor decking (see Figure 7.35) on supporting

members made by hot-rolled sections.

Design procedures for fired pin connectors are summarized in Table 7.14 and are similar to those for screwed connections.

Table 7.14 – Design resistance for cartridge fired pins

Pins loaded in shear:
<u>Bearing resistance:</u> $F_{b,Rd} = 3.2 \cdot f_u \cdot d \cdot t / \gamma_{M2}$
<u>Net section resistance:</u> $F_{n,Rd} = A_{net} \cdot f_u / \gamma_{M2}$
<u>Shear resistance:</u> Shear resistance $F_{v,Rd}$ to be determined by testing: $F_{v,Rd} = F_{v,Rk} / \gamma_{M2}$
Conditions: ³⁾ $F_{v,Rd} \geq 1.5 \cdot \sum F_{b,Rd}$ or $F_{v,Rd} \geq 1.5 \cdot F_{n,Rd}$
Pins loaded in tension:
<u>Pull-through resistance:</u> ¹⁾ - for static loads: $F_{p,Rd} = d_w \cdot t \cdot f_u / \gamma_{M2}$ - for wind loads and combination of wind loads and static loads: $F_{p,Rd} = 0.5 \cdot d_w \cdot t \cdot f_u / \gamma_{M2}$
<u>Pull-out resistance:</u> Pull-out resistance $F_{o,Rd}$ to be determined by testing.
<u>Tension resistance:</u> Tension resistance $F_{t,Rd}$ to be determined by testing.
Conditions: ³⁾ $F_{o,Rd} \geq \sum F_{p,Rd}$ or $F_{t,Rd} \geq F_{o,Rd}$
Range of validity: ²⁾
<u>Generally:</u> $e_1 \geq 4.5 \cdot d$ $3.7 \text{ mm} \leq d \leq 6.0 \text{ mm}$ $e_2 \geq 4.5 \cdot d$ for $d = 3.7 \text{ mm}; t_{sup} \geq 4.0 \text{ mm}$ $p_1 \geq 4.5 \cdot d$ for $d = 4.5 \text{ mm}; t_{sup} \geq 6.0 \text{ mm}$ $p_2 \geq 4.5 \cdot d$ for $d = 5.2 \text{ mm}; t_{sup} \geq 8.0 \text{ mm}$ $f_u \leq 550 \text{ N/mm}^2$ For tension: $0.5 \text{ mm} \leq t \leq 1.5 \text{ mm}$ $t_{sup} \geq 6.0 \text{ mm}$
¹⁾ These values assume that the washer has sufficient rigidity to prevent it from being deformed appreciably or pulled over the head of the fastener.
²⁾ Cartridge fired pins may be used beyond this range of validity if the resistance is determined from the results of tests.
³⁾ The required condition should be fulfilled when deformation capacity of the connection is needed. When these conditions are not fulfilled it should be proved that the required deformation capacity will be provided by other parts of the structure.

Table 7.15 shows, as an example, design data offered by HILTI (2005) (www.hilti.com).

Table 7.15 – Example of design data for HILTI fired pins

<p>X – ENP Siding and Decking Nail</p> <p>Carbon steel shank: HRC 58 Zinc coating: 8 – 16 µm</p> <p>(www.hilti.com)</p>		<p>Roof decking</p>																																																									
		<p>Floor decking</p>																																																									
		<p>Wall liners</p>																																																									
		<p>Characteristic loads – steel sheeting</p> <table border="1"> <thead> <tr> <th rowspan="2">Sheeting thickness t_s [mm]</th> <th colspan="2">Trapezoidal profile (symmetric loading)</th> <th colspan="2">Liner trays ¹⁾ (asymmetric loading)</th> </tr> <tr> <th colspan="2">Char. resistance according to ETA-04/0101</th> <th colspan="2">Char. resistance keeping to ETA-04/0101</th> </tr> <tr> <th>nominal</th> <th>Shear V_{Rk} [kN]</th> <th>Tension N_{Rk} [kN]</th> <th>Shear V_{Rk} [kN]</th> <th>Tension N_{Rk} [kN]</th> </tr> </thead> <tbody> <tr> <td>0.75</td> <td>4.70</td> <td>6.30</td> <td>3.30</td> <td>4.40</td> </tr> <tr> <td>0.88</td> <td>5.40</td> <td>7.20</td> <td>3.80</td> <td>5.00</td> </tr> <tr> <td>1.00</td> <td>6.00</td> <td>8.00</td> <td>4.20</td> <td>5.60</td> </tr> <tr> <td>1.13</td> <td>7.00</td> <td>8.40</td> <td>4.90</td> <td>5.90</td> </tr> <tr> <td>1.25</td> <td>8.00</td> <td>8.80</td> <td>5.60</td> <td>6.20</td> </tr> <tr> <td>1.50</td> <td>8.60</td> <td>8.80</td> <td>6.00</td> <td>6.20</td> </tr> <tr> <td>1.75</td> <td>8.60</td> <td>8.80</td> <td>6.00</td> <td>6.20</td> </tr> <tr> <td>2.00</td> <td>8.60</td> <td>8.80</td> <td>6.00</td> <td>6.20</td> </tr> <tr> <td>2.50</td> <td>8.60</td> <td>8.80</td> <td>6.00</td> <td>6.20</td> </tr> </tbody> </table> <p>• N_{Rk} and V_{Rk} are valid for steel sheet with minimum tensile strength ≥ 360 N/mm² (\geq S280 EN 10326). • For intermediate sheet thicknesses, use recommended load for next smaller thickness or linear interpolation.</p>	Sheeting thickness t_s [mm]	Trapezoidal profile (symmetric loading)		Liner trays ¹⁾ (asymmetric loading)		Char. resistance according to ETA-04/0101		Char. resistance keeping to ETA-04/0101		nominal	Shear V_{Rk} [kN]	Tension N_{Rk} [kN]	Shear V_{Rk} [kN]	Tension N_{Rk} [kN]	0.75	4.70	6.30	3.30	4.40	0.88	5.40	7.20	3.80	5.00	1.00	6.00	8.00	4.20	5.60	1.13	7.00	8.40	4.90	5.90	1.25	8.00	8.80	5.60	6.20	1.50	8.60	8.80	6.00	6.20	1.75	8.60	8.80	6.00	6.20	2.00	8.60	8.80	6.00	6.20	2.50	8.60	8.80
Sheeting thickness t_s [mm]	Trapezoidal profile (symmetric loading)			Liner trays ¹⁾ (asymmetric loading)																																																							
	Char. resistance according to ETA-04/0101		Char. resistance keeping to ETA-04/0101																																																								
nominal	Shear V_{Rk} [kN]	Tension N_{Rk} [kN]	Shear V_{Rk} [kN]	Tension N_{Rk} [kN]																																																							
0.75	4.70	6.30	3.30	4.40																																																							
0.88	5.40	7.20	3.80	5.00																																																							
1.00	6.00	8.00	4.20	5.60																																																							
1.13	7.00	8.40	4.90	5.90																																																							
1.25	8.00	8.80	5.60	6.20																																																							
1.50	8.60	8.80	6.00	6.20																																																							
1.75	8.60	8.80	6.00	6.20																																																							
2.00	8.60	8.80	6.00	6.20																																																							
2.50	8.60	8.80	6.00	6.20																																																							

Table 7.15 – Example of design data for HILTI fired pins (continues)

Recommended loads – steel sheeting				
Sheeting thickness t [mm]	Trapezoidal profile (symmetric loading)		Liner trays ¹⁾ (asymmetric loading)	
	Recommended loads		Recommended loads	
nominal	Shear V_{rec} [kN]	Tension N_{rec} [kN]	Shear V_{rec} [kN]	Tension N_{rec} [kN]
0.75	2.50	3.35	1.75	2.35
0.88	2.90	3.85	2.00	2.70
1.00	3.20	4.25	2.25	3.00
1.13	3.75	4.50	2.65	3.15
1.25	4.25	4.70	3.00	3.30
1.50	4.60	4.70	3.20	3.30
1.75	4.60	4.70	3.20	3.30
2.00	4.60	4.70	3.20	3.30
2.50	4.60	4.70	3.20	3.30

• N_{rec} and V_{rec} are valid for steel sheet with minimum tensile strength ≥ 360 N/mm² (\geq S280 EN 10326).
 • For intermediate sheet thicknesses, use recommended load for next smaller thickness or linear interpolation.
 • Recommended loads N_{rec} and V_{rec} are appropriate for Eurocode 1 wind loading design with a partial safety factor $\gamma_F = 1.5$ for wind load and a partial resistance factor $\gamma_M = 1.25$ for the fastening.

7.4.3 Design of welded connections

7.4.3.1 General design and workmanship consideration

EN1993-1-3 (CEN, 2006a) provides procedures to calculate the resistances of spot welds, fillet welds and arc spot welds. The provisions will be presented in the following paragraphs §§7.4.3.2 to §§7.4.3.4. They apply to thin materials only ($t < 3$ mm for spot welds, or $t < 4$ mm for fillet and arc spot welds). For thicker materials ($t > 4$ mm) the welds have to be designed according to EN1993-1-8 (CEN, 2005e), which provides design procedures for welded connections (that are not presented in this book). EN1993-1-8 also refers to groove butt and flare groove bevel welds.

The main difference between the strength of a welded connection in cold-formed steel and a welded connection in hot-rolled steel is the dominance of sheet/weld tearing as failure mode in cold-formed steel connections, as shown in §§7.2.2.3 (Figures 7.22 and 7.23). Although the design provisions provide guidance on the determination of weld strength, the design is generally limited by the tearing of the base metal. The design of welded connections must also consider workmanship, quality and inspection when determining if a weld is an appropriate connection method.

Provisions regarding welding consumables and welding are provided by §§1.2.5 (Reference Standards, Group 5) of EN1993-1-8.

Generally, it is stated that assembly and welding shall be carried out in such a way that the final dimensions are within the appropriate tolerances. The design project specifications must stipulate details pertaining to welded connections that require special loading procedures, special levels of quality control, special inspection procedures, or special tests procedures. When welding galvanized sheet, suitable ventilation shall be provided. Also, welding of steel sheets shall not be done when the ambient temperature is lower than -30°C , or when the surfaces are wet. The parts to be joined shall be brought into close contact to facilitate complete fusion. The importance of ensuring closeness of the connected parts cannot be over-emphasized, especially for arc spot welds. If any gap exists between the members prior to the spot welding, the strength of the weld may be substantially reduced. The design project specifications must define the special inspection procedures when made necessary by the choice of welding technology and erection conditions. Visual inspection is always necessary. Particular emphasis shall be placed on verifying the proper location, size and length of a weld, in addition to verifying bead shape, reinforcement and undercut.

7.4.3.2 Design of spot welds

Spot welds may be either resistance welded or fusion welded. However, for building construction spot welds are generally made using an arc welding procedure.

Spot welds may be used as rolled or galvanized parent material up to 4.0 mm thick, provided that the thinner connected part is not more than 3.0 mm thick. Table 7.16 summarises the design procedures for spot weld connections working in shear according to EN1993-1-3. The following notations are used:

A_{net}	is the net cross sectional area of the connected part;
n_w	is the number of spot welds in one connection;
t	is the thickness of the thinner connected part or sheet [mm];
t_1	is the thickness of the thicker connected part or sheet;
d_s	is the interface diameter (see Figure 7.37).

and the edge distances e_1 and e_2 and the spacings p_1 and p_2 are as defined in Figure 7.27a. The partial factor for calculating the design resistance of spot welds shall be taken as $\gamma_{M2} = 1.25$.

The interface diameter d_s of a spot weld shall be determined from the following:

- for fusion welding: $d_s = 0.5 \cdot t + 5 \text{ mm}$ (7.5a)

- for resistance welding: $d_s = 5 \cdot \sqrt{t}$ (7.5b)

Table 7.16 – Design resistance for spot welds

Spot welds loaded in shear:	
<u>Tearing and bearing resistance:</u>	
- if $t \leq t_1 \leq 2.5t$	$F_{tb,Rd} = 2.7 \cdot \sqrt{t} \cdot d_s \cdot f_u / \gamma_{M2}$ [with t in mm]
- if $t_1 \geq 2.5t$	$F_{tb,Rd} = 2.7 \cdot \sqrt{t} \cdot d_s \cdot f_u / \gamma_{M2}$, but $F_{tb,Rd} \leq 0.7 \cdot d_s^2 \cdot f_u / \gamma_{M2}$ and $F_{tb,Rd} \leq 3.1 \cdot t \cdot d_s \cdot f_u / \gamma_{M2}$
<u>End resistance:</u>	$F_{e,Rd} = 1.4 \cdot t \cdot e_1 \cdot f_u / \gamma_{M2}$
<u>Net section resistance:</u>	$F_{n,Rd} = A_{net} \cdot f_u / \gamma_{M2}$
<u>Shear resistance:</u>	$F_{v,Rd} = \frac{\pi}{4} \cdot d_s^2 \cdot f_u / \gamma_{M2}$
<u>Conditions:</u> $F_{v,Rd} \geq 1.25 \cdot F_{tb,Rd}$ or $F_{v,Rd} \geq 1.25 \cdot F_{e,Rd}$ or $\sum F_{v,Rd} \geq 1.25 \cdot F_{n,Rd}$	
Range of validity:	
$2 \cdot d_s \leq e_1 \leq 6 \cdot d_s$	$3 \cdot d_s \leq p_1 \leq 8 \cdot d_s$
$e_2 \leq 4 \cdot d_s$	$3 \cdot d_s \leq p_2 \leq 6 \cdot d_s$

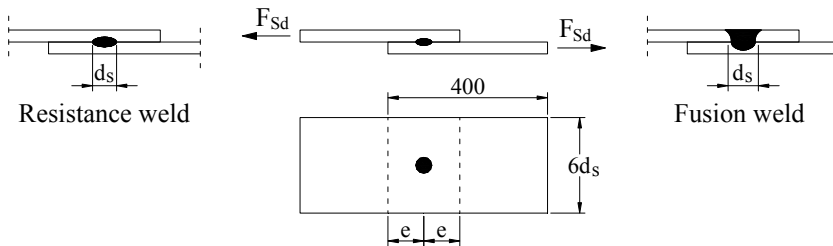
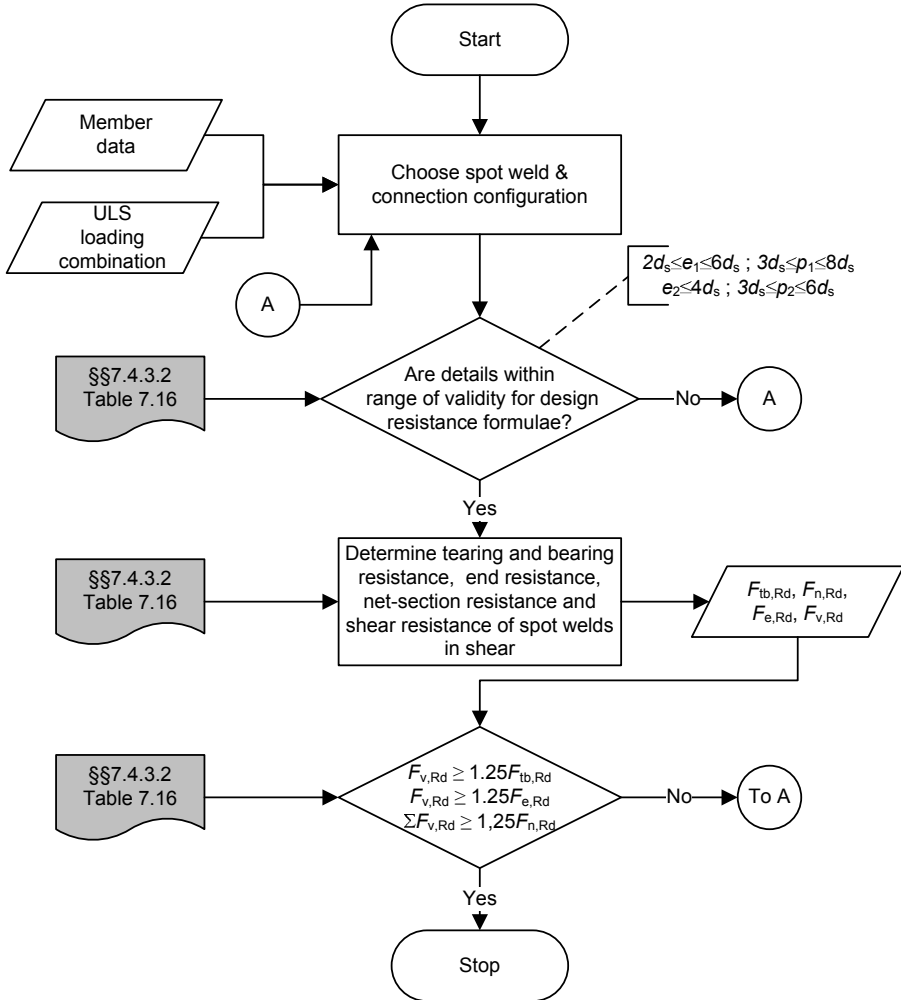


Figure 7.37 – Test specimen for shear test spot welds

The value of d_s actually produced by the welding procedure shall be verified by shear tests using single-lap test specimens as shown in Figure 7.37. The thickness t of the specimen should be the same as that used in practice.

Flowchart 7.3 presents schematically the calculation procedure for spot welds connections of cold-formed steel members.



Flowchart 7.3 – Design resistance of spot welds connections of cold-formed members

7.4.3.3 Fillet lap welds

The following procedure shall be used for the design of arc-welded lap welds where the parent material is 4.0 mm thickness or less. For thicker parent material, lap welds shall be designed using EN1993-1-8 (CEN, 2005e).

The weld size shall be chosen such that the resistance of the connection is governed by the thickness of the connected part or sheet, rather

than the weld. This requirement may be assumed to be satisfied if the throat size of the weld is at least equal to the thickness of the connected part or sheet. Based on research findings, the ultimate strength of a fillet weld connection has been found to occur by tearing the sheet, not failure of weld. In most cases, the higher strength of the weld material prevents the failure. The design resistance calculation procedures presented hereafter are based on sheet tearing.

The partial factor for calculating the design resistance of lap welds shall be taken as $\gamma_{M2} = 1.25$.

The design resistance $F_{w,Rd}$ of a fillet welded connection shall be determined from the following:

- for a side fillet that is one of a pair of side fillets:

$$F_{w,Rd} = t \cdot L_{w,s} \cdot (0.9 - 0.45 \cdot L_{w,s} / b) \cdot f_u / \gamma_{M2} \quad \text{if } L_{w,s} \leq b \quad (7.6a)$$

$$F_{w,Rd} = 0.45 \cdot t \cdot b \cdot f_u / \gamma_{M2} \quad \text{if } L_{w,s} > b \quad (7.6b)$$

- for end fillet:

$$F_{w,Rd} = t \cdot L_{w,e} \cdot (1 - 0.3 \cdot L_{w,e} / b) \cdot f_u / \gamma_{M2}$$

for one weld and if $L_{w,s} \leq b$ (7.6c)

where

- b is the width of the connected part or sheet, (see Figure 7.38);
- $L_{w,e}$ is the effective length of the end fillet weld, (see Figure 7.38);
- $L_{w,s}$ is the effective length of the side fillet weld, (see Figure 7.38).

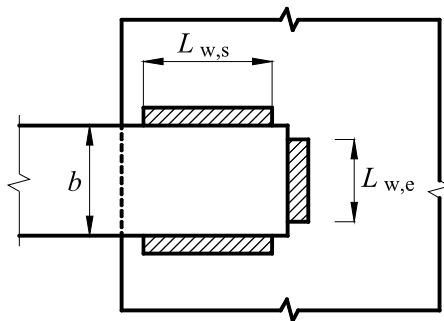


Figure 7.38 – Fillet welded lap connection

If a combination of end fillets and side fillets is used in the same connection, its total resistance shall be taken as equal to the sum of the resistances of the end fillets and the side fillets.

The effective length L_w of a fillet weld shall be taken as the overall length of the full-size fillet, including end returns. Provided that the weld is full size through this length, no reduction in effective length needs to be made for either the start or termination of the weld.

Fillet welds with effective lengths less than 8 times the thickness of the thinner connected part should not be designed to transmit any forces.

7.4.3.4 Arc spot welds

Arc spot welds and elongated arc spot welds should not be designed to transmit other forces than shear. Arc spot welded connections are often made by melting through the top sheet and fusing the sheets together with additional filler metal. Thus the spot welds should not be used through connected parts of sheets with a total thickness of more than 4 mm or when the thinnest connected part is more than 4 mm thick. Arc spot welds should have an interface diameter d_s of not less than 10 mm. To ensure a proper penetration and to avoid excessive burning of the sheet, if the thickness of the sheet is less than 0.7 mm, a weld washer should be used (see Figure 7.39).

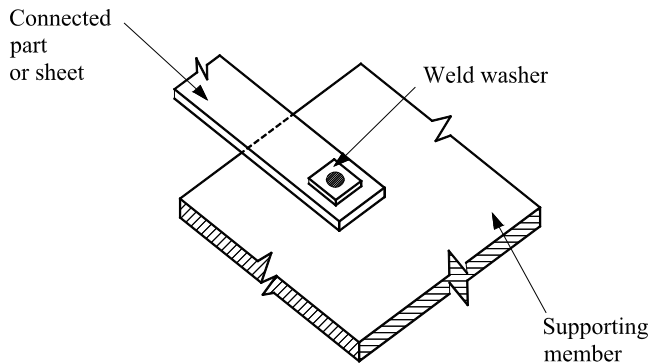


Figure 7.39 – Arc spot weld with weld washer

Arc spot welds should have adequate end and edge distance as given in the following:

- (i) The minimum distance measured parallel to the direction of the force transfer, from the centre line of an arc spot weld to the nearest edge of an adjacent weld or to the end of the connected part toward which the force is directed, should not be less than the value of e_{min} given by the following:

- if $f_u / f_y < 1.15$

$$e_{min} = 1.8 \cdot \frac{F_{w,Sd}}{t \cdot f_u / \gamma_{M2}} \quad (7.7a)$$

- if $f_u / f_y \geq 1.15$

$$e_{min} = 2.1 \cdot \frac{F_{w,Sd}}{t \cdot f_u / \gamma_{M2}} \quad (7.7b)$$

where $F_{w,Sd}$ is the design stress (load) induced by the design actions at the level of the fastener.

- (ii) The minimum distance from the centreline of a circular arc spot weld to the end or edge of the connected sheet should not be less than $1.5d_w$ where d_w is the visible diameter of the arc spot weld.
- (iii) The minimum clear distance between an elongated arc spot weld and the end of the sheet and between the weld and the edge of the sheet should not be less than $1.0d_w$.

529

Circular arc spot welds

The design shear resistance $F_{w,Rd}$ of a circular arc spot weld should be determined as follows:

$$F_{w,Rd} = (\pi / 4) \cdot d_s^2 \cdot 0.625 \cdot f_{uw} / \gamma_{M2} \quad (7.8)$$

where

f_{uw} is the ultimate tensile strength of the welding electrodes.

However, the strength $F_{w,Rd}$, calculated with eqn. (7.8), assesses the shear resistance of the weld itself, and in order to evaluate the design resistance of the connected sheet(s), the resistance should not be taken as greater than the peripheral resistance given by the following:

- if $d_p / \sum t \leq 18 \cdot (420 / f_u)^{0.5}$:

$$F_{w,Rd} = 1.5 \cdot d_p \cdot \sum t \cdot f_u / \gamma_{M2} \quad (7.9a)$$

- if $18 \cdot (420 / f_u)^{0.5} < d_p / \sum t < 30 \cdot (420 / f_u)^{0.5}$:

$$F_{w,Rd} = 27 \cdot (420 / f_u)^{0.5} \cdot (\sum t)^2 \cdot f_u / \gamma_{M2} \quad (7.9b)$$

- if $d_p / \sum t \geq 30 \cdot (420 / f_u)^{0.5}$:

$$F_{w,Rd} = 0.9 \cdot d_p \cdot \sum t \cdot f_u / \gamma_{M2} \quad (7.9c)$$

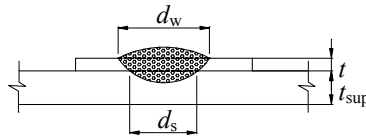
where $\sum t$ is defined in Figure 7.40.

The interface diameter d_s of an arc spot weld (see Figure 7.40), is the weld diameter, defined by the following equation based on the measured fusion diameter:

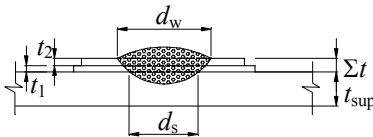
$$d_s = 0.7d_w - 1.5\sum t \text{ but } d_s \geq 0.55d_w \quad (7.10)$$

where:

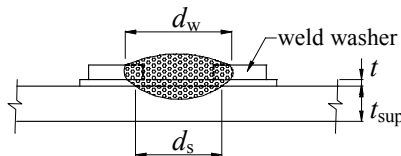
d_w is the visible diameter of the arc spot weld (see Figure 7.40).



a) Single connected sheet ($\sum t = t$)



b) Two connected sheets ($\sum t = t_1 + t_2$)



c) Single connected sheet with weld washer

Figure 7.40– Arc spot weld

The effective peripheral diameter d_p of an arc spot weld, which is essentially an average weld diameter through the thickness of the sheet(s) being welded, should be obtained as follows:

- for a single connected sheet or part of thickness t :

$$d_p = d_w - t \quad (7.11a)$$

- for multiple connected sheets or parts of total thickness $\sum t$:

$$d_p = d_w - 2\sum t \quad (7.11b)$$

Elongated arc spot weld

The behaviour of an elongated arc spot or seam weld (slotted weld) is similar to the behaviour of a circular arc spot weld.

The design shear resistance $F_{w,Rd}$ of an elongated arc spot weld should be determined from:

$$F_{w,Rd} = [(\pi/4) \cdot d_s^2 + L_w \cdot d_s] \cdot 0.625 \cdot f_{uw} / \gamma_{M2} \quad (7.12)$$

Similar to the case of a circular spot weld, $F_{w,Rd}$ should not be taken as greater than the peripheral resistance given by:

$$F_{w,Rd} = (0.5 \cdot L_w + 1.67 \cdot d_p) \cdot \sum t \cdot f_u / \gamma_{M2} \quad (7.13)$$

531

where

L_w is the length of the elongated arc spot weld, measured as shown in Figure 7.41.

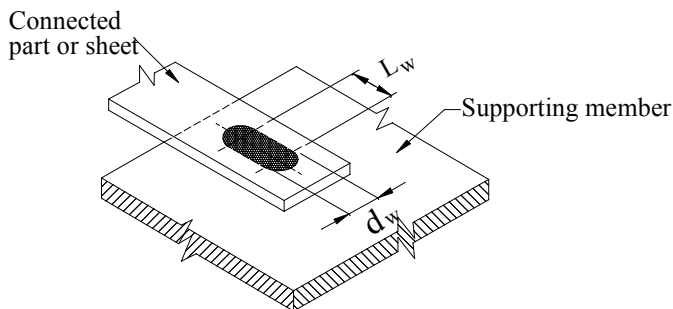


Figure 7.41 – Length of the elongated arc spot weld

End resistance:

$$F_{e,Rd} = 1.4 \cdot t \cdot e_1 \cdot f_u / \gamma_{M2} = 1.4 \cdot 1.0 \cdot 13 \cdot 430 / 1.25 / 1000 = 6.26 \text{ kN/weld}$$

Net section resistance:

$$F_{n,Rd} = A_{net} \cdot f_u / \gamma_{M2}$$

Corresponding to section *a-a* in Figure 7.42:

$$A_{net} = 1 \cdot (46 - 2 \cdot 5.5) = 35 \text{ mm}^2$$

$$F_{n,Rd} = 35 \cdot 430 / 1.25 / 1000 = 12.04 \text{ kN}$$

Weld shear resistance:

$$F_{v,Rd} = \frac{\pi}{4} \cdot d_s^2 \cdot f_u / \gamma_{M2} = \frac{\pi}{4} \cdot 5.5^2 \cdot 430 / 1.25 / 1000 = 8.17 \text{ kN/weld}$$

Checking ductility conditions:

$$F_{v,Rd} = 8.17 \text{ kN} > 1.25 \cdot F_{tb,Rd} = 6.39 \text{ kN}$$

$$F_{v,Rd} = 8.17 \text{ kN} > 1.25 \cdot F_{e,Rd} = 7.83 \text{ kN}$$

$$nF_{v,Rd} = 16.34 \text{ kN} > 1.25 \cdot F_{n,Rd} = 15.05 \text{ kN} (n_w = 2)$$

The total resistance of the connection is governed by the tearing and bearing resistance and is:

$$4 \text{ welds} \cdot 5.11 \text{ kN/weld} = 20.44 \text{ kN} \quad (n_w = 4)$$

533

Example 7.8: Arc spot weld lap joint

Determine the resistance of the arc spot weld lap joint presented in Figure 7.43.

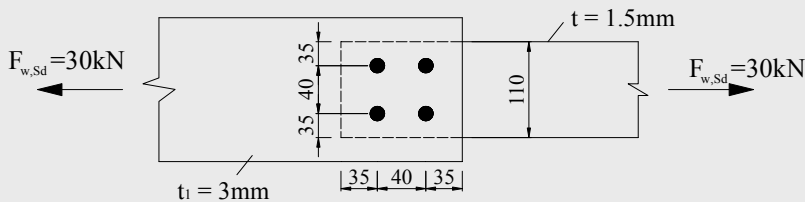


Figure 7.43 – Arc spot weld lap joint

7. CONNECTIONS

Given: Base material, Steel grade S355 MC, $f_y=355 \text{ N/mm}^2$, $f_u=430 \text{ N/mm}^2$, of thickness $t = 1.5 \text{ mm}$ and $t_1 = 3.0 \text{ mm}$. Additionally, the ultimate tensile strength of welding electrode, $f_{uw}=475 \text{ N/mm}^2$ and $d_w=20 \text{ mm}$.

Weld design dimension:

$$d_p = d_w - t = 18.5 \text{ mm}$$

$$d_s = 0.7d_w - 1.5 \cdot t = 11.75 \text{ mm} > 0.55 \cdot d_w = 11 \text{ mm}$$

Weld position:

$$e_1 = 35 \text{ mm} > 1.5 \cdot d_w = 30 \text{ mm}$$

$$e_2 = 35 \text{ mm} > 1.5 \cdot d_w = 30 \text{ mm}$$

The design shear resistance of a circular arc spot weld is:

$$\begin{aligned} F_{w,Rd} &= \frac{\pi}{4} \cdot d_s^2 \cdot 0.625 \cdot f_{uw} / \gamma_{M2} \\ &= \frac{\pi}{4} \cdot 11.75^2 \cdot 0.625 \cdot 475 / 1.25 / 1000 = 25.7 \text{ kN/weld} \end{aligned}$$

but, in order to evaluate the design resistance of the connected sheet, it should not be greater than the peripheral resistance of connected parts:

$$d_p / \sum t = 18.5 \text{ mm} / 1.5 \text{ mm} = 12.33 < 18 \cdot \sqrt{\frac{420}{f_u}} = 17.8$$

(One single connected sheet, $\sum t = t = 1.5 \text{ mm}$)

Formula (7.9a) of §§7.4.3.4 applies to calculate the peripheral resistance, i.e.

$$\begin{aligned} F_{w,Rd} &= 1.5 \cdot d_p \cdot \sum t \cdot f_u / \gamma_{M2} \\ &= 1.5 \cdot 18.5 \cdot 1.5 \cdot 430 / 1.25 / 1000 = 14.32 \text{ kN/weld} \end{aligned}$$

Thus, the peripheral resistance governs the connection resistance. The total capacity is:

$$4 \text{ welds} \times 14.32 \text{ kN/weld} = 57.28 \text{ kN}$$

Final check is for minimum edge distance. In Figure 7.43 the design load induced by the design actions is $F_{w,Sd} = 30 \text{ kN}$.

For $f_u / f_y = 430 / 355 = 1.21 > 1.15$

$$\Rightarrow e_{1\min} = 2.1 \cdot \frac{F_{w,Sd} / 4}{t \cdot f_u / \gamma_{M2}} = 2.1 \cdot \frac{30000 / 4}{1.5 \cdot 430 / 1.25} = 30.52 \text{ mm}$$

$$e_1 = 35 \text{ mm} > e_{1\min} = 30.52 \text{ mm}$$

Example 7.9: Fillet lap joint

Determine the design resistance of the lap side welded strap-to-gusset connection shown in Figure 7.44, in which $t_1 = 3 \text{ mm}$, $t = 1 \text{ mm}$ and $f_u = 420 \text{ N/mm}^2$. In order to ensure that the joint resistance is governed by the tearing of the sheet, the throat size is taken as equal to the strap thickness, $t = 1 \text{ mm}$.

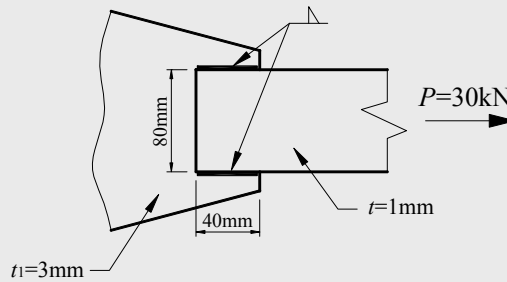


Figure 7.44 – Lap side welded strap-to-gusset

Design resistance of weld:

$$L_{w,s} = 40 \text{ mm} < b = 80 \text{ mm}$$

$$L_{w,Rd} = t \cdot L_{w,s} \cdot (0.9 - 0.45 \cdot L_{w,s} / b) \cdot f_u / \gamma_{M2}$$

$$= 1.0 \cdot 40 \cdot (0.9 - 0.45 \cdot 40 / 80) \cdot 420 / 1.25 / 1000 = 9.07 \text{ kN/weld}$$

The total welded connection resistance, for two sided fillet weld is:

$$2 \cdot 9.07 \text{ kN/weld} = 18.14 \text{ kN} < P = 30 \text{ kN}$$

In order to improve the resistance of the connection an end fillet is added, with a supplementary capacity of:

$$F_{w,Rd} = t \cdot L_{w,e} \cdot (1 - 0.3 \cdot L_{w,e} / b) \cdot f_u / \gamma_{M2}$$

$$= 1.0 \cdot 80 \cdot (1 - 0.3 \cdot 80 / 80) \cdot 420 / 1.25 = 18.82 \text{ kN}$$

The total resistance of connection in this case is:

$$18.14 \text{ kN} + 18.82 \text{ kN} \cong 37 \text{ kN}$$

Thus, the force $P = 30 \text{ kN} \leq 37 \text{ kN}$.

7.5 DESIGN ASSISTED BY TESTING OF COLD-FORMED STEEL CONNECTIONS

7.5.1 General

Testing plays an important role in defining reliable values for the design resistance of cold-formed steel fasteners.

Chapter 9 of EN1993-1-3 contains general provisions for “Design assisted by testing” and Annex A sets out appropriate standardised testing and evaluation procedures for a number of tests commonly required in cold-formed steel design. The test procedures refer to:

- tests on profiled sheets and linear types;
- test on cold-formed member;
- tests on structures and portions of structures;
- tests on torsionally restrained beams.

As can be seen, there are no standard procedures for testing fasteners, although some principles can be taken from those included in Annex A. For testing fasteners, Chapter 9 of EN1993-1-3 makes reference to older documents of ECCS–TC7, e.g. Publications no. 21 and no. 42. In 2008, an updated version of Publication 21 of ECCS was published (ECCS, 2008a).

Annex A of EN 1993-1-3 also contains a chapter devoted to the evaluation of test results to determine characteristics and design values.

In this section, procedures for testing fasteners working in shear and tension, according to ECCS–TC7, Publications no. 21 and 124 are summarised, as well as an example of application.

7.5.2 Fasteners in shear

The ECCS Recommendations (ECCS, 2008a) distinguish between tests to determine the strength and stiffness of the fastener itself and test to determine the properties of connections incorporating one or more fasteners.

It is important that test procedures and the interpretation of the results are standardised in this way. In the first place, such factors as the method and speed of testing can affect the results. Secondly, fastener test results can show a significant scatter so that it is necessary to repeat a given test several times and to use an appropriate statistical interpretation. A fastener test provides three pieces of information as defined in Figure 7.45, namely the strength, the stiffness and the deformation capacity. Designers are mainly concerned with strength of connections and this is reflected in the following parts of this chapter. However, it must also be appreciated that fasteners in light gauge steel tend to be less stiff than their counterparts in heavier construction so that connection flexibility can be significant in certain assemblies. Furthermore, as in any load bearing structure, it is important that connections are not brittle and this implies that there is adequate deformation capacity.

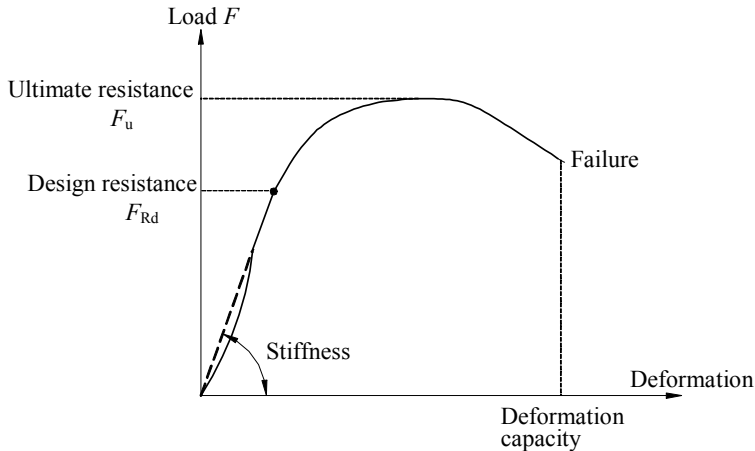


Figure 7.45 – Typical fastener test result: main parameters (ECCS, 2008a)

The standard shear test is known as the single lap joint shear test in which a two fastener lap joint of standard dimensions is placed in a tensile testing machine and loaded to failure. The standard dimensions are defined

in Figure 7.46 and Table 7.17. The standard shear test incorporates two fasteners and the results obtained are an average for the two fasteners concerned. In Figure 7.37, test specimen dimensions for shear tests on single spot weld lap joint specimens were presented.

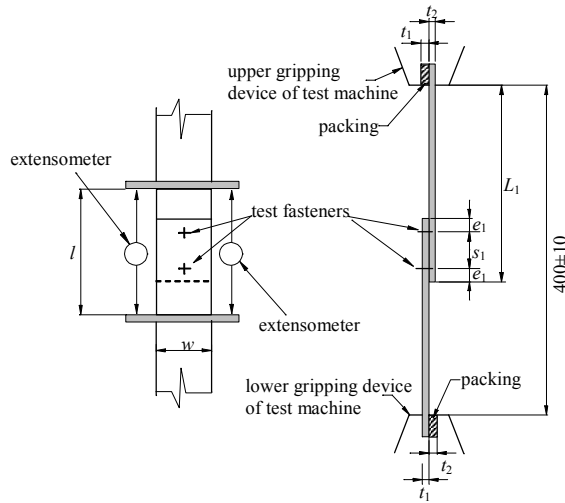


Figure 7.46 – Standard shear test (single lap joint shear test) (ECCS, 2008a)

In general, a test incorporating a single fastener lap joint will give similar results for fastener strength but a considerable reduction in flexibility as a result of the jamming effect of distortion due to eccentricities within the joint. The European Recommendations allow a single fastener test to be used where it is considered that such a test is more representative of the condition of the actual structure than a double fastener test.

During testing, it is specified that the rate of loading shall not exceed 1 KN/min and the rate of straining shall not exceed 1 mm/min. Faster rates of loading may lead to artificially high test results for both strength and stiffness.

Table 7.17: Specimen dimensions (ECCS, 2008a)

Fastener diameter <i>d</i> [mm]	Specimen dimensions [mm]				
	<i>w</i>	<i>L</i> ₁	<i>e</i> ₁	<i>s</i> ₁	<i>l</i>
< 6.5	60	260	30	60	150
> 6.5	10 <i>d</i>	200+10 <i>d</i>	5 <i>d</i>	10 <i>d</i>	20 <i>d</i> +30
Tolerance	±2	±5	±1	±1	±6

7.5.3 Fasteners in tension

The performance of connections in cold-formed steel structures is influenced not only by the fasteners themselves but also by the thickness and strength of the sheet material. In case of tests, strength values may also be influenced by the nature of the testing set-up, particularly if the fastener passes through a flange of high width-to-thickness ratio, or if distortion of the connected flange is likely to be significantly influenced by the webs.

The standard tension test fixture is the simplest among alternative set-ups and is shown in Figure 7.47. The standard test specimen for use in this apparatus is shown in Figure 7.48. The test fixture allows very easy clamping of the specimens, but the fixed dimensions together with the rigid clamping of the web means that it serves only as a model of real profiled sheeting. However, it has been found that this model gives satisfactory results for many sheeting profiles particularly those where the fastener passes through the narrower flange. The failure modes likely to occur during a tension test of a specimen are described in §§7.2.1.1 (see Figures 7.4 and 7.11).

Compared with tests on profiled sheeting, where the profile geometry may have a favourable effect, tests on flat sheets will generally give lower bound values of strength and may be conservatively applied to profiled sheeting.

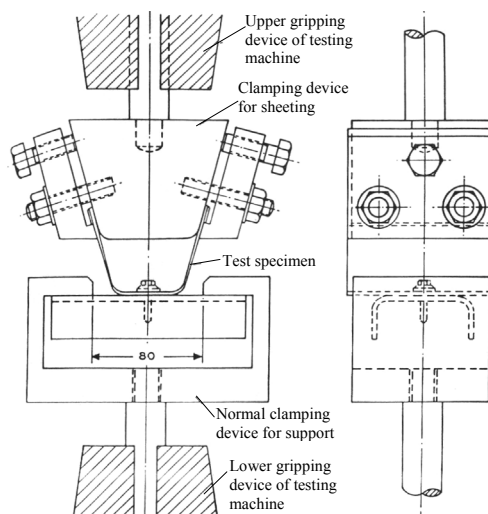


Figure 7.47 – Set-up and fixture for the standard tension test (ECCS, 2008a)

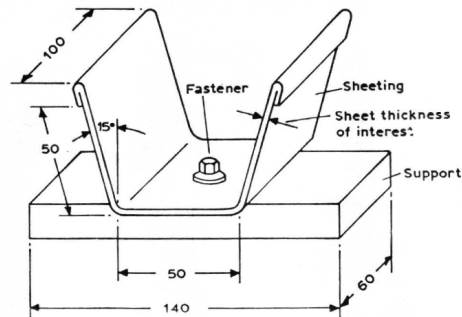


Figure 7.48 – Pull over/pull through test specimen (ECCS, 2008a)

7.5.4 Evaluation of test results

7.5.4.1 General

Both the European Recommendations (ECCS, 2008a) and Annex A of EN1993-1-3 (CEN, 2006a) provide procedures to evaluate tests results and to determinate the characteristic resistance, R_k , and the design resistance R_d . In the following both procedures will be presented.

A test specimen should be regarded as having failed if the applied load has reach its maximum value, or if the gross deformation exceeds specified limits. In case of connections specimens, it is not always easy to identify the ultimate test load. In the European Recommendations (ECCS, 2008a) it is established that “The ultimate load of fastening should be taken as the maximum load recorded during test or the load at which the first drop occurs in the load-deflection diagram”.

In the testing of connections, or of components in which the examination of large deformations is necessary for accurate assessments (for example, in evaluating the moment – rotation characteristics of sleeves), no limit need to be placed on the gross deformation during the test. For fasteners tested in shear, as a guidance, the following deformation capacity limits can be considered (Davies, 1991):

- for seam fasteners between adjacent cladding elements (screws, blind rivets): 0.5 mm;
- for other type of connections: 3.0 mm.

An appropriate margin of safety should be available between a ductile failure mode and possible brittle failure modes. This is often the case for connections.

7.5.4.2 Evaluation of tests results according to Annex A of EN1993-1-3

Adjustment of test results

- 1) Test results should be appropriately adjusted to allow for variations between the actual measured properties of the test specimens and their nominal values.
- 2) The actual measured basic yield strength $f_{yb,obs}$ should not deviate by more than -25% from the nominal basic yield strength f_{yb} , i.e. $f_{yb,obs} \geq 0.75f_{yb}$.
- 3) The actual measured thickness t_{obs} should not exceed the nominal material thickness t_{nom} by more than 12%.
- 4) Adjustments should be made in respect of the actual measured values of the core material thickness $t_{obs,cor}$ and the basic yield strength $f_{yb,obs}$ for all tests, except if values measured in tests are used to calibrate a design model then provisions of (5) need not be applied.
- 5) The adjusted value $R_{adj,i}$ of the test result for test “i” should be determined from the actual measured test result $R_{obs,i}$ using:

$$R_{adj,i} = R_{obs,i} / \mu_R \quad (7.14)$$

in which μ_R is the adjustment coefficient given by:

$$\mu_R = \left(\frac{f_{yb,obs}}{f_{yb}} \right)^\alpha \left(\frac{t_{obs,cor}}{t_{cor}} \right)^\beta \quad (7.15)$$

541

The core thickness, t_{cor} , is the material thickness, i.e. the actual thickness minus any protective coatings, such as galvanising. For a usual coating of 275g/m², the core thickness can be taken as $t_{nom} - 0.04$.

- 6) The exponent α for use in eqn. (7.15) should be obtained as follows:
 - if $f_{yb,obs} \leq f_{yb}$: $\alpha = 0$
 - if $f_{yb,obs} > f_{yb}$: $\alpha = 1$
- 7) The exponent β for use in eqn. (7.15) should be obtained as follows:
 - if $t_{obs,cor} \leq t_{cor}$: $\beta = 1$

- if $t_{obs,cor} > t_{cor}$:
 - for tests on profiled sheets on linear trays: $\beta = 2$
 - for tests on members, structures or portions of structures:
- if $b_p/t \leq (b_p/t)_{lim}$: $\beta = 1$
- if $b_p/t > 1.5(b_p/t)_{lim}$: $\beta = 2$
- if $(b_p/t)_{lim} < b_p/t < 1.5(b_p/t)_{lim}$: obtain β by linear interpolation.

in which the limiting width-to-thickness ratio $(b_p/t)_{lim}$ given by:

$$(b_p/t)_{lim} = 0.64 \sqrt{\frac{Ek_\sigma}{f_{yb}}} \sqrt{\frac{f_{yb}/\gamma_{M1}}{\sigma_{com,Ed}}} \cong 19.1\varepsilon \sqrt{k_\sigma} \sqrt{\frac{f_{yb}/\gamma_{M1}}{\sigma_{com,Ed}}} \quad (7.16)$$

where

- b_p is the notional flat width of a plane element;
- k_σ is the relevant buckling factor (see Tables 3.5 or 3.6);
- $\sigma_{com,Ed}$ is the largest calculated compressive stress in that element, at the ultimate limit state.

One can see there are no specific values of β for testing connections. By extension, the value $\beta = 1$ could be adapted when the measured thickness of the thinnest connected part, $t_{core,obs}$, is lower than the nominal value, t , and $\beta = 2$ when it is greater. This is an arbitrary and rough assumption.

Characteristic values

- 1) Characteristic values may be determined statistically, provided there are at least 4 test results, but a larger number is generally preferable, particularly if the scatter of results is relatively wide.
- 2) If the number of tests results available is 3 or less, the method based on a small number of tests may be used.
- 3) The characteristic minimum value should be determined using the following provisions. If the characteristic maximum value or the characteristic mean value is required, it should be determined by using appropriate adaptations of the provisions given for the characteristic minimum value.

- 4) The characteristic value of a resistance R_k determined on the basis of at least 4 tests may be obtained from:

$$R_k = R_m - k \cdot s \tag{7.17}$$

where

- s is the standard deviation;
- k is the appropriate coefficient from Table 7.18;
- R_m is the mean value of the adjusted test results R_{adj} .

- 5) The standard deviation s may be determined using:

$$s = \left[\sum_{i=1}^n (R_{adj,i} - R_m)^2 / (n-1) \right]^{0.5} \equiv \left[\left[\sum_{i=1}^n (R_{adj,i})^2 - (1/n) \left(\sum_{i=1}^n R_{adj,i} \right)^2 \right] / (n-1) \right]^{0.5} \tag{7.18}$$

where

- $R_{adj,i}$ is the adjusted test result for test “ i ”;
- n is the number of tests.

Table 7.18 – Values of coefficient k

n	4	5	6	8	10	20	30	∞
k	2.63	2.33	2.18	2.00	1.92	1.76	1.73	1.64

Characteristic values for families of tests

- 1) A series of tests carried out on a number of otherwise similar structures, portions of structures, members, sheets or other structural components, in which one or more parameters is varied, may be treated as a single family of tests, provided that they all have the same failure mode. The parameters that are varied may include cross sectional dimensions, spans, thicknesses and material strengths.
- 2) The characteristic resistances of the members of a family may be determined on the basis of a suitable design expression that relates the test results to all of the relevant parameters. This design expression may be either based on the appropriate equations of structural mechanics, or determined on an empirical basis.

- 3) The design expression should be modified to predict the mean measured resistance as accurately as practicable, by adjusting the coefficients to optimize the correlation. Information on this process is given in section 2.5 of EN1993-1-1 and in Annex D of EN1990.
- 4) In order to calculate the standard deviation “s”, each test result should first be normalized by dividing it by the corresponding value predicted by the design expression. If the design expression has been modified as specified in (3), the mean value of normalized test results will be unity. The number of tests n should be taken as equal to the total number of tests in the family.
- 5) For a family of at least four tests, the characteristic resistance R_k should then be obtained from eqn. (7.17) by taking R_m as equal to the value predicted by the design expression, and using the value of k from Table 7.18 corresponding to a value of n equal to the total number of tests in the family.

Characteristic values based on a small number of tests

- 1) If only one test is carried out, then the characteristic resistance R_k corresponding to this test should be obtained from the adjusted test result R_{adj} using:

$$R_k = 0.9 \cdot \eta_k \cdot R_{adj} \quad (7.19)$$

544

in which η_k should be taken as follows, depending on the failure mode:

- yielding failure: $\eta_k = 0.9$;
- gross deformation: $\eta_k = 0.9$;
- local buckling: $\eta_k = 0.8 \dots 0.9$ depending on effects on the global behaviour;
- overall instability $\eta_k = 0.7$;

Also the extension, for connection failure, $\eta_k = 0.9$, is suggested.

- 2) For a family of two or three tests, provided that each adjusted test result $R_{adj,i}$ is within $\pm 10\%$ of the mean value R_m of the adjusted test results, the characteristic resistance should be obtained using:

$$R_k = \eta_k \cdot R_m \quad (7.20)$$

- 3) The characteristic value of stiffness properties (such as flexural or rotational stiffness) may be taken as the mean value of at least two tests, provided that each test result is within $\pm 10\%$ of the mean value.
- 4) In the case of one single test, the characteristic value of the stiffness is reduced by 0.95 for favourite values and increased by 1.05 for non-favourite values.

Design values

- 1) The design value of a resistance R_d should be derived from the corresponding characteristic value R_k determined by testing using:

$$R_d = \eta_{\text{sys}} R_k / \gamma_M \quad (7.21)$$

where

- γ_M is the partial factor for resistance;
- η_{sys} is a conversion factor for differences in behaviour under test conditions and service conditions.

- 2) The appropriate value for η_{sys} should be determined in dependence of the modelling for testing.
- 3) For sheeting and for other well defined standard testing procedures η_{sys} may be taken as equal to 1.0. For tests on torsionally restrained beams, $\eta_{\text{sys}} = 1.0$ may also be used.
- 4) For other types of tests in which possible instability phenomena, or modes of behaviour, of structures or structural components might not be covered sufficiently by the tests, the value of η_{sys} should be assessed taking into account the actual testing conditions, in order to achieve the necessary reliability.
- 5) For a family of at least four tests, the value γ_M may be determined using statistical methods. Information on an appropriate method is given in section 2.5 of EN1993-1-1 and in Annex D of EN1990.
- 6) Alternatively γ_M may be taken as equal to the appropriate value of γ_M for design by calculation given in EN1993-1-3 e.g. $\gamma_M = 1.25$.
- 7) One can consider that while Annex A of EN1993-1-3 does not contain standard test procedures for connections, such procedures are defined in European Recommendations (ECCS, 2008a).

7.5.4.3 Evaluation of test results under static loads according to European Recommendations (ECCS, 2008a)

The European Recommendations (ECCS, 2008a) use the same eqn. (7.17) as in EN1993-1-3 to evaluate the characteristic value of resistance, R_k , in which:

R_m is the mean value of the adjusted test results R_{adj} from a minimum of five tests of:

- for tension: the ultimate load
- for shear: the maximum load reached at a deformation of 3 mm.

and the adjustment coefficient, μ_R , is given by:

$$\mu_R = \left(\frac{f_{u,obs}}{f_u} \right)^\alpha \left(\frac{t_{obs,cor}}{t_{cor}} \right) \quad (7.22)$$

where

$f_{u,obs}$ = the actual measured ultimate resistance;

f_u = nominal ultimate resistance;

$\alpha = 1$, if $f_{u,obs} > f_u$ and

$\alpha = 0$, if $f_{u,obs} \leq f_u$.

The design resistance of fastenings under static load is defined as the characteristic static resistance divided by an appropriate partial safety factor:

$$R_d = \frac{R_k}{\gamma_{M2}} \quad (7.23)$$

where

R_d = is the design resistance of a fastening;

R_k = is the characteristic resistance of a fastening under static load;

γ_{M2} = is the partial factor for resistance.

According to Annex D of EN1990, the partial factor of resistance, γ_{M2} , should be taken from the appropriate Eurocode provided there is sufficient similarity between the tests and the usual field of application of the partial factor as used in calculations. According to EN1993-1-3, the partial factor of resistance may be chosen $\gamma_{M2} = 1.25$ for fastenings.

The shear flexibility of a fastening, c_h , where this is required for the purpose of design, is given as a deflection per unit force, and can be obtained as:

$$c_h = \frac{1}{R_d / \gamma_1} \cdot \frac{\sum a_h}{n} \quad (7.24)$$

where

a_h = the slip of a fastening (corrected with the elongation of the test specimen over the measuring length) at a load equivalent to R_d / γ_1 ;

R_d = design resistance of a fastening;

γ_1 = an appropriate factor;

n = number of test specimens.

The shear flexibility shall be determined from sheet-to-sheet connection tests of using either a two fastener or a one fastener test set-up.

For fastening sheets to the substructure connections using the one-fastener test set-up the appropriate value of γ_1 is 1.5 corresponding to the partial load factor for wind action.

The shear flexibility is based on the averaged measured deformation obtained from shear tests. The level of applied shear force in the connection at which the deformation is obtained is the maximum force at working load level, i.e. the design resistance of the fastener divided by the partial factor of safety for the particular load in question. In the two fastener shear test, the applied load should be divided by two to determine the force at working load in a single fastener.

Example 7.10: Design assisted by testing of connections with self-tapping screws. Comparison with the analytical method of EN1993-1-3 (CEN, 2006a).

The goal of the experimental program was to evaluate the performance of two new¹ types of screws (see Table 7.19) proposed by the LINDAB Romania to be used in structural joints (Fülöp & Dubina, 2003).

¹ “new” type in the sense that fasteners have been just introduced in fabrication by the producer.

Table 7.19 – Types of proposed screws D3 and D6

	Symbol	D3
	Self-tapping screw with flat head	
	d_{nom}	4.8 mm
	d_{int}	3.5 mm
	Material quality	-
Applicability domain in accordance with producer's specifications		1...3 mm
	Symbol	D6
	Self-tapping screw with countersunk head	
	d_{nom}	6.3 mm
	d_{int}	4.8 mm
	Material quality	-
Applicability domain in accordance with producer's specifications		3...6 mm

For this purpose, several types of specimens selected to replicate the most frequent combinations of plate thicknesses, connected with self-tapping screws (see Figure 7.49), were tested in order to determine the shear capacity.

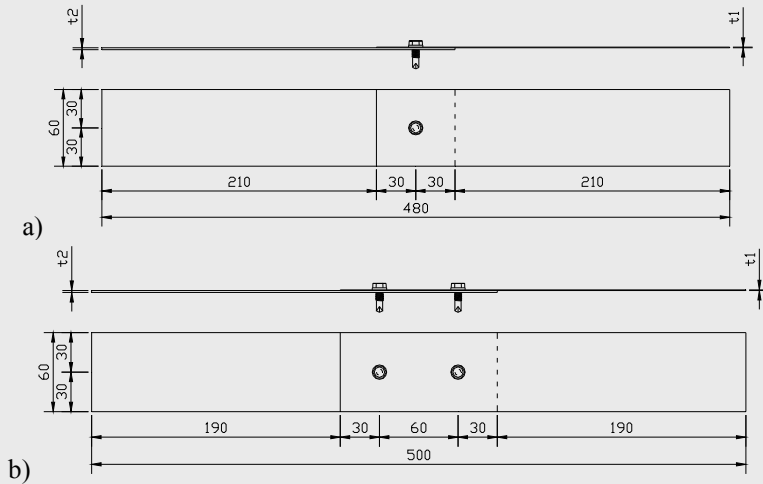


Figure 7.49 – Typical specimens: (a) Series I and, (b) Series II

The steel sheets used in the experimental tests were the common type used by LINDAB Romania, with $f_y=350 \text{ N/mm}^2$ and $f_u=420 \text{ N/mm}^2$, and with thicknesses varying from 1 to 3 mm. In these circumstances, given the limitations of the applicability of the screws, series of five tests were

proposed, according to Figure 7.50, so that the full range of thicknesses were tested, resulting in a total of 110 tests.

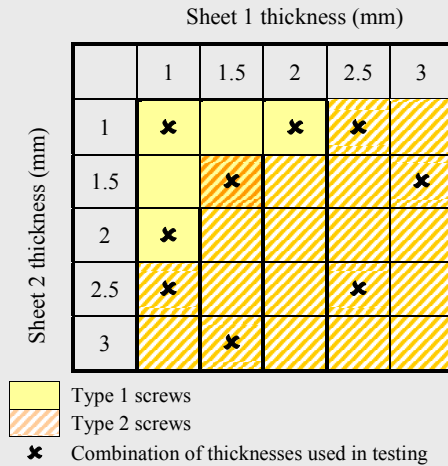


Figure 7.50 – Tested connection

Several combinations of plate thickness were used: (a) sheet plates with equal thickness, (b) thinnest sheet is next to the head of the screw as the EN1993-1-3 and AISI codes assume and (c) thickest sheet is next to the head of the screw, covered by the AISI code only.

The specimens were tested in the laboratory of the Steel Structures and Structural Mechanics Department at the “Politehnica” University of Timisoara. A UTS/TESTWELL machine was used. Data acquisition was performed using two extensometers placed on both sides of the specimens and their readings were taken automatically (see Figure 7.51).

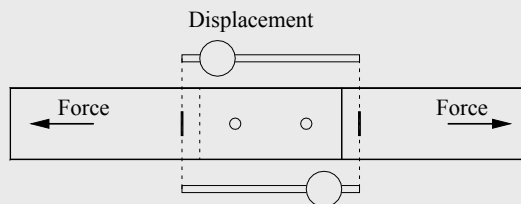


Figure 7.51 – Testing method

The specimens, tests and interpretation of results were performed according to "Recommendation for the European Steel Construction: The design and testing of Connections in Steel Sheeting and Sections" (ECCS, 1983a).

Extensometers were installed to measure the elongation over a length of 150 mm near the middle of the specimens. To simulate a quasi-static loading condition, as suggested in ECCS (1983a), the load was applied with a rate of 1 mm/min.

Experimental results. Interpretations

The primary experimental results obtained from the tests were force-displacement curves (thin solid lines in the left hand side diagrams of Figure 7.52) and the failure mode for each specimen, as shown in the right hand side of Figure 7.52.

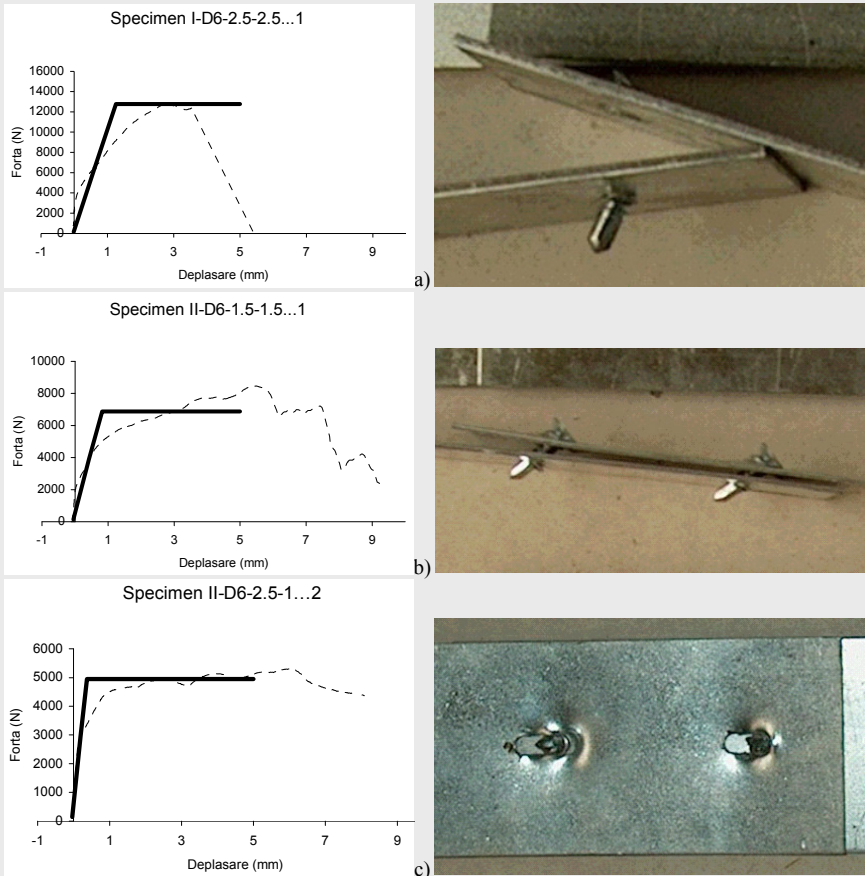


Figure 7.52 – Characteristic force – displacement curves and different failure modes

Typical failure modes expected for these types of joints are: (1) shear failure of the screw (Figure 7.52a) (brittle failure mode), (2) tilting and pull-out of fastener from the bottom steel sheet (Figure 7.52b) (ductile failure mode), (3) screw head pulling through the top sheet (ductile failure mode), (4) failure due to bearing resistance of the thinner sheet (Figure 7.52c) (ductile failure mode), (5) tearing of the thinner sheet edge (brittle failure mode). To these failure modes another one can be added that not necessarily refers to the joint i.e. (6) net section failure (brittle failure mode).

From the point of view of failure modes, design codes specify that only ductile failure modes are acceptable and brittle modes should be avoided. Thus net section failure should be avoided by appropriate choice of plate width and by ensuring adequate edge distance. The only brittle failure mode that can occur under this condition is the shear of the self-tapping screw.

Figure 7.53 shows the region of plate thickness pairs that can expect a brittle failure and may define the range of applicability of the studied screws. Based on the tested cases an extrapolation of probable failure modes was undertaken for the plate thicknesses for which no tests were performed.

Interpretation of experimental curves in order to determine the bearing capacity and stiffness was performed in accordance with the ECCS (1983a) guidelines. The characteristic value of the ultimate force, F_k , determined on the basis of tests was obtained from:

$$F_k = F_m - k \cdot s \quad (7.25)$$

where

- s is the standard deviation;
- k is the appropriate coefficient from Table 7.18;
- F_m is the mean value of the ultimate force, F_u .

The ultimate force was determined for each specimen as the (maximum) force at which the deformation capacity (displacement) of 3 mm was attained (ECCS, 1983a). It is recommended to test a minimum of five specimens, so that the values obtained can be assumed to be representative.

The shear flexibility can be calculated using the formula:

$$c_h = \frac{1}{F_d / \gamma_1} \cdot \frac{\sum a_h}{n} \tag{7.26}$$

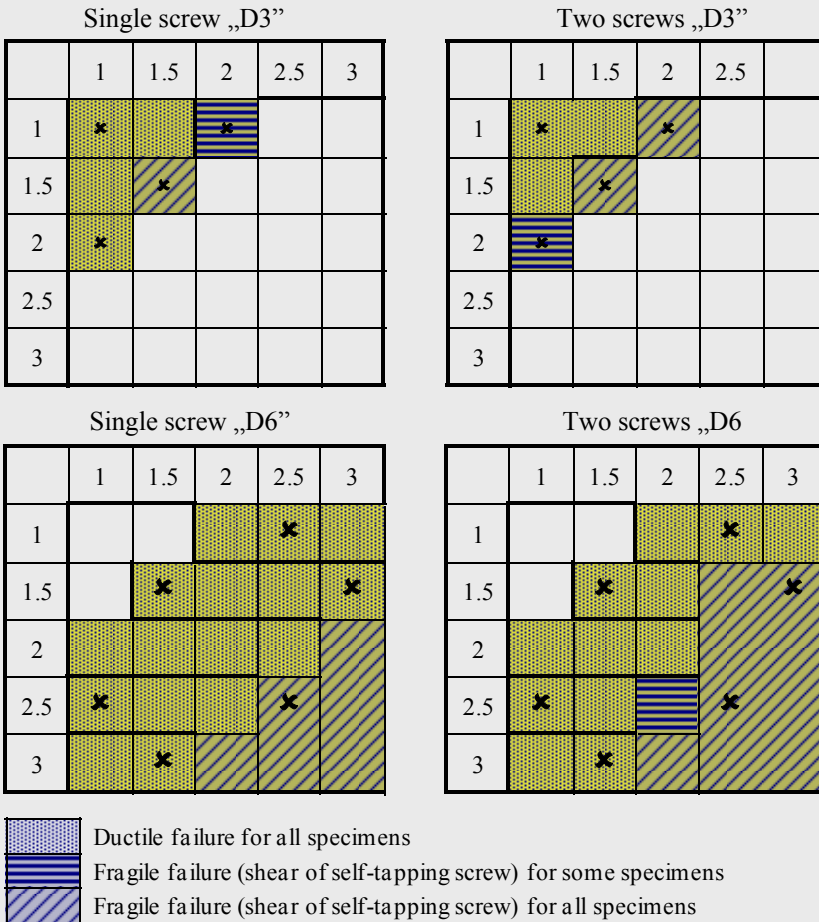
where

a_h = the slip of a fastening (corrected with the elongation of the test specimen over the measuring length) at a load equivalent to F_d / γ_1 ;

F_d = the design capacity of the fastening;

γ_1 = an appropriate factor. The recommended value for γ_1 is 1.5;

n = number of test specimens.



“D3” and “D6” defined in Table 7.19

Figure 7.53 – Failure modes distribution for specimens

In order to determine the stiffness it is recommended to use specimens with two self-tapping screws. Specimens with only one screw only can be used if they are considered more representatives from the point of view of position in the structure.

Applying the procedure to the tested specimens, Tables 7.20 and 7.21 present the characteristic values of shear strength and flexibility for both types of joints.

Table 7.20 – Results summary SERIES-I (single screw)

	I-D3 1-1	I-D3 1-2	I-D3 2-1	I-D3 1.5-1.5	I-D6 1.5-1.5	I-D6 1-2.5	I-D6 2.5-1	I-D6 1.5-3	I-D6 3-1.5	I-D6 2.5-2.5
P_m (N)	3618	5293	4361	5245	5551	5217	4363	8671	8906	12124
s (N)	311.2	157.3	503.8	724.1	470.6	490.3	411.9	1004.4	498.3	629.7
P_k (N)	2955	4958	3288	3703	4548	4172	3485	6532	7845	10782
K (kN/mm)	7.64	13.18	9.28	12.92	12.06	27.07	2.69	16.65	7.68	9.60
c_h (mm/kN)	0.131	0.076	0.108	0.077	0.083	0.037	0.372	0.060	0.130	0.104

Table 7.21 – Results summary SERIES-II (two screws)

	II-D3 1-1	II-D3 1-2	II-D3 2-1	II-D3 1.5-1.5	II-D6 1.5-1.5	II-D6 1-2.5	II-D6 2.5-1	II-D6 1.5-3	II-D6 3-1.5	II-D6 2.5-2.5
P_m (N)	3497	6102	4795	5919	6929	6184	4964	9533	10504	12442
s (N)	224.3	269.9	186.3	187.9	187.7	278.5	22.8	475.5	347.5	419.5
P_k (N)	3020	5527	4399	5518	6529	5591	4916	8520	9764	11548
K (kN/mm)	7.78	10.67	6.61	9.26	10.62	11.55	7.12	12.43	7.03	9.77
c_h (mm/kN)	0.128	0.094	0.151	0.108	0.094	0.087	0.141	0.080	0.142	0.102

Design method according to EN1993-1-3

Design codes have established formulas for determining the bearing capacity of joints with self-tapping screws, joint stiffness not being taken into account. Similar to the normal bolt connections it should be checked for multiple failure modes. From possible failure modes most of them can be avoided by appropriate constructive measures, the only remaining failure mode that refers literary to the connection being the bearing capacity.

According to EN1993-1-3 the bearing capacity of a joint depends on the nominal values of the thickness of the thinnest steel sheet (t), the self-tapping screw diameter (d), and the ultimate strength of the steel (f_u), i.e.:

$$F_{b,Rd} = \frac{\alpha \cdot d \cdot t \cdot f_u}{\gamma_{M2}} \quad (7.27)$$

where: α is a coefficient calibrated experimentally, which takes into account the relationship between sheet thickness and diameter of the screw, and $\gamma_{M2} = 1.25$ is the partial safety factor.

In order to avoid shear failure of the screw shaft, the screw must satisfy the relationship: $F_{v,Rd} \geq 1.2 F_{b,Rd}$ or $\Sigma F_{v,Rd} \geq 1.2 F_{n,Rd}$, where $F_{v,Rd}$ is the shear strength of screw shaft determined experimentally.

Table 7.22 presents the values of bearing capacity obtained using EN1993-1-3 for the combination of sheet thicknesses used for the tested specimens (see Figure 7.50).

Table 7.22 – Bearing capacity of self-tapping screw connection according to eqn. (7.27) (without γ_{M2})

t_1 (mm)	t_2 (mm)	α	d (mm)	$F_{b,Rd}$ (N)
1	1	1.460	4.8	2943
1	2	1.897	4.8	3824
2	1	-	4.8	²
1.5	1.5	1.789	4.8	5410
1.5	1.5	1.568	6.3	6173
1	2.5	2.1	6.3	5557
2.5	1	-	6.3	²
1.5	3	1.929	6.3	7656
3	1.5	-	6.3	²
2.5	2.5	2.016	6.3	13335

Comparison of experimental results with analytical calculations

Analysing the experimental results from Table 7.20 and Table 7.21, relative decrease of bearing capacity can be observed for joints with a single screw compared to those with two screws. This is primarily due to the fact that the results for these specimens are less consistent than those for the specimens with two screws. From this point of view, the design code recommends the use of specimens with two screws for determining the bearing capacity (compared to a single screw) and the connection stiffness.

² Cases not covered by EN1993-1-3

Comparing in terms of bearing capacity, the analytical results obtained with the formulas in EN1993-1-3 (see Table 7.22) with the experimental ones corresponding to the two screws specimens (see Table 7.21), one observes they are in the safety range (see Figure 7.54).

However D3 screws have a brittle failure even for thin thicknesses of sheets due to the weakening of the metal shank near the head of the screw (groove for screwdriver is affecting the metal strength), while D6 screws have a head shape less suitable for joining steel plates because they do not provide a contact surface of the screw head on the sheet metal. As a result, the failure begins by tilting of the screw shaft which affects the joint stiffness.

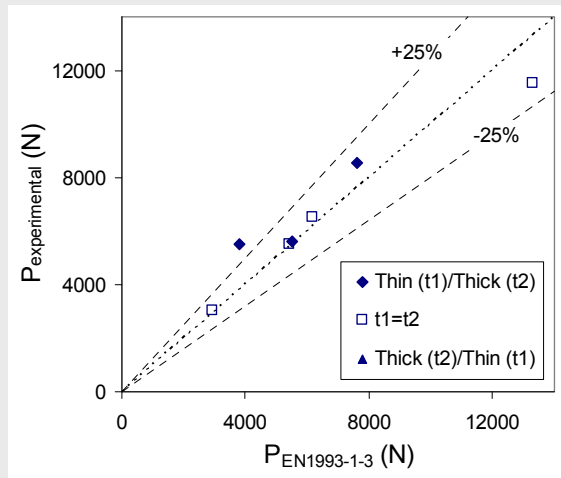


Figure 7.54 – Comparison of experimental and EN1993-1-3 bearing capacities

Chapter 8

BUILDING FRAMING

8.1 GENERAL INFORMATION

This chapter outlines how to design a residential building in cold-formed steel in agreement with the Eurocode 3 specifications. First of all, a general overview about the available construction systems is provided. Particular attention is paid to the stick-built system, which is, the most widespread construction system. Then, since the design of a house is a multicriterial problem, for which only an optimised compromise is possible, an overview on the architectural, structural and environmental aspects are presented. Finally, the detailed design of a one family house demonstrates the application of the Eurocodes.

557

8.2 INTRODUCTION

Cold-formed steel (CFS) systems have recently been identified as low-cost high performance solutions to residential buildings.

Cold-formed steel housing derives benefits from dry constructions (guaranteed quality of product, short execution time, and lower costs). Typical benefits of cold-formed steel systems are:

- wide variety of sections;
 - stability of shape in case of humidity;
 - easy assembling and disassembling;
 - easy integration of services (plumbing, cabling, ducting) inside of walls and partitions;
-

- lightness;
- high structural performance;
- flexibility.

Moreover, from an economic viewpoint, CFS structures are competitive in terms of cost. First of all, the lightness of the structure leads to smaller and more cost competitive foundations which can be built on regular or even poor soils, and allows concrete slabs to be used on sloping or steep sites, as well as regular flat sites. Also the prefabrication, that is typical for CFS constructions, is a decisive factor in terms of cost. A construction technique that makes assembly and erection simple often leads to more economical solutions than saving on the cost of materials. The fast erection time of CFS structures also leads to potential cost savings because it reduces the risk of delays to completing the construction, mortgage costs and fees.

Moreover, the industrial prefabrication ensures a guaranteed quality of building components that is realized in workshops protected from bad weather and subjected to constant quality checks.

From a sustainability viewpoint, the use of recyclable materials, the easy assembling and disassembling, the flexibility of systems and the possible reuse of elements ensure a low environmental impact.

The presented advantages of CFS housing have led to wide-spread use of these systems for new residential buildings, in regions that have traditionally been characterized by wood constructions like the United States of America and Australia (Watson, 2005), regions with difficult weather conditions like North Europe (LSK, 2005), as well as high seismicity like Japan (The committee on light gauge steel structures, 2004) and New Zealand.

8.3 CONSTRUCTION SYSTEMS

Residential buildings, despite their relatively small size and complexity, are very good products for an industrial production. Steel constructions, by their nature, are pre-fabricated to some degree and, in particular, three types of pre-fabrication have been developed for cold-formed steel housing: stick-built, panelised and modular constructions. In Chapter 1 (§§1.4.2), Figures 1.23 to 1.27 show different examples of cold-

formed steel frame residential buildings. On the following, some other examples will be presented, this time associated with different construction systems and technologies.

Stick-built constructions (see Figure 8.1) are obtained by assembling on site a modest number of members (studs, joists and rafters) and sheathing panels, which are fastened together by screws, nails or bolts. All elements are realised in the factory under a controlled environment and transported to the site, where the construction takes place without heavy lifting equipment. This gives rise to the use of a minimum volume of raw material and a reduction of energy to transport and erect the house. Dry constructions ensure less disruption and noise on site as well as minimum site waste. CFS houses, besides being made of light and standard elements, can be adaptable and flexible to different site conditions and to changing lifetime requirements. Moreover, high structural performance and good acoustic and thermal behaviour can be achieved by careful design. This produced flexibility offered by steel framing enables last minute changes and adjustments to the design. The stick-built system is particularly suitable for homes with unusual dimensions and design features.



Figure 8.1 – Stick built construction – Poland

Panelised constructions (see Figure 8.2) are made of bidirectional elements (wall and floor sub-frames and roof trusses), which are prefabricated in a factory. Thermal insulation and some of the lining and finishing materials may also be applied to the steel sub-frame to form panels, leading to a reduction of execution times. This system is particularly suited for houses characterized by a large number of repetitive elements.



Figure 8.2 – Panellised construction – Spain

Alternative forms of wall assembly used in low-rise steel framed construction are realised with light gauge steel cassettes (see Figure 8.3). The basic arrangement of this system consists of C-shaped cassettes that span vertically between top and bottom tracks to form high storey panels. The wall construction is then completed internally by insulation and dry lining (Trebilcock, 1994).



Figure 8.3 – Cassettes – Prototype for economic hotels – PARTAB – Sweden

Stick built and panellised systems can be assembled as Balloon Frame or Platform Frame systems. The Balloon Frame system was introduced by George Washington in 1830 for wooden structures (Sprague, 1981). In this system, the wall can be structuring continuous from foundation to roof and the floors are connected to the front or the side of the columns (Figure 8.4).

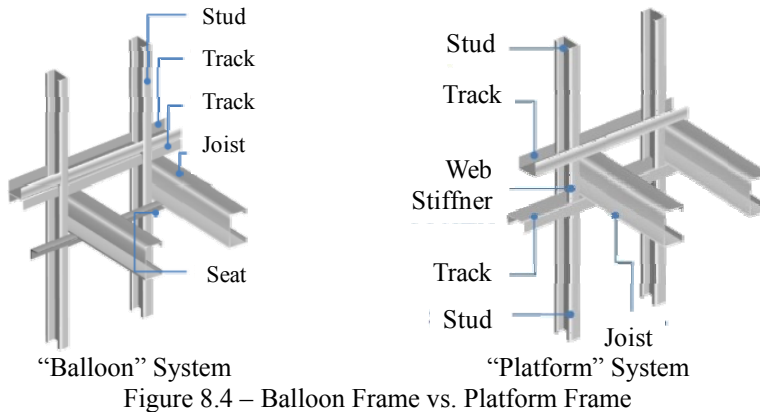


Figure 8.4 – Balloon Frame vs. Platform Frame

The joists are fixed into a track attached to the face of the stud wall. This attachment is usually a direct screw-fixed method or the floor system may be “hung” on the wall by means of a Z-section. Advantages of this method are the possibility to work on wide surfaces, the enhanced adaptability to tolerance “creep” and vertical alignment and it allows good air tightness. On the other hand, the difficulty of erecting wide surfaces on site represents a significant disadvantage.

In the Platform Frame system, the structure is built storey by storey, so that each storey can serve as working platform for the construction of the floor above. The walls are not structurally continuous and loads are transferred through the floor structure from the upper to the lower walls by means of mechanical connectors. Framing ensures the transfer of floor loads directly onto the studs but requires reinforcement of the joist webs in order to eliminate the possibility of web crippling.

Modular or volumetric constructions use pre-engineered modular units, which are transported from the factory to the site and installed as fitted out. Frames are welded together in the workshop by using cold-formed galvanized steel sections together with window and door openings which are formed at this stage. Two generic forms of modular construction exist: a) continuously supported modules, where vertical loads are transmitted through the walls to a continuous foundation (see Figure 8.5); b) open-sided or point-supported modules, where vertical loads are transmitted through corner and intermediate supports to point-foundations (see Figure 8.6). Point-supported modules require deeper edge beams than continuously

8. BUILDING FRAMING

supported modules. In both systems, forces are transferred by the module to module connections assisted by horizontal bracing, when necessary (Lawson & Ogden, 2008). Great importance has to be given to the junctions between the various members, because these determine the physical properties of the whole structure. The application of modular construction is the most economical solution for the repetitive production of a large number of similarly sized units. Modular toilets, bathrooms, lifts, service plants and roof-top extensions can also be introduced beside of existing buildings to create new spaces and improve the functionality of the building.



Figure 8.5 – Continuously supported module



Figure 8.6 – Modular unit by Kingspan

The different construction systems are often combined together in order to reduce the construction times without loss in terms of spatial organization. This is the case for Beaufort Court, where X-braced wall panels, floor cassettes and bathroom modules are combined together (see Figure 8.7).



Figure 8.7 – Beaufort Court by Feilden Cleegg Bradley – London, UK

8.4 STICK BUILT CONSTRUCTIONS

Among the different cold-formed construction systems, stick-built constructions are the most widespread, and their design methodology is quite codified. This system replaces more than any other the wood constructions systems, so that in numerous countries a large number of building companies turned their wood production into light gauge steel production. Stick built construction is composed with a repetitive number of structural elements (CFS profiles, sheathing panels, fasteners) that form structural diaphragms (walls, floors and roof) which are connected together by mechanical anchors. The main sub-systems are described in detail hereafter.

563

8.4.1 Foundation

Cold-formed steel housing does not need deep foundations because of their lightness. They can easily be set on poured concrete wall foundations (see Figure 8.8a) or slab-on-ground foundations (see Figure 8.8b). In particular, in the latter case, 300-500 mm thick slab foundations can be realized even on poor soils without deep digging. This is the simplest form of foundation for the most light steel residential structures. Using this form of foundation, bearing walls (see Figure 8.9) may be supported on thickened

8. BUILDING FRAMING

portions of the slab and changes in ground level can be easily accommodated.

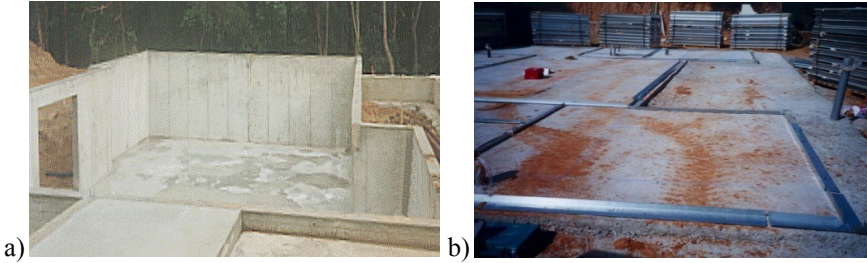


Figure 8.8 – Typical foundation systems

In areas where frost is a design issue, individual anchors and footers are extended to below the frost line and bear on earth below that depth. As an alternative to running the footers below the frost line, holes for the footers may be dug to the frost depth and then back filled to the surface with gravel or other material that will not retain moisture. Another option is to insulate the area around the crawl space. This would eliminate the need to run the anchors and footings below the frost depth.

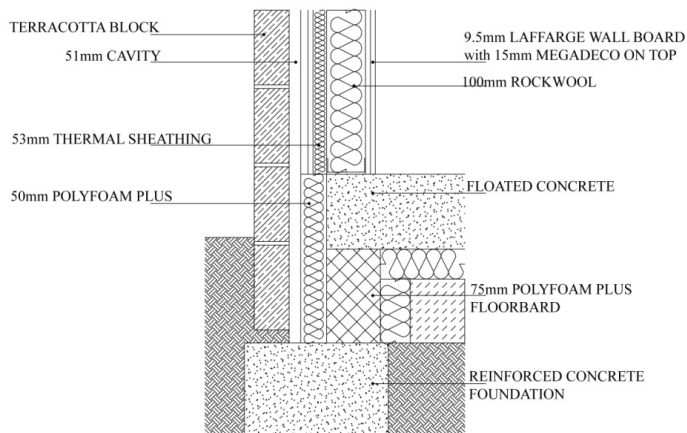


Figure 8.9 – Concrete slab on ground detail (SS025a-EN-EU, AccessSteel 2006)

8.4.2 Floors

Floors are realized with horizontal load bearing members (joists) sheathed with gypsum and wood-based panels. Joists are usually C- or Z-shaped members spaced at 300-600mm and fastened at each end to a floor

track (see Figure 8.10). Web-stiffeners are installed at both joists ends in order to strengthen the member against web-crippling. Floor spans will range from about 4 meters to 6 meters depending upon the depth and type of the joist (SS027a-EN-EU, AccessSteel 2006). The spans can be taken from manufacturer's published tables but should be checked by the responsible structural engineer. For the most part, spans are limited by vibration considerations, as presented in §§8.5.5. When the span is very large, C-shaped members (floor blocking) are installed in perpendicular direction to the joists, in order to stiffen them along the length, and flat straps are fastened to the bottom side to ensure continuity between joists and blocks.

To obtain adequate in-plane bracing, X-bracing realized by flat straps fastened on the bottom side or the sheathing itself can be adopted as bracing system. In particular, a drywall ceiling makes acceptable lower-flange bracing, but in a basement, the usual approach is to run a strip of steel strapping at the centre of the joist span for the entire length of the floor section, securing it to each joist with one screw. The blocking can be narrower than the joists themselves, and is, usually, fastened to the joists with clip angles.

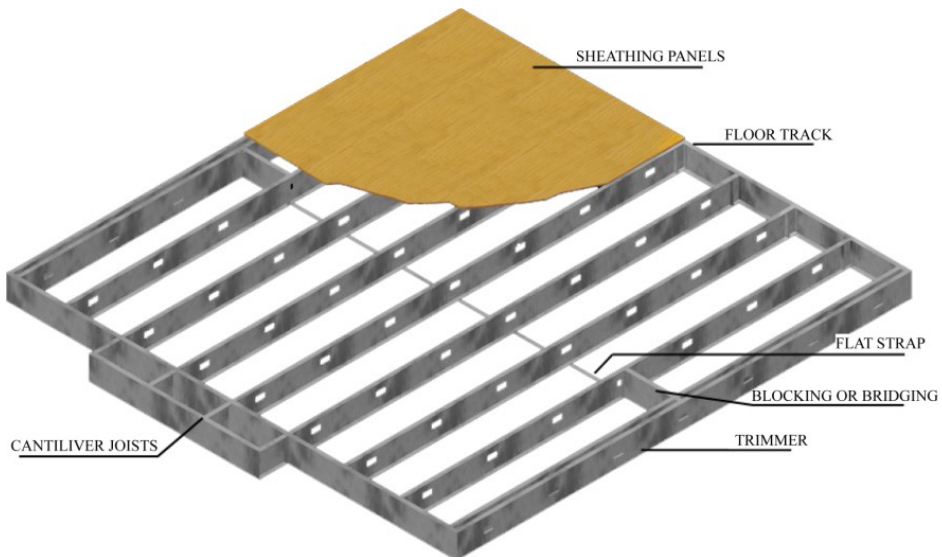


Figure 8.10 – Typical floor framing (Iuorio, 2009)

Moreover, cantilevered joists can be realized but they require a web stiffener where they pass over the supporting wall.

Services and piping can be accommodated by introducing holes along the joists (see Figure 8.11).



Figure 8.11 – Piping

Specific construction details have to be designed in case of openings. In fact, as shown in Figure 8.12, the presence of an opening requires the introduction of header joists, box sections that can be realized with a C-joist and a floor track, placed in the perpendicular direction to the adjacent joists and trimmer joists at the other two edges.

As described in the next sections, some technological details have to be designed to ensure soundproofing and reduce vibrations. In fact, although vibrations induced by human footsteps do not produce structural damage it can be a source of discomfort.

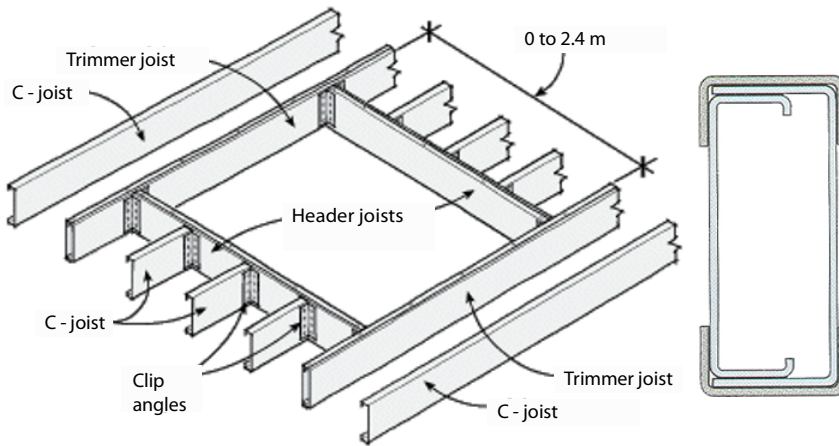


Figure 8.12 – Floor opening and header detail

8.4.3 Wall studs

Walls can be divided into load bearing walls and non-bearing walls. In the first case the principal structure is comprised of studs, i.e. vertical load bearing members spaced at 300-600 mm, in line with floor joists. The studs are fastened at each end to wall tracks, which have the function of supporting the studs laterally and distributing loads among the studs. In order to strengthen the stud along the height, it is quite common to introduce lipped channel profiles (blocking) at mid wall height (see Figure 8.13).

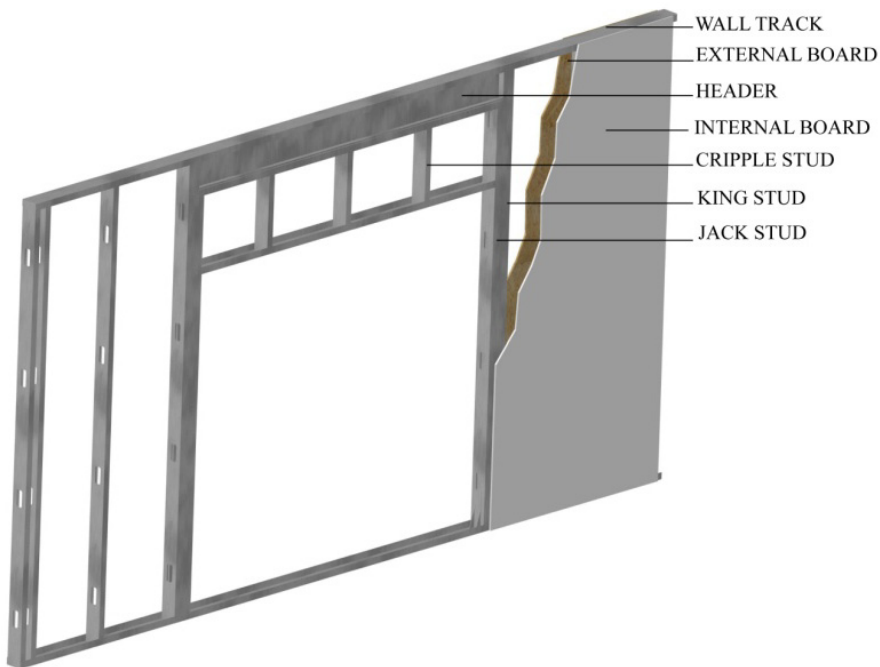


Figure 8.13 – Typical wall framing (Iuorio, 2009)

The wall design can change dependent of the function of the wall. When the walls represent the lateral load resisting system, they have to carry vertical loads transferred from upper floors and roof, as well as resist horizontal loads from wind and seismic actions. In particular, the ability to resist horizontal in-plane actions can be achieved by different systems: a) X bracing; b) installing horizontal steel strapping on both wall sides at mid-height and in-line blocking at ends of all straps; c) fastening structural

sheathing boards on one or both sides of the studs; d) introducing a structural sheathing on one side and horizontal steel strapping on the other side (mixed solution). In particular, structural sheathings have to be installed with the long direction parallel to the studs and have to cover the full height.

Moreover in order to prevent the wall from up-lift due to horizontal in-plane actions, hold down anchors have to be introduced at the end of each component wall.

The result is a sandwich construction where each panel can bear perpendicular pressure on its surface as well as in-plane loads. The internal wall cavity is ideal for inserting cables, pipes and insulation. An unlimited range of materials can be used as finishing of both the inner and the outer surface: paint, wallpaper, coating, fabric, etc. as suggested in Figure 8.14.

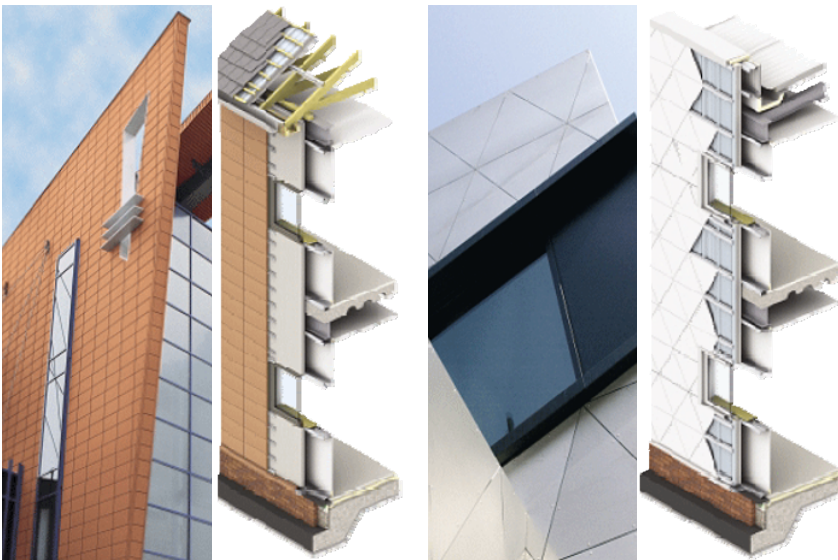


Figure 8.14 – Solutions for wall façade (Kingspan, 2007)

Depending on the adopted stratification, the external walls can vary in thickness from about 70mm to 300mm and the internal structural walls from 70 mm to 150 mm. Non-structural walls, room partitions, will range from about 40 mm to 100 mm. Section thickness for structural elements will range from 0.9 mm to 3.2 mm and for non-structural elements from 0.7 mm to 0.9 mm (SS026a-EN-EU, AccessSteel 2006).

8.4.4 Roof

Light steel building can present pitched or mono-pitched, flat or curved roofs. In any case, the main structural components of roof framing are: rafters, which are structural framing member (usually sloped) that supports roof loads (typically lipped channel sections), ceiling joists, i.e. horizontal structural cold-formed lightweight steel profiles that supports the ceiling and attic loads (typically lipped channel sections); ridge members, i.e. horizontal members placed at intersection between the top edges of two sloping roof surfaces and fascia, i.e. members attached to the rafter ends as edge members for the attachment of roof sheathing, exterior finishes, or gutter, as shown in Figures 8.15 and 8.16. Moreover, as for walls and floors, blocking and flat straps can be introduced to strengthen the in-plane members, and in case of roof openings, headers are installed. Where possible, the roof frames should be aligned with the studs of the supporting walls. Where this is not possible, the use of a robust, load carrying, top track will permit trusses or other roof framing to be located with a reasonable degree of flexibility (SS028a-EN-EU, AccessSteel 2006).

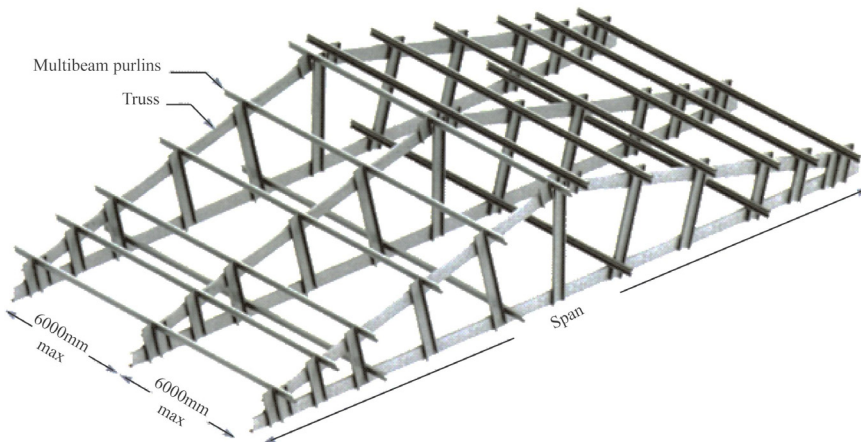


Figure 8.15 – Typical roof framing – Kingspan

Typically, the design of the ridge connection and the connection between trusses and walls are critical. Figure 8.16 shows some detailing solutions.

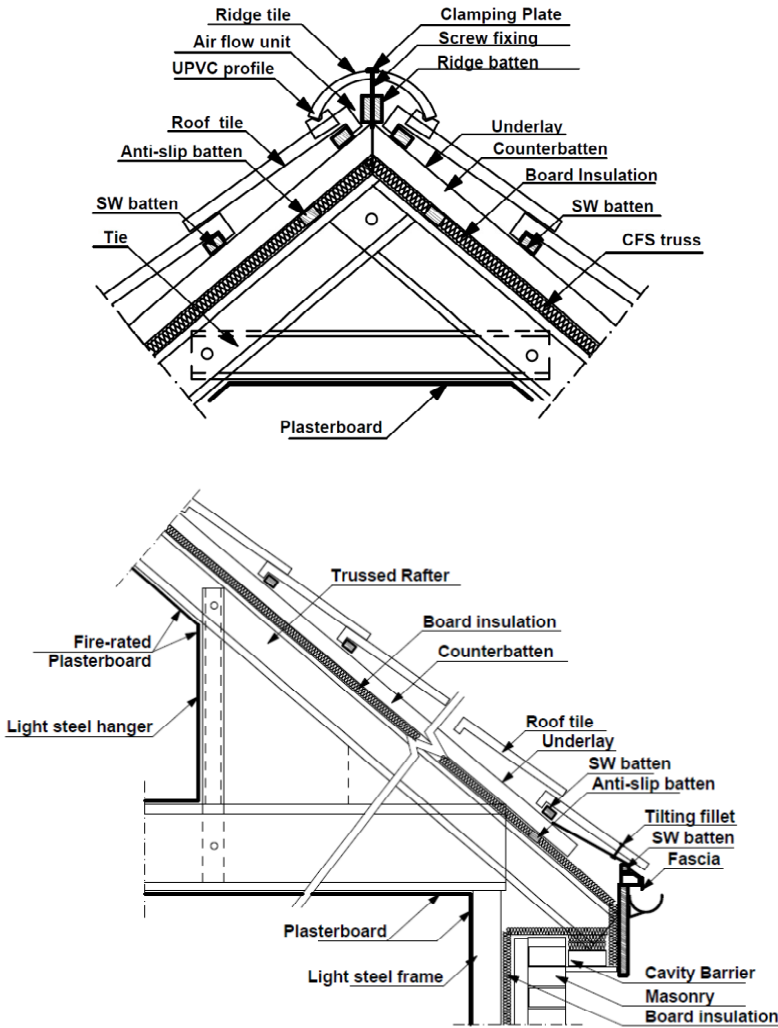


Figure 8.16 – Ridge and eaves details

8.4.5 On-site Construction

Short execution time is one of the advantages of using cold-formed steel structures to realize low-rise buildings. Figures 8.17 through 8.21 show the construction phases from the transportation on site of the structural profiles to the completion of the dwelling.

The storage on site of all the structural components starts the building site (see Figure 8.17).



Figure 8.17 – Phase I: Profiles are stored on site

A place for storing has to be allocated in order to avoid the corrosion of the members. According to the onsite conditions, the foundation is prepared (see Figure 8.18).



Figure 8.18 – Phase II: Foundation

The members can be fastened together by self-drilling screws (see Figure 8.19). New processes for fastening sheathing panels, like tacking and stapling, have been developed. Pneumatic fastening processes are simpler and quicker than screwing, but present the disadvantage of making on-site assembly defects relatively expensive to repair.



Figure 8.19 – Phase III: Walls are assembled on the floor and then lifted up in vertical position

When all walls of the first floor are completed (see Figure 8.20) and the structure is braced by means temporary diagonal elements, the second floor or roof can be built (see Figure 8.21). The temporary bracing system is required in order to strengthen the construction to provide an adequate working platform to construct the upper floors.

572



Figure 8.20 – Phase IV: Vertical structural elements of the first floor are completed

When the complete structural system is installed, piping and finishing materials are added.

As has been shown, the simplicity of the construction phases allows the dwelling to be erected by non-professional workers.



Figure 8.21 – Phase V: Roof trusses are assembled

8.5 CONCEPTUAL DESIGN

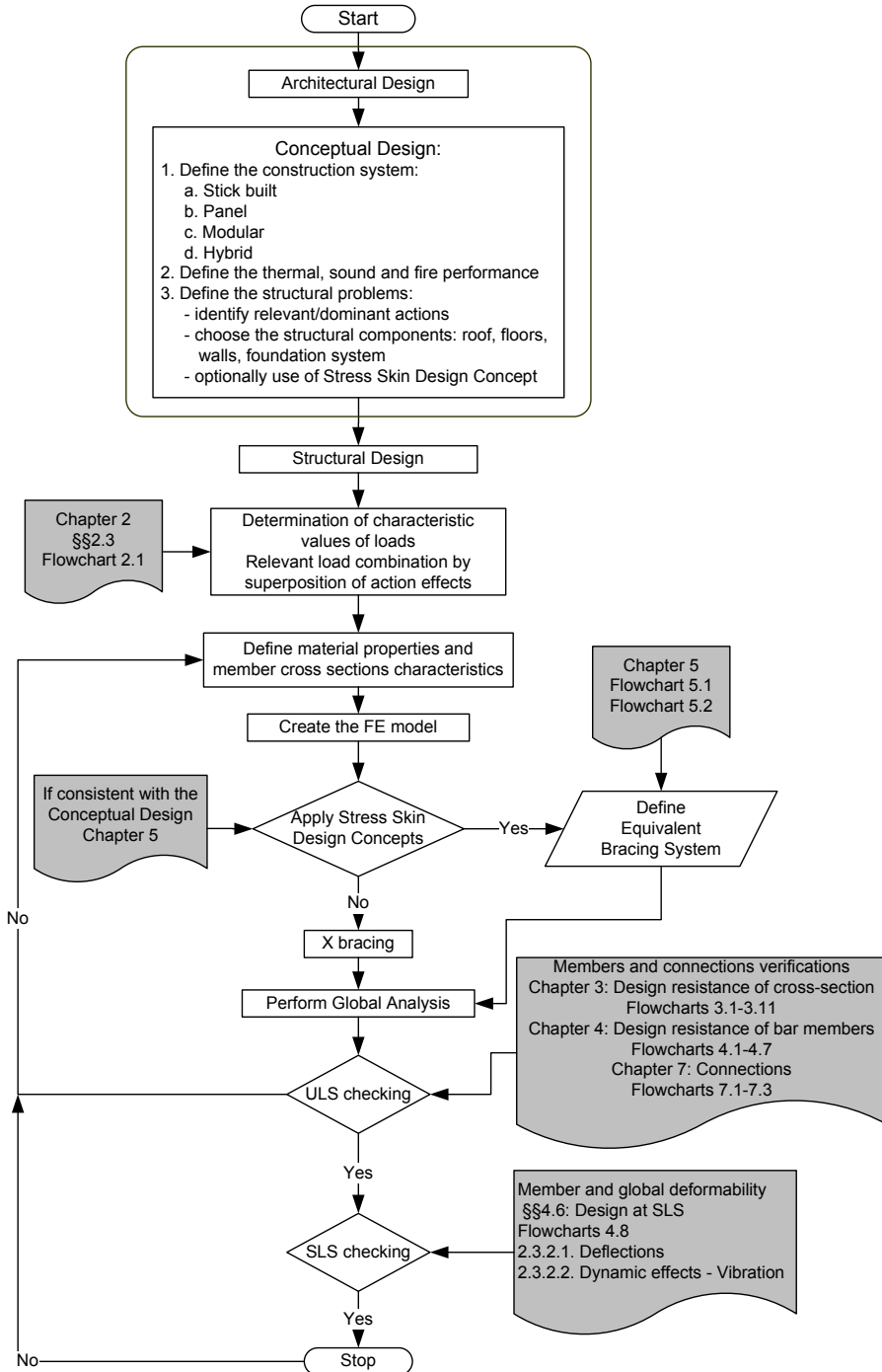
The conceptual design is one of the most important steps in the design of a CFS construction. In fact, the best design of a light gauge structure can be achieved when a holistic design approach is applied. A holistic approach requires the development of the architectural and structural design in parallel. Since the beginning, all the performance in terms of structural safety, thermal and sound insulation and fire protection have to be defined.

In this way, the members that best satisfy the structural requirements and, at same time, is compatible with the other technological requirements can be defined very early in the design process in order to reach the best solution with the minimum cost and time.

Once the conceptual design is defined and from a structural viewpoint the most relevant actions and the main structural components have been identified, then the structural design can be developed as summarized in the following Flowchart 8.1.

8.5.1 Architectural design

In the contemporary market, flexibility, adaptability to personal tastes and high quality are the main clients' requirements. The stick-built construction can very well satisfy these requirements. This system can be used for different building typologies: one or multi-storey housing, offices, hotels, restaurants, shopping centres, temporary structures, etc.



Flowchart 8.1 – Conceptual design

CFS systems can match the architectural requirements of social housing, as demonstrated by the current extensive use in the United Arab Emirates (see Figure 8.22), where large social housing compounds have been realized with this system, as well as, the system can fulfil more complex requirements as those defined for the recent school in Naples designed and built-up for the British Command of the Defence Estate (Landolfo, 2011; Landolfo *et al*, 2011; Iuorio *et al*, 2012).

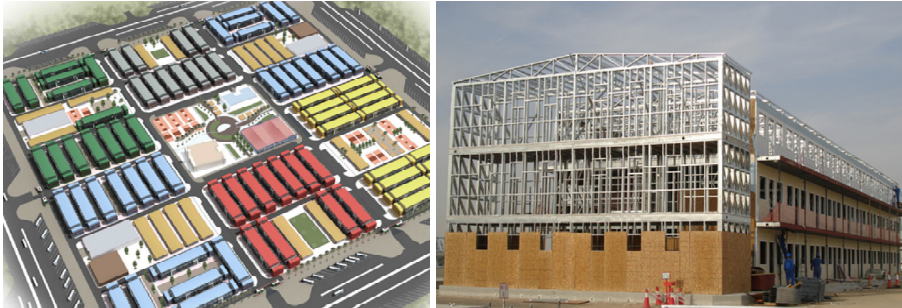


Figure 8.22 – CWR – Abu Dhabi – UAE



Figure 8.23 – Foundation and Primary Stage School – Naples – Italy

8. BUILDING FRAMING

In this second case, the adopted design solutions for the execution of the new “Foundation and Primary Stage School” (see Figure 8.23) on behalf of the British Force (BFS) of NATO in Naples are of great interest within the Italian construction sector. The adoption of a stick built system made of cold-formed steel walls braced by wooden sheathing panels has appeared as the most adequate to meet architecture solutions together with the high standards in terms of safety, durability and eco-efficiency required by the client. The final results is a building in covered area of about 3000 m² that reflects, in each its element, the integrated and coordinated work done by designers and technicians, from the conceptual design trough construction work and testing.

Moreover, construction companies, like Yorkon and Kingspan, are showing the architectural possibilities also in the case of very complex plan distributions, as in the case of Lingham Court (see Figure 8.24), where curved CFS panels and modular units are combined in order to distribute flats and gardens in two crescents.

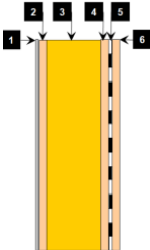
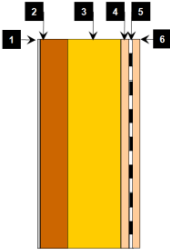
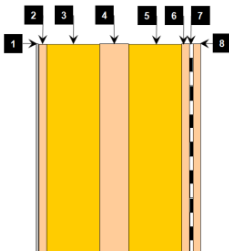


Figure 8.24 – Lingham Court – London, UK

8.5.2 Thermal insulation

In order to achieve a low energy house, thermal bridges and convection flows should be avoided and a good air tightness should be ensured. The presence of thermal bridges is usually the cause of heat losses and cold surfaces. Because steel is a high conductor of heat, it is extremely important to insulate the sections in external walls and the roof beams. Therefore, the space between wall surfaces must be filled with insulating materials like glass wool or Rockwool, that are both non-flammable materials with good thermal insulation capacity. Moreover, several insulation layers as well as thermal bridges breakage can be installed to obtain an extremely high insulation levels. In this regard, Table 8.1 shows the thermal transmittance values for some common type of wall assembly.

Table 8.1 – Transmittance values of some common wall assemblies (LSK, 2005)

Wall section		[mm]	U-value [W/m ²]	Fire resistance
	1. External layer (reinforced, mineral) 2. Plaster board 3. Mineral wool & stud 4. Plasterboard 5. Vapor barrier 6. Plasterboard	10 15 150 12.5 - 12.5	0.48	30min
	1. External layer (reinforced, mineral) 2. Wooden soft fibreboard 3. Mineral wool & stud 4. Plasterboard 5. Vapor barrier 6. Plasterboard	10 80 100 12.5 - 12.5	0.29	30min
	1. External layer (reinforced, mineral) 2. Plaster board 3. Mineral wool & stud 4. Mineral wool 5. Mineral wool & stud 6. Plasterboard 7. Vapor barrier 8. Plasterboard	10 15 100 50 100 12.5 - 12.5	0.18	30min

Moreover, in order to reduce the conductivity of the steel member, thermo profiles can be used. These special members shown in Figure 8.25 present longitudinal holes in the web that lengthen the path required to transfer heat, with a reduction of heat propagation.

In the same way, achieving correct air tightness improves room temperature, inside air quality and energy balance. Therefore, waterproof membranes are installed on the inner side of internal coatings.

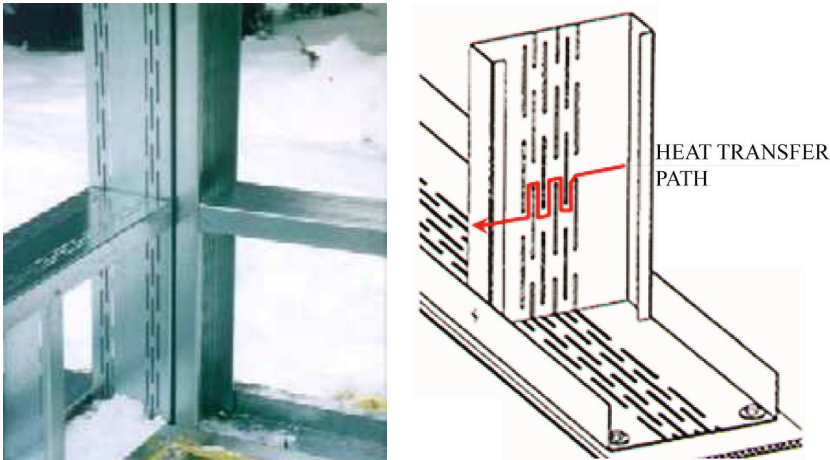


Figure 8.25 – Thermo profiles

A 9 mm thick gypsum board is ideal as wind baffle board. This board resists rain, frost and sun well without deformations and moisture will not make it warp. Other building boards that can be used as wind baffle boards include 12 mm or 25 mm thick porous wood fibre wind baffle board; 6.5 mm or 9 mm thick plywood or 12 mm thick bitulite. Moreover, if the interior coating is not sufficiently tight, hot air and vapour can penetrate and the resulting humidity can be a cause of corrosion, fungus, frost, etc. Hence, a suitable moisture barrier like a 0.2 mm polystyrene film with 1.83×10^{-12} $\text{kgm/m}^2\text{sPa}$ moisture permeability should be installed (Miettinen & Saarni, 2000).

8.5.3 Soundproofing

In CFS construction, the parameters that influence soundproofing are:
a) the board materials and spacing; b) typology, thickness and spacing of

steel elements (studs or joists); c) the typology of insulating material placed in the internal cavity and the connections and the assembly typology (see Figure 8.26).

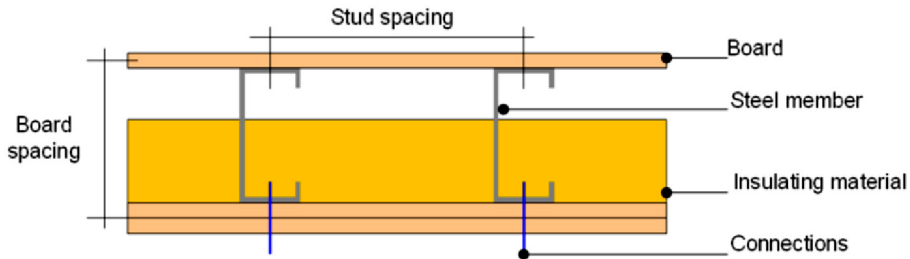


Figure 8.26 – Parameters influencing the soundproofing of walls

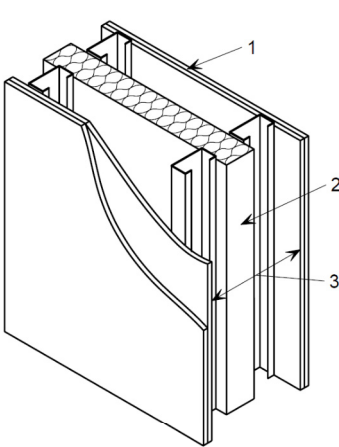
To obtain a good soundproofing, the sheathing should be “flexible” from an acoustic viewpoint. In this regard a 20 mm thick plasterboard or wood-based panel have good properties. Moreover to optimise sound insulation, two boards should be separated as much as possible. Otherwise, sections that have a deep fold or thermopurlins can be used.

Great importance has to be paid to the insulating material used to fill the internal wall cavity. In particular, when fibrous materials are used, the sound energy crossing the fibres is transformed into heat energy so that sound and thermal insulation can be achieved at the same time. The sound properties are also affected by the way the boards are fixed on the steel members and on the supports. Particular attention must be paid to acoustic problems when installing metal pipes. They must not come into contact with any stud to avoid sound transmission.

Moreover, in designing floor assemblies, footsteps and impact noise have to be considered. In this case, the propagation of footstep noise through the floor can be prevented by separating the topside as much as possible from the underside. This can be obtained by using floating floors and false ceiling. In particular, in the case of false ceiling, the use of resilient bars between the supporting members and the plasterboard reduces connection stiffness and consequently reduces the sound vibrations between joists and board.

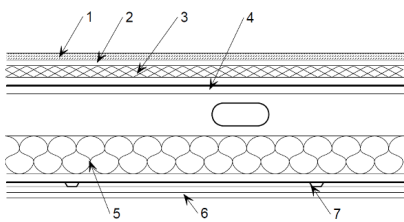
A typical separating wall detail is shown in Figure 8.27a. This detail illustrates the separation of the structural elements, mass of plasterboard and

mineral wool for absorption. An airborne sound reduction of 60 to 65 dB can be achieved, depending on the thickness and type of boards. The acoustic performance of separating floors is dependent on both maximising airborne sound reduction and minimising impact sound transmission. It is often control of impact sound which is more problematical, and a resilient layer on top of the floor is required to reduce direct sound transfer. A typical separating floor is shown in Figure 8.27b (SS032a-EN-EU, AccessSteel 2006).



1. Wall lining: 2 or more layers of gypsum based board
2. Absorbent material: 50 mm of approved material
3. Wall width: 200 mm minimum

a) Separating wall detail from Robust Details



1. 18 mm chipboard
 2. 15 mm sound resistant board
 3. 30 mm rigid insulation
 4. Floor cassette with 22 mm board
 5. 100 mm insulation
 6. 2 layers, 15 mm wall board fixed to resilient bars
 7. Proprietary resilient support
- b) Typical 'floating floor' construction to achieve satisfactory acoustic performance

Figure 8.27 – Example of efficient sound insulation solutions (SS032a-EN-EU, AccessSteel 2006; Robust Details, 2010)

Grubb & Lawson (1997) provides information and guidance on the construction of light steel framing systems in general building applications, both the domestic and commercial building market. They provide information related to acoustic insulation, fire protection, and structural

design. Clough & Ogden (1993) present details on the acoustic insulation of building elements constructed using cold-formed structural steel sections.

8.5.4 Fire resistance

Fire design is an essential part of the design procedure of a building. Fire design methods are used to ensure that a structure designed according to rules used for normal room temperatures can also withstand the additional effects induced by increasing temperature. The criterion commonly used for determining the fire resistance of a steel structure against fire is called fire resistance-time. Structures are classified into different groups of required fire resistance time as R-15, R-30, R-60, etc. The classification is based on the type, structural system and use of the structure. Calculation models for the fire design of steel structures, of class 1 and 2 cross-sections, are given in Eurocode 3, Part 1.2 (CEN, 2005d).

Steel members are incombustible (Class A, material) but they have to be protected against reacting the high temperature during a fire. In CFS structures, walls, floors and roof are generally built using a cold-formed steel member core as the principal load-bearing system, mineral or glass wool as thermal and sound insulation and sheathing boards on the outsides.

Because these elements act as separating elements between adjacent fire compartments, they should resist the spread of fire, heat and toxic fire gases into the next compartment.

The compartments of a lightweight steel structure and their locations determine the fire resistance category of the building. For both, walls and floors, the location of sheathing, the thickness and the number of coating layers as well as the width of the insulation determine the fire resistance category.

Thin sections of all the load-bearing members (studs, joists, rafters, etc.) must be covered with anti-fire materials such as plaster, plaster-fibre, or sand limestone, which should be attached to the flanges of the sections using screws at regular and sufficiently small intervals.

To understand what happens during a fire, the external walls may be considered assuming the fire on the inside. In these members, there would normally be a great difference in temperature between the two faces of wall under a fire. Typically, the fire side of the wall can easily be 200°C - 300°C

hotter than the external side not exposed to fire (Ranby 1999). This means that the material properties of the steel parts deteriorate much faster on the fire side than they do on the external side. The fire side of the steel members being hotter, the thermal elongation is also much greater on that side, causing the steel member to deflect towards the heat source.

The structural behaviour of individual studs changes as a function of temperature in this type of sheathed wall structure due to changes in the boundary conditions. At normal room temperature and at the beginning of the increase of temperature under fire, the restraining effect of the sheathing boards can be effective, but when the critical temperature (in case of gypsum boards the critical temperature is approximately 550°C) for the functionality of the wall is reached, the boards are calcined and their restraining effect is negligible (Ranby, 1999). Cracking and actual destruction of the gypsum boards will also take place. This means that torsional, torsional-flexural and distortional buckling modes may occur. However, the gypsum boards on the external (cooler) side remain in place after the fire side boards become calcined, unless the deflection induced by the thermal gradient and second-order effects causes the compressed gypsum boards on the external side to break. The falling off of gypsum boards on the fire side of the wall will naturally expose the steel studs directly to the fire. This will lead to a rapid reduction of the temperature gradient across the steel section, while other parts of the wall where the gypsum boards are still in place will continue to have strong temperature gradients. Consequently, adjacent steel studs may be exposed to substantially different conditions towards the later stages of a compartment fire. At this point, insulation placed in the internal wall cavity can play a key role, because once the fire side covering is destroyed, the insulation, that can have a melting temperature mayor of 1000°C, slows down the propagation of fire to the other side of the wall. Structural fire design model for steel wall studs have been presented by Klippstein (1978), Ranby (1999) and Kaitila (2000).

Figure 8.28 shows the fire resistance duration of some load bearing wall configurations.

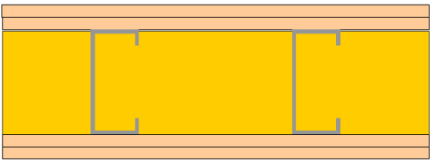
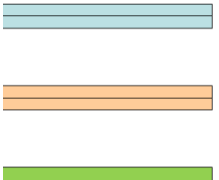
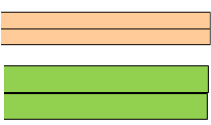
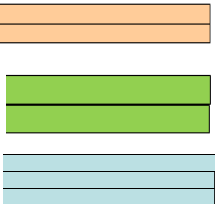
Fire resistance		
30 min		<ul style="list-style-type: none"> 2 × 12.5 mm Fire Proof Plasterboard 10 + 12.5 mm Gypsum Fibreboard 20 mm Fireboard
60 min		<ul style="list-style-type: none"> 2 × 15 mm Gypsum Plasterboard 2 × 15 Fireboard
90 min		<ul style="list-style-type: none"> 2 × 25 mm Gypsum Plasterboard 2 × 20 Fireboard 3 × 12.5 Gypsum Fibreboard

Figure 8.28 – Fire resistance duration of some wall assemblies

Moreover, studs or beams which are not integrated in the walls or floors must provide the required fire-resistance. Covering these members with fire-retardant panels or rough coats or insulating layers can be a good solution.

583

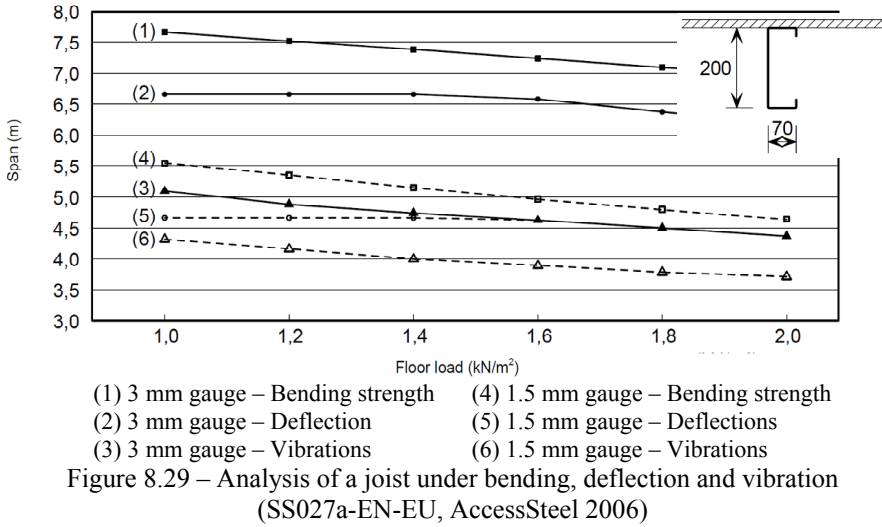
Finally, attention must be paid to the connections between the wall, floor and roof panels, because they may allow the fire to reach the internal cavities. To avoid it, the connections must be lined with incombustible mineral wool strips, mastic or expanded foam.

8.5.5 Vibration

Vibrations caused by human activity have long been recognized as significant serviceability concern for residential floor systems. In particular, steel framed floors are typically lighter and have less damping than other traditional floors. As a result, such systems designed for only strength may be more susceptible to excessive floor vibrations due to human footfalls (see

8. BUILDING FRAMING

Figure 8.29). Therefore, in the design stage, this problem has to be taken into account.



Document SN036a-EN-EU of Access Steel (2006) gives rules for the consideration of vibrations by simple (and thus conservative) approaches for verification. The procedure presented in SN036a-EN-EU is based on the recommendations and requirements given by ISO 10137 (2007), ISO 2631-1 (1997) and ISO 2631-2 (2003). For cases where the guidance in these Standards is unavailable, or incomplete, recommendations that have been developed in the RFCS project entitled “Vibration of Floors” (Project reference 7210-PR/314) were presented.

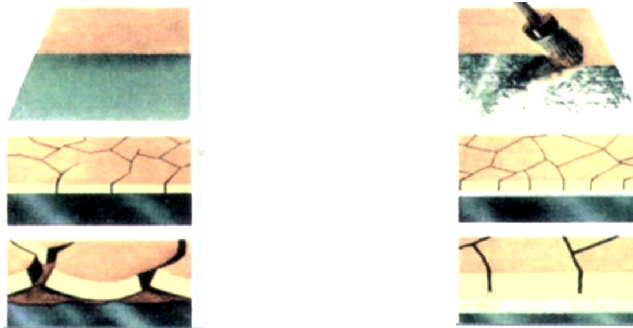
8.5.6 Durability

Residential homes are one of the few necessities that consumers expect to last a lifetime. It is critical therefore that the framing materials of residential homes perform satisfactory for as long as other components such as exterior and interior wall coverings and flooring. To last a lifetime, light gauge steel framing needs proper corrosion protection. The standard form of corrosion protection for cold-formed steel sections is the continuous dip zinc coating applied as a pre-coat to the rolling of the strip steel that forms the section.

Galvanizing has proven to be the most economical and effective way to protect steel (AISI, 2004). Galvanizing is a process whereby steel is immersed into a bath of molten zinc (450°C) to form a metallurgic bonded zinc coating.

The zinc coating is able to protect the steel much more reliably than paint coating because it passivates the steel, and is resistant to damage and effects of local moisture arising from condensation in transient conditions. The zinc adheres to the steel substrate and deforms around the bends during forming, even in complex section shapes, without cracking or becoming detached. For these reasons, galvanizing has become the standard method for corrosion protection of cold-formed steel members in a wide range of applications not subjected to direct weathering or exposed conditions. Moreover, galvanizing has the advantage that, when zinc coating is breached, for example at cut edges or drilled holes, or when the zinc has been eroded away locally, significant corrosion of the steel substrate will not necessarily occur. Only when the distance between the zinc and steel is large will the steel corrode.

Zinc coatings provide a barrier that prevents oxygen, moisture and other atmospheric pollutants from reaching the steel. Because many of the products formed are at least partially soluble in water, the zinc is consumed over a period of time in any damp location. In fact, zinc corrosion rates correlate with two major factors: time of wetness and concentration of air pollutants. The consumption of zinc and the life of zinc-coated steels can be calculated with reasonable accuracy for specific environments from research data.



a) paint coating

b) duplex: zinc and paint coating

Figure 8.30 – Comparison between paint coating and zinc and paint coating (AIZ, 2005)

Since residential steel framing should be dry almost all the time, zinc's corrosion rate will be very low.

Moreover, in a residential house, internal walls and floors are sheathed and insulated; therefore the steel components are kept above a certain temperature, minimising the risk of interstitial condensation and avoiding pattern staining on internal surfaces. The use of vapour barrier and thermal breaks should eliminate any significant moisture exposure to internal wall framing. For instance, a vapour barrier or sill gasket has to be installed between the track and the foundation to prevent underside corrosion in the event that the concrete substrate gets wet, or, a breather membrane is recommended in exposed locations where rain may penetrate the outer skin and would wet the insulation layer.

In cases of suspended ground floors, over-roofing of existing building, and joists built into solid masonry walls, the steel can be exposed to moisture over an extended period. In the cases, adequate ventilation should be ensured.

In more aggressive locations, such as externally, or with poor quality brickwork, rainwater can gradually remove the beneficial effect of the galvanizing layer. Therefore, galvanized steel is not recommended for long life applications in areas subjected to continuous wetting and drying, running rainwater over the surface, leakage from service pipes, corrosive or acidic materials or polluted atmospheres.

586

Good building practice, thermal insulation and proper ventilation ensure that the design of modern houses conforms to a warm dry environment, even though humidity is created by the occupants or activities inside.

Galvanising has the advantage that, where continuity of galvanized coating is broken, for example at cut edges or drilled holes, or when the zinc has been eroded away locally, no significant corrosion of the steel will occur. This is because zinc in the close proximity to the exposed steel will still corrode preferentially, acting as a consumable anode in an electrochemical cell (i.e. it protects the steel cathodically). The use of a sacrificial metallic layer is known as galvanic action. Only when the distance between the zinc and steel is too great will the steel begin to corrode.

Numerous monitoring studies carried out in Europe, USA, and Japan have showed that the environmental conditions present in warm frame

construction are such that moisture levels are very low and that galvanized steel components are not subjected to a risk of significant corrosion within the expected life of well-maintained modern buildings. Moreover, these studies suggested the monitoring of the internal environment and measurement of remaining zinc thickness on galvanized steel sections in various places of the building should be performed at least after 30 years of use.

8.5.7 Sustainability

Sustainability is one of the greatest challenges of the modern world. The construction sector plays an important role in sustainable developments of the world and national economies. Sustainable construction has different approaches and different priorities in various countries. Some of them identify economic, social and cultural aspects as part of sustainable construction, but these aspects are raised as major issues only in a few countries.

Sustainable construction can be regarded as a subset of sustainable development and contains a wide range of issue, i.e.: re-use of existing built assets, design for minimum waste, minimizing resource and energy use and reducing pollution.

Light gauge steel framing represents a valuable solution from an environmental point of view because it is a dry construction system without organic materials. Dry construction significantly reduces the risk of moisture problems and “sick building syndrome” (Burstrand, 2000). Furthermore, steel, gypsum and mineral wool are closed cycle materials, each of them can be 100% recycled. In fact, most steel members in a CFS construction are produced from recycled steel. The magnetic properties of the steel allows easy extraction from waste materials and all the collected elements can be fully recycled to produce new products with fine qualities. Therefore, the recycled steel is used to make members that are durable, separable, dismantlable and reusable. Moreover, the easy assembling and disassembling of cold-formed steel structures allow constructions to be erected and disassembled with a small amount of waste material. Light gauge steel framing means less energy consumption during production than equivalent housing with a framework of concrete poured on-site. Light

gauge steel framing only uses about a fourth of the amount of raw materials used for equivalent homes in concrete. Furthermore, the low dead weight of building components ensures a good working environment and leads to reduced transport needs.

Therefore, the competitiveness of a CFS house's ecological balance is mainly based on the use of recyclable materials, light gauge components, dry-construction, easy assembling and disassembling, reduced amount of wasted materials and reuse of elements (see Figure 8.31).

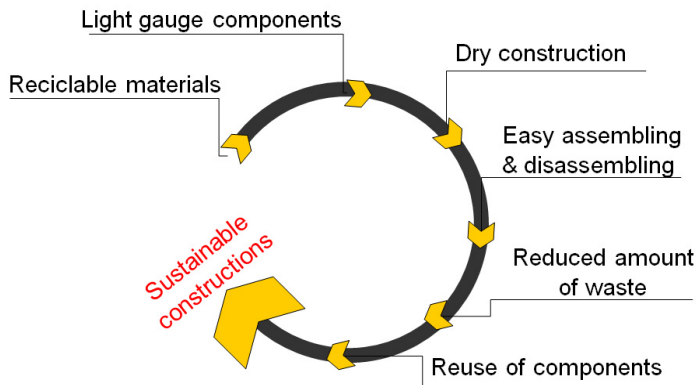


Figure 8.31 – Life cycle for cold-formed steel construction (Iuorio, 2009)

The sustainability of a residential building is also strongly correlated to the internal comfort and energy saving. Hence, the envelope design plays an important role and has to address some of the following issues:

- the exterior layer has to balance the need for protection of the elements, visual value and economics;
- the thermal insulation has to be compatible with the exterior layer and mechanically fastened to the structure;
- the consistency of the interior layer has a great influence on the indoor air quality. The trend today is to use gypsum board and vapour barrier on studs. Currently, some directions of research are towards focus on finding alternatives, i.e. new or traditional materials which allow for vapour migration to the wall cavity and could provide thermal inertia.

Moreover, as already seen in the previous sections, the envelope has to provide as much as possible a uniform “wrapping” of the steel structure in order to avoid and/or control thermal bridging.

8.6 STRUCTURAL DESIGN

8.6.1 Structural conception

As for structural design of a traditional building, also in the case of structures made with cold-formed steel profile, there are two main performance requirements: to transfer to the ground the vertical loads and the horizontal forces acting on the structure.

The design under vertical loads does not represent a very complex issue. In fact, considering that the construction systems consist of dry assemblies, in which panels and profiles are connected by pinned joints, the structural analysis for vertical loads is the resolution of a statically determined pendular scheme, where the internal forces for each element can be easily obtained by the acting loads.

An interesting feature is the possibility to carry out the structural checks according to two different approaches: “all-steel design” and “sheathing-braced design”. The first approach does not consider the presence of sheathing panels and the generic profile is assumed as isolated (free-standing) neglecting the interaction between the profile itself and the sheathing (see Figure 8.32a). In this case, the load bearing capacity of the member is calculated only considering the end conditions and intermediate restraints, if they are present. Therefore, the buckling length of member is evaluated neglecting the stabilizing effect provided by the sheathing panel. The advantage of this approach is its simply application, even if, in some cases, the provided results could be very conservative.

The latter approach calculates the load bearing capacity of member taking into account the presence of sheathing. In fact, when the sheathing has adequate strength and stiffness and it is effectively connected to steel profiles, the bending resistance (for beams) and the axial resistance (for studs) are increased because of the interaction with sheathing panels. This phenomenon is due to the bracing effect of sheathing on profiles (see Figure 8.32b), that improves mainly the strength against local and distortional buckling modes.

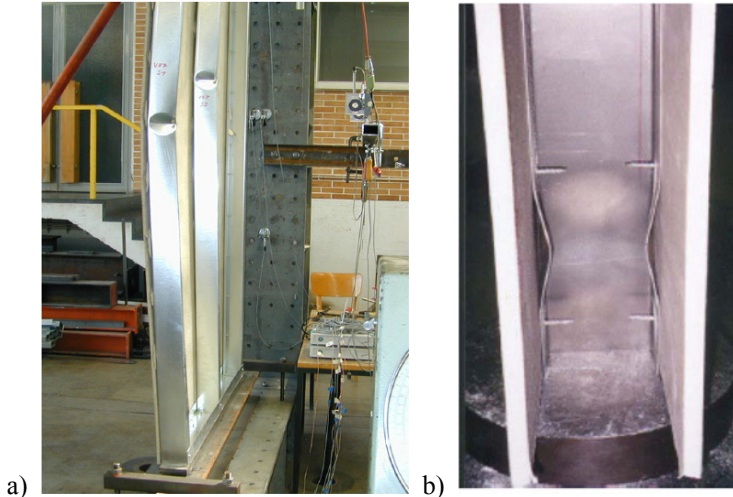


Figure 8.32 – (a) Global buckling of an “isolated” stud (Lange & Naujoksb 2006);
 (b) Local buckling of a sheathed profile (Telue & Mahendran, 2001)

The design under horizontal loads, mainly wind and seismic loads, represents a more delicate issue which represents the object of different studies carried out at University of Naples Federico II (Landolfo *et al*, 2006; 2010; Fiorino *et al*, 2007, 2009, 2011; Iuorio, 2007, 2009) and at the “Politehnica” University of Timisoara (Fülöp & Dubina 2004a,b, 2006). In fact, when the building is subjected to a horizontal load, floors and roofs have to be able to act as a diaphragm and transfer the loads to the walls which, in turn, have to resist to these loads and transfer them to the foundations (see Figure 8.33). Therefore, the global lateral response of the building is strongly connected to the structural behaviour of floors and walls under in-plane actions.

The in-plane resistance of these structures can be achieved either using steel bracing (usually X-bracing) or taking into account the sheathing-to-frame interaction. Therefore, as well as for vertical loads design, also for design under horizontal loads it is possible to identify the “all-steel design” and “sheathing-braced design” approaches.

When the in-plane resistance is assured by X-bracings, steel straps are generally used to obtain the diagonal elements. In floors and roofs, steel straps are connected to the bottom flanges of joists while, in walls they are connected to the external faces of studs (see Figure 8.34). In particular, the

flat straps used for bracings are made with hot coated steel sheet as well as those used to form the other members.

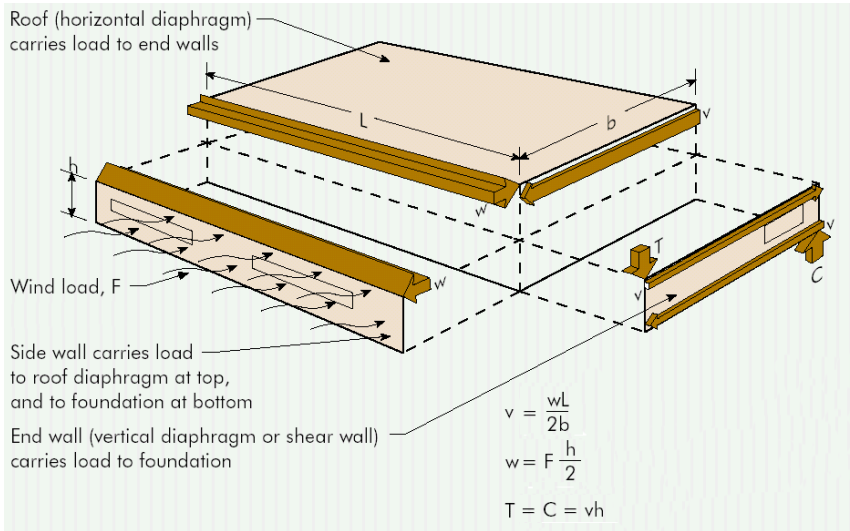


Figure 8.33 – Load pattern for horizontal loads (wind loads)

As an alternative to resist to horizontal loads, the effects of sheathing-to-frame interaction can be taken into account. On contrary, for the case of vertical loads, in which the presence of sheathings gives only a secondary stabilizing effect, in this case the interaction of steel framing, sheathing and their connections represents the real lateral resisting system. When this approach is used, floor and walls can be considered as diaphragms and the structural response depends on their elements and relevant connections (see Figure 8.35).

591

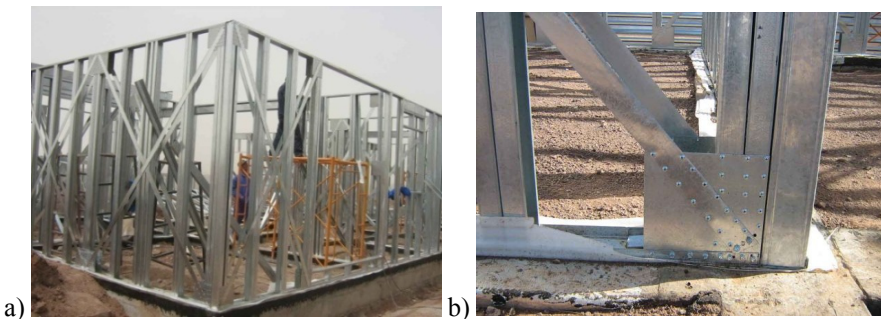


Figure 8.34 – a) Wall lateral bracing with steel straps (X-bracings); b) Detail of the connection between diagonal strap and steel framing

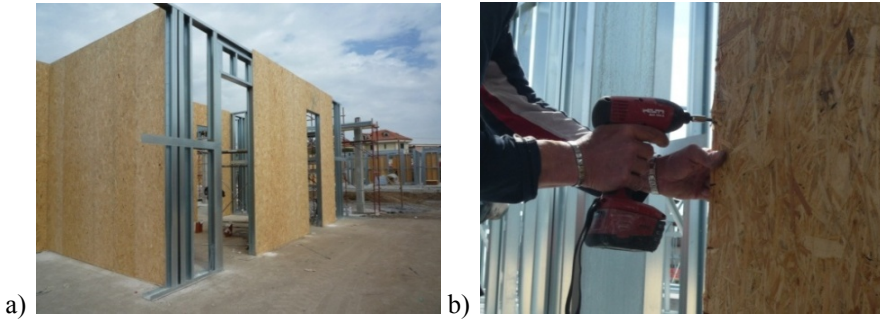


Figure 8.35 – (a) Wall lateral bracing given by sheathing-to-frame interaction;
(b) Application of the sheathing panel to the steel framing

When the load bearing capacity for both vertical and horizontal loads is evaluated taking into account the sheathing-to-frame interaction, in terms of structural performance, the advantages of using cold-formed steel profiles are clearly maximized. Indeed, in this case it is possible to assure an elastic behaviour of structure also under design earthquake of high intensity.

The typical features of cold-formed steel structures involved the development of specific codes for design under horizontal loads, such as “North American Standard for Cold-Formed Steel Framing – Lateral Design” (AISI S213-07/S1-099). In addition, in order to simplify the design procedure of this structural typology, several specific design manuals have been published such as “Prescriptive Method For Residential Cold-Formed” (NASFA, 2000) and “Workpack design for Steel House” (LSK, 2008).

8.6.2 Design under vertical loads

The design under vertical loads mainly consists in the selection of the load bearing elements of floors and walls. The structural design of cold-formed profiles generally regards C-, Z- and U cross-sections, in which the behaviour is generally governed by buckling phenomena, simple (local and distortional) and/or coupled with global modes (see Chapter 3: Behaviour and resistance of cross-section).

In the following Sections the main checks, according to Eurocode 3 – Part 1.3, for steel profiles of floors and walls are shown.

8.6.2.1 Design of floors

The main load bearing elements for floors are the joists, which have a structural scheme of simple supported beam under uniform load (see Figure 8.36).



Figure 8.36 – Structural elements for floors

At ultimate limit states, the structural design of joists consists in checking the resistance of the cross-section (bending, shear, and local transverse force) and instability of the member (lateral-torsional buckling), while, at serviceability limit states, the control of deflections and vibrations has to be carried out.

The bending resistance ($M_{c,Rd}$) at midspan cross-section of joists, which is the most stressed one in bending, can be determined by eqns. (3.83) in §§3.8.4 (see Flowchart 3.6), while for the check against the shear force acting at joist support the shear resistance ($V_{b,Rd}$) can be calculated considering only the web contribution and it can be evaluated through eqn. (3.91) in §§3.8.5 (see Flowchart 3.7). In addition, always at joist support, the resistance against the local transverse forces has to be checked according to eqn. (3.117) in §§3.8.7.1 (see Flowchart 3.6). This check can be neglected if specific reinforcing profiles, called “web stiffeners”, are attached to the web at joist ends (see Figure 8.37). Example 3.5 from Chapter 3 presents the design of a cold-formed steel member in bending.



Figure 8.37 – “Web stiffener” profile

The determination of the resisting moment against the lateral-torsional buckling can be carried out by applying the eqn. (4.56) in §§4.3.2.1 (see Flowcharts 4.3 and 4.4). Example 4.3 presents the design of a laterally unrestrained cold-formed steel beam in bending at the Ultimate Limit State. It has to be noticed that this check is strongly influenced by the arrangement of torsional restraints. In particular, at joist ends torsional restraints are represented by the “web stiffeners”, while, along the joists, the torsional restraints can be obtained by connecting a steel flat strap to the bottom flange of all joists and fixing at least one field between two joists by means of a profile called “blocking” (see Figure 8.38).



Figure 8.38 – Intermediate torsional restraints system for floors

At serviceability limit states, the calculation of maximum deflection needs to take into account the effects of local buckling. In fact, local buckling can influence the behaviour at serviceability limit states because in profiles with slender sections it can occur before to reach the maximum elastic stress. The effects of local buckling consist of a reduction of section

inertia, which depends on stress magnitude. Therefore, deflections can be calculated considering an effective second moment of area, which can be taken variable or uniform along the span or, alternatively, an uniform value based on the maximum acting bending moment can be assumed. The effective second moment of area at serviceability limit state can be calculated by eqn. (4.103) in §§4.6 (see Flowchart 4.8). Example 4.6 from Chapter 4 presents the serviceability limit state check of a cold-formed steel member in bending.

8.6.2.2 Design of walls

Load bearing walls can have many structural functions. Their primary function is to carry vertical load from the floors and roof and transmit them to foundations. In this case, the structural scheme consists in a pinned column subjected only to axial compression coming from the wall weight and the loads transmitted by the above structures (walls and floors). When walls have also a bracing function, they have also to resist in-plane to lateral loads, due to wind or earthquake, which have to be transmitted to foundations. In case of external walls, they also have to resist the lateral pressure action of the wind and transmit it to the floor and roof diaphragms. This action is usually schematized as an uniform load acting on the stud in the direction perpendicular to wall plane (see Figure 8.39).

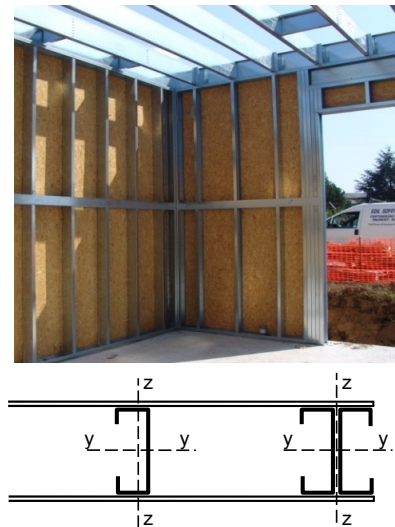


Figure 8.39 – Structural elements for walls (studs)

In general a C-section stud of an external wall is subjected to combined compression load and bending moments about the y - y and z - z axes. In fact, besides the bending moment about the direction perpendicular to the wall induced by wind loads ($M_{y,Ed}$), a bending moment about the wall plane due to the shift between the centroid of effective cross-section and that of gross cross-section ($\Delta M_{z,Ed}$) has to be considered in calculations (see Figure 3.43 in §§3.8.3). Therefore, at ultimate limit state the resistance of cross-section, which takes into account also the effects of local and distortional buckling, and the global buckling resistance under compression and bending moments have to be calculated.

The resistance of cross-section should be determined by eqns. (3.128) in §§3.8.9 (see Flowchart 3.9 and Example 3.6), while buckling resistance should be calculated through eqn. (4.61) in §§4.4.2 (see Flowcharts 4.5 and 4.6 and Example 4.4). In this case, the terms $M_{z,Ed}$ (due to the absence of in plane bending moment) and $\Delta M_{z,Ed}$ (due to the symmetry of section respect to the y - y axis) are equal to 0.

The buckling resistance is strongly influenced by buckling length. When studs have not torsional restraints, the buckling length for both in-plane and out of plane direction is equal to the length of profile. The sections typically used for walls are characterized by a small inertia in the wall plane and, in order to improve the behaviour of studs in this direction, studs can be restrained with a system similar to those used for floors. In particular, steel flat straps are lengthwise attached to stud flanges at mid-height of the wall. Also in this case, at least one field between two studs has to be fixed by a “blocking” profile (see Figure 8.40). This system allows to obtain a buckling length of studs equal to half wall height.



Figure 8.40 – Intermediate torsional restraints system for walls

At the ends of walls the studs are made with “back-to-back” coupled C-sections. In this case, due to double symmetry of section, the centroid of effective cross-section corresponds to that of gross cross-section. Therefore, a stud of an external wall is subjected to axial compression and bending moment perpendicular to the wall.

In case of internal walls, the bending moment due to wind is not present ($M_{y,Ed} = 0$) and C-section studs are subjected to compression and bending moment about the wall plane ($\Delta M_{z,Ed} \neq 0$), while “back-to-back” coupled studs, having doubly symmetric section, studs are subjected to uniform compression ($\Delta M_{z,Ed} = 0$ and $M_{y,Ed} = 0$).

8.6.2.3 Sheathing-braced design for vertical loads

As mentioned before, when bidimensional elements, such as panels and sheets, are connected to steel profiles of floors (joists) and walls (studs), the structural performance is improved because the influence of buckling modes is mitigated by constraining effect given by the sheathing.

In floors, depending on the arrangement of bidimensional element, the direction of loads and the structural scheme, the sheathing can restrain the steel profile on the flange in compression or in tension. In the first configuration (see Figure 8.41a), the stabilizing effect is the highest and it completely opposes to lateral-torsional buckling. In the latter configuration (see Figure 8.41b), the effect of sheathing is lower but, in any way, the load bearing capacity is increased by the torsional restraint provided by the sheathing-to-frame connections.

The evaluation of stabilizing effects needs specific design procedures because they depends on several factors such as shape and thickness of profile, flexural stiffness of sheathing, stiffness of sheathing-to-frame connections. Section 4.5 of this book provides information about beams restrained by sheathing.



a) Sheathing on flange in compression b) Sheathing on flange in tension
Figure 8.41 – Stabilizing effect of sheathing on C-profile under bending

For design of walls, a remarkable reference is represented by the “North American Standard for Cold-Formed Steel Framing – Wall Stud Design” (AISI S211-07), which provides a design methodology mainly based on the interpretation of the result of researches carried out in the United States (Miller, 1989; Lee, 1995). This methodology can be used only for design of walls sheathed on both sides with the same sheathing type.

The design approach takes into account the stabilizing effect given by sheathing reducing the buckling length only for global buckling in the wall plane. Therefore, for flexural buckling out of wall plane, the buckling length is considered conservatively equal to the stud length and the presence of sheathing is completely neglected whereas, for in-plane flexural and torsional buckling, the buckling length is assumed as two times the spacing of sheathing to stud connection. This assumption is based on the conservative hypothesis that every two connections one is ineffective (see Figure 8.42). In addition, in order to avoid the failure of connections, the maximum value of axial resistance is limited depending on the sheathing type and the spacing of connections.

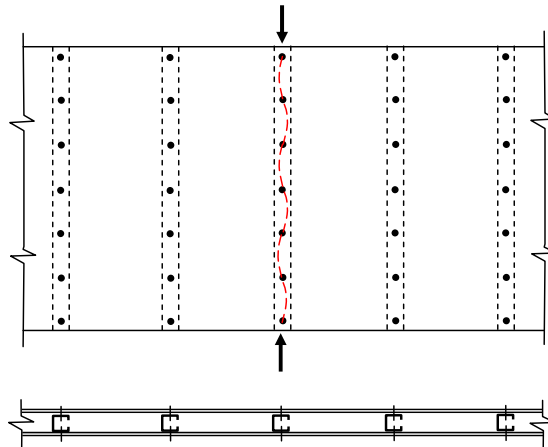


Figure 8.42 – In-plane buckling deformed shape of a stud in case of fully effective connections (AISI S211-07)

8.6.3 Design under horizontal loads

As observed above, the structural performance of cold-formed steel systems can be evaluated considering or not the favourable effect given by

sheathing. Hereafter the main steps to calculate displacements and strength according the two methodologies are shown. In particular, even if the explanation is mainly focused on the behaviour of vertical walls subjected to in-plane lateral loads, these methodologies can be applied also to evaluate to response of floor decks subjected to in-plane loads.

8.6.3.1 “All-steel” lateral bracing

If lateral bracing is obtained by only using steel elements and the presence of the sheathing is neglected, then the lateral resisting system consist usually in concentric diagonal X-bracing and the structural behaviour of both floors and walls is similar to that of a steel truss.

For walls, the main structural components are the steel frame composed by studs and tracks, the diagonal bracings, the diagonals-to-frame connections and the connections between steel framings and external structures. In particular, steel straps are used as diagonal bracings and, due to their great slenderness, they are considered active only in tension. Therefore, the lateral load applied on a wall is adsorbed only by the diagonal in tension, which transmits a significant axial compression force to the ends of wall. For this reason, the design of members and connection located at wall ends is very important, especially for end studs, diagonal connections and tension anchors (see Figure 8.43).

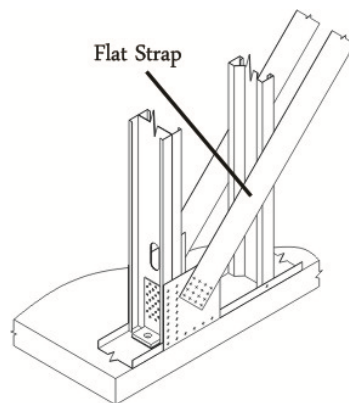


Figure 8.43 – Detail of a corner in “all-steel” walls (Fülöp & Dubina, 2004a)

The lateral displacement at the top of a wall subjected to a horizontal load (H) can be evaluated taking into account the contribution of main

structural components (see Figure 8.44): diagonal in tension (d_d), frame to foundation anchors (d_a) and diagonal to frame connections (d_c). In particular, the lateral wall displacement can be calculated as follows:

$$d = d_a + d_d + d_c \tag{8.1}$$

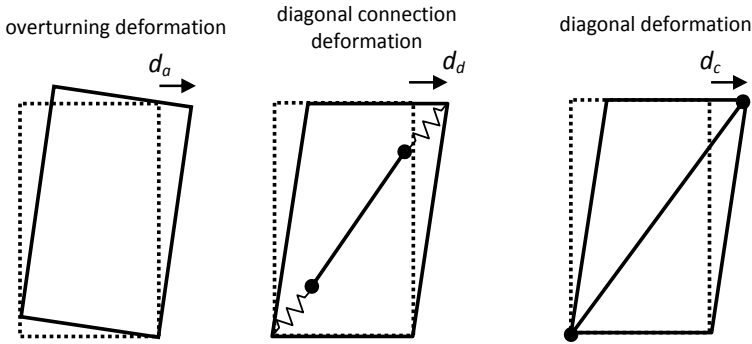


Figure 8.44 – Deformation contributions of an X-braced wall under lateral loads

As well as for the evaluation of displacements, the resistance of a wall subjected to in-plane loads can be evaluated through the strength associated to each wall component. In particular, for each wall component it is possible to individuate one or more failure mechanisms and the smallest associated strength value defines the lateral wall resistance. Therefore, the lateral wall resistance (H_c) is given by:

$$H_c = \min(H_{c,s}; H_{c,t}; H_{c,a}; H_{c,d}; H_{c,c}) \tag{8.2}$$

in which $H_{c,s}$, $H_{c,t}$, $H_{c,a}$, $H_{c,d}$ and $H_{c,c}$ are the strength associated to studs, tracks, frame to foundation anchors, diagonals in tension and diagonal to frame connections, respectively.

In case of wall under seismic actions, the current trends propose to design the resisting systems according to capacity design criteria, which consist in the achievement of the failure mechanism that maximize the wall ductility. In this case, the most ductile mechanism consists in the cross section yielding of diagonal in tension. Therefore, the fracture of net section at fastener holes has to be avoided and the frame, diagonal-to-frame connections and foundation anchors have to assure an appropriate

overstrength:

$$F_{n,Rd} > N_{t,Rd}; H_{c,s} > H_{c,d}; H_{c,a} > H_{c,d}; H_{c,c} > H_{c,d} \Rightarrow H_c = H_{c,d} \quad (8.3)$$

In order to satisfy these requirements, different technical solutions are used. In facts, the buckling failure of end studs can be avoided using C-profiles coupled “back-to-back”, which are more resistant than a single profile. In addition, in order to avoid strong deformation in bottom tracks and to transfer directly tension forces to foundations, special anchor devices, as known as “hold-down connectors”, are used (see Figure 8.45).

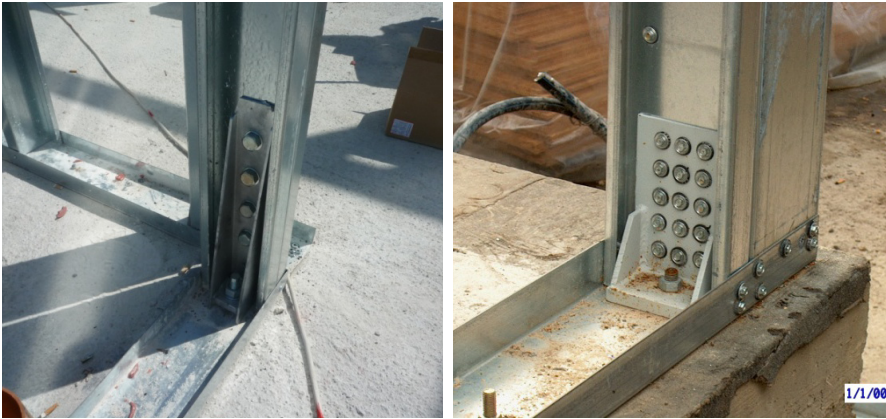


Figure 8.45 – Hold-down device

8.6.3.2 Structural behaviour of sheathed diaphragm

When the design is carried out according to “sheathing-braced” methodology, floor decks and walls act as diaphragm. In particular, floors can be considered as simple supported horizontal diaphragms subjected to a uniform load, while walls are cantilever vertical diaphragms subjected to uniform horizontal force acting on top edge (see Figure 8.46). The structural behaviour of diaphragm can be assumed as that of an I-beam, in which sheathing panels are the web and the chord profiles are the flanges. In particular, sheathing panels adsorb the shear actions, while the compression and tension axial load due to the bending are resisted by chord profiles.

Therefore, it is possible to individuate two main components: web panels and chords profiles. Both components are obtained as assembly of different elements. In facts, the sheathing system consists of several panels

connected each other and chord members can be obtained by coupling two profiles.

In addition, the connections between panels and chord profiles influence strongly the diaphragm behaviour and, then, the evaluation of their structural response represents an important step of the design procedure.

As mentioned before, with particular regards to walls, it is possible to individuate the main structural components such as steel frame, sheathing panels, sheathing-to-frame connections and connections between steel frame and external structures (see Figure 8.47). It is clear that the global structural response of the diaphragm (wall or floor) depends basically on the local structural response of its components.

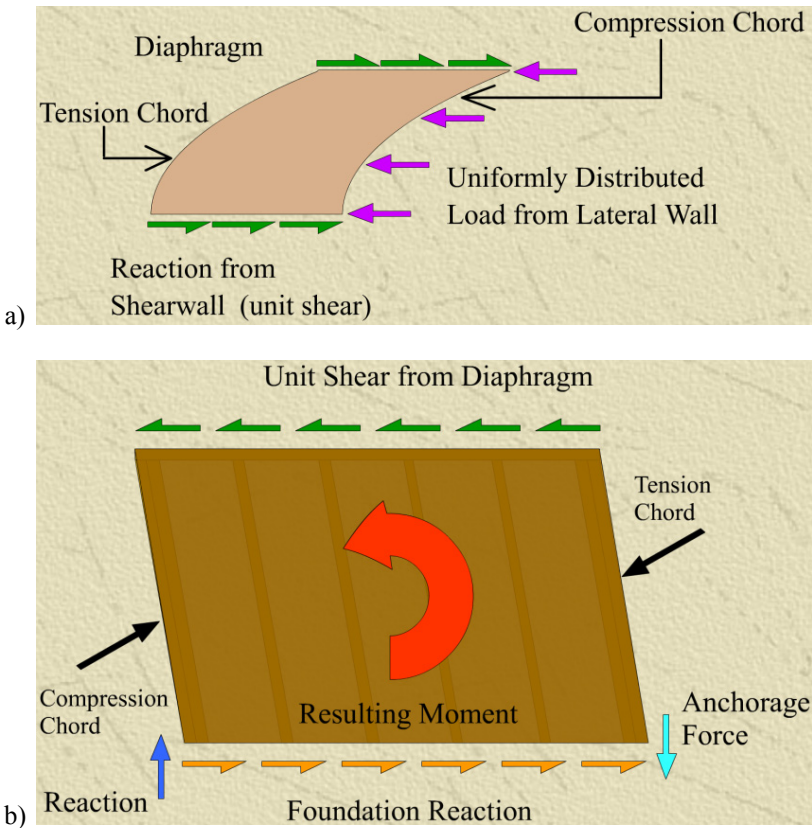


Figure 8.46 – Structural scheme of floor a) and walls b) diaphragms (<http://timber.ce.wsu.edu/Supplements/ShearWall/Loadpath.htm>)

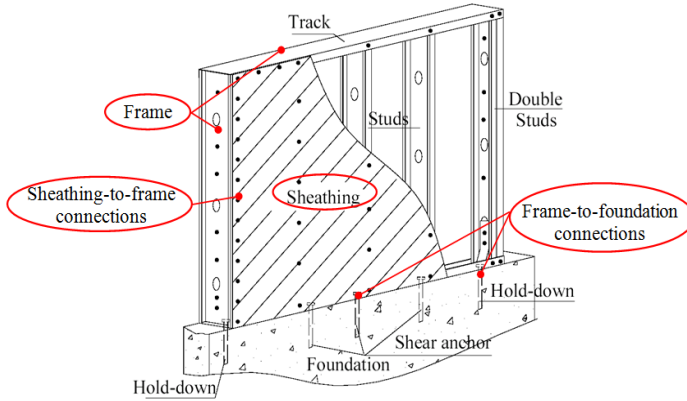


Figure 8.47 – Main wall structural components

As well as for “all-steel” design, the evaluation of lateral displacement at top wall under horizontal loads can be obtained by adding in series the deformation contribution of each structural component (see Figure 8.48) as follows:

$$d = d_s + d_a + d_p + d_f \tag{8.4}$$

in which d_s , d_a , d_p and d_f are the deformation contribution of steel frame, frame-to-foundation anchors, sheathing panels and sheathing-to-frame connections, respectively.

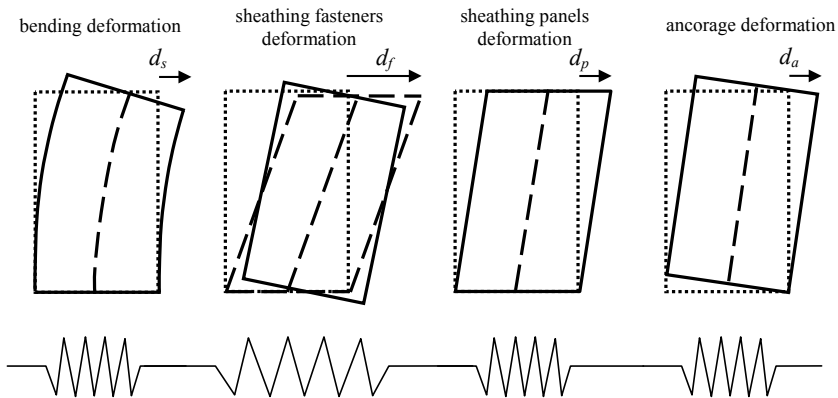


Figure 8.48 – Deformation contributions of a sheathed wall under lateral loads

If the local behaviour of sheathing to frame connections governs the global lateral response of walls, as it generally happens, the relevant

deformation produces wall lateral displacement greater than those produced by other components (see Figure 8.48):

$$d_s \ll d_f; \quad d_a \ll d_f; \quad d_p \ll d_f \quad (8.5)$$

The contribution d_s , d_a and d_p are linear functions of external lateral load (H) and they can be simply evaluated applying well known formulations.

Also the evaluation of wall lateral strength can be carried out in similar way to the case of the “all-steel” approach. Therefore, it can be obtained by the wall lateral strength associated to the failure of chords studs, frame-to-foundation anchors, panels and sheathing-to-frame connections as follows:

$$H_c = \min(H_{c,s}; H_{c,a}; H_{c,p}; H_{c,f}) \quad (8.6)$$



Figure 8.49 – Global collapse mechanism of a wall due to failure of sheathing to frame connections

Generally, the failure mechanism of sheathing to frame connections is the most ductile and, in order to follow the capacity design criteria, panels, anchors and steel framing have to be oversized (see Figure 8.50):

$$H_{c,s} > H_{c,f}; H_{c,a} > H_{c,f}; H_{c,p} > H_{c,f} \Rightarrow H_c = H_{c,f} \quad (8.7)$$

The solutions used to avoid the failure of chord studs in compression and anchors are the same used for “all-steel” walls, while the failure of sheathing panels can be avoided using panels with adequate mechanics properties and thickness (at least 9 mm thick wood-based panels and gypsum boards).

Beside the theoretical methodologies, the lateral wall resistance can be evaluated by means of an experimental approach, based on a large number of tests results carried out on full scale specimens having different configuration (see Figure 8.51). This approach consists in “design tables”, provided by codes that can be used only for walls consistent with fixed limitation depending on the reference experimental results (AISI S213-07).

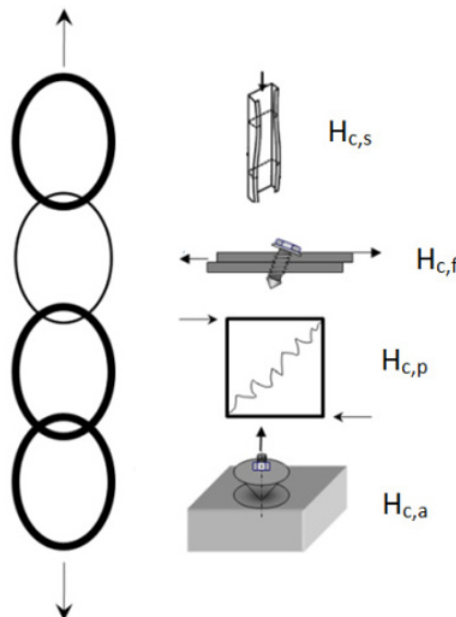


Figure 8.50 – Possible failure mechanism and capacity design criteria



Figure 8.51 – Typical shear tests of a wall (Fülöp & Dubina, 2004a)

8.6.4 Specific design manuals

606

The peculiarity of design and execution of cold-formed steel housing induced the demand of specific design manuals. In this direction, the North America Steel Framing Alliance published the “Prescriptive Method For Residential Cold-Formed Steel Framing” (NASFA, 2000), which provides tables for design of structural elements and a large number of construction details. In Europe, a similar work has been developed by Arcelor Research Liege and Bureau Greisch, which published the “Workpack design for Steel House” (LSK, 2008). This is a manual which provides general design specifications, an on-line design tool and a library of construction details.

8.6.4.1 Prescriptive method for residential cold-formed steel framing

The “Prescriptive Method For Residential Cold-Formed Steel Framing” (NASFA, 2000), developed by the North America Steel Framing Alliance, provides the guidelines for the design of little and middle

dwelling using cold-formed steel framings. The specifications given by the “Prescriptive Method” are given by means of tables, figures and information about design and execution.

These guidelines are valid for buildings consistent with fixed limitations: not more than two stories, maximum plan dimension 11×18 m, maximum wall height 3 m; maximum roof slope in the range from 20 to 100%, maximum cantilever span 610 mm. The range of validity in terms of acting loads is given in Table 8.2. In terms of materials, steel structural elements have to be obtained by cold forming of structural sheets according to the requirements of ASTM A653, ASTM A792 and ASTM A875.

Table 8.2 – Prescriptive Method for Residential Cold-Formed Steel Framing Range of validity for loads (NASFA, 2000)

Floor dead load:	0.48 kN/m ² (except roofs)
Roof dead load:	0.72 kN/m ²
Wall dead load:	0.48 kN/m ²
Design wind speed:	49 m/s
Wind exposure:	A/B (suburban and wooded) C (open terrain)
Ground snow load:	3.35 kN/m ²
Floor live load (First floor):	1.92 kN/m ²
Floor live load (Second floor):	1.44 kN/m ²
Roof live load:	3.35 kN/m ²

The “Prescriptive Method for Residential Cold-Formed Steel Framing” individuates and classifies the main sub-structures of building such as foundations, roofs, structural and non-structural walls and roofs. For each sub-structure, the manual provides comprehensive information for main elements, bracing and joining systems. All the information is enhanced with figures that show the different structures and the relevant construction details. Moreover, the manual gives several tables for sizing the main elements such as joists, studs, headers and connections. In addition, the manual provides information about plants installation, acoustic and thermal insulation and protection against corrosion and fire.

8.6.4.2 Workpack design for Steel House

The “Workpack design for steel house” (LSK, 2008) offers several “easy-to-use” tools for the design of low-rise dwellings. In particular, the workpack provides a manual containing design specification for building

with information about finishing, architectural details, thermal and acoustic insulation, a list of construction details and an on-line software for design according to EN1993-1-3 (Pastor & Etzenbach, 2008). The workpack has been developed for two stories dwellings with and without attic. The structure has to be designed using cold-formed steel members made with S350GD+Z coated steel grade, while self-drilling screw and bolts are used for connections.

The software allows to design the different building parts such as roof, floors and walls. The user enters the input parameters relating to geometry and loads of the element selected for design. Then the software gives the adequate profile section according to checks given in EN1993-1-3 (CEN, 2006a) and the reaction forces to be used for design of other elements. The software gives also the drawings of construction details.

8.7 CASE STUDY: RESIDENTIAL BUILDING

The planning stage is the ideal time to consider aspects such as health and safety as well as cost and appearance. In this section, the design of a one family house is developed. When designing cold-formed steel building structures, the designer has to manage four peculiar structural problems which characterize the behaviour and performance of thin-walled sections. These peculiarities have been summarized in the previous chapters and refer mainly to: stability and local strength of sections; connecting technology and related design procedures; reduced ductility and fire resistance. Chapters 3, 4 and 7 have been specifically devoted to the first two types of problems, while only a general overview is provided for the last two points.

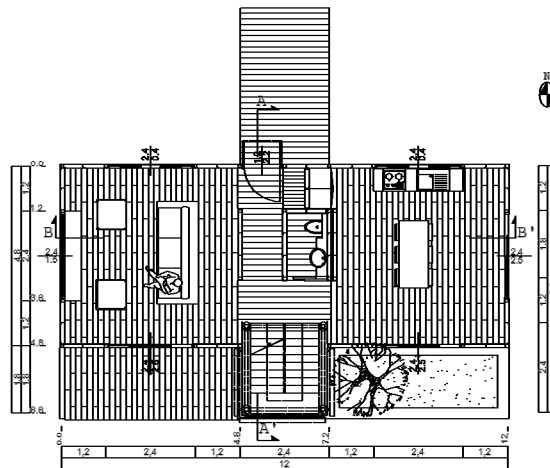
Hereafter, the design of a residential building is carried out considering architectural, technological and structural issues.

8.7.1 Architectural design

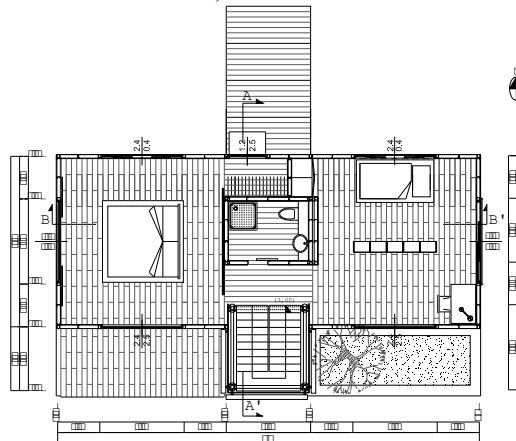
The architecture aims to be a prototype of a contemporary housing in which flexibility, environmental comfort and high structural performance are the keywords (Iuorio, 2009).

The dwelling develops in two floors and is organized in wide and regular spaces where the walls are concentrated along the perimeter and in

the centre of house, in order to ensure the maximum flexibility of the internal spaces (see Figure 8.52). A continuous space on two levels is articulated perpendicularly to the entrance axis, where closed toilet blocks and a small glazed stair tower are located. The common living and dining rooms are located at the ground floor of 60 m² that extends into 17 m² of external space, consisting of a small garden and a terrace (see Figure 8.52a). The bedrooms are on the first floor (see Figure 8.52b). Each room is wide and square, and according to Mies Van Der Rohe lesson “the less is more”, the furnishing is minimal. The result is a rectangular shaped house with a flat roof.



a) Ground floor



b) First floor

Figure 8.52 – Case study: plan views

8. BUILDING FRAMING

The opening distribution follows environmental requirements, introducing narrow openings on the northern front and wide and adequately shielded openings on the South and South-West elevations (see Figure 8.53 and Figure 8.54). Moreover, the particular opening locations in the fronts have been chosen so that the inhabitants can view the outer environment, and the inside life can be perceived from the outside.

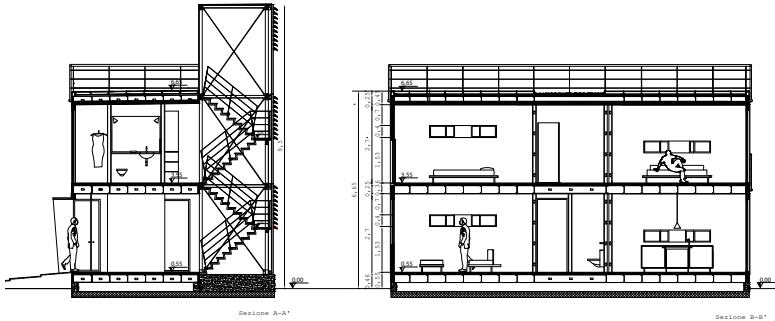


Figure 8.53 – Sections

In order to develop a holistic design, and in agreement with the Flowchart 8.1, material and components have been defined in order to provide adequate soundproofing, and heat and fire resistance consistent with a sustainable design.

610

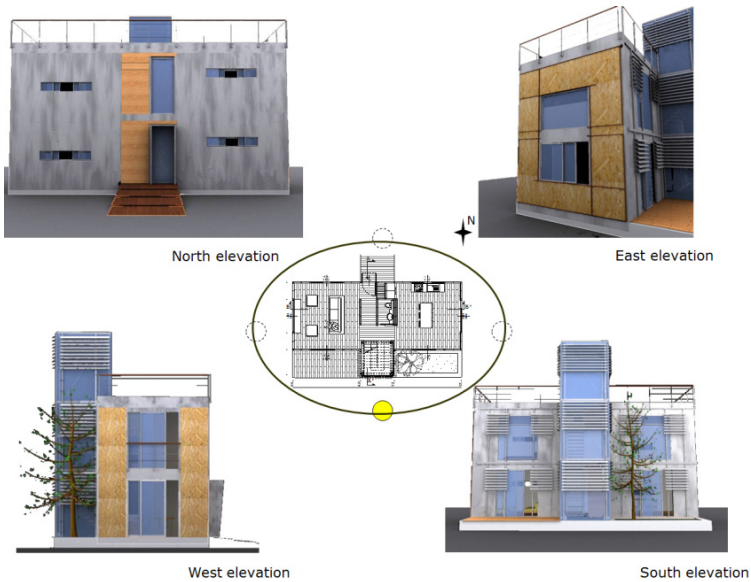


Figure 8.54 – Case study: opening distribution

The stair tower has been designed separately. It has an independent structure consisting of four CFS circular hollow section columns, connected at each storey by light gauge beams to which the glazed panels are fixed (see Figure 8.55). The steps are made by CFS beams on which wood panels are screwed. X bracings stiffen the vertical structure.

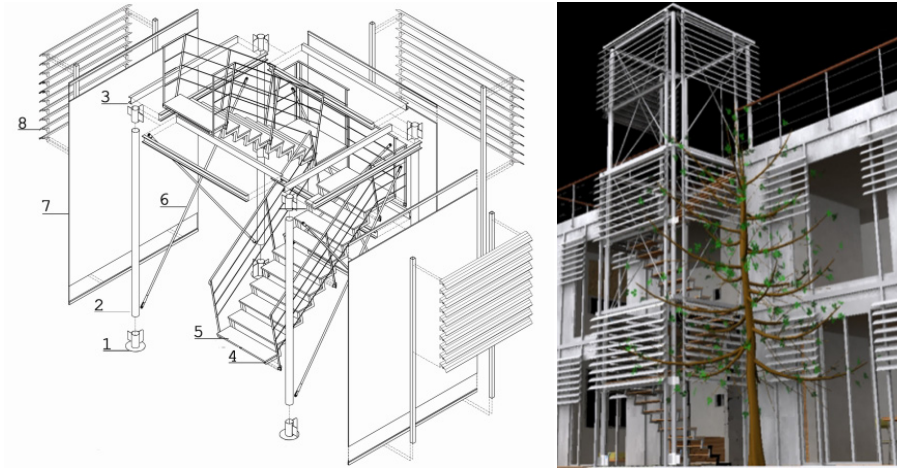


Figure 8.55 – Case study: stair tower

8.7.2 Conceptual Design

The construction is an interesting example of stick built construction. The structure is supported on a concrete slab, to which the steel frame is anchored by clip angles and post installed anchors. A 30 cm high air room is introduced between foundation and the above structure, in order to protect the ground floor from the moisture and reduce corrosion risks. The basic framing system has been designed as a platform system; hence, the system is characterized by discontinued walls, interrupted at each floor level by floor framing. A general description of the components and materials of the two main subsystems (floor and walls, see Figure 8.56) are specified in the following clauses. Table 8.3 summarizes the principal dimensions of the building.

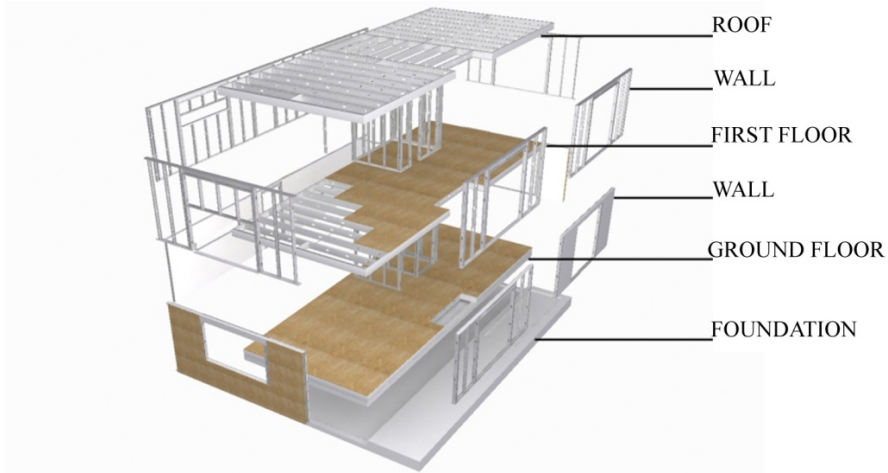


Figure 8.56 – Case study: subsystems

Table 8.3 – Principal physical characteristics

Building width	4.8 m
Building length	1.2 m
Wall height	2.7 m
Wall stud spacing	0.6 m
Floor joist spacing	0.6 m
Roof slope	Flat

8.7.2.1 Floor assembly

The floor framing is composed of joists spaced at 600 mm and aligned with vertical load bearing framing members. Joists are connected at each end by a floor track. Web stiffeners are installed at the end of bearing location of each joist to strengthen the member against web crippling and to ensure the continuity of vertical load bearing members (see Figure 8.57). Floor blockings are placed between the end joists. Flat straps (40 mm wide and 1 mm thick) run perpendicular to joists and connect blockings and joists together. The floor works as a diaphragm where the sheathing panels, realized with oriented strand board panels, constitute the horizontal bracing system.

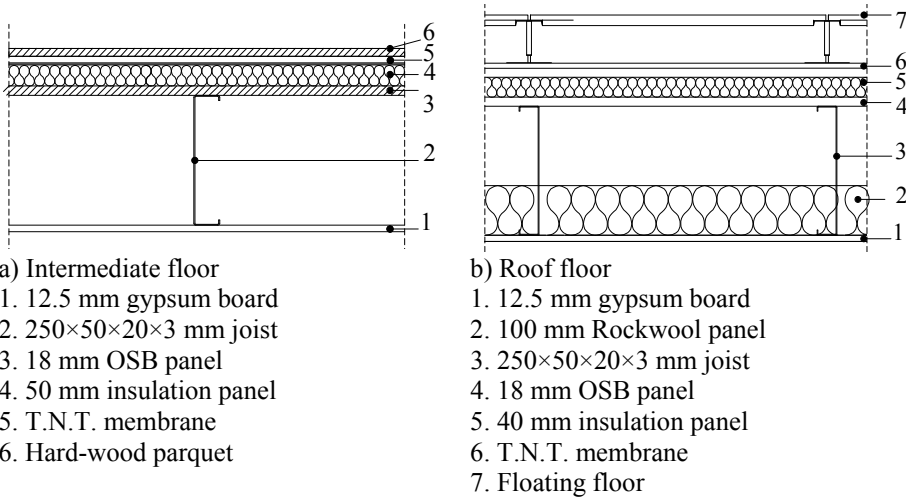


Figure 8.58 – Floor sections

8.7.2.2 Wall assembly

Walls of 2700 mm height are framed with studs realized with 100×50×20×1 mm lipped channel sections, spaced at 600 mm on centre. Each end of the studs is fastened to 100×40×1 mm wall track (see Figure 8.59). No blocking or cross bracing system is introduced in the wall framing.

In order to withstand horizontal action and to provide stiffness and strength, 9.0 mm thick Type 3 OSB (CEN, 1997) external panels and 12.5 mm thick standard GWB (ISO6308, 1980) internal panels have been adopted as bracing system.

At the end of each wall resistant segment S/HD10B metal-to-metal connectors by Simpson Strong-Tie Company (2007) and HIT-RE 500 with HIS-N 8.8 adhesive-bonded anchors by Hilti (2005) have been introduced as hold-down devices. HST M8 mechanical anchors by Hilti (2005) are used as shear anchors.

The wall thickness is 175 mm and consists of the following layers, from the interior to the exterior: 2 layers of 12.5 mm thick gypsum panels, 100×50×20×1 mm lipped channel section (stud), 100 mm thick rigid insulation panel, 9 mm thick oriented strand board panel, 40 mm of external thermal insulation and external finishing.

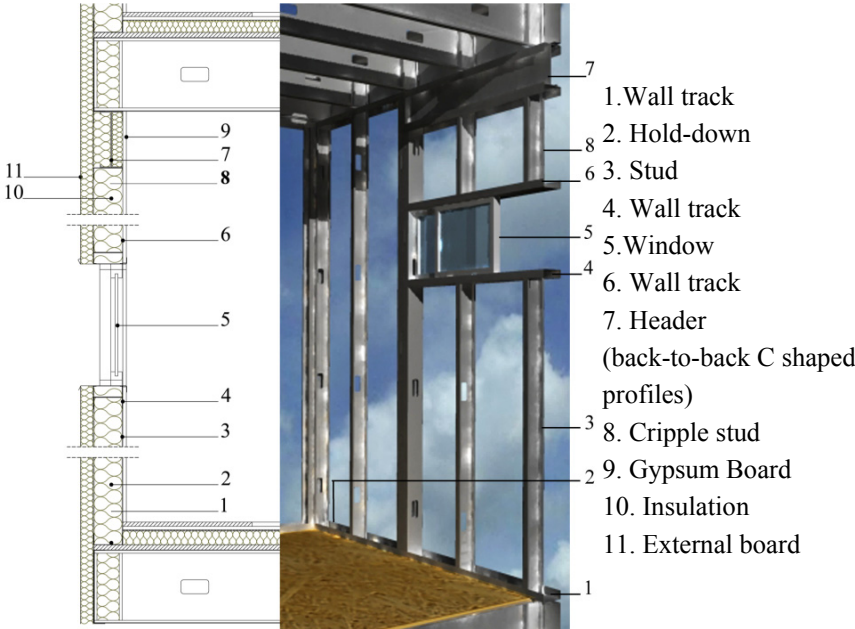
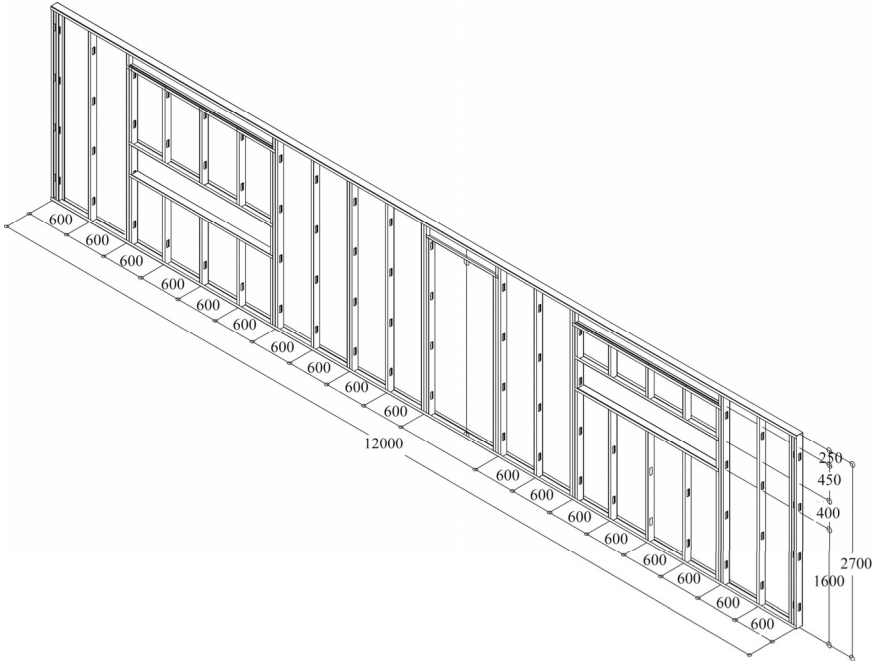


Figure 8.59 – Case study: wall section and perspective of structural components

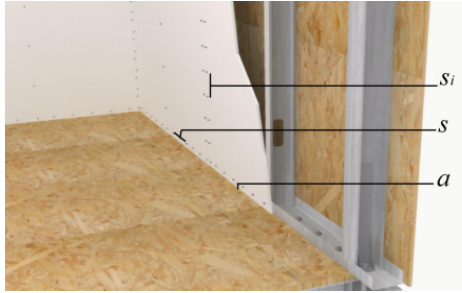


Figure 8.60 – Case study: sheathing-to-frame screw spacing

Particular care has been given to the design of openings (see Figure 8.61). In general, the studs placed at both ends of an opening are coupled with one or more King studs, i.e. vertical structural members which span the full height of the wall providing bearing for headers and with one or more Jack studs, vertical members which do not span the full height of the wall. Headers are installed above wall openings in all exterior and interior load-bearing walls, while they are not required in the interior non-load bearing walls. In this project, all openings have been realized with two King and one Jack stud per opening edge (both have the same stud section: 100×50×20×1 mm) and back-to-back headers (250×50×20×2 mm). Moreover, cripple studs are introduced to provide a backing to attach sheathing and finishing.

In conclusion, Table 8.4 summarizes the dimensions of the main structural components.

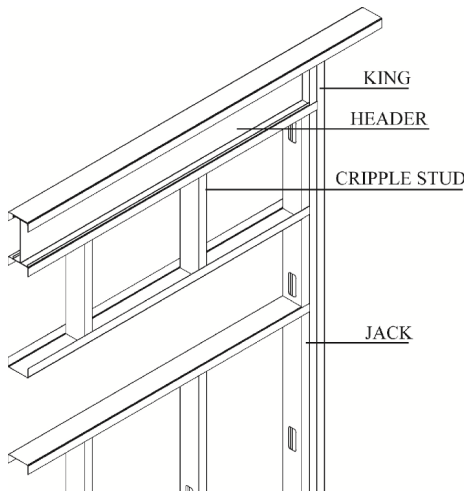


Figure 8.61 – Window design

Table 8.4 – Dimensions of the main structural components

Member	(web depth × flange width × lip depth × thickness) (mm)
Joist	250×50×20×3.0
Wall stud	100×50×20×1.0
Headers	250×50×20×2.0

8.7.3 Structural design

The building is assumed to be located in Southern Italy, which is a territory of moderate wind and snow. Earthquake loading has not been considered. The structure is designed only under vertical loads and the wind is considered only as local action on the walls. Joists and studs are checked taking into account the all-steel methodology in agreement with Section 8.6.2. The loading conditions and structural conception together with the sizes of the main structural components and specific details are presented hereafter.

8.7.3.1 Reference codes

Eurocode 0 (EN1990, 2002) and the set of EN 1991, *Eurocode 1* are used to define the loads and combination of loads (see also Chapter 2 of the book). Verifications of steel members and connections at the Ultimate and Serviceability Limit States (ULS and SLS, respectively) are undertaken according to EN1993-1-1 (CEN, 2005a), EN1993-1-3 (CEN, 2006a) and EN1993-1-5 (CEN, 2006b) and according to Chapters 3, 4 and 7 of the book, which also contain flowcharts and numerical examples.

8.7.3.2 Loads

Dead loads

Tables 8.5 to 8.7 summarize the respective weights of the structural and non-structural components of the house.

8. BUILDING FRAMING

Table 8.5 – Dead loads for roof floor

Typology	Floor	Description	Load (kN/m ²)
Structural elements	Sheathing	18 mm OSB panel	0.12
	Steel members	Light gauge steel	0.15
Non-structural elements	Floating floor	Wooden floor	0.25
	Insulation	Rock wool (100+40mm)	0.12
	Ceiling	12.5 mm Gypsum panel	0.10
Total load			0.74

Table 8.6 – Dead loads for external walls

Typology	Wall	Description	Load (kN/m ²)
Structural elements	Sheathing	9 mm OSB panel	0.06
	Steel profiles	Light gauge steel	0.11
	Internal board	2×12.5 mm Gypsum panel	0.20
Non-structural elements	Insulation	Rock wool	0.04
	Cladding system	Insulated wall system	0.15
Total load			0.56

Table 8.7 – Dead loads for internal walls

Typology	Wall	Description	Load (kN/m ²)
Structural elements	Steel profiles	Light gauge steel	0.08
	Boards	4×12.5mm Gypsum panel	0.40
Non-structural elements	Insulation	Rock wool	0.04
Total load			0.52

618

Live loads

The live loads have been defined in agreement with EN1991-1-1 (CEN, 2002b). The case study belongs to class A, therefore a Q_k value of 2 kN/m² has been adopted.

Wind loads

In order to evaluate the wind action, the basic wind velocity is assumed equal to $v_b = 27$ m/s, the reference height has been considered equal

to the building height ($z_e = 6.65\text{m}$) and a terrain category III has been assumed. Hence, the wind pressure has been defined consistent with the EN1991-1-4 (CEN, 2005b), as follows:

$$w_e = q_p(z_e) \cdot c_{pe} \quad (8.8)$$

where

$q_p(z_e)$ is the peak velocity pressure at reference height z_e calculated as:

$$q_p(z) = [1 + 7 \cdot I_v(z)] \cdot \frac{1}{2} \cdot \rho \cdot v_m^2(z) = c_e(z) \quad (8.9)$$

the exposure factor $c_e(z)$ has been evaluated as a function of the height using Figure 4.2 of EN 1990 and external pressure coefficients of 0.8 and 0.7 have been considered for walls and roof, respectively.

Therefore, a wind load of 0.51 kN/m^2 has been considered applied on the walls and a load of 0.44 kN/m^2 has been estimated for the floors.

Snow loads

The snow loads have been defined consistent with the EN1991-1-3 (CEN, 2003a), as follows:

$$s = \mu_i \cdot C_e \cdot C_t \cdot s_k \quad (8.10)$$

where

- μ_i is the snow load shape coefficient
- s_k is the characteristic value of snow load on the ground
- C_e is the exposure coefficient ($C_e = 1$ for normal topography)
- C_t is the thermal coefficient ($C_t = 1$).

A snow load of 1.60 kN/m^2 has been considered.

Table 8.8 summarizes all the defined variable loads for both the roof and the floors.

Table 8.8 – Variable Loads

Actions	Load (kN/m^2)
Live (Q)	2.00
Wind (Q_w)	Wall Roof
	0.51 0.44
Snow (Q_s)	1.60

Combination of actions

The loads are combined at the Ultimate Limit States as follow (§§2.3.1, eqn. (2.2), Flowchart 2.1):

$$\sum_{j \geq 1} \gamma_{G,i} G_{k,j} + \gamma_{Q,i} Q_{k,i} + \sum_{i > 1} \gamma_{Q,i} \psi_{0,i} Q_{k,i} \tag{8.11}$$

and at the Serviceability Limit States in agreement with the characteristic combination (§§2.3.1, eqn. (2.5), Flowchart 2.1), as:

$$\sum_{j \geq 1} G_{k,j} + Q_{k,i} + \sum_{i > 1} \psi_{0,i} Q_{k,i} \tag{8.12}$$

The partial safety factors for the Ultimate Limit State for actions on building structures are given in Table 2.3, i.e. $\gamma_G = 1.35$ for permanent loads and $\gamma_Q = 1.50$ for variable loads. The recommended values of ψ factors for the more common actions may be obtained from Table 2.4, and are summarised in Table 8.9.

Table 8.9 – ψ factors according to EN 1990

Actions	ψ_0	ψ_1	ψ_2
Category A: domestic, residential areas	0.7	0.5	0.3
Snow loads on building For sites located at altitude $H \leq 1000$ m	0.5	0.2	0
Wind loads on building	0.6	0.2	0

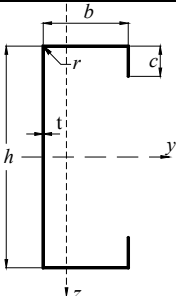
8.7.4 Design checking

In the following, a joist belonging to the roof floor and a stud of an external wall of the first floor are verified at the Ultimate Limit State and the joist deflection is checked at the Serviceability Limit States.

8.7.4.1 Joist

Main structural components of a floor framing are the joists. Hereafter a joist of the roof floor (Fig. 8.58a) is checked. Table 8.10 summarizes the geometry and the material properties of the structural member.

Table 8.10 – Joist geometry and material properties

Component	Material Properties
	<p>Geometry</p> <p> $h = 250 \text{ mm}$ $b = 50 \text{ mm}$ $c = 20 \text{ mm}$ $t_n = 3 \text{ mm}$ $t = 2.96 \text{ mm}$ $r = 3 \text{ mm}$ $L = 4800 \text{ mm}$ </p> <p> $E = 210000 \text{ N/mm}^2$ $f_{y,k} = 350 \text{ N/mm}^2$ $f_u = 420 \text{ N/mm}^2$ $\nu = 0.3$ which corresponds to S350GD+Z </p>

The joists have a span of 4.8 m and the lateral torsional restrains (flat straps and floor blocking) are located every 2.4 m. The loads applied on the roof and uniformly distributed on the joists are defined as follows:

- permanent actions: $q_G = 0.74 \cdot 0.6 = 0.44 \text{ kN/m}$
- live loads: $q_Q = 2 \cdot 0.6 = 1.2 \text{ kN/m}$
- snow load: $q_S = 1.6 \cdot 0.6 = 0.96 \text{ kN/m}$

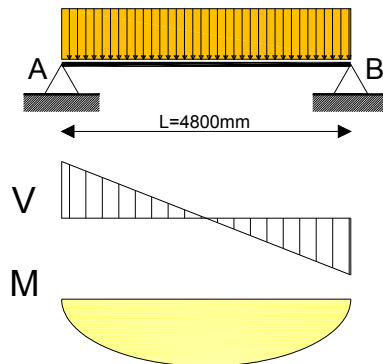


Figure 8.62 – Joist geometry and loading model

As load combination at ULS has been considered only the one that produces the most unfavourable effect which corresponds to the following:

$$q_{Ed} = \gamma_G \cdot q_G + \gamma_Q \cdot q_S + \gamma_Q \cdot \psi_{0Q} \cdot q_Q$$

$$q_{Ed} = 1.35 \cdot 0.44 + 1.5 \cdot 0.96 + 1.5 \cdot 0.7 \cdot 1.2 = 3.30 \text{ kN/m}$$

The maximum applied bending moment at mid-span about the major axis y - y is:

$$M_{Ed} = \frac{q_{Ed} \cdot L^2}{8} = \frac{3.30 \cdot 4.8^2}{8} = 9.50 \text{ kNm}$$

and the maximum applied shear is:

$$V_{Ed} = \frac{q_{Ed} \cdot L}{2} = \frac{3.30 \cdot 4.8}{2} = 7.92 \text{ kN}$$

The joists have been verified at ULS for bending and shear. In particular, the design moment resistance of the cross-section for bending, according to EN1993-1-3 and Chapters 3 of this book (§§3.8.4, eqns. (3.83), Flowchart 3.6), is:

$$M_{c,Rd} = \frac{W_{eff,y} \cdot f_{yb}}{\gamma_{M0}} = \frac{(78626 \cdot 350) \cdot 10^{-6}}{1} = 27.79 \text{ kNm}$$

Hence, the bending resistance verification is satisfied:

$$M_{Ed} / M_{c,Rd} = 9.50 / 27.79 = 0.34$$

The design buckling resistance moment of the joist is (§§4.3.2.1, eqn. (4.56), Flowcharts 4.3 and 4.4):

$$M_{b,Rd} = \frac{\chi_{LT} \cdot W_{eff,y} \cdot f_{yb}}{\gamma_{M1}} = \frac{(0.38 \cdot 78626 \cdot 350) \cdot 10^{-6}}{1} = 10.58 \text{ kNm}$$

Hence, the buckling verification is satisfied:

$$M_{Ed} / M_{b,Rd} = 9.50 / 10.58 = 0.90$$

The design shear resistance (§§3.8.5, eqn. (3.91), Flowchart 3.7) is:

$$V_{b,Rd} = \frac{h_w \cdot t \cdot f_{yb}}{\gamma_{M0}} = \frac{(247 \cdot 2.96 \cdot 143) \cdot 10^{-3}}{1} = 104.21 \text{ kN}$$

Hence, the shear resistance is verified:

$$V_{Ed} / V_{b,Rd} = 7.92 / 104.21 = 0.08$$

To avoid the occurrence of web crippling at the end of the joists where concentrated forces are located, some web stiffeners have been placed. Therefore, no local transversal force needed.

In order to verify the member at the serviceability limit states, in agreement to EN1993-1-3, two loading conditions have to be considered:

$$q_{d1} = q_G + q_S + \psi_{0Q} q_Q = 0.44 + 0.96 + 0.7 \cdot 1.2 = 2.24 \text{ kN/m}$$

$$q_{d2} = q_S + \psi_{0Q} q_Q = 0.96 + 0.7 \cdot 1.2 = 1.80 \text{ kN/m}$$

The second moment of area for SLS (§§4.6, eqn. (4.103), Flowchart 4.8) is:

$$I_{fic} = I_{gr} - \frac{\sigma_{gr}}{\sigma} \cdot (I_{gr} - I(\sigma)_{eff})$$

$$I_{fic1} = 9393759 - \frac{80.42}{350} \cdot (9393759 - 9393759) = 9393759 \text{ mm}^4$$

$$I_{fic2} = 9393759 - \frac{63.61}{350} \cdot (9393759 - 9393759) = 9393759 \text{ mm}^4$$

It can be noticed that for the selected case, C joist under an uniformly applied load equal to 2.24 kN/m and 1.80 kN/m (respectively for q_{d1} and q_{d2}), the second moment of area for SLS is equal to the second moment of area of the gross cross section ($I_{fic} = I_{eff} = I_{gr}$).

Therefore, the joist deflections are:

$$\delta_1 = \frac{5}{384} \cdot \frac{q_{d,1} \cdot L^4}{EI_{fic}} = \frac{5}{384} \cdot \frac{2.24 \cdot 4800^4}{210000 \cdot 9393759} = 7.86 \text{ mm}$$

$$\delta_2 = \frac{5}{384} \cdot \frac{q_{d,2} \cdot L^4}{EI_{fic}} = \frac{5}{384} \cdot \frac{1.80 \cdot 4800^4}{21000 \cdot 9393759} = 6.31 \text{ mm}$$

which correspond to the following span-to-deflection ratios:

$$\frac{L}{\delta_1} = \frac{4800}{7.86} = 610$$

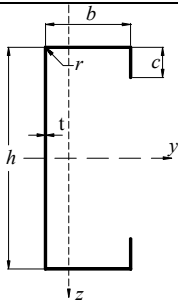
$$\frac{L}{\delta_2} = \frac{4800}{6.31} = 761$$

which is satisfactory enough.

8.7.4.2. Studs

A stud belonging to an external wall at the first floor of the building is verified. Table 8.11 summarizes the main geometry and material properties of the member. The verification of the stud (single C-lipped section) of the first floor is schematized in Figure 8.63.

Table 8.11 – Stud properties

Component	Material Properties
 <p>Geometry</p> <p> $h = 100 \text{ mm}$ $b = 50 \text{ mm}$ $c = 20 \text{ mm}$ $t_n = 1 \text{ mm}$ $t = 0.96 \text{ mm}$ $r = 3 \text{ mm}$ $H = 2700 \text{ mm}$ </p>	<p> $E = 210000 \text{ N/mm}^2$ $f_{y,k} = 350 \text{ N/mm}^2$ $f_u = 420 \text{ N/mm}^2$ $\nu = 0.3$ which corresponds to S350GD+Z </p>

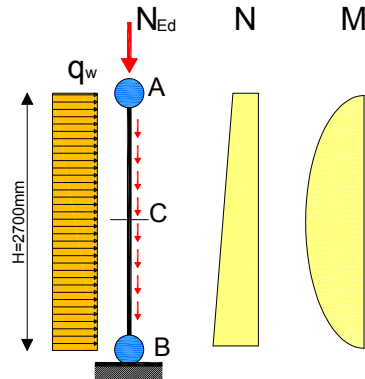


Figure 8.63 – Stud geometry and loading model

The loads applied on the roof and transferred to the studs as concentrated loads (N_{Ed}) are defined as follows:

- permanent actions: $q_{G,r} = 0.74 \cdot 0.6 \cdot 2.4 = 1.07 \text{ kN}$
- live loads: $q_Q = 2 \cdot 0.6 \cdot 0.6 \cdot 2.4 = 2.88 \text{ kN}$
- snow loads: $q_S = 1.6 \cdot 0.6 \cdot 2.4 = 2.30 \text{ kN}$
- wind loads: $q_w = -0.44 \cdot 0.6 \cdot 2.4 = 0.63 \text{ kN}$

Moreover, the studs are subjected to permanent load due to weight of the wall:

- permanent actions: $q_{G,w} = 0.56 \cdot 0.6 = 0.34 \text{ kN / m}$

and to a distributed load due to horizontal wind load:

- wind load: $q_{w,h} = -0.44 \cdot 0.6 \cdot 2.4 = 0.61 \text{ kN/m}$

The resistance verifications have been carried out by considering the less conservative load combination at the ULS for the bottom end (point B, see Figure 8.66) and the mid-height (point C, see Figure 8.66) stud cross-sections.

The bottom end cross-section is subjected to an uniform compression load equal to:

$$N_{Ed,B} = \gamma_G \cdot q_{G,r} + \gamma_G \cdot q_{G,w} \cdot H + \gamma_Q \cdot q_S + \gamma_Q \cdot \psi_{0,Q} \cdot q_Q + \gamma_Q \cdot \psi_{0,w} \cdot q_w$$

$$N_{Ed,B} = 1.35 \cdot 1.07 + 1.35 \cdot 0.34 \cdot 2.7 + 1.5 \cdot 2.3 + 1.5 \cdot 0.7 \cdot 2.88 = 9.14 \text{ kN}$$

625

and the mid-height cross-section is subjected to:

$$N_{Ed,C} = \gamma_G \cdot q_{G,r} + \gamma_G \cdot q_{G,w} \cdot H / 2 + \gamma_Q \cdot q_Q + \gamma_Q \cdot \psi_{0,S} \cdot q_S + \gamma_Q \cdot \psi_{0,w} \cdot q_w$$

$$N_{Ed,B} = 1.35 \cdot 1.07 + 1.35 \cdot 0.31 \cdot 1.35 + 1.5 \cdot 2.88 + 1.5 \cdot 0.5 \cdot 2.30 + 1.5 \cdot 0.6 \cdot (-0.63) = 7.53 \text{ kN}$$

Moreover, the stud is also subjected to a uniform distributed load due to the wind that produces a maximum moment at the mid-height of the stud equal to:

$$M_{Ed,max} = \gamma_Q \cdot q_{w,h} \cdot \frac{2.7^2}{8} = 1.5 \cdot 0.31 \cdot \frac{2.7^2}{8} = 0.28 \text{ kNm}$$

Therefore, at the end of the stud the resistance has been checked in agreement to Chapter 3, §§3.8.9, eqn. (3.128a) and Flowchart 3.9, as follows:

$$\frac{N_{Ed,B}}{N_{c,Rd}} + \frac{M_{y,Ed} + \Delta M_{y,Ed}}{M_{cy,Rd,com}} + \frac{M_{z,Ed} + \Delta M_{z,Ed}}{M_{cz,Rd,com}} \leq 1$$

$$\frac{9.14}{42.27} + \frac{0+0}{0.93} + \frac{0+0.01}{0.93} = 0.23$$

The resistance verification for the mid-height cross-section has been checked as follows:

$$\frac{N_{Ed,C}}{N_{c,Rd}} + \frac{M_{y,Ed} + \Delta M_{y,Ed}}{M_{cy,Rd,com}} + \frac{M_{z,Ed} + \Delta M_{z,Ed}}{M_{cz,Rd,com}} \leq 1$$

$$\frac{7.53}{42.27} + \frac{0.42+0}{1.92} + \frac{0+0.01}{0.93} = 0.40$$

The buckling verification has been carried out in agreement to Chapter 4, §§4.4.2, eqns. (4.61) and Flowchart 4.5, as follows:

$$\frac{N_{Ed}}{\chi_y \frac{N_{Rk}}{\gamma_{M1}}} + k_{yy} \frac{M_{y,Ed} + \Delta M_{y,Ed}}{\chi_{LT} \frac{M_{y,Rk}}{\gamma_{M1}}} + k_{yz} \frac{M_{z,Ed} + \Delta M_{z,Ed}}{\gamma_{M1}} \leq 1$$

$$0.819 \cdot \frac{7530}{42272} + 1.20 \cdot \frac{420000+0}{0.84 \cdot \frac{1916063}{1}} + 1.084 \cdot \frac{0+10000}{\frac{914840}{1}} \leq 1$$

$$\frac{N_{Ed}}{\chi_z \frac{N_{Rk}}{\gamma_{M1}}} + k_{zy} \frac{M_{y,Ed} + \Delta M_{y,Ed}}{\chi_{LT} \frac{M_{y,Rk}}{\gamma_{M1}}} + k_{zz} \frac{M_{z,Ed} + \Delta M_{z,Ed}}{\gamma_{M1}} \leq 1$$

$$\frac{7530}{0.634 \cdot \frac{42272}{1}} + 1.199 \cdot \frac{420000+0}{0.84 \cdot \frac{1916063}{1}} + 1.083 \cdot \frac{0+10000}{\frac{914840}{1}} = 0.61$$

8.7.5 Details

The main structural details of the presented case study are shown in Figure 8.64 through Figure 8.73. They are representative of widely used

details in cold-formed steel buildings, as demonstrated by the pictures of a Romanian house (Constantin House, SP024a-EN-EU, AccessSteel 2006).

FLOOR FRAMING and MATERIALS

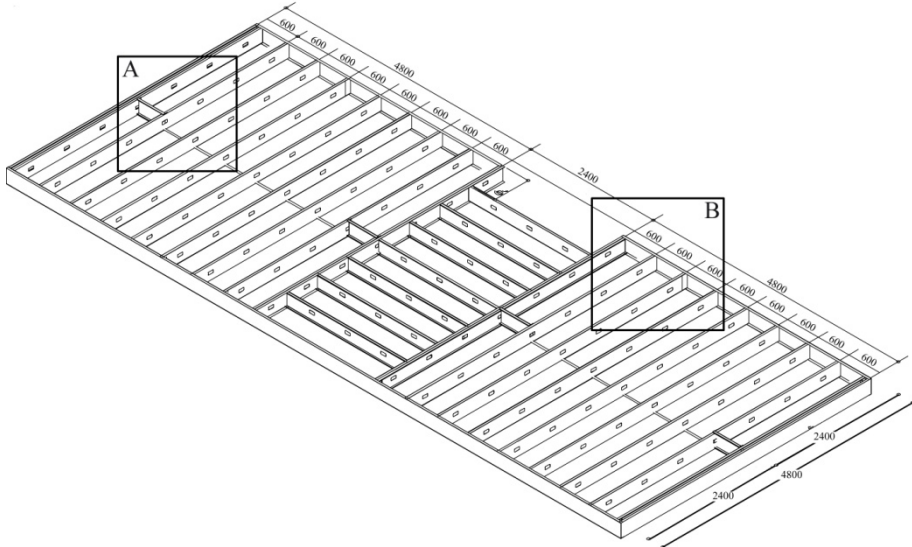


Figure 8.64 – Floor framing

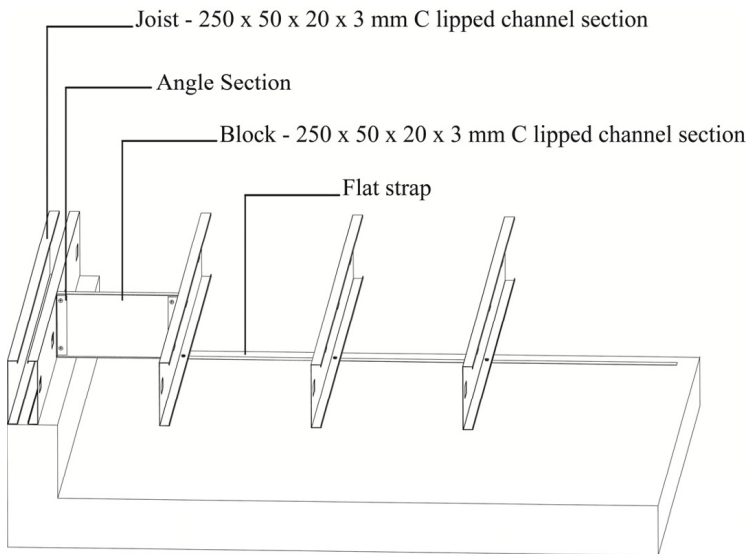


Figure 8.65 – Floor framing: Detail A – Blocking

8. BUILDING FRAMING

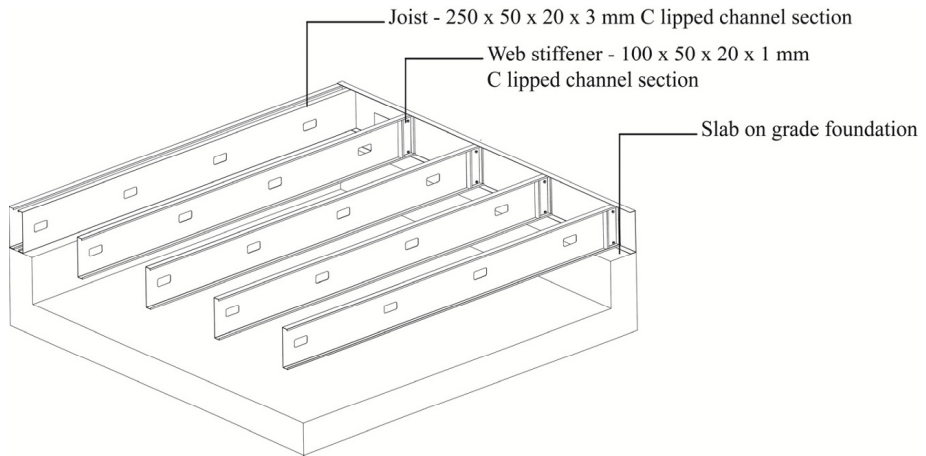


Figure 8.66 – Floor framing: Detail B



628



Figure 8.67 – Example of web stiffener and double joists at Constantin House (SP024a-EN-EU, AccessSteel 2006)

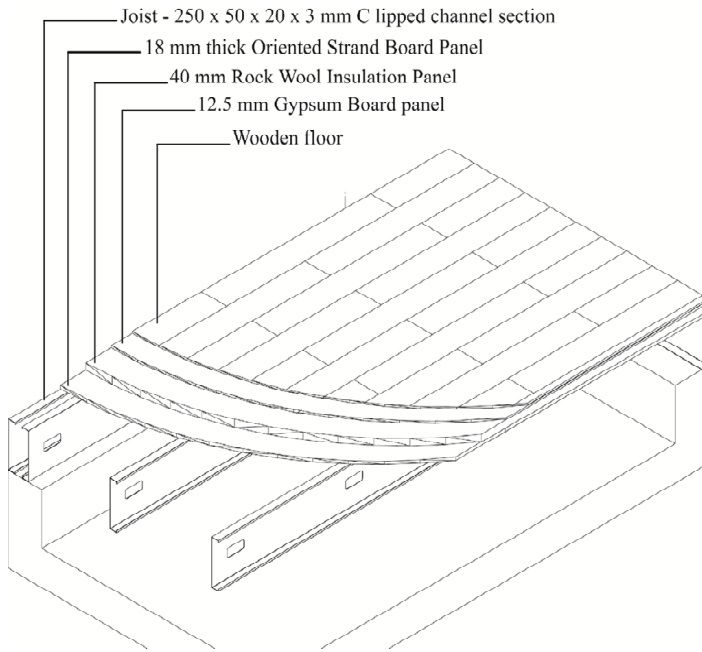


Figure 8.68 – Floor framing: stratification

WALL FRAMING and MATERIALS

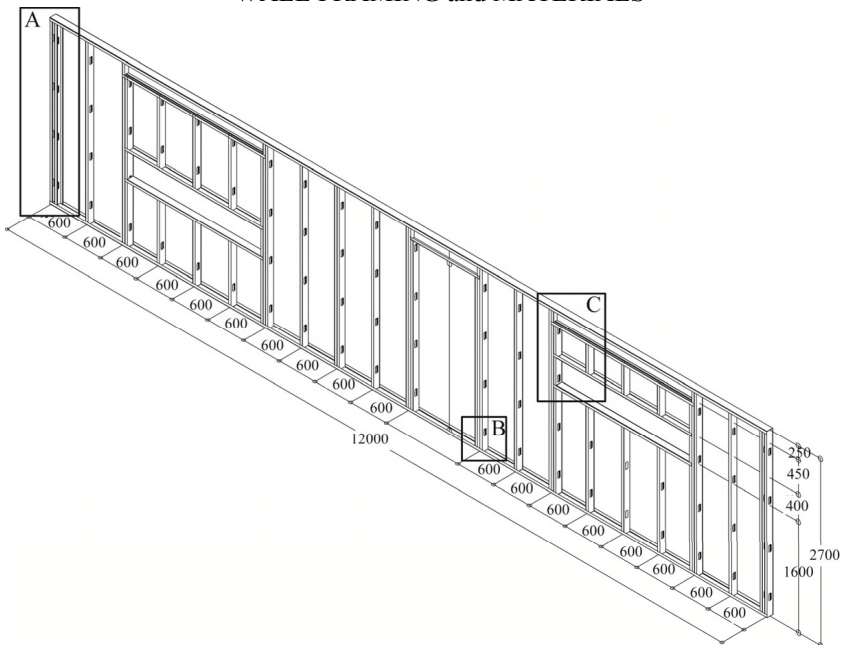


Figure 8.69 – Wall framing

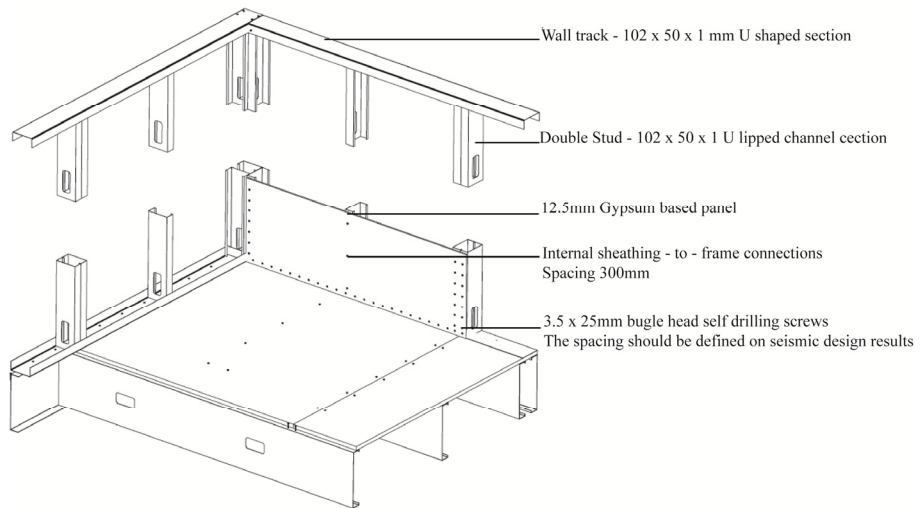


Figure 8.70 – Wall framing: Detail A: Wall corner



Figure 8.71 – Example of wall corner at Constantin House
(SP024a-EN-EU, AccessSteel 2006)

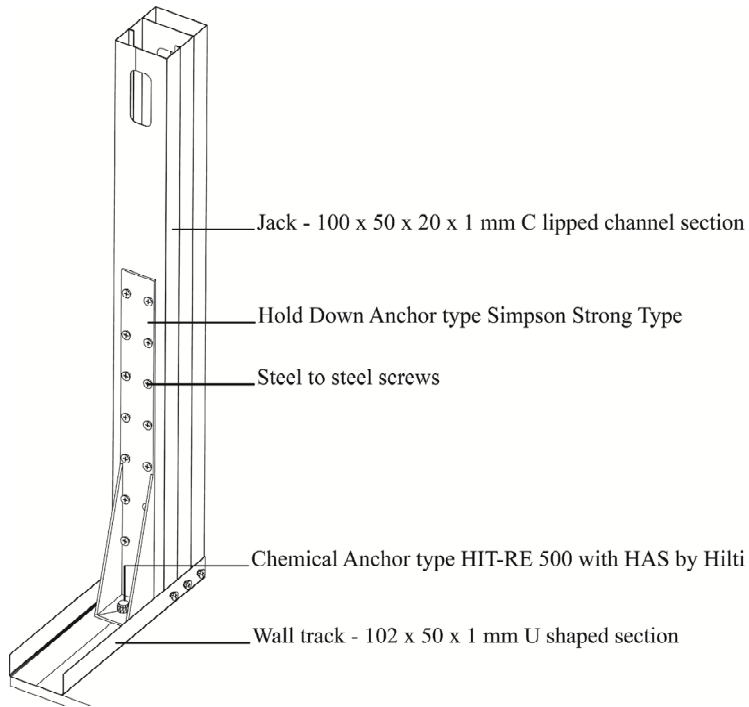


Figure 8.72 – Wall framing: detail B: Hold down anchor



Figure 8.73 – Example of Hold down anchor at Constantin House (SP024a-EN-EU, AccessSteel 2006)

8. BUILDING FRAMING

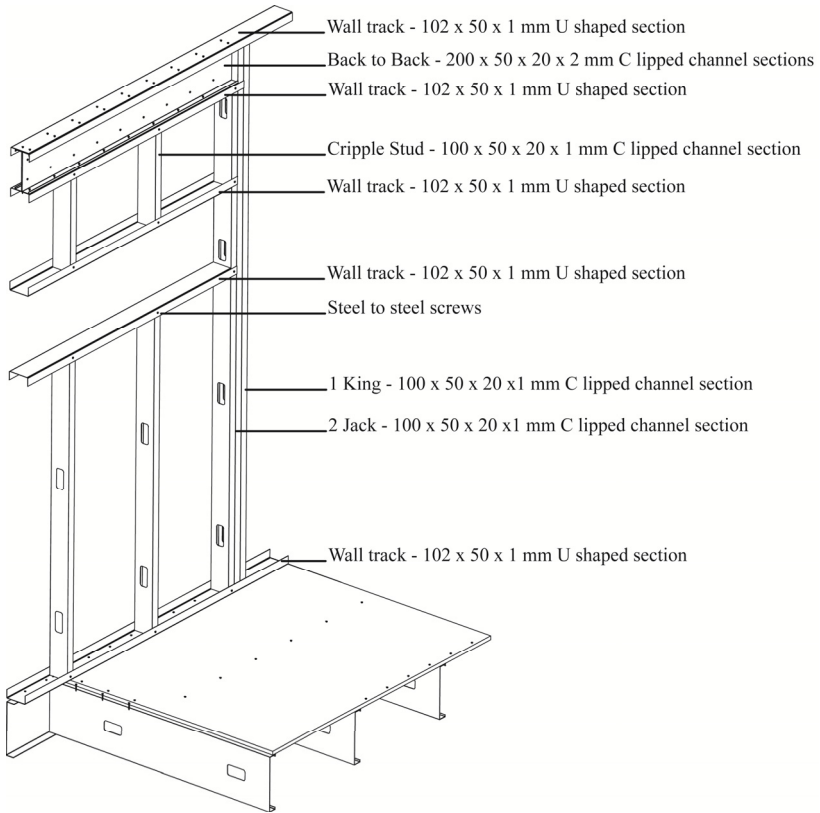


Figure 8.74 – Wall framing: detail C: Header

REFERENCES

Allen HG, Bulson PS (1980). *Background to Buckling*, McGraw-Hill Book Company Limited, Maidenhead, England.

Allen DE, Pernica G (1998). *Control of floor vibration*, Construction Technology Update, National Research Council of Canada, No. 22, Dec. 1998.

AISI (1996). Cold-Formed Steel Design Manual, *American Iron and Steel Institute. Washington, D.C.*

AISI (1999). Specification for the Design of Cold-Formed Steel Structural Members with Commentary, 1996 Edition, Supplement No. 1. *American Iron and Steel Institute. Washington, D.C.*

AISI (2001). North American Specification for the Design of Cold-Formed Steel Structural Members with Commentary, *American Iron and Steel Institute. Washington, D.C.*

AISI (2004). Supplement 2004 to the North American Specification for the Design of Cold-Formed Steel Structural Members, 2001 Edition: Appendix 1, Design of Cold-Formed Steel Structural Members Using Direct Strength Method. Publication SG05-1, *American Iron and Steel Institute, Washington, D.C.*

AISI (2004). Durability of Cold-Formed Steel Framing Members. 2nd Edition, *American Iron and Steel Institute, Washington, D.C.*

AISI S100-07 (2007). North American Specification for the Design of Cold-Formed Steel Structural Members, *American Iron and Steel Institute, Washington, D.C.*

AISI S100-07-C (2007). Commentary on North American Specification for the Design of Cold-Formed Steel Structural Members, *American Iron and Steel Institute, Washington, D.C.*

AISI S200-07 (2007). Standard for Cold-Formed Steel Framing – General Provisions, *American Iron and Steel Institute, Washington, D.C.*

AISI S201-07 (2007). North American Standard for Cold-Formed Steel Framing – Product Data, *American Iron and Steel Institute, Washington, D.C.*

AISI S210-07 (2007). Standard for Cold-Formed Steel Framing – Floor and Roof System Design, *American Iron and Steel Institute, Washington, D.C.*

AISI S211-07 (2007). Standard for Cold-Formed Steel Framing – Wall Stud Design, *American Iron and Steel Institute, Washington, D.C.*

AISI S212 (2007). Standard for Cold-Formed Steel Framing – Header Design, *American Iron and Steel Institute, Washington, D.C.*

AISI S213-07 (2007). Standard for Cold-Formed Steel Framing – Lateral Design, *American Iron and Steel Institute, Washington, D.C.*

AISI S214-07 (2007). Standard for Cold-Formed Steel Framing – Truss Design, *American Iron and Steel Institute, Washington, D.C.*

AISI S230-07 (2007). Standard for Cold-Formed Steel Framing – Prescriptive Method for One and Two Family Dwellings, *American Iron and Steel Institute, Washington, D.C.*

634

AIZ (2005). Zincatura a caldo, *Associazione Italiana Zincatura.*

AS 4100 (1990). Steel Structures, *Australian Standard. Homebush, Sydney, Australia.*

AS/NZS 4600:(2005): Cold-formed Steel Structures, *Australian Standard / New Zealand Standard, Sydney, Australia.*

Baehre R, Buca J (1986). *Die wirksame Briete des Zuggurtes von biegebeanspruchten Kassetten*, *Stahlbau* 55(9), 1986, 276-285.

Baehre R (1987). *Zur Schubfeldwirkung und-bemessung von Kassettenkonstruktionen*, *Stahlbau* 56(7), 197-202.

Baehre R, Buca J, Egner R (1990). *Empfehlungen zur Bemessung von Kassettenprofilen*, *R. Schardt Festchrift*, University of Darmstadt.

Bernard ES, Coleman R, Bridge RQ (1999). *Measurement and assessment of imperfections in thin-walled panels*, Thin Walled Structures. 33(1999), 103-126.

Bivolaru D (1993). *Numerical methods and technical experimentation in determination of residual stresses in cold-formed profiles*, Final work. University of Liege, Belgium.

Bjorhovde R (1972). *Deterministic and probabilistic approaches to the strength of steel columns*, PhD Dissertation, Lehigh University, PA.

Bleich F (1952). *Buckling strength of metal structures*, McGraw-Hill Book Company Inc., New York.

Boissonade N, Greiner R, Jaspart JP, Lindner J (2006). *New design rules in EN 1993-1-1 for member stability*, ECCS Technical Committee 8 – Structural Stability, P119, ECCS, Brussels.

Bourrier P, Brozzetti J (1996). *Construction metalique et mixte acier-beton*. Eyrolles, Paris, 222-227.

Bulson PS (1970). *The stability of flat plates*, Chatto and Windus, London.

Burstand H (2000): *Light gauge steel framing for housing*, SBI – Swedish Institute of Steel Construction, Publication 170, Stockholm, Sweden.

BS5950-1 (2000). The structural use of steelwork in building, Part 1: Code practice for design - Rolled and welded sections, *British Standards Institution*, London.

CEN (1992). ENV 1993-1-1:1992 - Eurocode 3: Design of steel structures, Part 1.1: General rules and rules for buildings, *European Committee for Standardization, Brussels, Belgium*.

CEN (1996). ENV 1993-1-3:1996 - Eurocode 3: Design of Steel Structures Part 1.3. General Rules. Supplementary rules for cold-formed thin gauge members and sheeting. (including the Corrigenda to ENV1993-1-3 of 1997-02-25), *European Committee for Standardization, Brussels, Belgium*.

CEN (1997). EN 300:1997 - Oriented strand boards OSB - Definitions, classification and specifications, *European Committee for Standardization, Brussels, Belgium*.

CEN (2001). EN 10002-1:2001 - Tensile testing of metallic materials. Method of test at ambient temperature, *European Committee for Standardization, Brussels, Belgium*.

CEN (2002a). EN 1990:2002 - Eurocode – Basis of structural design, *European Committee for Standardization, Brussels, Belgium*.

CEN (2002b). EN 1991-1-1:2002 - Eurocode 1: Actions on structures - Part 1-1: General actions-Densities, self-weight, imposed loads for buildings, *European Committee for Standardization, Brussels, Belgium*.

CEN (2002c). EN 1991-1-2:2002 - Eurocode 1: Actions on structures - Part 1-2: General actions - Actions on structures exposed to fire, *European Committee for Standardization, Brussels, Belgium*.

CEN (2003a). EN 1991-1-3:2003 - Eurocode 1: Actions on structures - Part 1-3: General actions - Snow loads, *European Committee for Standardization, Brussels, Belgium*.

CEN (2003b). EN 1991-1-5:2003 - Eurocode 1: Actions on structures - Part 1-5: General actions - Thermal actions, *European Committee for Standardization, Brussels, Belgium*.

CEN (2004). EN1998-1:2004 - Eurocode 8: Design of structures for earthquake resistance - Part 1: General rules, seismic actions and rules for buildings, *European Committee for Standardization, Brussels, Belgium*.

CEN (2005a). EN 1993-1-1:2005 - Eurocode 3: Design of steel structures - Part 1-1: General rules and rules for buildings, *European Committee for Standardization, Brussels, Belgium* (including EN1993-1-1:2005/AC, 2009).

CEN (2005b). EN 1991-1-4:2005 - Eurocode 1: Actions on structures - Part 1-4: General actions - Wind actions, *European Committee for Standardization, Brussels, Belgium*.

CEN (2005c). EN 1991-1-6:2005 - Eurocode 1: Actions on structures - Part 1-6: General actions - Actions during execution, *European Committee for Standardization, Brussels, Belgium*.

CEN (2005d). EN 1993-1-2:2005 - Eurocode 3: Design of steel structures - Part 1-2, Design of Steel Structures, General rules. Structural fire design, *European Committee for Standardization, Brussels, Belgium*.

CEN (2005e). EN1993-1-8:2005 - Eurocode 3: Design of steel structures. Part 1-8: Design of joints, *European Committee for Standardization, Brussels, Belgium*.

CEN (2006a). EN 1993-1-3:2006 - Eurocode 3: Design of steel structures. Part 1-3: General Rules. Supplementary rules for cold-formed thin gauge members and sheeting, *European Committee for Standardization, Brussels, Belgium* (including EN1993-1-3:2006/AC, 2009).

CEN (2006b). EN 1993-1-5:2006 - Eurocode 3: Design of steel structures - Part 1-5: Plated structural elements, *European Committee for Standardization, Brussels, Belgium* (including EN1993-1-5:2006/AC, 2009).

CEN (2006c). EN 1991-1-7:2006 - Eurocode 1: Actions on structures - Part 1-7: General actions - Accidental actions, *European Committee for Standardization, Brussels, Belgium*.

CEN (2007). EN 1993-1-6:2007 - Eurocode 3: Design of steel structures - Part 1.6: General rules - Strength and stability of shell structures, *European Committee for Standardization, Brussels, Belgium*.

CEN (2008). EN 1090:2008 - Execution of steel structures and aluminium structures - Part 2: Technical requirements for steel structures, *European Committee for Standardization, Brussels, Belgium*.

CSA (1994). S136 - Specification for Cold Formed Steel Structural Members. *Canadian Standards Association, Toronto, Ontario*.

Clough RH, Ogden RG (1993). *Building design using cold formed steel sections. Acoustic insulation*, Publication P128, The Steel Construction Institute.

CUFSM (2008). *Elastic Buckling Analysis of Thin-walled Members*, version 3.12. www.ce.jhu.edu/bschafer/cufsm312

Davies JM (1978). *A bibliography on the Stressed Skin Action of light gauge corrugated sheet cladding*, University of Salford, Dept. of Civil Eng., Rep. 75/63.

Davies JM, Bryan ER (1982). *Manual of stressed skin diaphragm design*, Granada Publishing.

Davies JM (1986). *A general solution for the shear flexibility of profiled sheets, I: Development and verification of the method, and II: Application of the method*, Thin Walled Structures, Vol. 4, No. 1, 41-68 and Vol.4, No.2, 151-161.

Davies JM, Fisher J (1987). *End failure in stressed skin diaphragms*, Proc. of the Institution of Civil Engineering's, Part 2, Vol. 83, 275-293.

Davies JM (1991). *Connections for cold-formed steelwork*. In: *Design of Cold-Formed Steel Members* (Rhodes J, Editor), Elsevier Applied Science, London and New York.

Davies JM, Leach P (1994a). *First-order generalised beam theory*, Journal of Constructional Steel Research, 31 (2-3) 187-220.

Davies JM, Leach P, Heinz D (1994b). *Second-order generalised beam theory*, Journal of Constructional Steel Research, 31 (2-3) 221-241.

638

Davies JM, Leach P, Kelo E (1995). *The case of light gauge steel in low and medium raised modular buildings*, Proceedings of the 3rd International Conference on Steel and Aluminium Structures, ICSAS'95, Istanbul, 24-26 May.

Davies JM, Jiang C (1996). *Design of thin-walled columns for distortional buckling*, Coupled Instabilities of Metal Structures – CIMS'96, Imperial College Press, London, 165-172.

Davies R, Predeschi R, Sinha BP (1996). *The shear behaviour of press-joining in cold-formed steel structures*, Thin-walled Structures, Vol. 25, No. 3, 153-170.

Davies JM, Dewhurst DW (1997). *The shear behaviour of thin-walled cassette sections infilled by rigid insulation*, Proceedings of International Conference on Experimental Model Research and Testing of Thin-Walled Structures. Prague, Czech Republic, September 1997, 209-216.

Davies JM, Lawson RM (1999). *Stressed skin design of modern steel roofs*, The Structural Engineers, Vol. 77, No. 21.

Davies JM (2001). *Lightweight sandwich construction*, Oxford, London, Edinburgh (UK). Blackwell Science Ltd.

Davies JM (2002). *Cassette wall construction*, Current Research and Practice – Advance in Steel Structures – ICASS'02, Vol. 1 (Chan SL, Teng JG and Chung KF, Eds.), Elsevier Science Ltd., Oxford, 57-68.

Davies JM, Fragos AS (2002). *The local shear buckling of thin-walled cassettes infilled by rigid insulations – 1. Tests*, Proceedings of 3rd European Conference on Steel Structures – Eurosteel 2002, Coimbra, Portugal, 19-20 September 2002, 669-678.

Davies JM, Fragos AS (2003). *Shear strength of empty and infilled cassettes*, Thin-Walled Structures, 41 (2003), 109–125.

Davies JM, Fragos AS (2004). *The local shear buckling of thin-walled cassettes infilled by rigid insulation*, Journal of Constructional Steel Research, 60(3-5):581-599.

Davies JM (2005). *Residential buildings – Chapter 7*. In: *Light gauge metal structures. Recent advances* (Rondal J & Dubina D, Eds.), CIMS Udine Courses and Lectures – No. 455. SpringerWienNewYork, 143-188.

Davies JM (2006b). *Light gauge steel cassette wall construction— theory and practice*, Journal of Constructional Steel Research, 62 (2006) 1077–1086.

Davies JM (2006a). *Developments in stressed skin design* (Tribute Edition to Rolf Baehre), Thin Walled Structures, Vol. 44, No. 12, 1250-1260.

Dubina D (1996). *Coupled instabilities in bar members – General Report*, Coupled Instabilities in Metal Structures – CISM'96 (Rondal J, Dubina D, Gioncu V, Eds.). Imperial College Press, London, 119-132.

Dubina D (2000). *Recent research advances and trends on coupled instability of bar members*, General Report – Session 3: Bar Members, Coupled Instabilities in Metal Structures - CIMS'2000 (Camotin D, Dubina D, Rondal J, Eds.). Imperial Colleague Press, London, 131-144.

Dubina D (2001). *The ECBL approach for interactive buckling of thin-walled steel members*, Steel & Composite Structures. 1(1):75-96.

Dubina D, Ungureanu V, Fülöp L, Nagy Zs, Larsson H (2001a). *LINDAB cold-formed steel structures for small and medium size non-residential buildings in seismic zones*, Proc. of the 9th Nordic Steel Construction Conference – NSCC2001, Helsinki, Finland, June 18-20, 2001, (Makelainen P *et al*, Eds.), 463-470.

Dubina D, Ungureanu V, Georgescu M, Fülöp L (2001b). *Innovative cold-formed steel structure for restructuring of existing RC or masonry buildings by vertical addition of supplementary storey*, Thin-Walled Structures “Advances and Developments”, Elsevier (Zaras J, Kowal-Michalska K, Rhodes J, Eds.), 187-194.

Dubina D (2005). *Peculiar problems in cold-formed steel design – Chapter 2*. In: *Light gauge metal structures. Recent advances* (Rondal J & Dubina D, Eds.), CIMS Udine Courses and Lectures – No. 455. SpringerWienNewYork, 5-15.

Dubina D, Ungureanu V (2002). *Effect of imperfections on numerical simulation on instability behaviour of cold-formed steel members*, Thin Walled Structures. Vol. 40, No. 3, 239-262.

640 Dubina D (2008). *Structural analysis and design assisted by testing of cold-formed steel structures*, Thin-Walled Structures, 46(7-9), 741-764.

ECCS (1976). *Manual on stability of steel structures*, Second edition, Publication P022, European Convention for Constructional Steelwork, Brussels, Belgium.

ECCS (1978). *European recommendations for steel construction*, Publication P023, European Convention for Constructional Steelwork, Brussels, Belgium.

ECCS (1987). *European recommendations for design of light gauge steel members*, Publication P049, European Convention for Constructional Steelwork, Brussels, Belgium.

ECCS (1983a). *European Recommendations for the Design and Testing of Connections in Steel Sheeting and Sections*, Publication P021, European Convention for Constructional Steelwork, Brussels, Belgium.

ECCS (1983b). *Mechanical fasteners for use in steel sheeting and sections*. Publication P042, European Convention for Constructional Steelwork, Brussels, Belgium.

ECCS (1995). *European Recommendations for the Application of Metal Sheeting acting as a Diaphragm*, Publication P088, European Convention for Constructional Steelwork, Brussels, Belgium.

ECCS (2000). *Preliminary worked examples according to Eurocode 3 Part 1.3*, Publication P114, European Convention for Constructional Steelwork, Brussels, Belgium.

ECCS (2001). *European Recommendation for Sandwich Panels*, Publication P115, European Convention for Constructional Steelwork, Brussels, Belgium.

ECCS (2008a). *The Testing of Connections with Mechanical Fasteners in Steel Sheeting and Sections*. Publication 124, European Convention for Constructional Steelwork, Brussels, Belgium.

ECCS (2008b). *Worked examples according to EN1993-1-3*. Publication 123, European Convention for Constructional Steelwork, Brussels, Belgium.

ECCS (2009). ECCS TC7 TWG 7.9 / CIB Working Commission W056. *Preliminary European Recommendations for the Testing and Design of Fastenings for Sandwich Panels*. Publication ECCS no. 127/CIB no. 320, Belgium.

Fiorino L, Della Corte G, Landolfo R (2007). *Experimental tests on typical screw connections for cold-formed steel housing*. Engineering Structures. Elsevier Science. Vol. 29, No. 8, 1761–1773.

Fiorino L, Iuorio O, Landolfo R (2009). *Sheathed cold-formed steel housing: a seismic design procedure*, Thin Walled Structures, Vol. 47, 919 – 930.

Fiorino L, Iuorio O, Landolfo R (2011). *Seismic Analysis of Sheathing-Braced Cold-Formed Steel Structures*, Engineering Structures, Vol. 34, 538–547.

Fischer M, Zhu J (1996). *The method of effective width and for bars with thin-walled cross-sections-remarks of insufficiencies and improvements*, Coupled Instabilities in Metal Structures-CISM'96, Imperial College Press, London, 141-148.

Fenster SMC, Girardier EV, Owens GW (1992). *Economic Design and the Importance of Standardised Connections*, In Constructional Steel Design: World Developments (Dowling PJ *et al*, Eds.). Elsevier Applied Science, Barking, Essex, UK, 541-550.

Fülöp L, Dubina D (2003). *Experimental program to evaluate the shear capacity two new types of screws. Research report* (in Romanian), PU Timisoara. Beneficiary LINDAB Romania Ltd.

Fülöp L, Dubina D (2004). *Performance of wall-stud cold-formed shear panels under monotonic and cyclic loading. Part I: Experimental research*, Thin-Walled Structures, Vol. 42(2), 321–338.

Fülöp L, Dubina D (2004). *Performance of wall-stud cold-formed shear panels under monotonic and cyclic loading. Part II: Numerical modelling and performance analysis*, Thin-Walled Structures, Vol. 42(2), 339–343.

Fülöp L, Dubina D (2006). *Design criteria for seam and sheeting-to-framing connections of cold-formed steel shear panels*, Journal of Structural Engineering, American Society of Civil Engineers - ASCE, Vol. 132(4), 582-590.

Galambos TV (1998). *Guide to Stability Design Criteria for Metal Structures*, 5th Edition, John Wiley and Sons.

Gardner L, Nethercot DA (2001). *Behaviour of cold-formed stainless steel cross-sections*, Proceedings of 9th Nordic Steel Construction Conference – NSCC2001, Helsinki, Finland, 18-20 June, 781-789.

Gerard G (1946). *Secant Modulus Method for determination of Plate Instability above the Proportional Limit*, Journal Aero Sci., Vol. 13(1), 38-44.

Gioncu V, Balut N, Dubina D, Moldovan A, Pacoste C (1992). *Coupled instabilities in mono-symmetrical steel compression members*, Journal of Constructional Steel Research, Vol. 21(1992), 71-95.

Gioncu V (1994). *General Theory of Coupled Instabilities*, Thin-Walled Structures, 19(2-4), 81-127.

Grubb PJ, Lawson RM (1997). *Building design using cold-formed steel sections: construction detailing and practice*, SCI Publication P165. Steel Construction Institute, Ascot, Berkshire, United Kingdom.

Hancock GJ (1997). *Light Gauge Construction*, Progress in Structural Engineering and Materials, Vol. I (I), 25-30.

Hancock GJ (1998). *Design of Cold-formed Steel Structures*, 3rd edition, Australian Institute of Steel Construction, Sydney.

Hancock GJ, Murray TM, Ellifritt DS (2001). *Cold-Formed Steel Structures to the AISI Specification*, Marcel Dekker, Inc., New York.

Hancock GJ (2007). *Design of cold-formed steel structures (to AS/NZS 4600:2005)*, 4th edition, Australian Steel Institute, Sydney.

Helenins A (2000). *Shear strength of clinched connections in light gauge steel*, VTT Research Notes 2029, Technical Research Centre of Finland.

Hilti (2005). *North American product technical guide*. www.hilti.com

Hirt MA, Bez R, Nussbaumer A (2006). *Construction Métallique: Notions fondamentales et méthodes de dimensionnement*, Traité de Génie Civil, Volume 10, PPUR, Lausanne, Switzerland.

ISO 6308 (1980). Gypsum plasterboard – Specification, *International Organization for Standardization*, Geneva, Switzerland.

ISO 2631-1 (1997). Mechanical vibration and shock – Evaluation of human exposure to whole-body vibration: Part 1: General requirements, *International Organisation for Standardization*, Geneva, Switzerland.

ISO 2631-2 (2003). Mechanical vibration and shock – Evaluation of human exposure to whole-body vibration: Part 2: Vibration in buildings (1 Hz to 80 Hz), *International Organisation for Standardization*, Geneva, Switzerland.

ISO 10137 (2007). Bases for design of structures - Serviceability of buildings and pedestrian walkways against vibration, *International Organisation for Standardization*, Geneva, Switzerland.

Iuorio O, (2007). *Cold-formed steel housing*, Pollack Periodica - An International Journal for Engineering and Information Sciences, Vol. 2-3, 97-108.

Iuorio O (2009). *Design Procedures for Cold-formed steel housing in seismic area*, PhD Thesis, University G. D'Annunzio, Pescara, Italy.

Iuorio O, Fiorino L, Macillo V, Landolfo R (2012). *Seismic design and experimental tests of an Italian cold-formed steel structure*, Proceeding of STESSA2012, Santiago de Chile, Chile.

John V (1991). *Durability of Galvanized Steel Building Components in Domestic Housing*, British Steel Technical - Welsh Laboratories.

Kaitila O (2000). *Cold Formed Steel Structures in Fire conditions*, Proceeding of Seminar on Steel Structures: Design of Cold-Formed Steel Structures, Finland.

644

Von Karman T (1910). *Fiestighetsproblem im Maschinenbau*, Encyclopaedie der Mathematischen Wissenschaften.

Von Karman T, Sechler EE, Donnel LH (1932). *Strength of thin plates in compression*, Trans ASME, 54-53.

Kidmann R, Mathias K (2011). *Steel Structures. Design using FEM*, Ernst & Sohn, Berlin.

Kingspan (2007). *Insulated Flat Architectural Wall & Facade Systems*. www.kingspan.com

Kirby PA, Nethercot DA (1979). *Design for structural stability*, Granada.

Klippstein KH (1978). *Strength of Cold-Formed Steel Stud Exposed to Fire*, Proceedings of the Fourth International Speciality Conference on Cold-Formed Steel Structures, St. Louis, Missouri, U.S.A.

König J (1978). *Transversally loaded thin-walled C-shaped panels with intermediate stiffeners*, Swedish Council for Building, Research Document D7, Stockholm, Sweden.

Landolfo R, Fiorino L, Della Corte G (2006). *Seismic behaviour of sheathed cold-formed structures: physical tests*, Journal of Structural Engineering, ASCE, Vol. 132, Issue: 4, 570-581.

Landolfo R, Fiorino L, Iuorio O, (2010). *A Specific Procedure for Seismic Design of Cold-Formed Steel Housing*, Advanced Steel Construction, Vol. 6, No. 1, 603-618.

Landolfo R (2011). *Cold-formed steel structures in seismic area: research and applications*, Proceedings of VIII Congresso de Construção Metálica e Mista, Guimarães, Portugal.

Landolfo R, Fiorino L, Iuorio O, (2011). *Progetto, Realizzazione E Collaudo Della Nuova Scuola BsF In Lago Patria – Napoli*, Costruzioni Metalliche, n. 6.

Lange J, Naujoksb B (2006). *Behaviour of cold-formed steel shear walls under horizontal and vertical loads*, Thin-Walled Structures Vol. 44, 1214–1222.

Law SCW, Hancock GJ (1987). *Distortional Buckling Formulas for Channel Columns*, Journal of Structural Engineering, ASCE, Vol. 113, No. 5, 1063-1078.

Lawson RM, Ogden RG (2008). *Hybrid light steel panel and modular systems*, Thin-walled Structures, July-Sept 2008, Vol. 46, pp.720-730.

Lee YK (1995). *Analysis of Gypsum-Sheathed Cold-Formed Steel Wall Stud Panels*, Engineering Report in partial fulfillment of the degree Masters of Science, Department of Civil Engineering, Oregon State University, Corvallis, OR, USA.

Lim J (2001). *Joint effects in cold-formed steel portal frames*, PhD Thesis, University of Nottingham, UK.

Lindner J (2003). *Simplified design of purlins*, ECCS TC8, Rep. TC8-2003-016.

Lindab Systemline. *Industrial halls – Application guide*.

LSK (2005). *European Lightweight Steel-Framed Construction*, LSK and Arcelor publication, Luxemburg.

LSK (2008). *Guide WiSH: Workpack design for Steel House - Memento pour l'Habitat à Ossature Acier*, 1st Edition, LSK (European Light Steel Construction Association). www.euro-steel.com

MacGinley TJ, Ang TC (1992). *Structural Steelwork: Design to Limit State Theory*, Butterworth-Heinemann Ltd; 2nd Edition, Oxford.

Makelainen P, Kesti J (1999). *Advanced method for lightweight steel joining*, Journal of Constructional Steel Research, Vol. 49, No. 2, 107-116.

Marguerre K (1938). *Zur Theorie der gekremmter Platte grosser Formaenderung*, Proceedings of 5th Congress for Applied Mechanics, Cambridge.

Maquoi R, Rondal J (1978). *Mise en equation des nouvelles courbes Europeenes de flambement*, Construction Metallique, 1(1978), 17-30.

646 Martin LH, Purkiss JA (2008). *Structural Design of Steelwork to EN 1993 and EN 1994*, 3rd Edition, Butterworth-Heinemann – imprint of Elsevier, UK.

Mazzolani FM, Sylos Labini F (1984). *Skin frame interaction in seismic resistant structures*, Construzioni Metalliche, No. 4, 3-16.

Mazzolani FM, Piluso V (1996). *Theory and Design of Seismic Resistant Steel Frames*, E & FN Spon, London.

Miettinen E, Saarni R (2000). *Use of steel in house building*, The Finnish Constructional Steelwork Association Ltd., Helsinki.

Miller TH (1989). *Studies on the Behavior of Cold-Formed Steel Wall Stud Assemblies*, Ph.D. Thesis, Department of Civil Engineering, Cornell University.

Murray NW (1985). *Introduction to the theory of thin-walled structures*, Clarendon Press, Oxford.

NASFA (2000). *Prescriptive Method for Residential Cold-Formed Steel Framing*, 2000 Edition, North American Steel Framing Alliance.

Nethercot DA (1991). *Limit states design of structural steelwork*, Chapman & Hall, London, UK.

NBC (1995). *User's Guide – Structural Commentaries (Part 4). Commentary A: Serviceability Criteria for Deflections and Vibrations*.

Pastor N, Etzenbach C (2008). *WISH*: Workpack design for steel house. The new European easy-to-use tool for cold-formed steel building design*, Proceedings of EUROSTEEL 2008, Graz, Austria.

Plank R, Dowling (2003). J. Sustainable Constructions. *Steel Buildings*, 1st ed.; The British Constructional Steelwork Association Ltd, British Library, Publication No. 35/03.

Pekoz T, McGuire W (1980). *Welding of Sheet Steel*, Proceedings of Fifth International Speciality Conference on Cold-formed Steel Structures, St. Louis, Missouri, November 1980.

Predeschi RF, Sinha DP, Davies R (1997). *Advance Connection Techniques for Cold-Formed Steel Structures*, Journal of Structural Engineering (ASCE), 2(123), 138-144.

Quach WM, Teng JG, Chung KF (2004). *Residual stresses in steel sheets due to coiling and uncoiling: a closed-form analytical solution*, Engineering Structures 26(2004), 1249–1259.

Ranby, A, (1999). *Structural Fire Design of Thin Walled Steel Sections*, Licenciate Thesis, Division of Steel Structures, Department of Civil and Mining Engineering, Luleå University of Technology, Sweden.

Rasmussen KJR, Hancock GJ (1988). *Geometric Imperfections in Plated Structures Subject to Interaction between Buckling Modes*, Thin Walled Structures, 6(1988), 433-452.

Rasmussen KJR, Hancock GJ (1993). *Design of cold-formed stainless steel tubular members. I: Columns*, Journal of Structural Engineering, ASCE, 119(8): 2349-2367.

Rhodes J (Ed.) (1991). *Design of Cold-formed Steel Members*, Elsevier Applied Science, London and New York.

REFERENCES

Rondal J, Maquoi R (1979a). *Formulation d'Ayrton-Perry pour le flambement des barres métalliques*, Construction Métallique, 4, 41-53.

Rondal J, Maquoi R (1979b). Single Equation for SSRC Column Strength Curves, ASCE J. Struct. Div., Vol. 105, No. ST1, 247-250.

Rondal J (1988). *Thin-walled structures – General Report*, Stability of Steel Structures (Ivanyi M. Ed.), Akademiai Kiado, Budapest, Vol. 2, 849-866.

Rondal J, Dubina D, Bivolaru D (1994). *Residual stresses and the behaviour of cold-formed steel structures*, Proceedings of 17th Czech and Slovak International Conference on Steel Structures and Bridges, Bratislava, Slovakia, September 7-9, 193-197.

Rotter JM (2011). *Challenges in the generalisation of structural buckling assessments to all structures and load cases*, Proceedings of the 6th International Conference on Thin Walled Structures – ICTWS 2011 (Dubina D, Ungureanu V, Eds.), Timisoara, Romania, 3-5 September 2011, 71-86.

Robust Details (2010). *Part E - Resistance to the passage of sound*, The Building Regulations. http://www.planningportal.gov.uk/uploads/br/BR_PDF_ADE_2003.pdf

648 RFCS-7210-PR/314 (2003). Research Fund for Coal and Steel. *Generalisation of criteria for floor vibrations for industrial, office, residential and public building and gymnastic halls*, Final report.

RFS2-CT-2007-00033 (2007). Research Fund for Coal and Steel. *Human induced Vibrations of Steel Structures (HIVOSS). Vibration Design of Floors. Guideline*, Background Document.

Schafer BW, Peköz T (1998a). *Computational modelling of cold-formed steel characterising geometric imperfections and residual stresses*, Journal of Constructional Steel Research, 47(1998), 193-210.

Schafer BW, Grigoriu M, Peköz T (1998b). *A probabilistic examination of the ultimate strength of cold-formed steel elements*, Thin Walled Structures, 31(1998), 271-288.

Schafer BW, Peköz T (1998c). *Direct Strength Prediction of Cold-Formed Steel Members using Numerical Elastic Buckling Solutions*,

Proceedings of the Fourteenth International Specialty Conference on Cold-Formed Steel Structures. St. Louis, Missouri, 69-76.

Schafer B, Peköz T (1999). *Local and Distortional Buckling of Cold-formed Steel Members with Edge Stiffened Flanges*, Light-weight Steel and Aluminium Structures, Proceedings of the 4th Int. Conf. on Steel and Aluminium Structures, ICSAS'99, Espoo, Finland, 89-97.

Schafer BW (2001). *Direct Strength Prediction of Thin-Walled Beams and Columns*, Research Report, John Hopkins University, USA.

Schafer BW (2006). *Designing cold-formed steel using the Direct Strength Method*, Proceeding of the 18th International Specialty Conference on Cold-Formed Steel Structures, Orlando, FL., U.S.A., October 2006.

Schafer BW, Ádány S (2006). *Buckling analysis of cold-formed steel members using CUFSM: conventional and constrained finite strip methods*, Eighteenth International Specialty Conference on Cold-Formed Steel Structures, Orlando, FL. October 2006.

Schardt R (1989). *Verallgemeinerte Technische Biegetheorie*, Springer-Verlag, Berlin.

Sedlacek G, Müller C (2006). *The European standard family and its basis*, Journal of Constructional Steel Research, 62(2006), 1047-1059.

Seeka MW, Murray TM (2008). *Lateral restraint forces in Z-section roof systems using the component stiffness method*, Journal of Constructional Steel Research 64(12), 1366–1378.

Sfintesco D (1970). *Fondement expérimental des courbes européennes de flambement*, Construction Métallique. 3(1970), 5-9.

daSilva LS, Simoes R, Gervasio H (2010). *Design of Steel Structures, Eurocode 3: Design of Steel Structures, Part 1-1: General rules and rules for buildings*, Ernst & Sohn – A Wiley Company. ECCS Eurocode Design Manuals.

Silvestre N, Camotim D (2002a). *First-order generalised beam theory for arbitrary orthotropic materials*, Thin-Walled Structures, 40 (9) 755-789.

Silvestre N, Camotim D (2002b). *Second-order generalised beam theory for arbitrary orthotropic materials*, Thin-Walled Structures, 40 (9) 791-820.

Silvestre N, Camotim D (2003). *Nonlinear Generalized Beam Theory for Cold-formed Steel Members*, International Journal of Structural Stability and Dynamics. 3 (4) 461-490.

Sprague PE (1981). *The Origin of Balloon Framing*, Journal of the Society of Architectural Historians, Vol. 40, No. 4, 311-319.

Stark JWB, Soetens F (1980). *Welded Connections in Cold-formed Sections*, Proceedings of Fifth International Speciality Conference on Cold-formed Steel Structures, St. Louis, Missouri, November 1980.

Stowell EZ (1948). *A Unified Theory of Plastic Buckling of Column and Plates*, NACA, Report 898.

SSEDTA (1999). Structural Steelwork Eurocodes –Development of a Trans-National Approach. *Course: Eurocode 3. Module 4: Member design. Lecture 12: Unrestrained Beams.*

SSEDTA (1999). Structural Steelwork Eurocodes –Development of a Trans-National Approach. *Course: Eurocode 3. Module 4: Member design. Lecture 14: Beam-Columns.*

650

Steel Deck Institute: *Diaphragm Design Manual*, 3rd Edition, 2004.

SF012a-EN-EU. *Governing combination of actions – Flow Chart*. Access Steel 2006. www.access-steel.com

SF038a-EN-EU: *Calculation of effective section properties for cold-formed steel lipped channel sections under compression or bending – Flow chart* (created by Ungureanu V., checked by Dubina D.) Access Steel 2006. www.access-steel.com

SF039a-EN-EU. *Design of a cold-formed steel member in compression – Flow chart* (created by Ungureanu V, checked by Dubina D) Access Steel 2006. www.access-steel.com

SF040a-EN-EU: *Design of a cold-formed steel lipped channel member in tension – Flow chart* (created by Ungureanu V., checked by Dubina D.) Access Steel 2006. www.access-steel.com

SF041a-EN-EU: *Design and serviceability limit state check of a cold-formed steel member in bending– Flow chart* (created by Ungureanu V., checked by Dubina D.) Access Steel 2006. www.access-steel.com

SF042a-EN-EU. *Design of a cold-formed steel wall stud in combined compression and uniaxial bending – Flow chart* (created by Ungureanu V, checked by Dubina D) Access Steel 2006. www.access-steel.com

SF043a-EN-EU: *Design resistance of screwed connections of cold-formed members– Flow chart* (created by Ungureanu V, checked by Dubina D) Access Steel 2006. www.access-steel.com

SF044a-EN-EU. *Buckling verification of non-uniform members in portal frames – Flow chart.* Access Steel 2006. www.access-steel.com

SFS Intec AG (2011). *Pitched roofing and cladding: Innovative fastening systems and application expertise.* <http://www.sfsintec.biz>

SN036a-EN-EU. *NCCI: Vibrations.* Access Steel 2006. www.access-steel.com

SN032a-EN-EU. *NCCI: General method for out-of-plane buckling in portal frames.* Access Steel 2006. www.access-steel.com

SP024a-EN-EU. *Case Study: Constantin's Family House, Ploiesti, Romania.* Access Steel 2006. www.access-steel.com

SS025a-EN-EU. *Scheme Development: Foundations for Light Steel Residential Structures.* Access Steel 2006. www.access-steel.com

SS026a-EN-EU. *Scheme Design: Walls in Light Steel in Residential Structures.* Access Steel 2006. www.access-steel.com

SS027a-EN-EU. *Scheme Development: Intermediate Floors in Light Steel Residential Structures.* Access Steel 2006. www.access-steel.com

SS028a-EN-EU. *Scheme development: Roofs for light steel residential structures.* Access Steel 2006. www.access-steel.com

SS032a-EN-EU. *Scheme development: Acoustic performance in residential construction with light steel framing.* Access Steel 2006. www.access-steel.com

Simpson Strong-Tie Company (2007). <http://www.strongtie.com>

Telue Y, Mahendran M (2001). *Behaviour of Cold-formed Steel Wall Frames Lined with Plasterboard*, Journal of Constructional Steel Research 57(4), 435-452.

Thomasson PO (1978). *Thin-walled C-shaped panels in axial compression*, Swedish Council for Building Research, Research Document D1, Stockholm, Sweden.

Timoshenko SP, Gere JM (1961). *Theory of elastic stability*, McGraw-Hill, New York.

Toma T, Sedlacek G, Weynand K (1993). *Connections in Cold-Formed Steel*, Thin Walled Structures, 16, 219-237.

Trahair NS, Bradford MA (1988). *The behaviour and design of steel structures*, 2nd Edition, Chapman and Hall.

Trahair NS (1993). *Flexural-torsional buckling of structures*, E & FN SPON, London.

Trebilcock PJ (1994). *Building design using cold formed steel sections: an architect's guide*, Publication P130. The Steel Construction Institute.

652 The Committee on Light-gauge Steel Structures (2004). The Japan Iron and Steel Federation and Steel-Framed House Association. *Steel-framed Houses - Development and Growing Construction in Japan*, Steel Construction Today & Tomorrow, 9, 1-8.

THIN-WALL (1996). *Cross-section analysis and Finite Strip Buckling Analysis of Thin-Walled Structures*, Centre for Advanced Structural Engineering, University of Sydney.

<http://timber.ce.wsu.edu/Supplements/ShearWall/Loadpath.htm>

Ungureanu V, Dubina D (1999). *Single and interactive buckling modes for unstiffened thin-walled steel sections in compression*, Stability and Ductility of Steel Structures, SDSS'99 (Dubina D & Ivanyi M, Eds.), Elsevier Science Ltd., Oxford, 543-550.

Ungureanu V, Dubina D (2004). *Recent research advances on ECBL approach. Part I: Plastic-elastic interactive buckling of cold-formed steel sections*, *Thin-walled Structures*, 42(2), 177-194.

Ungureanu V, Ciutina A, Tuca I, Dubina D, Grecea D, Fulop L (2011). *Structural and Environmental Performance of Steel Framed Houses: A Case Study*. Summary report of the Cooperative Activities, Cost Action C25. Volume 1: Integrated approach towards sustainable constructions. Department of Civil & Structural Engineering, Faculty for the Built Environment, University of Malta, Malta.

Vayas I, Dubina D (2004). *Cold-formed steel structures* (in Greek), Kleidarithmos Publ., Athena.

Vlasov VZ (1961). *Thin-Walled Elastic Beams*. transl. by Y. Schechtman, Israel Program for Scientific Translations, Office of Technical Services, U.S. Department of Commerce, Washington, DC.

Voutay PA, Davies JM (2002). *Analysis of Cassette Sections in Compression*, Current Research and Practice – Advance in Steel Structures – ICASS’02, Vol. 1 (Chan SL, Teng JG and Chung KF, Eds.), Elsevier Science Ltd, Oxford, 401-408.

Vyberg G (1976). *Diaphragm action of assembled C-shaped panels*, Swedish Council for Building, Research Document D9, Stockholm, Sweden.

Watson K (2005). *Steel Framed Housing*, National Association of Steel-Framed Housing Inc, Australia.

Way AGJ, Popo-Ola SO, Biddle AR, Lawson RM (2009). *Durability of Light Steel Framing in Residential Building*, Publication P262, 2nd Edition. The Steel Construction Institute.

Winter G (1940). *Stress distribution in and equivalent width of flanges of wide thin-wall steel beams*, NACA Technical, Note 784.

Winter G (1970). *Commentary on the 1968 Edition of the Specification for the Design of Cold-formed Steel Structural Members*, American Iron and Steel Institute, New York, NY.

REFERENCES

Wong MF, Chung KF (2002). *Structural behaviour of bolted moment connections in cold-formed steel beam-column sub-frames*, Journal of Constructional Steel Research, Vol. 58, Issue 2, 253-274.

Xu L, Ling Z, Xie WC, Liu Y, Schuster RM (2000). *Dynamic behaviour of floors with cold-formed steel joists*, The 15th International Specialty Conference on Cold-Formed Steel Structures, St. Louis, Missouri USA, October 19-20.

Yu W-W, Toma T, Baehre R, Eds. (1993). *Cold-Formed Steel in Tall Buildings*, Chapter 5: Connections in Cold Formed Steel (Author: Toma T), 95-115. Council on Tall Buildings and Urban Habitat. Committee S37. McGraw-Hill, New York, 184 p.

Yu W-W (2000). *Cold-formed Steel Design* (3rd Edition), John Willey & Sons, New York.

Zadanfarrokh F, Bryan ER (1992). *Testing and design of bolted connections in cold-formed steel sections*, Proceedings of the 11th International Speciality Conference in Cold Formed Steel Structures, St. Louis, Missouri, USA, October 20-21.

Zaharia R, Dubina D (2000). *Behaviour of cold-formed steel truss bolted joints*, Proceedings of the 4th International Workshop of Connections in Steel Structures, Roanoke, USA, October 23-25, 443-453.